

*Operation*

# HARDTACK

*Preliminary Report*

19991012 014

TECHNICAL SUMMARY OF MILITARY EFFECTS  
PROGRAMS 1-9, *sanitized version*

Issuance Date: September 23, 1959

HEADQUARTERS FIELD COMMAND  
DEFENSE ATOMIC SUPPORT AGENCY  
SANDIA BASE, ALBUQUERQUE, NEW MEXICO

Reproduced From  
Best Available Copy

Classification *CANCELLED. THIS VERSION ONLY.*  
By Authority of *ED 12958. Coordinated with DOE, Navy, Air Force.*  
By *[Signature]* Date *2/23/99*

[Redacted]

Statement A  
Approved for public release;  
Distribution unlimited. *per NTPR Review*  
*[Signature]*

68-008627

This is a preliminary report based on all data available at the close of this project's participation in Operation HARDTACK. The contents of this report are subject to change upon completion of evaluation for the final report. This preliminary report will be superseded by the publication of the final (WT) report. Conclusions and recommendations drawn herein, if any, are therefore tentative. The work is reported at this early time to provide early test results to those concerned with the effects of nuclear weapons and to provide for an interchange of information between projects for the preparation of final reports.

When no longer required, this document may be destroyed in accordance with applicable security regulations.

DO NOT RETURN THIS DOCUMENT



[REDACTED]

ITR-1660

OPERATION HARDTACK PRELIMINARY REPORT

*TECHNICAL SUMMARY OF MILITARY EFFECTS  
PROGRAMS 1-9*

Deputy Chief of Staff  
Weapons Effects Tests  
Field Command, AFSWP  
Sandia Base, Albuquerque, New Mexico

RESTRICTED  
[REDACTED]  
[REDACTED]  
[REDACTED]

[REDACTED]

D-3538/1

## ABSTRACT

Although more than 70 devices were detonated during the two phases of Operation Hardtack, principal activity by DOD projects was limited to eleven shots. Five of these were DOD shots and six were developmental.

Two series of tests were conducted to develop immediate tactical doctrines. Underwater shots were fired in two environments, one in relatively deep water, and one on the bottom of Eniwetok Lagoon at a depth of about 150 feet. Although there had been previous underwater shots, many gaps existed in the knowledge of effects from weapons actually available in stockpile. General objectives of this series were attained. Another series of four developmental shots was heavily instrumented by DOD projects.

Only theory, based on extrapolation from much-higher-yield devices, or from high-explosive tests, existed regarding effects from a 1-to-20 ton nuclear device. Yields from these four shots ranged from no nuclear yield, to about 20 tons. Although all of the specific objectives of this program were not realized, knowledge of effects has been enhanced in the area of sub-kiloton detonations.

The very-high-altitude shots were possibly the most important tests during Operation Hardtack. Three shots were fired at altitudes from 85,000 to 250,000 feet. No previous shots had been made at these altitudes. Principal considerations were partition of energy, and, of immediate tactical and strategic concern, the effects on long-range communications, and on ICBM's in the immediate area. Most objectives were attained, although the need for further investigations in this region exists.

Many individual projects participated in the low-yield, underwater, and high-altitude events. In addition, investigations on developmental shots were made in the fields of aircraft response, nuclear-blast detection, world-wide fallout, underground structures, and neutron flux.

Operation Hardtack was the most extensive operation ever engaged in by the DOD. In general, the operation was successful, although there were some individual objectives which were not achieved. Knowledge of the effects of underwater and very-low-yield surface and near-surface shots was vastly increased. Much basic knowledge of very-high-altitude effects was gained. Aircraft and underground structures programs were successful.

## *PREFACE*

Operation Hardtack was concluded on 30 October 1958 with the approach of the Nuclear Test Suspension. Members of the DOD test organizations had been in the field for 10 months. This report, as written, is of necessity a Preliminary Report and much of the data is based on project ITR's and early calculations. It is believed, however, that the information contained herein will be of value. It is emphasized that much of the data is subject to change, as results are analyzed by the operating projects.

The report is a summary of the seven technical programs which operated during the three phases (EPG, Johnston Island and NTS) of Operation Hardtack. In addition, a summary of the activities of the staffs of the Commanders at the various operating locations is included.

Individual chapters and sections of this publication were written by members of the Weapons Effects Test Group who were most concerned with the activities reported.

In many cases, this report discusses an overall program, and results of individual projects are not considered separately. For more detailed information on Hardtack results, the reader is referred to the Preliminary and WT Reports of the projects.

TABLE A SUMMARY OF SHOT DATA AND ENVIRONMENTAL CONDITIONS FOR ENIWETOK PROVING GROUND

SHOT			YIELD			
Code Name	Device Name	Sponsor	Predicted	Radiochemical (Fission)	Hydrodynamic (Total)	Total Recommended
Yucca		AFSWP			—	1.7 kt**
Cactus		LASL			16.9 = 1.6 kt	17.5 = 1.5 kt
Fir		UCRL			1.36 = 0.03 Mt	1.36 = 0.03 Mt
Butternut		LASL			53.5 = 5.4 kt	52 = 6 kt
Koa		LASL			1.30 = 0.08 Mt	1.30 = 0.08 Mt
Wahoo		AFSWP			—	10.5 = 1.5 kt
Holly		LASL			5.72 = 0.39 kt	5.9 = 0.5 kt
Nutmeg		UCRL			22.4 = 1.0 kt	25.0 = 1.3 kt
Yellowwood		LASL			330 = 27 kt	320 = 25 kt
Magnolia		LASL			57.3 = 3.6 kt	57 = 4 kt
Tobacco		LASL			11.6 = 0.8 kt	11.3 = 1 kt
Sycamore		UCRL			91.3 = 6.0 kt	91.3 = 6.0 kt
Rose		LASL			15.3 = 1.1 kt	15 = 1 kt
Umbrella		AFSWP			—	9 = 1.5 kt
Maple		UCRL			204 = 10 kt	213 = 10 kt
Aspen		UCRL			319 = 8 kt	319 = 8 kt
Walnut		LASL			1.46 = 0.09 Mt	1.46 = 0.09 Mt
Linden		LASL			10.2 = 0.8 kt	11 = 1 kt
Redwood		UCRL			412 = 7 kt	412 = 7 kt
Elder		LASL			887 = 57 kt	900 = 60 kt
Oak		LASL			9.01 = 0.65 Mt	8.9 = 0.6 Mt
Hickory		UCRL			13.4 = 0.4 kt	13.2 = 1.4 kt
Sequoia		LASL			4.95 = 0.39 kt	5.1 = 0.4 kt
Cedar		UCRL			220 = 15 kt	220 = 15 kt
Dogwood		UCRL			397 = 10 kt	397 = 10 kt
Poplar		UCRL			9.3 = 0.3 Mt	9.3 = 0.3 Mt
Pisonia		LASL			256 = 20 kt	256 = 25 kt
Juniper		UCRL			63.5 = 4.0 kt	65.0 = 3.5 kt
Olive		UCRL			202 = 7 kt	202 = 7 kt
Pine		UCRL			2.0 = 0.1 Mt	2.0 = 0.1 Mt
Teak		AFSWP			—	3.8 Mt**
Quince		AFSWP			0	0
Orange		AFSWP			—	3.8 Mt**
Fig		AFSWP			13 = 4 tons	21 = 1 tons

\* Not corrected for transmission time.

† Tide in feet above mean low low water.

‡ Estimated from dry runs. World time clock not triggered.

§ Depth of device was 500 feet in 3,200 feet of water.

¶ Depth of device was 150 feet on lagoon bottom.

TABLE A SUMMARY OF SHOT DATA AND ENVIRONMENTAL CONDITIONS FOR ENIWETOK PROVING GROUND (CONT.)

Code Name	Date (EPG)	Time * (EPG)	Device Environment	TIME AND LOCATION		
				Height of Burst ft	Atoll	Site
Yucca	28 Apr	1440:00.256 ± 0.001	Free Balloon	85,000	Bikini	USS Boxer 60 mi W of Bikini
Cactus	6 May	0615:00.142 ± 0.001	Ground Surface	3	Eniwetok	Yvonne
Fir	12 May	0550:00.148 ± 0.001	Barge	9.88	Bikini	Charlie
Butternut	12 May	0615:00.113 ± 0.001	Barge	10.13	Eniwetok	Yvonne
Koa	13 May	0630:00.145 ± 0.001	Ground Surface in 10' water tank	3.0	Eniwetok	Gene
Wahoo	16 May	1330:00.5 = 0.1 †	Underwater	- 500 ‡	Eniwetok	SW of Irvin
Holly	21 May	0630:00.116 ± 0.001	Barge	13.06	Eniwetok	Yvonne
Nutmeg	22 May	0920:00.151 ± 0.001	Barge	12.11	Bikini	Tare
Yellowwood	26 May	1400:00.1345	Barge	10.52	Eniwetok	Janet
Magnolia	27 May	0600:00.1096	Barge	13.88	Eniwetok	Yvonne
Tobacco	30 May	1415:00.1507	Barge	9.06	Eniwetok	Janet
Sycamore	31 May	1500:00.1457 ± 0.001	Barge	11.64	Bikini	Charlie
Rose	3 Jun	0645:00.1123	Barge	15.43	Eniwetok	Yvonne
Umbrella	9 Jun	1115:00.244 ± 0.001	Underwater (lagoon bottom)	- 150 †	Eniwetok	NNE of Henry
Maple	11 Jun	0530:00.1417 ± 0.001	Barge	11.58	Bikini	Fox
Aspen	15 Jun	0530:00.1361 ± 0.001	Barge	10.82	Bikini	Charlie
Walnut	15 Jun	0630:00.1401 ± 0.001	Barge	7.21	Eniwetok	Janet
Linden	18 Jun	1500:00.1160 ± 0.001	Barge	8.25	Eniwetok	Yvonne
Redwood	28 Jun	0530:00.1373	Barge	10.79	Bikini	Fox
Elder	28 Jun	0630:00.130 = 0.020	Barge	9.17	Eniwetok	Janet
Oak	29 Jun	0730:00.1467	Barge	6.5	Eniwetok	Alice
Hickory	29 Jun	1200:00.1455	Barge	12.11 ±	Bikini	Tare
Sequoia	2 Jul	0630:00.1320	Barge	6.5	Eniwetok	Yvonne
Cedar	3 Jul	0530:00.1369	Barge	10.84	Bikini	Charlie
Dogwood	6 Jul	0630:00.2445	Barge	12.25	Eniwetok	Janet
Poplar	12 Jul	1530:00.141	Barge	11.66	Bikini	Charlie
Pisonia	15 Jul	1100:00.123	Barge	6.5	Eniwetok	Yvonne
Juniper	22 Jul	1620:00.139	Barge	12.11	Bikini	Tare
Olive	23 Jul	0830:00.224	Barge	8.0 Est	Eniwetok	Janet
Pine	27 Jul	0830:00.232	Barge	8.0 Est	Eniwetok	Janet
Teak	31 Jul	2350:05.597	Redstone Missile	250,000	Johnston	—
Quince	6 Aug	1415:00.155 = 25	Surface	—	Eniwetok	Yvonne
Orange	11 Aug	2330:08.607	Redstone Missile	141,000	Johnston	—
Fig	15 Aug	1600:00.2516	Surface	—	Eniwetok	Yvonne

\* Not corrected for transmission time. † Tide in feet above mean low low water.

‡ Estimated from dry runs. World time clock not triggered. ‡ Depth of device was 500 feet in 3,200 feet of water.

† Depth of device was 150 feet on lagoon bottom.

\*\* Recommended yield based on similar device previously tested. (Yield not measured on this shot.)

TABLE A SUMMARY OF SHOT DATA AND ENVIRONMENTAL CONDITIONS FOR ENIWETOK PROVING GROUND (CONT.)

Code Name	Station Number	Holmes and Narver Coordinates		METEOROLOGICAL CONDITIONS (Surface)							
				Air Pressure	Air Temperature	Dew Point	Visibility	Tide at Zero Time †	Wind		Relative Humidity
									mb	F	
Yucca	42	—	—	1,011.5	78.2	69.6	10	3.2	055	20	75
Cactus	20	106,370.00	124,215.00	1,010.5	80	72	10	4.8	070	13	76
Fir	5	170,600.00	76,200.00	1,009.2	80.0	73.0	10	3.0	070	17	80
Butternut	33	100,811.78	123,319.35	1,008.6	80.6	74.0	10	2.6	090	12	80
Koa	21	149,360.00	71,120.00	1,010.5	81.0	74.0	10	2.0	050	16	79
Wahoo	44	29,550.45	61,514.78	1,013.1	87.5	73.0	10	3.4	090	15	63
Holly	34	01,834.10	124,942.76	1,010.2	80.6	75.0	10	4.4	090	16	83
Nutmeg	11	99,949.89	110,951.12	1,012.5	81.3	72.5	10	3.1	080	11	76
Yellowwood	28	143,993.96	78,161.29	1,010.8	87.0	73.0	10	2.0	090	14	63
Magnolia	32	101,343.99	124,160.63	1,010.5	80.0	72.0	10	2.1	090	14	76
Tobacco	30	145,137.26	79,778.65	1,010.2	84.0	75.0	7	4.1	080	12	74
Sycamore	5	170,600.00	76,200.00	1,008.1	83.4	74.0	10	5.0	080	15	73
Rose	29	100,810.98	123,315.00	1,008.1	80.9	74.0	10	4.2	090	22	79
Umbrella	43	42,614.65	76,029.01	1,010.8	86.0	72.0	10	2.9	050	20	63
Maple	8	169,298.97	126,799.01	1,010.5	80.7	74.0	10	2.4	070	22	81
Aspen	7	170,601.07	76,071.05	1,011.1	81.3	74.0	10	2.8	050	18	78
Walnut	3	143,995.91	78,168.42	1,011.0	80.8	76.0	10	3.0	090	17	84
Linden	23	101,876.77	125,011.80	1,010.2	88.1	77.5	10	3.2	090	13	71
Redwood	9	169,333.30	126,787.28	1,010.1	81.2	78.5	10	2.2	065	10	92
Elder	2	145,136.42	79,789.53	1,008.7	81.3	74.0	10	1.2	090	17	78
Oak	25	124,981.45	36,108.02	1,009.5	81.1	76.5	10	1.4	120	14	87
Hickory	12	99,950.35	110,951.78	1,010.1	82.0	81.3	10	2.3	090	8	84
Sequoia	24	101,870.70	124,999.56	1,007.3	80.9	76.0	10	3.3	090	17	83.5
Cedar	3	170,600.45	76,203.93	1,010.2	83.2	76.3	10	5.0	070	16	79
Dogwood	2	145,135.10	79,786.30	1,008.9	81.3	77.0	10	3.6	090	17	85
Poplar	4	169,650.45	72,870.51	1,008.1	82.3	81.9	10 to 7	2.3	070	11	99
Pisonia	22	103,212.29	114,678.21	1,011.5	80.3	74.9	4 to 1	0.7	020 to 200	4 to 7	83
Juniper	13	99,950.77	110,949.79	1,009.5	87.5	78.9	10	0.9	090	17	76
Olive	16	145,137.81	79,790.26	1,009.7	79.6	76.0	8	3.5	130	13	89
Pine	10	142,548.79	76,109.98	1,009.3	80.1	75.5	10	1.3	220	16	85
Teak	—	—	—	—	—	—	—	—	—	—	—
Quince	15	103,950.00	126,185.00	1,009.9	89.7	77.5	10	—	090	12	67
Orange	—	—	—	—	—	—	—	—	—	—	—
Fig	15	103,950.00	126,185.00	1,007.8	86.1	78.0	10	—	080	16	77

\* Not corrected for transmission time. † Tide in feet above mean low low water.

‡ Estimated from dry runs. World time clock not triggered. § Depth of device was 500 feet in 3,200 feet of water.

¶ Depth of device was 150 feet on lagoon bottom.

\*\* Recommended yield based on similar device previously tested. (Yield not measured on this shot.)



TABLE B. SUMMARY OF SHOT DATA AND ENVIRONMENTAL CONDITIONS FOR NEVADA TEST SITE

NA, not applicable.

Code Name	Device Name	Sponsor	Predicted	Radiochemical	YIELD	Hydrodynamic	Total Recommended	Date (PST)	Time (PST)	Device Environment	TIME AND LOCATION		Nevada State Grid Coordinates		Device Elevation, MSL	
											Height of Burst	Area	Station Number	North		East
Eddy	[REDACTED]	LASL	[REDACTED]	[REDACTED]	[REDACTED]	[REDACTED]	83 ± 3 tons	19 Sep	0600:00.15 ± 0.1	Balloon	500	7	7b	851,124.94	687,540.14	4,686.47
Mora	[REDACTED]	LASL	[REDACTED]	[REDACTED]	[REDACTED]	[REDACTED]	2.0 ± 0.1 kt	29 Sep	0605:00.077 ± 0.001	Balloon	1,500	7	7b	851,124.94	687,540.14	5,686.47
Tamblains	[REDACTED]	UCRL	[REDACTED]	[REDACTED]	[REDACTED]	[REDACTED]	72 ± 10 tons	8 Oct	1400:00.131 ± 0.010	Underground	Tunnel	12	12b.02	899,430.07	635,789.38	6,616.00
Quay	[REDACTED]	LASL	[REDACTED]	[REDACTED]	[REDACTED]	[REDACTED]	81 ± 6 tons	10 Oct	0630:00.142 ± 0.001	Steel tower	100	7	7c	854,123.94	687,540.18	4,344.62
Lea	[REDACTED]	LASL	[REDACTED]	[REDACTED]	[REDACTED]	[REDACTED]	1.25 ± 0.1 kt	13 Oct	0520:00.136 ± 0.001	Balloon	1,500	7	7b	851,124.94	687,540.14	5,686.47
Hamilton	[REDACTED]	AFSWP	[REDACTED]	[REDACTED]	[REDACTED]	[REDACTED]	1.17 ± 0.06 tons	15 Oct	0800:00.15 ± 0.1	Timber tower	50	FF	F1	747,820.44	715,028.82	3,132.31
Logan	[REDACTED]	UCRL	[REDACTED]	[REDACTED]	[REDACTED]	[REDACTED]	5.0 ± 0.2 kt	15 Oct	2200:00.140 ± 0.005	Underground	Tunnel	12	12a.02	886,350.04	635,615.11	6,141.00
Dona Ana	[REDACTED]	LASL	[REDACTED]	[REDACTED]	[REDACTED]	[REDACTED]	36 ± 4 tons	16 Oct	0620:00.144 ± 0.001	Balloon	450	7	7b	851,124.94	687,540.14	4,636.47
Itu Arriba	[REDACTED]	LASL	[REDACTED]	[REDACTED]	[REDACTED]	[REDACTED]	92 ± 9 tons	18 Oct	0625:00.120 ± 0.001	Timber tower	72.5	3	3s	834,517.11	687,007.14	4,082.13
Socorro	[REDACTED]	LASL	[REDACTED]	[REDACTED]	[REDACTED]	[REDACTED]	6.3 ± 0.6 kt	22 Oct	0530:00.15 ± 0.1	Balloon	1,450	7	7b	851,124.94	687,540.14	5,636.47
Wrangell	[REDACTED]	UCRL	[REDACTED]	[REDACTED]	[REDACTED]	[REDACTED]	116 ± 12 tons	22 Oct	0850:00.115 ± 0.001	Balloon	1,500	FF	Fa	746,249.98	716,000.29	4,576.71
Rushmore	[REDACTED]	UCRL	[REDACTED]	[REDACTED]	[REDACTED]	[REDACTED]	188 ± 10 tons	22 Oct	1540:00.129 ± 0.001	Balloon	500	9	9a	868,633.69	682,418.34	4,714.20
Sanford	[REDACTED]	UCRL	[REDACTED]	[REDACTED]	[REDACTED]	[REDACTED]	4.9 ± 0.3 kt	26 Oct	0220:00.132 ± 0.001	Balloon	1,500	FF	Fa	746,249.98	716,000.29	4,576.71
DeBaca	[REDACTED]	LASL	[REDACTED]	[REDACTED]	[REDACTED]	[REDACTED]	2.5 ± 0.3 kt	26 Oct	0800:00.141 ± 0.001	Balloon	1,500	7	7b	851,124.94	687,540.14	5,686.47
Evans	[REDACTED]	UCRL	[REDACTED]	[REDACTED]	[REDACTED]	[REDACTED]	55 ± 30 tons	28 Oct	1600:00.15 ± 0.1	Underground	Tunnel	12	12a.04	899,231.74	634,545.26	6,829.19
Matzema	[REDACTED]	UCRL	[REDACTED]	[REDACTED]	[REDACTED]	[REDACTED]	0	29 Oct	0320:00.15 ± 0.1	Steel tower	50	9	9d	865,633.89	682,379.36	4,252.47
Humboldt	[REDACTED]	AFSWP	[REDACTED]	[REDACTED]	[REDACTED]	[REDACTED]	7.8 ± 0.7 tons	29 Oct	0645:00.107 ± 0.001	Timber tower	25	3	3v	836,984.24	687,377.67	4,053.65
Santa Fe	[REDACTED]	LASL	[REDACTED]	[REDACTED]	[REDACTED]	[REDACTED]	1.25 ± 0.13 kt	29 Oct	1900:00.119 ± 0.001	Balloon	1,500	7	7b	851,124.94	687,540.14	5,686.47
Blanca	[REDACTED]	UCRL	[REDACTED]	[REDACTED]	[REDACTED]	[REDACTED]	19.0 ± 1.5 kt	30 Oct	0700:00.15 ± 0.1	Underground	Tunnel	12	12a.05	866,986.27	635,352.96	6,138.59

\* One-point safety test shots not included.

TABLE C SUMMARY OF METEOROLOGICAL CONDITIONS FOR SHOTS AT NEVADA TEST SITE

NA, not applicable; NM, not measured. All data was taken at Yucca Flat Weather Station (3,924 MSL).

Shot	On Surface *					At Approximate Elevation of Ground Zero MSL					At Approximate Height of Burst MSL								
	Barometric Pressure mb	Air Temperature C	Dew Point C	Relative Humidity pct	Wind Direction deg	Wind Velocity knots	Air Pressure mb	Air Temperature C	Dew Point C	Relative Humidity pct	Wind Direction deg	Wind Velocity knots	Air Pressure mb	Air Temperature C	Dew Point C	Relative Humidity pct	Wind Direction deg	Wind Velocity knots	
Eddy	882	9.2	-11.0	22		Calm	875	14.2	-7.9	21		Calm	868	21.4	-3.2	19		Calm	
Mora	880	7.5	2.3	70		Calm	874	11.8	6.5	70		Calm	826	17.3	5.0	43		330	3
Tamapais	882	30.1	-6.2	9	290	12	NA	NA	NA	NA	NA	NA	NA	NA	NA	NA	NA	NA	NA
Quay	886	15.0	-2.0	31	290	4	876	15.3	-2.7	29	320	8	870	15.6	-2.9	28	330	9	
Lea	886	3.3	-15.8	23	180	1	878	13.4	-4.3	29	220	1	831	18.3	-1.0	27	190	9	
Hamilton	891	15.7	-1.4	31	360	1	NM	NM	NM	NM	NM	NM	NM	NM	NM	NM	NM	NM	NM
Logan	887	12.8	-5.3	28	160	4	NA	NA	NA	NA	NA	NA	NA	NA	NA	NA	NA	NA	NA
Dona Ana	887	7.1	-8.2	33	360	02	880	13.7	-2.7	32	005	4	862	19.9	-0.7	25	013	6	
Rio Arriba	883	5.0	-12.4	27		Calm	879	9.3	-10.3	24		Calm	878	9.4	-10.7	23		Calm	
Socorro	883	-7.7	-20.8	34		Calm	874	4.7	-14.7	23	027	4	836	9.3	NM	13	095	6	
Wrangell	884	8.3	-19.0	18	290	2	NM	NM	NM	NM	NM	NM	863	11.1	NM	13	070	7	
Rushmore	880	18.3	-11.6	12	135	4	873	17.8	NM	12	141	4	857	16.3	NM	12	165	6	
Sanford	884	3.4	3.1	98	135	1	NM	NM	NM	NM	NM	NM	864	9.4	5.7	78	061	1	
Debeca	885	7.8	5.6	86		Calm	879	8.3	5.1	80		Calm	829	7.6	2.1	68	028	2	
Evans	884	20.0	-5.8	17	010	16	NA	NA	NA	NA	NA	NA	NA	NA	NA	NA	NA	NA	NA
Mazama	886	7.6	-6.6	36	340	6	876	10.0	-6.4	31	380	11	NM	NM	NM	NM	NM	NM	
Humboldt	887	7.2	-3.4	47	345	5	885	7.4	-3.2	46	343	6	NM	NM	NM	NM	NM	NM	
Santa Fe	884	10.5	-6.7	29	340	4	876	12.1	-7.4	25	350	6	828	11.6	-11.3	19	030	14	
Bianca	887	7.9	-8.6	30	330	10	NA	NA	NA	NA	NA	NA	NA	NA	NA	NA	NA	NA	NA

\* Visibility unrestricted for all shots.

## CONTENTS

ABSTRACT -----	4
PREFACE -----	5
CHAPTER 1 INTRODUCTION -----	25
1.1 Background -----	25
1.2 Objectives -----	25
1.3 Summary of Shot Data -----	27
1.4 Project Participation -----	27
1.5 Organization -----	27
1.6 Personnel -----	31
1.7 Administration -----	31
1.8 Security and Classification -----	31
1.9 Operations -----	31
1.10 Communications -----	32
1.11 Timing Signals and Voice Countdown -----	33
1.12 Supplies and Equipment -----	33
1.13 Construction -----	34
1.14 Fiscal -----	34
1.15 Organization and Logistics at NTS -----	35
1.16 Support Photography -----	36
1.17 Reports -----	39
CHAPTER 2 SHOT WAHOO -----	40
2.1 Introduction -----	40
2.1.1 Objectives -----	40
2.1.2 Background -----	40
2.1.3 Procedure -----	44
2.1.4 Preparatory Operations -----	49
2.1.5 Test Operations -----	49
2.2 Wahoo Blast and Shock -----	53
2.2.1 Wahoo Oceanography -----	53
2.2.2 Hydrodynamic Yield Determination -----	55
2.2.3 Underwater Shock Pressures -----	56
2.2.4 Visible Surface Phenomena -----	61
2.2.5 Air Overpressures -----	62
2.2.6 Deep-Water Waves -----	65
2.3 Nuclear Radiation Effects -----	69
2.3.1 General -----	69
2.3.2 Objectives -----	69
2.3.3 Background -----	69
2.3.4 Experimental Method -----	70

2.3.5 Results and Discussion - - - - -	76
2.3.6 Conclusions - - - - -	86
2.4 Ship Response and Damage Studies - - - - -	86
2.4.1 Introduction - - - - -	86
2.4.2 Preliminary Hardtack Tests of Tapered-Charge Technique - - - - -	88
2.4.3 Hull Response and Damage Studies on Surface Ships - - - - -	91
2.4.4 Hull Response Studies of Submarines - - - - -	100
2.4.5 Shipboard Machinery and Equipment Shock Damage Studies - - - - -	102
2.4.6 Summary - - - - -	114
 CHAPTER 3 SHOT UMBRELLA - - - - -	 117
3.1 Introduction - - - - -	117
3.1.1 Objectives - - - - -	117
3.1.2 Background - - - - -	117
3.1.3 Procedure - - - - -	117
3.1.4 Preparatory Operations - - - - -	117
3.1.5 Test Operations - - - - -	118
3.2 Blast and Shock - - - - -	122
3.2.1 Umbrella Preshot and Postshot Bathymetric Surveys - - - - -	122
3.2.2 Hydrodynamic Yield Determination - - - - -	125
3.2.3 Underwater Shock Pressures - - - - -	125
3.2.4 Visible Surface Phenomena - - - - -	130
3.2.5 Air Overpressures - - - - -	133
3.2.6 Water Waves - - - - -	138
3.3 Nuclear Radiation Effects - - - - -	141
3.3.1 General - - - - -	141
3.3.2 Objectives - - - - -	141
3.3.3 Background - - - - -	141
3.3.4 Experimental Method - - - - -	141
3.3.5 Results and Discussion - - - - -	144
3.3.6 Conclusions - - - - -	152
3.4 Ship Response and Damage Studies - - - - -	153
3.4.1 Introduction - - - - -	153
3.4.2 Hull Response and Damage Studies of Surface Ships - - - - -	154
3.4.3 Hull Response Studies of Submarines - - - - -	162
3.4.4 Shipboard Machinery and Equipment Shock Damage Studies - - - - -	166
3.4.5 Summary - - - - -	175
3.5 Naval Mine Field Clearance by Atomic Underwater Bursts - - - - -	177
3.5.1 Objective - - - - -	177
3.5.2 Background - - - - -	178
3.5.3 Instrumentation - - - - -	178
3.5.4 Feasibility of Wide Area Clearance of Naval Influence Mines by Nuclear Weapons - - - - -	186
3.5.5 Data Requirements - - - - -	186
3.5.6 Playback System - - - - -	192
3.5.7 Results - - - - -	196
 CHAPTER 4 SHOT YUCCA - - - - -	 199
4.1 Objectives - - - - -	199

4.1.1	Background	199
4.1.2	Operation	201
4.1.3	Results	201
4.1.4	Summary and Conclusion	201
4.2	Blast Measurements	201
4.2.1	Objectives	201
4.2.2	Background	202
4.2.3	Theory	202
4.2.4	Instrumentation	203
4.2.5	Results	205
4.3	Nuclear Measurements	206
4.3.1	Objectives	206
4.3.2	Background and Theory	206
4.3.3	Experimental Plan	207
4.3.4	Results and Discussion	207
4.3.5	Conclusions	207
4.4	Thermal Radiation Measurements	208
4.4.1	Introduction	208
4.4.2	Background	208
4.4.3	Methods	208
4.4.4	Instrumentation	208
4.4.5	Positioning Methods	209
4.4.6	Results	210
4.4.7	Conclusions	217
CHAPTER 5 SHOTS TEAK AND ORANGE		218
5.1	Background and Objectives	218
5.1.1	Operations	218
5.1.2	Results	219
5.2	Pressure Measurements for High-Altitude Bursts	219
5.2.1	Objective	219
5.2.2	Background	219
5.2.3	Method of Experimentation	222
5.2.4	Field Layout of Equipment	222
5.2.5	Results	224
5.2.6	Discussion	224
5.2.7	Conclusions	229
5.3	Neutron Flux from Very-High-Altitude Bursts	230
5.3.1	Objectives	230
5.3.2	Background	230
5.3.3	Method of Experimentation	232
5.3.4	Reliability of Data	234
5.3.5	Results	234
5.3.6	Summary	237
5.3.7	Conclusions and Recommendations	239
5.4	Chorioretinal Burn Studies	240
5.4.1	Objective	240
5.4.2	Background	240
5.4.3	Theory	241

5.4.4	Procedure	241
5.4.5	Instrumentation	242
5.4.6	Results and Conclusions	243
5.5	Electromagnetic Attenuation Studies	244
5.5.1	Background	244
5.5.2	Objectives	245
5.5.3	Experimental Plan	245
5.5.4	Results	246
5.6	Thermal Radiation Measurements	249
5.6.1	Introduction	249
5.6.2	Background	249
5.6.3	Instrumentation	251
5.6.4	Results	251
5.7	Destructive Effects of Very-High-Altitude Detonations	265
5.7.1	Objectives	265
5.7.2	Background	266
5.7.3	Method of Experimentation	267
5.7.4	Results	272
5.7.5	Conclusions	272
5.8	Temperature, Density, and Pressure of the Upper Atmosphere During a Very-High-Altitude Nuclear Detonation	272
5.8.1	Objectives	272
5.8.2	Background	272
5.8.3	Experimental Plan	273
5.8.4	Results	275
5.8.5	Conclusions	275
5.8.6	Recommendations	275
CHAPTER 6 BLAST AND SHOCK		276
6.1	Introduction	276
6.2	Crater Measurements	279
6.3	Air Blast	279
6.4	Ground Motion	288
6.4.1	Accelerations	288
6.4.2	Displacement	292
6.4.3	Soil Pressure	293
6.4.4	Shock Spectra	296
6.4.5	Results	298
CHAPTER 7 NUCLEAR RADIATION		299
7.1	General	299
7.2	Neutron Flux from Large-Yield Bursts	299
7.2.1	Objectives of Project 2.4	299
7.2.2	Background and Theory	299
7.2.3	Experimental Method	299
7.2.4	Results and Discussion	301
7.2.5	Conclusions	304
7.3	Aircraft and Rocket Fallout Sampling	304



7.3.1 Objectives of Project 2.8	304
7.3.2 Background and Theory	304
7.3.3 Experimental Method	306
7.3.4 Results and Discussion	307
7.3.5 Conclusions	309
<b>CHAPTER 8 STRUCTURES AND EQUIPMENT</b>	<b>310</b>
8.1 Objective	310
8.2 Background (Land Structures)	310
8.3 Response of Earth-Confined Flexible Arch-Shell Structures in High-Pressure Region	310
8.3.1 Objectives	310
8.3.2 Background	311
8.3.3 Structure Description and Construction	311
8.3.4 Instrumentation	312
8.3.5 Results	315
8.3.6 Conclusions	321
8.4 Behavior of Deep Reinforced-Concrete Slabs in High-Pressure Regions	321
8.4.1 Objectives	321
8.4.2 Background	321
8.4.3 Structure Description and Construction	322
8.4.4 Instrumentation	322
8.4.5 Results	325
8.4.6 Conclusions	326
8.5 Damage to Existing EPG Structures	326
8.5.1 Objective	326
8.5.2 Background	326
8.5.3 Procedures	327
8.5.4 Results and Discussion	327
8.5.5 Conclusions	330
8.6 Summary	330
<b>CHAPTER 9 EFFECTS ON AIRCRAFT STRUCTURES</b>	<b>332</b>
9.1 Background and Theory	332
9.2 Objectives	333
9.3 Procedure	333
9.4 Results	333
9.5 Conclusions and Recommendations	345
<b>CHAPTER 10 TEST OF SERVICE EQUIPMENT AND MATERIALS</b>	<b>346</b>
10.1 Objectives	346
10.2 Background	346
10.3 Wave Form of Electromagnetic Pulse from Nuclear Detonations	346
10.4 Effects of Nuclear Detonations on the Ionosphere	350
10.5 Effects of Nuclear Radiation on Electronic Fuze Components and Materials	355

CHAPTER 11 THERMAL RADIATION-----	363
11.1 Introduction-----	363
11.2 Effects on Materials and Skin-Simulant Experiments-----	363
11.3 Instrumentation-----	363
11.4 Results-----	364
11.5 Infrared Correlation Measurements-----	368
11.6 Material Ablation and Neutron Studies-----	368
Chapter 12 SHOTS QUINCE AND FIG-----	370
12.1 Introduction-----	370
12.1.1 Objectives-----	370
12.1.2 Background-----	370
12.1.3 Planning and Operations-----	370
12.2 Blast Measurements-----	372
12.2.1 Objectives-----	372
12.2.2 Background-----	372
12.2.3 Instrumentation-----	372
12.2.4 Results-----	373
12.2.5 Discussion-----	376
12.2.6 Conclusions-----	376
12.3 Crater Measurement-----	376
12.4 Nuclear Radiation-----	377
12.4.1 Introduction-----	377
12.4.2 Operations and Instrumentation-----	377
12.4.3 Results and Discussion-----	380
12.4.4 Conclusions-----	384
12.5 Thermal Radiation from a Very-Low-Yield Burst-----	384
12.5.1 Objectives-----	384
12.5.2 Background-----	384
12.5.3 Instrumentation-----	385
12.5.4 Chemical Warfare Laboratory Instrumentation-----	385
12.5.5 Naval Radiological Defense Laboratory Instrumentation-----	386
12.5.6 Naval Material Laboratory Instrumentation-----	387
12.5.7 Results-----	387
12.5.8 Conclusions-----	388
CHAPTER 13 NEVADA TEST SITE PHASE-----	389
13.1 Nuclear Radiation and Effects-----	389
13.1.1 Introduction-----	389
13.1.2 Objectives-----	391
13.1.3 Background-----	391
13.1.4 Procedure-----	392
13.1.5 Results and Discussion-----	394
13.1.6 Shot Hamilton-----	394
13.1.7 Shot Humboldt-----	400
13.1.8 Conclusions-----	400
13.2 Effects of a Fractional Kiloton Shot on a Biological Specimen-----	401
13.2.1 Introduction-----	401

13.2.2 Objectives -----	401
13.2.3 Background-----	402
13.2.4 Operational Procedure -----	402
13.2.5 Results -----	403
13.3 Operational Analysis of the Dazzle Effect on Combat Personnel -----	405
13.3.1 Introduction -----	405
13.3.2 Operational Procedure -----	405
13.3.3 Results-----	406
13.4 Evaluation of Air-Blast Gages and Supporting Air-Blast Measurements -----	406
13.4.1 Objectives -----	406
13.4.2 Method of Experimentation -----	406
13.4.3 Results-----	408
13.4.4 Conclusions -----	410
13.5 Proof Test of AN/TVS-1 (XE-3) Flash-Ranging Equipment -----	410
13.5.1 Objectives -----	410
13.5.2 Background -----	410
13.5.3 Theory-----	410
13.5.4 Method of Experimentation -----	410
13.5.5 Results -----	411
13.5.6 Conclusions and Recommendations -----	412
13.6 Thermal Radiation from Low-Yield Bursts -----	412
13.6.1 Objective -----	412
13.6.2 Background-----	412
13.6.3 Shot Participation -----	412
13.6.4 Method of Experimentation -----	412
13.6.5 Data Obtained -----	413
13.6.6 Discussion -----	413
13.7 Electromagnetic Pulse Measurements of Low-Yield Bursts -----	416
13.7.1 Objectives-----	416
13.7.2 Background -----	416
13.7.3 Method of Experimentation -----	416
13.7.4 Data Obtained -----	417
APPENDIX -----	418
REFERENCES-----	451
FIGURES	
1.1 Organization of Joint Task Force 7 -----	29
1.2 Task Unit 7.1.3 organization -----	30
1.3 Task Unit 3 personnel deployment-----	37
2.1 Early planning array for Shot Wahoo -----	42
2.2 DD-592 Ex-USS Howorth -----	45
2.3 EC-2 Ex-Michael Moran -----	45
2.4 USS Bonita (SSK-3) being placed in the Umbrella array. -----	46
2.5 Barges used in the Wahoo array to moor the target ships and to provide project instrument platforms -----	46
2.6 Coracle, moored around the shot area -----	47
2.7 Shot Wahoo: active ships around surface zero -----	48
2.8 Wahoo target array at shot time, showing approximate water depths -----	50

2.9	Wahoo array looking from near surface zero down the destroyer line -----	52
2.10	Placing the Wahoo device-----	52
2.11	Comparison of BT observations at 1100 and 1200 of Shot Wahoo minus 6 days-----	54
2.12	Extrapolated sound velocity cross section along the array at Wahoo shot time -----	55
2.13	Underwater pressures versus range, Shot Wahoo-----	58
2.14	Comparison of peak underwater pressures with predicted contours, Shot Wahoo-----	59
2.15	Underwater shock-wave records, Shot Wahoo-----	59
2.16	Growth of Shot Wahoo plume-----	63
2.17	Plume collapse and base surge-----	64
2.18	Air overpressure records, Shot Wahoo-----	66
2.19	Water-wave measurement stations, Shot Wahoo-----	67
2.20	Subsurface pressure as a function of time, Station 160.03, Site James, Shot Wahoo-----	68
2.21	Inundation elevations for Site Irwin-----	68
2.22	The GITER Model 103 instrument with the outer water-tight case cover removed-----	71
2.23	Coracle-----	71
2.24	Various types of floating film packs-----	72
2.25	Map of Wahoo array, showing coracles, floating film packs, and target ships-----	73
2.26	Location and designation of GITER stations on target destroyers-----	74
2.27	Instrument locations on DD-592-----	75
2.28	Dose rate versus time for std-GITER. Coracle at DRR 7.2 (277 deg T, 6,920 feet) Tape 080-----	77
2.29	Dose rate versus time for std-GITER. Coracle at DL 7.2 (231.5 deg T, 7,100 feet) Tape 94-----	78
2.30	Dose rate versus time for std-GITER. Coracle at D 8.0 (251 deg T, 7,580 feet) Tape 123-----	79
2.31	Map of Wahoo array showing doses received at coracle stations within one minute after shot time-----	80
2.32	Dose rate versus time for GITER at Station 1, Pilot House on EC-2-----	81
2.33	Dose rate versus time for GITER at Station 1 on DD-593-----	81
2.34	Plots of film-pack doses and estimated solid angle of radioactive cloud subtended at film packs at various locations on main decks of DD-474, DD-592, DD-593, Shot Wahoo-----	82
2.35	Total gamma doses on deck of DD-593 after Shot Wahoo-----	85
2.36	Transit gamma doses on deck of DD-593 after Shot Wahoo-----	85
2.37	Comparison of shock waves of tapered charge and conventional charge of identical weight at the same distance-----	89
2.38	Special charge studies, preliminary Shot Wahoo-----	90
2.39	Tapered charge rigging plan-----	90
2.40	Armed tapered charge I before lowering for second test-----	91
2.41	Second test-----	94
2.42	Loading and basic target response for surface ships-----	94
2.43	EC-2 gage locations-----	95
2.44	Recording equipment on EC-2 instrument platform-----	97

2.45 Overall phenomena in Shot Wahoo (EC-2) -----	97
2.46 Hull loading and hull response, EC-2 (Shot Wahoo) -----	98
2.47 Cross-section distribution of EC-2 hull response, Shot Wahoo -----	98
2.48 Longitudinal distribution of response in DD-593, Shot Wahoo -----	99
2.49 Response distribution upward through DD-593, Shot Wahoo -----	99
2.50 Inboard profile and section views, showing locations of strain gages on the USS Bonita (SSK-3) -----	102
2.51 Oscillogram of bottom-reflected shock wave on the USS Bonita (SSK-3) for Shot Wahoo -----	104
2.52 Shock studies of shipboard machinery and equipment -----	106
2.53 Recording equipment on resiliently mounted table in recording center -----	108
2.54 Typical installation of a velocity meter and a shock-spectrum recorder -----	108
2.55 Typical installation of high-speed motion-picture cameras -----	109
2.56 Oscillogram of direct shock wave on SS Michael Moran (EC-2) for Shot Wahoo -----	110
2.57 Comparison of shock spectra on the three target destroyers for Shot Wahoo -----	113
3.1 Squaw, scale-model submarine construction, previously used during Operation Wigwam, being placed in the target array for Shot Umbrella -----	118
3.2 Early planning target array for Shot Umbrella -----	119
3.3 Target array for Shot Umbrella -----	121
3.4 Preshot hydrographic survey of the Umbrella area -----	123
3.5 Bottom profiles through surface zero prior to and after Shot Umbrella -----	124
3.6 Instrumentation for early time-of-arrival data -----	126
3.7 Pressure versus distance for Umbrella and Wigwam -----	126
3.8 Shock-wave record -----	128
3.9 Arrival times versus horizontal distance, Shot Umbrella -----	128
3.10 BC gage peak pressures at various depths versus distance, Shot Umbrella -----	129
3.11 EPT and MPT gage peak pressures at various depths versus distance, Shot Umbrella -----	129
3.12 Shock-wave durations at various depths versus distance, Shot Umbrella -----	131
3.13 Shock-wave peak-pressure comparisons, Shot Umbrella -----	131
3.14 Development of throwout, Shot Umbrella -----	132
3.15 Base surge upwind and downwind extent, at early times, Shot Umbrella -----	134
3.16 Rocket, camera, and radar ship stations -----	135
3.17 Details of pressure probe -----	135
3.18 General layout of dart -----	135
3.19 Three Ultradyn gage records -----	136
3.20 Summary of mechanical gage results, Shot Umbrella -----	137
3.21 Comparison of Umbrella surface data with estimated high- explosive data (maximum pressure data) -----	137
3.22 Water-wave measurement stations, Shot Umbrella -----	139
3.23 Subsurface pressure as a function of time near stations, Shot Umbrella -----	140
3.24 Wave record for Station 160.01, Site Henry, Shot Umbrella -----	140
3.25 Location and designation of GTR stations on target destroyers -----	143

3.26	Instrument locations on DD-592 -----	145
3.27	Dose rate versus time for std-GITR -----	146
3.28	Map of Umbrella array showing doses received at coracle (and SIO skiff) stations within one minute after shot time -----	146
3.29	Total gamma doses on decks of target destroyers after Shot Umbrella -----	148
3.30	Plots of film pack dose and estimated solid angle of radioactive cloud subtended at film packs at various locations on main deck of DD-474, Shot Umbrella -----	148
3.31	Total gamma dose rates on decks of target destroyers after Shot Umbrella -----	150
3.32	Transit gamma dose rates on decks of DD-592 and DD-593 after Shot Umbrella -----	150
3.33	Gamma dose rates in water below DD-593 after Shot Umbrella -----	151
3.34	Gamma-ionization decay of contaminant collected in 6-inch-thick lead cave on DD-592 after Shot Umbrella, values corrected for background -----	152
3.35	Overall underwater phenomena, DD-474, Shot Umbrella -----	156
3.36	Overall pressure phenomena, DD-592, Shot Umbrella -----	156
3.37	Overall pressure phenomena, DD-593, Shot Umbrella -----	157
3.38	Overall underwater phenomena, EC-2, Shot Umbrella -----	157
3.39	Cross-section distribution of initial hull response, EC-2, Shot Umbrella -----	158
3.40	Longitudinal distribution of bottom (keel) velocities, DD-474, Shot Umbrella -----	158
3.41	Response distribution upward along bulkhead, DD-474, Shot Umbrella -----	159
3.42	Vertical displacements on DD-474, Shot Umbrella -----	160
3.43	Vertical displacements on EC-2, Shot Umbrella -----	161
3.44	Squaw submarine hull instrumentation response -----	164
3.45	SSK-3 instrumentation and hull response -----	165
3.46	Pressures measured under the bow and near the bottom of the ballast tanks in Squaw-29 during Shot Umbrella -----	167
3.47	Oscillogram of direct shock wave on the Squaw-29 for Shot Umbrella -----	168
3.48	Oscillogram of direct shock wave on the USS Bonita (SSK-3) for Shot Umbrella -----	169
3.49	Oscillogram of direct shock wave on SS Michael Moran (EC-2) for Shot Umbrella -----	172
3.50	Shock spectra obtained near the bottom of a bulkhead on each of the surface targets, Shot Umbrella -----	173
3.51	Vertical velocities of turbine foundation and subbases in USS Fullam (DD-474), for direct shock wave from Shot Umbrella -----	176
3.52	Layout of mine field -----	180
3.53	Damage to mines Mark 25-2 at 1,380 feet -----	181
3.54	Damage to mines Mark 25-2 at 1,980 feet -----	181
3.55	Peak pressures computed from mechanical-pressure-gage deformations, assuming step response -----	188
3.56	Location of instrument platforms relative to surface zero for Shots Umbrella, Wahoo, Yellowwood, and Tobacco -----	189



3.57 Schematic of underwater instrumentation and mines relative to Platform 1 (Station 681.01) -----	190
3.58 Block diagram of pressure measuring system -----	193
3.59 Block diagram of monitor system for mine Mark 25 Mod 0 -----	193
3.60 Idealizer for magnetic mines -----	195
3.61 View of LCU 1317, Platform 1 -----	195
3.62 Typical mine installation -----	196
4.1 Yucca in-flight configuration -----	200
4.2 Canister with pressure transducer -----	204
4.3 Trace of direct telemetering, Canister 5 -----	205
4.4 Positioning technique used by AOC-CIC -----	210
4.5 Shot Yucca thermal pulse from FUV No. 77, 2,000 to 2,500 Å, Project 8.2, AFCRC -----	211
4.6 Shot Yucca thermal pulse from NUV No. 14, 2,500 to 3,950 Å, Project 8.2, AFCRC -----	211
4.7 Shot Yucca thermal pulse from VIS No. 27, 3,950 to 5,000 Å, Project 8.2, AFCRC -----	211
4.8 Shot Yucca thermal pulse from IR No. 44, 5,000 to 10,000 Å, Project 8.2, AFCRC -----	212
4.9 Shot Yucca thermal pulse from the bolometer (A/C 15750), Project 8.2, AFCRC -----	212
4.10 Shot Yucca fireball versus time, Project 8.3, EG&G -----	214
4.11 Shot Yucca temperature and brightness, Project 8.3, EG&G -----	215
5.1 Johnston Island layout -----	219
5.2 Redstone missile -----	220
5.3 Planned Redstone missile trajectories; Shot Orange, left and Shot Teak, right -----	221
5.4 Statham pressure gage -----	223
5.5 Field layout of electronic recording system -----	223
5.6 Tower station -----	225
5.7 Base of tower station -----	225
5.8 After-the-fact station layout for Shot Teak -----	226
5.9 After-the-fact station layout for Shot Orange -----	226
5.10 Overpressure time record from Station 172.02, 34-foot tower, Shot Orange -----	227
5.11 Overpressure time record from Station 172.02, ground level, Shot Orange -----	227
5.12 Arrival time versus slant range for Teak and Orange -----	227
5.13 Positive phase duration versus slant range for Teak and Orange -----	227
5.14 Surface level overpressures versus slant range for Teak and Orange -----	229
5.15 Missile and pod trajectories for Shot Teak -----	232
5.16 Missile and pod trajectories for Shot Orange -----	233
5.17 Pod 3C dose rate, Shot Teak -----	236
5.18 Pod 3 neutron flux 14.35 km, Shot Teak -----	237
5.19 Pod 2 dose rate, Shot Orange -----	238
5.20 Pod 2 neutron flux 8.25 km, Shot Orange -----	238
5.21 Pod 4 dose rate, Shot Orange -----	239
5.22 Array for ionospheric absorption measurements -----	245
5.23 Array for radar reflection measurements -----	246
5.24 Typical communication circuit input versus time records -----	248

5.25	Typical rocket trajectory for determining Shot Orange attenuation region -----	248
5.26	Shot Teak fireball -----	252
5.27	Shot Orange fireball -----	253
5.28	Streak records, Shot Teak -----	254
5.29	Streak records, Shot Orange -----	255
5.30	Shot Teak diameter-time data -----	256
5.31	Shot Teak thermal pulse from FUV No. 57 (far-ultraviolet), 2,000 to 2,500 Å -----	256
5.32	Shot Teak thermal pulse from NUV No. 78(d) (near-ultraviolet), 2,500 to 3,950 Å -----	257
5.33	Shot Teak thermal pulse from VIS No. 23 (visible), 3,950 to 5,000 Å -----	257
5.34	Shot Teak thermal pulse from IR No. 48 (infrared), 5,000 to 10,000 Å -----	258
5.35	Shot Teak thermal pulse from Bolometer No. 2 -----	258
5.36	Shot Orange thermal pulse from FUV No. 57, 2,000 to 2,500 Å -----	259
5.37	Shot Orange thermal pulse from NUV No. 78(d), 2,500 to 3,950 Å -----	259
5.38	Shot Orange thermal pulse from VIS No. 31, 3,950 to 5,000 Å -----	259
5.39	Shot Orange thermal pulse from IR No. 16, 5,000 to 10,000 Å -----	260
5.40	Shot Orange thermal pulse from Bolometer No. 2 -----	260
5.41	Approximate thermal pulse, 3.8 Mt air burst -----	261
5.42	Fireball radius versus time, Shot Teak -----	262
5.43	Fireball radius versus time, Shot Orange -----	263
5.44	Spectral irradiance versus time, Shot Orange -----	264
5.45	Streak spectra of Shot Teak -----	264
5.46	Streak spectra of Shot Orange -----	265
5.47	Nose cone and instrument canister -----	269
5.48	Photograph of single piston device -----	269
5.49	Front face of instrument casting (Shot Teak) -----	270
5.50	Side view of instrument casting (Shot Teak) -----	271
5.51	Illustration of thermal-intensity device -----	271
5.52	Complete sphere assembly -----	273
5.53	Head assembly, exploded view -----	274
5.54	Aspen vehicle in firing position -----	274
6.1	Instrumentation location, Shot Cactus -----	277
6.2	Instrumentation location, Shot Koa -----	278
6.3	Cactus: Preshot and postshot surveys -----	280
6.4	Koa: Preshot and postshot surveys -----	280
6.5	Cactus preshot aerial photograph -----	281
6.6	Cactus postshot aerial photograph -----	281
6.7	Koa preshot aerial photograph -----	282
6.8	Koa postshot aerial photograph -----	282
6.9	Crater radius versus height of burst, scaled to 1 kt -----	283
6.10	Crater depth versus height of burst, scaled to 1 kt -----	283
6.11	Scaled pt data, Shots Cactus and Koa, with free-air 1 kt curve (from TM 23-200) scaled to 1.6 kt -----	285
6.12	Pt wave forms -----	286
6.13	Scaled VLP data -----	287
6.14	Maximum slap acceleration versus depth, Shot Koa -----	290
6.15	Maximum slap acceleration versus depth, Shot Cactus -----	291
6.16	Typical acceleration records -----	292

6.17	Displacement records -----	293
6.18	Drum layout for Shot Cactus -----	294
6.19	Underground pressures, Shot Cactus -----	295
6.20	Underground pressures, Shot Koa -----	295
6.21	Self-recording reed gage -----	297
6.22	Low-frequency self-recording gage -----	297
7.1	Station layout, Project 2.4, Shots Yellowwood and Walnut -----	300
7.2	Station array with ground cable and anchors -----	301
7.3	Neutron flux measured by fission foils times slant distance squared versus slant distance, Shot Yellowwood -----	302
7.4	Neutron flux measured by fission foils times slant distance squared versus slant distance, Shot Walnut -----	302
7.5	Predicted and measured dosages for Shot Yellowwood -----	303
7.6	Predicted and measured dosages for Shot Walnut -----	303
7.7	Air-sampling rocket -----	308
8.1	Typical non-drag-sensitive earthwork configuration -----	312
8.2	One of the 25-foot-span arch shells -----	313
8.3	Structure 3.2d, endwall reinforcing by steel tie-rods and concrete deadman anchorage -----	313
8.4	Earth configuration, 25-foot-span structure -----	314
8.5	Earth configuration, 38-foot-span structure -----	314
8.6	Completion of earthwork construction, Structure 3.2b -----	316
8.7	Postshot view of horizontal plate joint in Structure 3.2a -----	316
8.8	Structure 3.2b, postshot -----	317
8.9	Aerial view Structure 3.2d, postshot -----	318
8.10	Structure 3.2d, postshot -----	319
8.11	Structure 3.2d, postshot -----	319
8.12	Structure 3.2d, postshot -----	320
8.13	One-way slab supports at the 600-psi location -----	323
8.14	Two-way slab support -----	324
8.15	Posttest view of two-way slabs at range of 1,830 feet, looking away from ground zero, depicting the evidence of foundation failure -----	326
8.16	Peak air overpressure for a 1-kt surface burst, with observed points -----	328
8.17	Reduced vertical ground acceleration 10 feet below ground surface for a 1-kt surface burst, with observed points -----	329
8.18	Damage to wood-frame camp structures for a surface burst -----	329
9.1	Location of the B-52 for each shot participation -----	335
9.2	Overpressure and time-of-shock-arrival correlation -----	336
9.3	Orientation angle and overpressure coverage -----	337
9.4	Correlation of measured and calculated percent design limit bending moment -----	351
9.5	Correlation of measured and calculated direct radiant exposure -----	338
9.6	Correlation of measured and calculated temperature rise -----	338
9.7	Correlation of measured and actual temperature rise using the measured vertical component of the radiant exposure ( $Q_N$ ) -----	339
9.8	Measured variation of bending-moment stress at right-wing Station 17.5 for FJ-4 139467; Shot Koa -----	339
9.9	Measured normal load factor near the airplane center of gravity for FJ-4 139310; Shot Butternut -----	339

9.10	Chordwise overpressure distribution at 0.002-second intervals following shock arrival at the tail at Wing Station 175.75 for FJ-4 139310; Shot Butternut -----	340
9.11	Chordwise overpressure distribution at 0.002-second intervals following shock arrival at the tail at Wing Station 175.75 for FJ-4 139467; Shot Koa -----	341
9.12	Incremental section lift, following shock arrival at the tail, at Wing Station 175.75 for FJ-4 139310; Shot Butternut-----	343
9.13	Incremental section lift, following shock arrival at the tail, at Wing Station 175.75 for FJ-4 139467; Shot Koa-----	343
10.1	Wave form: Shot Yucca, 2 kt, 440 miles; Kusaie -----	348
10.2	Wave form: Shot Yucca, 2 kt, 440 miles; Kusaie -----	348
10.3	Wave form: Shot Cactus, 17 kt, 240 miles; Wotho -----	349
10.4	Wave form: Shot Cactus, 17 kt, 240 miles; Wotho -----	349
10.5	Wave form: Shot Cactus, 17 kt, 240 miles; Wotho -----	351
10.6	Wave form: Shot Fir, 1.36 Mt, 100 miles; Wotho-----	351
10.7	Wave form: Shot Fir, 1.36 Mt, 100 miles; Wotho-----	352
10.8	Wave form: Shot Nutmeg, 22.5 kt, 100 miles; Wotho -----	352
10.9	Wave form: Shot Nutmeg, 22.5 kt, 100 miles; Wotho -----	353
10.10	Component magnetic recorder, showing electronic and power decks open for servicing -----	357
10.11	Component magnetic recorder, showing plug-in circuit elements-----	357
10.12	Exposure pod for dynamic test of components-----	358
10.13	Interior of exposure pod, showing method of mounting components for test-----	358
10.14	Station map, Site Tare -----	359
10.15	Station map, Site Fox-----	360
11.1	Temperature histories of the NML simulant bare and blackened -----	365
11.2	Temperature histories of the NML simulant in contact with the hot-wet assembly -----	366
11.3	Temperature histories of the NML simulant in contact with the gray uniform assembly -----	366
12.1	Blast line layout for Shots Quince and Fig, Site Yvonne -----	373
12.2	Peak dynamic pressure versus ground range, Shot Fig -----	374
12.3	Comparison of Fig overpressure data with the 1-kt free-air overpressure curve scaled to 1.6 kt and then to 21.5 tons -----	374
12.4	Neutron dose, Shot Fig -----	382
12.5	Gamma doses versus distance-----	382
12.6	Composite decay curve of fallout samples, Shot Fig -----	383
13.1	DOD organization, NTS phase of Operation Hardtack-----	390
13.2	Station array, Shot Hamilton-----	395
13.3	Station array, Shot Humboldt -----	395
13.4	Neutron dose as measured by the threshold detector technique times slant distance squared versus slant distance for Shot Hamilton and Shot Humboldt-----	396
13.5	Neutron dose, $RD^2$ versus slant distance, from sulfur activation on 0-degree axis -----	396
13.6	Neutron dose, $RD^2$ versus slant distance, from sulfur activation on 85-degree axis-----	397
13.7	Initial gamma dose rate versus time at 550 yards, 85-degree axis -----	397

13.8	Initial gamma dose rate versus time at 750 yards, 85-degree axis	398
13.9	Initial gamma dose versus distance	399
13.10	Summary of initial gamma, $RD^2$ versus slant distance	399
13.11	Overpressures versus ground range, Shot Hamilton	407
13.12	Maximum total head pressure versus ground range, Shot Hamilton	408
13.13	Overpressures versus ground range, Shot Humboldt	409
13.14	Maximum total head pressure versus ground range, Shot Humboldt	409
13.15	Peerless flash-ranging set, AN/TVS-1 (XE-3), showing camera with 5-inch lens, automatic actuator, camera mount, leveler, tripod, control box, and battery box	411

#### TABLES

A	Summary of Shot Data and Environmental Conditions for Eniwetok Proving Ground	6
B	Summary of Shot Data and Environmental Conditions for Nevada Test Site	7
C	Summary of Meteorological Conditions for Shots at Nevada Test Site	8
1.1	Project Participation, Pacific Phase	28
2.1	Projects and Agencies Participating in Shots Wahoo and Umbrella	43
2.2	Funding for Underwater-Test Projects	43
2.3	Funding for Support Items of Underwater Shots	44
2.4	Distances of Target Array Units from Surface Zero, Shot Wahoo	51
2.5	Summary of EPT and MPT Underwater Shock Data, Shot Wahoo	60
2.6	Direct Shock Wave Durations, Shot Wahoo	61
2.7	Bottom Reflection Coefficients, Shot Wahoo	62
2.8	Summary of Air Blast Data, Shot Wahoo	65
2.9	Comparison of Peak Air Overpressures with Predictions	65
2.10	Average 24-hour Gamma Doses Aboard Target DD's Based upon Film Badge Data, Shot Wahoo	83
2.11	Ratios of Gamma Dose in Compartments to Dose on Weather Deck, Based on Average Film Badge Data, Shot Wahoo	83
2.12	Comparison of Early Target Response at Tapered Charge Test with Atomic Explosion Data	92
2.13	Strains on the USS Bonita (SSK-3) from Shot Wahoo	103
2.14	Velocities, Rise Times, and Average Accelerations on SS Michael Moran (EC-2) from Shot Wahoo	111
2.15	Velocities, Rise Times, and Average Accelerations on USS Killen (DD-593) from Shot Wahoo	112
2.16	Vertical Velocities of Hull for Direct Shock Wave from Shot Wahoo	114
3.1	Target-Ship Distances from Surface Zero for Shot Umbrella	120
3.2	Summary of Early Hydrodynamic Data, Shot Umbrella	127
3.3	Summary of First Wave Data, Shot Umbrella	138
3.4	Average 24-hour Gamma Doses Aboard Target Ships Based upon Film-Badge Data	149
3.5	Strains on Squaw-29 from Shot Umbrella	170
3.6	Strains on the USS Bonita (SSK-3) from Shot Umbrella	170
3.7	Velocities, Rise Times, and Average Accelerations on SS Michael Moran (EC-2) from Shot Umbrella	174
3.8	Velocities, Rise Times, and Average Accelerations on USS Fullam (DD-474) from Shot Umbrella	175

3.9	Effects of the Nuclear Detonation on the Mine Field	182
3.10	Effect of Shot Umbrella on Mine Field	185
3.11	Actuations Recorded During the Test	187
3.12	Array Specifications for Platform 1, Station 681.01	191
3.13	Shot and Platform Locations	197
4.1	Command Tones and Tone Functions	204
4.2	Irradiance Data from Shot Yucca	212
4.3	Shot Yucca Geometry	216
5.1	Overpressure Measurements, Shot Teak	228
5.2	Overpressure Measurements, Shot Orange	228
5.3	Tabulation of Arrival Times and Positive-Phase Durations, Shots Teak and Orange	229
5.4	Trajectory Data	234
5.5	Predicted and Estimated Actual Slant Ranges to Pods	235
5.6	Preliminary Estimates of Pod Performances	235
5.7	Attenuation Data	237
5.8	Positioning of Rabbits and Thermal Recording Devices for Shots Teak and Orange	241
5.9	Cloud Cover, Shot Teak	242
5.10	Condition of Rabbits' Eyes at Exposure Time, Shot Teak	242
5.11	Cloud Cover, Shot Orange	243
5.12	Condition of Rabbits' Eyes at Exposure Time, Shot Orange	243
5.13	Estimated Thermal Intensities at Various Exposure Stations	244
5.14	Positions of Aircraft for Shots Teak and Orange	250
5.15	Neutron Intensity Measurements	272
6.1	Gage Locations for Each Project 1.8 Station	289
7.1	Summary of Aircraft Samples	309
8.1	Summary of Structural Results	315
8.2	Peak Surface Overpressures	325
9.1	Peak Responses of Stabilizer and Fin, Project 5.1	334
9.2	Thermal Input and Response Data, Project 5.1	334
9.3	Measured and Calculated Values of Overpressure and Time of Shock Arrival	342
9.4	Measured and Calculated Values of Maximum Temperature Rise	344
10.1	Wave Form and Shot Parameters	354
10.2	First Disturbance above Kusaie, Shot Fir	354
11.1	Maximum Temperature Rise of the Skin Simulants, Shot Yellowwood	367
11.2	Maximum Temperature Rise of the Skin Simulants, Shot Walnut	367
12.1	Subkiloton Yield Nuclear Device, Shots Quince and Fig	371
12.2	Results of Pressure-Time Gages, Shot Fig	375
12.3	Results of Dynamic-Pressure Gages, Shot Fig	376
12.4	Neutron Dose, Shot Fig	381
12.5	Ground Station Instrumentation	385
12.6	Radiant Exposure Data	387
13.1	Project Participation, Nevada Phase	391
13.2	Foxhole Dosimetry, Shot Humboldt	404
13.3	M-59, Armored Personnel Carrier, Dosimetry, Shot Humboldt	405
13.4	Station Bearing, Slant Range, Elevation, and Burst Altitude	413
13.5	Predicted versus Measured Fireball Time History	414
13.6	Measured versus Scaled Irradiance	415



TOP SECRET

## Chapter I INTRODUCTION

### 1.1 BACKGROUND

In memorandums of 5 June 1956, 24 January 1957, and 4 February 1957, the Joint Chiefs of Staff approved incorporation of the following special shots in Operation Hardtack: (1) a very-high-altitude, balloon-borne detonation (90,000 feet) of about 2 kt (Shot Yucca); (2) a very-high-altitude, missile-borne detonation (250,000 feet) of about 4 Mt (Shot Teak); (3) an additional missile-borne detonation (125,000 feet) of about 4 Mt (Shot Orange); (4) an underwater event of about 10 kt detonated at 500 feet below the surface in 3,000 feet of water (Shot Wahoo); and (5) an additional underwater event detonated on the bottom of Eniwetok Lagoon in 150 feet of water (Shot Umbrella).

The Joint Chiefs of Staff also authorized the Armed Forces Special Weapons Project (AFSWP) to plan and implement, in coordination with the various services and the AEC, appropriate test programs to be conducted in conjunction with the aforementioned detonations, and to select appropriate nuclear devices.

The Chief, AFSWP, formulated these plans, and also a number of separate projects to be conducted in conjunction with selected development shots. Projects were designated with various private and governmental laboratories as project agencies.

During the final planning and operational phases of the operation, the number of scheduled shots was increased from 25 to 35 and some projects were added and a few deleted. (See Table 1.1 for final operating projects and agencies). Most shot additions had little effect on Department of Defense (DOD) participation with the exception of Shots Quince and Fig, development shots predicted to be approximately 10 to 50 tons in yield. They were of great interest to the DOD and extensive participation was authorized. Another change which vitally affected planning and organization was the movement of Shots Teak and Orange from Bikini Atoll to Johnston Island, and the resulting delay of three months.

A second phase of Operation Hardtack was conceived near the end of the Pacific Operation. Tests involved in this phase were conducted at the Nevada Test Site (NTS). Primary DOD interest again centered around very-low-yield devices.

The overall Research and Development costs, including the major changes noted, were budgeted at \$28,662,074.

The operational phase opened with the firing of Shot Yucca between the Eniwetok and Bikini Atolls on 28 April 1958, and ended at 2400, 30 October at the NTS when, by Presidential decree, an atomic test suspension became effective.

### 1.2 OBJECTIVES

All EPG detonations during Operation Hardtack were barge shots except the five DOD shots mentioned in Section 1.1 and four surface shots (Cactus, Koa, Quince and Fig). NTS shots included balloon, tower and underground detonations. Major DOD efforts were concentrated on Shots Yucca, Cactus, Koa, Wahoo, Umbrella, Teak, Orange, Quince, Fig, Hamilton, and Humboldt, although individual projects participated in other shots.

Department of Defense program participation was of a greater magnitude than on any previous operation. Most experiments conducted in the EPG were of a nature that could not be carried out at the NTS, due to yield or environmental requirements.

Program 1 was designed to determine air blast, underground shock, and underwater shock

TOP SECRET

parameters and effects. Primary participation included the underwater shots, Wahoo and Umbrella; three surface shots, Koa, Cactus, and Fig; and the very-high-altitude shot, Yucca. Underwater and air-blast pressures from the underwater events provided input data to assist the individual services in determining safe-delivery ranges for ships and aircraft, and to support the target-response projects of Program 3. Ground-shock measurements from the surface bursts provided design criteria for hard underground structures and missile sites. Air-blast information from the very-high-altitude shot provided data to check theoretical estimates of energy partition at high altitude. In addition, blast and crater measurements made on a very-low-yield weapon will be of particular interest to the ground forces.

Program 2 objectives were of a diversified nature.

(a) Participation in the underwater events was developed to determine the gross radiological hazards resulting from underwater bursts. Included were free-field measurements, deck and selected compartment contamination, and ingestion and inhalation hazards from contamination entering the ships via ventilation and combustion air systems.

(b) Neutron-energy-spectrum data collected will be used to supplement the presently inadequate knowledge of neutron-energy spectrums from thermonuclear weapons.

(c) Prompt-neutron measurements were to be determined from a very-high-altitude, small-yield weapon and the neutron-energy spectrum and gamma-ray dose at several distances from the two very-high-altitude, megaton-yield detonations were to be determined.

(d) Radiation measurements in the nuclear cloud were to be made to obtain better data concerning the contribution of radioactive debris to world-wide contamination.

(e) Neutron and prompt-gamma measurements, as well as close-in fallout data, were to be obtained from a very-low-yield device.

Program 3 was designed for determination of the effects of underwater bursts on surface and subsurface vessels, and for the study of several types of land structures under various loading conditions. Information obtained from underwater bursts will aid in formulation of operational doctrine regarding delivery ranges and tactics for both surface and subsurface ships. Information obtained on the response of ship's structures will provide criteria for future designs. Data obtained from various earth-covered flexible arches tested under both long and short duration air blasts, and deep reinforced-concrete slabs, tested under blast loading, will assist in determining construction criteria for future underground structures.

Program 4 was activated during the operational phase to determine the extent of chorioretinal damage caused by direct exposure to very-high-altitude, high-yield nuclear detonations at distances from 50 to 350 naut mi from ground zero, and to relate experimental results to theoretical calculations. An extensive program was conducted at NTS to determine effects on animals located in field fortifications and armored vehicles near a very-low-yield burst.

Nuclear weapon delivery by manned aircraft is often limited by weapon blast and thermal effects on the delivery aircraft, and by nuclear radiation of the crew. Test data has indicated that blast inputs and skin-temperature rise can be predicted within satisfactory limits, but that prediction of the response of the aircraft to these inputs is much less reliable. In order to perfect delivery tactics in the ranges of critical safety margins, B-52D, A4D-1, and FJ-4 aircraft were to fly several missions each, collecting data on the results of various inputs for Program 5. In addition to immediate problems of delivery tactics, much of the experimental data will provide information to modify and refine prediction methods for more general application to all aircraft types.

Program 6 was assigned highly diversified objectives. They can be roughly divided into four categories.

(a) Electronic equipment located at various distances from the zero point was to collect data to determine the feasibility of using the electromagnetic pulse from a nuclear blast as a detector of future bursts over long and short ranges, and to study the fireball and nuclear cloud by radar

to determine ground zero and yield for use in tactical situations.

(b) Investigations were to be made of the ionization effects of high-altitude detonations on communications systems dependent on the ionosphere for propagation, and to determine whether ICBM or antimissile missiles could be detected or controlled in the vicinity of a recent high-altitude detonation.

(c) Investigations of the deleterious effects on fuses and their components as a result of gamma rays and neutrons from nuclear explosions were to be made.

(d) On underwater shots, experiments were to be made to determine the feasibility of using nuclear explosions to clear Naval mine fields. This information will be of great interest to the Navy for both offensive and defensive warfare.

One of the objectives of Program 8 was the evaluation of laboratory methods for determining the effects of thermal radiation on materials, a continuation of studies begun during Operation Plumbbob. The most important objective of current and urgent concern to the national defense was the investigation of damage-producing parameters associated with thermal radiation from high-altitude detonations. Of these, the thermal X-radiation was particularly important as a possible means of destroying incoming ICBM's. The program also assisted Program 4 in the study of retinal burns and made measurements of the thermal radiation from very-low-yield detonations.

Program 9 was assigned a support mission, including documentary photography and support photography for all projects requiring this service. In addition, several projects were created to provide the carriers (balloons and missiles) for the high-altitude events. Special assistants to the Commander, TU-7.1.3, were designated to coordinate these activities with various project agencies.

### 1.3 SUMMARY OF SHOT DATA

Yields, meteorological data, and environmental data at firing time are shown at the beginning of this report. These yields must be considered preliminary and are subject to change.

### 1.4 PROJECT PARTICIPATION

Table 1.1 indicates the shots on which each project participated.

### 1.5 ORGANIZATION

Under the authority of Secret letter, file SWPWT/960, Chief, AFSWP, dated 2 June 1953, subject: "Tests Involving Nuclear Detonations Participated in or Conducted by Agencies of the Government of the United States Outside the Continental United States," the responsibility of the Preparation, Operation, and Post-Operation Phases of Operation Hardtack was assigned to Commander, Field Command, AFSWP.

The Director, Test Division, Weapons Effects Test Group, a staff agency under the Commander, Field Command, AFSWP, was assigned the function of detailed planning and field implementation of the military weapon-effect program, Operation Hardtack.

At the onset of Operation Hardtack, organization planning for the Task Unit 7.1.3 (TU-7.1.3) staff had been completed and was subdivided into two operating sections. The largest section was to be on Eniwetok Atoll where the majority of projects were located. A smaller composite staff was to be based at Bikini Atoll where the principle objectives were concerned with the three very-high-altitude shots. A deputy commander was designated for each atoll, thus allowing the Commander, TU-7.1.3, freedom of action in supervising DOD efforts for the entire operation.

TABLE 1.1 PROJECT PARTICIPATION, PACIFIC PHASE

Project	ENIWETOK SHOTS													BIKINI SHOTS																						
	Cactus	Koa	Butternut	Wahoo	Holly	Yellowwood	Magnolia	Tobacco	Rose	Walnut	Umbrella	Oak	Elder	Linden	Sycamore	Pine	Prunus	Quince	Fig	Sycamore	Fir	Huning	Poplar	Aspen	Maple	Cedar	Hickory	Redwood	Juniper	Dogwood	Pine	Olive	Yucca	Teak	Orange	
1.1																																				
1.2																																				
1.3																																				
1.4																																				
1.5																																				
1.6																																				
1.7																																				
1.8																																				
1.9																																				
1.10																																				
1.11																																				
1.12																																				
1.13																																				
2.1																																				
2.2																																				
2.3																																				
2.4																																				
2.6																																				
2.7																																				
2.8																																				
2.9																																				
2.10																																				
2.11																																				
2.14a,b,c																																				
3.1																																				
3.2																																				
3.3																																				
3.4																																				
3.5																																				
3.6																																				
3.7																																				
3.8																																				
4.1																																				
5.1																																				
5.2																																				
5.3																																				
6.3																																				
6.4																																				
6.5																																				
6.6																																				
6.7																																				
6.8																																				
6.9																																				
6.10																																				
6.11																																				
6.12																																				
6.13																																				
8.1																																				
8.2																																				
8.3																																				
8.4																																				
8.5																																				
8.6																																				
8.7																																				
8.8																																				
9.1d																																				
9.2																																				
9.3																																				

\* Shot Yucca was a high altitude balloon shot from the USS Boxer, 60 miles west of Bikini. Shots Teak and Orange were high altitude missile shots from Johnston Island.

Organizational and personnel planning had all been based on the two-staff concept, with both staffs in supporting distance of each other.

In January 1958, personnel of the advance party began to arrive at the Eniwetok Proving Ground (EPG). TU-7.1.3 was organized as a part of Joint Task Force 7 to conduct approved weapons-effects tests under the operational control of CTG-7.1 and the technical direction of the Chief, AFSWP (see Figure 1.1). It was activated on 15 March 1958, being completely operational on that date, with the organization functioning as outlined in the preceding paragraph. This organization functioned smoothly until the first week in May. At that time, for valid reasons, higher authorities decided to move the launch sites for Shots Teak and Orange, the missile-borne, very-

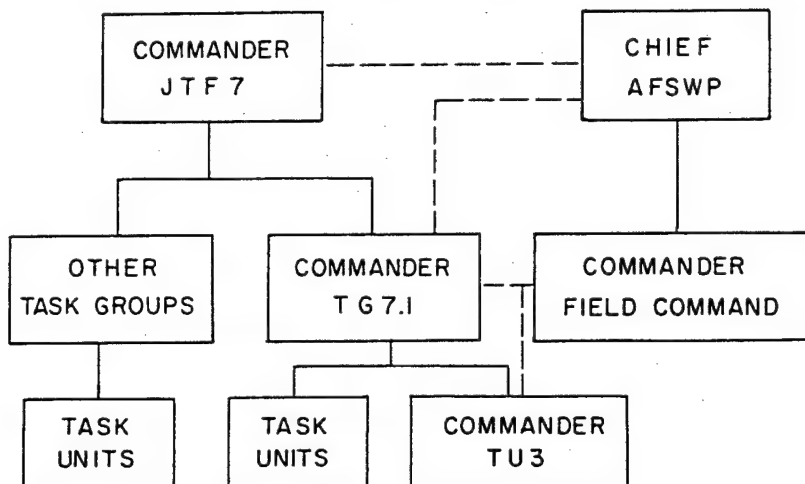


Figure 1.1 Organization of Joint Task Force 7.

high-altitude detonations, from Bikini Atoll to Johnston Island. The problems created in moving project personnel and equipment after completion of most construction and instrumentation will not be discussed here. However, the creation of a new staff necessary to man Johnston Island taxed the TU-7.1.3 headquarters personnel to the limit. At that time, fortunately, most project participation at the Bikini Atoll had been completed. This staff was reduced to one officer and one enlisted man. Personnel thus relieved formed the nucleus of the TU-7.1.3 Headquarters Staff at Johnston Island. Additional personnel were necessary, however, due to three facts: (1) the need for rapid construction, (2) a major change in the participation of many projects due to the shortage of land stations, and (3) Johnston Island was beyond the distance for direct support of some of the staff agencies on Eniwetok. Additional personnel were furnished by the Eniwetok staff and by sending additional personnel into the field from the Sandia Base office of the DC/S Weapons Effects Tests. A deputy for the Commander TU-7.1.3 was appointed for Johnston Island (Figure 1.2).

Midway in the Operation, an additional shot of great interest to the DOD, a very-low-yield device, was added. A reduced TU-7.1.3 staff was required in the EPG for an additional six weeks. Offices on Johnston Island were closed on 23 August, and on Eniwetok on 26 August. However, some personnel remained at both sites for several additional days to complete roll-up activities.

Prior to return of all personnel from the Pacific, the NTS phase of Operation Hardtack came into being. The organization followed the DOD NTS pattern. The DC/S, Weapons Effects Tests, became the Military Deputy Test Manager, and the DOD Test Group, having similar functions to TU-3 in the Pacific, became the operating agency for Weapons Effects Tests. The final detona-

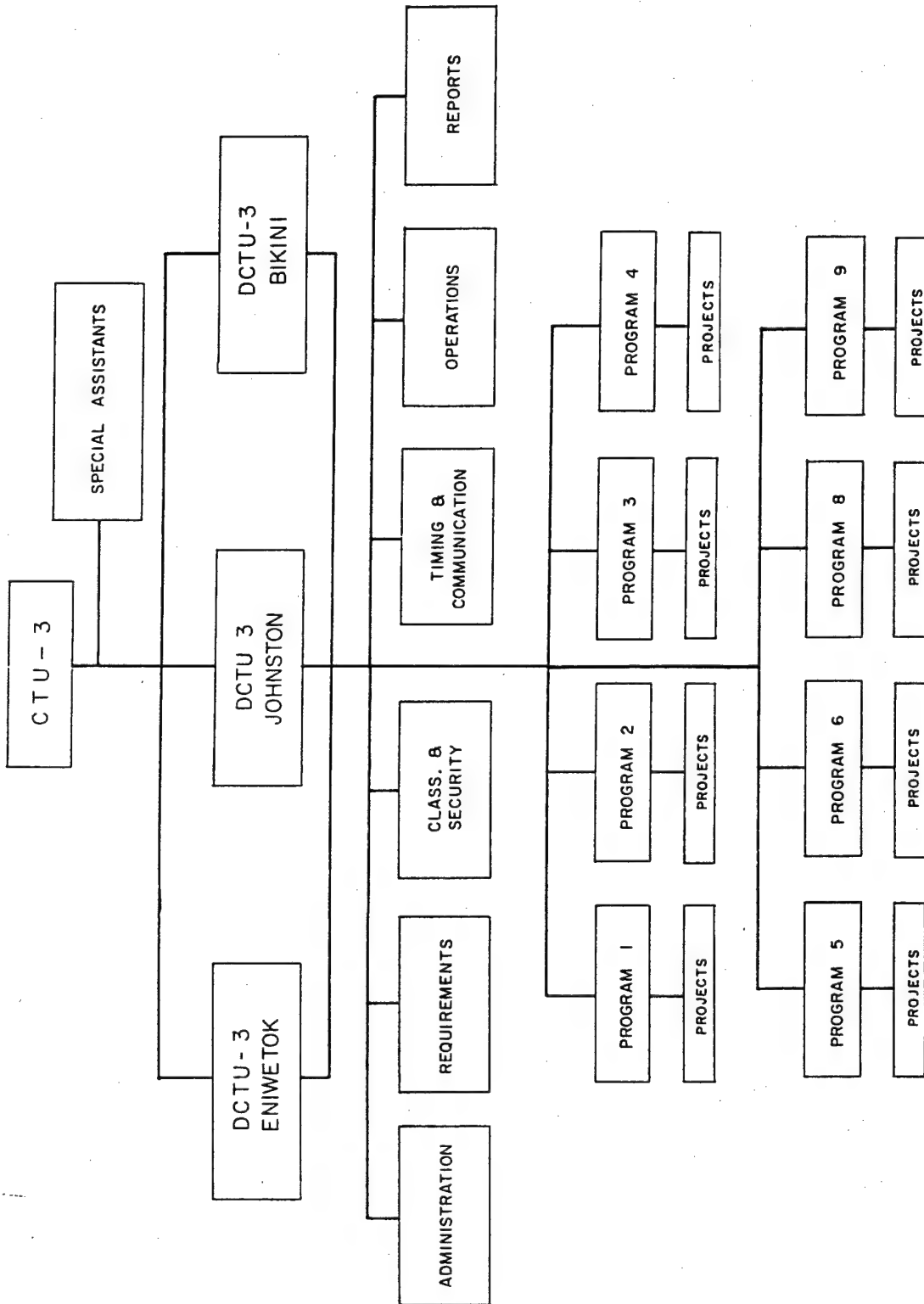


Figure 1.2 Task Unit 7.1.3 organization.

tion at the NTS occurred on 30 October 1958.

In summation, the staffs supervised seven programs consisting of 47 projects in the EPG proper, six programs with 18 projects at Johnston Island, and five programs of 11 projects at NTS.

#### 1.6 PERSONNEL

It was considered advisable for the Personnel and Administration Officer from the Support Division, Weapons Effects Tests, FCWT, to augment the TG-7.1 Staff as an Assistant Adjutant General at an appropriate time, primarily for the issuance of overseas travel orders, inasmuch as the plans and problems of TU-3 personnel (approximately half of TG-7.1) were more familiar to FCWT. All administrative procedures relative to requests for orders, issuing of Civilian Identification Cards, and Military Air Transport Service (MATS) reservations for DOD agencies were processed through FCWT and coordinated with Program Directors and the FCWT Security Officer. Request for travel orders for TU-3 personnel continued to be processed through FCWT at Albuquerque, New Mexico, even after TU-3 was activated at the EPG. Figure 1.3 shows the TU-3 personnel strength as a function of time during the Hardtack operational phase. Section 1.15 discusses the personnel arrangements at the NTS.

#### 1.7 ADMINISTRATION

The Administrative Section of TU-3 maintained offices at Eniwetok, Bikini and Johnston Island. Each office provided the following services for those TU-3 personnel on its respective locations: (1) distribution of official and personal mail with related systems for suspense files, locator files, and correspondence logs; (2) maintenance of TU-3 central files; (3) maintenance and supervision of the control and receipt system for classified documents; (4) processing of outgoing correspondence; (5) mustering of personnel; (6) assistance in the preparation and dissemination of administrative practices directed by higher headquarters; (7) assistance in correspondence of service members with their parent organizations on military matters; and (8) reports and reservations for air and surface transportation for return to the Continental United States. The administration at NTS is discussed in Section 1.15.

#### 1.8 SECURITY AND CLASSIFICATION

As during Operation Redwing, only certain aspects of the overall security function were assumed by the TU-7.1.3 office for the EPG phase of Operation Hardtack. These aspects consisted primarily of TU-3 badge-request processing, the maintenance of TU-3 security clearance records, and security liaison with TG-7.1 and TG-7.5, responsible for physical security functions.

The TU-3 and TG-7.1 Classification Officers operated a joint facility during the Eniwetok portion of the Operation. However, for the Johnston Island portion, these functions were separated.

For the NTS phase, personnel of the Security Office, FCWT, were integrated into a Joint AEC-DOD Pass and Badge Office on 4 September 1958. The primary mission of the DOD Security Office was the certification of military clearances and the assignment of appropriate sigma categories. Unlike previous continental tests, certain clearance formalities were eliminated, due to lack of time. This office ceased operations at the NTS on 4 November 1958, at which time clearance action reverted to the FCWT Office at Sandia Base, New Mexico.

#### 1.9 OPERATIONS

During the planning phase of Operation Hardtack, the Operations Branch of Weapons Effects Tests (WET) was occupied with reviewing project plans, consolidating and coordinating operational requirements, and coordinating and publishing general planning information. Summaries



involving the requirements for ships, aircraft, sample return flights, timing signals, communications facilities, navigational aids, weather information, and radiological safety, were prepared. Requirements information was extracted from project status reports, and with the experience from previous operations, formed the basic concept for Operation Hardtack operational planning. FCWT planning directives and SOP's assisted in providing guidance to projects on operational planning.

During the operational phase, the Program Directors handled the direction and implementation of project participation. The Operations Section reviewed, consolidated, and coordinated event data, daily transportation needs, communications and timing requirements, and maintained continuous liaison with the J-3 Section of TG-7.1 in supplying these requirements. Current operational schedules, weather data, timing schedules, and current situation information was maintained by Operations Branch, and Program Directors and Staff Agencies of TU-3 were kept advised of all changes. Other operational functions such as reports, postshot information, general operational assistance, etc., were provided through Operations Branch. The Operations Officer with TU-3 offices at Bikini provided similar assistance to Bikini projects.

Planning for the high-altitude events (Shots Teak and Orange) had been completed and carried almost to completion when the site location was changed from How Island, Bikini, to Johnston Island. Planning was begun immediately at Eniwetok on notification of the new site and continued at WET at Sandia Base during May and June 1958. Consolidations of requirements involving ships, aircraft, sample return and film processing flights, timing signals, rocket firing, manned stations, weather data, practice rehearsals, etc., were prepared from review of revised project-status reports and the initial status reports of added projects.

On Johnston Island and at Hawaii, projects were grouped under composite Program Directors, who accomplished a large part of the operations work within the projects.

The Operations Section within TU-3 assisted as requested, published information and schedules as necessary, coordinated matters affecting more than one program, and performed normal operations functions.

#### 1.10 COMMUNICATIONS

The primary communications function was to determine those facilities and/or services necessary to sustain military-effects programs and initiate action through support agencies for implementation.

Eniwetok-Bikini Atoll. TG-7.2 operated terminal telephone and teletype facilities at Eniwetok-Fred Island providing service to all activities. TG-7.5 provided all other inter- and intra-island communications support, including cryptographic, within the complex. Individual projects operated their own scientific communications equipment.

Inter- and intra-island telephone systems were adequate for routine command and administrative purposes, but could not support remote-area, off-atoll, and shipboard activities of TU-3 programs and projects. This latter requirement was provided through a series of six radio networks with 63 stations at Eniwetok and three radio networks with 49 stations at Bikini. Radio Sets AN/VRC-18 and AN/PRC-10 were utilized, and operated satisfactorily in these nets.

JTF-7 coordinated and allocated all frequencies to support operations. TU-3 programs and projects, utilizing 55 frequencies from 0 to 9,800 Mc in support of their scientific effort, experienced no major interference problems.

Johnston Island. JTF-7 operated all base and terminal communications facilities, including cryptographic. Due to the concentrations of scientific stations, wire circuits were utilized primarily for intra-island service with radio relegated to a secondary roll.

JTF-7 allocated 58 frequencies from 0 to 10,125 Mc for the TU-3 scientific programs and projects. Frequency interference from all conceivable sources was a continuing problem through-



out this phase of operations. Adequate means for determining interference sources were lacking. Although electromagnetic-countermeasure (ECM) equipment was available, it was relatively ineffective, due to equipment and antenna design limitations. Generally, ECM receiver sensitivity was far below that of scientific equipment. ECM equipment of the latest design should be available for future operations involving large scale radio-frequency radiations.

NTS. The AEC, through their contractor organizations, provided all telecommunications service to support the military-effects programs. Overall requirements were minor, and included normal administration telephones, and one radio network with two base stations and 15 mobile stations. Scientific frequencies were not required, and no problems were encountered.

#### 1.11 TIMING SIGNALS AND VOICE COUNTDOWN

The TU-3 Electronics Staff Officer was responsible for the implementation of all timing signal requirements requested by DOD projects. These timing signals actuated project test instrumentation at specific times prior to, and at shot time. Requirements requested in Project Monthly Status Reports were reviewed, consolidated, and forwarded to all interested agencies.

Timing Signals and Voice Countdown were provided by Edgerton, Germeshausen and Grier (EG&G), an AEC civilian contractor. All timing equipment was provided and maintained by this firm. Installation of all wire from the timing-distribution stations to project location was provided by Holmes and Narver (H&N), another AEC civilian contractor.

Timing signals were received by means of hardwire and radio-tone receivers. Hardwire signals were available at most of the land stations, while radio-tone receivers were utilized at remote stations. Timing signals on ship stations were provided by a central radio station on each major ship, and then by wire to project stations. On the missile-borne very-high-altitude events, service to the distant project sites created new problems involving transmission of timing signals and voice countdown over long distances, availability of suitable transmission facilities within limited frequency allocations, and transmission of security event time information requiring immediate action. These distant project sites were provided voice countdown service transmitted by single-side band equipment.

Timing signal dry runs were provided twice daily to give maximum assurance of instrument reliability at shot time. All projects were urged to participate on as many dry runs as possible. Additional timing signal dry runs were provided when necessary.

#### 1.12 SUPPLIES AND EQUIPMENT

Standing Operating Procedure 40-1, 26 July 1957, was published to provide logistic information and to delineate logistical areas of responsibility to DOD projects. Projects were requested to anticipate their technical supply requirements for the entire operation and to procure these supplies for shipment to EPG, or to request assistance from FCWT. In most cases, the projects performed this action in a most complete manner. Emergency channels for the procurement of supplies were arranged either through the J-4 section of TG-7.1 or the equipment section of the AEC contractor. Normal housekeeping, office and limited technical requirements were obtainable through J-4, TG-7.1, and as supplemented by expendable office supplies furnished by FCWT.

Standing Operating Procedure 40-2, 10 September 1957, was published to assist DOD projects to properly prepare, mark and ship supplies and equipment to, from, and within the EPG. Distribution of these SOP's included separate mailing to each agency's transportation office, plus a copy to the Project Officer. Reports from the port officials indicated some equipment was still received with improper or incomplete marking. However, it was noted that there was a marked improvement over past operations. The shipment of supplies and equipment from the EPG to the United States was monitored by the J-4 Section and a representative of TU-3. Consequently, retrograde shipments progressed more smoothly and with a decrease in lost or mis-

routed supplies. This was true, in spite of the necessity to divert shipment to Johnston Island, and later to divert equipment to NTS for the second phase of Operation Hardtack.

### 1.13 CONSTRUCTION

The initial requirements for construction were originally requested from all approved projects by Headquarters, AFSWP early in June 1957. As the requirements for construction were received by Chief, AFSWP, they were transmitted to FCWT, which was still in the field in Operation Plumbbob. Since many participating agencies were also engaged in Operation Plumbbob, very few construction requirements were actually received until approximately mid-September 1957. From this time until approximately early December 1957, construction requirements were received in good order although somewhat late under an ideal time table. The architect-engineer produced the preliminary and final drawings promptly after submission of criteria, and there was no hold-up in the field for lack of drawings.

Operation Hardtack, like the preceding overseas operation, involved a considerable amount of ship modification work in a number of Naval shipyards. In order to coordinate this work and maintain an effective control over both costs and progress, an experienced Naval officer was assigned to FCWT and stationed at the Long Beach Naval Shipyard. From this location, the work at all West Coast shipyards was coordinated and controlled. This arrangement worked exceptionally well, and resulted in substantial savings in time and money, as compared to previous operations.

It was found that all DOD construction, with the exception of certain Army Ballistic Missile Agency (ABMA) facilities on How Island, was in excellent shape from the standpoint of progress and schedules when it arrived in the field. The work on How Island was completed reasonably close to schedule, but only after expenditure of excessive overtime. All other test construction for DOD project participation elsewhere in the EPG was completed well within scheduled dates. This was a marked contrast to the previous operation.

Construction of support facilities, such as new barracks and laboratories, was from three to four weeks behind schedule and was never made up. The effects of this situation were minimized to a degree by moving projects around to utilize existing space assigned to late arriving projects.

The decision to transfer the two ABMA shots to Johnston Island required a major amount of redesign and site adaptation of already-constructed facilities on How Island. Since all interested personnel were at the EPG, the redesign was accomplished by the architect-engineer at the EPG. One member of the G-6 staff of FCWT was detached and sent to Johnston Island to supervise the TG-7.1 construction at that site.

Soon after return of the FCWT group from the EPG and Johnston Island, the second phase of Hardtack was initiated at NTS. The total DOD construction requirement for this operation was not large, compared to previous Nevada operations. However, the time schedule was extremely short and tight, requiring extensive effort on the part of all participating agencies to meet test schedules. All of the design was done in the field with construction closely following, and in many cases with no formal drawings.

The cost of test construction at the EPG was approximately \$1,650,000. The cost of construction at Johnston Island was approximately \$617,000. Support work-order costs in the EPG were listed at \$85,000 and at Johnston Island as \$103,000. Construction at the Nevada Test Site was listed at \$49,000, with approximately \$22,000 for field-support work.

### 1.14 FISCAL

1. The following information will deal almost exclusively with Research and Development Funds under the control of CHAFSWP, as information is not available to Commander FCAFSPW with respect to expenditures by other services. However, on 10 September 1957, a summary of

expected expenditures was reported and is listed here to indicate the magnitude of this type of operation.

<u>Agency</u>	<u>R&amp;D Funds</u>	<u>Other Funds</u>	<u>Totals</u>
AFSWP	\$18,970,000	\$13,000,000	\$31,970,000
Army	3,758,250	—	3,758,250
Navy	2,291,000	8,109,000	10,400,000
Air Force	425,000	3,650,000	4,075,000
Grand Total	\$25,444,250	\$24,759,000	\$50,203,250

2. As noted above, \$18,970,000 was budgeted by AFSWP in September 1957. Following is a list of increases necessitated by increase in scope of approved projects, additional projects, and the move to Johnston Island.

<u>Source</u>	<u>Project</u>	<u>Amount</u>
AFSWP	6.5	\$ 800,000
AFSWP	6.11	600,000
AFSWP	Johnston	2,962,576
AFSWP	Quince	677,000
AEC	2.8	240,000
Air Force	1.8	117,500
Air Force	1.12	10,000
Air Force	1.7	50,000
Air Force	1.9	64,000
Air Force	8.6	30,000
Air Force	Very high altitude	400,000
Total		5,951,076
AFSWP		18,970,000

Grand Total,  
R&D Funds Controlled by AFSWP, 24,921,076

From economies effected in the field it is anticipated that approximately \$110,000 will be returned to the Air Force, plus \$500,000 to \$600,000 made available to finance the NTS portion of Operation Hardtack.

3. Terminating cost figures will not be available until the final test reports are submitted by the laboratories. However, it appears that R&D expenditures for EPG, Johnston Island and NTS will be:

Laboratory Expenses	\$19,000,000
Field Costs (Construction, Photo, Timing, etc.)	4,075,000
Grand Total	\$23,075,000

#### 1.15 ORGANIZATION AND LOGISTICS AT NTS

Support Group. The DOD Support Group (Support Division, Weapons Effects Tests, Field Command, AFSWP) functioned as an element under the Office of the Test Manager. The Military Deputy Test Manager (Deputy Chief of Staff, Weapons Effects Tests) exercised supervision over the Support Group. The mission was to provide administrative and logistical support to DOD/AFSWP participating agencies. In addition, logistical support was furnished the AEC per instructions to the Commander, Field Command, AFSWP, from the Chief, AFSWP, for implementing the Operation.

**Supply and Procurement.** The General Supply Branch of the Support Group began operations 25 August 1958. The President's announcement on 22 August that test operations would be suspended 31 October 1958 was the implementing order. The mission was to provide depot, post camp and station supply support to DOD/AFSWP agencies. Requisitions from technical service sources and General Services Administration (GSA) for the period 25 August 1958 to 15 December 1958 totaled approximately \$15,000. Reynolds Electrical and Engineering Company (REECO) supply facilities were utilized to a greater extent than in past operations because of the short preparatory phase for the Operation. Supplies and services obtained through REECO totaled approximately \$10,000. A local purchasing and contracting office was operated on a part-time basis at 1734 South Main Street, Las Vegas, Nevada, where transactions totaling approximately \$40,000 were conducted.

**Religious Services.** An Auxiliary Catholic Chaplain for Lake Mead Base and a Protestant Chaplain assigned to Indian Springs Air Force Base were assisted by one enlisted man on a part-time basis furnishing scheduled services at the Site. Personnel of the Jewish faith were afforded government transportation to Las Vegas.

**Personnel.** DOD/AFSWP agencies provided military and civilian personnel to implement their test objectives. The foregoing agencies were augmented for administrative and logistical support by personnel assigned to Weapons Effects Tests Group, Field Command, AFSWP, plus 2 officers and 35 enlisted personnel procured on a temporary basis. Personnel comprised a headquarters for the Test and Support Groups, Finance, Security, Supply, Motor Pool, Motor Maintenance and a dispensary. See Figure 1.3 for graph of personnel strength.

**Billeting.** Housing of DOD/AFSWP sponsored agencies was administered by the Field Command Support Group. Two dormitories and 52 house trailers were allocated by the AEC. The peak period, 13 October 1958, reflected an overload of 50 percent when 256 personnel were being billeted.

**Motor Pool Operation.** The DOD Motor Pool was activated 1 September 1958. Motor vehicles and trailers comprised 187 units. Vehicles were dispatched on a daily basis, with the exception of weekly dispatches, when justified. Seventy-one vehicles were on loan during the Operation (63 to AEC and 8 to Indian Springs Air Force Base). Three rental sedans were acquired from REECO for command administrative support. Twenty-four hour capability was established when necessary and all commitments met.

**Commercial Traffic Activity.** Operations were routine with no appreciable increase pertaining to the issue of travel requests, bills of lading, etc.

**Vehicle and Generator Maintenance.** Fourth-echelon maintenance plus machine shop services were accomplished as capability permitted. Vehicles in long-term storage were put into operational use by DOD maintenance personnel and restoraged by contractor personnel at the termination of the Operation. Fifteen generators were used, and necessary maintenance was performed by REECO. Warehouse issue, Las Vegas local Purchasing and Contracting Office, and REECO served as parts agencies.

**Fiscal.** Authorizations totaling \$400,000 were allotted by AFSWP for extra-military costs. Expenditures consisted of six object classes as follows:

02	\$71,000	07	\$ 500
03	2,500	09	55,000, and
04	2,000	99	219,000

(AFSWC \$49,000, OA NTS \$55,000, and AEC \$115,000).

#### 1.16 SUPPORT PHOTOGRAPHY

The mission of Program 9 was to provide documentary and technical photographic support

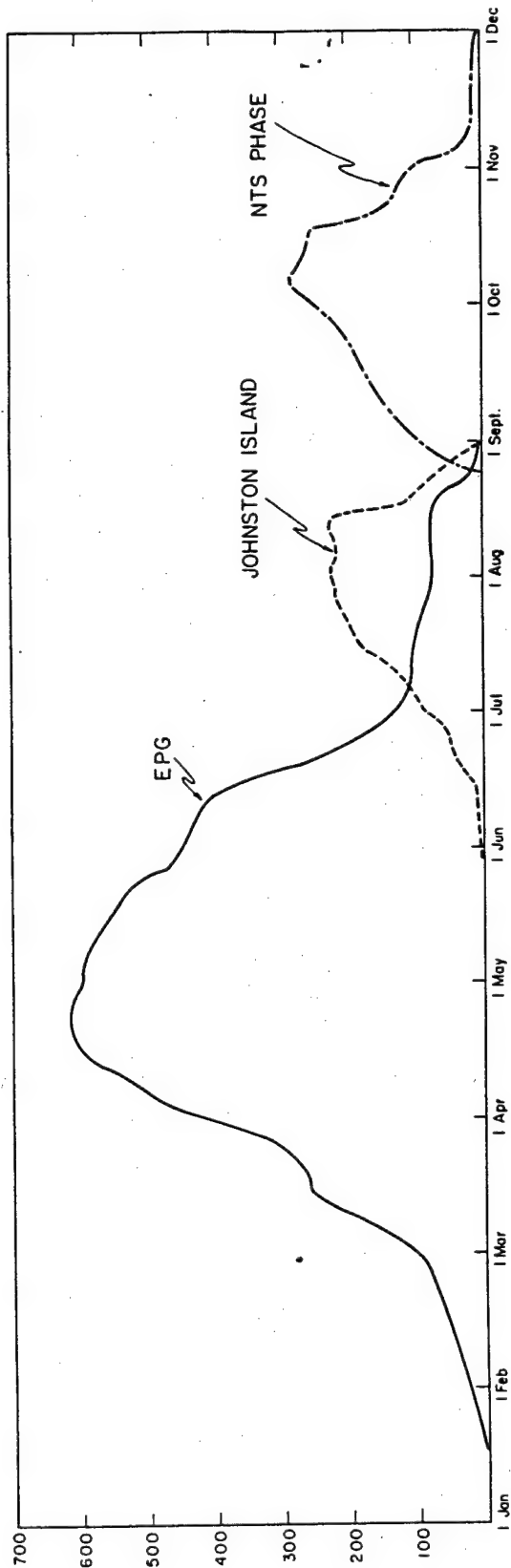


Figure 1.3 Task Unit 3 personnel deployment.

to participating DOD agencies. The documentary support consisted of both still and motion-picture coverage of project activities to depict the scope of the project's effort, and to show significant results of their effort, for historical and report purposes. Still photography, in support of projects for illustrating preliminary and final reports, was conducted by TU-7.1.1. Motion-picture coverage to be used in the production of a Weapons Effects Film was provided by JTF-7. Technical photography, such as high-speed, time-lapse, and function-of-time photography, was furnished by TU-5 (EG&G).

During the planning phase of Operation Hardtack, it became evident that the needs of the various projects for photographically-collected data would fall on the five military-effects events: two high-altitude-rocket detonations, one high-altitude-balloon detonation, and two underwater detonations. Because of the varied nature and location of the detonations, more extensive and sophisticated camera installations were needed than on any prior operation. As the test series proceeded, additional shots of military interest were added to further increase the complexity and number of camera stations.

For the high-altitude-balloon detonation, RB-36's were used with a back-up camera installation mounted on the USS Boxer. For Shots Teak and Orange, the RB-36's were used with back-up surface and ground stations.

The photographic equipment used for all three high-altitude detonations consisted of streak, high- and medium-speed motion picture, rapid-sequence still, and Zenith cameras, utilizing both color and black-and-white film.

The photographic instrumentation for the two underwater shots was basically the same for each shot. The stations common to both shots consisted of a camera station on Site Elmer; camera stations on Site Glenn; an LCU camera station anchored in the lagoon; an RB-50 aircraft directly over surface zero at 25,000 feet altitude; three C-54 aircraft orbiting at 20,000 feet range at altitudes of 1,500 feet, 9,000 feet, and 10,000 feet; and one RB-50 aircraft which provided vertical aerial photographic coverage of the target array before and after each shot.

For Shot Wahoo, an additional camera station was installed in the hold of the EC-2 to record effects of a deep-water detonation on the ships' structure.

For Shot Umbrella, in addition to the basic installations, a camera station was installed on a barge 20,000 feet from surface zero, another camera station was installed on Site Henry to photograph rocket firings, and a trimetrogon-camera array was installed on a H-19 helicopter to photograph wave action at two surface instrument platforms.

In addition to the major portion of the photographic effort on the five military effects shots, a somewhat smaller effort was expended on some of the AEC diagnostic shots. A camera station was installed to record the effects of the thermal pulse on certain materials. Several aerial photographic surveys of craters produced by land surface detonations were accomplished; aerial surveys were made to locate strings of gages placed in the water prior to several shots; and mosaics were flown on Johnston Island, and all the islands of both Bikini and Eniwetok Atolls, for planning purposes.

Before the five original military-effects shots had all been detonated, two additional shots of DOD interest were added to the program: two very-low-yield surface bursts on Site Yvonne at the Eniwetok Atoll. This necessitated the establishment of two camera stations to cover the Yvonne events, and the addition of some still and motion picture documentary coverage of the two events. In all, the documentary coverage consisted of about 66,000 feet of original 35-mm Eastman color negative film from which a military-effects motion-picture film report will be prepared after the operation.

For historical and report purposes, approximately 3,500 black and white still negatives were exposed during the operation.

## 1.17 REPORTS

For the Interim Test Report program of Operation Hardtack, the Reports Office was responsible for (1) coordination of the preparation of technical reports in accordance with AFSWP requirements; (2) administration of the review and approval process; (3) review of certain aspects of the overall technical content; and (4) detailed editorial review of all reports for organization, writing and printing style, and presentation of tables, illustrations, and equations.

The Reports Office also provided limited library service of published technical reports concerned with military effects, and some drafting and illustrating service for project personnel and others connected with the DOD test organizations.

Operation Hardtack produced the largest AFSWP report program of any nuclear test to date, some 80 reports. A special system of publication was designed to cover those projects whose shot participation was extended in time and geographical location. To expedite early distribution of the first phase of such project's activities, some ITR's were published as basic reports with later supplements, for example: ITR-1612-1, ITR-1612-2, etc. (The final reports of these projects will be under one cover, numbered, for example, WT-1612.)

Each ITR draft was first reviewed by the appropriate Program Director, then by the Analysis Officer and by the Editor of the Reports Office, and lastly for final approval by the CTU-3 (for EPG projects) or the Director, DOD Test Group (for NTS projects) and by the Technical Director, DC/S WET, FC AFSWP. Final security classification of the approved manuscript was then determined by the Classification Officer and an appropriate distribution selected by the Reports Office, both based on joint AEC-DOD and AFSWP criteria.

After completion of this test-site processing, the approved and classified manuscript was transmitted to Reports Branch, FCWT, at Sandia Base, where the report was prepared for printing (preparation of camera copy), a process that included additional drafting and illustrations and complete type composition, proofreading, and makeup into pages. (No changes in content were made after release of the report from the test site.) This camera copy was then transmitted to the Technical Information Service Extension, US AEC, Oak Ridge, Tennessee, for printing and distribution.



## Chapter 2

### SHOT WAHOO

#### 2.1 INTRODUCTION

Shot Wahoo was the underwater detonation of a 10-kt nuclear device in the ocean off the southwestern sector of Eniwetok Atoll. The device was detonated on 16 May 1958 at a depth of 500 feet over a sloping bottom, which had a depth of 3,000 feet at the shot location. A target array, consisting principally of three destroyers and an EC-2 liberty ship, was moored in deep water at varying ranges and orientations from surface zero. In addition, manned destroyers and two manned and submerged submarines were operating near the test area.

2.1.1 Objectives. There was a distinct need in the Navy for information regarding effects of nuclear explosions. In particular, [REDACTED]

[REDACTED] In order to build ships and submarines to deliver these weapons, to know more about the radiological effects and damage that ships will receive from underwater nuclear explosions, and in order to develop tactics for delivery of the new weapons, a great deal of information was needed. The underwater tests during Operation Hardtack were designed to supply the needed information.

In order to achieve this general primary objective, the following specific objectives were established for the various participating projects: (1) measurement of the pressure-time histories of the underwater shocks as a function of distance and depth in support of ship damage studies and of the effects of refraction; (2) measurement of air blast and surface phenomena; (3) determination of the hydrodynamic yield of the weapon through a study of the time of arrival of the shock wave at intervals close to the weapon; (4) study of the vulnerability of ships to radiation; (5) study of contamination ingress into ships; (6) determination of the characteristics of the radiological environment; (7) determination of the hull loading and the response of surface and subsurface ships resulting from the underwater shock waves; (8) determination of the machinery response and damage by nuclear shock-induced hull motions; and (9) demonstration of a safe-delivery range for this specific burst depth.

The test objectives of the underwater program, in summary, were to document the basic effects data with regard to initial and residual radiation, air overpressures, underwater shock pressures, crater measurements, mechanics of base surge, and radiological contaminants and to document the response of selected targets to underwater shock pressures. The purpose of the objectives was to provide information that would permit determination of safe minimum standoff distances for delivery of nuclear antisubmarine warfare weapons by existing vehicles and improvement in predictions of the lethal range of nuclear antisubmarine warfare weapons against submarine type and surface ship targets in shallow and in deep water.

2.1.2 Background. Prior to Operation Hardtack there had been only two underwater nuclear bursts, Shot Baker (Operation Crossroads) and the Operation Wigwam detonation. Crossroads Baker was a  $23 \pm 3$  kt burst at a 90-foot depth in 180 feet of water. A major array, consisting of battleships, carriers, cruisers, destroyers, submarines (both surface and submerged), and merchant ships was subjected to the effects of this shot.

The scarcity of scientific data obtained, however, seriously restricted the applicability of the observed damage to the general problem. This is particularly so, since the pressure pulse



in the shallow water at Crossroads Baker was made complex by multiple reflection from the bottom and surface, and was completely nonrepresentative of the deep-water cases. In addition, the machinery of these ships was not operating, making extrapolation of damage to operating ships highly uncertain. During Operation Wigwam, a  $32 \pm 3$  kt device was detonated at a depth of 2,000 feet in approximately 16,000 feet of water. Here the emphasis was upon the determination of submarine lethality. Three model submarines (Squaws) having diameters and scantlings four-fifths the size of the SS-567 submarine, were employed. These models had only simulated equipment. Damage to operating equipment was not considered. Surface ships in the Wigwam array were limited to instrument barges, and the shock motions recorded on these barges cannot be reliably interpreted in terms of damage to Navy ships.

Considered from the attitude of safe delivery, the two previous detonations yielded little usable data. A major uncertainty existed in predicting the degree of response levels which would cause damage to operating equipment. Other questions existed regarding the response level generated by shallow-angle-of-attack shock waves; on the transmission of the shock motions of the hull to the rest of the ship; and on other phenomena that had assumed new importance in nuclear weapon effects, such as radiation, refraction, cavitation, and reflection influences. Safe ranges established in operational doctrine prior to Shot Wahoo were affected by these uncertainties, as well as the uncertainties regarding radiation effects. Removal of the uncertainties would result in establishing the minimum safe ranges that would permit the development of the full delivery potential of ships and submarines.

Planning for the underwater shots of Operation Hardtack began shortly after the end of Operation Wigwam. The Chief of Naval Operations appointed a group, (William J. Thaler, of the Office of Naval Research, as chairman) to draw up plans for further underwater tests as a part of Operation Hardtack. The title of the group was Special Weapons Effects Test Planning Group (SWET) with representatives from Navy Bureaus, and the Chief of Naval Operations (CNO). Representatives of AFSWP and of various laboratories and other agencies were invited to participate and supply advice to the SWET Group.

In order to make underwater weapon-effect predictions for surface ships and submarines under general conditions, it was necessary to understand more about radiation effects, as well as the entire range of transition from the production of free-field pressures in the water through final hull and equipment damage to the ship.

This range of transition can be divided into the following phases: (1) generation of free-field pressures; (2) relation between the free-field pressures and both the loading and initial response of the hull (the interaction problem); (3) transmission of the hull motions to the remainder of the ship (the shock pattern throughout the ship); (4) relation between the hull velocities and the type and amount of damage produced in the ship's hull (hull damage); (5) relation between the magnitude of shock level which is observed in the shock pattern throughout the ship and the resulting equipment damage (shock damage).

In planning the underwater shots, it was considered desirable to have as ideal a shock wave as possible for at least the first several ship locations in order to obtain the most optimum relationships between the shock wave and ship response. Furthermore, the shot geometry should be such that it would answer as many questions as feasible. The location of Shot Wahoo had to meet these requirements and, in addition, had to present a feasible operational situation.

After consideration of many plans, it was decided that three destroyers and an EC-2 liberty ship would comprise the array. The destroyers would be placed at locations where effects would range from moderate-equipment damage to no damage. The EC-2 would be placed at a severe-hull-damage range. The array would include barges, for mooring ships and for support of project activities, and coracles, for data collection (Figure 2.1).

In early test planning, Shot Wahoo was called Little Wigwam. After many meetings of the Special Effects Test Planning Group (SWET Group) and reports (SWET-1, 2, 3, 4, 5), the

SWET-4 report was tentatively accepted by CNO in December 1956. Compromises regarding funds available, ships that could be used in the target array, and shot dates were made, and SWET-5 was approved by CNO, the Joint Chiefs of Staff, and the Secretary of Defense (Reference 1). The date for Shot Wahoo was established in April 1957 as 1 June 1958.

Meanwhile, there were international considerations, disarmament proposals, and the possibility that nuclear tests would be stopped. These factors caused a decision to be made to advance the date of Shot Wahoo by two weeks. This was done despite the advice of oceanographers, aer-

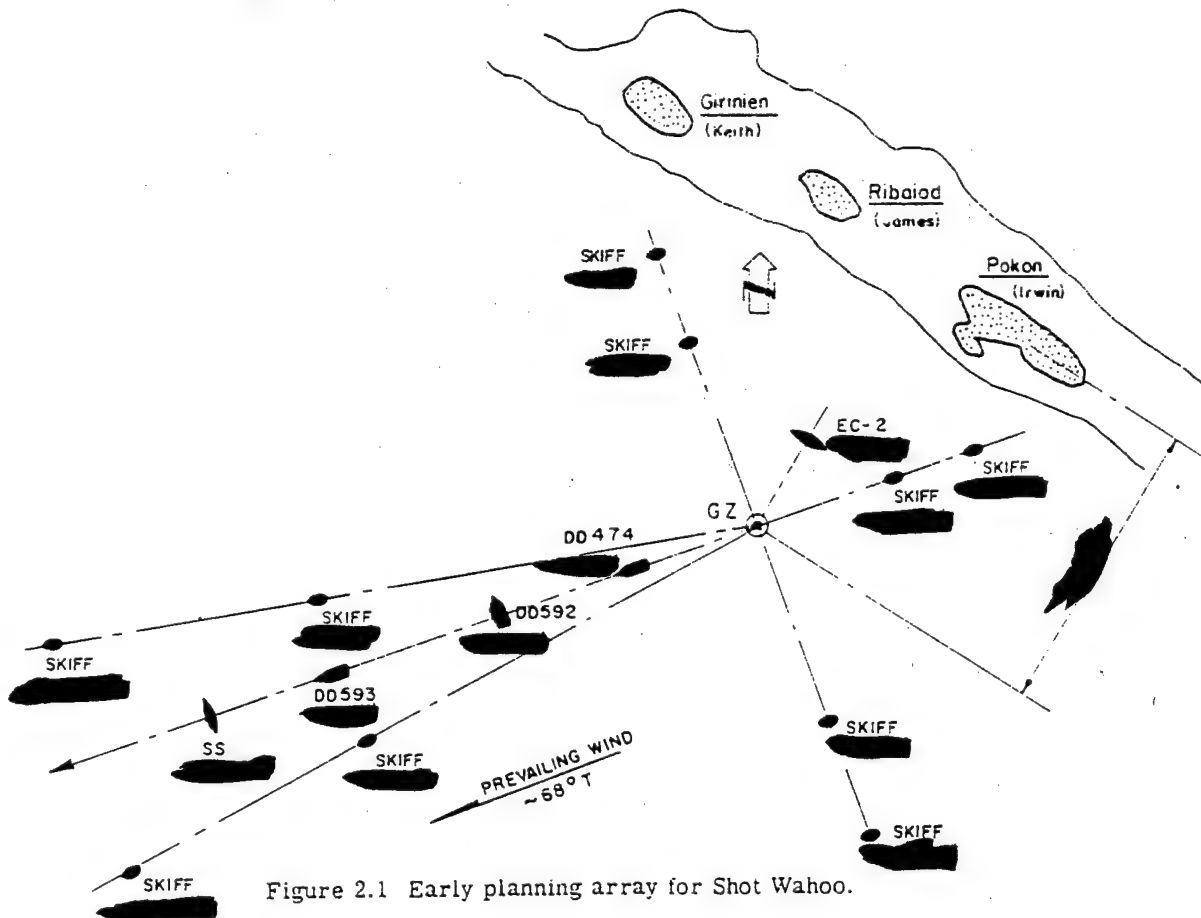


Figure 2.1 Early planning array for Shot Wahoo.

ographers, and naval experts who predicted extreme difficulties due to weather, heavy seas, and strong winds before 1 June. The directed date for Shot Wahoo was set at 15 May 1958.

In May 1957, the Assistant Secretary of Defense directed that a drastic reduction, from about \$28 million to \$20 million, be made in the DOD research funds for Operation Hardtack. This, in turn, meant a cutback in the underwater program.

The program as finally approved, shown in "Operation Hardtack Weapons Effects Program," (Reference 2), was published by Headquarters, AFSWP, in August 1957 and sent to Field Command, AFSWP, for final planning and implementation. Shot Wahoo was to simulate [redacted] weapon detonated 500 feet below the surface, in water 3,000 feet deep.

Approved objectives, projects, project agencies and funding breakdown are shown in Tables 2.1, 2.2, and 2.3. No attempt has been made to separate the costs of the two underwater shots, Wahoo and Umbrella; therefore, participation and funding for both are indicated in the tables.

In June 1957, as a result of a meeting of certain Buships and AFSWP personnel and project officers at the Long Beach Naval Shipyard, the USS Fullam (DD-474), USS Howorth (DD-592)

TABLE 2.1 PROJECTS AND AGENCIES PARTICIPATING IN SHOTS WAHOO AND UMBRELLA

Project	Title	Agency
1.1	Underwater Pressure Measurements	Naval Ordnance Laboratory
1.2	Air Blast Measurements	Naval Ordnance Laboratory
1.3	Surface Phenomena Measurements	Naval Ordnance Laboratory
1.5	Free-Field Pressure Measurements	Naval Electronics Laboratory
1.6	Water-Wave Measurements	Scripps Institute
1.11	Yield Measurement	Armour Research Foundation
1.13	Hydrographic Survey	Office of Naval Research
2.1	Shipboard Radiation on Vulnerability	Naval Radiological Defense Laboratory
2.2	Shipboard Contamination Ingress	Naval Radiological Defense Laboratory
2.3	Characteristics of the Radiological Environment	Naval Radiological Defense Laboratory
3.1	Special Charge Studies	Underwater Explosives Research Division
3.3	Shock Studies of Ships Machinery and Equipment	David Taylor Model Basin
3.4	Loading and Basic Target Response (surface ships)	Underwater Explosives Research Division
3.5	Hull Response (submarine)	David Taylor Model Basin
3.8	Damage Assessment	Bureau of Ships
6.7	Mine Clearance Studies	Naval Ordnance Laboratory
6.8	Underwater Influence and Mine Reactions	Mine Defense Laboratory

TABLE 2.2 FUNDING FOR UNDERWATER-TEST PROJECTS

Project	Title	AFSWP	Navy	Total
1.1	Underwater Pressure Measurements	592,000	800,000	1,392,000
1.2	Air Blast Measurements	472,500	625,000	1,097,500
1.3	Surface Phenomena Measurements	30,000	136,000	166,000
1.5	Free-Field Pressure Measurements	400,000	—	400,000
1.6	Water-Wave Measurement	89,000	—	89,000
1.11	Yield Measurement	150,000	—	150,000
1.13	Hydrographic Survey	60,000	—	60,000
2.1	Shipboard Radiation Vulnerability	486,400	—	486,400
2.2	Shipboard Contamination Ingress	273,300	—	273,300
2.3	Characteristics of the Radiological Environment	681,800	260,000	941,800
3.1	Special Charge Studies	89,000	211,000	300,000
3.3	Shock Studies of Ships Machinery and Equipment	600,000	—	600,000
3.4	Loading and Basic Target Response (surface ships)	1,051,000	89,000	1,140,000
3.5	Hull Response (submarine)	300,000	—	300,000
3.8	Damage Assessment	100,000	—	100,000
6.7	Mine Clearance Studies	100,000	—	100,000
6.8	Underwater Influence and Mine Reactions	300,000	100,000	400,000
Support		1,890,000	500,000	2,390,000
Grand Total		7,665,000	2,720,000	10,385,000
Ships and Facilities, Navy (Target preparation)				10,400,000
Task Group 7.3 services			No dollar value	
Target Array			No dollar value	

(Figure 2.2), USS Killen (DD-593), and SS Michael Moran (EC-2) (Figure 2.3) were selected from the reserve fleet as target ships. At this meeting of project officers, the shipyard was given preliminary information on what would be required.

The Bureau of Ships was responsible for readying the ships, as such, activating the necessary ships' machinery, and preparing for mooring the array. The individual projects were responsible for their own planning, funding, instrument installation, and readiness. TG-7.3 was re-

TABLE 2.3 FUNDING FOR SUPPORT ITEMS OF UNDERWATER SHOTS

Items	AFSWP	Navy	Total
Squaw rehabilitation	200,000	—	200,000
Mooring targets	540,000	500,000	1,040,000
Technical photography	450,000	—	450,000
Weapon suspension and firing	300,000	—	300,000
Timing signals	400,000	—	400,000
	1,890,000	500,000	2,390,000

sponsible for the operational problem of assembling the ships, barges, and equipment at the EPG and getting the target array moored.

This division of responsibility required that close liaison and good working relationships be established early. To fill this obligation, the Bureau of Ships and Field Command, AFSWP, each sent resident representatives to the Long Beach Naval Shipyard as coordinators of the work. This arrangement was most beneficial in working out the many problems associated with the work being done.

To assist the Commander, Field Command, AFSWP, in selecting proper target distances to accomplish the objectives of the tests, a panel of experts was appointed with membership from BuShips, ONR, and Headquarters, AFSWP, under a chairman from Field Command, AFSWP. This group had the title "Target Positioning Advisory Panel."

About 1 August, CNO designated the USS Bonita (SSK-3) (Figure 2.4) as the submarine target for Shot Wahoo. The destroyers and the EC-2 were taken into the Long Beach Naval Shipyard on 1 September 1957. The Bonita was taken to the San Francisco Naval Shipyard in November 1957.

For Shot Wahoo it was planned to use eight Navy YC barges as mooring platforms for the target ships and as floating instrument stations for various projects. The barges were procured by the Bureau of Ships, towed to Hawaii, and modified as necessary in the Pearl Harbor Naval Shipyard.

**2.1.3 Procedure. The Array.** Shot Wahoo was fired against an array consisting of target ships and barges. The latter served doubly as mooring points for the targets and as floating stations for various projects (Figure 2.5). Also included in the array were the coracles (Figure 2.6), a new type of station evolved from the skiffs used during Operations Wigwam and Redwing. The planned distances and orientations of the major targets are shown in Figure 2.1.

**The Nuclear Device.** The suspension and firing systems for the nuclear devices were considerably simplified to reduce cost. Instead of the large barge used during Operation Wigwam, telephone buoys were to be used for suspension. The firing panels were to be mounted in LCM hulls secured near the buoys. Firing signals were received by radio and transmitted for the LCMs to the devices by instrument cables (Reference 2).

**Fleet Support.** In addition to the target ships, there were 23 other ships present in the vicinity of Wahoo at shot time (Figure 2.7). Of these, the destroyers Mansfield, Benner, and

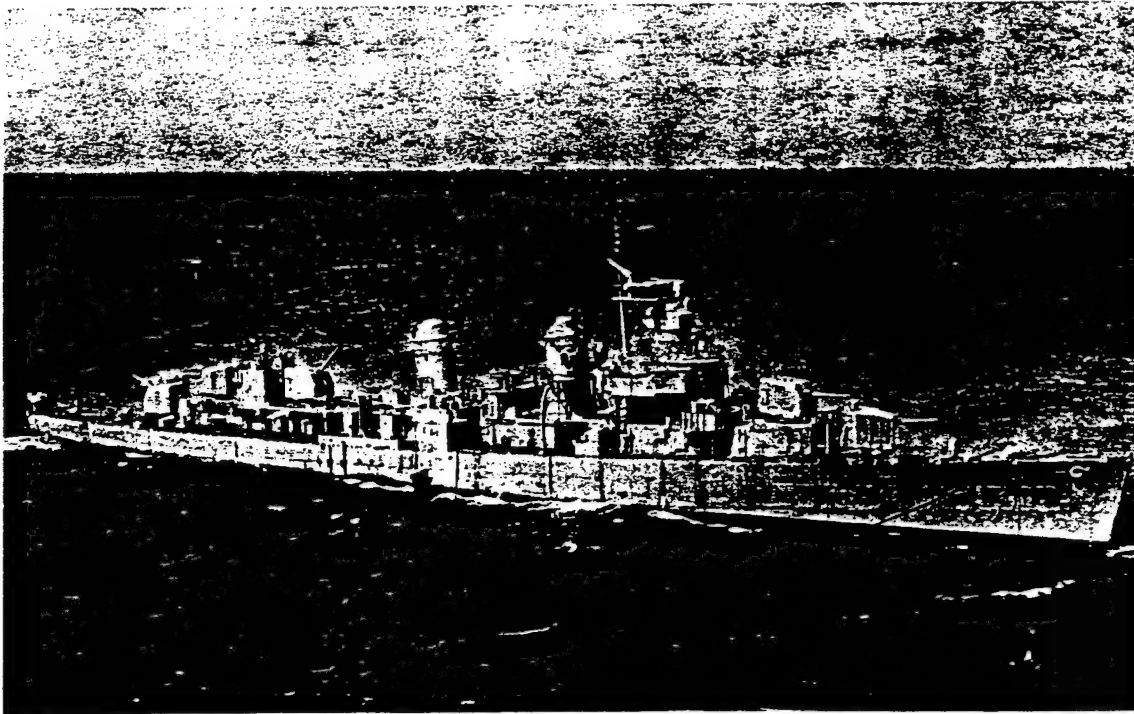


Figure 2.2 DD-592 Ex-USS Howorth. Shown in the Wahoo array with washdown in operation just prior to shot time. Surface zero was off the starboard beam of this ship.

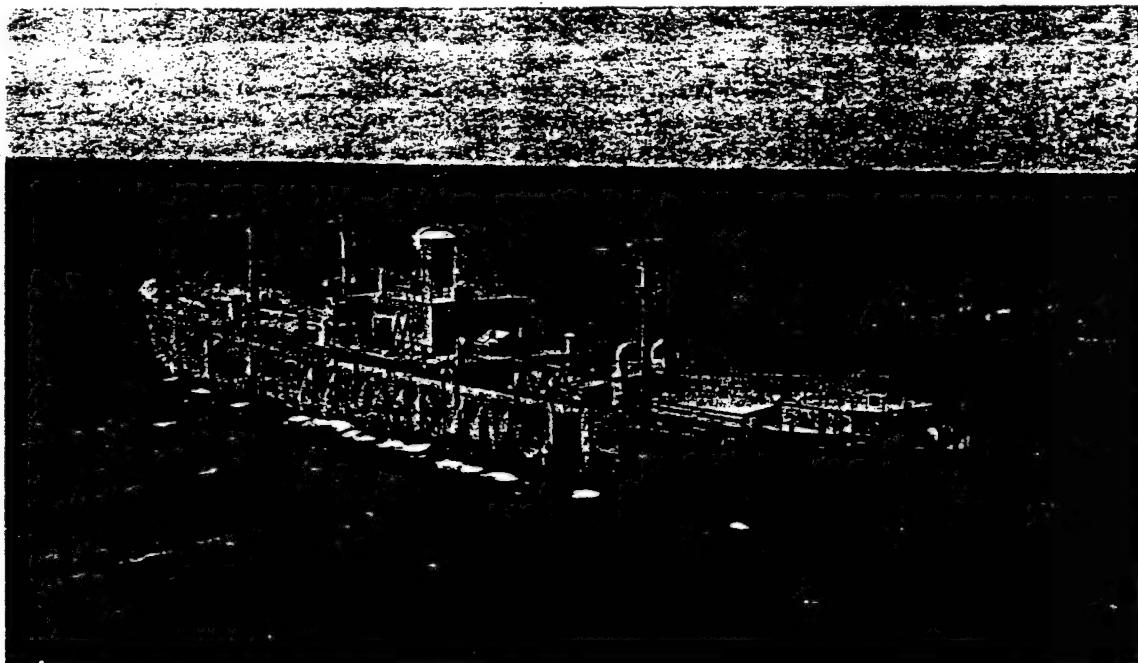


Figure 2.3 EC-2 Ex-Michael Moran. Shown in the Wahoo array with washdown in operation. Right center is the Number 2 barge with surface zero just off the right edge of the picture.

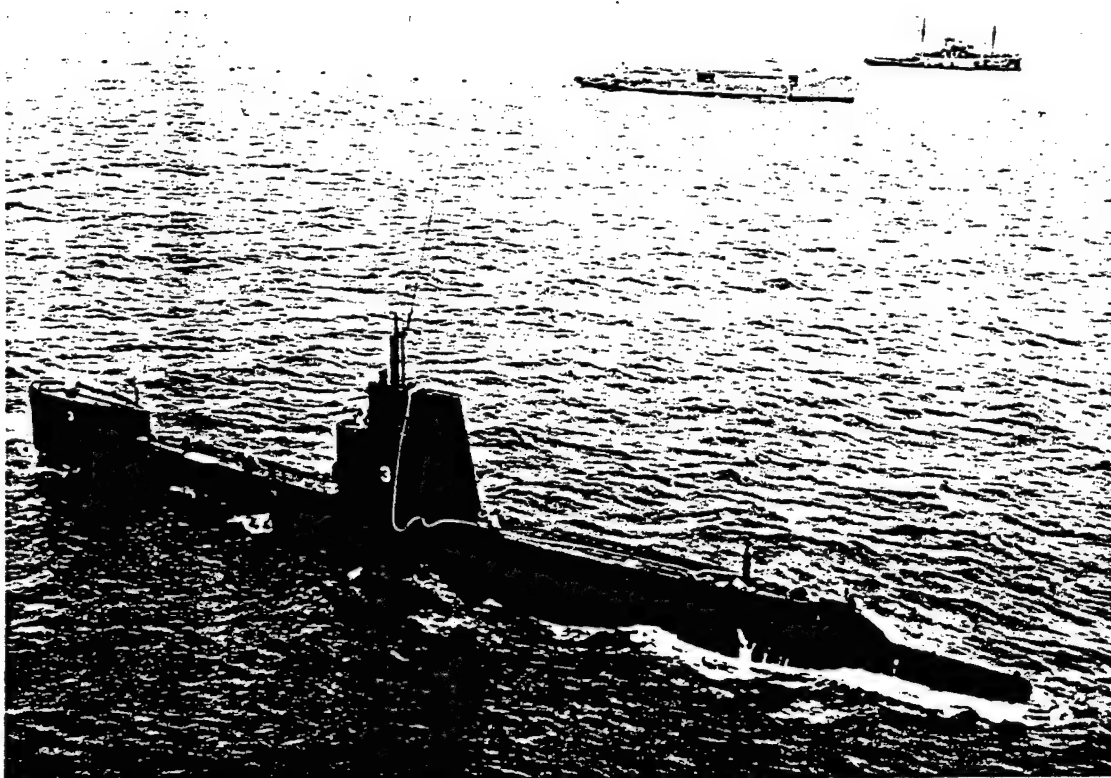
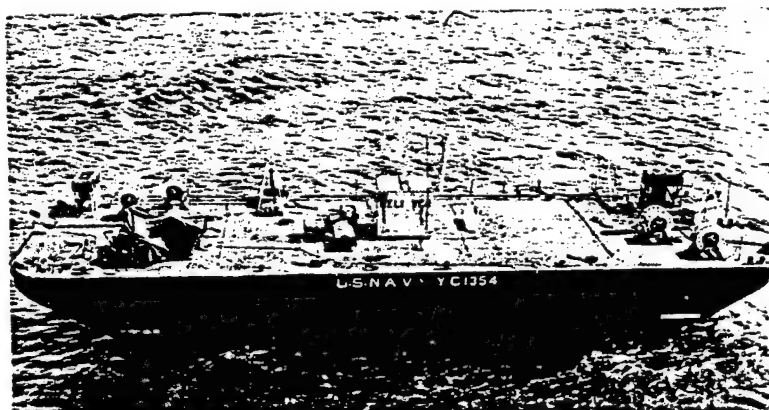
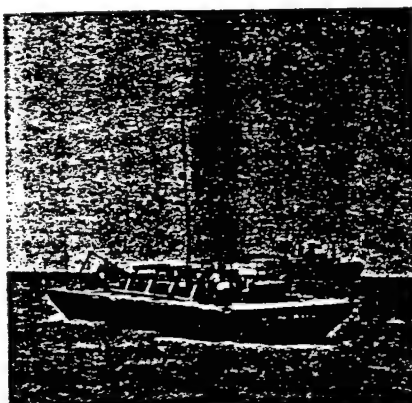


Figure 2.4 USS Bonita (SSK-3) being placed in the Umbrella array. In the background can be seen the YFNB-12 which acted as the instrument platform for the submerged Squaw and the USS Bolster, one of the work tugs of TG 7.3. The line of buoys to left of the YFNB supported the instrument cable to the submerged Squaw.



and to provide project instrument platforms.



Orleck and the submarine, Sterlet, participated in a training exercise during the shot. The Bonita was not moored in the array, as had been intended, because of difficulties in mooring, due to rough weather. The other ships present were part of TG-7.3 and included the command ship, USS Boxer; the USS Monticello, used as a center of boat operations; the USS Renville, which was equipped to function as the radiological safety center; and the tugs and salvage ships used in mooring and which stood by for emergency target recovery, or salvage, if needed.

**Air Support.** Aircraft participated in the photographic missions necessary for technical

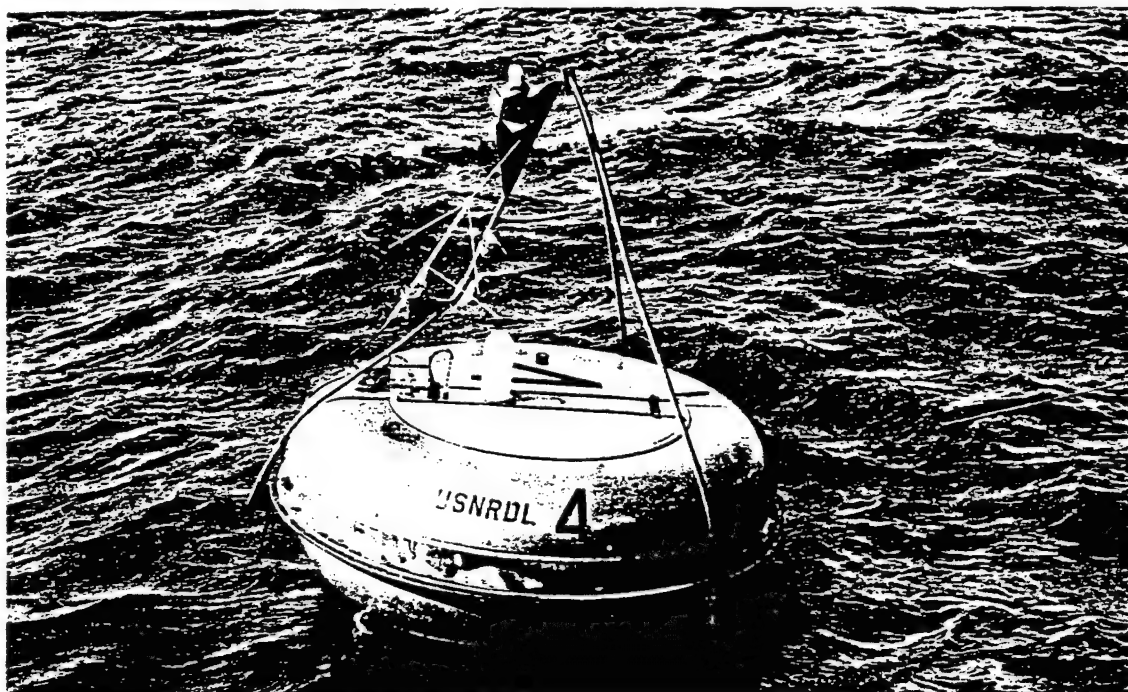


Figure 2.6 Coracle, moored around the shot area. These special stations supported projects collecting radiation information.

photography. Other assistance provided by TG-7.3 and TG-7.4 included helicopters for radiological surveys, recovery of data, transportation of samples and personnel; and aircraft for cloud sampling and for air-sea rescue.

**Preparation of Targets.** The scientific objectives of the underwater shots imposed several special requirements on the preparation of the target array. Some of these requirements were unique in the history of weapons testing.

One special requirement was for mooring the Shot Wahoo array in deep water. Small skiffs had been moored during Operations Redwing and Wigwam, and large ships had been anchored in very deep water. Shot Wahoo was different because it required the mooring of a large number of ships, barges, and buoys in 3,000 to 6,000 feet of water and, yet, with such precision that some horizontal distances were specified to within 100 feet. The shot location selected was in the lee of Eniwetok Atoll, and, though some shelter from rough seas was thus obtained, the conditions were essentially representative of the open sea. The mooring operations were planned and executed by TG-7.3 with the assistance of personnel from the Bureau of Ships (Reference 3).

Another requirement was for unattended operation of ships' main and auxiliary machinery for long periods. Target ships in previous tests had all been in a cold-iron condition. The YAG's

used during Operation Castle were prepared for remote operation, but were not target ships and had simpler machinery systems. Since the shock damage to a piece of machinery is presumed to be more severe when the machinery is operating, and since personnel could not be kept aboard in the lethal radiation fields expected, automatic controls had to be devised and installed. This was accomplished on the three destroyer targets under instructions issued by BuShips and under the supervision of Project 3.8.

A third requirement arose from the expected near-lethality of the shock the EC-2 would sustain. Should the ship sink in 3,000 feet of water, the scientific data collected, including the evidence presented by the damaged ship itself, and many tens of thousands of dollars of instrumen-

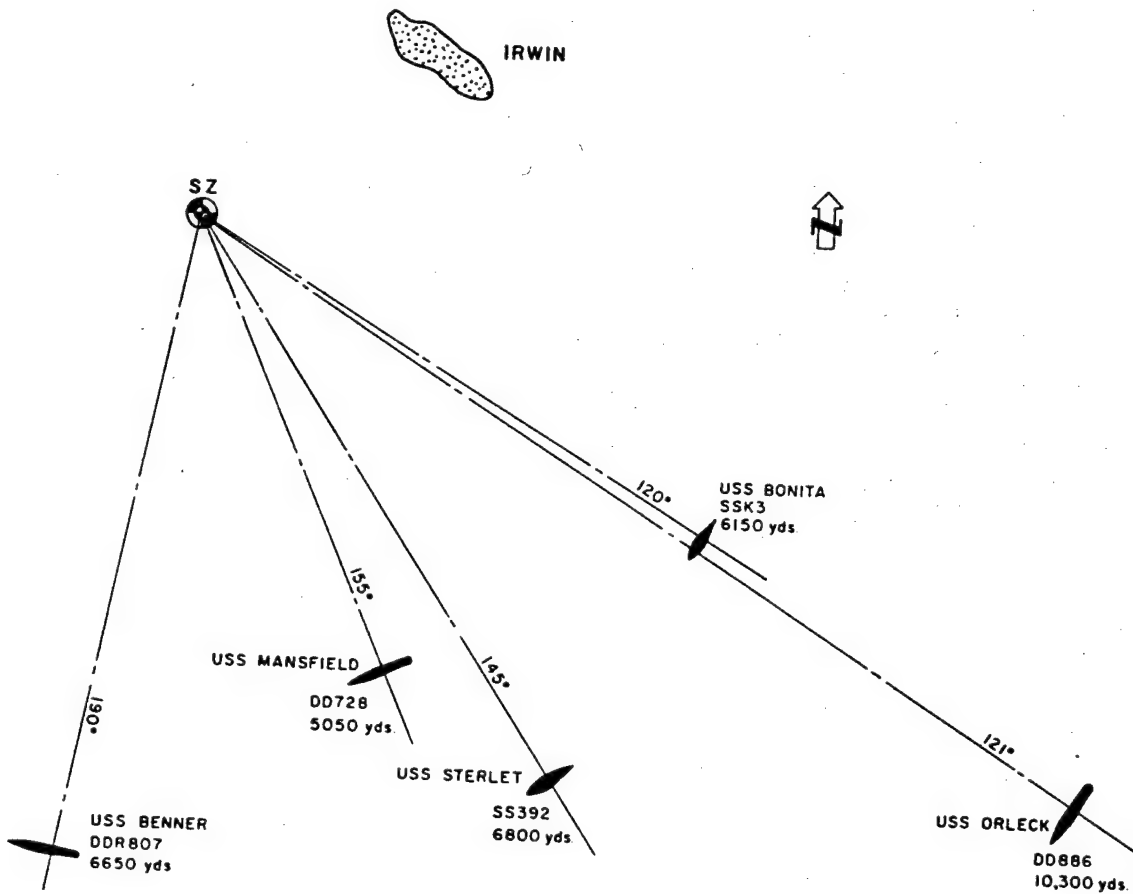


Figure 2.7 Shot Wahoo: active ships around surface zero.

tation, would be lost. To prevent this, the ship was given enough reserve buoyancy to float with the holds flooded. This was done by filling the holds with empty oil drums and improving the general watertightness of the ship. To provide stability and, at the same time, to simulate cargo, the holds were ballasted with water, concrete, and gravel. In this ship no machinery was activated.

Part of the preparation of the target array was to provide washdown systems on the ships and



on the instrumented barges. This accomplished three objectives: (1) early boarding for recovery of data, (2) reduction of the magnitude of the decontamination effort required, and (3) simulation of the radiological condition aboard delivery destroyers, in a downwind location.

2.1.4 Preparatory Operations. Three operations of significance were conducted before the operational phase began: (1) In November 1957 there was a trial of the barge mooring and of the device placement system off Oahu, Hawaii, in a depth of water approaching that expected in the EPG, 500 to 1,000 fathoms. These tests were successful and supported the feasibility of the plans. (2) During October 1957, a bottom survey in the area of the Wahoo and Umbrella sites was conducted, and other oceanographic data was obtained to assist in selecting the best positions for surface zero. This survey was arranged through ONR and later became a part of Project 1.13. (3) The high-explosive tapered-charge tests, Project 3.1, with the DD-592 as target, were conducted off Santa Cruz Island, California, in January 1958.

These tests served to confirm the adequacy of planning before the targets were towed to the EPG and, in the case of the DD-592, fulfilled the high-explosive part of the objective of Project 3.1 in comparing the shock motions produced by tapered-charge with those produced by nuclear detonation. All these tests were conducted by units of TG-7.3 except the oceanographic survey, which was done by ONR. The tapered-charge tests were under the technical direction of the Project 3.1 officer and under the technical control of Field Command, AFSWP.

The tapered-charge tests were conducted from 17 to 25 January, and the DD-592 was returned to Long Beach Naval Shipyard for final preparation, prior to being towed to Eniwetok.

Work on the USS Bonita (SSK-3) was completed in the San Francisco Naval Shipyard on 29 January. The Bonita was then sent to San Diego for final preparation at the Naval Repair Facility before departure for EPG.

Following the tapered-charge tests, a meeting of the Target Positioning Advisory Panel was held in Washington. Distances to the target ships from Shot Wahoo surface zero were set as: EC-2, 2,300 feet; DD-474, [redacted] feet; DD-592, [redacted] feet; and DD-593, [redacted] feet (Figure 2.8). In detailed planning of the mooring of the target ships by TG-7.3 and BuShips, it was determined that Barge 3 was not needed. It was decided to merely omit this number, rather than confuse all previous planning by renumbering the other barges. Barges then would be, from the atoll, Numbers 1, 2, 4, 5, 6, 7, 8, and 9.

2.1.5 Test Operations. The operational phase of Operation Hardtack began with the movement of personnel and equipment from the United States to the EPG. Ships, barges, and equipment were towed or transported from their respective shipyard or port.

Towing of the EC-2 began on 3 February and was completed at EPG on 1 March. Similarly, towing of the DD-474, DD-592, and DD-593 began in early March. The Bonita proceeded on her own power. All vessels arrived about 15 April.

The barges readied by the Pearl Harbor Naval Shipyard were towed as completed, with the first tow beginning about 1 January. Heavy weather caused minor delays in the tow schedules. In general, however, the schedules were adhered to. The after engine room of the DD-592 flooded during tow, because of a corroded pipe plug, which was open to the sea. Heavy weather prevented immediate corrective action, but the engine room was later pumped out. Little damage to instrumentation was done, since only a few gages were installed there. The camera mountings remained watertight. The zero buoy and the barge were scheduled to be moored from 25 March 1958 to 1 May.

TG-7.3 began mooring barges in late March and continued this work until just a few days before the scheduled shot date, 15 May. Winds of 25 to 35 knots and seas 10 to 20 feet high were most unfavorable. Extreme difficulty was encountered in accomplishing the mooring, and the project work on various barges of the array. Since the barge decks had to be kept clear of

equipment until after mooring, delays in installing and checking out equipment resulted. Transfer of material to the barges was hazardous to personnel and equipment. Some supplies were lost over the side, and some personnel fell in the water while being transferred from boats.

To assist in target preparations, TG-7.3 had a repair ship, USS Hooper Island (AR 17), moored near Site Elmer. The three destroyers and Bonita were nested alongside the Hooper Island during the late field preparations. The EC-2 was moored close by.

The USS Monticello, (LSD-35), and the boats assigned from the TG-7.3 Boat Pool provided transportation to the target array area and boat service between the barges and ships. Fre-

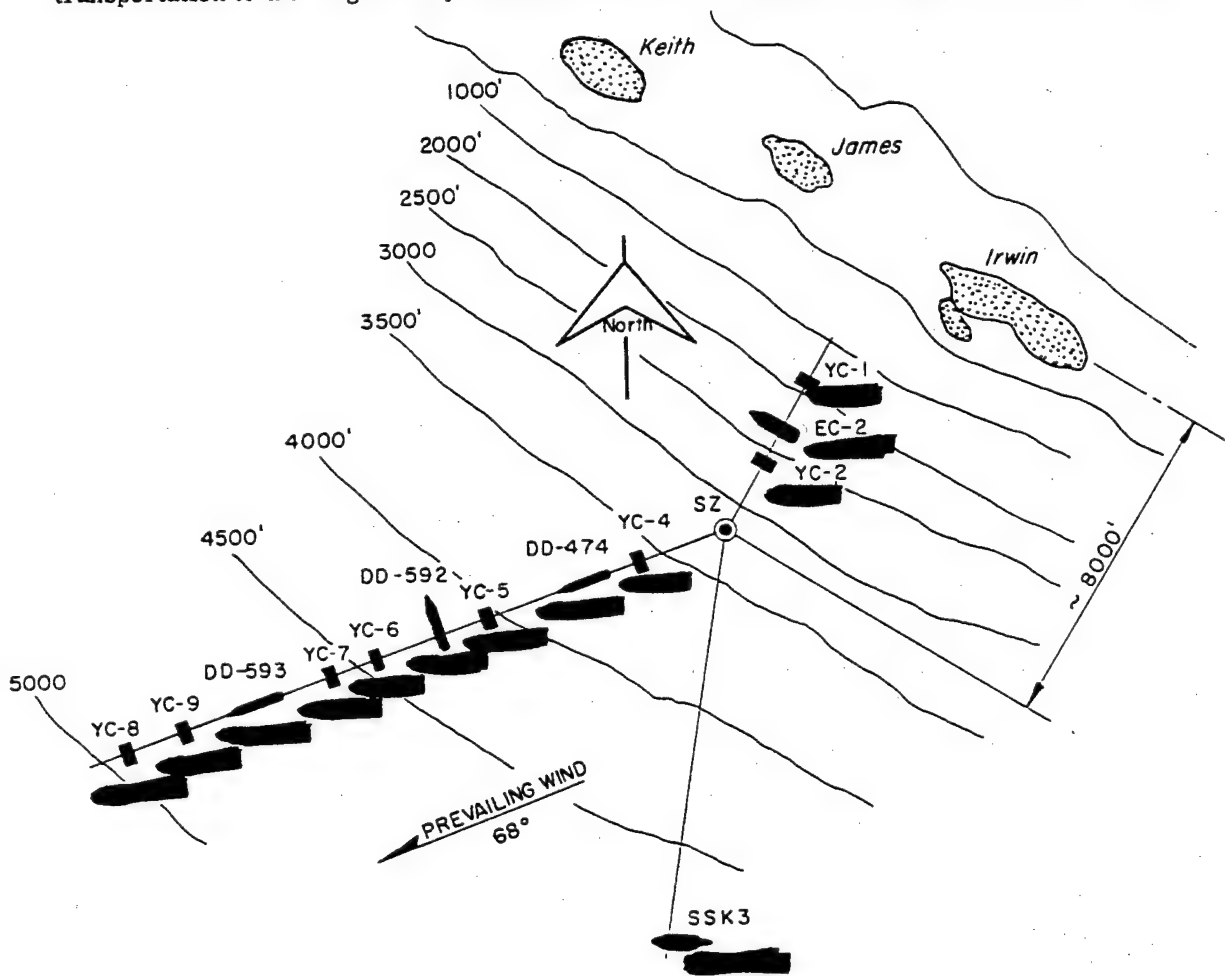


Figure 2.8 Wahoo target array at shot time, showing approximate water depths.

quent changes in schedules, due to bad weather, had to be made to adjust to unexpected situations; delays in getting on station were occasioned by the possibility of contamination from other shots; failure to get information resulted from overloaded communications and conflicting requirements. In the rush of last-minute preparations, two items assumed great importance: (1) Shot Wahoo zero hour of 1100, 15 May, was established, and (2) about a week before shot date, it became apparent to operational personnel that, due to difficult weather, it would be dangerous, if not impossible, to remotely submerge Bonita. Resurfacing would be hazardous, possibly leading to loss of the ship. Accordingly, CTG-7.3 made CNO aware of this concern

and advised CNO that it was planned to place Bonita to southeast of surface zero as a manned station at a safe range. The CNO concurred. Since TG-7.3 had already moored Barge 9, and Barge 8 was still to be moored, it was decided to simply tie Barge 8, which was completely instrumented, to Barge 9, allowing the wind and sea to stream Barge 8 to seaward. Thus, the positions of Barges 8 and 9 were transposed.

Earlier it had been planned for the target ships to be moored in the array about four days before shot time, but due to bad weather, this was not possible. Full-power runs of machinery, washdown systems, and timing signals were conducted in the lagoon. On 13 May, one critical anchor leg of a barge failed, and it was necessary to move the shot date to 16 May to repair this broken mooring.

On 14 May all target ships were towed to the vicinity of the shot area for further tests of machinery, washdown systems, and timing runs. They remained under tow overnight. The EC-2

TABLE 2.4 DISTANCES OF TARGET ARRAY UNITS FROM SURFACE ZERO, SHOT WAHOO

Ship	Distance from	Distance from	True Headings of Ships
	Surface Zero	Mean Centerline	
	ft	ft	
YC-1	[REDACTED]	142 S	—
EC-2	[REDACTED]	0	308° 30'
YC-2	[REDACTED]	24 S	—
SZ-	[REDACTED]	0	—
Z Barge	[REDACTED]	47 N	—
YC-4	[REDACTED]	114 S	—
DD-474	[REDACTED]	149 N	249° 30'
YC-5	[REDACTED]	232 S	—
DD-592	[REDACTED]	232 S	329° 00'
YC-6	[REDACTED]	95 S	—
YC-7	[REDACTED]	47 N	—
DD-593	[REDACTED]	320 N	242° 00'
YC-9	[REDACTED]	166 S	—
YC-8	[REDACTED]	64 S	—

was placed in her moor on 14 May. On 15 May the destroyers were placed in the array moor, and the full-scale trial of the device placement was accomplished (Figure 2.10). The USS Grasp remained over surface zero during the night.

During the late timing runs on 15 May, the lockout signal was, through error, not used, and all Project 2.3 coracle stations were triggered. In order to save the experiment, Project 2.3 worked throughout the night, and a two-hour delay, until 1300, was called to give adequate time to rearm.

Starting at 0900 on 16 May, the weapon was lowered into position, final evacuation of the target array was begun, and the USS Grasp left the zero-buoy area about 1100, while ships and boats moved to pre-selected positions south of surface zero to await the detonation. Several operational ships were deployed to the south of surface zero. Project personnel had permission to place limited instrumentation in the USS Orleck, USS Benner, and USS Mansfield. The approximate locations of the target-array stations and the manned ships are shown in Figure 2.7, Figure 2.8, Figure 2.9 and Table 2.4.

Between 1130 and 1145 the arming and firing party over surface zero asked for two 15-minute



Figure 2.9 Wahoo array looking from near surface zero down the destroyer line.

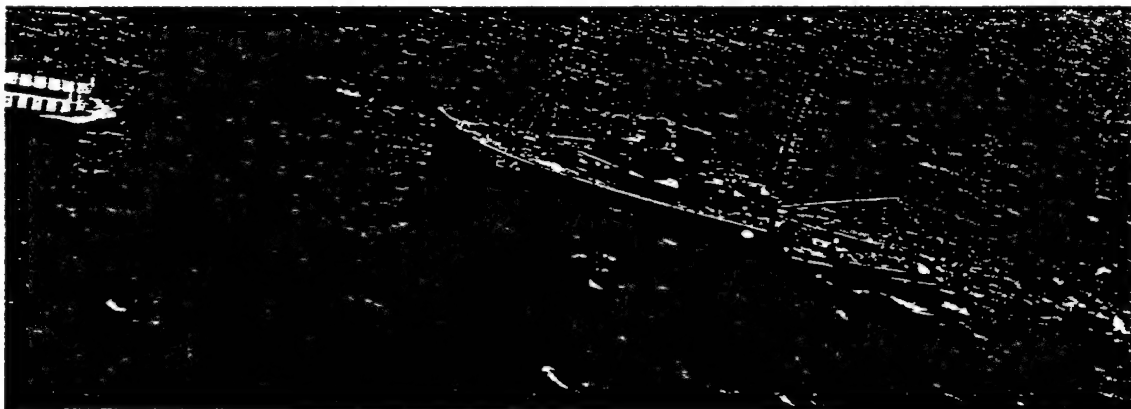


Figure 2.10 Placing the Wahoo device. The USS Grasp is moored stern to the zero buoy in the process of transferring the device to the buoy. At the left can be seen the LCM platform which housed the firing racks and the small buoys supporting the instrument cable to the device.

delays to correct radio difficulties. Their difficulties corrected, the party was evacuated by an aircraft rescue boat at 1230.

At 1330 on 16 May 1958 Shot Wahoo was detonated.

Early recovery of some data, particularly that of a radiological nature, was accomplished before dark on 16 May.

On 17 May the target ships were hosed down, monitored, and data was recovered as safety considerations permitted. When all projects were ready, the ships were taken from their moorings and towed into an anchorage near Site Fred where decontamination was performed, using teams from the USS Renville. This was accomplished in about 4 days.

## 2.2 WAHOO BLAST AND SHOCK

An accurate knowledge of free-field blast and shock phenomena from underwater detonations is one of the basic ingredients needed for determining lethal and safe-delivery ranges and for design of ship structures and machinery. Seven projects were involved in obtaining blast and shock or supporting data on Shot Wahoo: underwater pressure-time histories for use by ship damage projects; visible surface phenomena such as the spray dome, water column, base surge and water waves; air overpressures versus time; yield determination; and area oceanography. Data obtained was generally to be examined together with that of Operation Wigwam and of high-explosive tests in order to provide an ability to predict shock phenomena for any underwater-burst geometry.

2.2.1 Wahoo Oceanography. In order to allow intelligent planning of the target array, including positioning of the device and anchoring of the target array, it was necessary to ascertain the composition and characteristics of bottom sediments and the relief and slope of the ocean bottom, well in advance of Shot Wahoo. This work was accomplished during September and October 1957, by personnel from ONR, Columbia University Geophysical Field Station (CUGFS), U. S. Naval Mine Defense Laboratory (USNMDL) and the U. S. Navy Hydrographic Office (HyDro), with the U. S. Fish and Wildlife Service Motor Vessel, Hugh M. Smith. Some of the 1957 work was reported in the ITR of Project 1.13 (Reference 4), ITR-1608, which encompassed additional oceanographic work in the Shot Wahoo surface-zero vicinity. The final WT report by this project will cover the entire oceanographic picture.

Bottom Survey. Difficulties experienced during Operation Wigwam with a towed-target array made an anchored array on Operation Hardtack desirable. Work accomplished with the motor vessel Hugh M. Smith showed that the ocean floor was composed of fine-to-coarse coral sand which would permit anchoring of the array. Additional samples were taken from the USS Rehoboth during the operational phase of Operation Hardtack with Kullenberg and Phleger corers. These samples again showed the bottom consisted of blocks of coral and calcareous algae near the atoll shore, grading into a fine calcareous sand beyond the 600-fathom depth.

Ocean Depth. The bathymetric survey conducted by the Columbia University Field Station showed the Shot Wahoo site bottom to be smooth, with a very steep slope. Depth of water along the array is shown in Figure 2.8. Surface zero, as shown by this figure, was at a water depth of about 3,200 feet.

Sound Velocity. HyDro made preshot bathythermograph (BT) observations from barges YC-4, YC-5, and YC-7 and obtained additional BT profiles from the DD-593 at minus 15, minus 5 and minus 1 minutes. Target ship locations are shown in Figure 2.8. Data, similar to that from the DD-593, were lost for the DD-592 and DD-474 due to failure to receive timing signals. Preshot data showed significant changes can occur within a short time interval. Figure 2.11 shows such changes between 1100 and 1200 hours on D-6. Figure 2.12 presents the extrapolated sound-velocity distribution along the array at shot time. At the DD-593, the cross section was

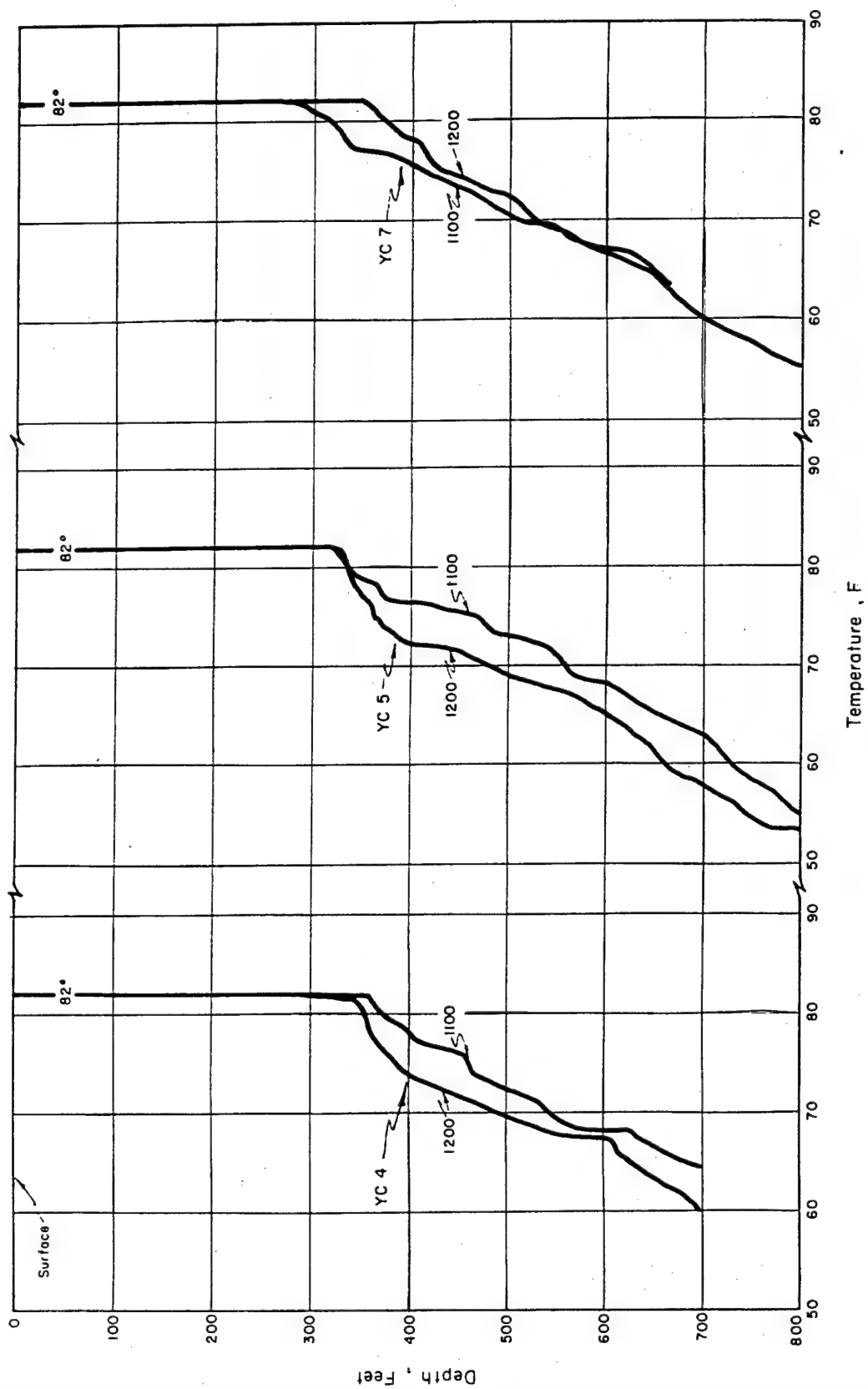


Figure 2.11 Comparison of BT observations at 1100 and 1200 of Shot Wahoo minus 6 days.

based on the minus-1-minute BT trace. The remaining portions of the cross-section were extrapolated, utilizing information on periodicity of temperature changes obtained from previous observations.

**2.2.2 Hydrodynamic Yield Determination.** General experimental procedure for determining hydrodynamic yield is described in Section 3.2.2. On Shot Wahoo, Armour Research Foundation (ARF) failed to obtain necessary data on shock-arrival times close-in to the device. Three weeks' effort was lost in trying to place telemetering and other equipment in the buoy which was to support the weapon. Normal transportation difficulties associated with large ship movements,

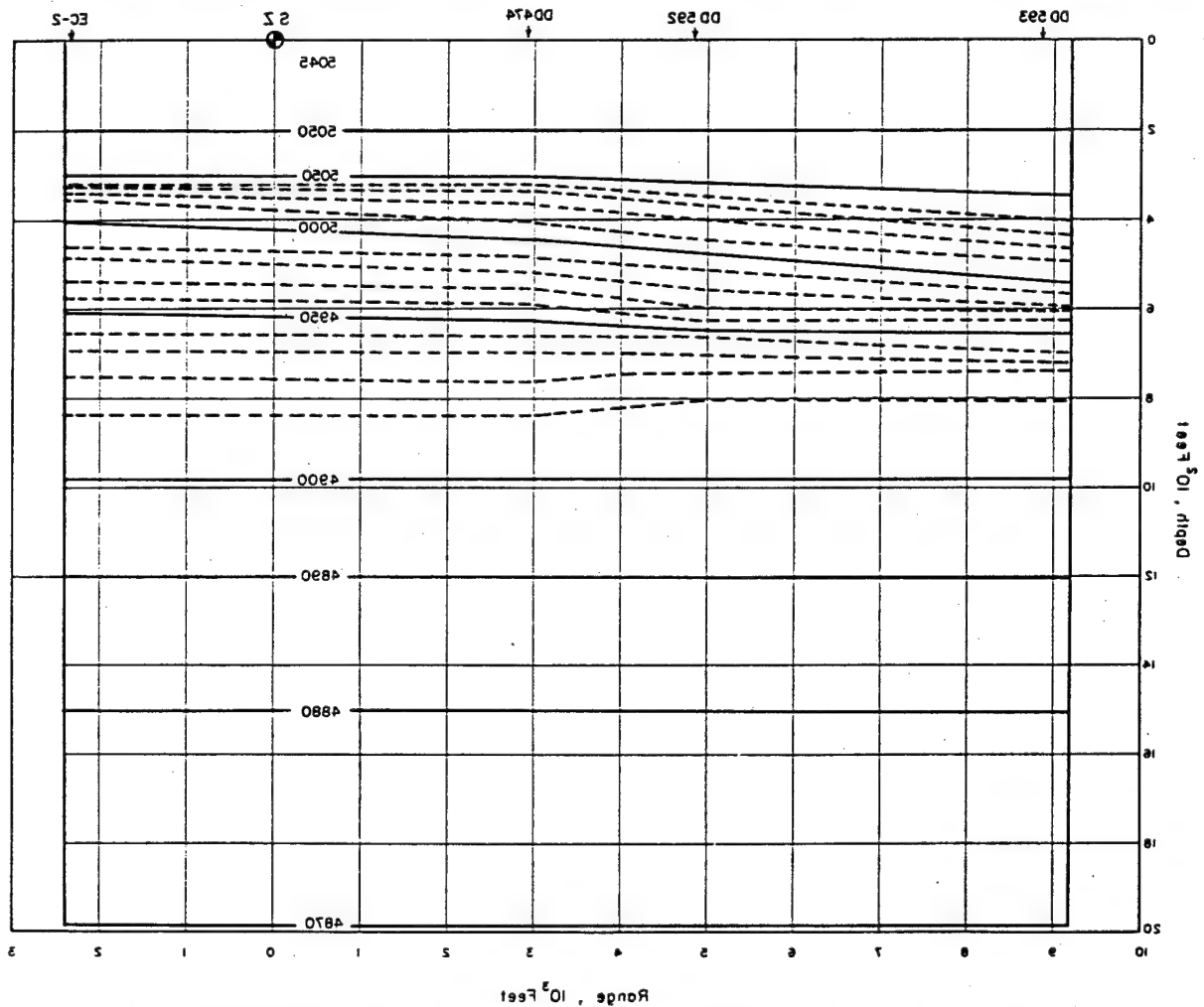


Figure 2.12 Extrapolated sound velocity cross section along the array at Wahoo shot time.

frequent inability to work due to sea conditions, and necessary restrictions of work to daylight hours, all combined to seriously limit work accomplished in the buoy. The project did succeed in instrumenting another surface-zero platform, a barge section, starting on D-11. However, after the barge section was moved from dry land to the shot site early on D-1, reception was questionable. Finally, the telemetering system was joined to the pressure-switch strings in the hope that reception would improve, once a nearby tug, used for lowering the weapon, de-

parted. During the attachment process, the delicate doppler cable was crimped between the barge and tug, and rendered useless. It was still hoped that the pressure-switch system would provide data, but reception remained inadequate through shot time, despite continued attempts to improve the signals. No data were obtained.

2.2.3 Underwater Shock Pressures. Free-field underwater-pressure data were needed primarily for ship-damage projects. The source, intensity, and time history of all pressure pulses near target vessels were desired, since this data forms the first step in the sequence of free-field pressure to loading to response to damage. In addition, pressure-time (p-t) measurements at various depths and ranges from the burst were desired in order that the effects of refraction, reflection, and cavitation could be studied.

Background. Shot Wigwam was the only previous underwater nuclear shot in deep water. Pressure-time histories, as measured during Operation Wigwam, were in good agreement with theoretical predictions (Reference 5). It was considered, therefore, that satisfactory predictions of the most important shock-wave parameters could be made for isovelocity water conditions. Shot Wahoo data were desired, nevertheless, to check Shot Wigwam results. Approximate equations for isovelocity water obtained from Shot Wigwam data for the shock-wave parameters of peak pressure and impulse were:

$$P_{\max} = 4.38 \times 10^6 \left( \frac{W^{1/3}}{R} \right)^{1.13} \quad \text{psi} \quad (2.1)$$

$$I = 1.176 \times 10^4 W^{1/3} \left( \frac{W^{1/3}}{R} \right)^{0.91} \quad \text{psi-sec} \quad (2.2)$$

Where W is the yield expressed in kt and R is the slant range in feet (NavOrd 4500).

Operation Wigwam results broadly confirmed the shape and values of the peak-pressure field predicted, considering refraction effects. However, predictions of a large pocket of pressures well over 800 psi in the range between 12,000 and 17,000 feet were not confirmed as data was not obtained in this region. Accordingly, full verification of the importance of refraction and of the prediction methods of Brockhurst and others was not obtained. It was hoped that Shot Wahoo would provide this verification.

Pressure waves reflected from the air-water surface are negative, and reduce the pressure behind them to a point where cavitation can take place. The region near the surface will, therefore, be momentarily filled with bubbles whose collapse may produce a pressure pulse as great as the direct shock in areas close to the cavitation region. A number of TNT tests have shown definite evidence of this pulse and a few measurements of cavitation collapse were obtained on Operation Wigwam. Since the exact mechanism of collapse, and size of pulse duration and amplitude were not known, measurement and interpretation of the cavitation pulse were objectives on Shot Wahoo.

During Operation Wigwam, the shock wave reflected from the bottom had a greater apparent effect on ships at a 30,000-foot range than did the direct shock. While neither shock was damaging at 30,000 feet, there appeared to be small regions of focusing at 15,000 feet and closer, where the reflected wave could have been damaging. Shot Wahoo was expected to provide additional information about the importance of reflected waves. Also of interest was any screening effect of the cavitation bubbles upon the bottom reflection.

Experimental Plan. Two projects, Navy Electronics Laboratory (NEL) and the Naval Ordnance Laboratory (NOL), participated in measuring Wahoo underwater pressures at ten lo-



cations. Four of the NEL stations were on barges (YC's) at ranges of [REDACTED] downwind and the fifth was on the DD-593 at [REDACTED]. NOL stations were on the YC-1, EC-2, DD-474, DD-592, and DD-728 at ranges of [REDACTED] feet respectively.

NEL used the same equipment as on Operation Wigwam, except for new magnetic-tape recorders. Recording equipment was self contained in 7-by-7-by-8-foot huts. After the barges had been moored, the huts, along with booms, winches, and gage strings had to be placed aboard. NOL instrumentation was also similar to that used on Wigwam; the circuitry and packaging of the magnetic recording units had been improved, and electronic gages were somewhat modified.

The primary measuring instruments used by NOL were tourmaline-piezoelectric gages. Twelve to fourteen gages were equally spaced, down to 2,000-foot depths. A few Wienko variable-reluctance gages were also used on the electronic-gage strings. NOL used ball-crusher gages at depths of 50, 100, and 150 feet, and mechanical pressure-time gages down to depths of 140 feet to augment data in the near-surface regions. NEL, at its YC-4 station, used 16 piezoelectric gages, spread at 50-foot intervals, down to 800 feet. Data from this station was telemetered, since there was a possibility the barge would not survive. At the other four NEL stations, ten piezoelectric and variable-reluctance gages were alternated at 100-foot intervals down to 1,000 feet. Three ball-crusher gages were also attached at each electronic-gage position at these four stations.

Results. Both NEL and NOL experienced considerable loss of data. Failures in ships' circuits between EG&G timing-signal stations and power supply caused loss of all electronic data on the two close-in destroyers. One of two NOL recorders on the EC-2 failed to operate, due to water leakage from the washdown. MPT data on DD-474 was lost on D-1 when a tug pre-initiated the gages during the process of repositioning the destroyer. NEL magnetic recorders failed to record properly on YC-5 and YC-6 for unknown reasons. On the YC-8, generators failed prior to shot time. Only one string of NEL ball-crusher gages, DD-593, survived the shot. This string was lost during recovery operations.

The variation with slant range of peak underwater overpressures obtained on Shot Wahoo are shown in Figure 2.13. Peak pressures ranged from 45 to 1,840 psi. Ball-crusher peaks were somewhat smaller than electronic data at comparable depths. The correlation of data from close-in deep gages with the free-water curve (10 kt) confirms scaling Equation 2.1 for isovelocity conditions developed from Wigwam data, since at deep levels and short ranges one would expect little refraction or surface effects on peak pressures. Figure 2.14 shows a plot of the data and predicted peak overpressure contours based on an average thermal structure for the Eniwetok area. It remains to be seen whether a better fit will result when contours are computed, based on the more realistic thermal structure shown in Figure 2.12. However, Wahoo data are too scanty to make a good evaluation of current techniques for computing departures from isovelocity values, due to refraction effects.

Pressure-time histories at several locations are shown in Figure 2.15. It is to be noted that the wave form at the EC-2 is much as expected ideally, whereas those at the DD-593 show considerable distortion due to the refraction influence. For the DD-593 records, the origin of the time scale was taken as the arrival time of the main shock at the 100-foot depth.

EPT and MPT data obtained on Shot Wahoo are summarized in Table 2.5. Bottom reflections had peaks around one seventh of the main pulse at the EC-2 range, but were about equal in strength to the main pulse at the DD-593. However, surprisingly, no bottom reflection was noted on the DD-593 records for depths less than 400 feet. Pulses due to cavitation collapse were much weaker than reflected pulses at a range of 2,000 and 3,000 feet, and were not observed at the range of the DD-593.

Table 2.6 compares measured durations from shock-wave arrival to cut-off against computed isovelocity water values for selected EC-2 and DD-593 gages. Cut-off times were arbitrarily

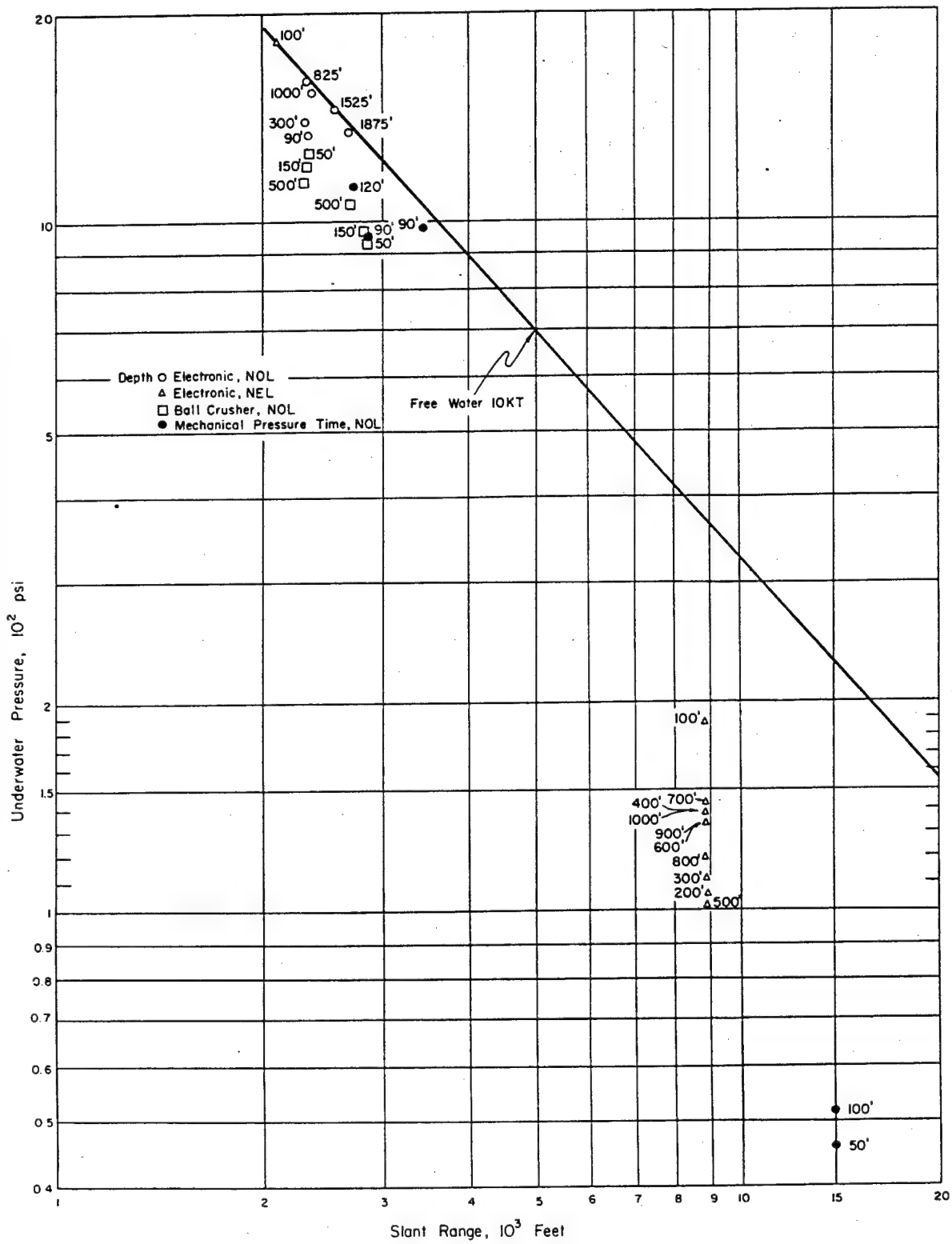


Figure 2.13 Underwater pressures versus range, Shot Wahoo.

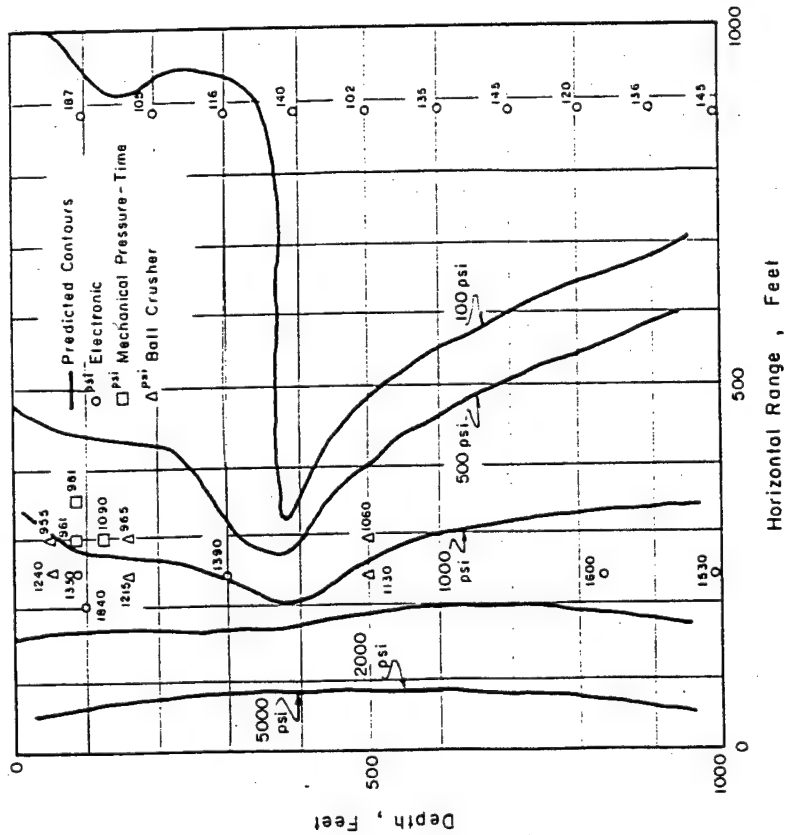


Figure 2.14 Comparison of peak underwater pressures with predicted contours, Shot Wahoo.

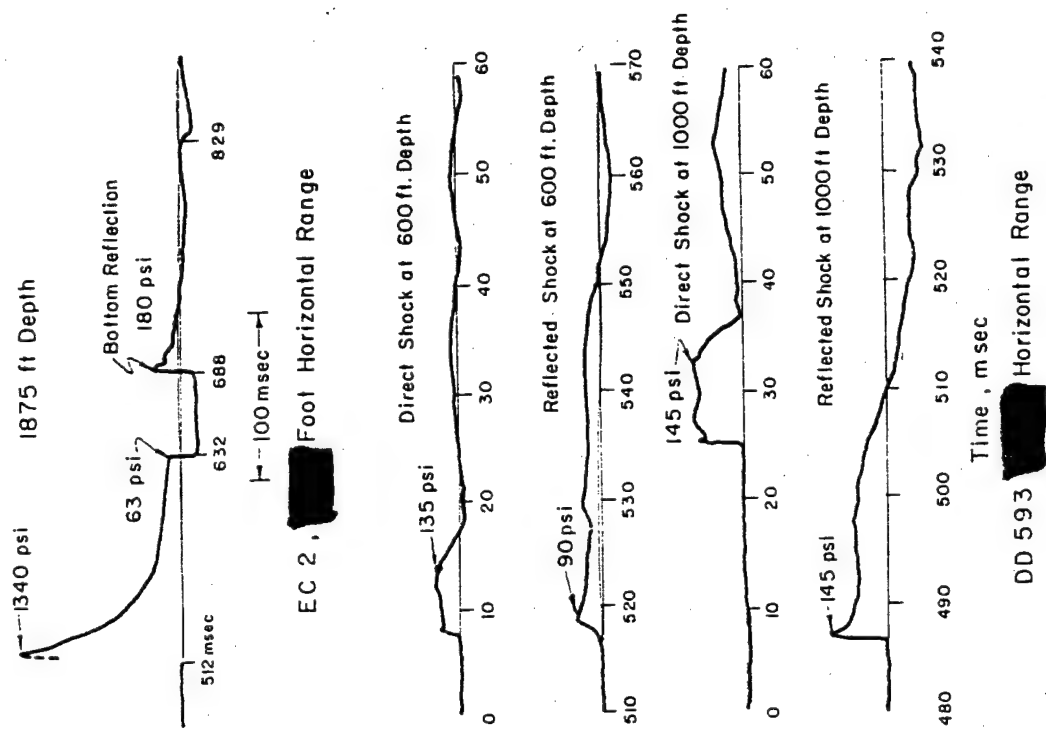


Figure 2.15 Underwater shock-wave records, Shot Wahoo.

TABLE 2.5 SUMMARY OF EPT AND MPT UNDERWATER SHOCK DATA, SHOT WAIHO

Horizontal Range	Gage Depth	Peak Pressure	Main Shock		Cavitation Pulse		Bottom Reflection	
			Time of Arrival	Duration of Positive Phase	Peak Pressure	Time of Arrival	Peak Pressure	Time of Arrival
ft	ft	psi	msec	msec	psi	msec	psi	msec
(YC-4)	100	1,840	—	10.1	—	—	—	—
(EC-2)	90	1,330	440	—	—	—	—	—
(EC-2)	300	1,390	430	22	124	644	188	1,000
(EC-2)	825	1,600	437	59	47	740	226	896
(EC-2)	1,000	1,530	447	71	15	782	220	861
(EC-2)	1,525	1,460	483	102	—	—	240	752
(EC-2)	1,875	1,340	512	120	45	960	180	688
(DD-474)	90*	961	—	—	—	—	—	—
(DD-474)	120*	1,090	—	—	—	—	—	—
(YC-1)	90*	981	—	—	—	—	244	455†
(DD-593)	100	187	—	1.1	—	—	—	—
(DD-593)	200	105	—	—	—	—	—	—
(DD-593)	300	110	0.6†	3.6	—	—	—	—
(DD-593)	400	140	2.3†	4.3	—	—	118	532.9†
(DD-593)	500	102	5.1†	5.2	—	—	140	527.7†
(DD-593)	600	135	7.9†	5.6	—	—	90	517.1†
(DD-593)	700	145	11.5†	—	—	—	105	508.7†
(DD-593)	800	120	16.1†	6.2	—	—	170	500.3†
(DD-593)	900	136	21.2†	—	—	—	113	496.2†
(DD-593)	1,000	145	25.1†	7.6	—	—	145	468.3†
(DD-728)	50*	45	—	1.9	—	—	102	465†
(DD-728)	100*	52.4	—	1.6	—	—	104	460†

\* MPT gages.

† After arrival of main shock at 100-foot station at same range.

‡ After arrival of main shock.

taken as the time the pressure returned to zero in cases where the arrival of the surface reflection was uncertain. Isovelocity values were obtained from graphically-computed differences in path length of the direct and reflected waves assuming a constant wave velocity of 5,000 ft/sec and ideal reflection. The agreement between the measured and computed durations was rather good at the EC-2 (foot range), but was poor at the DD-593 (foot range) and increasingly so, with depth. Inspection of Figure 2.12 indicates that many of the differences can be ex-

TABLE 2.6 DIRECT SHOCK WAVE DURATIONS, SHOT WAHOO

Gage Depth	Computed (msec)		Measured (msec)	
ft				
100	—	2.2	—	1.1
300	25	6.8	22	3.6
500	—	13.2	—	5.2
800	—	19.8	—	6.2
825	66	—	59	—
1,000	73	22.0	71	7.6
1,525	109	—	102	—
1,825	125	—	120	—

plained by the velocity structure of the water. For example, the direct ray, in going to DD-593 gage points below a depth of 400 feet, apparently must travel through the strong velocity gradient of the thermocline so that strong refraction may increase its trajectory length. On the other hand, the reflected ray will travel at a higher velocity and with less refraction, since a great portion of its trajectory is in the 5,050 ft/sec isovelocity region above the thermocline.

In order to provide a rough estimate of a bottom-reflection coefficient, calculations were made of bottom-reflected pressures expected, based on Equation 2.1. The distance traveled by the bottom-reflected wave was calculated by adding slant range to the hypothetical distance found by multiplying the difference in arrival time of the main shock and reflected wave by an assumed sound velocity of 5,000 ft/sec. Results shown in Table 2.7 indicate an average reflection coefficient of 0.30 for EC-2 gages and 0.48 for DD-593 gages. Since errors in the computed distance traveled by the bottom reflection are much more probable for the DD-593 gages, the value of 0.30 for reflection coefficient is preferred.

**2.2.4 Visible Surface Phenomena.** It would be desirable to be able to predict the size of the spray dome, water column, plumes, base surge, and other visible-surface phenomena from a deep water shot. The amount of water forced up is important because it has a definite bearing on the water waves formed, which can cause damage to nearby land areas; and because it is the source of the base surge, which flows out following water collapse. It is felt that base surge is primarily responsible for deposits of contamination from an underwater explosion.

Visible-surface phenomena were recorded by timed technical photographs from four surface stations and four aircraft flying around, or directly over the burst. Viewed from the air, the first visible evidence of the Wahoo burst was an expanding disk on the water surface, consisting of a white patch with a dark fringe, which indicated arrival of the shock wave. The dark fringe was the direct shock-wave slick, whereas the white patch, which reached a maximum radius of 1,600 feet, was the spray dome thrown up by the direct shock wave. At about 0.58 second after first appearance of visible surface effects (SZT), a jagged white ring appeared at a radius of about 2,100 feet and grew rapidly inward to a 1,500-foot radius at 0.71 second, leaving a white annulus around the spray dome. It is believed that this jagged white ring and ensuing annulus were spray thrown up by the cavitation pulse; time of occurrence is in rough agreement with cavitation-pulse time observed by underwater pressure gages at the EC-2.

At about one second after surface-zero time, additional dark slicks and white-spray patches,

due to shock-wave reflections from the ocean bottom, appeared in the neighborhood of the EC-2. These slicks expanded rapidly but unsymmetrically from their points of origin, leaving isolated white patches of spray in the region between the burst and the reef. These scattered patches are believed to have been points where the bottom-reflected shocks were focused by bottom irregularities.

From surface stations, first visible effect was the shock wave transmitted to the air above the water-air interface. Immediately thereafter, a ball-shaped dome of spray was visible. Figure 2.16 shows the development of the dome, which reached a maximum height of 940 feet at about 7 1/2 seconds. First evidence of the formation of the primary plumes appeared at about 1 to 2 seconds after surface zero time in the midst of the spray dome at an altitude of 300 to 400

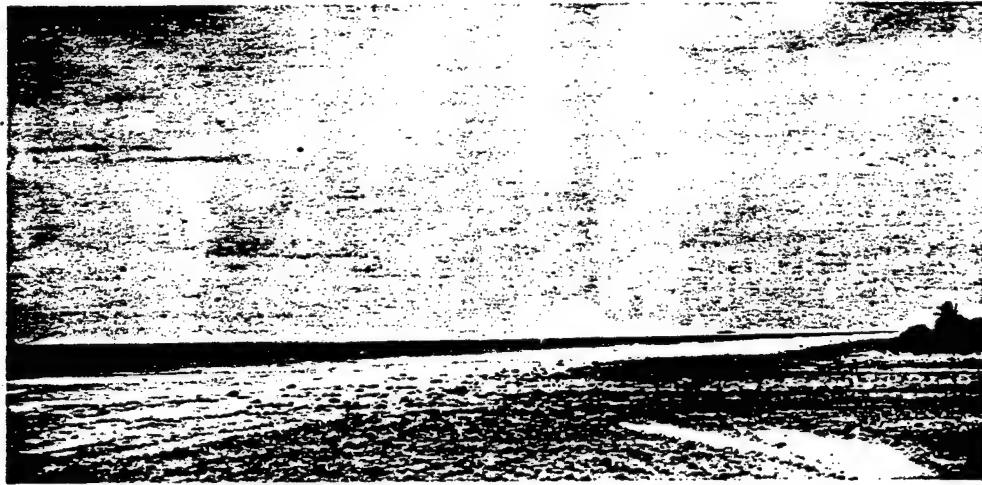
TABLE 2.7 BOTTOM REFLECTION COEFFICIENTS, SHOT WAHOO

Vessel	Gage Depth	Slant Range	Distance Traveled by Bottom Reflection	Calculated Bottom Reflection Pressure	Measured Bottom Reflection Pressure	Pressure Ratio
	ft	ft	ft	psi	psi	
EC-2	300	[REDACTED]	5,160	670	188	0.28
EC-2	825		4,630	740	226	0.31
EC-2	1,000		4,430	790	220	0.28
EC-2	1,875		3,560	1,000	337	0.34
DD-593	400		11,544	265	118	0.45
DD-593	500		11,505	266	140	0.53
DD-593	600		11,435	267	90	0.34
DD-593	700		11,372	269	105	0.39
DD-593	800		11,317	271	170	0.63
DD-593	1,000		11,208	275	145	0.53

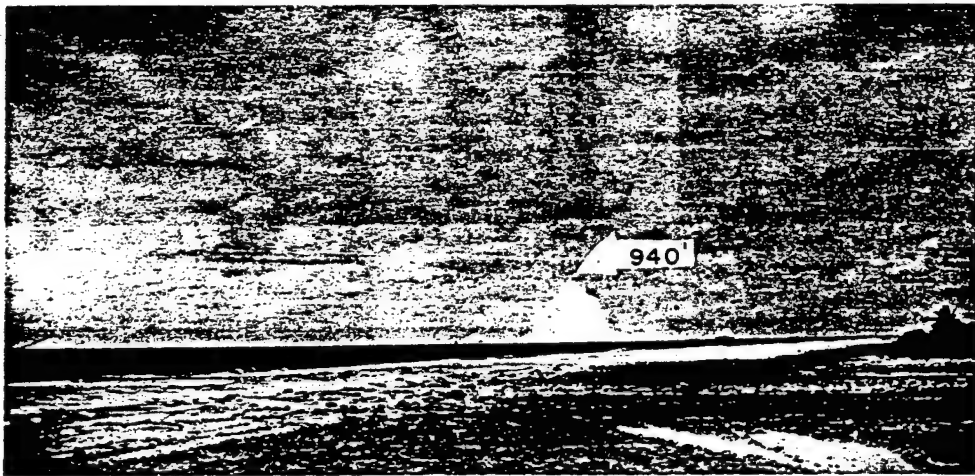
feet. Growth of the plumes is shown in Figure 2.16. The plumes reached a maximum height of about 1,760 feet and diameter of about 3,400 feet at 15 1/2 seconds. Plume collapse is shown in Figure 2.17, with the bulk of the water falling back into the ocean. The portion remaining air-borne, known as base surge, was clearly distinguishable 25 seconds after surface zero time. It was roughly circular in shape. As the surge clouds progressed outward (Figure 2.17), they thinned out considerably and became quite patchy. Patches of the surge cloud were still visible at 12 minutes.

With passage of the base surge, the well defined white-circular patch of Figure 2.17 was observed around surface zero. This patch had a radius of about 3,800 feet at 3 minutes. A foam ring was still barely visible at 17 minutes, with a radius of 4,300 feet. This residual ring was believed to be due to a strong circulation caused by the gravity rise of the shot bubble. Water spread out radially from surface zero, resulting in an accumulation of foam at the edge of the patch as seen in Figure 2.17. It is reasonable to assume that the residual patch coincided with the region of contaminated surface water.

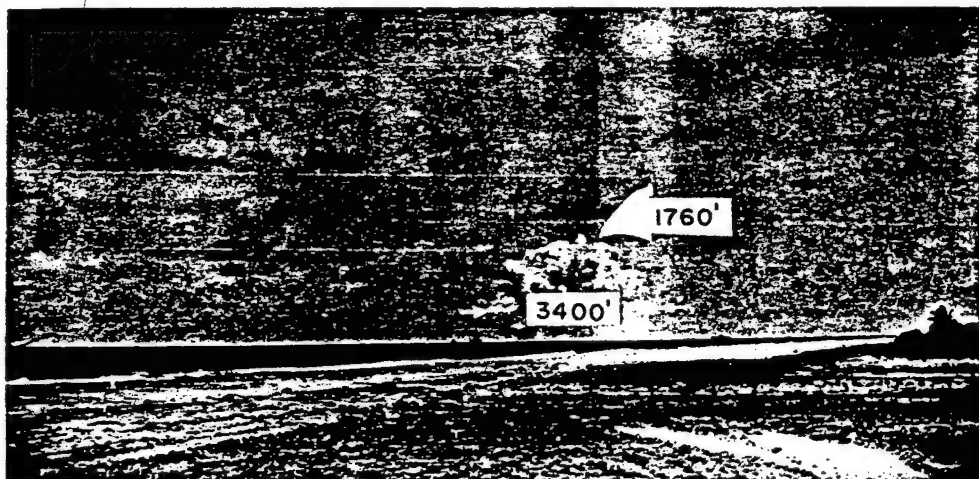
**2.2.5 Air Overpressures.** The air-overpressure field developed by underwater detonations is of particular interest for definition of ranges at which low-flying aircraft can safely direct atomic attacks against submarines. The only available overpressure data for deep-water shots had been from high explosive tests. During Shot Wahoo, NOL obtained air-overpressure data by employing two near-surface stations at the EC-2 and DD-474, and two balloons anchored on the EC-2 and YC-1, with mechanical gages at 500- and 1,000-foot altitudes. Electronic gages used were ultradyne type, diaphragm-inductance gages. The mechanical-gage-pressure system was the same as that used on rockets during Shot Umbrella and is described in Section 3.2.5.



4.6 sec



7.2 sec



15 sec

Figure 2.16 Growth of Shot Wahoo plume.





45.3 sec



6.2 min



17.7 sec



86 ± 3 sec

Figure 2.17 Plume collapse and base surge.



Results. Air-blast data obtained on Shot Wahoo is summarized in Table 2.8. The two balloon-borne gages at the EC-2 were lost, because the balloon broke away prior to recovery. The near surface, ultradyne gage at the DD-474 did not record, due to failure of power supply to the central timing-signal center. Maximum pressure recorded was 0.21 psi, at 30-foot altitude and [redacted] foot ground range. At least two peaks of approximate like values were observed. The first pulse is thought to have been produced by the underwater-shock wave being transmitted across the water-air interface. The second pulse is thought to have been produced by the explosion bubble, the air shock being created either by bubble movement of the water or venting of hot gases from bubble to air, or both. The second peak on the mechanical-gage record at 30-foot level at the EC-2 was obscured by many oscillations in the record. This was probably due to the whipping of the boom on which the gage was mounted. The electronic-pressure-time rec-

TABLE 2.8 SUMMARY OF AIR BLAST DATA, SHOT WAHOO

Gage	Location	Range	Altitude	First	Second	First	Second
				Shock	Shock	Shock	Shock
		ft	ft	psi	psi	sec	sec
Ultradyne	EC-2	[redacted]	30	0.18	0.11	0.48	1.08
Mechanical	EC-2	[redacted]	30	0.21	Obscured	0.52	Obscured
Mechanical	YC-1	[redacted]	500	0.12	0.17	1.10	1.58
Mechanical	YC-1	[redacted]	1,000	0.08	0.14	1.40	1.92

ord at the same EC-2 station is shown in Figure 2.18, along with the first and second pulses from the 500-foot balloon gage at the YC-1. These wave forms are similar to those produced by high-explosive-underwater explosions. Shot Wahoo air-blast pressures of the first shock pulse are compared with predictions based on high-explosive work in Table 2.9. These predictions were made by cube-root scaling of extrapolated 32-pound TNT data. There is good agreement between

TABLE 2.9 COMPARISON OF PEAK AIR OVERPRESSURES WITH PREDICTIONS

Gage	Range	Altitude	Shot Wahoo	HE
			Pressure	Pressure
	ft	ft	psi	psi
Ultradyne	[redacted]	30	0.18	0.22
Mechanical	[redacted]	30	0.21	0.22
Mechanical	[redacted]	500	0.12	0.11
Mechanical	[redacted]	1,000	0.08	<0.01

measurements and predictions. However, no firm conclusions on scaling high explosives to nuclear data can be drawn because of the small amount of data available.

**2.2.6 Deep-Water Waves.** One of the deep-underwater-shot objectives was to document water waves and inundation caused by the detonation. The data was desired to further understand generative processes, propagation characteristics, and inundation. Operation Wigwam, the only previous nuclear deep-water test, yielded a limited amount of wave data.

**Experimental Plan.** Water-wave-measurement stations established by the Scripps Institution of Oceanography (SIO) for Shot Wahoo are shown in Figure 2.19. The pressure-time (p-t) station near the Site James shore line was simply a strain-gage pressure transducer con-

nected by electric cable to a shore-based strip-chart recorder. The transducer was installed in 52.7 feet of water and operated as a differential gage with reference to sea-level changes. This unit, Mk VIII wave recorder, was identical to those used on Operations Castle and Redwing. Five other underwater p-t sensors (compliant bladders) were attached to deep-sea moorings at 100-to-150-foot depths. The bladders were connected by a pressure-transmitting hose to a modified BRL self-recording gage. The BRL gage had an aneroid-type sensor which drove a recording stylus over a battery-driven, chronometrically-governed, glass disk. The normal speed of the disk was changed and the units were accessorized with a pressure-reserve tank, solenoid-actuated air valves, suitable plumbing, battery-power supply and circuits for receiving

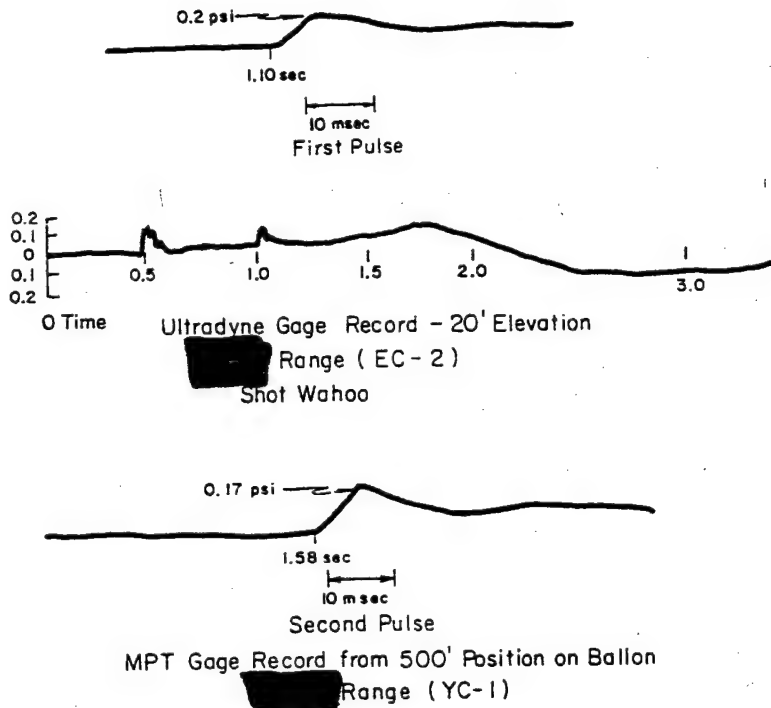


Figure 2.18 Air overpressure records, Shot Wahoo.

timing signals. The entire recording package was installed in NRDL coracles (doughnut-shaped floats, about 10 feet in diameter) and connected to the hose leading to the bladder below. Two pitch-and-yaw systems were installed on destroyers; these were essentially a set of gyros which fed information to a strip-chart recorder. The gyro systems were capable of measuring pitch variations up to  $\pm 30$  degrees and yaw to  $\pm 60$  degrees. Finally, several cameras were installed on sites to photograph wave action on target ships or on wave poles installed on reefs. Figure 2.19 shows the camera station on Site James.

Results. The Mk VIII record, Figure 2.20, shows the first water-wave disturbance radiating from surface zero to be a trough about 0.6 foot in depth. None of the other subsurface p-t units or gyro units provided any data, due primarily to timing-signal problems. However, photographs of ship motion confirm that the initial disturbance, as in Operation Wigwam, was a trough; at the EC-2, it was six feet in depth and arrived at H + 24 seconds. Figure 2.20 also shows that the third and fourth troughs were considerably deeper than the following crests. This unbalance may have been caused by loss of water due to passage over the reef into the lagoon, and/or a reflectance effect.

As shown by Figure 2.20, the highest wave crest was about 10 feet, near the reef line. Photographs of wave poles in the same vicinity show maximum-wave heights had increased to 18 feet above tide stage over the reef. As a result, Site Irwin and the southeast part of Site James

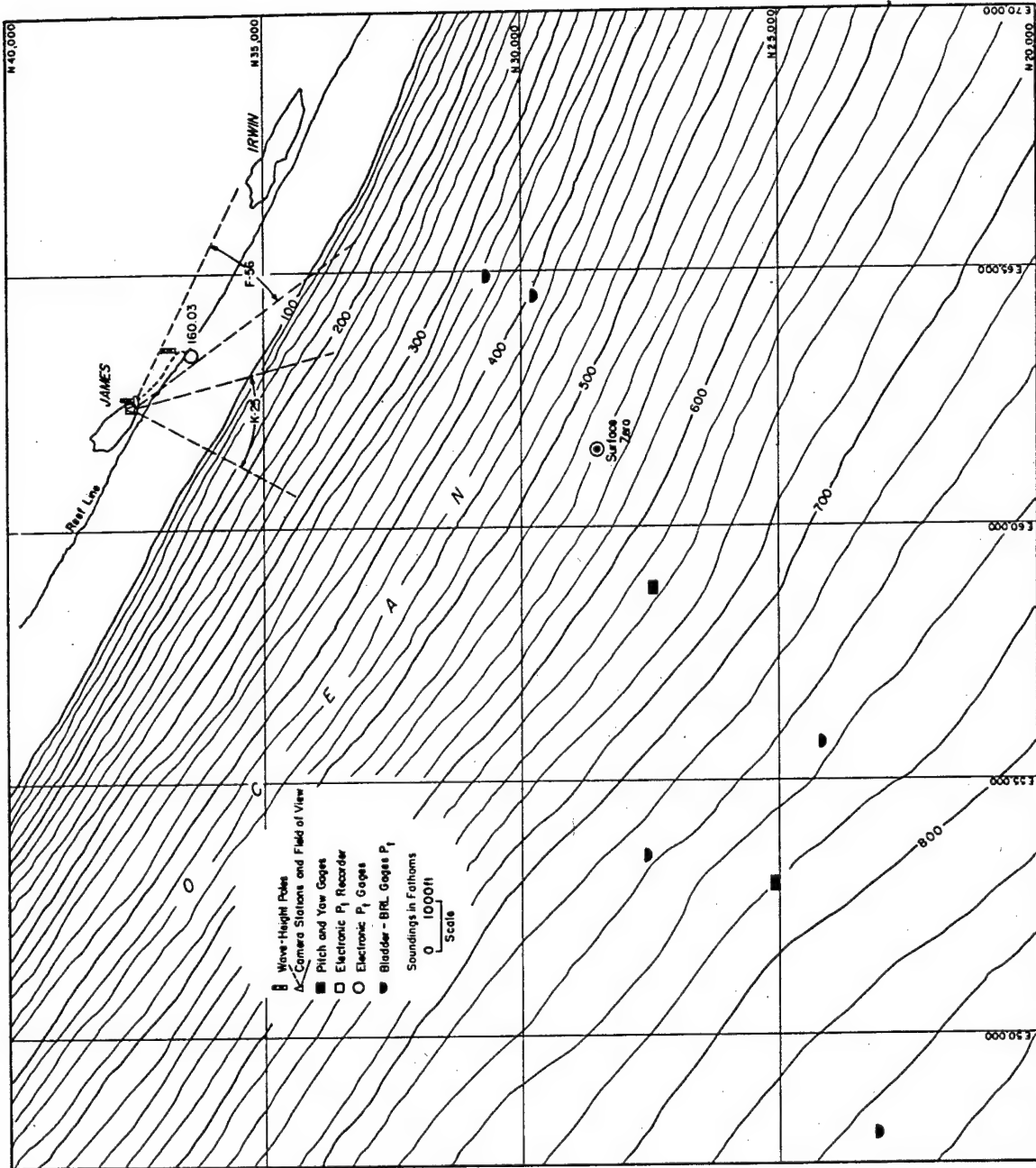


Figure 2.19 Water-wave measurement stations, Shot Wahoo.

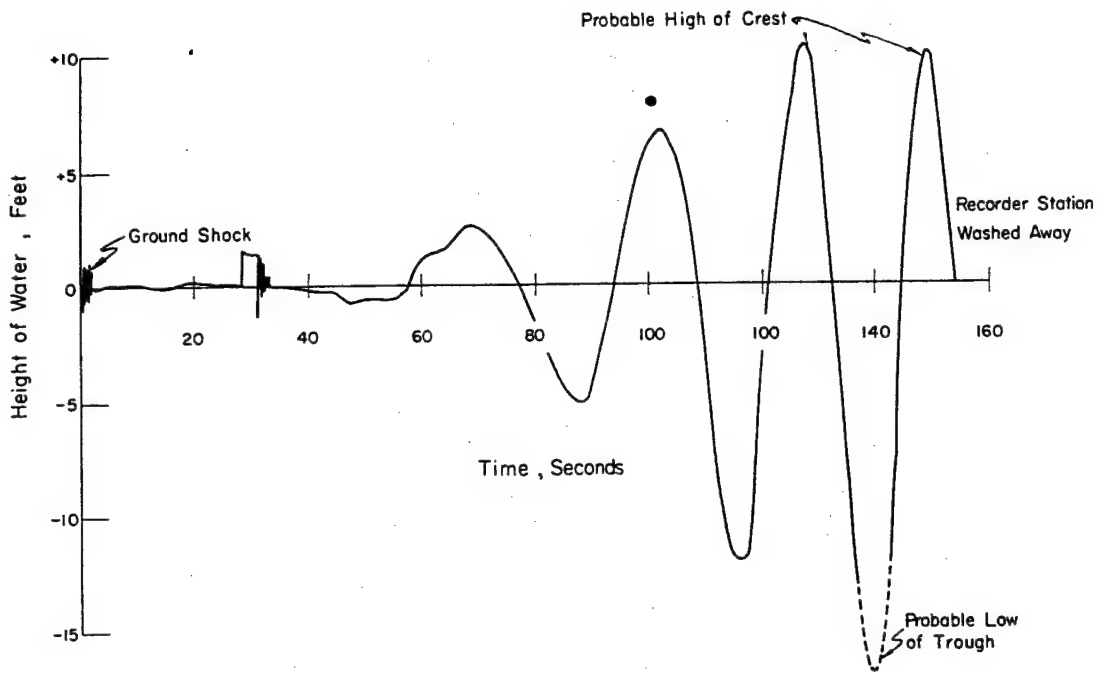


Figure 2.20 Subsurface pressure as a function of time, Station 160.03, Site James, Shot Wahoo. Test was at 1330 on 16 May 1958; tide stage was plus 3.5 feet; depth of transducer was 52.7 feet; range from surface zero was 7,025 feet on bearing of 7 degrees 26 minutes true.

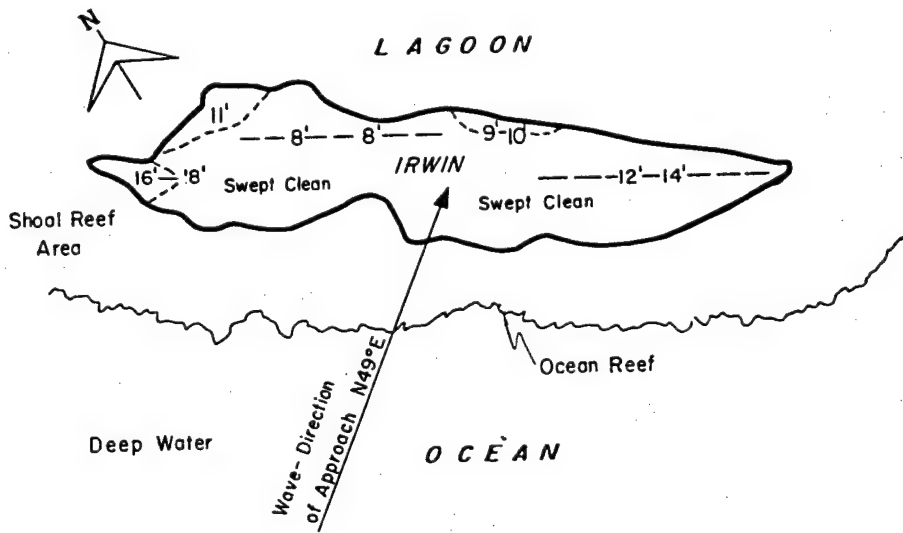


Figure 2.21 Inundation elevations for Site Irwin. Elevations are in feet above tide stage. Average elevation of island above tide stage was plus 6 feet. Range was 8,000 feet.

received considerable inundation damage. Results of a postshot survey of Site Irwin are shown in Figure 2.21. As can be seen from this figure, waves reaching Site Irwin approached approximately along a line normal to the reef. Inundation effects decreased rapidly with increasing angles away from the normal to the reef line, to the point where sites such as Glenn received negligible flooding.

## 2.3 NUCLEAR RADIATION EFFECTS

2.3.1 General. Three projects of Program 2 were devoted to the documentation of nuclear-radiation phenomenology from underwater detonations. Basically, it was the purpose of these projects to document the gross gamma free-fields produced about the points of burst, to measure the consequent dose rates and dosages generated on destroyer-type-target ships, and to evaluate the hazards generated by the ingress of the resultant contaminants into the interior of these ships.

2.3.2 Objectives. The particular objectives of the nuclear-radiation projects were to: (1) measure the complex gamma field at a number of positions within 10,000 yards of the underwater detonations as a function of time, (2) collect samples of the air-borne debris produced, (3) document the gamma-radiation fields aboard three moored destroyers exposed to the radiological environment at locations of possible operational interest, (4) determine the shipboard transit (remote source) and contaminated water gamma-radiation fields, (5) measure the gamma-ionization decay of a fallout sample collected on a destroyer a few minutes after shot time, (6) determine if an inhalation hazard existed within a destroyer-type ship due to ingress of contaminants via ventilation or combustion air systems, (7) estimate the external gamma-radiation dose and dose rate due to ingress of contaminants, and (8) measure particle-size distribution of ingress contaminants in an attempt to correlate biological dosimetry and physical measurements.

2.3.3 Background. With the advent of nuclear weapons for antisubmarine warfare, it became essential that the effects of underwater detonations of such weapons on surface-delivery craft be experimentally determined. The definition of a safe standoff distance with respect both to physical damage and nuclear radiation was of prime importance in the development of tactical doctrine involving these weapons. To obtain sufficient data to permit an eventual operational analysis to determine the safe radiological standoff distance for various tactical maneuvers, measurements of both the gamma free field and resultant shipboard phenomena were required.

Prior to Operation Hardtack the only underwater nuclear detonations were Shot Baker of Operation Crossroads and the one shot of Operation Wigwam. Neither of these two shots yielded measurements of gamma dose rate or gamma dose as a function of time and distance which were sufficiently detailed to permit reliable prediction of these phenomena in other situations. Although some gamma-field data was obtained during Operation Crossroads (References 6 and 7) and Operation Wigwam (Reference 8), the available pre-Hardtack information was fragmentary and insufficient for accomplishment of a satisfactory operational analysis. In general, early time-based data was lacking, and too few data points were available for the construction of reliable gamma-dose contours.

The available data in the area of shipboard radiation effects from underwater detonations was also limited. For the purpose of an operational analysis, extensive and detailed information was required on: (1) the various radiation sources generated by the underwater detonation, including remote, enveloping or surrounding, and shipboard sources; (2) the attenuation afforded by ships' structures and machinery, and (3) the ingress of contamination into the ships' interior and resultant radiological hazards.

Although investigations of gamma-radiation sources outside the ship had been performed for a fallout environment during Operation Castle (Reference 9) and Operation Redwing (Reference 10) and to a limited extent on the Wigwam underwater detonation (Reference 11), the information obtained was neither sufficiently complete nor, in some cases, directly applicable to the underwater weapon-delivery problem.

Ship radiation-shielding studies conducted prior to Operation Hardtack (Reference 10) indicated that radiation attenuation was dependent on ship geometry, the changing geometry of the several radiation sources with respect to the ship, and the gamma-energy spectra, which changes with time and weapon. In order to extend the range of relationships between shipboard situation and radiological environment to cover conditions directly applicable to the weapon delivery problem, it was necessary that typical delivery ships (destroyers) be instrumented and exposed to the dynamic radiological phenomena resulting from the underwater detonations of Operation Hardtack.

The contamination-ingress problem first became apparent after the Baker Shot of Operation Crossroads. Eighteen months after this shot, studies of the after-engine-room ventilation system of the USS Crittenden indicated that personnel in this compartment would have been exposed to lethal quantities of radiation due to ingress of radioactive aerosol, had the ventilation system been open or operating (Reference 12). As a result of this finding and those of other supporting laboratory and theoretical studies, tests were conducted on the ventilation and boiler-air systems of ships (YAG 39 and 40) subjected to fallout from surface megaton detonations during Operation Castle (Reference 9). It was learned that the average activity concentration in unprotected ventilation cubicles was of the order of 0.02 percent of the average weatherside concentration and that it could be reduced substantially by use of paper filters or electrostatic precipitation devices. These findings, however, pertained only to a fallout environment and could not validly be applied to the underwater burst, where the nature of the contaminating aerosol would be different.

In general, some information existed prior to Operation Hardtack on almost all aspects of free-field and shipboard radiation phenomena. This information, however, was extremely limited and, in most cases, not directly applicable to the underwater burst situation. Thus, there was an urgent need to document the radiological environment generated by underwater detonations and to determine the radiological effects and consequent hazards produced by the environment on delivery ships in the vicinity of the detonation. It is important to note that it was not the purpose of the projects to perform an operational analysis of the weapon delivery problem, but to gather sufficient experimental data to permit such an analysis to be performed.

2.3.4 Experimental Method. Documentation of Gross Gamma Fields. The primary documentation of the gamma fields generated by the underwater nuclear detonation was accomplished by means of a newly-developed Gamma-Intensity-Time Recorder (GITR). This instrument was a portable, self-contained unit consisting of a radiation detector and amplifier with time base, a recording system, a battery pack, and miscellaneous instrument control switches and associated circuitry. The GITR is shown in Figure 2.22. For close-in regions where very-high-dose rates were expected, a high-range, high-time resolution, gamma dose-rate versus time detector-recorder instrument was used. The high-range instruments were modifications of the Gustave I detectors developed by the Army Signal Engineering Laboratories (ASEL) for use on Operation Plumbbob (Reference 13). The gamma-dose-rate-versus-time instruments were mounted throughout the area of interest on coracle floating platforms as well as on major target ships. The coracle-mounting platform is shown in Figure 2.23. Coracles were developed as the result of experience gained with deep-moored skiff stations used in the fallout program of Operating Redwing.

The time-dependent measurements described above were supplemented with total-dose measurements made with NBS film-pack dosimeters. The film packs were distributed throughout the target array on coracles, as floating film packs (FFP), and at various positions aboard the three target destroyers and the EC-2. The floating film packs consisted of a film pack mounted in a small styrofoam float, which was connected to a larger identifier float made of the same material. For Shot Wahoo, a free-floating version of the FFP was used, while on Shot Umbrella

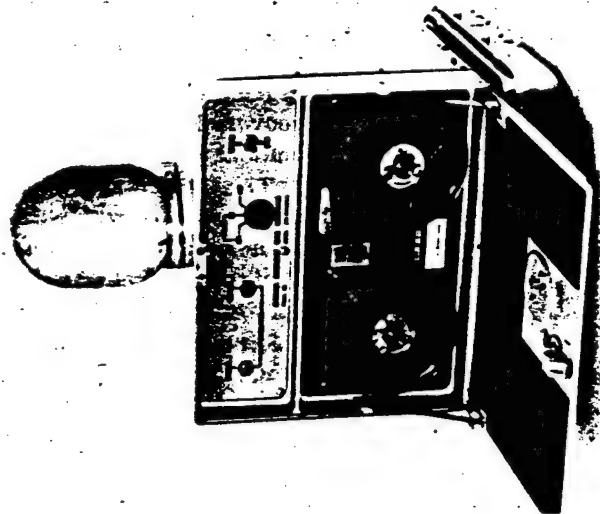


Figure 2.22 The GTR Model 103 instrument with the outer water-tight case cover removed. The detector is shown mounted on main instrument assembly.

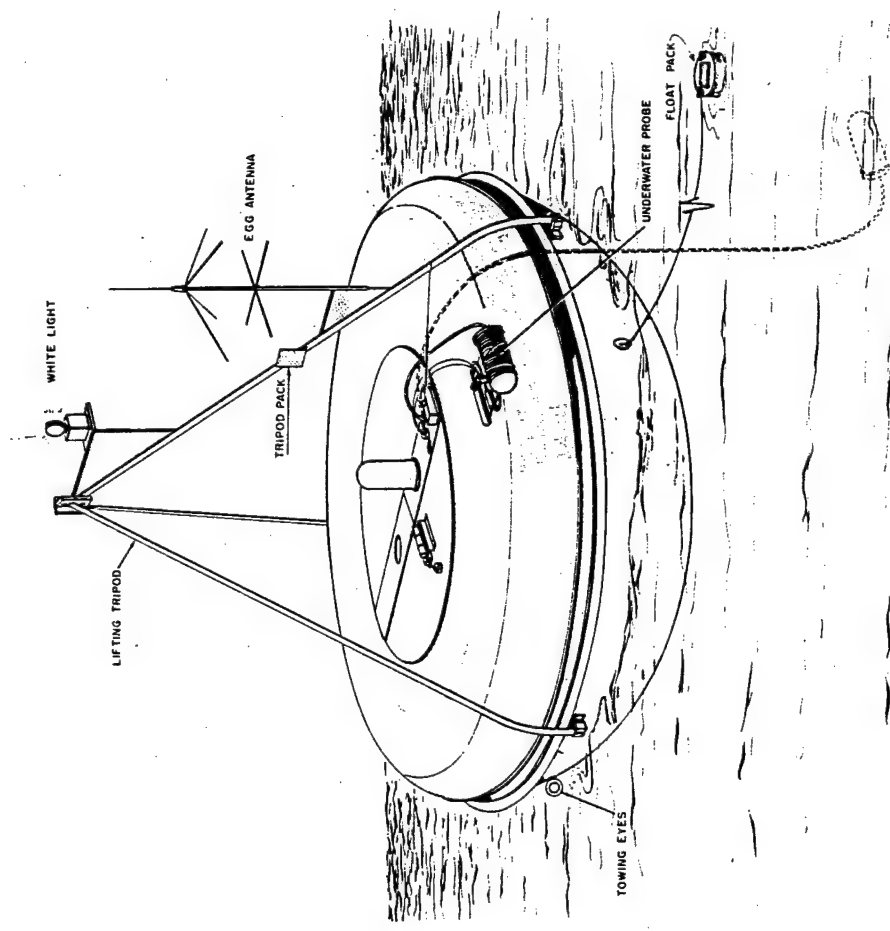


Figure 2.23 Coracle.

most of the FFP's were moored. Both versions of the FFP are shown in Figure 2.24.

Samples of radioactive debris deposited from the transit cloud were obtained through use of incremental collectors located both at coracle and ship stations. The physicochemical information obtained from the collected samples was intended primarily for use in obtaining corrections for application to the GTR dose-rate records.

The Shot Wahoo instrument array, showing the coracle, ship, and floating-film-pack locations is presented in Figure 2.25. This array included 21 deep-moored coracle stations, the three destroyers and the EC-2, and approximately 70 FFP's distributed through the array. It should be noted that not all FFP's are shown on Figure 2.25, since FFP's not recovered are omitted.

The coracle stations were deep moored in advance of the detonation and activated by radio-timing signals just prior to the event. For Shot Wahoo, the FFP's were dropped from aircraft, both prior to and after the event, in order to discriminate between the dose accrued during the

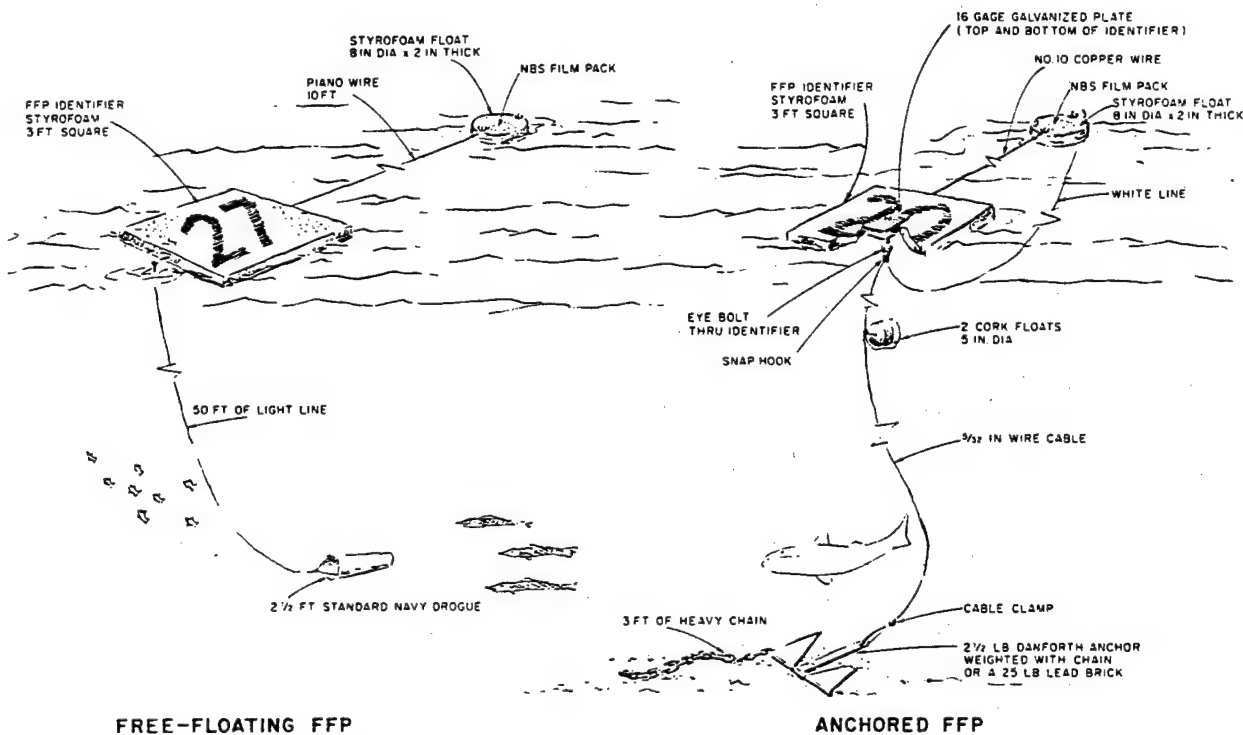


Figure 2.24 Various types of floating film packs.

dynamic portion of the burst sequence and that accrued from residual contamination.

Following the detonation, all instrumentation was recovered as early as radiological and operational conditions permitted, and the data was read out and analyzed.

**Documentation of Shipboard Radiation.** The three target destroyers (DD) were instrumented with GTR's to obtain gamma-dose-rate histories and with NBS film packs for total dose documentation. GTR's with unshielded detectors and film packs were installed at locations representing major battle stations. GTR instruments which had been fitted with directionally shielded detectors were installed on the fantail of each destroyer to record transit, i. e., remote-source radiation. Special underwater GTR's capable of automatic postshot submersion were also mounted on the fantails of the ships to obtain data on the dose rates which existed in the water surrounding these ships. The location of the various GTR's is shown in Figure 2.26.

To provide early decay information, a fallout collector connected to a fully-shielded GTR was employed. This installation was on the DD-592 only and its location is also shown in Figure 2.26.

The project instrumentation was installed on the destroyers prior to the event, and checkouts



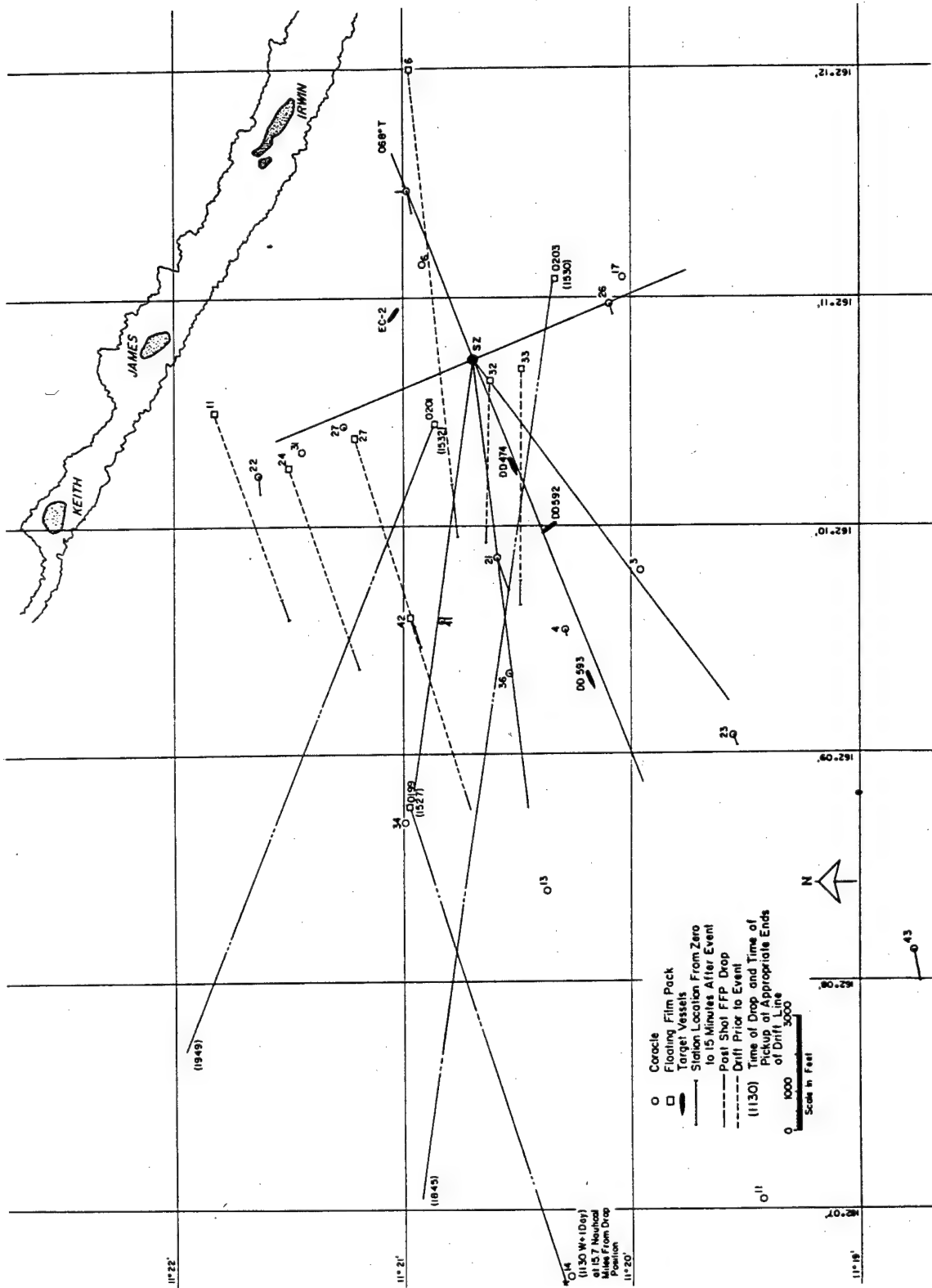
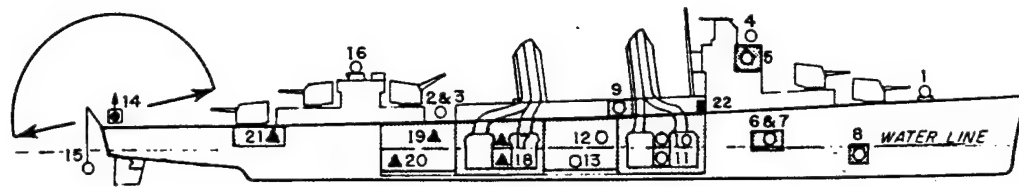
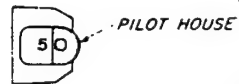
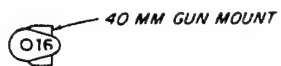
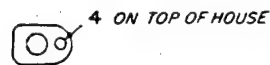


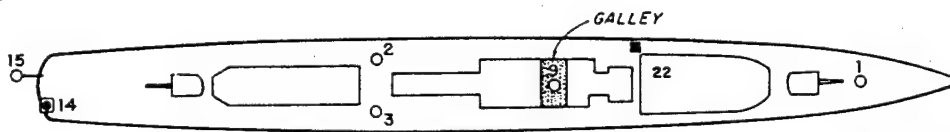
Figure 2.25 Map of Wahoo array, showing coracles, floating film packs, and target ships. Drift of coracles and floating film packs (where it occurred) is indicated.



- ◻ SHIELDED STATION, DIRECTION OF VIEW
- UNSHIELDED STATION ON ALL DD'S
- ▲ UNSHIELDED STATION ON DD592 ONLY
- DECAY UNIT ON DD592 ONLY
- ▭ INSTRUMENTED COMPARTMENT



O2 LEVEL



MAIN DECK

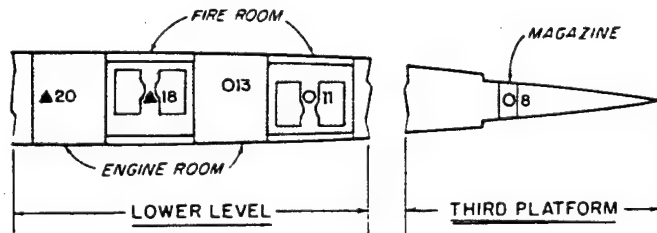
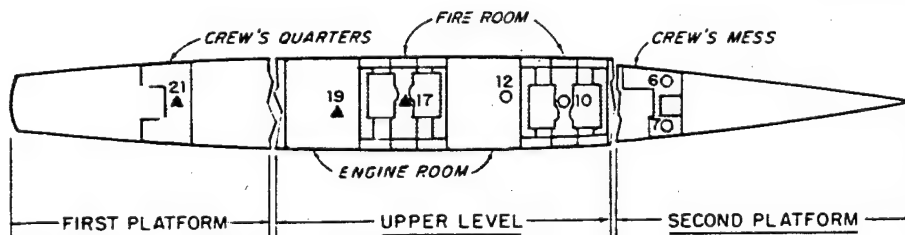


Figure 2.26 Location and designation of GATR stations on target destroyers.

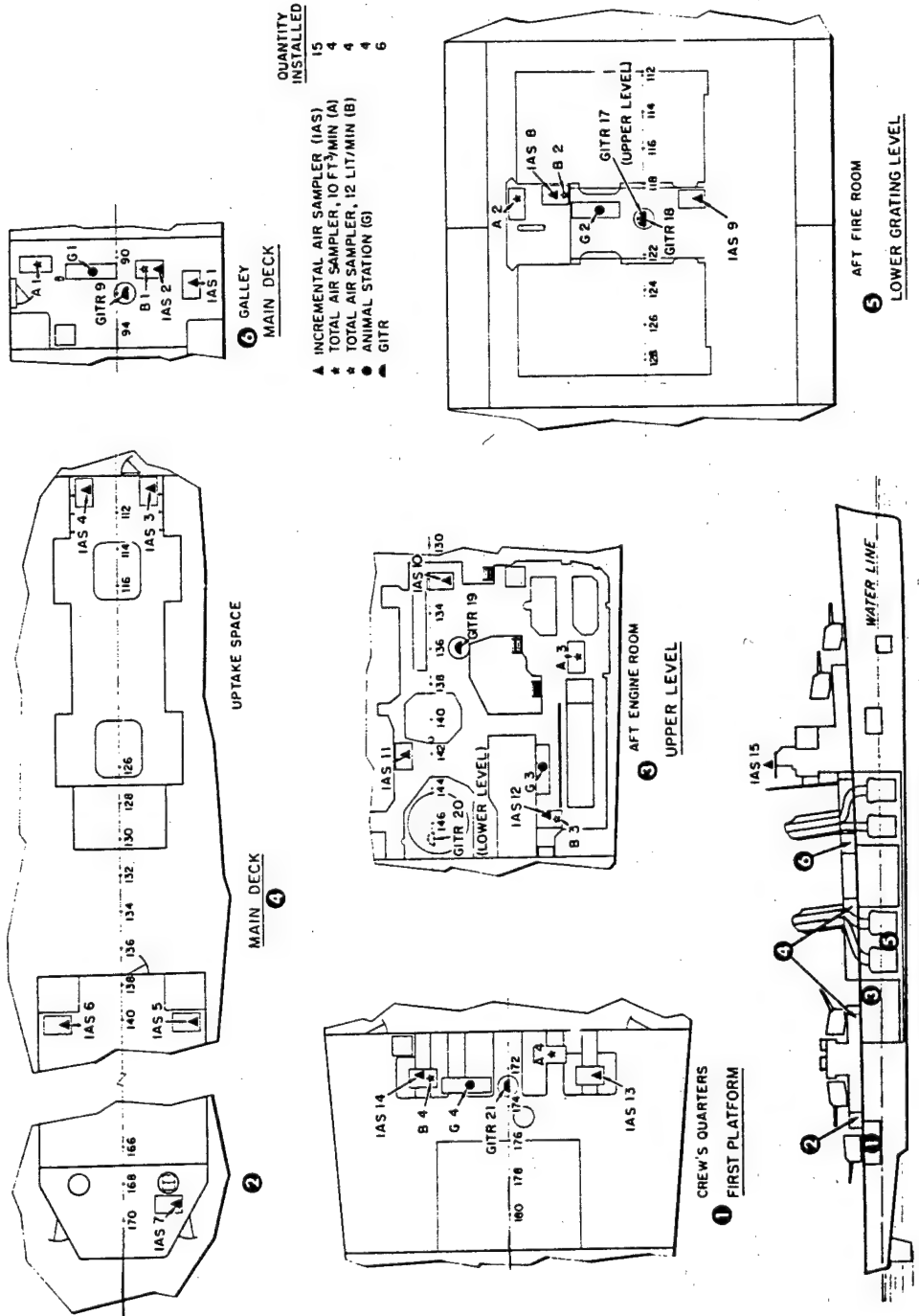


Figure 2.27 Instrument locations on DD-592.

were performed through D - 1. The GTR's were designed to be started by means of an H - 5-second-timing signal from the ship timing-control center. During the period of instrument operation, the ship's washdown system was operating to simulate normal tactical conditions. The GTR instruments had running times of 12 or 60 hours depending on type, and the GTR record tapes and film badges were recovered as soon after these times as feasible.

**Contamination Ingress Documentation.** For purposes of evaluating the inhalation and external gamma-radiation hazards due to ingress of contamination into the ship's interior, the USS Howorth (DD-592) was utilized. Three compartments, galley, after-engine room, and after crew's berthing, and their associated ventilation system, and the after fireroom, in which a full power airflow was maintained through an unfired boiler, were used as test spaces. Gamma-intensity recorders, incremental air samplers, total air samplers, surface (deposition) samplers, and small animals (mice and guinea pigs) were placed in selected locations within these compartments. The instrument locations are shown in Figure 2.27.

To simulate air-flow conditions typical of a ship under atomic-warfare conditions, 20 percent of rated air flow was to have been maintained through the test ventilation systems, while the remainder of the ship was closed. The 20 percent rated-flow condition provided a known situation that represented a maximum air flow for a ship with blowers off. Full-power air flow was maintained through an unfired boiler for the fireroom test.

To obtain data on weatherside phenomena, an air sampler and an animal station were installed above the washdown on the top of a platform above the forward gun director.

Consistent with radiological safety, the collected samples and animals were recovered as soon after the detonation as possible. Following recovery, the animals were sacrificed on a predetermined schedule and tissue counts were made. Air and surface samples were also to have been counted. Records from the GTR instruments were recovered upon expiration of their running times.

**2.3.5 Results and Discussion.** The gross-gamma field documentation effort during Shot Wahoo was adversely affected by an accidental transmission of a radio timing signal at 1600 hours on D - 1. As a result of this transmission, the GTR's and sampler instruments aboard the 21 coracles were activated and began to run down. Since this would have neutralized the gamma-field documentation array, an emergency rearming effort was initiated with the objective of rearming as many of the critical coracles as possible in the time remaining before the shot. As a result of this effort, 14 coracle stations were rearmed, and despite the increased probability of instrument failure inherent in an emergency operation of this type, 9 of the 12 more critical coracle stations showed a high percentage of proper instrument operation.

**Gamma Field Documentation.** The gamma-versus-time traces obtained during Shot Wahoo revealed that no gamma radiation was observed at the time of venting of the shot. This finding is demonstrated in Figure 2.28, which shows a representative gamma-dose-rate record. In the first 30 seconds after the shot, which could be defined as the period of initial radiation, no gamma radiation was observed, even at stations as close as 3,900 feet to surface zero. It was apparent that direct gamma radiation, either from the nuclear detonation or from shine directly from the resultant water column or plumes, was either extremely low or completely non-existent. After about 30 seconds, a significant rise in gamma activity did occur at the close-in stations. This was indicative of the arrival of the highly radioactive aerosol known as the base surge. However, with its passage over downwind stations, the gamma activity did not show an abrupt drop off but, instead, followed this initial dose-rate peak with a series of succeeding peaks as shown in Figure 2.29. The resulting complex curve could be resolved into a series of individual curves to show the passage of distinct dose-rate-activity peaks at downwind stations. This resolution of the experimental curve is demonstrated in Figure 2.30. The activity continued for a period of about 10 minutes as the peaks passed. The complexity of gamma traces was most apparent at downwind stations but was also evident to a lesser degree at crosswind stations.

The complete reason for the complex traces is presently undetermined; however, it appears to have been caused by a number of successive base surges inherent in the mechanism of the

cloud formation after venting. This, in turn, could be further complicated by a reversal of the upwind base surge through action of the existing surface winds and by breaking up of the original coherent mass of radioactive aerosol through turbulence and variations in wind structure. These perturbations of the initial base surge by wind effects allowed the downwind stations to monitor

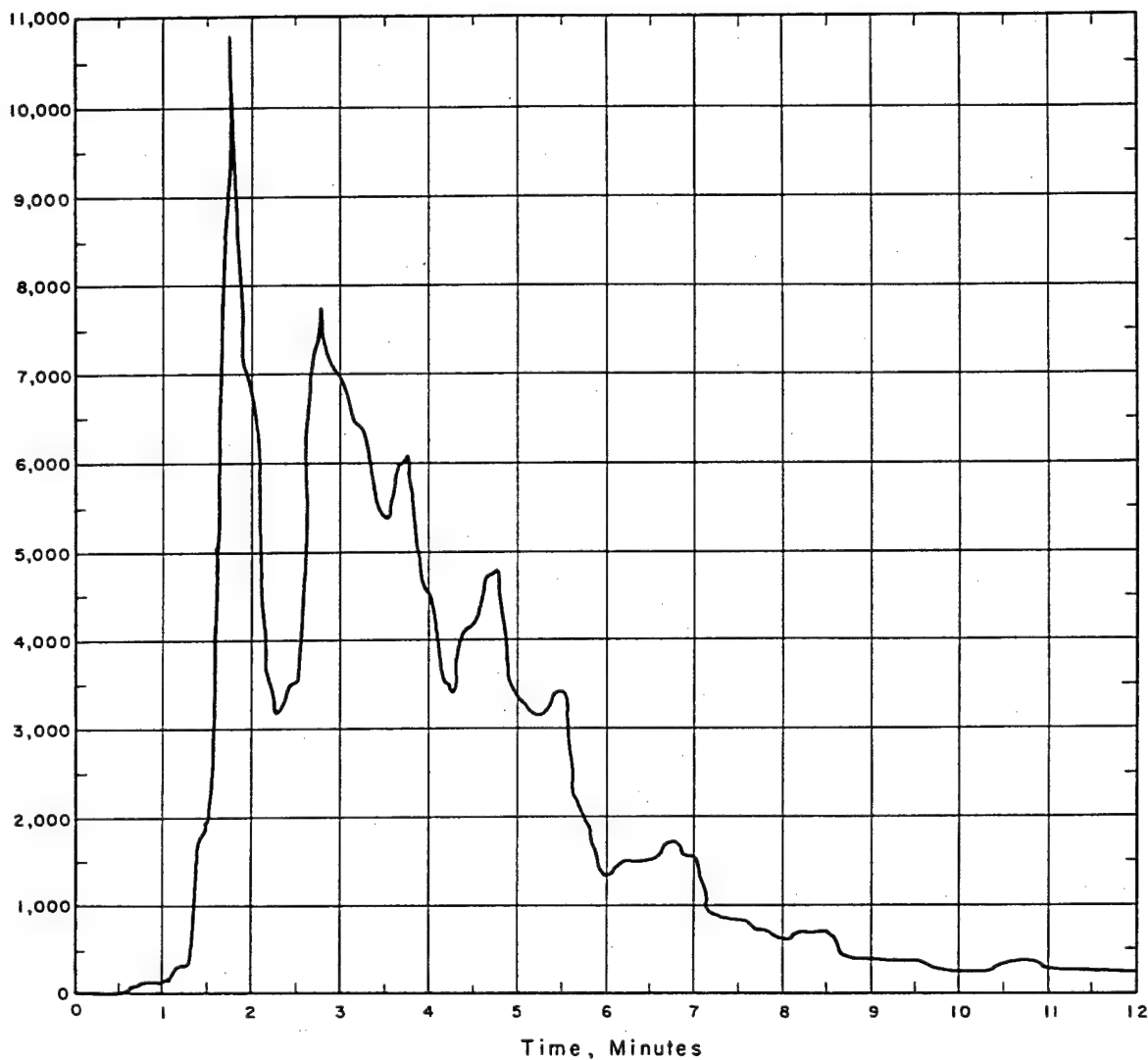


Figure 2.28 Dose rate versus time for std-GTR. Coracle at DRR 7.2 (277 deg T, 6,920 feet) Tape 080. Cumulative dose from GTR trace: 1 min 0.55 r; 3 min 184 r; 5 min 356 r; 8 min 442 r; 12.5 min 470 r. Film pack dose: tripod 435 r, float 340 r, Shot Wahoo. Warning: Increase values read from this gamma trace by 10 percent.

not only the original downwind base surge, but also the complex surge structure incident to the reversal of the upwind base surge.

For distances less than about 7,000 feet, the arrival of the gamma-activity peak indicated that the radioactive material moved outward from surface zero with a velocity of the order of 100 ft/sec. However, because of the complexity of the gamma traces, the mechanism of transport of this material was not fully explained.

For distances greater than about 7,000 feet, the comparison of arrival time with the known distance from surface zero indicated that the surface winds were primarily responsible for the movement of radioactive debris. Therefore, winds-aloft data and hydrographic plotting do not

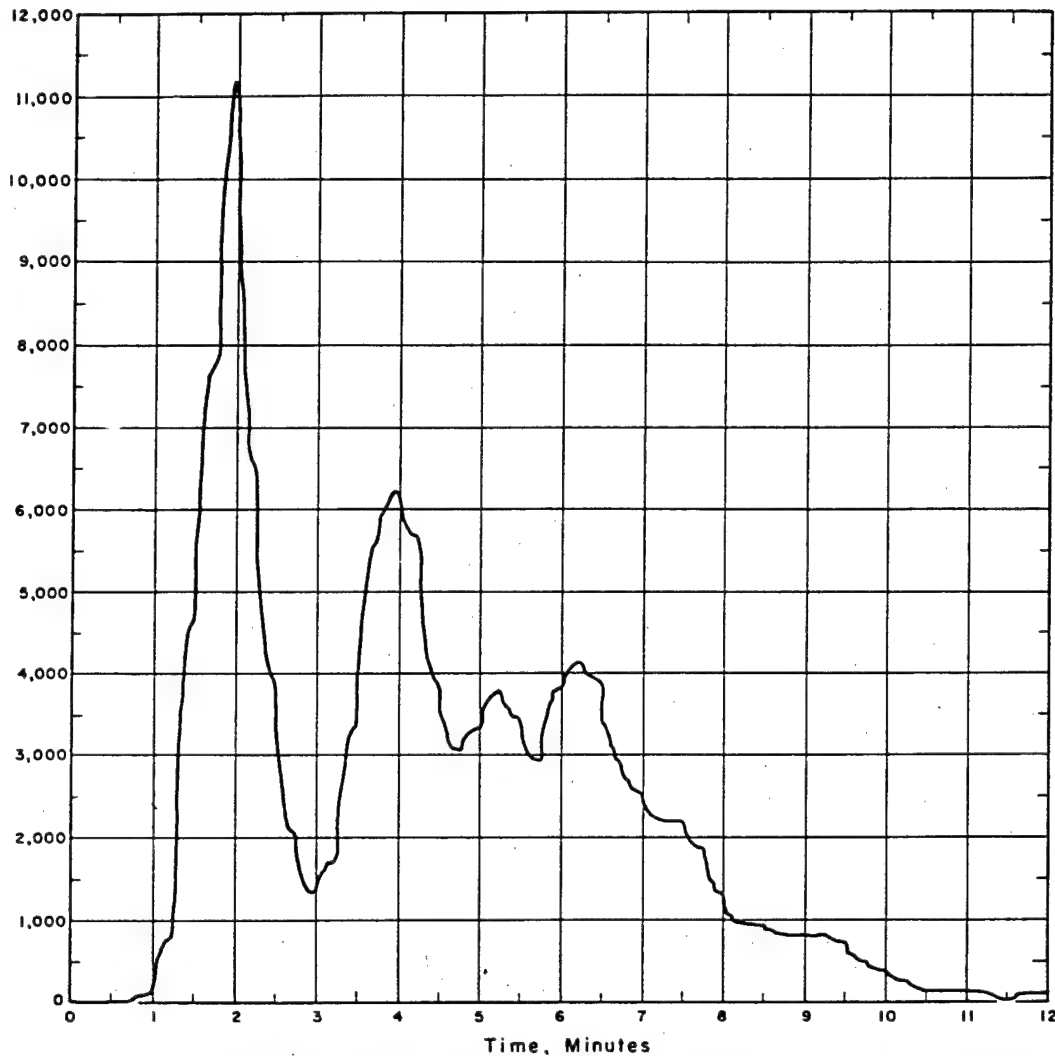


Figure 2.29 Dose rate versus time for std-GTR. Coracle at DL 7.2 (231.5 deg T, 7,100 feet) Tape 94. Cumulative dose from GTR trace: 1 min 0.7 r; 3 min 164 r; 5 min 306 r; 8 min 444 r; 12.5 min 472 r. Film pack dose: tripod 390 r, float 390 r, Shot Wahoo.

appear to be required for prediction of radiological fields resulting from this type of shot.

At all points of observation, the free-field gamma activity was essentially over about 15 minutes after zero time.

Total gamma-dose data from the floating film packs was roughly correlated to data from the GTR's; however, precise comparison was not possible because of the present lack of information on the exact location of film packs during exposure. This data should become available from analysis of the preshot and postshot photographs of the array.

A map of the Shot Wahoo array, showing the total dose received at various stations within one

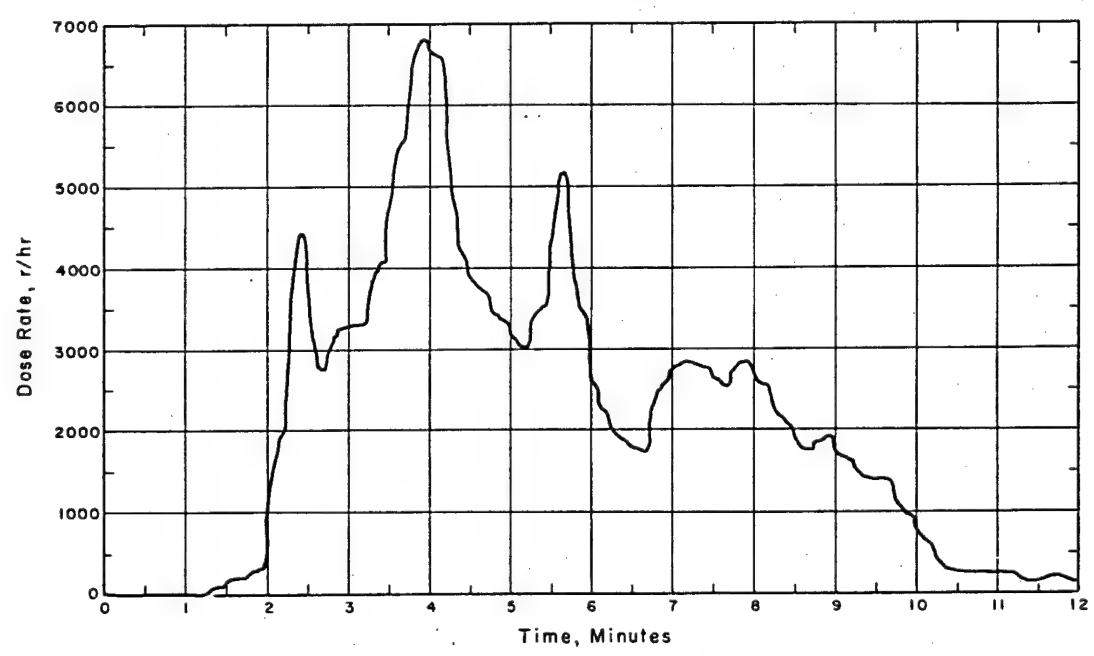
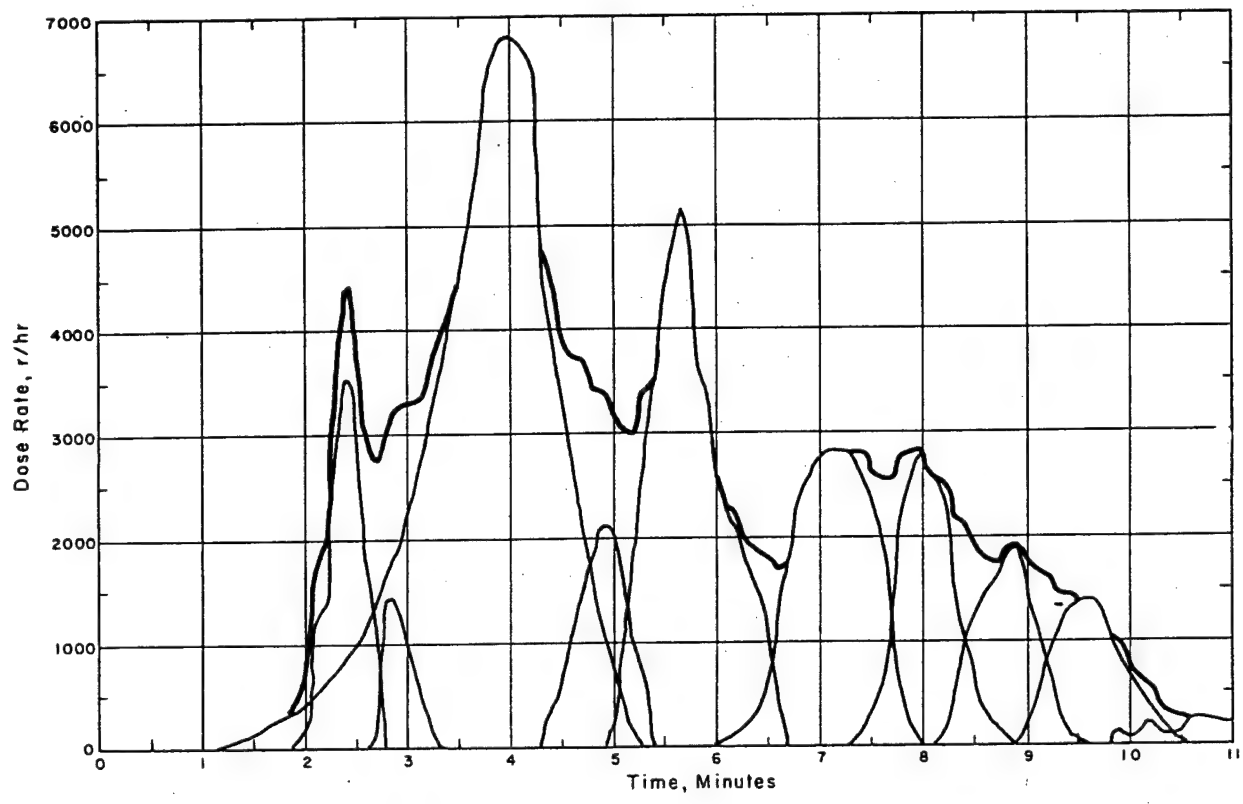


Figure 2.30 Dose rate versus time for std-GITR (lower graph). Coracle at D 8.0 (251 deg T, 7,580 feet) Tape 123. Cumulative dose from GITR trace: 1 min 0 r; 3 min 65.4 r; 5 min 235 r; 8 min 398 r; 12.5 min 468 r. Film pack dose: tripod 340 r, float 0 r, Shot Wahoo. Warning: Increase values read from this gamma trace by 10 percent. The upper graph of this figure shows the resolution (peeling) of the GITR trace into individual peaks. Coracle at D 8.0 (251 deg T, 7,580 feet) Tape 123. All values should be increased by 10 percent. The heavy black line represents sums of dose rates due to two or more overlapping peaks, Shot Wahoo.

minute after detonation, is shown in Figure 2.31.

**Incremental Sampling of Deposited Debris.** Samples of deposited debris were taken in an attempt to determine the activity contribution of contamination deposited on the coracles and ship surfaces to the total gamma fields measured by the GTR's. Since it was originally considered that the field from deposited contamination could represent a substantial fraction of the total measured field, some method of separating the two components was considered essential. However, the amount of deposited radioactive material proved so slight as to be negligible, and no correction was required. This is evidenced by the fact that GTR traces returned to background after final passage of the cloud. The radioactive debris collected by the incremental col-

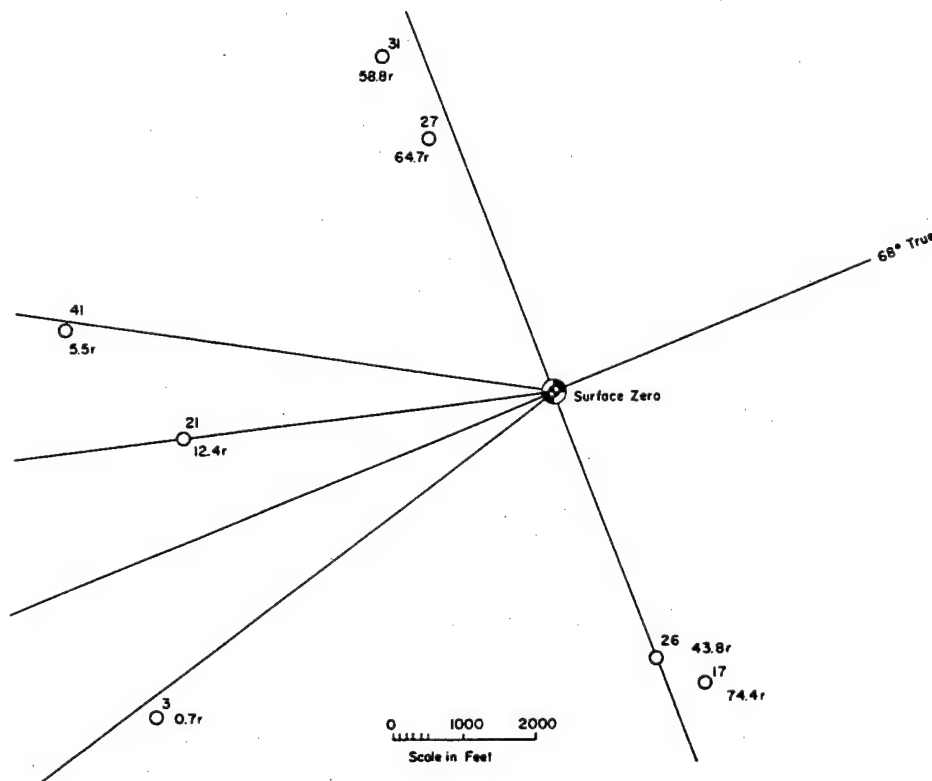


Figure 2.31 Map of Wahoo array showing doses received at coracle stations within one minute after shot time.

lectors was, therefore, used to determine the debris-deposition rate and decay rate for the various locations throughout the array. The deposition period was found to be usually short in the upwind and crosswind positions, and the longest deposition duration was found to occur at downwind stations, but even there, it did not exceed 10 minutes.

**Shipboard Gamma Radiation Fields.** Gamma traces recorded on the decks of the ships revealed approximately the same data as recorded at nearby coracle stations. A significant rise in weather-deck gamma activity did not occur until about 30 seconds to one minute after zero time, again indicating the arrival of the highly radioactive base surge. The complexity of downwind traces, as recorded by the coracle stations monitoring air-borne debris, was again evident in the traces of weather-deck gamma activity. A typical upwind trace is shown in Figure 2.32, and a typical downwind trace is shown in Figure 2.33.



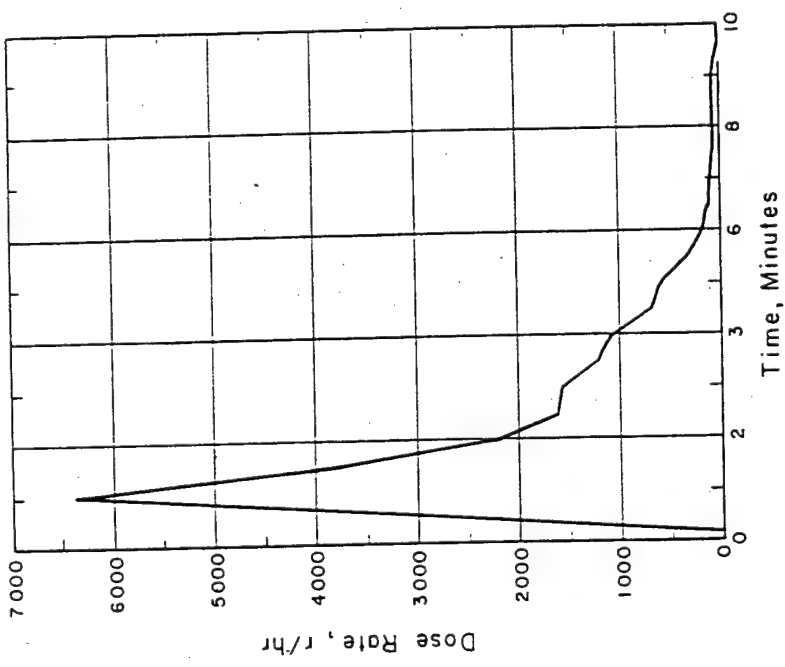


Figure 2.32 Dose rate versus time for GTR at Station 1, Pilot House on EC-2. EC-2 at 029.5 deg T, [redacted], Tape 081. Cumulative dose from GTR trace: 1 min 44 r; 3 min 153 r; 5 min 190 r; 8 min 201 r; 12.5 min 202 r. Film pack dose: 95 r, Shot Wahoo. Warning: Increase values read from this gamma trace by 10 percent.

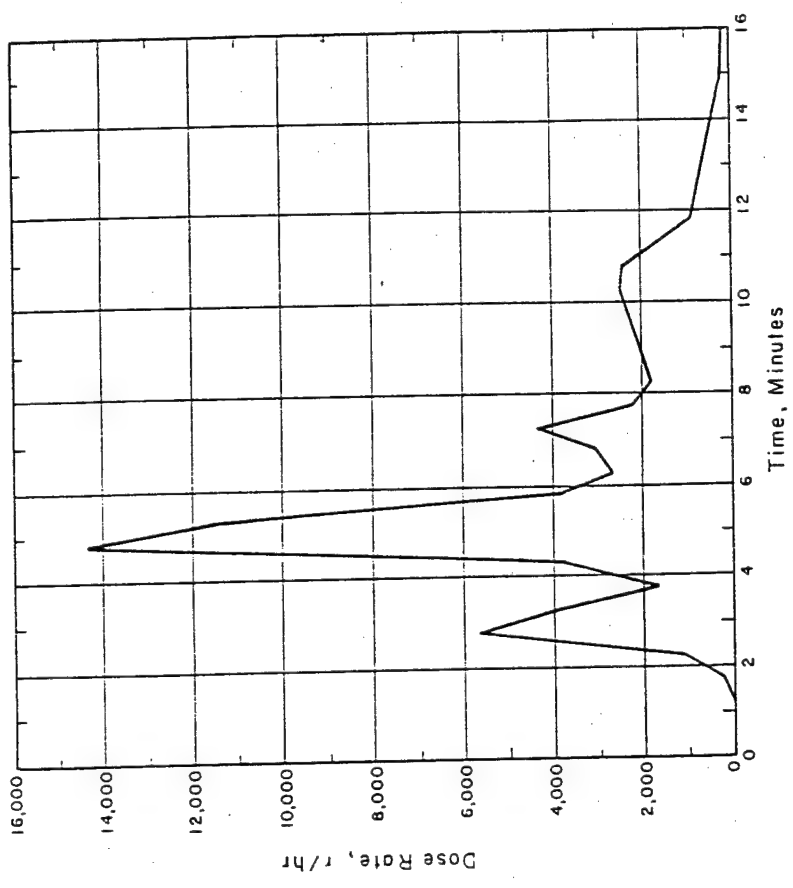


Figure 2.33 Dose rate versus time for GTR at Station 1 on DD-593. DD-593 at 249.8 deg T, [redacted], Tape 033. Cumulative dose from GTR trace: 1 min 0 r; 3 min 62.9 r; 5 min 287 r; 8 min 569 r; 12.5 min 722 r; 25 min 748 r. Film pack dose: 330 r, Shot Wahoo. Warning: Increase values read from this gamma trace by 10 percent.

The shipboard washdown systems were operating throughout the time of passage of the airborne debris.

The influence of the superstructure on external radiation fields is shown by inspection of Figure 2.34. As can be seen, the total dose measured by the film packs varies directly with the solid angle of radioactive cloud subtended at the film pack position. There appears to be a char-

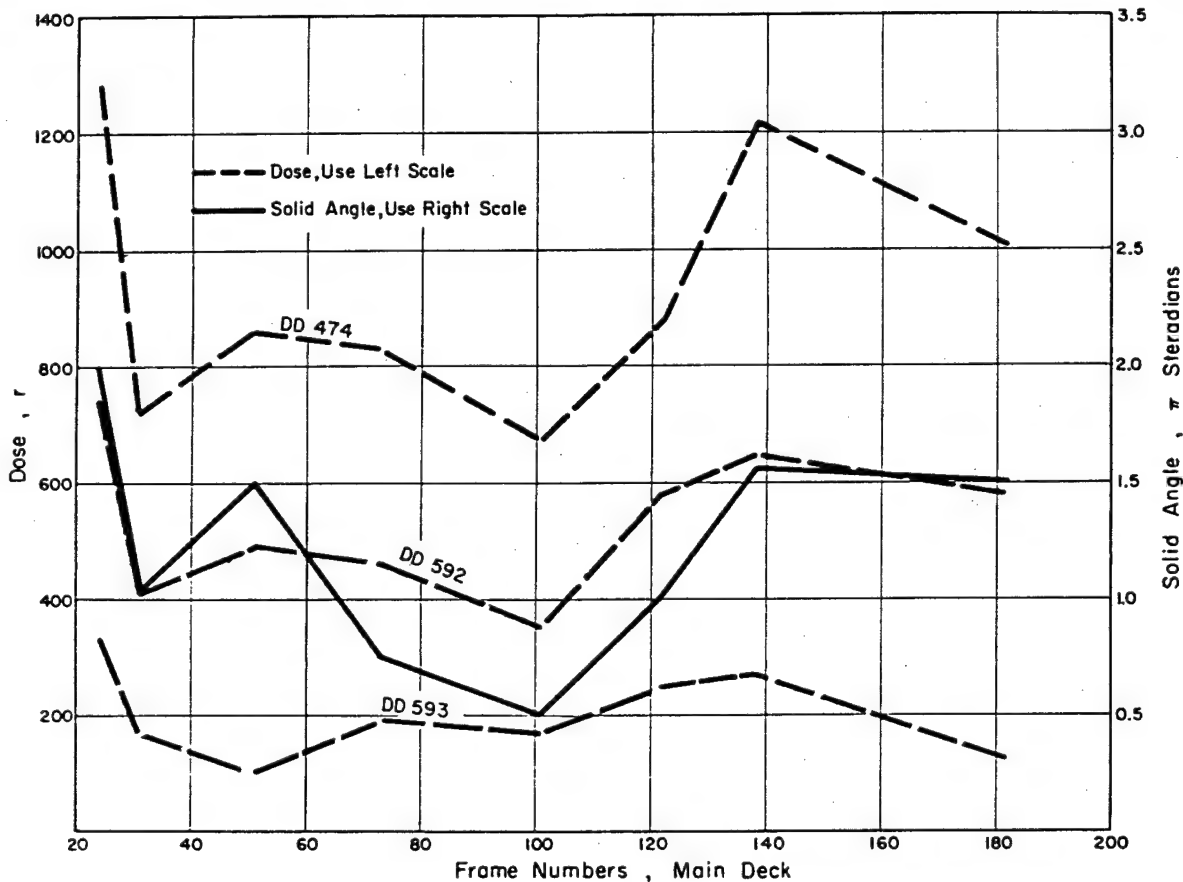


Figure 2.34 Plots of film-pack doses and estimated solid angle of radioactive cloud subtended at film packs at various locations on main decks of DD-474, DD-592, DD-593, Shot Wahoo.

acteristic curve shape for the three ships, regardless of their attitude or distance from surface zero.

In order to appreciate the intensity of the dose rate, it should be noted that the average total accumulated gamma dose on the weather-deck of a ship located 9,000 feet from surface zero reached 300 r in less than 12 minutes as demonstrated in Figure 2.35. Since the deposit radiation sources contributed a negligible amount to this total accumulated dose, it is safe to assume that transit doses present the only significant danger from gamma radiation on the deck of a ship when the washdown system is operating.

Below decks, the gamma radiation was attenuated to varying degrees, depending on the specific location. The best protection was afforded at locations below the water line. Table 2.10 shows that the total dose on the bridge complex was about two-thirds the main deck dose, while the total dose in the portion of the aft engine room below the waterline was about one-tenth the

TABLE 2.10 AVERAGE 24-HOUR GAMMA DOSES ABOARD  
TARGET DD's BASED UPON FILM BADGE DATA, SHOT WAHOO

Compartment or Area	DD-474	DD-592	DD-593
Above Waterline, 33 Feet	610	420	180
Bridge Complex			
Above Waterline, 11 to 16 Feet	650	420	160
Fwd Quarters	580	400	150
Radio Central	730	460	200
Galley	1,000	630	340
Main Deck	730	500	170
Crew's Washroom			
Above Waterline, 2 to 4 Feet	400	210	72
Crew's Mess	290	170	67
Fwd Fire Room	230	110	45
Fwd Engine Room	—	180	—
Aft Fire Room	—	170	—
Aft Engine Room	590	370	140
Aft Quarters	490	300	98
Steering Gear Room			
Below Waterline, 3 to 6 Feet	310	210	65
Magazine	110	37	19
Fwd Fire Room	76	29	10
Fwd Engine Room	—	54	—
Aft Fire Room	—	66	—
Aft Engine Room			

TABLE 2.11 RATIOS OF GAMMA DOSE IN COMPARTMENTS TO DOSE  
ON WEATHER DECK, BASED ON AVERAGE FILM BADGE  
DATA, SHOT WAHOO

Compartment or Area	DD-474	DD-592	DD-593
Above Waterline, 33 Feet	0.61	0.67	0.53
Bridge Complex			
Above Waterline, 11 to 16 Feet	0.65	0.67	0.47
Fwd Quarters	0.58	0.63	0.44
Radio Central	0.73	0.72	0.59
Galley	0.73	0.78	0.51
Crew's Washroom			
Above Waterline, 2 to 4 Feet	0.40	0.33	0.21
Crew's Mess	0.29	0.26	0.20
Fwd Fire Room	0.23	0.17	0.13
Fwd Engine Room	—	0.29	—
Aft Fire Room	—	0.27	—
Aft Engine Room	0.59	0.58	0.41
Aft Quarters	0.49	0.47	0.29
Steering Gear Room			
Below Waterline, 3 to 6 Feet	0.31	0.33	0.19
Magazine	0.11	0.06	0.06
Fwd Fire Room	0.08	0.05	0.03
Fwd Engine Room	—	0.09	—
Aft Fire Room	—	0.11	—
Aft Engine Room			

main deck dose. It can be noted from the doses presented for the DD-474 and DD-592 that any location on or above the main deck for a ship located within a mile downwind of surface zero would subject an individual to an accumulated gamma dose of more than 400 r. Since it has been previously shown that essentially all of the 24-hour dose was sustained in a time period of less than 20 minutes after shot, it can be assumed that the indicated doses were primarily accrued during this interval. A complete listing of the ratios of gamma dose in various compartments to the dose on the main deck is shown in Table 2.11.

**Shipboard Transit and Contaminated Water Radiation Fields.** By comparing Figures 2.35 and 2.36, it is seen that transit radiation is the only significant source of radiation at shipboard positions. The total gamma dose, including transit sources and deposit sources, is hardly distinguishable from the total gamma dose due to transit sources alone. It could be surmised that the washdown systems were extremely effective in reducing the gamma dose due to deposit sources to a negligible value and that, as a result, only transit dose was recorded at washed stations. However, film-pack dose data from stations above the washdown area show approximately the same results as those stations in the washdown area, thereby indicating that even at the unwashed locations, a high percentage of the total dose was due to remote-source radiation. Also, it is seen from Figure 2.35 that practically all the total accumulated dose was received within 14 minutes after zero time on a ship located 8,900 feet downwind from surface zero and that contribution by deposited contamination after this time was essentially negligible.

Because of the failure of timing signals, no data concerning contaminated water radiation fields was obtained on this shot.

**Shipboard Fallout Gamma Decay.** An attempt was made to record the gamma-ionization decay of a shipboard-collected fallout sample; however, no data was obtained because of the general shipboard timing signal failure, which resulted in the specially-shielded decay GTR not being activated.

**Inhalation Hazards Due to Ingress of Contaminants.** The results of doses received by animals on DD-592 show that acute internal doses received during the first 50 hours after shot, as a consequence of exposure at unprotected weatherside locations, were 168 rads (1 rad = unit of absorbed dose of 100 ergs/gm) for mice and 336 rads for guinea pigs. This ship was located [redacted] downwind from surface zero.

The highest 0-to-50-hour internal dose received in an interior compartment was 47 rads. This dose was sustained by guinea pigs in the galley. All other animals except the guinea pigs in the crew's quarters sustained internal doses between 1.5 and 15 rads during the first seven days after the shot. The guinea pigs in the crew's quarters sustained about 0.5 rad during the same period.

Although the ventilation system was to have been operated at 20 percent of rated air flow, the ship-power failure which occurred during Shot Wahoo resulted in the shutdown of all blowers. The exposures noted above were, therefore, sustained under unknown air-flow conditions. Induced air flow was probably quite high at the time of passage of the rapidly-moving base surge, but with the blowers not operating, there would have been little subsequent air flow to scavenge the compartments. These conditions may have contributed to the rather high internal doses found during Shot Wahoo.

**External Gamma Radiation Due to Ingress of Contaminants.** Within test compartments, no dose rate data were obtained on the external gamma activity due to ingress of contaminants for this shot, because of the failure of ship's power to receive the timing signals which were to have activated the GTR instruments. Although compartment surface samplers were recovered as soon as the radiological situation permitted, their activity at time of recovery was too low to count because of high local background. Therefore, only radiological survey data were obtained within the compartments on Shot Wahoo.

**Particle Size Distribution of Contaminants.** Since the total and incremental air samplers depended upon timing signals for activation, again, because of power failure, no air samples were collected.

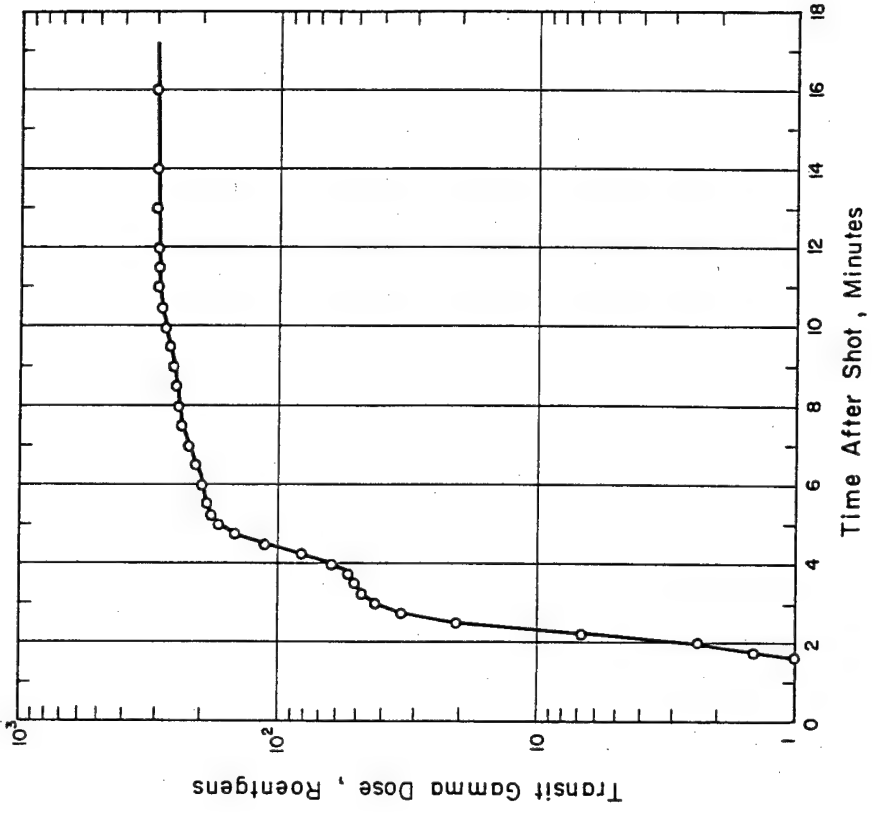


Figure 2.36 Transit gamma doses on deck of DD-593 after Shot Wahoo. Transit doses result only from radiation sources remote from the ship.

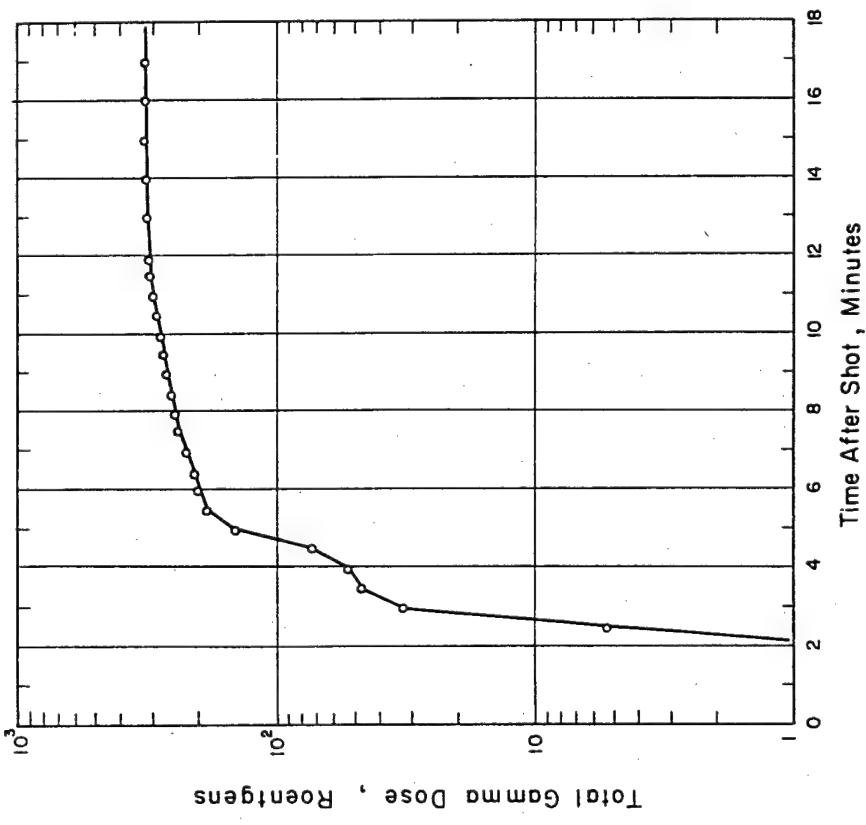


Figure 2.35 Total gamma doses on deck of DD-593 after Shot Wahoo. Values are averages of data from GTR stations 2, 3, and 4 which include effects from both transit and deposit radiation sources.

**2.3.6 Conclusions.** It was evident from the data obtained during Shot Wahoo that the primary source of radiation from a deep underwater burst of this type and depth was a transit source, the radiation from the base surge as it passed a particular location. This was not an immediate effect, but was dependent on the distance of the point of observation from surface zero. The base surge had a velocity of approximately 100 ft/sec to about 7,000 feet from surface zero. At more distant stations, the time of arrival appeared to be dependent on the direction and velocity of surface winds.

Free-field gamma activity virtually ceased at all locations by H + 15 minutes, thereby permitting normal operations as soon as the base surge had passed. During this initial period, doses in excess of 100 r were expected at locations less than three miles downwind from surface zero, while doses in excess of 400 r were expected at downwind locations of less than one mile. In order to receive no more than 25 r total dose, the standoff distance should have been on the order of four miles, while the safest approach direction would naturally have been from upwind of surface zero.

Aboard ships, the free-field gamma activity was modified by the superstructure. Even on weather decks, some degree of protection was afforded by the superstructure during passage of the base surge. Better protection was naturally afforded at interior locations, with dose reduction factors up to five or six in locations above the waterline and reduction factors between 9 and 30 in locations below the waterline.

Internal radiation doses of animals for the first 50 hours after shot ranged from 336 rads, received by guinea pigs exposed on the unprotected director platform, to 0.5 rad received by the guinea pigs in the crew's compartment. The highest 0-to-50-hour dose sustained in an interior compartment was the 47-rad dose received by guinea pigs exposed in the galley. These doses were received for an open-air system without fans operating, although the fireroom maintained a full combustion power air flow. It is to be noted that animals at all stations except the crew's compartment received doses in excess of 0.9 rad during the first seven days following exposure. By comparison of the external doses produced on the ship by the transit cloud with the internal doses sustained, it is evident that the primary consideration in the weapon delivery situation is reduction of the external dose received during the first several minutes. If this reduction is accomplished by distance, the ingress of contaminants should become completely insignificant. If, on the other hand, dose reduction is accomplished by additional ship shielding and the ship operates at a distance comparable to that at which the DD-592 was exposed, the ingress of contaminants may require some consideration.

## 2.4 SHIP RESPONSE AND DAMAGE STUDIES

**2.4.1 Introduction.** With the incorporation into the fleet of nuclear antisubmarine weapons deliverable by surface ships and submarines, it was necessary that a re-evaluation of the ship response and damage predictability for underwater nuclear explosions be made. It was found that the means were insufficient to give the needed answers to questions regarding a safe range for such delivery of underwater nuclear weapons by surface ships and submarines.

In developing atomic age tactical-delivery doctrine, it was necessary to answer the question of what is the safe standoff distance for a destroyer, for instance, delivering an atomic depth bomb. It is important to note at the outset that there was no single answer to this question, because a large number of variables were involved, each of which could have a pronounced effect on the answer. These principal variables were the yield of weapon, depth of burst, depth of water, reflection characteristics of sea bottom, abrupt temperature gradients with depth of the water which produce refraction of the shock waves, the structural type of the ship, the draft of ship, the type of machinery installed, and the orientation of the ship with respect to the underwater detonation.

To properly represent the effects of these parameters on the safe-standoff-delivery range, it was necessary that a family of curves be prepared for each general type of ship. Likewise, other various degrees of damage, i. e., light, moderate, and severe, would require appropriate additions to the above family of curves. Although abbreviated, approximate or gross curves of the above type had been prepared prior to Operation Hardtack. The meager data upon which they were based, however, did not satisfactorily answer the questions posed. In brief, safe ranges estimated prior to the Hardtack shots, of necessity, contained sizable safety allowances because of the lack of data. The limited data available came from two previous full-scale nuclear underwater tests, some model and theoretical work, and prior conventional high-explosive-underwater tests.

The two previous full-scale nuclear underwater tests, Operation Crossroads Baker and Operation Wigwam, had given indicative, but not definitive, answers. The geometry is discussed in Section 2.1.

To supplement the meager full-scale data from those two shots, theoretical and model-ship studies were conducted, and previous underwater conventional high-explosive test data were re-examined. From the results of these studies, as well as the high-explosive test data, predictions on the response of various ship types to the pressure field generated by an underwater nuclear detonation were developed. These predictions, however, included many generalizations which, until proven valid, cast considerable doubt upon the results. Thus, a full-scale check was needed.

Also, it was clear that damage to shipboard operating equipment required a test of operating vessels; because previous tests had included only ships' machinery and equipment in a non-operating, or cold-iron condition, the shock response of which could be considerably different under operational conditions. In addition, the final step of correlating response to damage required considerable amounts of test data to permit adequate statistical correlation. This information in turn would be useful in the shock-hardening design of future ships, including future ship machinery. To help satisfy this requirement for a large amount of test data within economical limits, the tapered-charge technique had been conceived. This technique proposed the use of relatively inexpensive high-explosive detonations of a type which would simulate the early phases of a nuclear generated shock wave against full-scale ships. However, this proposed technique also required a full-scale underwater nuclear test for confirmation.

The need was therefore established for a full-scale underwater nuclear test, in relatively deep water, exposing target ships with ships' machinery and equipment in operation. The deep underwater event, Shot Wahoo configuration, was thus selected. The ship target array chosen for Shot Wahoo consisted of three destroyers (DD-474, DD-592 and DD-593), a merchant ship (EC-2 type), and a submarine (SSK-3).

Because of the previously listed number of contributing variables which had to be considered in the nuclear depth bomb safe-delivery-range problem, it was essential to document the response of each vessel as completely as feasible. The target ships, therefore, were relatively highly instrumented to document the loading and response of the hull structure and ships' machinery. This would permit subsequent correlation with the underwater free-field phenomena measurements, and with the ship hull and machinery damage recorded. Thus, from the expected full-scale underwater nuclear test results, together with related ship model and tapered charge work, it was believed that safe delivery ranges for other yields and burst geometries could also be developed.

The Program 3 effort on Shot Wahoo consisted of four general categories: (1) pre-Wahoo, preliminary Hardtack tests of tapered-charge technique; (2) hull response and damage studies of surface ships; (3) hull response studies of submarines; and (4) shipboard machinery and equipment shock damage studies. Each of these categories is successively described in Sections 2.4.2 through 2.4.5.

**2.4.2 Preliminary Hardtack Tests of Tapered-Charge Technique.** Prior to Operation Hardtack, a series of explosion tests employing high explosive tapered charges against one of the Hardtack target ships, the destroyer DD-592, was conducted in January 1958 off Santa Cruz Island, California. One of the primary purposes was to provide a full-scale test on the tapered-charge technique of simulating an underwater nuclear detonation, which could subsequently be checked by Shot Wahoo.

**Objectives.** All the objectives of the Hardtack Project 3.1 tests were closely related to the subsequent tests of effects of underwater nuclear bursts on ships, which were conducted later in the summer of 1958 at the EPG during Operation Hardtack. Thus, the main objectives of the tapered-charge tests were: (1) to provide a pretest experimental check on the target damage predictions for Shot Wahoo, in order that optimum placement of the ship targets could be achieved for the later Hardtack effort; (2) to calibrate instrumentation on the target ships and check out the adequacy of the recording-equipment installations and shock mountings which were designed by the participating agencies for the later Hardtack effort; and (3) to develop and check the high explosive tapered-charge technique as a method of simulating and determining the effects of underwater nuclear detonations on ships.

**Background.** Considerable interest had been generated in the proposed high explosive tapered-charge technique, because, if successful, it would enable the Navy to obtain much effects data on ships without recourse to future full-scale nuclear testing. The tapered-charge technique was thus conceived as a long-range method of determining shock effects of underwater atomic detonations on ships; more specifically, to provide an economical method of obtaining large quantities of data which could be the basis for a statistical study of shock response versus damage.

The technique utilizes specially formed (i. e., tapered) high explosive charges to simulate a reproduction of shock-wave forms of underwater nuclear detonations against ships. An example of the initial shock wave from such a tapered high explosive charge, which simulates the initial shock wave from a nuclear detonation, as compared to the same yield of conventional high explosive charge, is shown in Figure 2.37. Limitations of the technique are that the later underwater shock loading phases, such as the bottom reflections, surface cavitation reloadings, and bubble pulses, are not as equally well represented as the direct shock wave. However, even the representation of these later shock-loading phases can afford a qualitative insight into the physical processes involved. In any event, it was hoped the technique could become a valuable tool to supplement full-scale tests.

The degree of validity and/or the limitations of the tapered-charge technique, as tested by preliminary Hardtack Project 3.1, were not expected to be available for comparative analysis until after the subsequent full-scale underwater Shot Wahoo results.

**Procedure.** Pressure measurements taken during Operation Wigwam showed that the underwater shock wave resulting from an atomic explosion is equal to that obtained from a TNT charge weight, equal to two thirds of the rated yield of the nuclear device. Since the expected yield of Wahoo was 10 kt, these test-tapered charges were designed to simulate the underwater shock wave of a charge of 6.7 kt of TNT. For these tests, a series of four large, tapered charges weighing from 1,400 to 4,400 pounds were to be used to simulate underwater nuclear attack against the DD-592. The test charges were to be detonated to produce successively increasing shock severity, starting with a mild attack corresponding to a peak underwater shock velocity on the target of 2.5 ft/sec. The DD-592 was one of three destroyers to be used subsequently as target ships at the EPG during Shots Wahoo and Umbrella. All instrumentation aboard the DD-592 was operative and calibrated for the tapered-charge tests.

Utilizing such instrumentation, the following Hardtack projects actually participated on the Project 3.1 test series:

UERD Project 3.1, tapered charge studies.



DTMB Project 3.3, shock studies on shipboard machinery and equipment.  
 UERD Project 3.4, hull loading and response of surface ships.  
 BUSHIPS Project 3.8, ship damage assessment.  
 NOL Project 1.1, underwater free-field pressure measurements.

Figure 2.38 indicates the test site orientation, including the DD-592 anchored off Santa Cruz Island in approximately 260 feet of water, and the high explosive tapered charge suspended from pontoon floats. The distances from the charge to broadside of the DD-592 were to vary from ap-

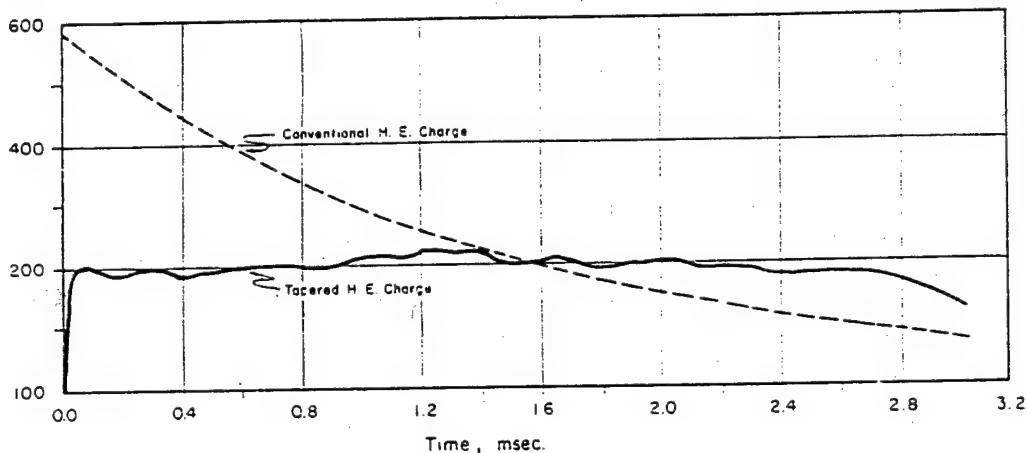


Figure 2.37 Comparison of shock waves of tapered charge and conventional charge of identical weight at the same distance. Charge weight 1,420 pounds HBX-1, distance 315 feet.

proximately 500 to 250 feet. Figure 2.39 shows the tapered charge rigging plan. Figure 2.40 is a photograph of a tapered charge before lowering into the water for the second test. Figure 2.41 is a photograph taken during the second test.

**Results.** These tapered-charge tests were actually carried to the threshold of shock damage to shipboard machinery and equipment. The tests were stopped after detonation of the third charge to avoid the probability of serious damage to the DD-592, prior to the full-scale nuclear test at EPG. Apparent significant shear yielding of the support bolts for the main propulsion turbines, failure of which would have dropped the turbine into the bilge and seriously jeopardized the later full-scale nuclear effort, was the principal damage item concerned. The peak ship-bottom velocities on the target resulting from each of the three tapered charges tested were 2.3, 3.5, and 5.2 ft/sec, respectively.

Table 2.12 shows an interesting comparison between the early target response at the tapered-charge test and full-scale nuclear data estimated from Shot Wahoo. The fair agreement of the peak ship-bottom velocities measured with the predicted values should be noted. The predictions were based on small-scale model tests and extrapolation to full scale was somewhat difficult. The confirmation of these values afforded by the tapered-charge tests gave increased confidence in the velocity predictions for Shot Wahoo. Also, the tests permitted an indication that the safe region of a destroyer from an atomic depth charge is defined by a peak velocity of approximately 6 to 8 ft/sec. Based on the increased confidence derived from these tapered-charge tests, it is significant that the Wahoo array range distances for the two close-in destroyers originally planned for [redacted] feet and [redacted] feet were subsequently revised to [redacted] feet and [redacted] feet from surface zero, respectively.

**Conclusions.** The conclusions of this test series on which the various participating projects appeared to agree were: (1) the attempt to simulate pressure histories of the direct shock

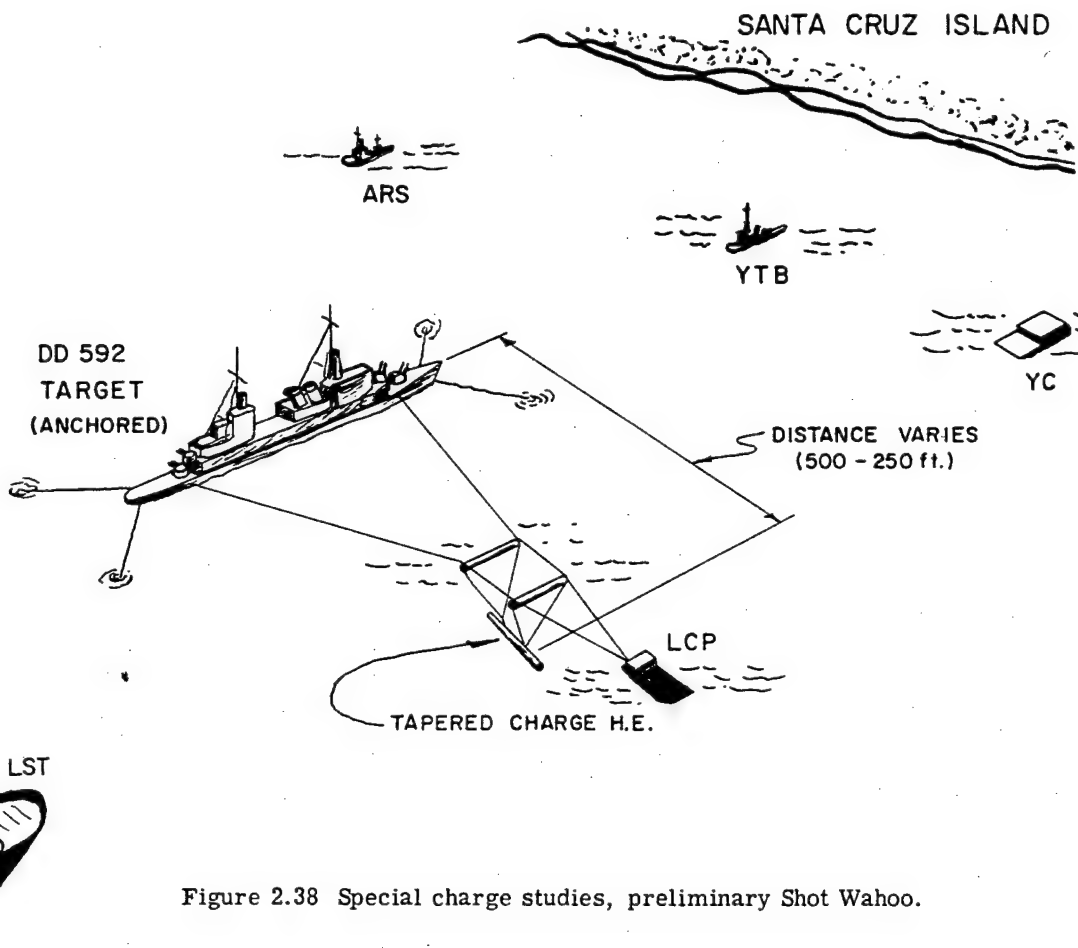


Figure 2.38 Special charge studies, preliminary Shot Wahoo.

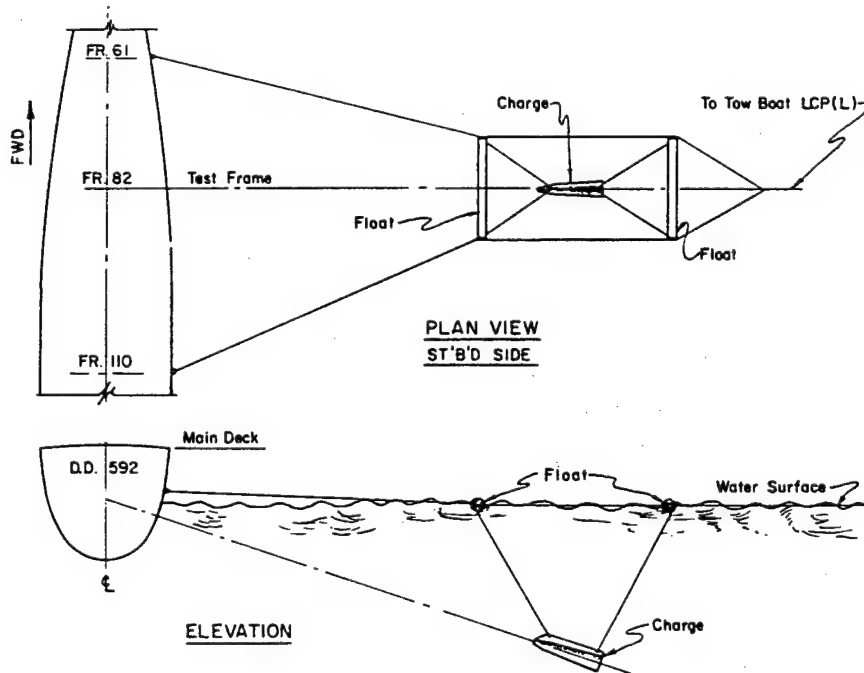


Figure 2.39 Tapered charge rigging plan.

waves of underwater atomic detonations by means of tapered charges was successful; (2) during the first two tapered-charge tests the bottom-reflected wave caused a stronger response of the target than the direct shock wave; (3) at the third test the bottom-reflected wave was considerably attenuated by the surface cavitation; (4) the target bottom velocity measured at the three tapered-charge tests was approximately twice the surface particle velocity resulting from the shock wave reflection; (5) the body velocity of the target was slightly less than the surface par-

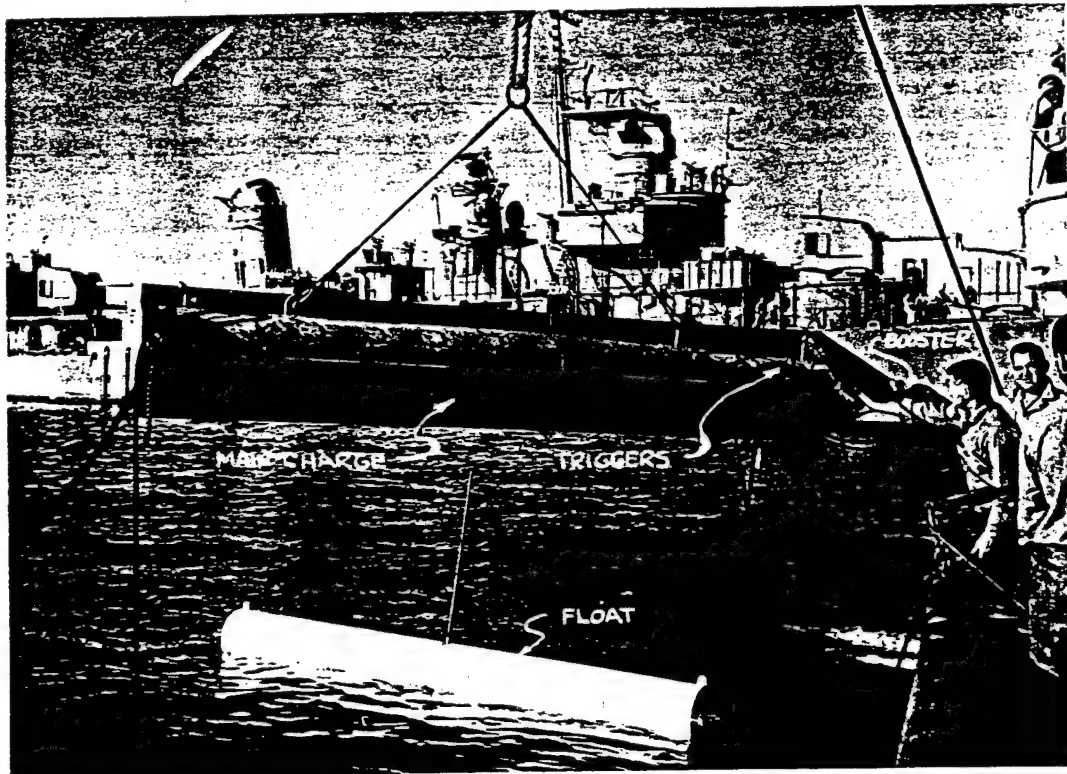


Figure 2.40 Armed tapered charge I before lowering for second test.

ticle velocity; (6) in general, the instrumentation installed to measure ship response for the later Hardtack tests performed satisfactorily; (7) the automatic equipment for unmanned operation of the propulsion plant of the DD-592 satisfactorily withstood the shock severities of the Project 3.1 test series; (8) improvement in the design of ship equipment by proper consideration of mass distribution and shock mounting would increase the capability of ships to withstand shock; (9) a decision as to whether the tapered-charge tests conducted simulated the target response to an atomic underwater explosion satisfactorily would have to await the results and evaluation of Shot Wahoo, and would be included in the final WT report; and (10) any future high-explosive tapered-charge tests for the purpose of simulating nuclear attack against the DD-592 or a similar target should provide for inputs well into the severe damaging range.

2.4.3 Hull Response and Damage Studies on Surface Ships. Objectives. The objectives of these studies on Shot Wahoo were to: (1) determine from the hull deflection standpoint, the safe-delivery range for surface-ship delivery of an underwater nuclear weapon in deep water; (2) determine from the hull deflection standpoint, the lethal range for merchant ships attacked by an underwater nuclear weapon in deep water; (3) obtain basic information on hull response as

related to free-field pressures and loading measurements in deep water, to provide check points for model experiments and high-explosive shaped-charge tests.

**Background.** In order to make underwater nuclear-weapon-effects predictions for surface ships under general conditions, it is necessary to understand the entire range of transition from the production of free-field pressures in the water, to the final hull and equipment damage within the ship. This range can be broken into the following phases: (1) the generation of free-

TABLE 2.12 COMPARISON OF EARLY TARGET RESPONSE AT TAPERED CHARGE TEST WITH ATOMIC EXPLOSION DATA

Test Number	Slant Standoff of 6.7 kt TNT for Best Match of Tapered Charge Shock Wave (attack angle 15 deg)	Peak Bottom Velocity *		Bodily Velocity †	
	ft	Estimated for Atomic Explosion ‡	Measured at Tapered Charge Test	Estimated for Atomic Explosion §	Measured at Tapered Charge Test
		ft/sec	ft/sec	ft/sec	ft/sec
1	22,800	2.5	2.3	1.0	0.7
2	16,150	3.5	3.4	1.4	1.2
3	10,260	5.6	5.2	2.4	2.3

\* Peak bottom velocity in this instance is defined as the highest velocity of the ship's bottom resulting from the direct shock wave impact.

† Bodily velocity in this instance is defined as the highest velocity averaged over the transverse section of target at test frame.

‡ Peak bottom velocity, estimated - is based on UERD ship model tests.

§ Bodily velocity, estimated - is assumed to be equal to the water surface particle velocity.

field pressures, (2) the relation between the free-field pressures and both the loading at the hull and the initial hull response (the interaction problem), (3) the transmission of the initial hull motions to the remainder of the ship (the shock pattern throughout the ship), (4) the relation between the initial hull velocities (hull response) and type and amount of damage produced in the ship's hull (hull damage), and (5) the relation between the magnitude of shock level, which is observed in the shock pattern throughout the ship, and the resulting equipment damage (shock damage).

Items 1, 2, and 3 were basic investigations relating the ship response to the loading and free-field pressures, while Items 4 and 5 concerned the structural and mechanical damage to the ship and equipment. The latter phases were also aimed at establishing scales, or rules, relating the initial hull response to degrees of damage to the ship and equipment aboard.

In considering ship hull response as related to underwater free-field shock pressures and loading measurements, it must be recognized that a modern ship is a complex elastic structure, whose hull plating, frames, bulkheads and decks generally constitute a complex, statically indeterminate structure, because of the ship's continuous-type welded and riveted-steel construction.

As discussed earlier in this chapter, the two previous full-scale underwater tests, Crossroads Baker and Wigwam, offered little data by which a generalized answer to the safe-delivery range tactical problem for surface ships in deep water could be made. Furthermore, little theoretical knowledge was available that would enable reliable predictions of the effect of underwater nuclear bursts on surface ships to be made. The phenomena were not well enough understood to allow the limited test results to be extrapolated with confidence to all general tactical situations. Even though the direct shock wave near the water surface could be reasonably predicted for very deep water geometries, many practical operational situations were likely where the water depth ranged between 500 to 5,000 feet (i. e., neither shallow nor very deep). With such water depths, it appeared probable that the ocean-bottom-reflected shock would cause a more severe ship shock response than that from the direct shock wave. Also, the pressure loading resulting from the formation and closure of a cavitating surface layer of water, while not well understood, would be of some secondary response importance. The screening effect of the cavitating layer on the bottom-reflected shock, under certain circumstances, was also believed to have considerable significance.

However, even if the underwater free-field phenomena or pressures in the water about the ship were known, there was no reliable theoretical means of predicting the loading pressures at the hull, the initial velocity motions in the hull, the shock pattern throughout the ship, or the hull damage and equipment damage produced by the shock. The lack of firm workable theoretical concepts concerning the generation of damage in surface ships by nuclear underwater bursts emphasized the importance of Objective 3 of this study, i. e., obtaining basic information on hull response as related to free-field pressures and loading measurements.

Other than full-scale nuclear tests, one source of information was provided by tests on small-scale models. An extensive series of instrumented model tests was conducted by UERD during 1955 and 1957 using a 1/35 scale model of a C-2 merchant ship and a 1/22 scale model of a cruiser. Both were tested under a great variety of attack charge weight and geometries, and these model data were expected to be valuable in extrapolating the results of the Hardtack full-scale tests to other tactical situations and other types of surface ships.

Other sources of information, high-explosive tests and the use of the proposed tapered-charge technique, have already been discussed in Section 2.4.2. These later tests held promise as another tool to supplement full-scale nuclear test data relating to equipment damage, as well as hull response.

It was clear, however, from a review of previous data from full-scale tests, model tests, theory, high-explosive and tapered-charge tests, that a full-scale nuclear test in relatively deep water was required to gather data on hull response and damage of surface ships.

Procedure. For the hull response and damage studies, the hulls of the target ships EC-2, DD-593, DD-592 and DD-474, were relatively highly instrumented. The locations of these target ships for Shot Wahoo were respectively, broadside at [redacted] stern-on at [redacted] broadside at [redacted] and stern-on at [redacted] feet from surface zero as shown in Figure 2.8. Instrumentation of the hulls, of course, included the ships' hull plating, hull frames, bulkheads, decks and superstructures. It was the intent to measure the response of the target ship throughout its complete time history, to measure the phases of response at all representative locations on the ships, and to record this with high-fidelity electronic recording equipment.

Thus, it was planned to measure pressure loading time histories at the hulls of the ships, velocity time histories at the hulls of the ships, bodily velocity time histories (both horizontal and vertical) of the ships as a whole, bodily displacements of the ships, hull deflection histories (of the EC-2), strain histories of the hull plating (of the EC-2), and of the flexing of the ship as a whole (of the DD's), and the rolling and pitching histories of the ships. Approximately 35 dynamic-measurement gages were installed on each of the three destroyers, and 50 gages were installed on the EC-2. The general location of these gages is indicated by Figure 2.42. As a minor effort, six dynamic-measurement gages were installed on one of the YC barges used for mooring the EC-2. Three high-speed motion picture cameras were installed to record hull and bulkhead deflections within the EC-2, to illustrate the motion, and to aid in analysis of other records.

The gages used were basically of the same types that were successfully employed in previous underwater tests. The underwater loading pressure gages used on the outside of the hulls were of the piezoelectric, tourmaline-crystal type. The velocity measurements, the principal instrumentation, were made by velocity meters consisting of a bar magnet, seismically mounted within a coil of wire. Relative movement of the coil, which is attached to the hull point being investigated, with respect to the seismically suspended magnet induces a voltage in the coil proportional to the relative velocity of the motion. This is a relatively simple, but rugged instrument, from which displacements or accelerations can also be obtained by appropriate computation. The deflection gages were of a type consisting of electrical resistance wire wound on a rod, with a sliding contact, so that movement of the rod with respect to the contact caused a change in resistance directly proportional to the deflection. Displacement gages were essentially of the same type, but with the sliding contact attached to a seismically suspended mass. Figure 2.43 shows the installation of three velocity meters and one displacement gage in a ship compartment area. Strain gages were the standard commercial (SR-4) resistance wire type, bonded directly to metal surface under test. Roll and pitch gages were rigidly mounted electrical potentiometer types, with pendulum.



Figure 2.41 Second test.

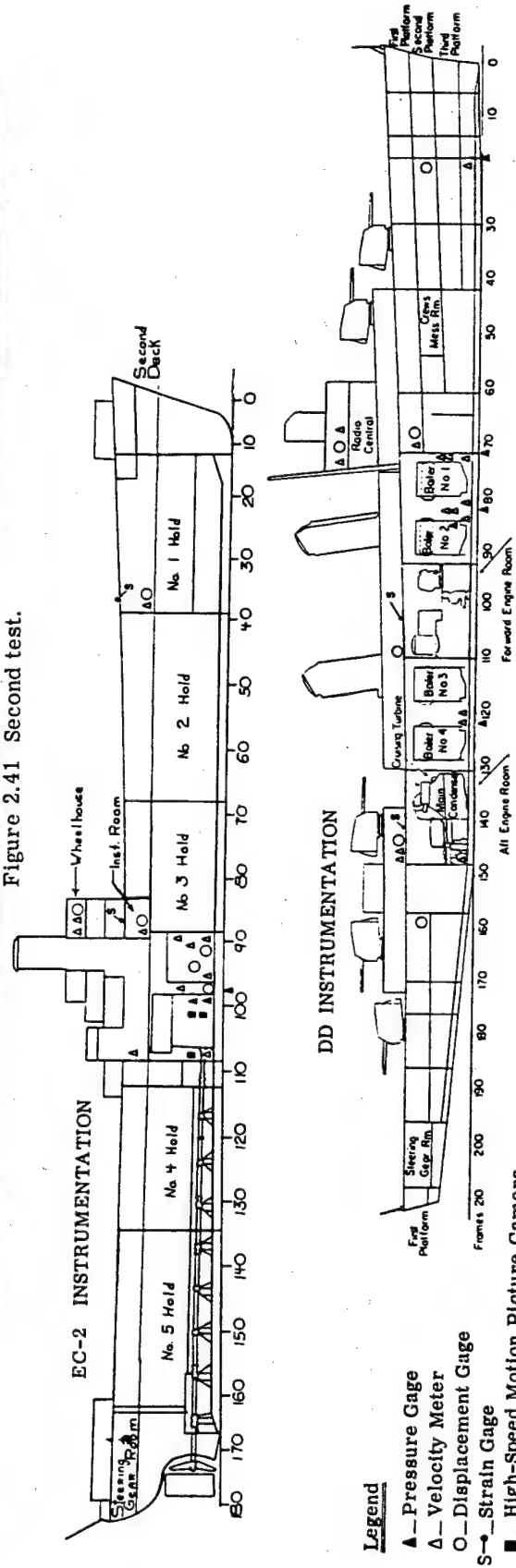


Figure 2.42 Loading and basic target response for surface ships.

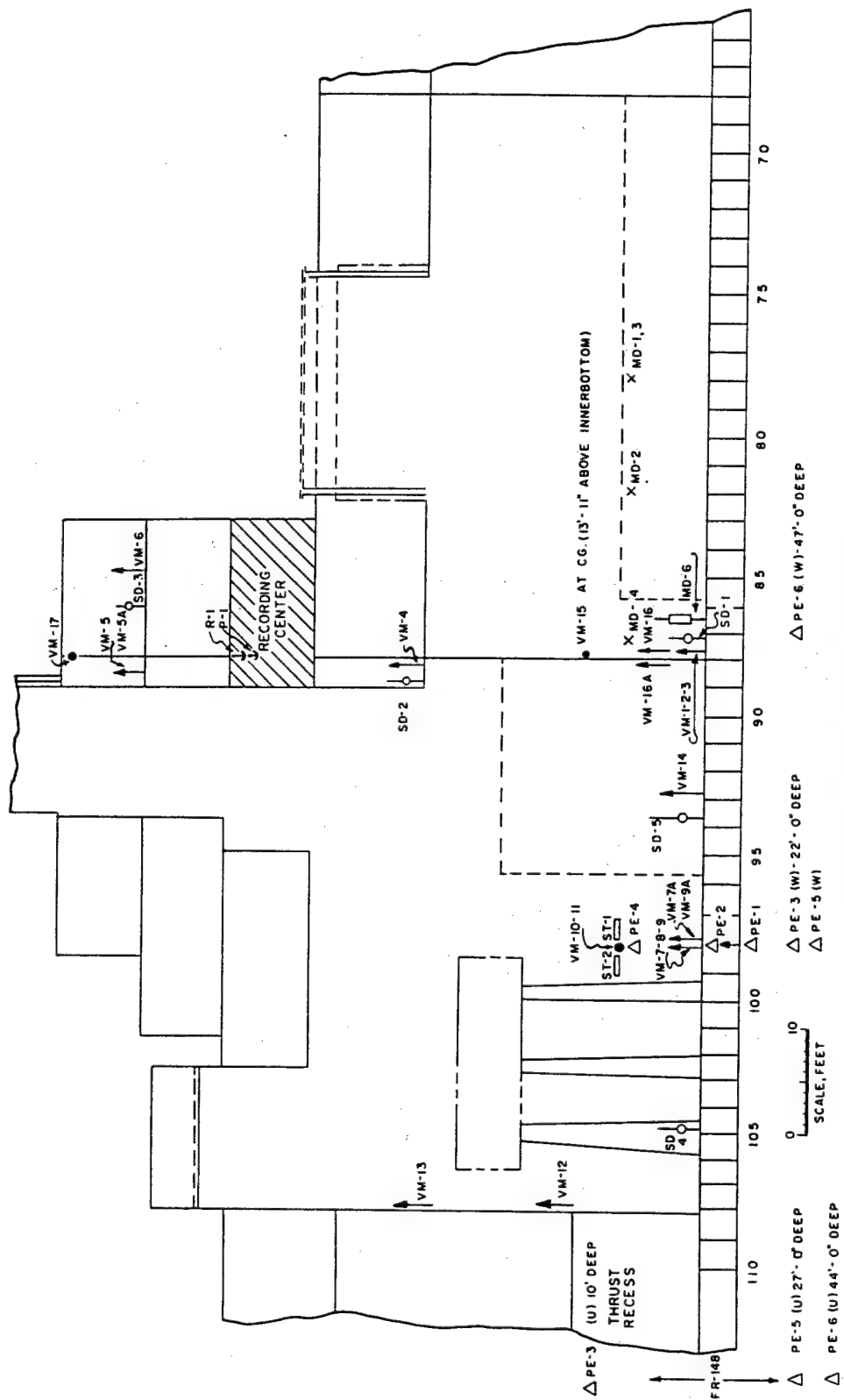


Figure 2.43 EC-2 gage locations.



All dynamic-gage measurements were recorded on magnetic tape recorders, and to a minor extent, on photographically sensitive visicorders, located in a recording center compartment near the middle of the ship. To protect the electronic recording units from severe shock damage, they were mounted on a steel frame suspended from the ship structure by a system of aeroid and steel springs. Figure 2.44 is a view of the recording center on the EC-2. Air conditioning and humidity-control equipment were installed in the recording center space on each ship to adequately protect the electronic equipment. Electric power for the instrumentation was supplied from 60-kw diesel generators especially installed on each of the four ships. The recording units were activated by wire timing signals from an EG&G radio-activated timing signal center on each of the ships.

**Results.** For Shot Wahoo, the electronic measurements of hull response on the EC-2 and the DD-593 were entirely successful. Measurements on both ships were uniformly of good quality. Because the recording-unit platform went beyond the motion anticipated and hit the overhead deck, some minor distortion of records was noticeable on the EC-2 as a result of severe mechanical shock motions on the recording equipment. However, no vital information on the EC-2 was lost.

Due to failure of the timing signal systems because of malfunctions of auxiliary ships' power, the electronic measurements of hull response were not obtained on the DD-592 or DD-474. As a result, data on hull response on these ships will have to come from the self-recording shock-spectrum recording gages which were also installed in the ships as back-up instrumentation. The high-speed motion picture cameras in the EC-2 hull functioned satisfactorily.

A few of the records from the EC-2 and DD-593 are shown on a compressed time scale in order to reveal an overall view of the response to underwater phenomena (Figure 2.45). The main phases of the response are marked on the figures, i. e., direct shock wave, cavitation re-loading subsequent to direct shock wave, and bottom-reflected wave.

The hull loading and response of the EC-2 are shown in Figure 2.46. The maximum recorded ship's bottom vertical velocity was about 14 ft/sec as shown. The velocities measured over the cross section of the EC-2 hull are shown in Figure 2.47. The maximum recorded side frame horizontal velocity was about 37 ft/sec, which corresponds to the maximum side frame displacement discussed below.

The longitudinal distribution of the response along the length of the DD-593 is illustrated in Figure 2.48. It can be seen that the maximum response from the reflected shock is two to three times as great as that from the direct shock for this particular shot geometry. Of some interest is the sea-bottom-induced precursor pressure wave, which produces a response prior to that due to the directly reflected pressure wave.

The response upward through the DD-593, as indicated by a few velocity records at positions on the forward fire-room bulkhead, is shown in Figure 2.49. The maximum response of about 2 ft/sec at each level from the reflected wave is shown. However, the longer rise times indicated at the higher decks would reduce the acceleration and damage effects at the higher decks.

The damage survey of the EC-2 hull indicated that a maximum transient displacement near the ship's center, of approximately four inches in the hull side frames, produced a maximum permanent hull side-frame displacement of about  $1\frac{1}{2}$  inches. In the same side area, maximum permanent hull-plating deformations between frames were about  $\frac{3}{4}$  inch. As a result of the side-frame deformation, many of the brackets connecting the side frames with the double bottom were buckled. Considerable damage resulted in the propeller-shaft-alley tunnel, which bowed inward about six inches, at the same time producing completely disabling shock damage to the propeller-shaft bearings. Examination of the ship's bottom revealed maximum hull plating dishes of about one inch. An open split seam about eight feet in length occurred at EC-2, Frame 120. Minor hull flooding caused by leaks in the engine room, holds, and shaft-alley tunnel was controllable by periodic pumping.





Figure 2.44 Recording equipment on EC-2 instrument platform.

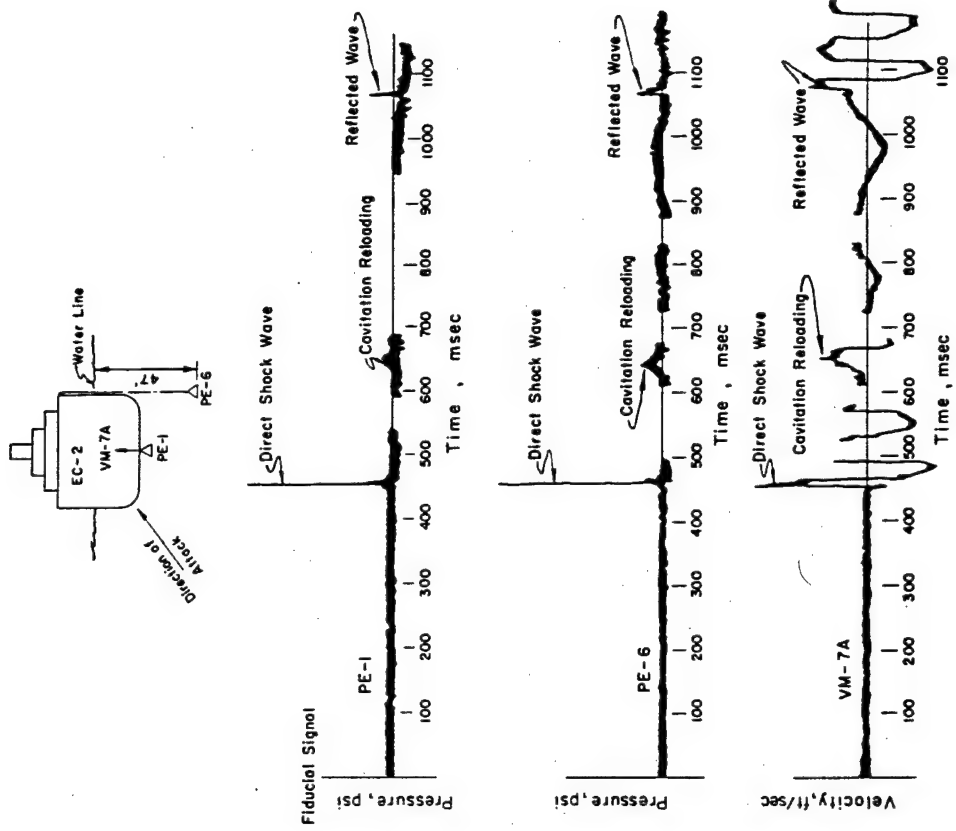


Figure 2.45 Overall phenomena in Shot Wahoo (EC-2).  
Note: Relative amplitudes are incorrect.

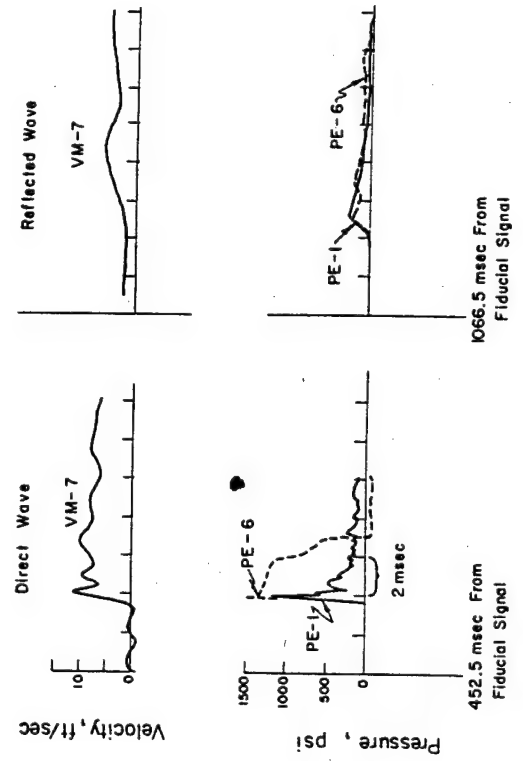
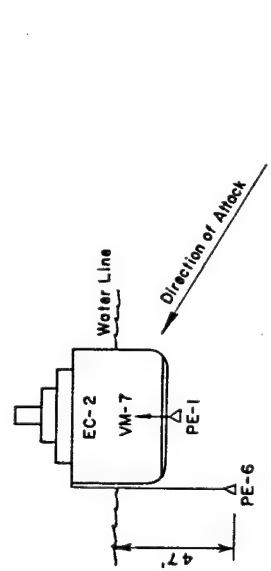
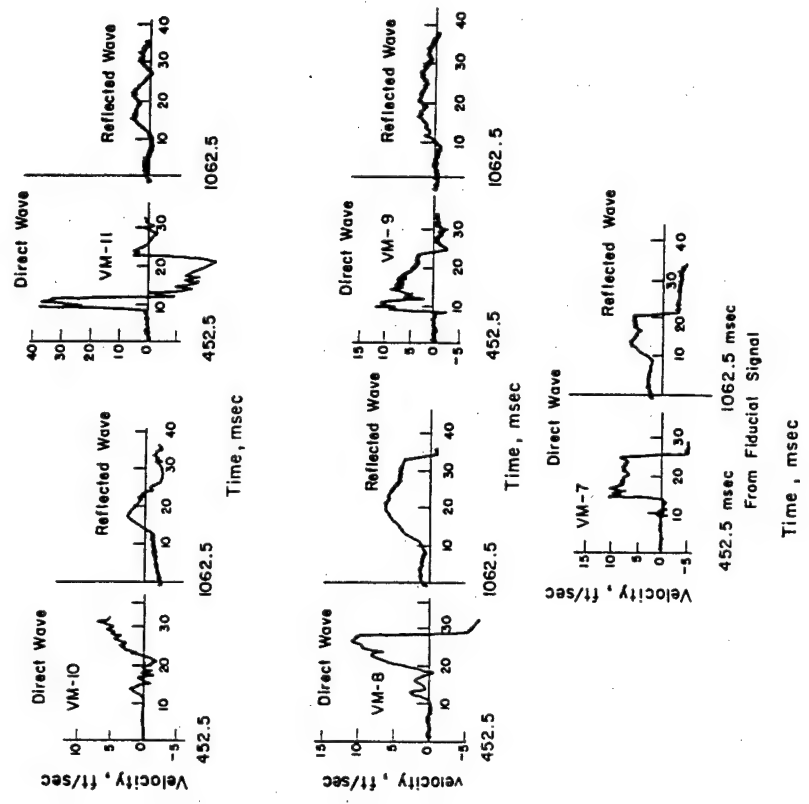
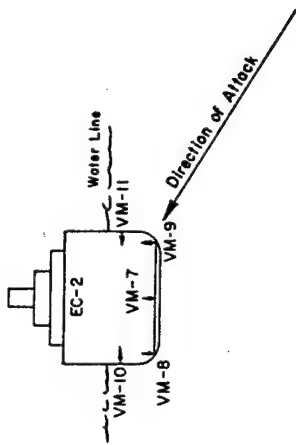


Figure 2.46 Hull loading and hull response, EC-2 (Shot Wahoo).

Figure 2.47 Cross-section distribution of EC-2 hull response, Shot Wahoo.

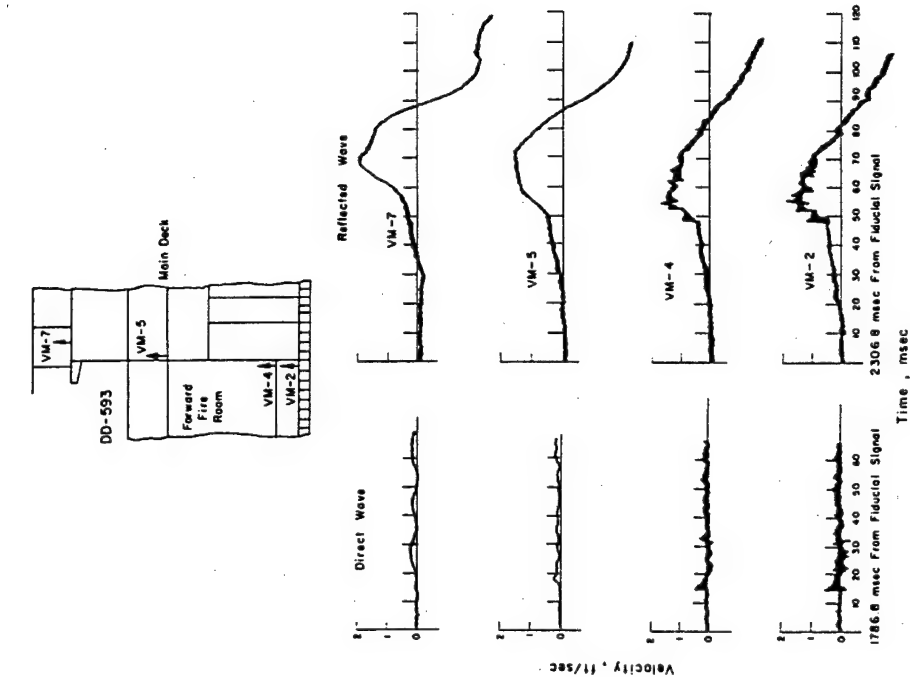


Figure 2.48 Longitudinal distribution of response in DD-593, Shot Wahoo.

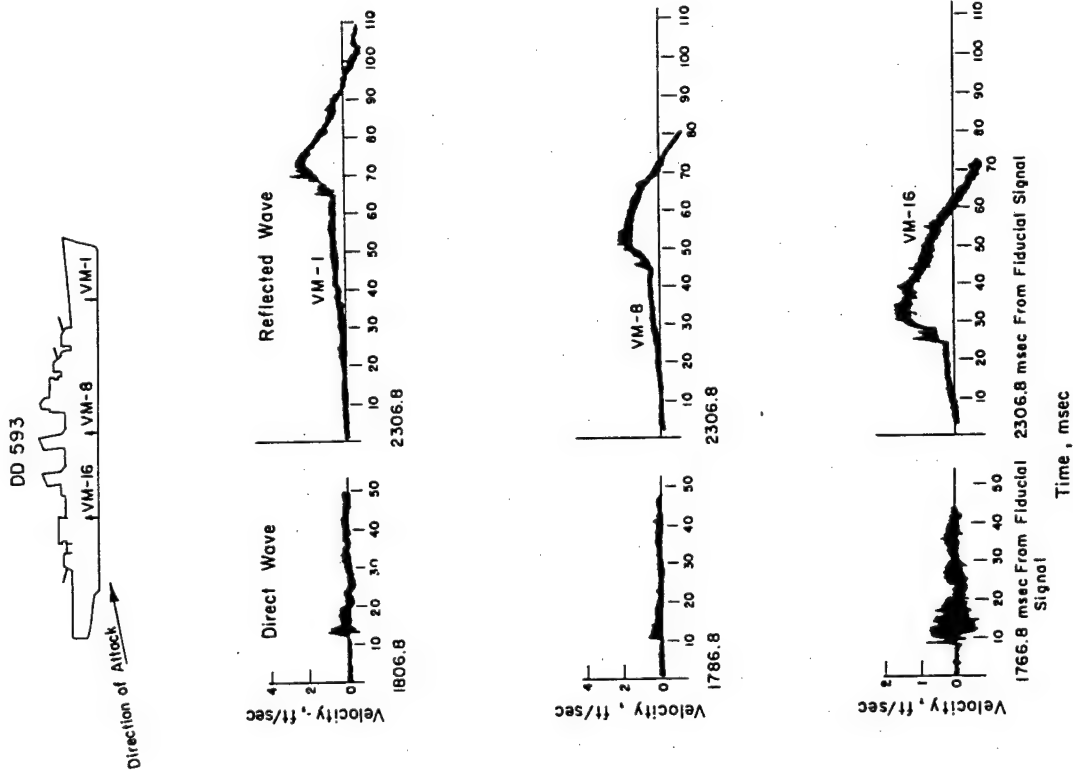


Figure 2.49 Response distribution upward through DD-593, Shot Wahoo.

A careful examination of the hulls of the DD-474, DD-592 and DD-593 revealed no hull damage, dishing, or other permanent hull deformation that could definitely be ascribed to Shot Wahoo.

Conclusions. The hull responses and damages of the surface ships EC-2, DD-593, DD-592 and DD-474 were somewhat less than predicted for Shot Wahoo. Apparently, this was due to a reduction in the free-field underwater pressures encountered from those predicted, due to stronger than expected refraction or bending of the shock waves, in turn caused by the abrupt temperature gradient with depth in the water at the Wahoo site. However, further detailed data study on this matter and the rest of the data collected is required. The following conclusions, however, apply to the hull response and damage studies on surface ships in deep water on Shot Wahoo. It should be understood that Wahoo conditions included yield, shot geometries, and, to a lesser extent, bottom reflection and water-temperature gradient characteristics for this test.

1. From the standpoint of hull deflection, a safe-delivery range for destroyers of [redacted] feet for Wahoo conditions has been demonstrated. The minimum safe-delivery range, from the standpoint of hull deflections, is considerably smaller than the above.

2. From the standpoint of hull deflection, it can now be estimated that the lethal range for the EC-2 is [redacted] feet under Wahoo conditions.

3. Considerable basic information on hull response as related to free-field pressures and loading measurements was obtained. This has provided check points for small-scale ship model experiments which confirm developed theories, which upon further analysis, are expected to prove valuable in extrapolating results of Wahoo to other conditions. The loss of electronically-recorded data on the DD-592 on Wahoo makes direct correlation with the full-scale, high-explosive, tapered-charge tests more difficult; however, it is expected that analysis of shock-spectra data available will permit such correlation. Some of the other preliminary features of the basic information obtained are given in the additional conclusions below.

4. The keel bottom velocities at the EC-2 position caused by the direct shock wave were, by far, the most significant, being about three times as great as the sea-bottom-reflected shock wave. The bulk cavitation reloading shock wave response at the EC-2 position was small.

5. The keel bottom velocities caused by the reflected shock wave at the DD-593 position, in contrast to the EC-2 position, were three times as great as those for the direct-shock wave.

6. Under side-on attack, the bottom vertical and horizontal velocities are not uniform over the length of the ship; despite uniformity of loading, velocity response was critically dependent upon precise locations of the structure to which the gages were attached.

7. Vertical velocities measured at the keels of the target ships were higher than corresponding water particle velocities. The maximum vertical bottom velocities measured were: 14 ft/sec for the EC-2; 2 ft/sec for DD-593.

8. The severity of the shock motions in a surface ship diminishes considerably from bottom to the superstructure decks. The damaging initial accelerations can be reduced by a factor of 20 or more, even though the peak velocities are the same because of the slower rise time at the higher deck levels.

9. The character of the EC-2 hull damage was similar to small-scale tests on the C-2 models. The magnitude of side damage may be predicted, therefore, with an accuracy sufficient for predicting lethal ranges, on the basis of these small scale model tests.

2.4.4 Hull Response Studies of Submarines. Objectives. The principal effort of the hull response studies on submarines was on Shot Umbrella, and it will be discussed in the chapter dealing with that event. However, as a result of the inclusion of the submarine SSK-3 in the Wahoo array, the following objective was added for these studies: determination of the response of the hull of a submarine in a simulated attack position in deep water.

The submarine SSK-3 was included in the Wahoo array primarily to demonstrate a safe-

delivery range for an underwater nuclear weapon in deep water. Although it was believed that shock damage to the submarine machinery and equipment would control the safe range, it seemed desirable to simultaneously study the response of the hull. This consisted of a few strain measurements made on the pressure-hull plating in a typical bay and at a previously determined weak spot in the forward torpedo room. The measurements were intended to provide a comparison of effects of dynamic and static pressure loading of the hull.

**Background.** Shot Baker of Operation Crossroads first tested submerged submarines (SS-212 and SS-285 class) exposed to underwater nuclear attack, and valuable information on lethal radii was obtained for attack in shallow water. However, the lack of pressure-time measurements in the water and of hull response-time measurements made extrapolation of these results to other targets, other depths of water, other burst geometries and other types of sea bottom difficult.

Operation Wigwam was specifically designed to determine the lethal range of submerged submarines exposed to underwater nuclear attack in very deep water. Submarine models (Squaws), 4/5 full-scale SS-563 class submarine in cross sectional dimensions, were utilized for these tests. The Wigwam results enabled reasonably confident establishment of safe ranges for submarines in very-deep water.

The pressures in such a very-deep water test were essentially those in a free-field, except for linear surface cutoff and refraction effects. For a detonation in water between 500 to 5,000 feet, i.e., neither shallow such as Shot Baker of Operation Crossroads nor very deep as in Wigwam, the effect of the bottom reflection shock wave could be expected to be more than on Wigwam but less than on Shot Baker of Operation Crossroads. Therefore, it was apparent that information on submarine-hull response from underwater nuclear detonation with Shot Wahoo geometry would be desirable in determining the minimum safe-delivery range of such weapons under such deep-water conditions.

**Procedure.** The operational submarine SSK-3, with crew aboard, was broadside at [redacted] foot range during Shot Wahoo and was submerged to periscope depth (50 feet to keel) in a simulated attack position. This range greatly exceeded that considered safe. Preliminary plans called for the SSK-3 to be located at [redacted] feet, moored and suspended between pontoons, without the crew aboard. Difficulties during the preparation of the mooring, including loss of some other target array mooring cables as a result of rougher seas than anticipated, required the change in plans. At the [redacted] foot range, the predicted dynamic-peak pressures during both the direct shock wave and during the bottom-reflected wave were much less than the estimated static collapse pressure of the hull.

The inner pressure hull of the SSK-3 was circular, with a diameter of 15 feet, a thickness of 7/8-inch medium steel with a yield strength of 34,000 psi; frames were external, spaced at 36 inches.

Strain gages were installed on the SSK-3 hull to measure the deformation of hull plating and stiffeners and were supplemented with high-speed motion picture cameras to aid in interpretation of the hull deformation data records. The location of the seven strain gages (SR-4 type) and three motion-picture cameras is shown in Figure 2.50. The signals from the gages were recorded on an oscillograph recorder in the submarine, with the sequence timer for Wahoo started manually by a crew member aboard listening to a radio voice timing signal.

**Results.** All instrumentation functioned well on the SSK-3, and good strain records and high-speed photography were obtained. As expected, no hull damage occurred. The records of the strain from the reflected shock wave are shown in Figure 2.51, and the peak values of strain are shown in Table 2.13. Of the three distinct pulses of strain, the second from the ocean-bottom-reflected shock was of the largest magnitude. The pressure from this reflected wave was lower than that from the direct wave, but the duration was longer. The origin of the third pulse was not definitely established but was probably from the cavitation reloading.

It will be noted that the maximum strain recorded was 390  $\mu\text{in}/\text{in}$ , which is below the hull yield strain of 1,100  $\mu\text{in}/\text{in}$ . The equivalent depth of submergence at which such hull strains would occur is about 200 feet. This equivalent depth is only half of the operating depth of the SSK-3 and only  $\frac{2}{7}$  of the estimated collapse depth of 700 feet.

The estimated static collapse pressure for the SSK-3 hull is about 300 psi (equivalent to 700-foot depth). Under Wahoo conditions, that value of dynamic pressure was estimated for SSK-3 at the 7,000-foot range at periscope depth. Therefore, this range can tentatively be considered a safe range at periscope depth, since it is clear that much higher pressures may be sustained without failure under short-duration dynamic conditions. Moreover, since Wahoo results in-

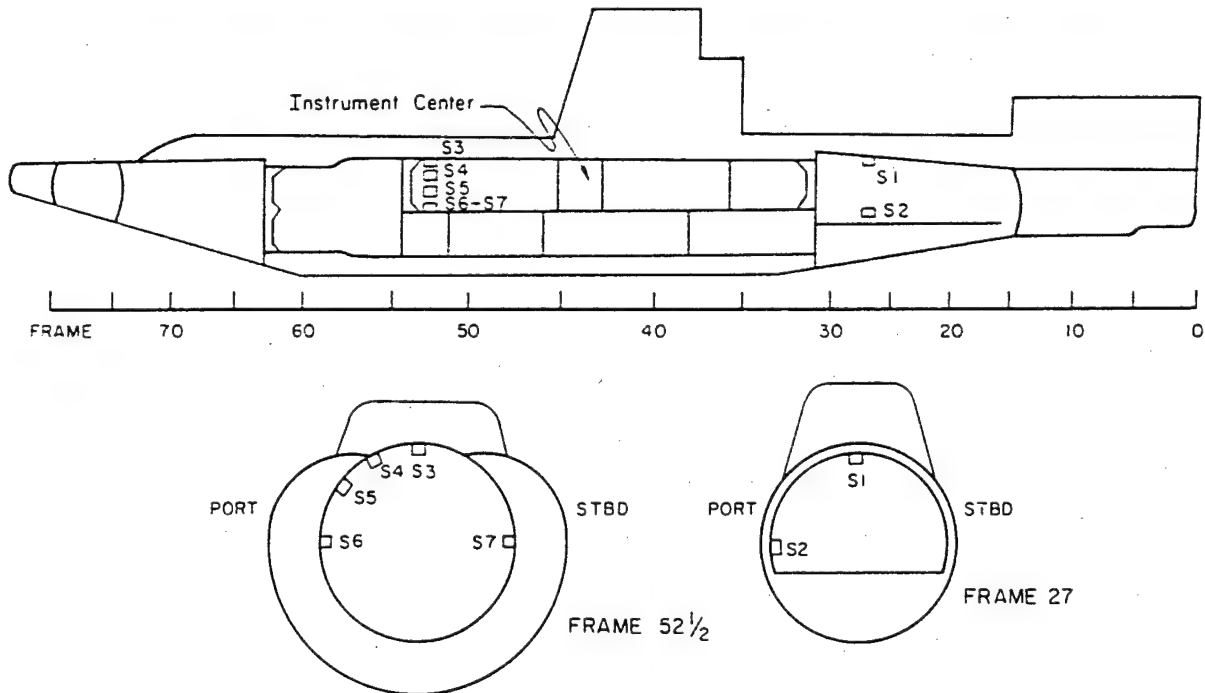


Figure 2.50 Inboard profile and section views, showing locations of strain gages on the USS Bonita (SSK-3).

indicated that the ocean bottom reflection characteristics were such that reflected wave pressures were less than expected, a better prediction of the minimum-safe range will be possible after detailed study of Wahoo pressure-time measurements and more consideration of the dynamic structural conditions required for collapse.

**Conclusions.** The following are the preliminary conclusions of the submarine hull study on Shot Wahoo. It should be understood that in the following, Wahoo conditions include yield, shot geometries, and to a lesser extent the bottom reflection characteristics and water-temperature gradients for this test.

Based on a comparison of static collapse pressure of the hull with estimated applied dynamic pressure of the same magnitude, it is estimated that a safe range for the SSK-3 submarine hull under Wahoo conditions is [REDACTED]. This comparison is quite conservative and therefore is not to be considered the minimum safe range, a better estimate of which will be made in the final report.

2.4.5 Shipboard Machinery and Equipment Shock Damage Studies. Objectives. The over-

all purpose of these studies was to obtain data on the effects of underwater nuclear detonations on ships, from the standpoint of shock damage to machinery and equipment, that could be used to check theory and to increase the knowledge of shock phenomena and effects. This would permit more reliable predictions of shock effects, including extrapolation to other attack geometries, and provide design information necessary for shock hardening of future ships' machinery and equipment. The specific objectives on the Wahoo shot were to:

1. Determine safe range and moderate damage ranges for delivery of antisubmarine nuclear

TABLE 2.13 STRAINS ON THE USS BONITA (SSK-3) FROM SHOT WAHOO

Position Number	Location *	Maximum Strains in $\mu$ in/in			Equivalent Depth †
		First Shock	Second Shock	Third Motion	
					ft
S1	Frame 27 at crown	50	240	190	200
S2	Frame 27, 90 deg port	90	-390	-190	220
S3	Frame 52 1/2 at crown	-40	170	100	130
S4	Frame 52 1/2, 26 deg port	30	180	100	140
S5	Frame 52 1/2, 45 deg port	60	210	90	170
S6	Frame 52 1/2, 90 deg port	30	-110	50	120
S7	Frame 52 1/2, 90 deg stbd	-30	120	100	70

\* All gages measured circumferential strain. Compression is recorded as positive strain.

† Change in depth of submarine which would produce same static strain as the largest dynamic strain observed. Strain gages were calibrated during deep-dive trials.

weapons by destroyers in deep water, from the standpoint of shock damage to machinery and equipment important to combat capability.

2. Determine safe ranges for delivery of antisubmarine nuclear weapons by submarines in deep water, from the standpoint of shock damage to machinery and equipment important to combat capability.

3. Determine the intensity and character of equipment shock motions on an EC-2 merchant ship at quasi-lethal range for the hull, under nuclear attack in deep water.

4. In general, obtain shock-motion data on ships' machinery, equipment, and foundations for correlation with free-field phenomena, hull loading and theories so that the results of nuclear tests in deep water can be extrapolated to other burst geometries and ships.

Background. By underwater explosion of a chemical or nuclear weapon, a ship may be either (1) destroyed by rupture of its hull or (2) rendered inoperative by the disruption of vital machinery and equipment by mechanical shock. For most surface ships and submarines, there was evidence that the shock damage to vital machinery and equipment was the most critical problem insofar as maintaining the ships' combat capability was concerned.

At the beginning of World War II, the machinery and equipment shock-damage problem was brought sharply into focus when German influence mines caused disabling ship-equipment damage. Subsequent high-explosive tests subjecting a submerged submarine and several destroyers to simulated attack by depth charges provided some data and indicated the large scope of the equipment shock-damage problem. It became clear that there are many variables involved: type of construction and materials used in ship equipment, type of structure to which equipment is attached on ship, type of ship, size of weapon, depth of burst, depth of water, type of sea bottom, and attack geometry. It became obvious that the complexity of the problem, as indicated by the parameters involved, required a systematic approach.

Shot Baker of Operation Crossroads provided only limited data on the equipment shock damage to surface ships. More data on shock from an underwater nuclear weapon was obtained on Operation Wigwam. However, this test was specifically designed to determine submarine lethality, with little effort expended to determine surface ship equipment-shock damage. The simplified submarine targets (Squaws) did contain weights simulating main machinery on which shock mo-

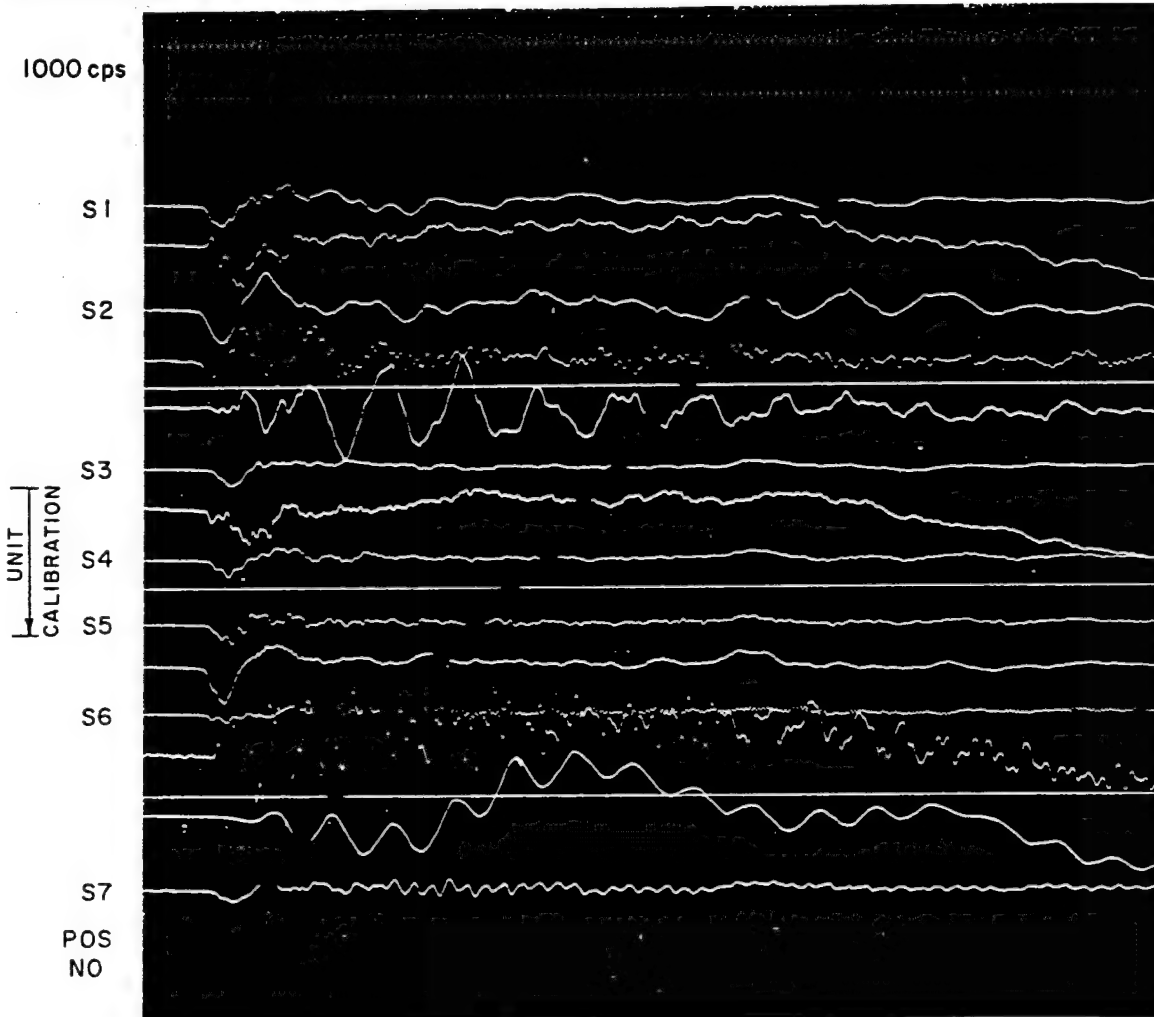


Figure 2.51 Oscillogram of bottom-reflected shock wave on the USS Bonita (SSK-3) for Shot Wahoo.

tion was extensively recorded, but the only surface ships in the test array were the YFNB instrument barges, which were instrumented.

Other underwater shock tests conducted with high-explosive charges on submarines and a variety of surface ships during the period of 1952 to 1957 have furnished additional data on shock response. The latest of these high-explosive tests, in December 1957, were the underwater explosion tests conducted on the new guided missile destroyer DDG-1 (USS Gyatt) to evaluate the shock strength of the missile system. In most of these tests, however, it was not practical to carry the tests into the severe shock damage ranges, since the targets involved were commissioned ships which were not expendable. Nevertheless, such tests have confirmed that both



operating submarines and surface ships can be disabled as a result of equipment shock damage at considerably greater distances than required to damage the hull. In addition, recent model studies using high explosives have also helped considerably in predicting the response of surface ships to a given underwater pressure loading.

However, the question of correlation between the response from a full-scale nuclear detonation and the occurrence of damage to various shipboard machinery and equipment, especially with the latter under actual operational conditions, was still unanswered. This shipboard machinery and equipment shock damage question could only be satisfactorily answered by having vessels, with vital shipboard equipment actually in operation, subjected to a pressure loading encountered in an underwater nuclear attack.

**Procedure.** To accomplish the objectives of the shipboard machinery and equipment shock damage studies, the shock motions of actual and simulated equipment, their foundations and supporting structures (including hull, bulkheads, decks and superstructures of the ships) were to be recorded as a function of time using electromagnetic velocity meters. In addition, at the same representative ship locations, the shock spectra associated with the movement of these structures were to be recorded by shock-spectra (reed-type) recorders.

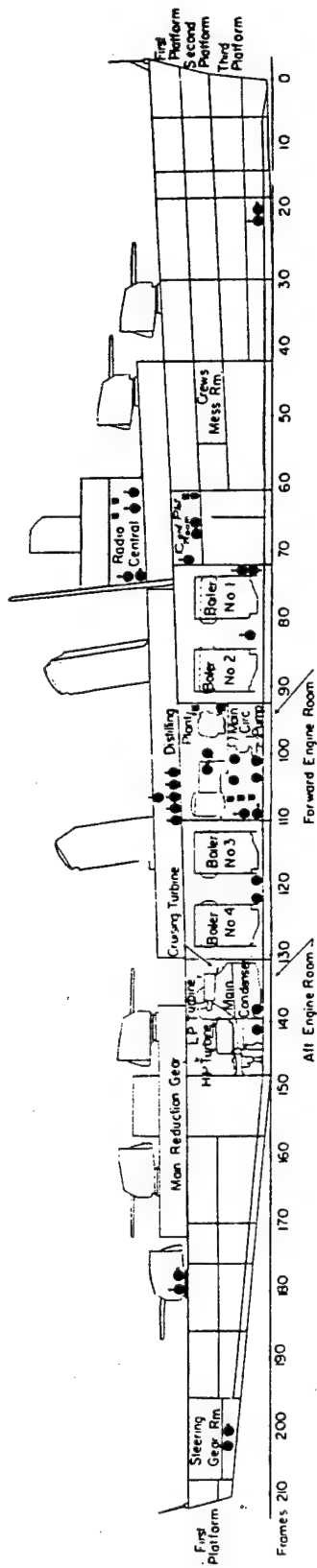
The DD-593, DD-592, DD-474 and the EC-2 were the principal target ships, and all were relatively highly instrumented for the equipment shock damage studies. The locations of these target ships from Shot Wahoo surface zero were respectively stern-on at [redacted] broadside at [redacted] stern-on at [redacted] and broadside at [redacted] feet, as indicated by Figure 2.8. A manned operational submarine, the SSK-3, was also instrumented and located at [redacted] foot range. As a supplementary effort, two manned operational destroyers, DD-728 and DD-886, containing minimal instrumentation, were exposed during Shot Wahoo at relatively long ranges from the burst [redacted] feet). Another manned operational submarine, the SS-392, without instrumentation, was located at [redacted] foot range.

For the three target destroyers, extensive instrumentation was located principally in the forward engine and fire rooms where the main machinery was in operation, as well as in radio central, in the CIC, gunfire control and gyrocompass rooms. The operation of machinery and equipment in the forward engine and fire rooms, without personnel aboard, was accomplished by installation of automatic controls in these three destroyers. The starboard propeller on each destroyer was replaced with a disk of the same diameter to allow the shaft to rotate at normal 400 rpm destroyer cruising speed without thrust. Unlike the DD's, the machinery on the EC-2 was not activated, although the instrumentation was located principally in the engine and fire room, as well as at other key locations such as on the bridge by steering control equipment.

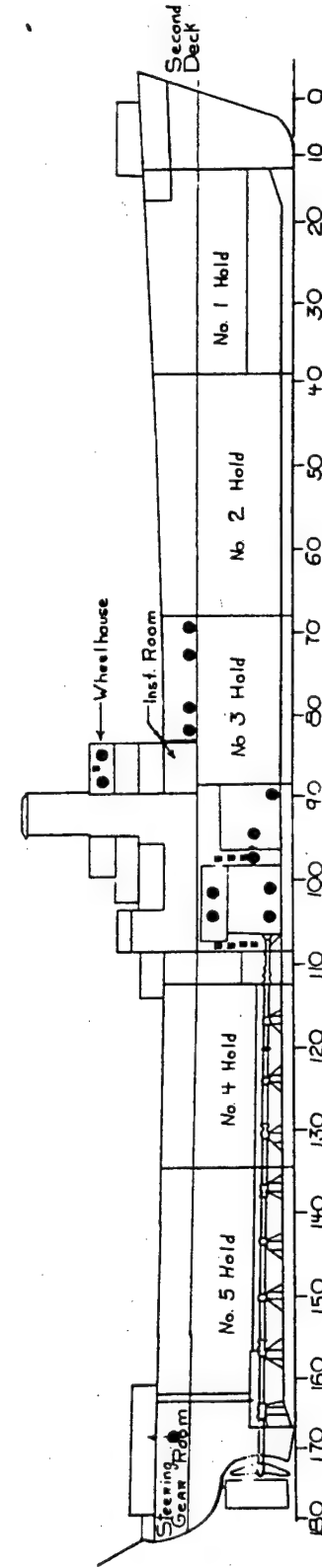
Approximately 50 velocity meter gages, and 50 shock-spectrum-recorder gages were installed on each of the three DD's; approximately 30 of each type gages were installed on the EC-2. Eight of each type were mounted on the SSK-3, and six velocity-meter measurements were taken on each of the two operational DD's (DD-728 and DD-886). Thus, a total of over 350 gages was installed for the machinery- and equipment-shock studies.

In addition to the above shock-measurement gages, a total of 40 high-speed, 1,000 frames per second, motion-picture cameras were installed on the three target destroyers, the EC-2 and SSK-3. These high-speed cameras were located to give a pictorial record of selected machinery response and damage to aid in analysis of the data measurements. The general locations of these gages and cameras on the target DD's and EC-2 are indicated by Figure 2.52.

The gages used were substantially the same types previously utilized on other underwater tests. The basic velocity measurements were made by velocity meters. This was a simple, rugged-type gage consisting of a spring-mounted-bar magnet mounted inside a cylindrical coil. The latter was attached rigidly to the equipment base whose shock motion was to be measured; motions of the base produced a voltage in the coil proportional to the relative velocity between the coil and the magnet. The time histories of the velocities so measured were recorded di-



DD INSTRUMENTATION



EC-2 INSTRUMENTATION

Legend

- - Velocity Meter, Shock-Spectrum Recorder
- - High-Speed Motion Picture Camera

Figure 2.52 Shock studies of shipboard machinery and equipment.

rectly on an oscillograph recorder located in a recording center compartment near the center of the ship. These recorder units were protected from radiation-film fogging by a lead shielding three inches thick. The recording equipment units were also mounted on steel spring cylinders to protect the recording units from severe shock damage, as shown in Figure 2.53. Air conditioning equipment was installed in the recording center compartments on each ship to adequately protect the electronic equipment from high humidity conditions.

The shock-spectrum-recorder gages consisted of 10 weighted, cantilever reeds, each of a particular natural frequency from 20 to 450 cps. When exposed to shock, displacements of each reed are scribed on a waxed paper. From peak displacements, the maximum acceleration of each reed can be computed; maximum acceleration plotted as a function of reed frequency is called shock spectrum. Shock spectrum specifications have been commonly utilized for several years by designers of shock-sensitive machinery and electronic equipment to resist shock environments. The basic shock-spectrum recorder is an autographic, self-contained, self-recording instrument which requires no power or time initiation. For the first time on Operation Hardtack, a few of the recorders were powered with an electric motor to drive the waxed paper, to thus separate versus time, the records produced by the successive direct, reloading, and reflected shock pulses. Figure 2.54 shows a shock-spectrum recorder.

Each of the 40 high-speed cameras used for these shock studies was protected against film-radiation fogging by being mounted within a special cylindrical shield of lead three inches thick, in turn resiliently mounted in a specially-designed frame. Figure 2.55 shows a typical camera installation.

**Results.** On five of the seven instrumented ships in the array, records of shock motions versus time were successfully made with all instruments installed. On the DD-592 and DD-474, the two target destroyers closest to the burst point, no electronic time-based records were obtained because of failure of the timing signal system on those two ships, which resulted from auxiliary ships' power malfunctions. The shock motions on these two ships, therefore, were recorded only on the self-recording shock-spectrum recorders. These mechanical instruments, installed to produce shock-response data and as a backup for the time-based instruments, functioned excellently on all ships. All high-speed cameras on those ships on which timing signals were received operated, and good quality films were obtained.

Figure 2.56 shows a typical oscillogram record from one of the targets, this of the response from the direct-shock wave on the EC-2. Table 2.14 and Table 2.15 show a tabulation of the velocities, rise times, and average accelerations for both direct and reflected-shock waves on the EC-2 and DD-593. These tabulations interestingly indicate the general range of response motions on various items of machinery and foundations. The maximum vertical velocity of about 14 ft/sec on the EC-2 and two ft/sec on the DD-593 compare well with similar measurements taken for the hull studies.

The shock-spectrum recorder data requires some data reduction and computation prior to presentation. However, a few records have been read and reduced and are shown in graphical form in Figure 2.57. The shock-spectrum data on the DD-474 and DD-592, upon analysis, is expected to make the principal shock motions on those two ships available, even though the electronic response instrumentation did not function.

The ship's machinery and equipment damage to the EC-2, located broadside at [redacted] feet from surface zero, was serious and crippling. Propulsion and auxiliary plants were seriously damaged. A variety of equipment, primarily cast-iron components, failed. In the propulsion plant, the main shaft bearings were broken from their pedestals. Mounting feet on fuel oil service pumps fractured; main condenser-holding bolts were sheared off. Auxiliary and ship's electrical service failed because of pipe-casting failures and failure of casting supports. The ship was made completely inoperable, by machinery and equipment shock damage, and would have required much shipyard work to return it to operating condition.

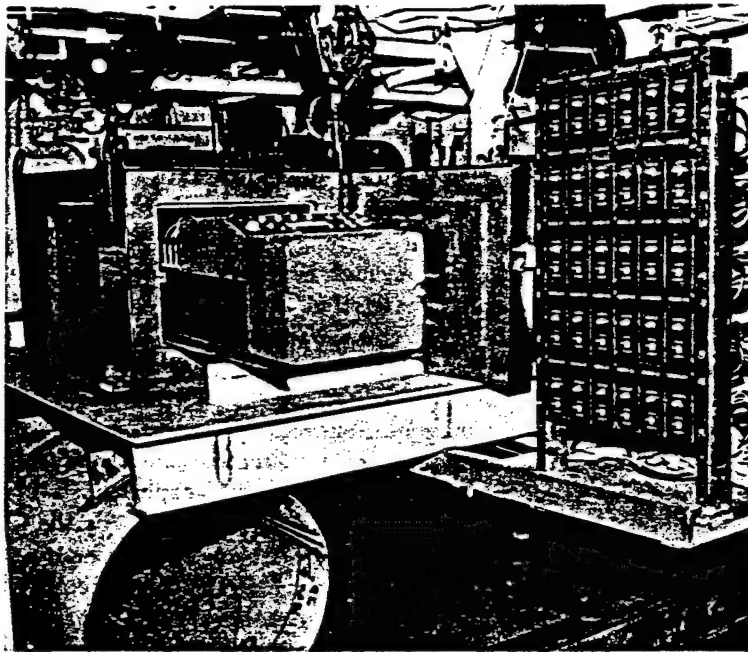


Figure 2.53 Recording equipment on resiliently mounted table in recording center. The oscillograph, partly removed from its lead-lined housing, can be seen. Another oscillograph in a similar housing is hidden behind the velocity-meter control and calibration panels cantilevered from the table. One of the two thin-walled 24-inch-diameter cylinders which support the table is visible in the lower left corner of the photograph. The cylinders are designed to yield under shock loading so as to limit accelerations of the table to around 4 g.

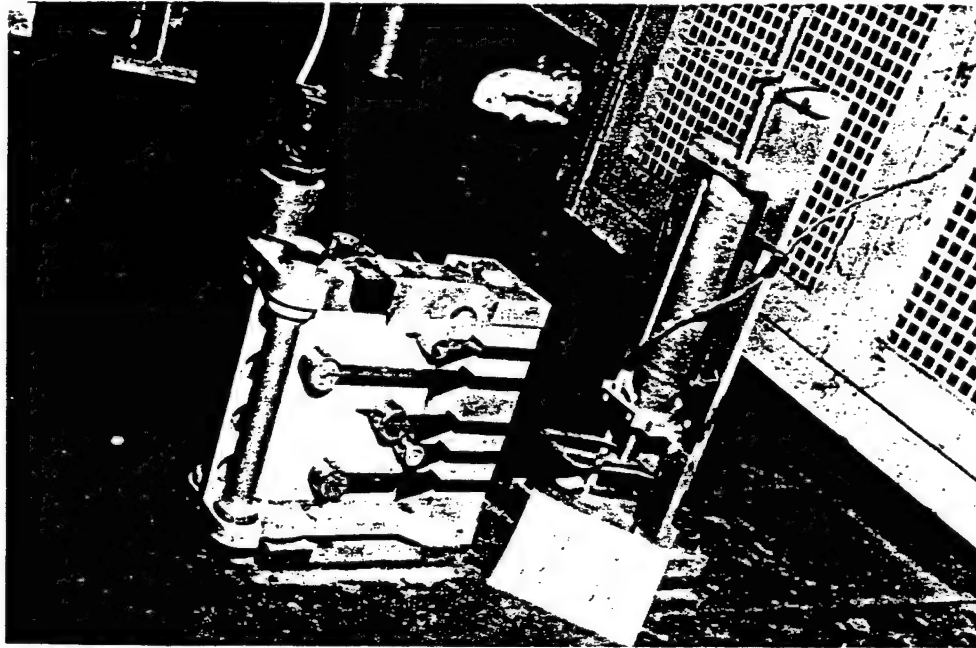


Figure 2.54 Typical installation of a velocity meter and a shock-spectrum recorder. The velocity meter at the right is connected by a cable to a galvanometer channel in the oscillograph shown in Figure 2.53. The shock-spectrum recorder at this location is equipped with a motor, which drives the recording paper. The protective cover has been removed from the shock-spectrum recorder to show five of the ten weighted cantilever reeds.



The ship's machinery and equipment damage to the DD-474, located [redacted] feet from surface zero, could be classified as light but beginning to approach the moderate damage range. The flexure plate bolts which support the foundations to the main turbines were appreciably deformed in both shear and bending. Misalignment between the turbines and the propulsion shaft resulting from the deformation of these bolts was taken up in the couplings. Although the turbines were still operable, misalignment would result in excessive wear in the couplings. Complete failure of these flexure plate bolts would drop the turbine into the bilge and at normal turbine speeds could result in severe damage to the ship. Thus indications are that the differ-

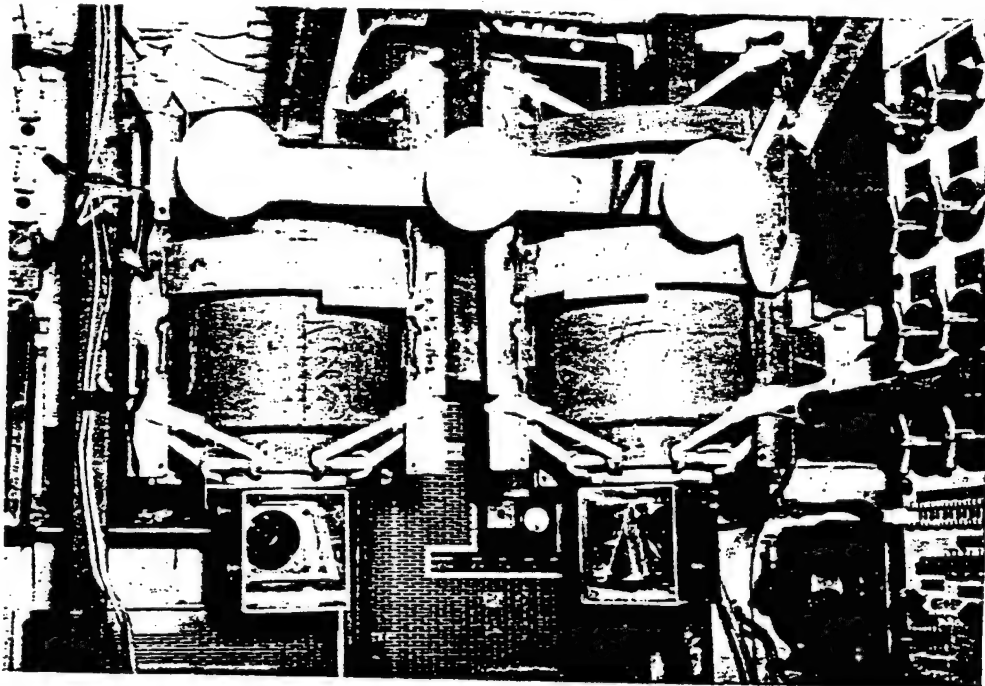


Figure 2.55 Typical installation of high-speed motion-picture cameras. Each camera is housed vertically inside a heavy lead-lined cylinder. The cylinder is seismically suspended by means of three pairs of rubber (shock) cords from a special frame. In order to take pictures horizontally, an adjustable mirror is used. It is seen below the housing reflecting an image of the camera lens. Lights for illuminating the subject are resiliently mounted.

ence in range may be small between light, moderate and severe damage. Brick work on the floor of one boiler was damaged, and a five-inch ammunition hoist was disabled by bolt failures.

The shock damage was negligible on the DD-592 and DD-593 at [redacted] feet, respectively. On the DD-728 and DD-886 at [redacted] feet, respectively, some electronic equipment failed. In addition, gearing in the rocket-thrown-torpedo (RATT) system jammed. It is of significance to note that these latter manned commissioned destroyers, unlike the target destroyers, had modern electronic equipment on board. Had the target ships closer to the burst point been outfitted with such electronic equipment, this undoubtedly would also have been damaged.

Shock damage to the SSK-3, [redacted] feet from surface zero, was negligible, consisting only of momentary power loss due to a circuit breaker trip and minor failures of electronic and ordnance equipment. The operating submarine SS-392, at [redacted] feet, reported a minor malfunc-

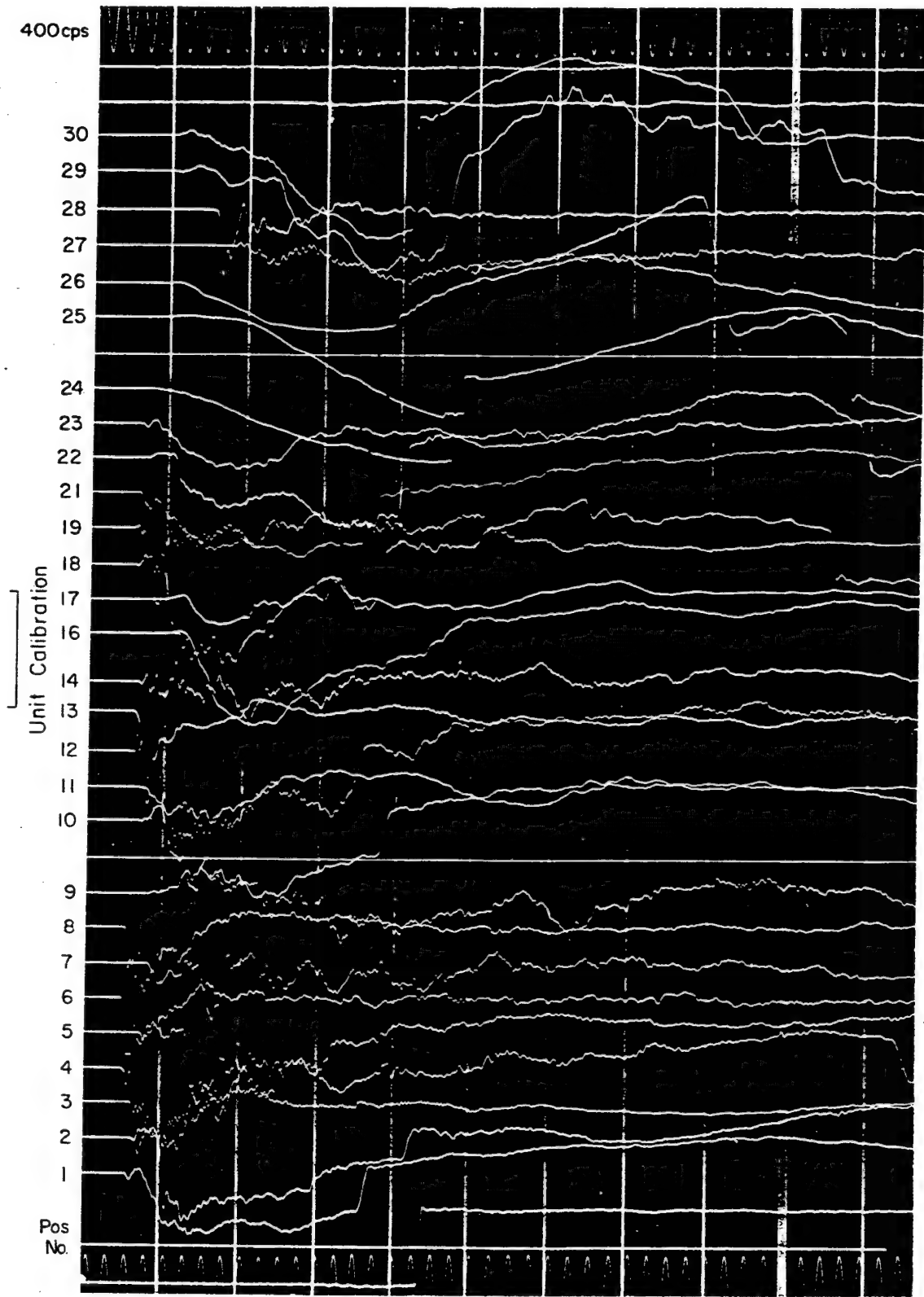


Figure 2.56 Oscillogram of direct shock wave on SS Michael Moran (EC-2) for Shot Wahoo.

TABLE 2.14 VELOCITIES, RISE TIMES, AND AVERAGE ACCELERATIONS ON SS MICHAEL MORAN (EC-2)  
FROM SHOT WAHOO

Position Number	Orientation *	Location	Direct Shock Wave			Reflected Shock Wave		
			Peak Velocity ft/sec	Rise Time msec	Average Acceleration g	Peak Velocity ft/sec	Rise Time msec	Average Acceleration g
1	V	Bottom center Bulkhead 88	8.4	6	44	4.7	7	21
2	V	Bottom center Frame 97	11.2	3	110	4.5	3	43
3	A	Bottom center Frame 97	7.7	1	240	0.8	1	31
4	V	Bottom stbd Frame 97	11.4	7	49	4.4	3	45
5	V	Bottom port Frame 97	9.7	2	180	5.2	3	50
6	A	Low stbd Frame 97	27.7	1	1,200	4.9	3	58
7	A	Low port Frame 97	7.6	2	120	-2.8	5	-18
8	A	Higher stbd Frame 97	28.7	3	330	3.8	8	15
9	A	Higher port Frame 97	-5.1	7	-22	-4.4	5	-29
10	V	Subbase main engine	10.0	4	72	4.8	14	10
11	A	Subbase main engine	5.9	9	20	1.5	13	3
12	V	Foundation Caterpillar diesel	12.2	4	86	4.7	3	47
13	A	Foundation Caterpillar diesel	13.0	2	220	1.0	3	11
14	V	Foundation steam-generators	6.0	3	64	5.3	15	11
16	V	Top of main engine	13.2	9	45	4.9	10	16
17	A	Top of main engine	3.4	4	26	-2.0	14	-4
18	V	Caterpillar diesel	13.7	10	43	7.9	11	22
19	A	Caterpillar diesel	6.6	2	110	1.8	3	19
21	V	Platform deck Bulkhead 88	8.2	10	27	4.2	5	27
22	V	Platform deck Frame 83	6.4	6	33	7.0	35	6
23	A	Platform deck Frame 83	4.7	10	14	2.3	43	2
24	V	03 level Frame 89	9.7	35	8	5.0	28	5
25	V	Wheelhouse	12.7	27	15	5.0	20	7
26	A	Wheelhouse	4.4	19	7	1.1	35	1
27	V	Steering gear room	5.0	11	14	3.6	35	3
28	V	Shaft alley	15.5	1	690	3.5	11	10
29	V	Foundation operating diesel	12.2	11	34	7.5	13	18
30	V	Operating diesel	14.3	22	20	5.4	13	13

\* Direction of measurement of motion: V, Vertical (motion upward is positive); A, Athwartship (motion to port is positive).

TABLE 2.15 VELOCITIES, RISE TIMES, AND AVERAGE ACCELERATIONS ON USS KILLEN (DD-593)  
FROM SHOT WAHOO

Position Number	Orientation *	Location	Direct Shock Wave			Reflected Shock Wave		
			Peak Velocity ft./sec	Rise Time msec	Average Acceleration g	Peak Velocity ft./sec	Rise Time msec	Average Acceleration g
1	V	Keel Frame 22	0.6	1	29	1.8	8	7
4	V	Foundation battery control	0.2	8	1	1.5	11	4
5	V	Battery control	0.2	6	1	1.6	13	4
6	V	Radio central Bulkhead 72	0.1	3	1	1.5	24	2
13	V	Keel Frame 99	0.5	1	30	1.6	9	5
17	V	Keel Bulkhead 110	0.3	1	22	1.3	8	5
18	L	Keel Frame 109	0.1	1	4	-0.2	12	-1
19	V	Flex plate Bulkhead 92 1/2	0.2	3	2	1.3	8	5
20	V	Foundation reduct gear, forward	0.2	1	6	1.1	9	4
21	V	Foundation reduct gear, after	0.2	1	16	1.3	11	4
22	V	Foundation turbogen, forward	0.2	3	2	1.6	14	4
23	A	Foundation turbogen, forward	0.0	11	0	0.3	13	3
24	V	Foundation turbogen, after	0.2	1	6	1.2	18	1
25	A	Foundation turbogen, after	-0.1	1	0	0.2	8	1
26	V	Reduction gear	0.2	6	1	1.5	10	5
27	V	Subbase HP turbine	0.2	10	1	1.8	20	3
28	V	Subbase LP turbine	0.2	15	1	2.0	25	2
29	V	Subbase turbogen	0.3	9	1	2.0	14	5
31	V	Main deck Bulkhead 110	0.1	1	4	1.6	18	3
33	V	Main deck Frame 107	0.1	6	1	1.5	18	3
34	V	Deckhouse top	0.2	10	1	2.2	18	4
46	V	Foundation 5-in. gun	0.2	3	4	1.4	11	4
48	V	Steering gear room	0.3	1	20	1.4	7	6
49	A	Steering gear room	-0.1	1	-3	0.3	10	1
50	L	Steering gear room	0.0	2	1	-0.2	17	-1
51	V	5-in. gun	0.2	10	1	2.1	18	4

\* Direction of measurement of motion: V, Vertical (motion upward is positive); A, Athwartship (motion to port is positive); L, Longitudinal (motion forward is positive).



tion in that release of torpedos occurred in two tubes as a result of raising of the stop bolts from the shock.

Table 2.16 shows the vertical velocities caused by the direct shock wave averaged for the EC-2 and DD-593, by various types of positions, and computed average ratios of velocity to water velocity. For shipboard machinery and equipment, these computed average ratios show that the velocities larger than surface-water velocity are associated with light load positions, while heavily loaded positions more closely approximate the surface-water velocity.

Conclusions. The shock damage to ship machinery and equipment on the target ships, although reasonably severe on the EC-2 and light approaching moderate on the DD-474, was

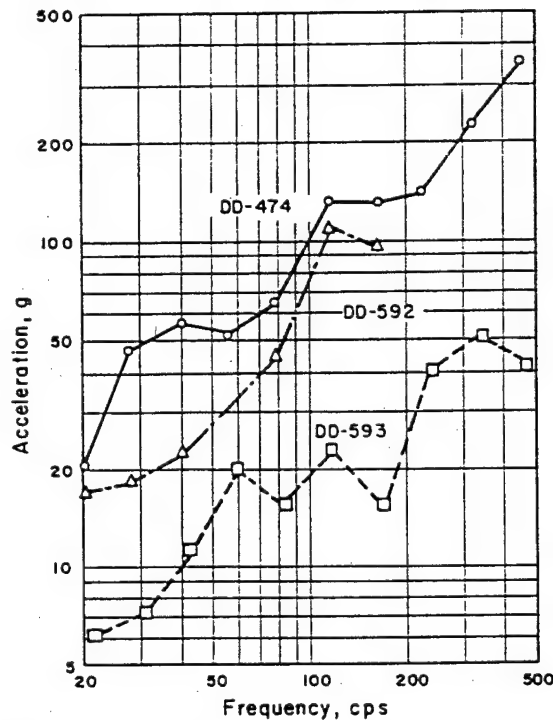


Figure 2.57 Comparison of shock spectra on the three target destroyers for Shot Wahoo. The spectra shown are for Position 17, measuring vertical motion of Bulkhead 110 at a point near the keel, and are the spectra for all the shock motions which occurred.

somewhat less than expected for Shot Wahoo. This was apparently due to a reduction in free-field pressures encountered from those predicted. This may have been caused by a stronger water-temperature gradient-refraction effect in the water than expected at the Wahoo site, although more detailed data study of this point is required. The following conclusions, however, apply to the ship machinery and equipment shock damage studies on Shot Wahoo. It should be understood that Wahoo conditions include yield, shot geometries, and to a lesser extent, bottom reflection and water-temperature gradient characteristics for this test.

1. From the standpoint of equipment shock response, the minimum safe range for delivery of an antisubmarine weapon by destroyers is [redacted] feet for Wahoo conditions. Damage or malfunction of particularly delicate equipment, i. e., some types of electronic equipment, may occur at larger ranges.

2. From the standpoint of equipment shock response, the range for moderate damage for delivery of an antisubmarine weapon by destroyers is between [redacted] feet for Wahoo conditions.

3. From the standpoint of equipment shock response, the minimum safe range for a submarine is less than [REDACTED] under Wahoo conditions. The estimated maximum submarine hull velocity at that range was about 2.5 ft/sec, which is considerably less than the velocity necessary to cause significant equipment damage. Therefore, [REDACTED] feet is a conservatively safe range, although malfunction of particularly delicate equipment (i. e. electronic) may occur at larger distances. In the final report it is expected that analysis will permit an estimate of the minimum safe range to be made.

4. Shock data defining the intensity and character of the shock motions on merchant ships

TABLE 2.16 VERTICAL VELOCITIES OF HULL FOR DIRECT SHOCK WAVE FROM SHOT WAHOO

Magnitude of Inertia Loading	Positions	Average Peak Velocities *		Ratio to Velocity of Surface Water	
		EC-2 ft/sec	DD-593 ft/sec	EC-2	DD-593
Heavy	Bulkheads at locations near keel	8.4	0.2	1.0	1.0
Intermediate	Foundations of propulsion machinery	10.0	0.2	1.2	1.0
Light	Foundations of light equipment and unloaded positions	12.0	0.5	1.4	2.5
Light	Highest velocity recorded (shaft alley of EC2, Frame 22 of DD593)	15.5	0.6	1.8	3.0
—	Computed velocity of surface water	8.5	0.2	—	—

\* Numerical averages of recorded peak velocities. Accuracy is low for data from DD-593 because the velocities are small compared to the peak velocities expected from the reflected wave. No time-history records were obtained from DD-474 or DD-592.

were obtained on an EC-2 at [REDACTED] feet from Shot Wahoo. At this range, the ship was totally disabled by machinery and equipment shock damage.

5. Sets of shock motion data were obtained on all seven of the target ships during Shot Wahoo. Time-based shock motion data were not obtained on the two target destroyers closest to the burst. However, data from self-recording mechanical shock-spectrum recorders were obtained on all targets. It is believed that sufficient data are at hand to provide check points to correlate with observed pressures and times so that the results of nuclear tests available can be extrapolated to other geometries and ships. It is hoped such generalizations can be developed for inclusion in the final report.

6. For Shot Wahoo, the direct shock wave, rather than the reflected shock wave, was the primary cause of shock damage at the close ranges of interest.

7. The safe range and damage range for submarine and surface ship targets, under Wahoo conditions, is determined by shock damage to ships machinery and equipment rather than by hull damage.

2.4.6 Summary. In summary, it is concluded that the results obtained from the projects in Program 3 on Shot Wahoo were generally successful in achieving the main objectives of the program.

The pre-Wahoo tests of high-explosive-tapered charges against the DD-592 in January 1958 successfully showed that the direct shock waves of an underwater nuclear detonation could be simulated by means of tapered charges. The decision as to whether this tapered-charge tech-

nique also properly simulates target response must await evaluation of shock-spectra-gage data from Shot Wahoo.

On Shot Wahoo, the response and damage to hulls, ships' machinery, and equipment of the surface ships EC-2, DD-593, DD-592 and DD-474 were somewhat less than predicted. Apparently, this was due to a greater reduction in the free-field underwater pressures from a stronger-than-expected refraction effect on the underwater shock waves, which, in turn, was due to the pronounced thermocline or abrupt temperature gradient with depth in the water at the Wahoo site. However, considerable detailed data study will be required prior to preparation of firm conclusions which are expected to appear in the final report.

In consonance with the less-than-expected ship response on Shot Wahoo, the EC-2 merchant ship, located broadside at 2,300 feet from surface zero at a predicted quasi-lethal range for the hull, actually sustained only light hull damage. A maximum transient displacement of about four inches in the hull side frames near the ship's center produced a maximum permanent hull side displacement of about one and one half inches. Maximum permanent hull-plate dishing between frames was about  $\frac{3}{4}$  inch. Minor hull flooding, caused by leaks due to minor seam cracks, was controllable by pumping. In contrast to the EC-2 hull, the ship machinery and equipment damage was severe, so as to make the ship completely inoperable, and would have required much shipyard work to return the EC-2 to an operating condition.

As expected, there was no hull damage to the DD-474, the destroyer closest to surface zero at [redacted] foot range, oriented stern-to. The ship's machinery and equipment damage to the DD-474 could be classified as light but beginning to approach the moderate damage range. The flexure plate bolts, which support the foundations for the main turbines, were appreciably deformed in both shear and bending. Misalignment between the turbine and propulsion shaft resulting from the bolt deformation was taken up in the coupling. Although the turbine was still operable and did operate at the normal 400 rpm propeller-shaft cruising speed through and after shot detonation, this misalignment would result in excessive wear in couplings. Complete failure of these deformed flexure plate bolts would have dropped the turbine in the bilge and at normal turbine speeds would have resulted in severe damage to the ship. Thus, indications are that the difference in range distance may be small between light, moderate, and severe damage ranges.

Although hull and shock damages on the other Shot Wahoo target ships were considered negligible, two manned operational destroyers at [redacted] foot range had some electronic equipment failures. In addition, gearing in the late model rocket-thrown-torpedo system jammed. It is also significant to note that these manned commissioned destroyers, unlike the target destroyers, had modern electronic equipment on board. If the target destroyers which were closer to the burst point had also been so outfitted, such electronic equipment undoubtedly would also have been damaged.

It is expected that analysis of the volume of self-recorded and electronically-recorded shock response data available, even though the electronically-recorded data on the DD-474 and DD-592 was not obtained on Shot Wahoo because of ship's power and timing signal malfunctions, will permit correlation of hull and equipment response with free-field pressures on all target ships.

From the results obtained, there was confirmation that the safe range and damage range for submarine and surface-ship targets under Shot Wahoo conditions is determined by shock damage to ship's machinery and equipment, rather than by hull damage.

The following additional preliminary conclusions drawn from Shot Wahoo data with respect to both hull and shock damage to ship's machinery and equipment are considered significant. It should be understood that these apply to the deep-water Shot Wahoo conditions, which include yield, shot geometries, and to a lesser extent, bottom reflection and temperature gradient characteristics for this test:

1. From the standpoint of hull deflection, the estimated lethal range for an EC-2 merchant ship is [REDACTED] feet for Shot Wahoo conditions.

2. The severe or crippling shock-damage range for machinery and equipment of an EC-2 merchant ship is [REDACTED] feet, under Shot Wahoo conditions.

3. The minimum safe range for repeated delivery of an antisubmarine weapon by destroyers is [REDACTED] feet for Shot Wahoo conditions.

4. The minimum safe range for single delivery of an antisubmarine weapon by destroyers, with shipyard availability soon after, is [REDACTED] feet for Shot Wahoo conditions.

5. The minimum safe range for delivery of an antisubmarine weapon from a submarine is [REDACTED] for Shot Wahoo conditions. Although this is a conservatively safe range, malfunction of particularly delicate equipment (i. e., electronic equipment) may occur at such range. It is expected that complete analysis of data will permit an estimate of the minimum safe range in the final report.

6. Considerable basic information of hull response on surface ships as related to free-field pressures and loading measurements was obtained. This data has provided check points for small-scale ship model experiments which confirm developed theories, which upon further analysis are expected to prove valuable in extrapolating results of Shot Wahoo to other geometries and ships. The loss of electronically-recorded data on the DD-592, as a result of ship's power and timing signal malfunctions, makes direct correlation with the high-explosive tapered-charge tests more difficult; however, it is expected that analysis of available self-recording shock-spectra response data will permit such correlation.

7. From the standpoint of ship damage important to combat capability, the safe range in deep water for surface ships likely to deliver nuclear underwater weapons in the foreseeable future is determined by shock damage to machinery and equipment, rather than damage to the hull.

## Chapter 3

# SHOT UMBRELLA

### 3.1 INTRODUCTION

Shot Umbrella was the underwater detonation of a 10-kt nuclear device in the southwestern part of Eniwetok Lagoon. The device was detonated 9 June 1958 on the bottom in about 148 feet of water. A target array, consisting principally of three destroyers, an EC-2 liberty ship, a submarine (SSK-3) and a submarine model (Squaw), was moored at various ranges and orientations from surface zero. In addition, naval mines were planted in the vicinity to determine mine reactions to nuclear detonations.

3.1.1 Objectives. The objectives of this test are presented in paragraph 2.1.1. In addition, there was the added objective of determining the mine-crushing capability of a nuclear detonation and the mine-actuating influences of such a detonation.

The test objectives and expected test results may be summarized as follows: (1) document the basic-effects data with regard to initial and residual radiation, air overpressures, underwater-shock pressures, crater measurements, mechanics of base surge, and radiological contaminants; (2) document the response of selected targets to underwater shock pressures; and from these objectives to (1) determine safe minimum-standoff distances for delivery of nuclear antisubmarine warfare weapons by existing vehicles; (2) improve predictions of the lethal range of nuclear antisubmarine warfare weapons against submarine type and surface-ship targets in shallow and in deep water; and (3) determine the mine-field-clearance capability of underwater-burst nuclear weapons.

3.1.2 Background. The background of this test is presented in Section 2.1.2. After consideration of many array plans it was finally decided that three destroyers, placed at ranges from moderate-equipment damage to no damage, an EC-2 liberty ship, and the Squaw (Figure 3.1), placed at a severe hull-damage range, would comprise the array (Figure 3.2). An operational submarine (Bonita) was later added to the array. Barges were included for support of project activities. Coracles collected data around the array.

About 1 August 1957, Chief, Naval Operations (CNO) designated the USS Bonita (SSK-3) as the submarine target for Shot Wahoo. The destroyers and the EC-2 were taken into the Long Beach Naval Shipyard on 1 September 1957. The Squaw and YFNB-12 were made ready at the Naval Repair Facility, San Diego, with work starting about 1 September. For Shot Umbrella, it was planned to use standard mooring buoys and anchors to hold the targets in place.

Tables 2.1, 2.2, and 2.3 list the approved projects, project agencies and funding for the two underwater shots, Wahoo and Umbrella. No attempt has been made to separate the costs between the two underwater shots. Therefore, participation and funding for both are indicated in the tables.

Figure 3.1 and Figures 2.2 through 2.6 show the targets and barges used during Shot Umbrella.

3.1.3 Procedure. The procedure used in preparation for Shot Umbrella is discussed in Section 2.1.3.

3.1.4 Preparatory Operations. The preparatory operations described in Section 2.1.4 are

applicable to Shot Umbrella. In addition, a test of the Squaw submergence system was conducted off San Diego, California, in November 1957.

Following the Special Charge Studies, Project 3.1, a meeting of the Target Positioning Advisory Panel was held in Washington. Distances to the target ships from surface zero were set as: EC-2, [REDACTED]; DD-474, [REDACTED] feet; DD-592, [REDACTED] feet; DD-593, [REDACTED] feet; and Squaw, [REDACTED] feet (Figure 3.2).

During the time between the test of the Squaw and the time it was towed to the EPG, the David

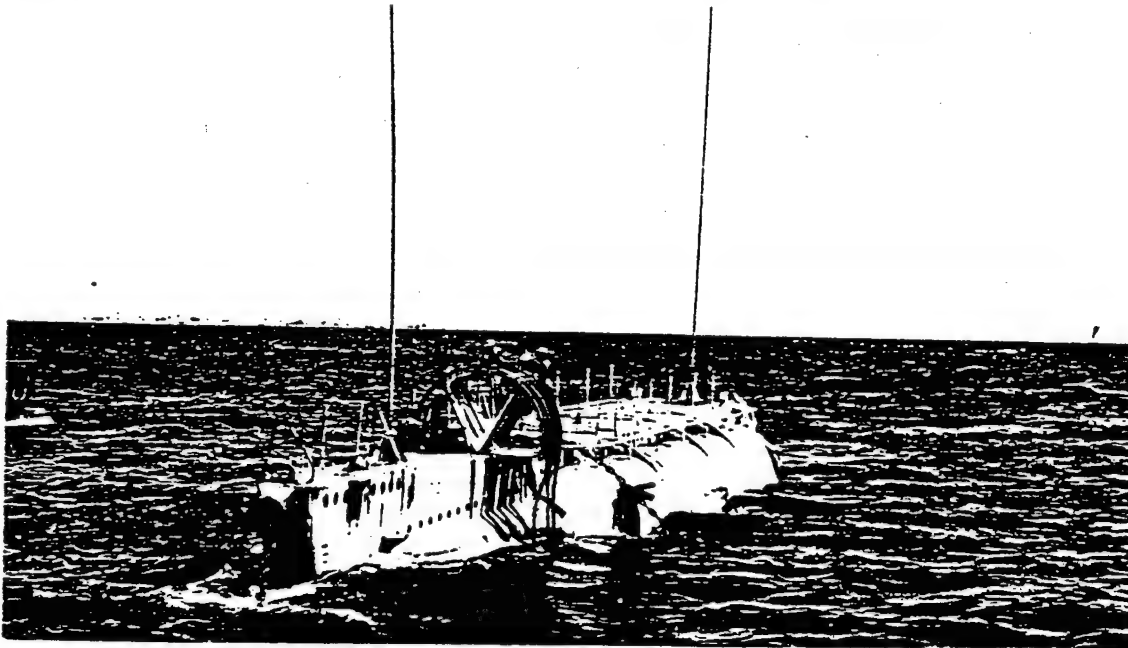


Figure 3.1 Squaw, scale-model submarine construction, previously used during Operation Wigwam, being placed in the target array for Shot Umbrella.

Taylor Model Basin was engaged in installing its instrumentation in the Squaw at the Naval Repair Facility, San Diego, California.

3.1.5 Test Operations. The operational phase of Hardtack began with the movement of personnel and equipment from the United States to the EPG. Ships, barges and equipment were towed or transported from their respective shipyards or ports. More details of the movement of target vessels are found in the previous chapter.

Shot Umbrella was scheduled to follow Shot Wahoo. At 1330 on 16 May 1958, Shot Wahoo was detonated. Early recovery of some data, particularly of a radiological nature, was accomplished before dark on 16 May.

On 17 May the target ships were hosed down, monitored, and data was recovered as safety considerations permitted. When all projects were ready, the ships were taken from their moorings and towed into an anchorage near Site Fred where decontamination was performed using teams from the USS Renville. This was accomplished in about four days.

To assist in target preparation, TG-7.3 again had the repair ship, USS Hooper Island (AR-17),

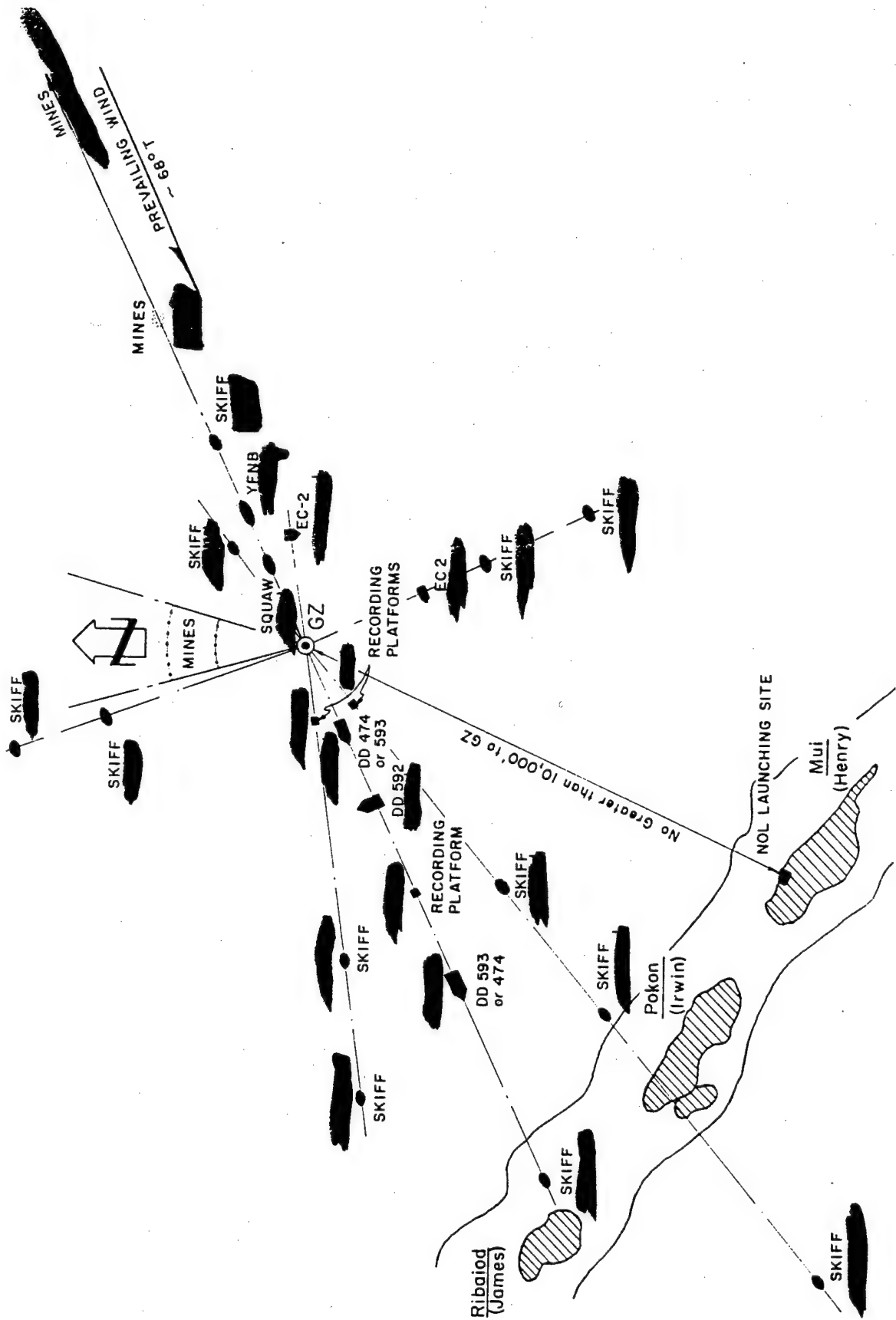


Figure 3.2 Early planning target array for Shot Umbrella.

**SECRET**

moored near Site Elmer. The three destroyers and Bonita were nested alongside the USS Hooper Island for the final field preparations for Shot Umbrella.

While project personnel were readying the targets and other instrumentation, TG-7.3 anchored buoys and barges and made other preparations to place the Shot Umbrella array in proper position.

On 15 April, the Chief, AFSWP, directed that the USS Bonita (SSK-3) be submerged in the Umbrella array at [redacted] feet, bow toward surface zero.

Task Group 7.3 had moored the Umbrella zero buoy on 1 May 1958, to assist those projects making early installations for Shot Umbrella.

On 23 May, the Target Positioning Advisory Panel held a meeting and decided on the following revised distances for the target ships from surface zero: EC-2, [redacted] feet; Squaw, [redacted] feet; DD-474, [redacted] feet; DD-592, [redacted] feet; and DD-593, [redacted] feet. These distances were accepted by the Chief, AFSWP (Table 3.1). Best estimates of exact ranges from surface zero at shot time are shown in Figure 3.3.

Beginning 4 June, the USS Monticello (LSD-35) and the boats assigned from TG-7.3 Boat Pool

TABLE 3.1 TARGET-SHIP DISTANCES FROM SURFACE ZERO FOR SHOT UMBRELLA

All distances shown are horizontal, in feet, from surface zero to the nominal centerline of the ship concerned.

EC-2	[redacted]	Squaw	[redacted]
DD-593	[redacted]	YFNB-12	[redacted]
DD-592	[redacted]	SSK-3	[redacted]
DD-474	[redacted]		

provided transportation to the target-array area and boat service between the barges and ships. The concept was good, but the daily operations were again beset by a series of minor but annoying problems, similar to those encountered prior to Shot Wahoo.

Since some data was lost on Shot Wahoo because of failure to get timing signals, much thought was given to assuring signals during Shot Umbrella. The radio timing central was given two independent sources of power and, in addition, a visual-indicator system was devised to show when a ship lost power supply.

Zero hour of 1100, 8 June, was established.

Following Shot Wahoo, in discussions with technical personnel, it was decided that, if possible, a more stable platform with more antenna room should be provided for the arming and firing operations and for Project 1.11. Investigation disclosed that a surplus LCU was available. Into the well of this LCU, the LCM, with its already installed instrumentation, was placed. Project 1.11 occupied one of the rooms on the starboard quarter of the LCU. The LCU was checked out at Site Elmer and taken on 4 June to the zero buoy where it remained until shot time.

The Squaw and YFNB were moored in the array on 31 May.

The EC-2, DD-474, DD-592, and DD-593 were moored in the array on 1 and 2 June.

On 4 June, a complete rehearsal of procedure of Shot Umbrella was conducted. Token groups of personnel were evacuated from the target array, washdown was in operation, a dummy device was placed in position, the full-frequency full-power dry run was made, and the procedure for early reentry, including the rad-safe survey, was followed. All aircraft missions for U-day were also flown.

Due to an accumulation of delays, it was decided to postpone shot day to 9 June 1958. The remaining days and nights were devoted to last-minute checks and rechecks of instruments,



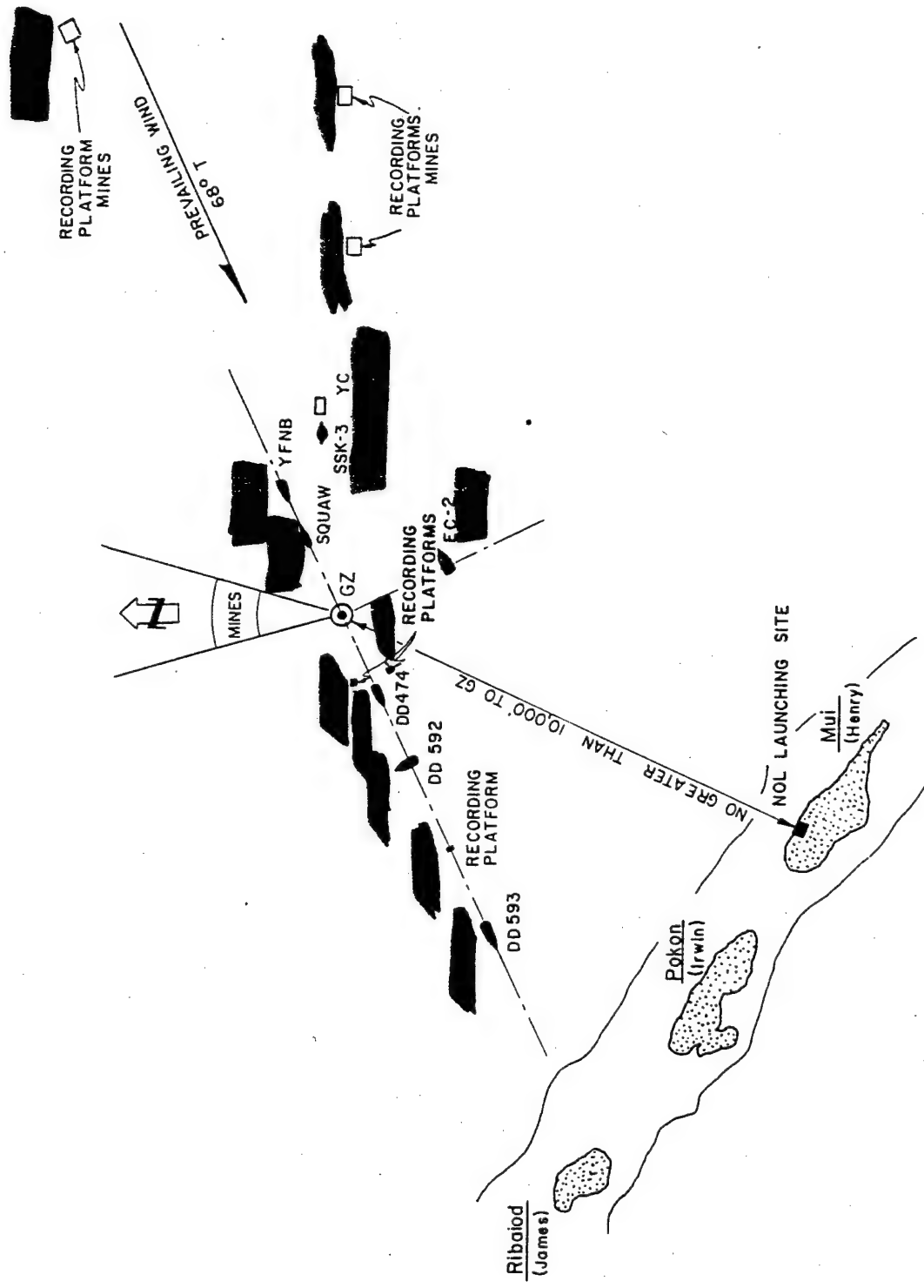


Figure 3.3 Target array for Shot Umbrella.

timing-signal runs, loading cameras, arming coracles, etc.

The Bonita was placed in position on 8 June.

At 0600 on 9 June, the device was lowered into position, final evacuation of the target array was begun, and the USS Grasp left the zero-buoy area about 0900, while ships and boats moved to pre-selected anchorages, generally east of surface zero, to wait for the detonation.

About 1030 a fifteen-minute delay was called to wait for better cloud conditions.

At 1115, 9 June 1958, the Umbrella device was detonated.

It was soon determined that there was not as much radiological contamination as had been anticipated. Using a prearranged entry plan, the early recovery of data and instrumentation was begun within two hours after shot time. By 1600 on 10 June, the early-data recovery was completed and the ships were broken from their moorings. The ships were taken to Site Elmer where the remaining project data was removed, damage surveys were conducted, and the ships made ready for return to the United States.

The EC-2 was found to be too badly damaged for economical repair. Permission was obtained to dispose of the ship, and it was sunk by gunfire in deep water off Eniwetok Atoll.

The USS Bonita was returned to the United States under its own power.

The DD-474, DD-592, DD-593 and Squaw YFNB were towed to the United States.

### 3.2 BLAST AND SHOCK

Study of free-field blast and shock phenomena from the shallow water shot, Umbrella, was accomplished by six projects. Their general objective was to correlate data obtained with results from Shot Baker of Operation Crossroads and high-explosive tests, with the aim of improving methods of predicting blast and shock phenomena for any underwater burst geometry in shallow water.

3.2.1 Umbrella Preshot and Postshot Bathymetric Surveys. A preshot bathymetric survey was made of a selected area of Eniwetok Lagoon to facilitate selection of the shot site and for use in placement of equipment and analysis of data. This survey was accomplished under the general direction of the Columbia University Geophysical Field Station in September and October 1957; however, Project 1.13 increased the density of data around surface zero during Operation Hardtack, using a TG-7.3 LCM equipped with a fathometer. Combined results shown in Figure 3.4 indicate the lagoon has an average depth of about 23 fathoms, with numerous coral heads one or two fathoms high.

Interest in the Shot Umbrella crater stemmed from possible use of bottom bursts in such civil applications as harbor construction and possible side benefits from military use of a weapon, such as formation of a crater lip which would make harbors inoperative. A postshot bathymetric survey was, therefore, made to ascertain the extent of the Umbrella crater and lip. An LCM, equipped with a fathometer, was used to document postshot water depths, starting on D + 1 day. Positioning and control of the boat were accomplished by cross bearings from known stations on Sites Keith and Glenn, and appropriate radio communications. Some lead-line soundings were also taken, and these showed little difference from fathometer readings. Four cross sections through ground zero are shown in Figure 3.5. Because of the extremely uneven preshot terrain, values for maximum crater depth and radius can only be grossly estimated. Crater depth appears to be less than 15 feet but is as much as 30 feet in regions where preshot high points existed. Crater radius appears to be about 900 feet. Crater lip height, if any, was too small to be measured by a fathometer. The crater was shallower and wider than TM 23-200 predictions of 100-foot depth and 550-foot radius, thus indicating need for further studies of craters from water-contained explosions.

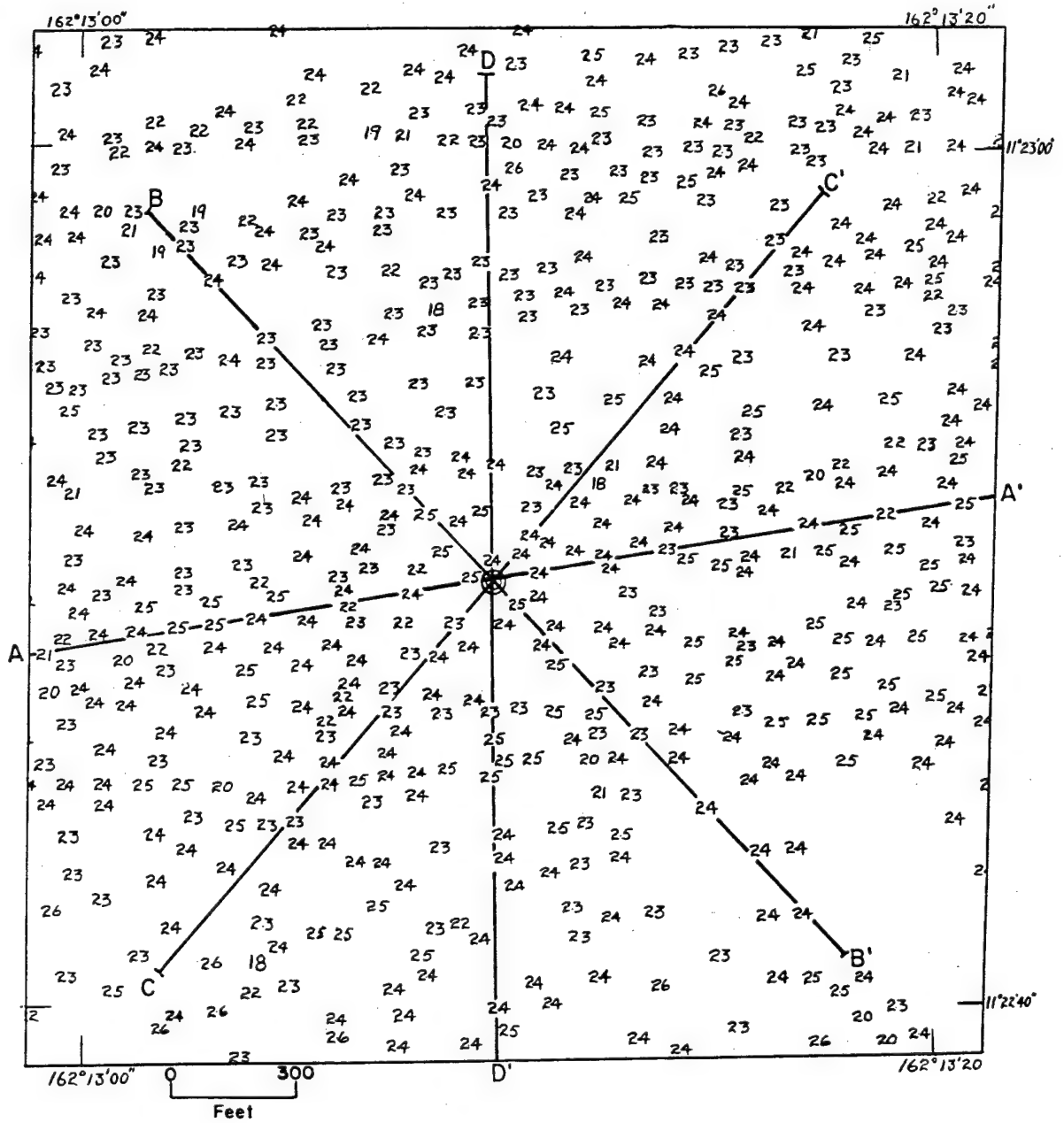


Figure 3.4 Preshot hydrographic survey of the Umbrella area. Soundings in fathoms.

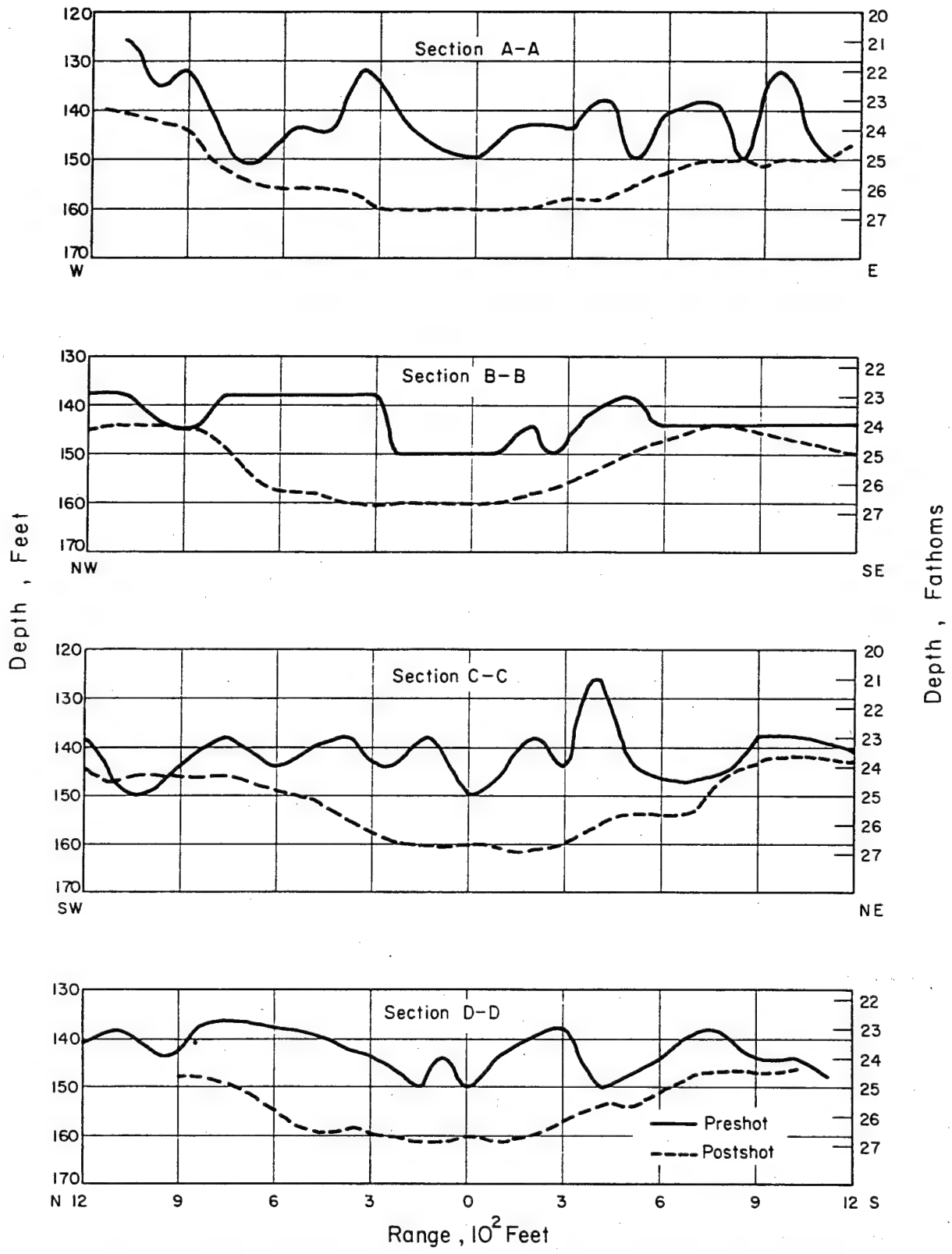


Figure 3.5 Bottom profiles through surface zero prior to and after Shot Umbrella.



3.2.2 Hydrodynamic Yield Determination. During Operation Wigwam, Armour Research Foundation (ARF) measured the time of arrival of the shock wave at selected points between the underwater shot point and the water surface. From the shock arrival data, ARF computed the shock-wave velocity versus range and then obtained the total-energy release of the device on the basis of theoretical considerations (Reference 14). For Operation Wigwam, the yield computed from this approach was considered to be quite reliable. The Operation Wigwam technique was re-instituted on Shot Umbrella primarily to provide a check on the energy partition between water and ground for the bottom-burst geometry. Shot Wahoo was to provide the free-water pressure-distance curve for the device. Secondary objective on Shot Umbrella was to provide a check on total yield.

Experimental Plan. Instrumentation, as shown in Figure 3.6, was essentially the same as used on Operation Wigwam. Two strings of pressure switches and a doppler cable were attached to the weapon-suspension cable. Closure of the pressure switches by the shock wave triggered a pulse generator whose response was telemetered to a receiving station. Shock-wave velocities were to be determined from the time interval between closures. A doppler coaxial cable was also installed to provide a measurement of shock velocity. A signal from a radio-frequency oscillator, transmitted down this cable, was to be reflected at the end crushed by the shock wave. The reflected signal and oscillator signal were to be mixed, amplified, and telemetered to the receiving station. This telemetered signal, the doppler frequency, would be directly proportional to the shock-wave velocity.

Preshot tests showed considerable interference with reception of telemetered signals from surface zero at Site Parry and adjacent islands. Therefore, a receiving station was set up on an LCU. Use of the LCU permitted movement to a good zone of reception, approximately [redacted] feet north of surface zero.

Results. Of two sets of pressure switches and one coaxial cable installed, only one set of pressure switches provided data. Measured times of shock arrival and computed values of shock velocity, overpressure, and total yield are shown in Table 3.2. As can be seen, a consistent yield was not obtained. At Gage 29, shock velocity was approaching sound velocity, so value of yield computed for this point can be disregarded. An average of the remaining points gives a total yield of 6.45 kt or effective yield of  $6.45 \times 1.6 = 10.3$  kt. This compares to the expected total yield of 10 kt and expected effective yield of 16 kt.

Figure 3.7 compares the Umbrella pressure-distance curve with that predicted from Operation Wigwam. The measured curve crosses the predicted decay line in such a manner that in one half of the region of interest the effective yield appears below, and in the other half above the 16 kt expected. Determination of energy partition between coral and water must await an adequate explanation of this unexpected slope of the measured curve.

3.2.3 Underwater Shock Pressures. Information from peak-pressure measurements and from limited amounts of pressure-time data obtained on Shot Baker of Operation Crossroads was inadequate to enable predictions of loading to ships and submarine targets from underwater shots in shallow water. Work with high explosives indicated general agreement with peak-pressure results of Shot Baker, Operation Crossroads, but left considerable uncertainty as to predictions of impulse for a nuclear shot. As a result, there was a real need for a substantial program for measuring underwater pressures as a function of time and distance from Shot Umbrella. These measurements were to be used by ship-damage projects to provide characteristic loading functions on target ships and so, when correlated with information on ship response and damage, provide a sound basis for determination of pertinent operational techniques. Naval Ordnance Laboratory (NOL) was the project agency for obtaining the pressure-time histories.

Experimental Procedure. NOL established 16 stations, with gages at depths of 10 to 130 feet, at ranges from 473 to 7,900 feet. The primary electronic gages were backed up by

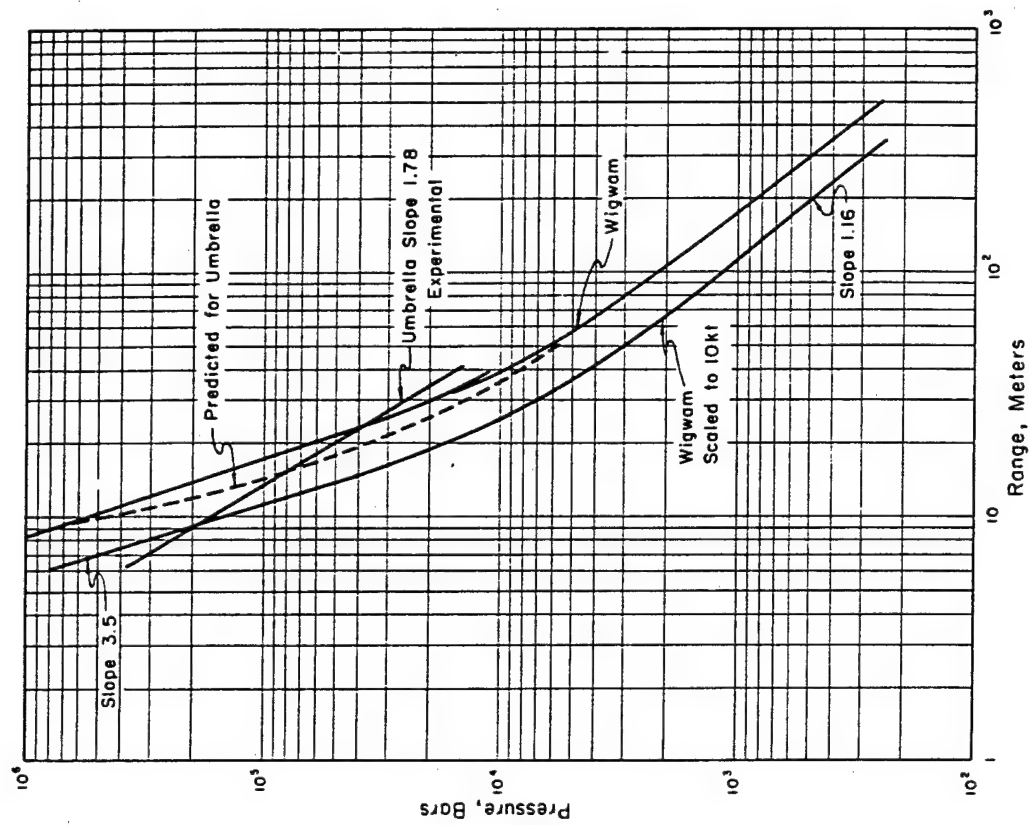


Figure 3.7 Pressure versus distance for Umbrella and Wigwam.

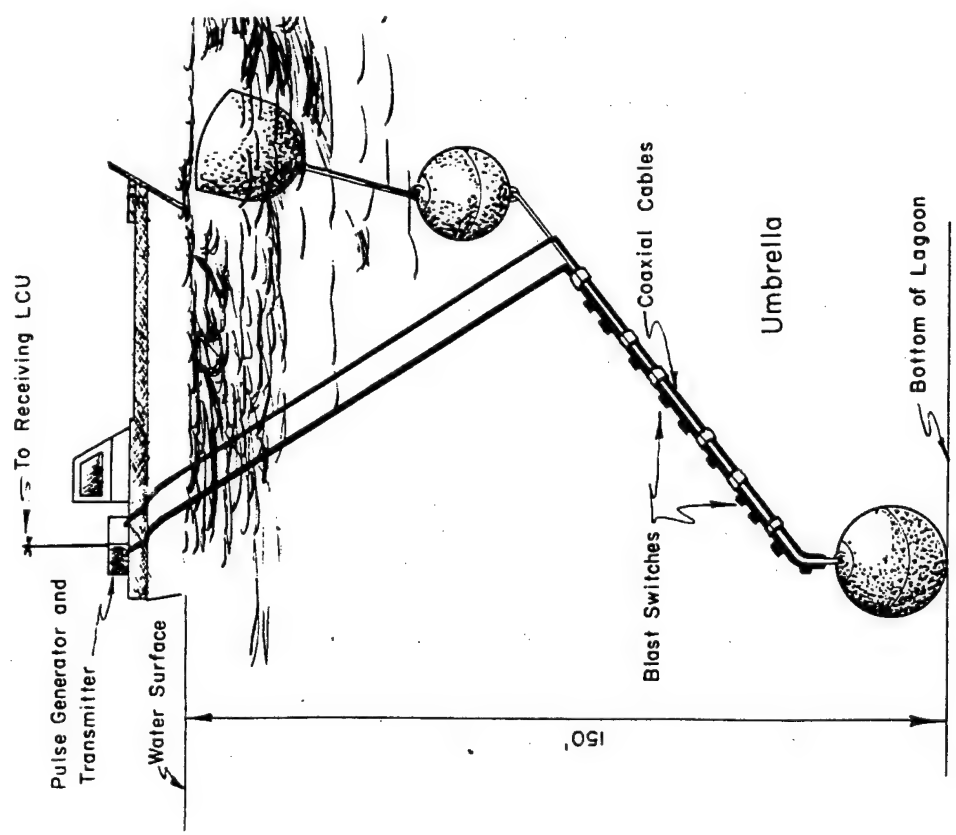


Figure 3.6 Instrumentation for early time-of-arrival data.

both mechanical pressure-time (p-t) and ball-crusher (b-c) gages. Vertical gage strings were deployed from all three destroyers, the YFNB, EC-2, 5,500-foot barge, and two close-in linear arrays composed of buoys and barges. Electronic strings, suspended from the close-in buoys, reported to recorders in barges at ranges of [redacted] feet. Alternate electronic gages from each string reported to separate recorders to insure against complete loss of data from any one station.

Results. A typical electronic p-t record obtained is shown in Figure 3.8. Mechanical pressure-time (mpt) and electronic pressure-time (ept) records were in good agreement. The low-amplitude pulse in advance of the main shock, reaching an overpressure of three psi, was found on almost all records. It was due to energy traveling first through the ocean bottom and then transferring into the water and is referred to herein as the ground wave. The direct shock wave was followed by a negative phase during which cavitation occurred. The second positive pulse of 61 psi was caused by cavitation closure. Although not shown, the cavitation pulse was

TABLE 3.2 SUMMARY OF EARLY HYDRODYNAMIC DATA, SHOT UMBRELLA

Gage Number	R = Radius from Bomb meters	t = Time of Arrival μsec	n *	U = Velocity m/sec	P = Pressure bars	R/W <sup>1/3</sup> meter/kt <sup>1/3</sup>	W = Total Yield kt
11	4.51	16	—	—	—	—	—
15	7.15	238	0.30	9.0 × 10 <sup>3</sup>	4.0 × 10 <sup>5</sup>	4.4	4.25
17	9.00	451	0.35	6.98 × 10 <sup>3</sup>	2.2 × 10 <sup>5</sup>	6.3	3.4
21	14.20	1,311	0.45	4.87 × 10 <sup>3</sup>	8.5 × 10 <sup>4</sup>	8.3	5.0
23	17.9	2,111	0.48	4.08 × 10 <sup>3</sup>	5.6 × 10 <sup>4</sup>	9.4	6.8
27	28.1	4,951	0.53	3.03 × 10 <sup>3</sup>	2.45 × 10 <sup>4</sup>	12.0	12.8
29	35.2	7,331	0.54	2.59 × 10 <sup>3</sup>	2.14 × 10 <sup>4</sup>	12.5	22.0

$$* n = \frac{\log (R_2/R_1)}{\log (t_2/t_1)} = U \frac{t}{R}$$

followed by numerous small pulses, more pronounced at greater ranges, which may have been the result of waves reflected or refracted from ground layers deep beneath the ocean bottom. In general, the pressure-time records were similar in shape to those from high-explosive tests.

Arrival times of the main shock, cavitation, and ground-wave pulses versus ground range are shown in Figure 3.9. A weak ground wave was found at all but the 473-foot station. Cavitation pulses were also found at all but the 473-foot station; however, at ranges inside 1,700 feet identification was difficult because of the presence of many small amplitude pulses. Figure 3.9 shows the main shock arrived at greater time intervals after the ground wave as ranges increased. The cavitation pulse appeared first about 500 msec after detonation, approximately 2,000 feet from surface zero, and propagated away in both directions. At ranges beyond 3,000 feet, the cavitation pulse appeared within a few milliseconds after the main shock.

Selected b-c gage peak pressures versus distance are plotted in Figure 3.10. The large variations in pressure observed from Operation Crossroads ball-crusher results were not found. For the first 70 to 80 feet down, pressures, with a few exceptions, were essentially constant. Below 70 to 80 feet, pressures decreased with depth. Pressures at the deepest gages, 130 feet, were 15 to 25 percent less than those near the surface. Readings at like depths and ranges showed a scatter of 10 to 15 percent.

Selected ept and mpt gage peak overpressures versus distance are plotted in Figure 3.11. Ept gage pressures from 25 feet down to mid-depth, 60 to 80 feet, were fairly constant at all stations. Ten-foot-deep ept gages at all stations recorded pressures lower than gages below. Below mid-depth, peak pressures decreased with depth at most ept stations. Shallowest mpt

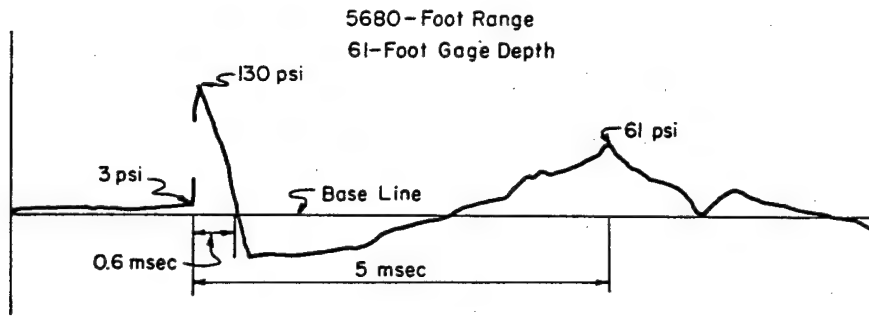


Figure 3.8 Shock-wave record.

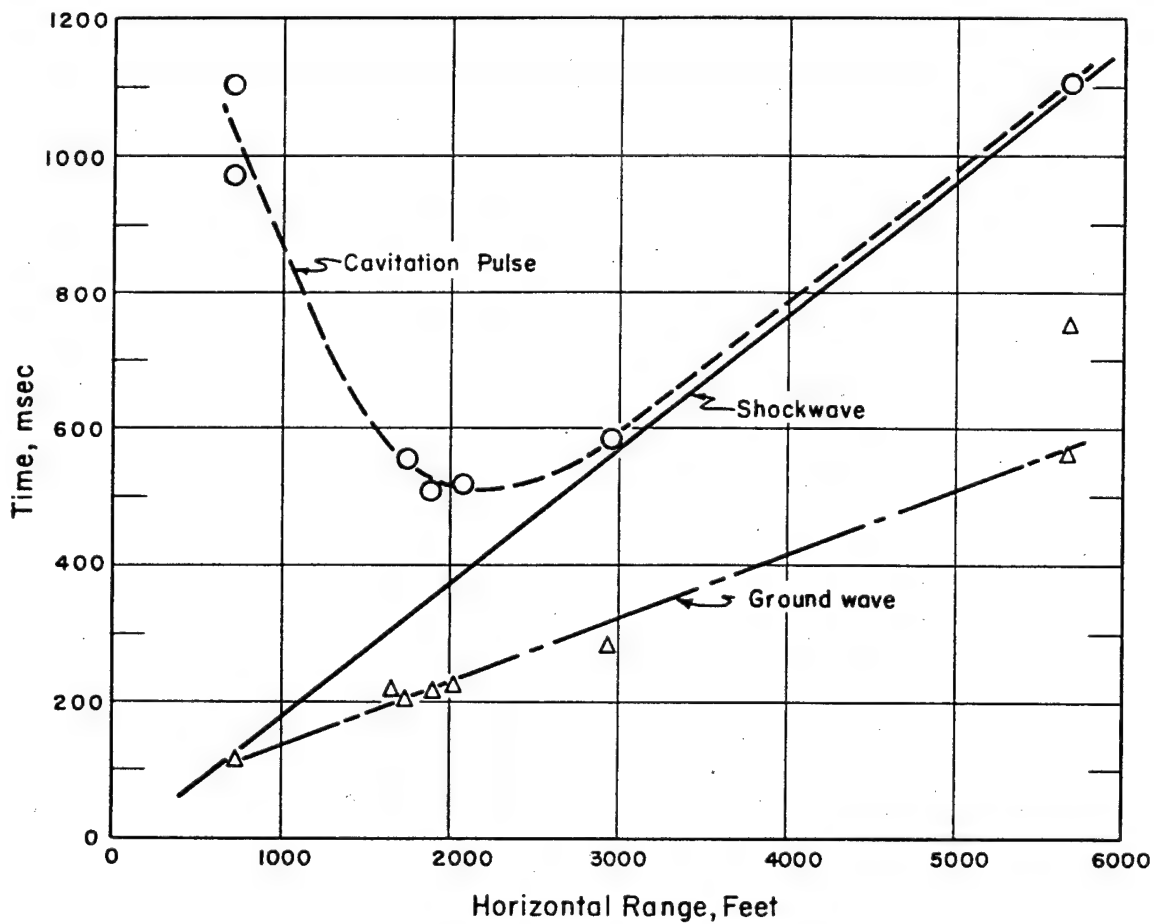


Figure 3.9 Arrival times versus horizontal distance, Shot Umbrella.



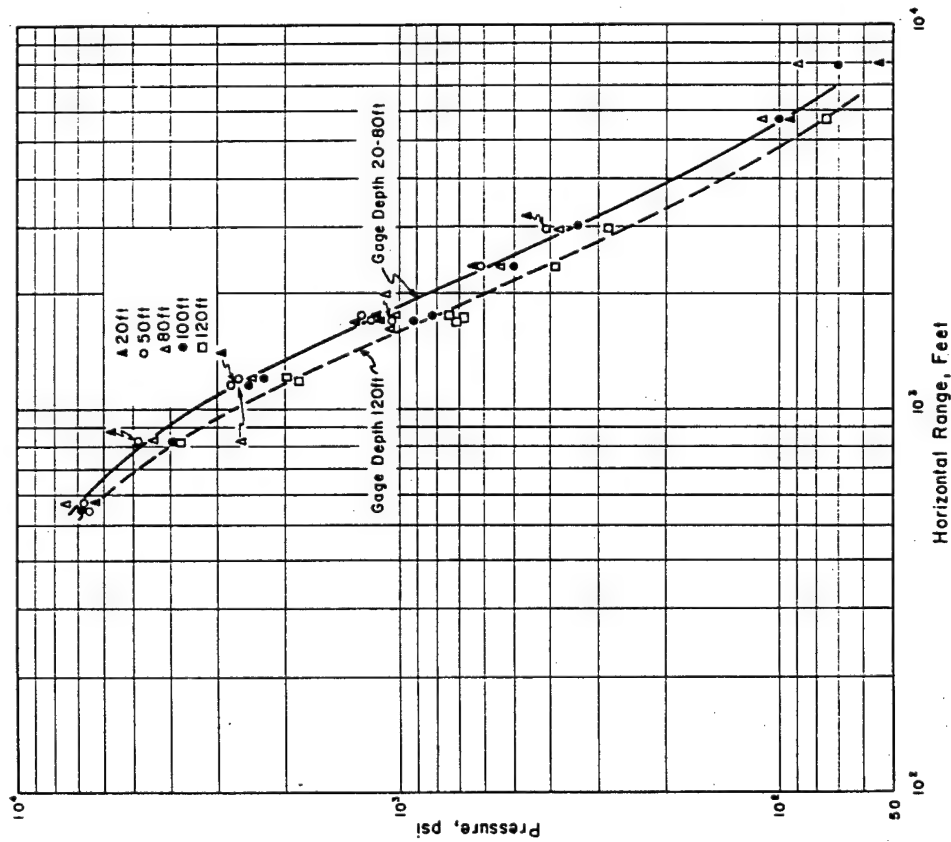


Figure 3.10 BC gage peak pressures at various depths versus distance, Shot Umbrella.

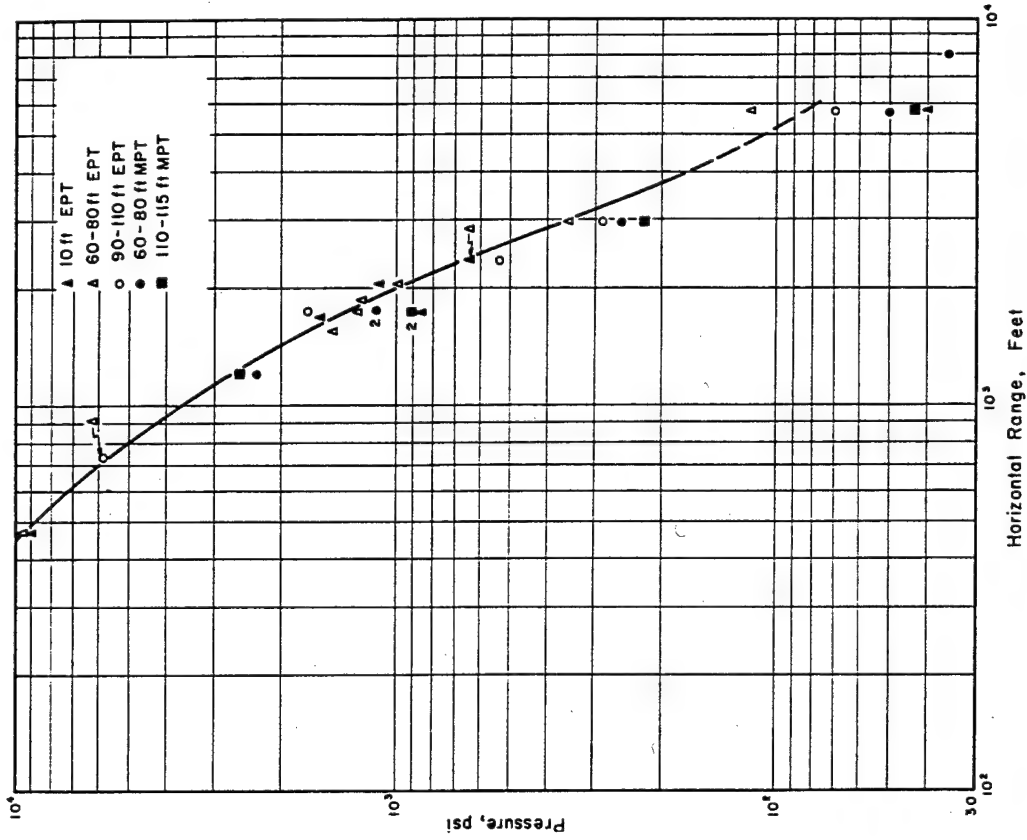


Figure 3.11 EPT and MPT gage peak pressures at various depths versus distance, Shot Umbrella.

gages were at 17 feet; one only of three showed a lower pressure than mid-depth readings. Most mpt stations showed the decrease in pressure in the bottom half of the string found on b-c and mpt results.

Figure 3.12 shows shock-wave durations as a function of distance, as measured on ept records. Duration increased regularly with depth and decreased with range.

Peak overpressures from mid-depth ept gages are compared with predictions and cube root scaled Baker b-c results in Figure 3.13. Plotted circles, values which were predicted by NOL for a 10-kt radiochemical yield under Umbrella conditions, are seen to be in excellent agreement with results.

In summary, Umbrella p-t and b-c gages from 473 to 7,900 feet from surface zero, at depths from 10 to 130 feet, recorded peak pressures ranging from 19 to 9,640 psi. Peak pressures at mid-depths were in agreement with predictions. Pressures decreased with depth in the lower half of the lagoon. A weak ground wave preceding the main pulse was observed on almost all records. Main shock durations at 70-foot depths decreased with range from about ten milliseconds at 474 feet to fractions of a millisecond beyond 5,000-foot range. Shock wave durations increased regularly with depth. A second pulse, due to cavitation, was observed at all but the 474-foot station. This pulse appeared first near 1,900-foot range and then moved toward and away from surface zero. Maximum cavitation pressure recorded was 314 psi, at 1,900-foot ranges.

**3.2.4 Visible Surface Phenomena.** Main military interest in water thrown up by an underwater burst is in the role it plays in spreading radioactive contaminants. The cauliflower cloud from a shallow burst may be the source of high energy initial gamma radiation. Clouds and base surge may transport contaminants downwind for several miles. It is important, therefore, that the source of these phenomena be understood and that reliable scaling laws be established. Most of existing theory and scaling laws for slicks, water columns, plumes, fallout, base surge, and foam rings are based on high-explosive data. The limited nuclear data which was available from Shot Baker of Operation Crossroads exhibited some pronounced differences from high-explosive results, so extrapolation of high-explosive-developed equations to the nuclear situation was uncertain. NOL accordingly undertook, with photographic support from Edgerton, Germeshausen and Grier (EG&G), to document the formation, growth, and dissipation of the visible surface phenomena of Shot Umbrella with the objective of improving existing scaling techniques. As on Shot Wahoo, visible surface phenomena were recorded by timed technical photography from four surface stations and four aircraft.

**Results.** From the air, subsurface luminosity was visible within two or three milliseconds after detonation and lasted about 10 milliseconds. An expanding white circular patch with dark fringe became visible about 15 milliseconds after detonation. The white patch was the spray thrown up by the impact of the direct shock wave, and the dark fringe, or slick, was the intersection of the direct-shock wave with the air-water surface. The dark fringe was visible out to a radius of 2,200 feet. At about 0.5 second, spray, believed to have been thrown up by the cavitation pulses, began to form with a radius of approximately 1,800 feet. This annulus of spray grew inwardly and merged at 1.01 seconds with the inner, solidly white, spray area at a radius of about 1,300 feet, forming a solid white patch with a radius of approximately 1,800 feet.

Viewed from the surface, the first effect seen was the air shock wave; this was visible for 80 to 100 msec. A bell-shaped dome of spray then began to form. Three stages of development of water throwout are shown in Figure 3.14. During a few tenths of a second, the bell-shaped dome was transformed into a vertical plume formation. Driven rapidly upward by expanding steam generated by the burst, the top of the plume formation reached 3,500 feet at 5 seconds, 5,000 feet at 10 seconds, and a maximum height of 5,800 feet at 25 seconds after surface zero time.

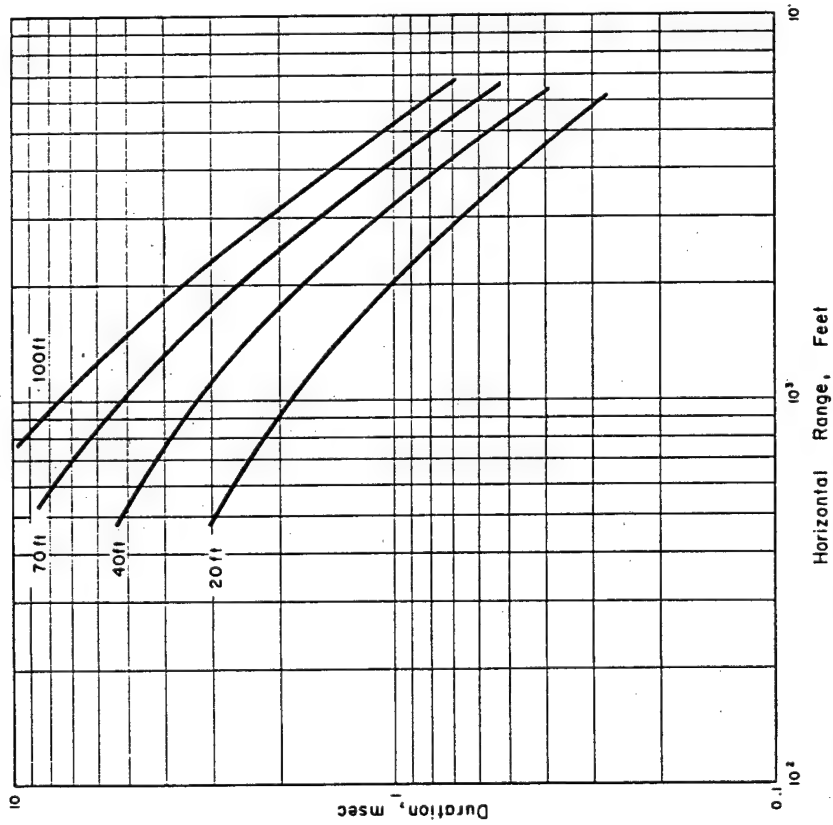


Figure 3.12 Shock-wave durations at various depths versus distance, Shot Umbrella.

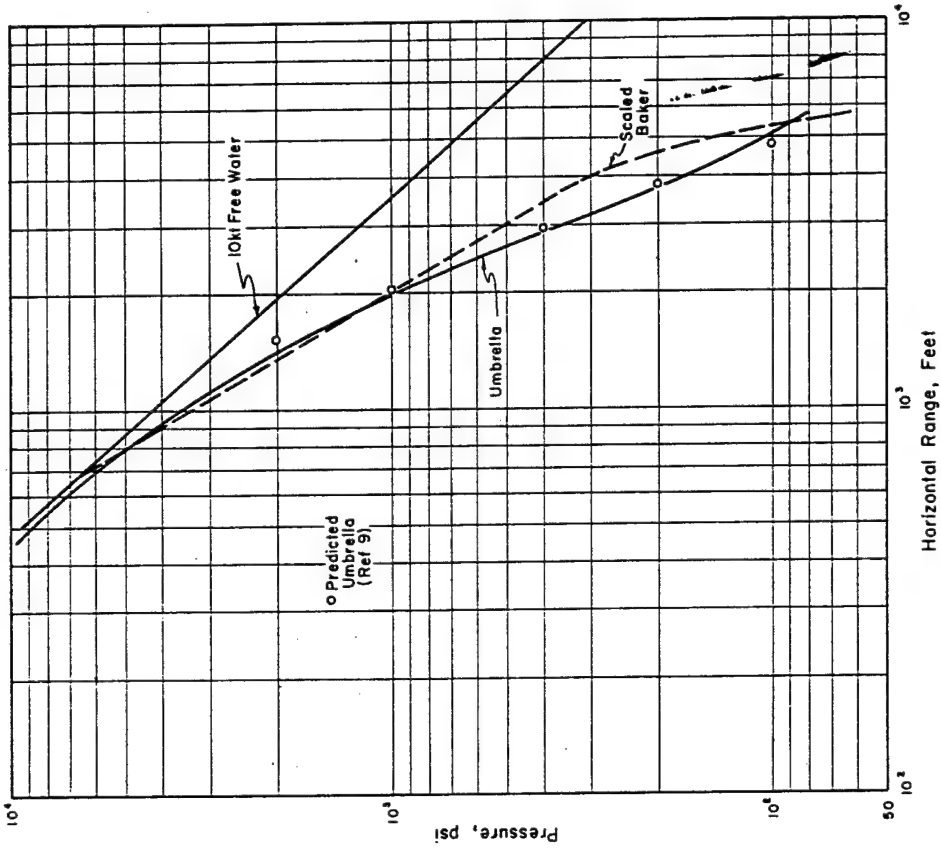
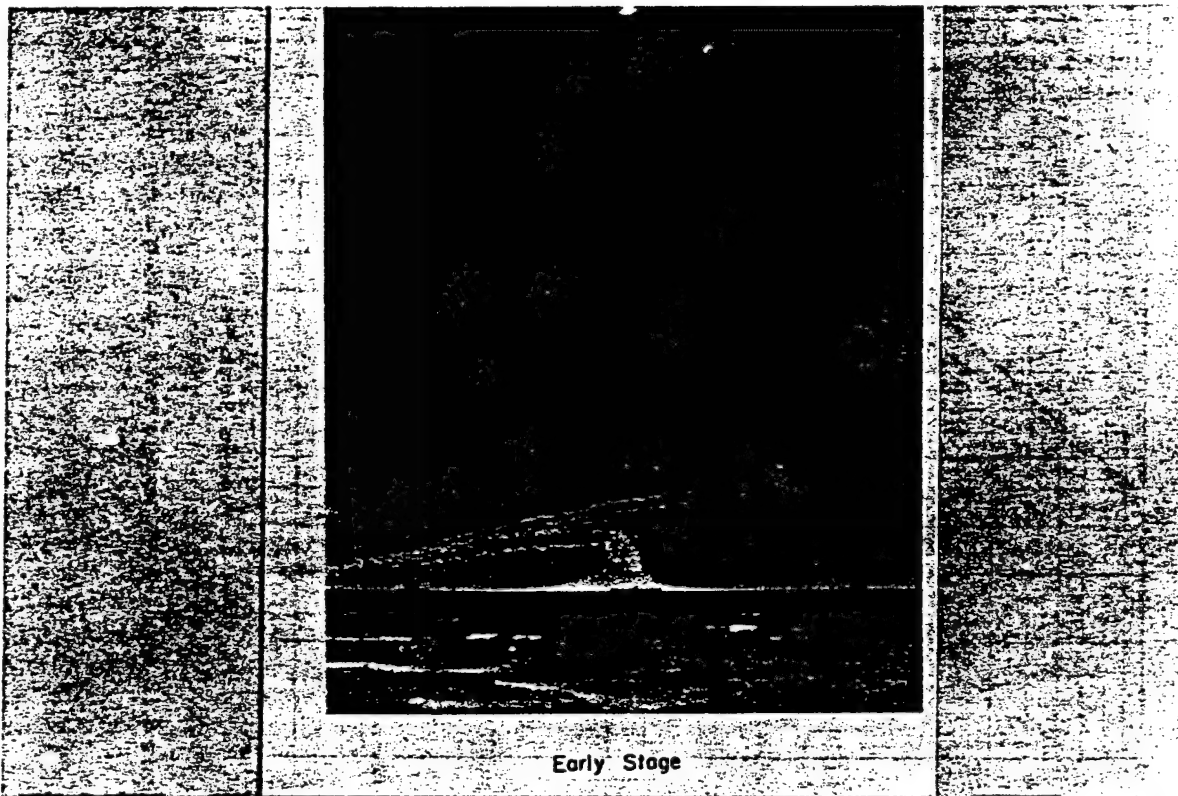
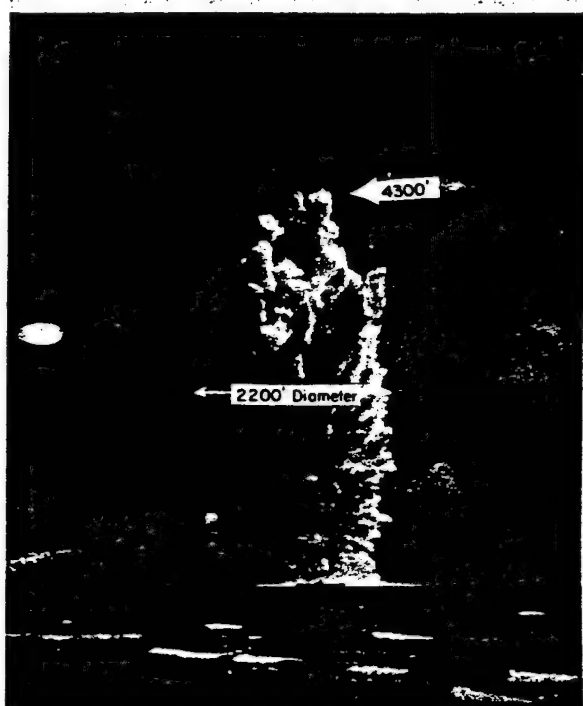


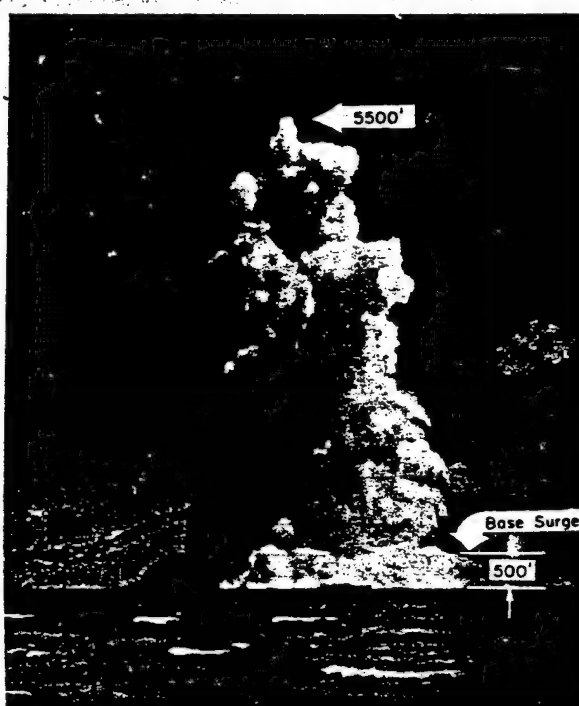
Figure 3.13 Shock-wave peak-pressure comparisons, Shot Umbrella.



Early Stage



Just Prior to Collapse



Collapse and Formation of Base Surge

Figure 3.14 Development of throwout, Shot Umbrella.

First indication of base surge was seen about 13 seconds after surface zero time. The surge was roughly circular in shape but not smooth in outline. By 42 seconds, it was 5,000 feet downwind and 3,400 feet upwind (Figure 3.15) and appeared as an outward moving elliptical ring. At 25 minutes, the longest available record, the surge was still visible as a well defined toroidal cloud.

In crosswind direction, base surge progressed outward at average radial velocity of 55 knots from 20 to 40 seconds, 21 knots from 40 to 120 seconds, and 9 knots from 2 to 5 minutes after surface zero time. By 7 minutes after surface zero time, the dynamic stage of base-surge expansion appeared to have ended, with a crosswind radius of some 9,700 feet having been attained. This was followed by a further, very gradual, expansion by turbulent diffusion.

The height of the surge cloud increased steadily; at 20 seconds after surface zero time, highest parts were at 500 feet, at 40 seconds at 900 feet, and at 75 seconds at 1,850 feet.

Since most of the plume formation falls back into the water rather than into a surge formation, the extent of this fallout was of interest. Visible fallout was observed to extend some 1,000 to 1,500 feet upwind and crosswind of surface zero. As the larger drops fell out, the settling cloud became more and more of a tenuous mist. Fallout mist, distinct from base surge, was visible until three minutes after surface zero time; visible fallout area extended downwind about 7,000 feet in a path some 2,000 to 3,000 feet wide.

A white circular patch of water shown at the top of Figure 3.15 became visible at surface zero as the mist cleared and base surge moved out. Patch diameter was about 5,300 feet at 2.5 minutes, 7,200 feet at 8 minutes, and 8,300 feet at 23 minutes. It was still clearly visible in the last picture taken at 25 minutes, probably because of suspension of considerable amounts of pulverized bottom material in the water.

3.2.5 Air Overpressures. Military interest in air blast from an underwater shot stemmed primarily from the potential use of aircraft for atomic attacks against submarines. Shot Baker of Operation Crossroads provided considerable overpressure data, and a few pressure-versus-time records were obtained near the level of the target-ship decks. Shot Baker data was insufficient by itself, however, to check the validity of scaling relationships developed from more numerous high-explosive test data. It was hoped that comparison of Shot Umbrella underwater and p-t data would lead to an understanding of the mechanism by which energy is transmitted across the water-air interface. This knowledge and comparison of nuclear and high-explosive data were expected to provide better predictions of air blast from nuclear shots in shallow water.

Experimental Plan. The major NOL effort to measure air blast on underwater shots was on Shot Umbrella. Ultradyne and mpt gages were mounted on vertical masts rising 15 feet or more above ship decks, or on horizontal spars extending out from ships. These near-surface gages were on the DD's 474 and 593, EC-2, buoy at [redacted] feet, and barges at [redacted] and [redacted] feet from surface zero. Mpt gages were suspended at 500 and 1,000-foot altitudes from five balloons moored on the three destroyers, and on the [redacted] and [redacted] foot barges. Thirty-two canisters containing mpt gages were deployed by rockets to altitudes up to 15,000 feet, and ground ranges to 8,000 feet. Figure 3.16 shows the two rocket-launching stations, DD-592 and Site Henry, and the photo and radar stations for determining canister positions. Finally, five rockets launched from the DD-592 provided smoke trails. High-speed photographs were taken of the shock interaction with the trails, and direction of flow behind the wave front.

Details of the mpt gage are shown in Figure 3.17. Each gage was calibrated dynamically in a shock tube. Rise times, when critically damped, were found to be 7 msec for 1-psi gages and 3 msec for 5-psi gages. Very little distortion of the applied wave form was found. Also, changes in gage orientation with respect to the shock wave produced negligible changes in readings for pressures less than 2 psi.

The overall rocket canister containing the pressure unit and other elements is shown in Fig-

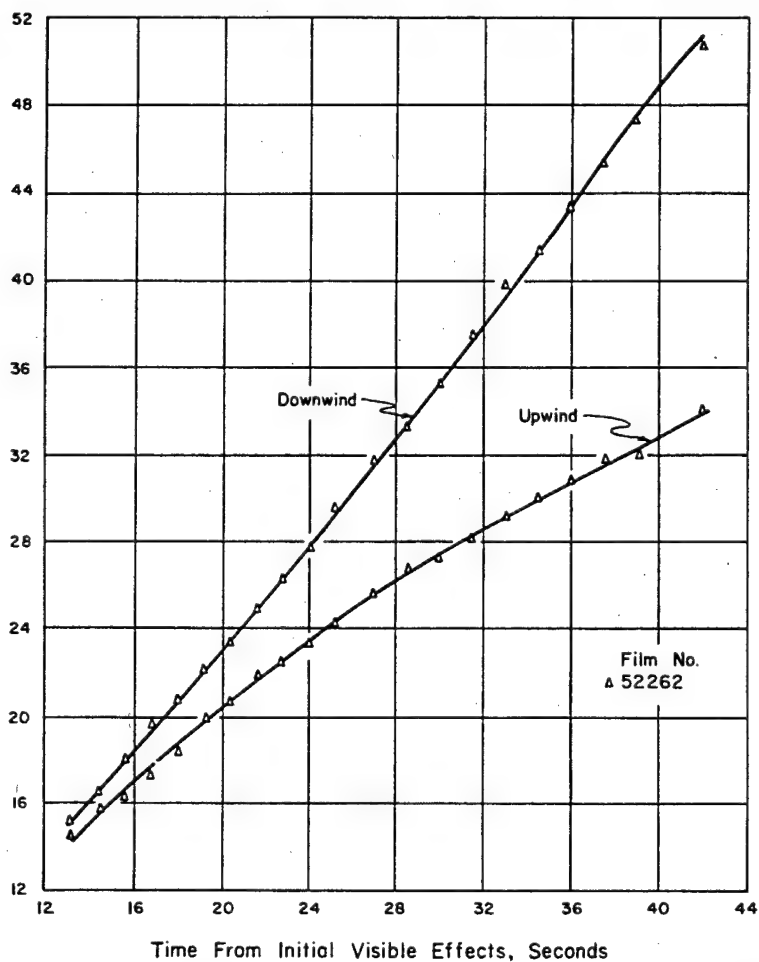


Figure 3.15 Base surge upwind and downwind extent, at early times, Shot Umbrella.



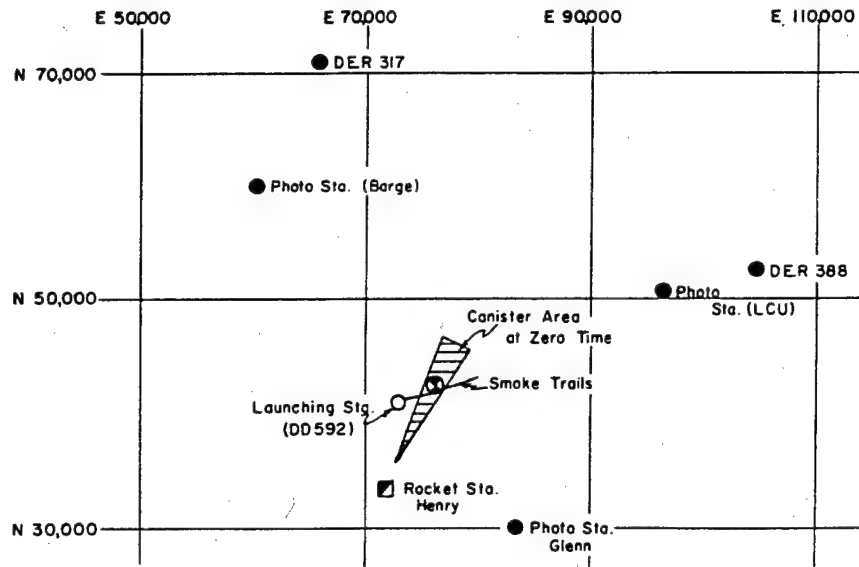


Figure 3.16 Rocket, camera, and radar ship stations.

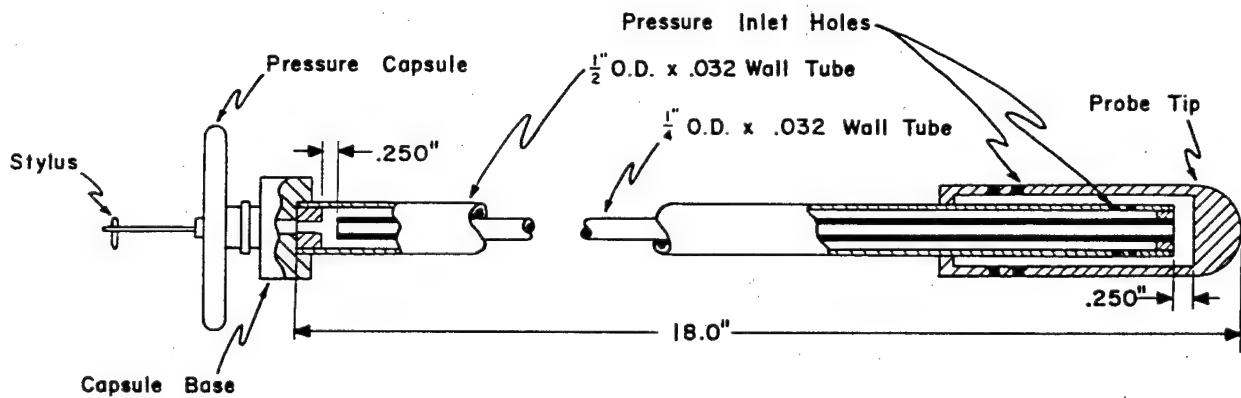


Figure 3.17 Details of pressure probe.

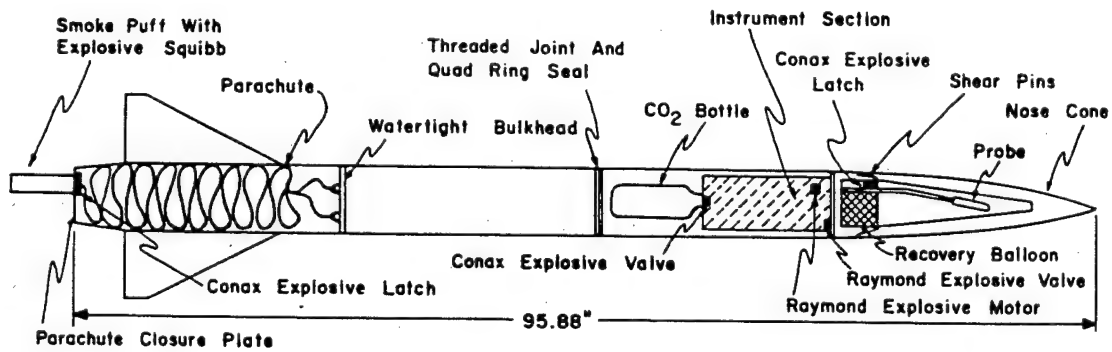


Figure 3.18 General layout of dart.

ure 3.18. The watertight section was to keep the canister afloat. The balloon in the forward compartment was inflated with CO<sub>2</sub>, with the explosive valve being set off by a sea switch. The balloon was used to assist in sighting the canister during recovery operations. An antenna was attached so that it would be free of the water when the balloon was inflated. This antenna fed a UHF locator beacon of approximately sardine-can size, which was located in the instrument section.

Results. Three LCM's and one LCU equipped with a DUKW were in the impact area by H + 1 hour and recovered 20 of the 32 rockets deployed. These vessels were assisted by an L-20, equipped with radio-direction-finder (RDF) gear, and an H-21 helicopter. The majority of the units were sighted from the air and marked by smoke flares dropped from the H-21; RDF equipment was used only to recover one unit. It is believed the missing units were damaged and sank. The surface craft also recovered the balloon gages from the DD-592. Of the four other balloons, three were carried away by gusty 35-knot winds prior to shot time, and one broke away immediately after the shot.

Photographic triangulation on the test was successful, although data has not yet been reduced.

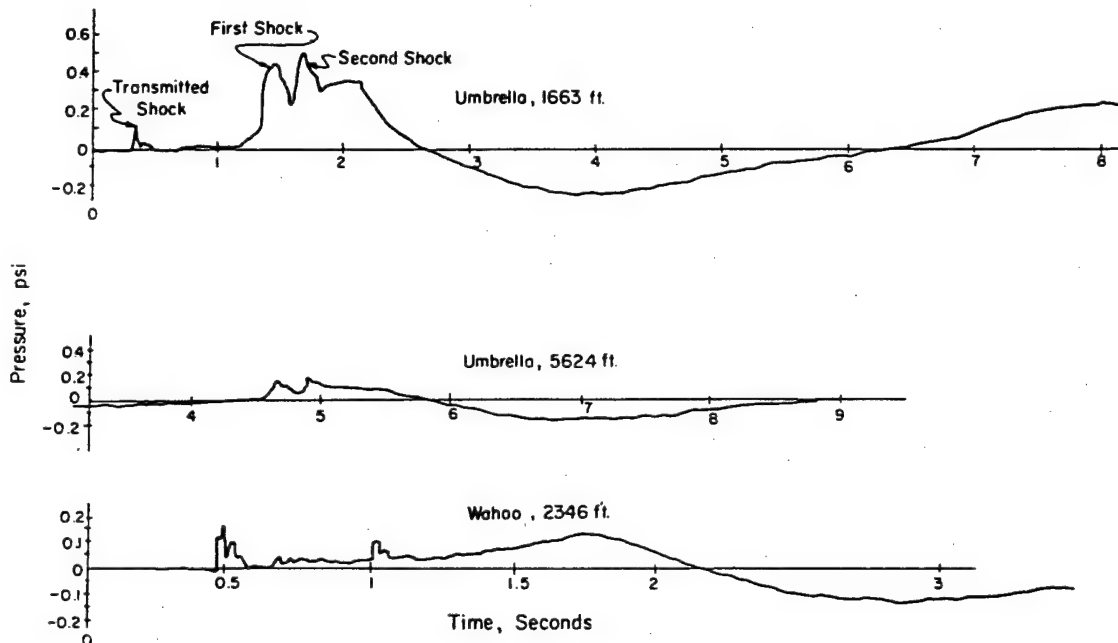


Figure 3.19 Three Ultradyne gage records.

Radarscope photography provided by two DER's failed to show parachute blips until M + 3 minutes because of cluttering by strong side-lobe echoes from other surface vessels.

Mpt records on Shot Umbrella showed only one distinct shock pulse. The typical canister record, which requires correction for fall of the canister, showed slow decay from the peak. Ultradyne records, Figure 3.19, all showed at least two pressure maxima of about the same magnitude, spaced about 230 msec apart, and a gradual descent to a negative-pressure minimum between 4 to 7 seconds after zero time.

Peak mpt overpressures shown in Figure 3.20 were almost all low compared to the high-explosive curves which were based on one-pound charges of TNT fired at scaled depths of 145 feet. High-explosive data were scaled to 10 kt by the cube-root law. Indicated gage positions shown are based on ballistic data and may be radically changed when photographic data becomes



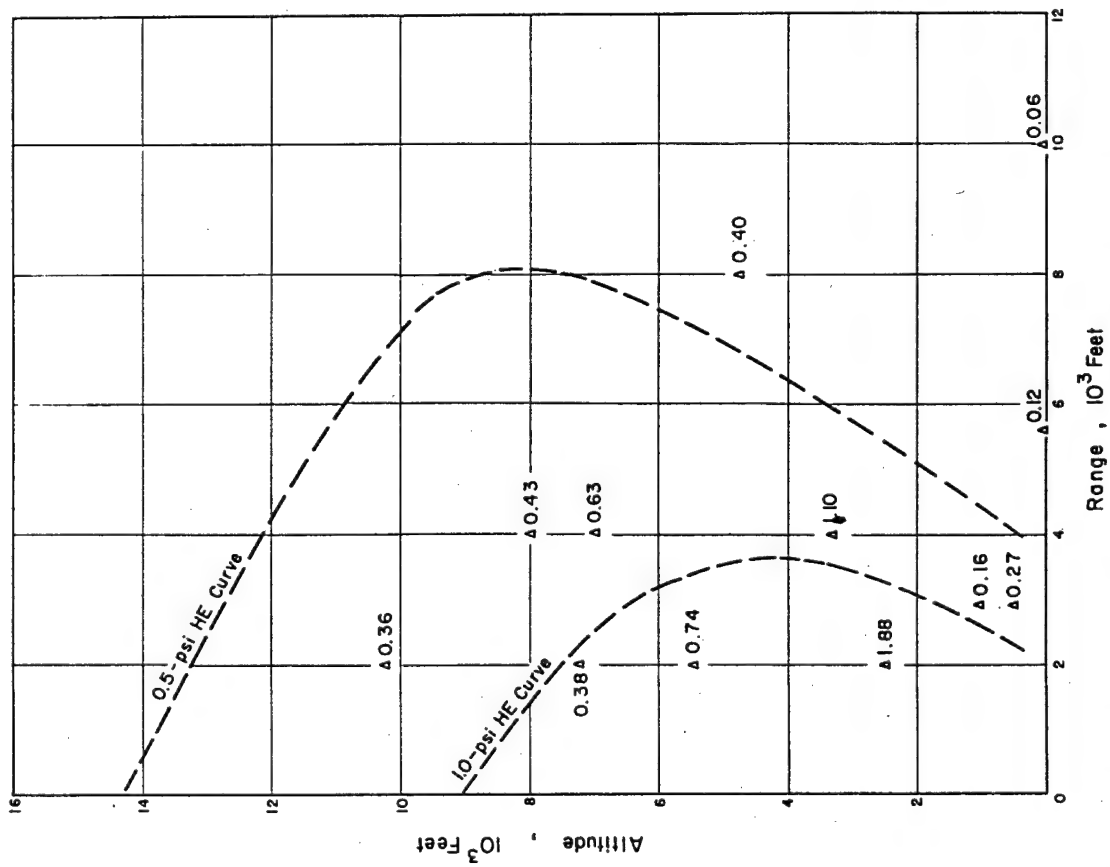


Figure 3.20 Summary of mechanical gage results, Shot Umbrella.

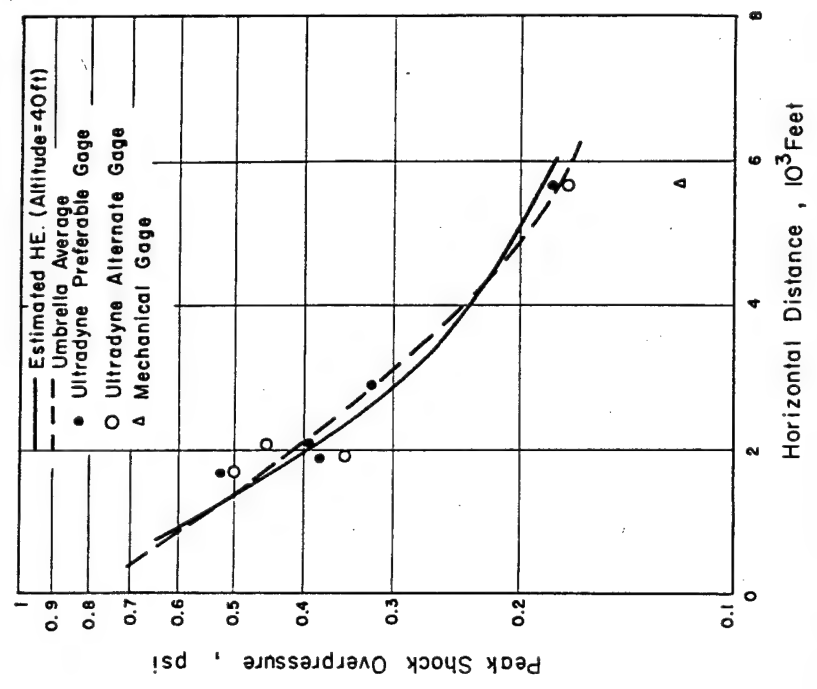


Figure 3.21 Comparison of Umbrella surface data with estimated high-explosive data (maximum pressure data).

available. In contrast, near-surface data compare favorably with predictions from high-explosive data, as seen from Figure 3.21. The predictions themselves involved extrapolations, since very low height high-explosive data were not available. Therefore, any conclusion that underwater chemical and nuclear explosions are completely equivalent in producing air-blast should be viewed with caution.

**3.2.6 Water Waves.** An objective on Shot Umbrella was to document water waves and inundation of nearby islands. Shot Baker of Operation Crossroads had provided the only available data from an underwater nuclear shot in shallow water. Considerable data was available from barge shots near the water surface and high-explosive shots.

**Experimental Plan.** Wave-measuring stations are shown in Figure 3.22. The three self-recording gages (turtles) placed on the lagoon bottom at ranges of 1,350 to 1,750 from sur-

TABLE 3.3 SUMMARY OF FIRST WAVE DATA, SHOT UMBRELLA

Depth of device submergence = 150 ft. Preliminary yield = 10 kt.

$$\frac{H_1}{H_2} = \left(\frac{d_2}{d_1}\right)^{1/4}, \text{ where, } d = \text{Water depth, ft.}$$

H = Height of first crest to following trough, ft.

Station	Range from	First Crest	First Trough	First Wave	Depth	Wave Height*	Time of First
	Surface Zero	Height	Depth	Height	of Water	Water Depth	Crest Arrival
	ft	ft	ft	ft	ft	150 ft	min:sec
163.02	[REDACTED]	+10.0	-17.7	27.7	152	27.7	:21
163.01	[REDACTED]	+11.0	-12.5	23.5	162.2	23.5	:27
163.03	[REDACTED]	+10.7	-11.0	21.7	154.8	21.7	:21
160.01	[REDACTED]	+4.7	-5.1	9.8	64.9	7.9	1:45
DD 593 †	[REDACTED]	+3.0	-2.0	5.0	114.0	4.7	1:42
Project G.3 No. 1	[REDACTED]	+2.3	-3.8	6.1	140.0	15.1	1:58
Project G.3 No. 2	[REDACTED]	—	—	—	145.0	—	4:51
Project G.3 No. 3	[REDACTED]	+1.1	-1.9	3.0	152.0	3.0	9:58
160.02	[REDACTED]	+0.59	-1.12	1.7	44.3	1.2	12:57

\* Wave heights from the various depths of measurement were adjusted to common water depth of 150 ft by Green's

† Amplitude data subject to revision upon further analysis.

face zero consisted of bourdon tubes which moved a stylus over clock-driven smoked-aluminum disks. The recording unit was shock mounted within a high-pressure steel case, which was embedded in a 1,000-pound-lead fairing for locational stability. Instrumentation other than the turtles was identical to that used on Shot Wahoo and described in Section 2.2.6.

**Results.** The three bottom turtle pressure records are shown in Figure 3.21. These and other subsurface pressure records have not been corrected for gage depth and wave period; actual wave heights at the surface may be about 25 percent higher for 150-foot-depth measurements. The initial disturbance shown in Figure 3.23 was a crest which arrived at the 1,750-foot station first, indicating considerable wave asymmetry. First crest heights at the two stations near 1,700 feet were essentially the same, as were first trough depths. In fact, there was considerable similarity between all three records.

Data on the first wave at each measurement station is tabulated in Table 3.3. A wave record from the Mk VIII wave recorder, Station 160.01, is shown in Figure 3.24. At this [REDACTED] foot range, the second crest had started to gain prominence. Pitch and yaw records from the DD-593, [REDACTED] foot range (also shown on Figure 3.24) indicated the second crest was the highest. Inspection of other records indicates the highest wave shifted progressively to later crests with increasing distance from surface zero. At the southwest end of Site Fred, 40,450-foot range, the fifth crest was the highest.

Postshot survey of islands to the south of the shot showed that inundation was negligible and

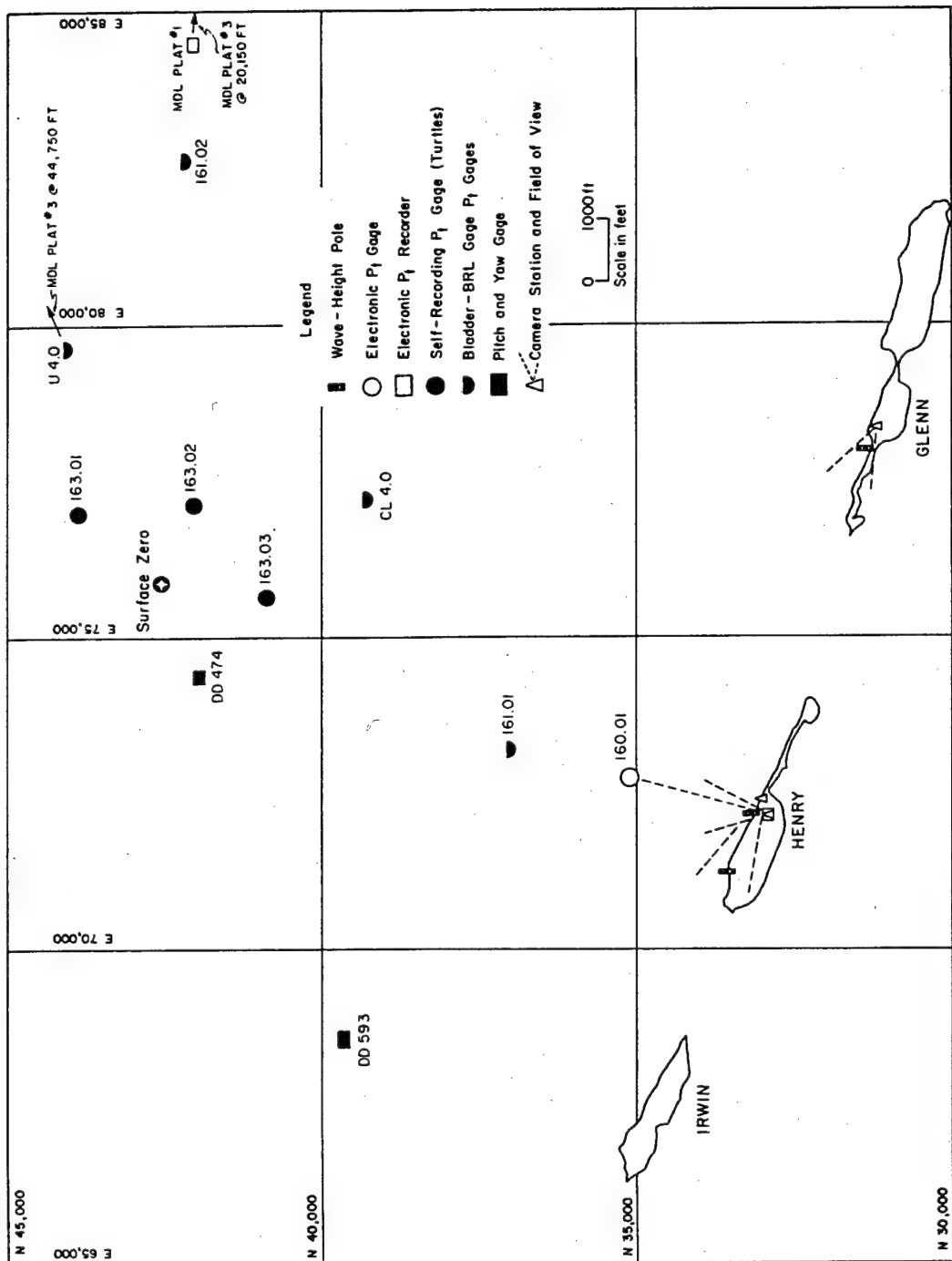


Figure 3.22 Water-wave measurement stations, Shot Umbrella.

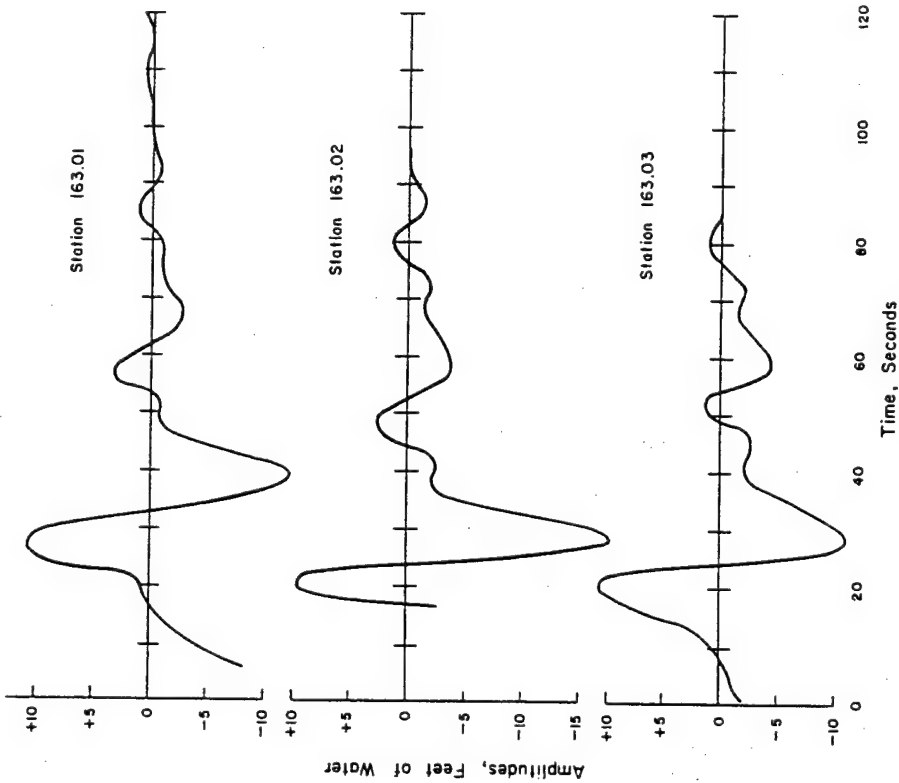


Figure 3.23 Subsurface pressure as a function of time near stations, Shot Umbrella. Surface-zero latitude, 11 deg 22 min 49.9 sec north; longitude, 162 deg 13 min 9.6 sec east. Shot time was 1115 on 9 June 1958. Station 163.01; bearing, 39 deg 26 min true; range, [redacted] feet; instrument depth, 162.2 feet. Station 163.02; bearing 112 deg 50 min true; range [redacted] feet; instrument depth, 152.0 feet. Station 163.03; bearing 189 deg true; range [redacted] feet; instrument depth, 154.85 feet.

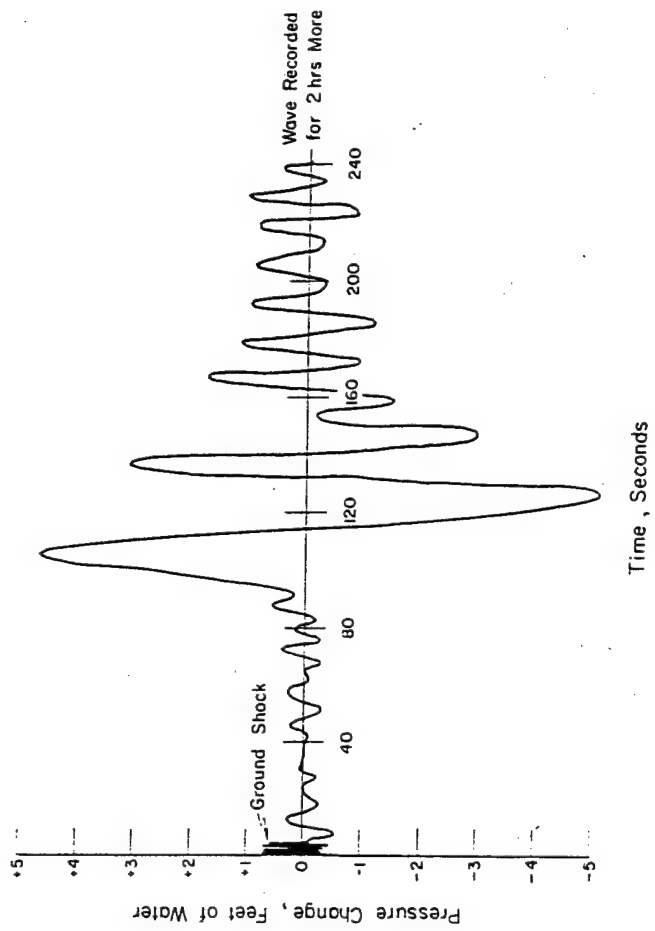


Figure 3.24 Wave record for Station 160.01, Site Henry, Shot Umbrella. Time was 1115 on 9 June 1958; range from surface zero was [redacted] feet on bearing 157 deg 38 min true; tide stage at shot time was plus 3.1 feet; depth of transducer was 64.9 feet.

generally less than that which occurs with high tides. It appears the shoal area adjacent to the islands effectively shielded them from inundation. Photographs indicate the waves broke between 2,000 to 3,000 feet from the Site Henry shore line. Breaking was not continuous along the advancing wave front, and it appears first breaking was initiated by coral heads in advance of the shoal area.

### 3.3 NUCLEAR RADIATION EFFECTS

3.3.1 General. The Nuclear Radiation and Effects Program had basically the same objectives and participation during Shot Umbrella as it had during Shot Wahoo. The general purpose of the three nuclear-radiation projects was again to document the gross-gamma-free fields about the point of burst, to measure the consequent dose rates and dosages generated on destroyer-type target ships, and to evaluate the hazard generated by the ingress of the resultant contaminant into the interior of these ships. Although certain modifications were made as the result of experience gained on Shot Wahoo, these modifications were generally minor in nature and were primarily concerned with improving instrumentation reliability and obtaining more complete instrumentation coverage of critical areas.

3.3.2 Objectives. The specific objectives of the nuclear radiation projects for Shot Umbrella were the same as those presented in Section 2.3.2 for Shot Wahoo.

Although the project objectives were identical for both shots, the results to be obtained were not expected to be the same because of the inherent differences in shot conditions. Shot Wahoo simulated a deep underwater burst on the open sea, while Shot Umbrella was to approximate a bottom burst in relatively shallow water.

3.3.3 Background. Since less than two months separated Shots Umbrella and Wahoo, the state of knowledge pertaining to underwater-shot nuclear-radiation effects was essentially the same as it had been prior to Shot Wahoo. Little data had been reduced from the first shot by the time preparations were essentially complete for Shot Umbrella. Furthermore, the differences between Shots Wahoo and Umbrella were of such a nature that the results of one would probably give no sound basis for predicting the effects of the other. Therefore, both shots were required on the basis of obtaining extensive and detailed information for operational analysis of a deep-water, open-sea-type burst and a shallow-water bottom-type burst.

Although some gamma-field data was obtained during Operation Crossroads (References 15 and 16) on a shallow lagoon shot, the available pre-Hardtack information was fragmentary and insufficient for accomplishment of a satisfactory operational analysis. Any projections of gamma-dose contours from pre-Hardtack data would have been unreliable. The specific information, therefore, required from Shot Umbrella was the documentation of: (1) the various radiation sources generated by an underwater detonation on the bottom of a lagoon, including remote, enveloping or surrounding, and shipboard sources; (2) the attenuation afforded by ship's structures and machinery; and (3) the ingress of contamination into the ship's interior and resultant radiological hazards incident thereto.

3.3.4 Experimental Method. The experimental method for Shot Umbrella was essentially the same as for Shot Wahoo, with minor modifications dictated by experience gained from Shot Wahoo. A mechanical safety was installed on each coracle to prevent accidental activation of the instruments during timing-signal dry runs. More-accurate data concerning preshot and postshot instrument positions were obtained by using radar positioning on Shot Umbrella, instead of the photomosaic mapping used on Shot Wahoo. Helicopter recovery of floating film packs was also developed and utilized, thereby greatly improving the recovery probability of those instruments.

Because of the relatively short duration of the gamma radiation phenomena on Wahoo compared to the recording time on the GTR's, it was decided to manually activate the shipboard GTR's upon evacuation of the ships before the shot. This provided additional reliability, in that no dependence was placed on radio-timing signals.

Documentation of the Gross Gamma Fields (Project 2.3). As in Shot Wahoo, the primary documentation of the gamma fields generated by Shot Umbrella was accomplished by the use of the GTR and high-range, high-time resolution recorders described in Section 2.3.4. These instruments were located at 26 coracle stations and on the major target ships. The use of coracles had proven highly successful on Shot Wahoo, and the number of coracles used was increased by five for Shot Umbrella in order to obtain more complete instrument coverage of critical areas. This increased coverage was permitted through use of coracles which had been retained as spares.

Twenty-one coracles were moored inside the lagoon by standard Naval techniques at depths less than 30 fathoms, while the other five coracles were deep moored outside the lagoon in a manner identical to that used for Shot Wahoo. After the last timing-signal dry run and before evacuation, all coracles were manually armed. The coracle instrumentation was activated by radio-timing signals just prior to the event.

The time-dependent measurements were again supplemented with total-dose measurements made with NBS film-pack dosimeters. The film packs were distributed throughout the target array on coracles, as floating film packs (FFP), and at various positions aboard the three target destroyers and the EC-2. The FFP's placed inside the lagoon prior to the shot were anchored in place, while those in deep water were free floating as they had been for Shot Wahoo. Self-anchoring FFP's were also air dropped into the array after the shot. To achieve a more complete recovery of the FFP's than that achieved on Shot Wahoo, helicopter recovery was utilized. This proved to be a highly successful recovery method and a high percentage of the Shot Umbrella FFP's were recovered.

Fallout samples were again taken by means of incremental collectors (IC) located on the coracles and ships.

The Shot Umbrella instrument array included 26 coracle stations, the three target destroyers and the EC-2, and approximately 70 FFP's distributed throughout the array.

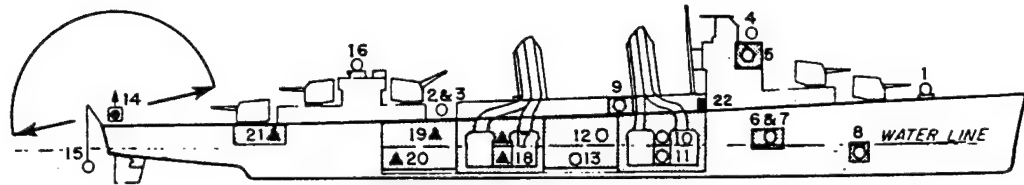
Following the detonation, all instrumentation was recovered as early as radiological and operational conditions permitted. In contrast to Shot Wahoo, the FFP's for Shot Umbrella were located by radar before and after the shot, and as has previously been noted, recovery was accomplished by helicopters.

Documentation of Shipboard Radiation. The instrumentation for the measurement of shipboard gamma-radiation fields was essentially the same as for Shot Wahoo. The gamma-radiation-dose rates and doses aboard the three target destroyers were measured by GTR's and NBS film packs, respectively, at locations representing major battle stations. Unshielded detectors were again located on weather decks and in several compartments to obtain total-radiation fields at these locations. A directionally-shielded detector was located on the fantail of each destroyer to measure remote-source (transit) radiation. Another detector was suspended underwater beneath the fantail of each destroyer to measure radiation in the nearby water. Figure 3.25 presents the location of GTR detector stations aboard the destroyers.

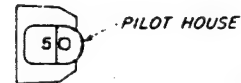
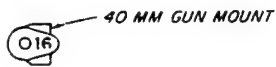
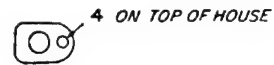
To provide early-decay information, a fallout collector connected to a fully shielded (6-inch lead) GTR was employed. This installation was on the DD-592 only.

The GTR's were started manually at H - 3 hours. All recorders had at least a 12-hour running time, at which time they shut off automatically as their recording tape ran out. As soon after as was feasible, the record tapes and film badges were recovered and processed for data reduction.

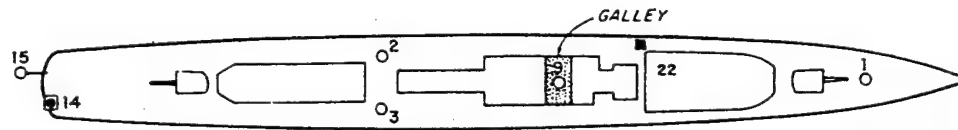
Contamination Ingress Documentation. For the purpose of evaluating the inhala-



- ◻ SHIELDED STATION, DIRECTION OF VIEW
- UNSHIELDED STATION ON ALL DD'S
- ▲ UNSHIELDED STATION ON DD592 ONLY
- ▣ DECAY UNIT ON DD592 ONLY
- ▭ INSTRUMENTED COMPARTMENT



O2 LEVEL



MAIN DECK

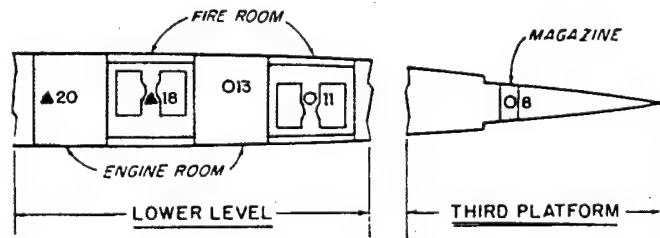
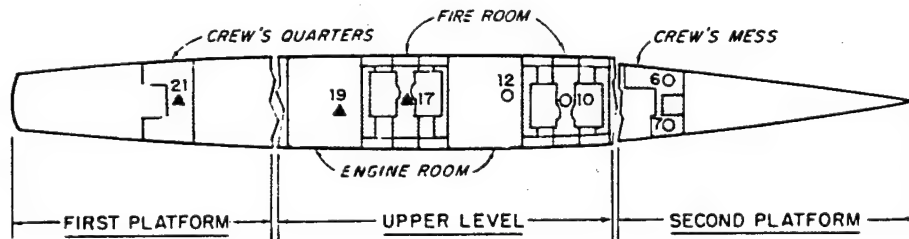


Figure 3.25 Location and designation of GTR stations on target destroyers.

tion and external gamma-radiation hazards from contamination ingress into a ship's interior, the DD-592 was again instrumented with GTR's, incremental air samplers, total air samplers, and surface samplers. As before, guinea pigs and mice were used for inhalation studies. Test spaces represented or simulated stations that would be manned under general quarters. The ventilation system was maintained at 20 percent of rated air flow to simulate a blowers-off condition, wherein the only air flow would be due to the movement of the ship. Full-power air flow was maintained through the unfired boiler to represent maximum operation of the boiler system. Instrument locations are shown in Figure 3.26.

The washdown system, activated before shot time, washed the entire weather surfaces of the ship, with the exception of an instrument platform above the forward gun director. This gun-director instrumentation was to provide data on the basic weatherside phenomena, while the washdown system was to minimize the effect of deposited radioactive debris on the shipboard gamma-radiation measurements.

Consistent with radiological safety, the animals and collected samples were recovered as soon after the detonation as possible. Following recovery, the animals were sacrificed on a predetermined schedule, and tissue counts made. The air and surface samples were counted as soon as they were received at the project-counting facility. GTR tapes were recovered after instrument run down.

**3.3.5 Results and Discussion.** After inspection of the partially reduced data, it was estimated that approximately 78 percent of the maximum possible data was recovered from the coracle and FFP array. Aboard the ships, satisfactory data was obtained on shipboard radiation and contamination ingress from all the instrumented ships.

**Gamma Field Documentation.** As in Shot Wahoo, no gamma radiation was observed at the time of venting of the shot bubble. A typical gamma trace is shown in Figure 3.27. Inspection of this trace revealed that, for about the first 30 seconds after detonation, no gamma radiation was observed at a station located approximately one-half mile downwind from surface zero, indicating that direct gamma radiation, either from the nuclear reaction or from shine directly from the water column or plumes, was either extremely low or completely non-existent. As on Shot Wahoo, the dose-rate peak became apparent at the time that the base surge reached a particular location, usually within a minute at stations out to one mile from surface zero. In this respect Shots Wahoo and Umbrella show marked similarity. However, it should be noted that, whereas Shot Wahoo produced many successive dose-rate peaks following the initial arrival of the base surge, Shot Umbrella produced basically one peak, after which the activity rapidly decreased, essentially to zero. For close-in stations, the Shot Umbrella dose rates appeared to be somewhat higher than the Shot Wahoo dose rates, but the total dose was somewhat lower. This is understandable because of the longer duration of the radiation phenomena for Shot Wahoo. A map of the Shot Umbrella array, showing the total dose received at various stations within one minute after detonation, is shown in Figure 3.28. The use of a one-minute dose is arbitrary in view of the continuity of the contributing event. However, at stations within a half mile, most of the total dose was received within one minute. At all points of observation, the free-field gamma activity was over about 17 minutes after zero time.

The outermost instrument location was over four miles from surface zero, and at that point the total dose received was of the order of 30 r.

Although the difference in the gamma traces of Shots Wahoo and Umbrella indicate dissimilar mechanisms of cloud formation, both shots indicated that surface winds are the primary means of transport of the radioactive cloud at distances greater than 7,000 feet. At distances less than 7,000 feet, the Shot Umbrella cloud appeared to move radially outward from surface zero at approximately 100 ft/sec, as had been observed on Shot Wahoo.

**Incremental Sampling of Deposited Debris.** The collection of samples of ra-



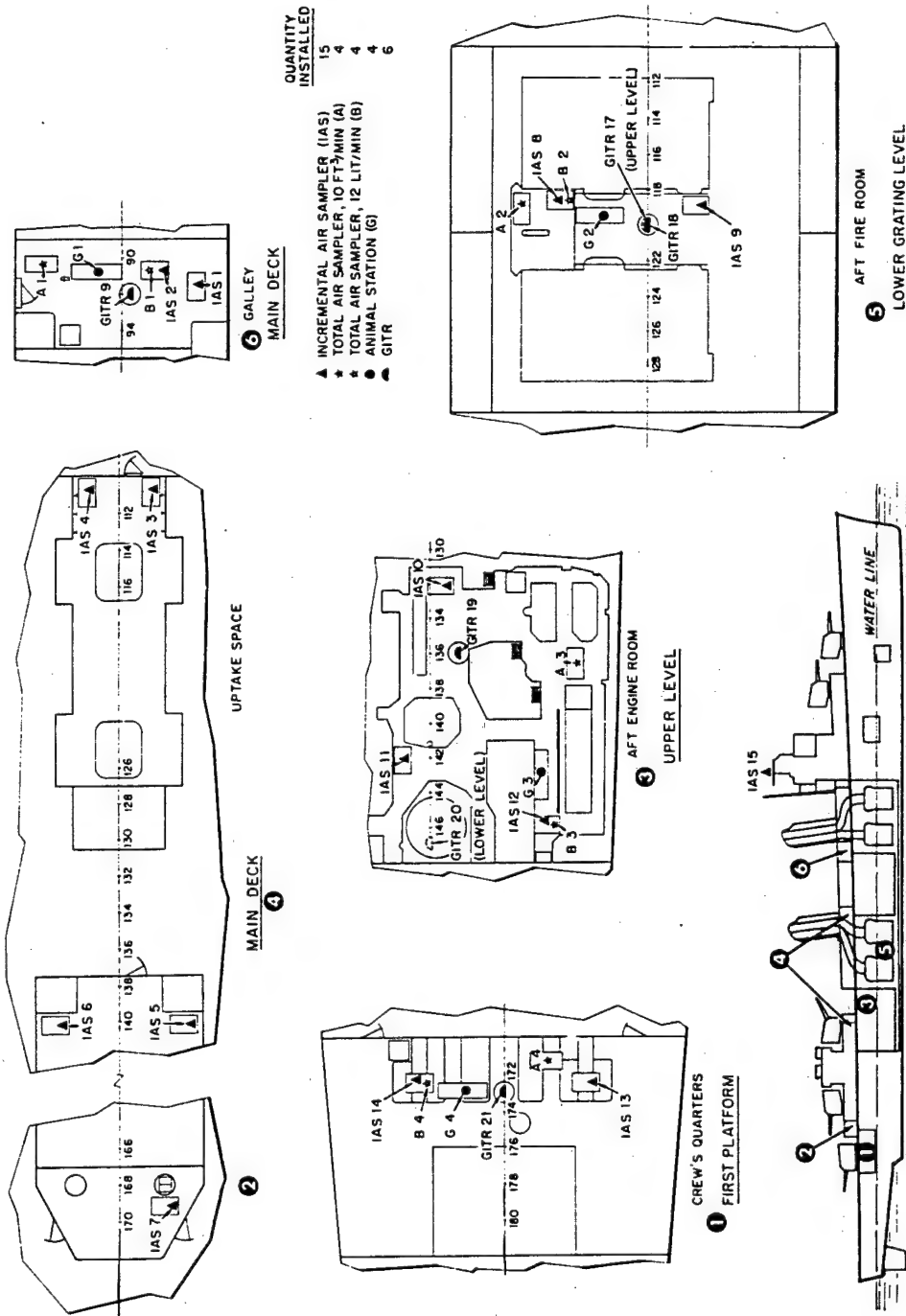


Figure 3.26 Instrument locations on DD-592.

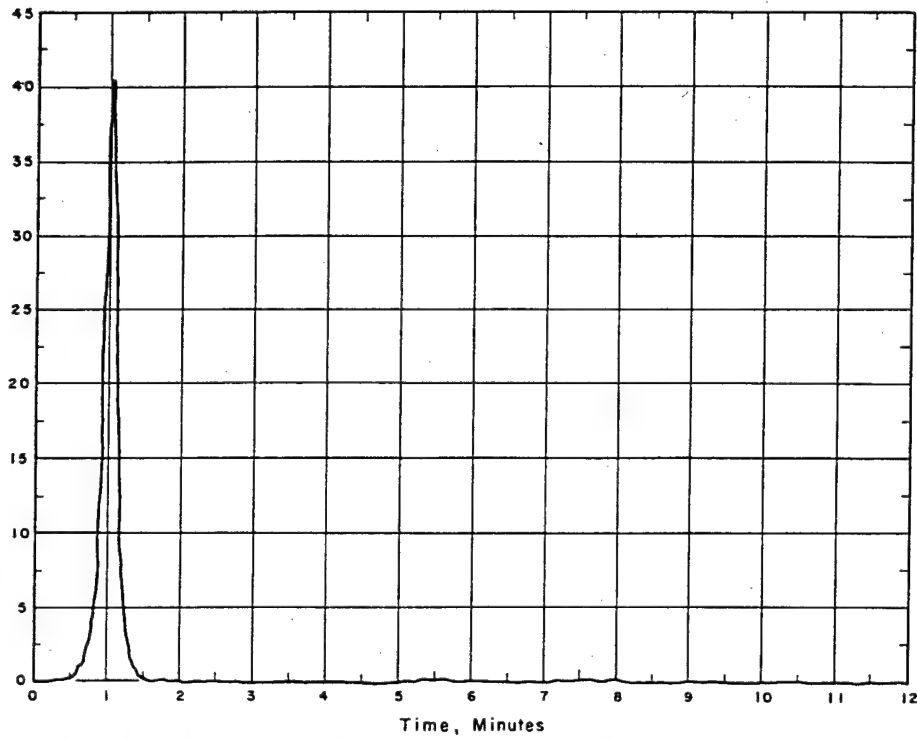


Figure 3.27 Dose rate versus time for std-GITR. Coracle at D 4.5 (247.9 deg T, 4,770 feet) Tape 450. Cumulative dose from GITR trace: 1 min 67.2 r; 3 min 123 r; 5 min 123 r; 8 min 127 r; 12.5 min 127 r; 25 min 128 r. Film pack dose: tripod 85 r, float 145 r, Shot Umbrella. Note: this coracle capsized.

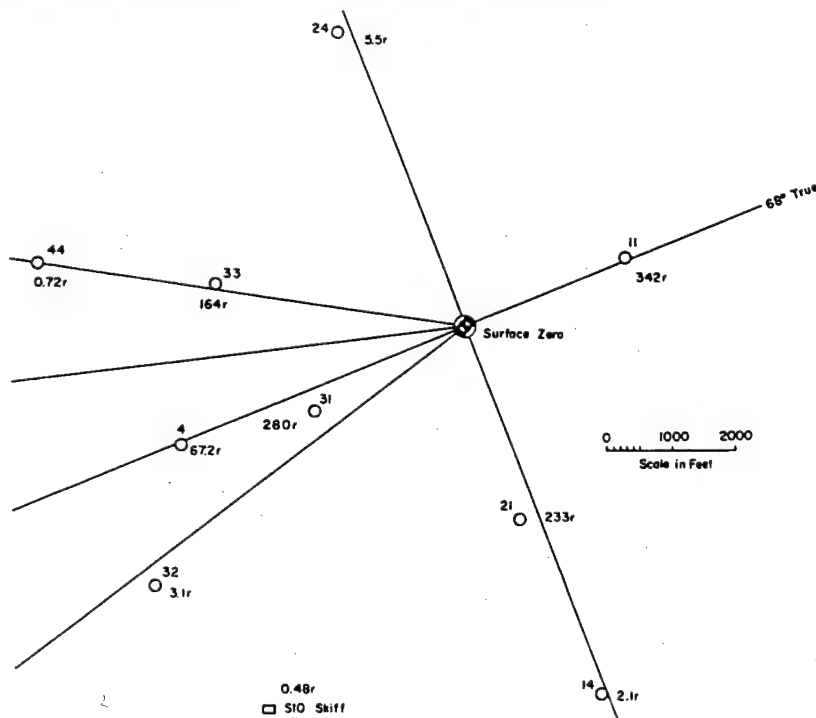


Figure 3.28 Map of Umbrella array showing doses received at coracle (and SIO skiff) stations within one minute after shot time.

radioactive debris deposited on coracle and ship surfaces was repeated on Shot Umbrella. As before, the collected samples were to have been used to correct the GTR readings if the dose-rate contribution to the measured total-dose rate was found to be significant. The deposited debris-dose rate proved to be negligible, and the collected samples were used to study the deposit of activity throughout the array and to obtain decay data. As on Shot Wahoo, the period of deposition was found to be short in the upwind and crosswind directions. Unlike Shot Wahoo, however, a single peak in deposition rate was found at practically all stations, and no deposition period exceeded 7 minutes.

**Shipboard Gamma-Radiation Fields.** Gamma traces recorded on the weather decks of the target ships again compared favorably with those dose-rate traces obtained on nearby coracles. A significant rise in gamma activity occurred from 30 seconds to one minute after zero time, again indicating the arrival of the highly radioactive base surge.

The salient feature of the total dose curves (Figure 3.29) shows the rapid acculation of essentially the complete dose. For example, it is observed that the total dose of over 700 r was accumulated on the weather deck of DD-474 within one minute after detonation. This ship was located about [redacted] feet from surface zero. Comparison of Shot Wahoo (Figure 2.35) presented in Section 2.3.5 with the previously mentioned Figure 3.29 shows a faster build-up but smaller accumulation of dose on DD-593 after Shot Umbrella. The DD-593 was located [redacted] feet downwind from surface zero on Shot Wahoo and [redacted] feet downwind from surface zero on Shot Umbrella.

The shipboard washdown systems were operating throughout the time of passage of the airborne debris, thus greatly reducing the probability of the instruments' being affected significantly by deposited contamination.

The influence of the superstructure on external radiation fields is demonstrated by comparison of the total dose measured and estimated solid angle of cloud subtended at film pack locations as shown in Figure 3.30. It can be seen that the superstructure definitely modifies the free-field doses and dose rates at different locations on the weather deck. As indicated by this comparison, the modification appears to be dependent on the cloud solid angle seen at each position.

Below decks, the gamma radiation was attenuated to varying degrees, depending on the specific location. In all cases, locations anywhere except on the main deck afforded some degree of protection from radiation, while the best protection was offered at locations below the waterline. Table 3.4 shows the doses received at film-badge locations on each ship for Shot Umbrella. The Shot Wahoo doses are also presented for comparison purposes. It is obvious from inspection of this table that the doses received from Shot Umbrella were much less than those for Shot Wahoo, and in each case the corresponding ship was closer to surface zero in Shot Umbrella than it was in Shot Wahoo. Approximate exposure distances are given below:

<u>Target Ship</u>	<u>Shot Wahoo</u>	<u>Shot Umbrella</u>
	feet	feet
DD-474	[redacted]	[redacted]
DD-592	[redacted]	[redacted]
DD-593	[redacted]	[redacted]

For comparison, it might be noted that the DD-474 on Shot Wahoo was approximately the same distance from surface zero as was DD-592 on Shot Umbrella. In contrast to Shot Wahoo, where the main-deck dose of the DD-474 at a distance of [redacted] feet was 1,000 r, the main-deck dose on the DD-592 located at [redacted] feet for Shot Umbrella was only 430 r.

It can also be observed from Table 3.4 that the main-deck dose on the DD-474 at less than one

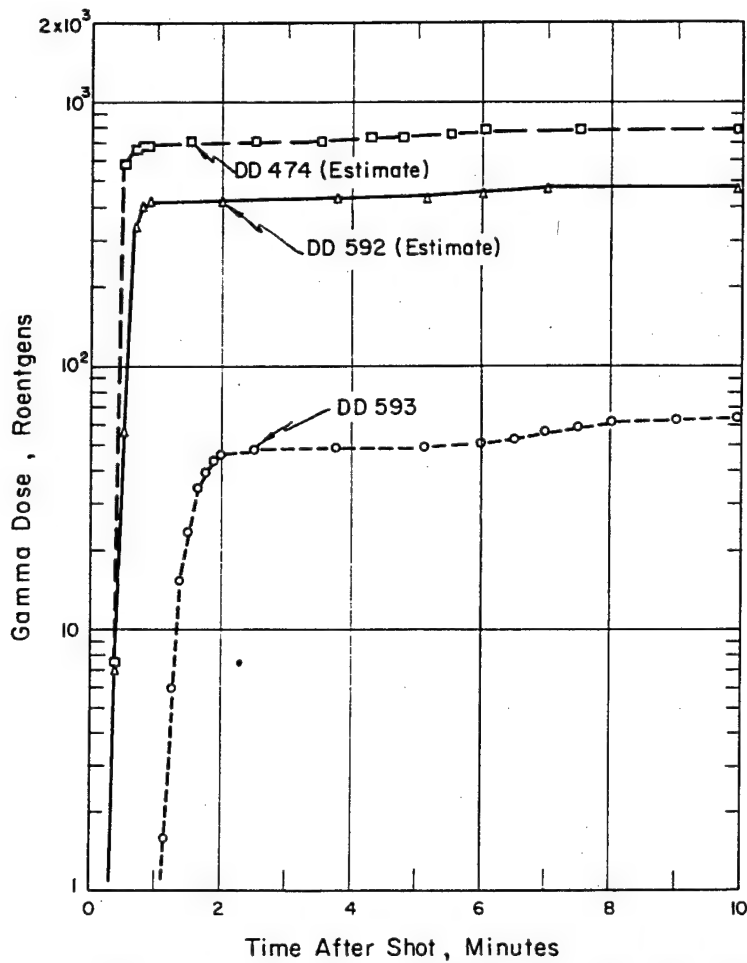


Figure 3.29 Total gamma doses on decks of target destroyers after Shot Umbrella. These values also represent estimates of transit doses.

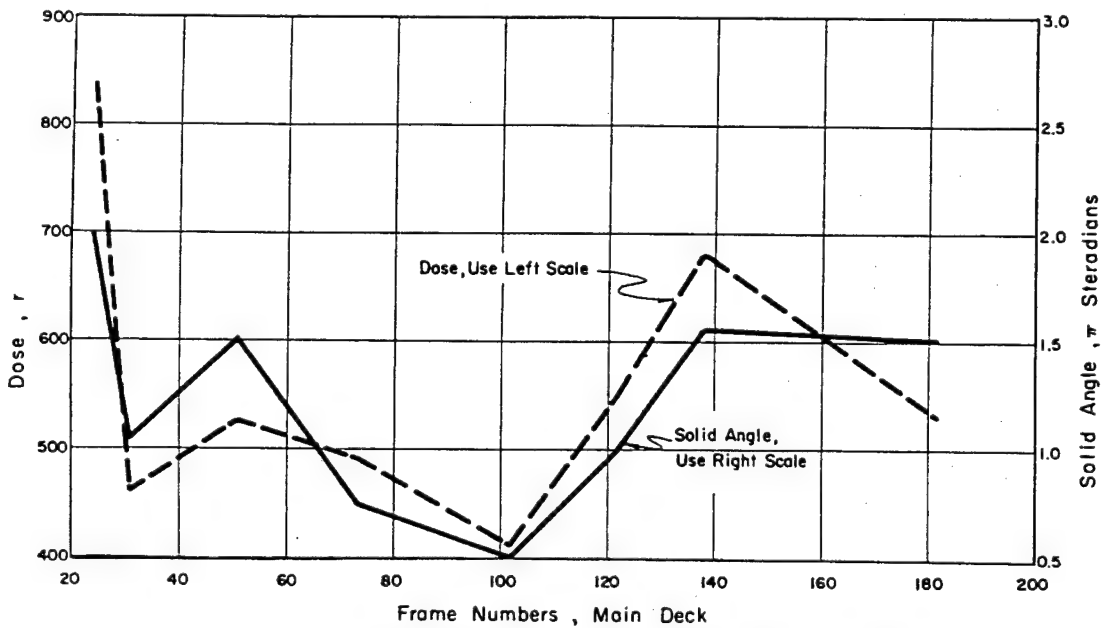


Figure 3.30 Plots of film pack dose and estimated solid angle of radioactive cloud subtended at film packs at various locations on main deck of DD-474, Shot Umbrella.

half mile for Shot Umbrella was comparable to that measured on the DD-593 located at a distance of approximately one and one half miles for Shot Wahoo.

Shipboard Transit and Contaminated Water Radiation Fields. By comparing Figures 3.31 and 3.32, it is seen that the transit-radiation source is the only significant radiation source. Total gamma-dose rates (Figure 3.31), including those from transit sources and

TABLE 3.4 AVERAGE 24-HOUR GAMMA DOSES ABOARD TARGET SHIPS BASED UPON FILM-BADGE DATA

Compartment or Area	Shot Wahoo			Shot Umbrella		
	DD-474	DD-592	DD-593	DD-474	DD-592	DD-593
	r	r	r	r	r	r
Above Waterline, 33 ft						
Bridge Complex	610	420	180	310	220	28
Above Waterline, 11 to 16 ft						
Forward Quarters	650	420	160	300	190	26
Radio Central	580	400	150	230	180	23
Galley	730	460	200	300	270	35
Main Deck	1,000	630	340	360	430	57
Crew's Washroom	730	500	170	260	290	31
Above Waterline, 2 to 4 ft						
Crew's Mess	400	210	72	160	87	13
Forward Fire Room	290	170	67	140	90	14
Forward Engine Room	230	110	45	89	100	12
Aft Fire Room	—	180	—	—	96	—
Aft Engine Room	—	170	—	—	110	—
Aft Quarters	590	370	140	220	210	28
Steering Gear Room	490	300	98	180	210	23
Below Waterline, 3 to 6 ft						
Magazine	310	210	65	160	81	12
Forward Fire Room	110	37	19	41	19	2.6
Forward Engine Room	76	29	10	17	12	1.9
Aft Fire Room	—	54	—	—	22	—
Aft Engine Room	—	66	—	—	39	—

deposit sources, are hardly distinguishable from dose rates due to transit sources alone (Figure 3.32). The curves could virtually be superimposed on one another within the limits of accuracy of the as yet incomplete data.

Because the ships' washdown systems were operating, it could be surmised that the washdown systems were highly effective in removing deposit sources from the ship before they could contribute significantly to the total gamma dose. However, film-pack dose data from stations above the washdown area show approximately the same results as those in the washdown area, thereby indicating that a high percentage of the total dose was due to remote-source radiation.

Attempts to measure radiation in adjacent water met with little success. Underwater detectors were submerged off the fantail of each target destroyer at the time of evacuation. The instruments on DD-474 and DD-592, however, were damaged by shock before any data was recorded. Therefore, data was obtained from DD-593 only. Figure 3.33 presents the results, which may be slightly overestimated because of arbitrary corrections made for shielding and geometry.

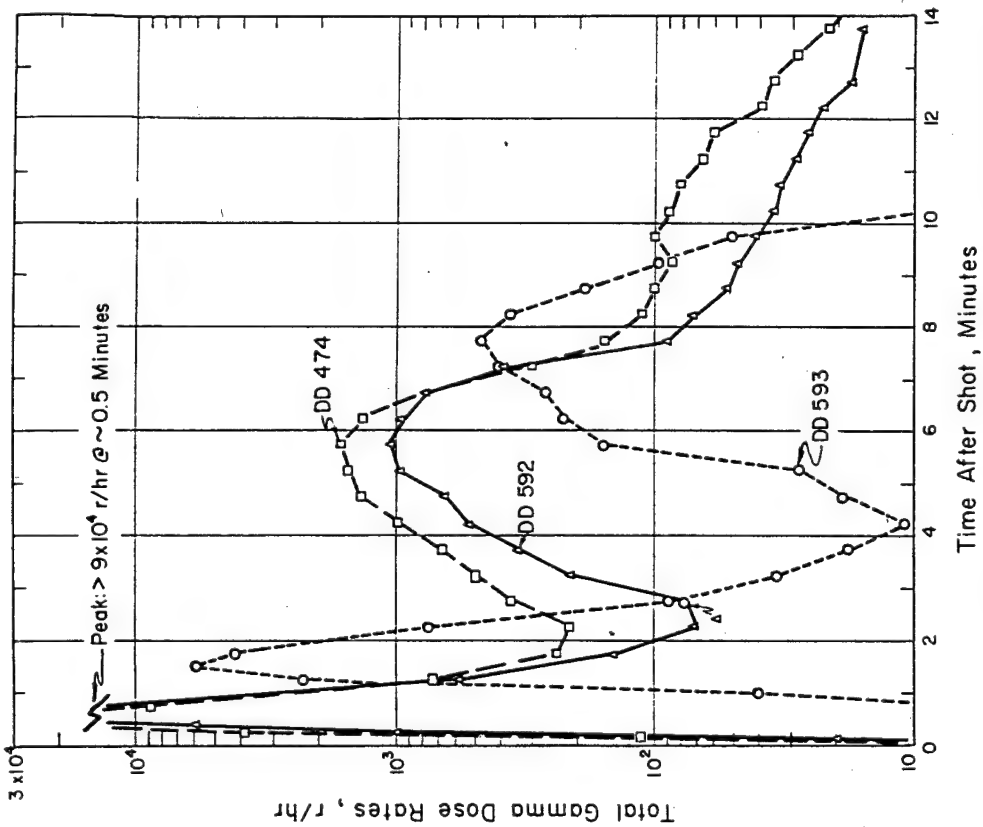


Figure 3.31 Total gamma dose rates on decks of target destroyers after Shot Umbrella. Averaged data from GTR stations 1, 2, 3, and 4 which include effects from both transit and deposit radiation sources.

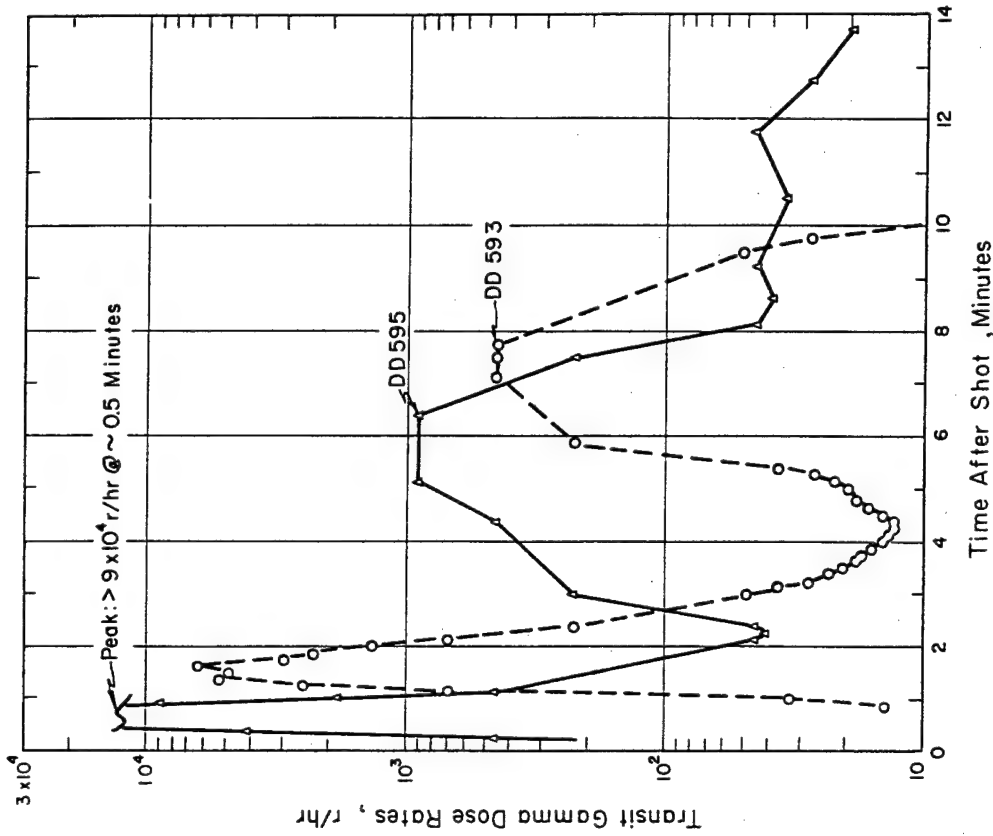


Figure 3.32 Transit gamma dose rates on decks of DD-592 and DD-593 after Shot Umbrella. Transit dose rates result only from radiation sources remote from the ships.

The first two series of peaks are probably due to fallout, while the peaks after six hours are likely caused by the contaminated water drifting past the ship. The low dose rates measured appear to be of little significance.

**Shipboard Fallout Gamma Decay.** Figure 3.34 shows the curve for gamma-ionization decay of a debris sample collected in a six-inch-thick lead cave on DD-592 after Shot Umbrella. It is seen that a smooth plot was obtained when deck-dose rates were subtracted from the fallout-dose rates. Later times than those shown in the figure yielded the following results: from 8 to 11.5 hours after shot time the slope of the decay curve was  $-0.61$ , and from 23.2 to 34.8 hours the slope of the decay curve was  $-1.46$ .

**Inhalation Hazards Due to Ingress of Contaminants.** For Shot Umbrella, contamination hazards were again studied aboard DD-592, which was located 3,000 feet from

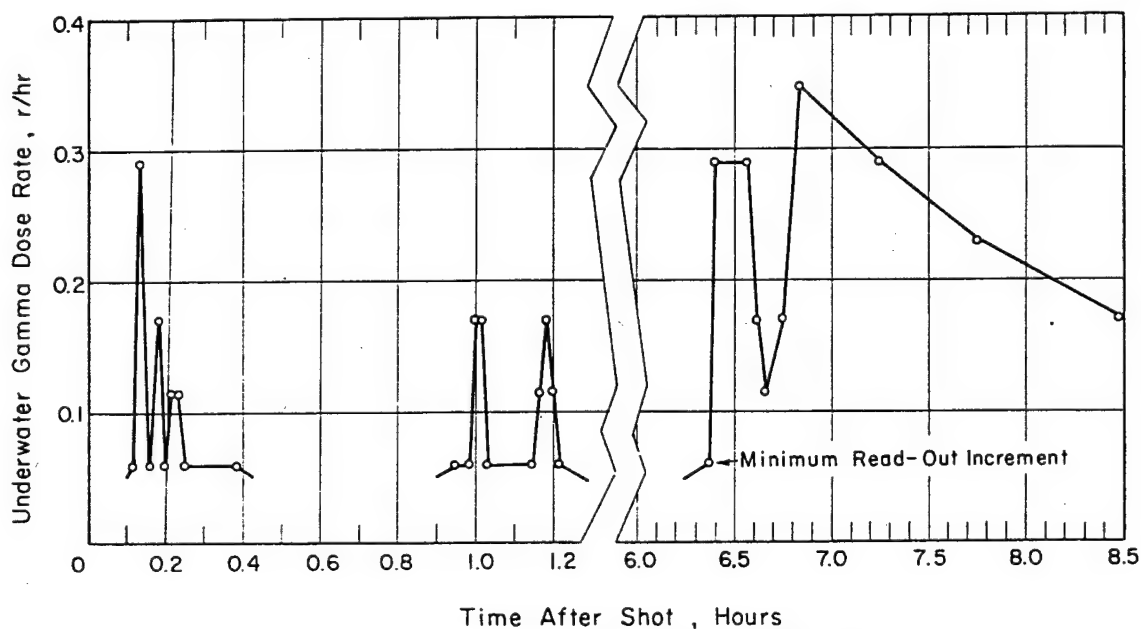


Figure 3.33 Gamma dose rates in water below DD-593 after Shot Umbrella. Detector was submerged 15 feet below water surface.

surface zero. Mice and guinea pigs were exposed at various locations aboard the ship and subsequently sacrificed on a predetermined schedule.

At unprotected weatherside locations, zero to 50 hour internal doses received by the mice were about six rads, as compared to about one rad sustained internally by the guinea pigs. All zero to 50 hour internal doses sustained at interior locations were 0.9 rad or less.

It is interesting to note that the internal doses received from Shot Umbrella were much less than those received from Shot Wahoo, even though the target ship was located closer to surface zero for this event. It may have been that the ventilation system, which operated at 20 percent of rated air flow for Shot Umbrella, scavenged the compartments of some of the contaminated air after passage of the base surge. All Shot Umbrella doses were lower than those sustained during Shot Wahoo, including those internal doses received at unprotected weatherside locations.

**External Gamma Radiation Due to Ingress of Contaminants.** External radiation due to ingress of contaminants was estimated from the sum of the radiation from airborne activity and the radiation from deposited activity within various compartments aboard the DD-592. At ten minutes after zero time, the following dose rates were recorded: galley, 17 r/hr; aft fireroom, 6.2 r/hr; aft engine room, 12 r/hr; aft crew's quarters, 24 r/hr. At H+2

hours, the dose rates had decayed to 0.8 r/hr, 0.12 r/hr, 0.03 r/hr, and 0.04 r/hr in the respective compartments. By comparing these dose rates with the total dose rates discussed in Section 3.3.5, it is readily seen that contamination ingress does not contribute significantly to the total external gamma-dose rates as recorded in the same compartments.

**Particle Size Distribution of Contaminants.** While the incremental air sampler did not function to yield time-dependent particle-size information, the percentage of contam-

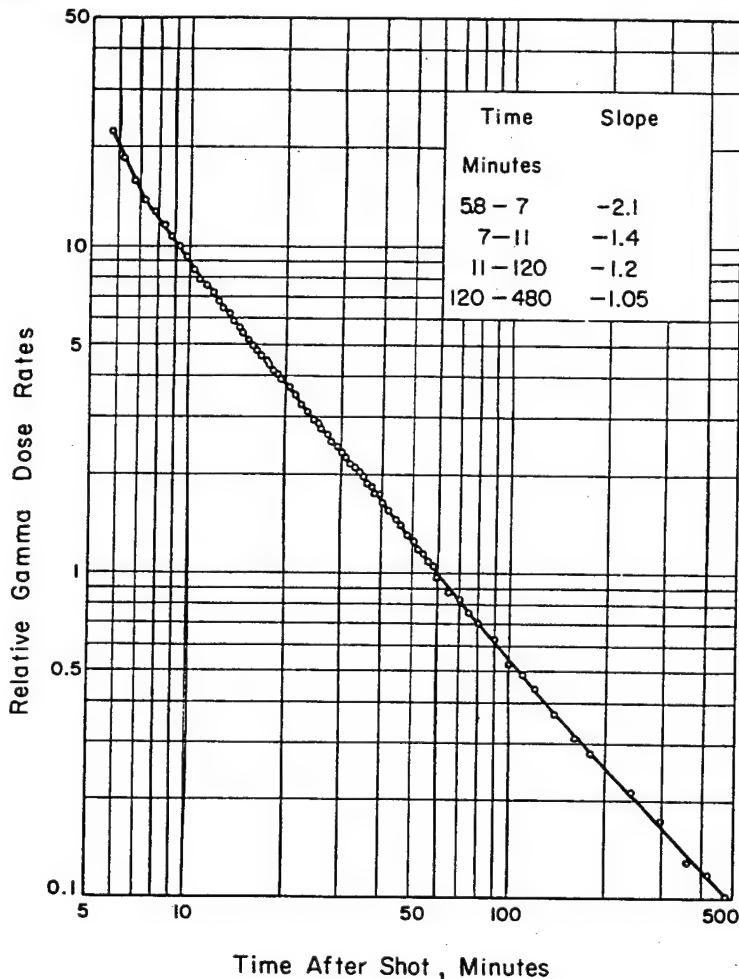


Figure 3.34 Gamma-ionization decay of contaminant collected in 6-inch-thick lead cave on DD-592 after Shot Umbrella, values corrected for background.

inants passing the filters indicated that most of the particles were below one micron in size, in the total air samples obtained. It can be seen that the contaminant was readily air-borne and in the respirable-size range.

**3.3.6 Conclusions.** As was the case during Shot Wahoo, the primary radiation from Shot Umbrella was found to be the radiation from the base surge as it passed a particular location. The intensity and time of arrival of this radiation was dependent on the distance from ground zero, the nature of the surface winds, and, to some extent, on the nature of the shot. In a shallow-harbor type burst, similar to Shot Umbrella, there appears to be less transport of the gamma-



radiation sources than from a deep-water burst. This may be due to the large-size particles which are picked up from the lagoon bottom by the burst. These relatively large particles absorbed a great amount of radioactive material and, because of their weight, settled quite rapidly before they were carried any considerable distance. This would account for the rapid decrease in activity of the base surge at increasing distances from surface zero. In contrast, Shot Wahoo picked up no particles from the ocean bottom; therefore, the radioactive material was carried by the base surge in a suspended state, and settlement of this mist was much slower than if there had been solid particles contained therein.

Normal sea operations can be resumed after passage of the base surge, which would be within 20 minutes at locations less than four miles from surface zero. During passage of the base surge, some protection from radiation is afforded at interior locations of a ship, but at distances less than one half mile the gamma activity from the base surge is so high that even the protective environment of a ship will not reduce this activity to acceptable levels.

Shipboard-contaminant deposition appears to have contributed little to the total gamma dose, and this hazard can be all but eliminated by an effective washdown system on all weather surfaces. Contamination ingress is not particularly important as a contributor to the total gamma dose below decks, but this ingress acquires some significance when inhalation hazards are considered. Particle sizing information revealed that most of the ingress particulate could be easily inhaled. The internal exposure at all animal stations below decks was 0.9 rad or less, in the first 50 hours after the shot. Above decks, the internal exposure reached six rads for mice and one rad for guinea pigs during the same period.

Gamma doses in excess of 100 r will be sustained in the open at distances less than about two miles downwind from surface zero. Because the surface winds appear to be the primary mechanism of transport of the base surge at distance greater than about 7,000 feet, the 100-r dose distance will probably be substantially reduced in the upwind direction. A study of the downwind gamma records would indicate a tentative conclusion that a downwind distance of approximately 23,000 to 28,000 feet from surface zero should be maintained in order to assure a total free-field dose of less than 25 r.

### 3.4 SHIP RESPONSE AND DAMAGE STUDIES

**3.4.1 Introduction.** The general need for a re-evaluation of ship response and damage predictability for underwater nuclear explosions, to give required answers to questions of the safe range for delivery of such nuclear weapons by surface ships and submarines, has been discussed in Section 2.4.1.

The Shot Umbrella geometry, a nuclear shot detonated on the ocean bottom in relatively shallow water (i. e., 148-foot depth), represented an operationally important environment. Many important strategic areas, such as the North American continental shelf, the European North Sea approach, etc., are of approximately this same water depth. Thus, information regarding safe ranges for delivery of nuclear weapons in such water configurations was also vitally required.

Previous small scale underwater high-explosive tests and theory predicted that pressure pulses for this shallow water geometry would be markedly different from the deep-water case. The closeness of both the air-water surface interface and the sea-bottom-reflection boundaries for the shallow water burst geometry influenced the pressure histories to such an extent as to make theoretical and small scale high-explosive treatment quite complex and difficult. Therefore, the full-scale pressure pulses from a nuclear detonation as predicated by theory and small-scale high-explosive tests were subject to much question.

These uncertainties in the prediction of the underwater free-field pressures for a shallow water shot made predictions of ship damage ranges doubly uncertain. Surface ship and submarine responses to the complex shallow water pressure pulses could not be readily extrapolated from

the deep-water case, i. e. Shot Wahoo geometry, even if the actual pressure pulses could be predicted.

Shot Baker of Operation Crossroads was the only prior underwater nuclear detonation in this shallow environment, but that detonation was at mid-depth in a 180-foot depth of water and, as discussed in Section 3.1, left many questions to be answered.

In addition to the safe-delivery problem of nuclear weapons by surface ships or submarines in shallow water, the submarine lethality ranges in shallow water were uncertain. Submarine-lethality predictions for the very-deep-water-geometry case were verified on Operation Wigwam. However, theory was inadequate to reliably extrapolate the lethality ranges to a submarine hull in shallow water.

Of the submarine hull-lethality prediction methods proposed and available, the so-called excess impulse method appeared to be the most promising. The excess impulse is defined as the impulse delivered by that portion of the shock overpressure which is in excess of the static hull-collapse pressure minus the hydrostatic pressure. The applicability of this method is partly theoretical and partly intuitive. It is reasoned that some amount of excess impulse is needed to collapse a submarine hull, the exact value of which is not overly critical since the variation of excess impulse with range is quite rapid. Therefore, it would be expected that with any reasonable assumed value, the range computed should be within the other uncertainties inherent to the problem. As an example, one value of excess impulse which has been used to define lethality for a submarine-like model, the Squaw, is 2.5 psi-sec. Such value is intended to indicate the range where there is a 50 percent probability the submarine will be lethally damaged.

However promising the excess-impulse method appeared for submarine lethality predictions, differing opinions existed on the applicability of its concept, especially with the very short-duration pressure pulses. Therefore, to provide a check point for submarine lethality predictions in shallow water, it was considered necessary to place a submarine-like model, the Squaw, target at a range predicted to be near-lethal to assess the reliability of the prediction methods. The shallow-water depth was such that it would also be possible to retrieve the damaged Squaw subsequent to the shot for study of the mode of failure.

Therefore, the shallow water event, Shot Umbrella, was required to determine both the safe ranges for surface ships and submarine delivery of underwater nuclear weapons and the lethality range for submarines in shallow water. Shot Umbrella simulated the firing of an antisubmarine nuclear depth charge or torpedo in waters of depth representative of our North American continental shelf and other strategically important areas. It was intended that the answers obtained from Shot Umbrella, of course, eventually be such as to cover not only the particular geometry of this one shallow water shot but other shallow water geometries, other yields, other types of ships, and other orientations.

The Program 3 effort on Shot Umbrella consisted of three general categories: (1) hull response and damage studies of surface ships, (2) hull response studies of submarines, and (3) shipboard machinery and equipment shock damage studies. Each of these categories is described successively in the following sections.

**3.4.2 Hull Response and Damage Studies of Surface Ships. Objectives.** The objectives of the hull response and damage studies of surface ships on Shot Umbrella were similar to those on Shot Wahoo, except that their application was to shallow-water geometries. The objectives on Shot Umbrella, therefore, were to: (1) determine from the hull-deflection standpoint, the safe-delivery range for surface-ship delivery of an underwater nuclear weapon in shallow water; (2) determine from the hull-deflection standpoint, the lethal range for merchant ships attacked by an underwater nuclear weapon in shallow water; (3) obtain basic information on hull response as related to free-field pressures and loading measurements in shallow water, so as to provide check points for model experiments and high-explosive shaped-charge tests.

**Background.** The problem of making predictions of response and damage from underwater nuclear-weapon effects for surface-ship hulls under general conditions has been previously discussed in Section 2.4.3. The increased difficulty in making such predictions when the surface ship is in relatively shallow water, compared with deep water, has been further discussed in Section 3.4.1. The closeness of both the air-water interface and the ocean-bottom-reflection boundaries for the shallow-water burst geometry influence the pressure histories to such an extent as to make theoretical and small-scale explosive treatment quite complex and difficult.

**Procedure.** For the hull response and damage studies on Shot Umbrella the same surface target ships were exposed as for Shot Wahoo, i. e., the DD-593, DD-592, DD-474 and the EC-2. These ships were located stern-on at [redacted] feet, broadside at [redacted] feet, stern-on at [redacted] feet, and broadside at [redacted] feet from surface zero, as shown on Figure 3.3. The three destroyers were the principal targets; the EC-2 was a contingency target for Shot Umbrella. Since it had sustained only light, rather than lethal hull damage on Shot Wahoo, it was possible to re-expose the EC-2 on Shot Umbrella. On Shot Umbrella, the EC-2 was exposed with its port side toward surface zero. On Shot Wahoo, the starboard side was exposed.

The relatively highly instrumented hulls of these four target surface ships included the same gages and gage-recording equipment for Shot Umbrella that had been previously installed for Shot Wahoo. The description of this instrumentation has been included in Section 2.4.3. The only modification was to transfer several of the hull-side-deflection gages in the EC-2 from the starboard to port side of the ship, since that was the side exposed to the burst on Shot Umbrella. It was not feasible, however, to similarly reorient the three heavy lead shields for the high-speed cameras which had been installed to record hull and bulkhead deflections within the EC-2 on Shot Wahoo. On the other hand, the other 40 high-speed cameras installed in the target ships primarily for the purpose of recording shock damage to machinery and equipment were installed so that they did function on Shot Umbrella as they had previously on Shot Wahoo. These cameras are described in Section 3.4.3. In general, all hull instrumentation installed for Shot Wahoo was also used for Shot Umbrella.

**Results.** For Shot Umbrella, good quality records of measurements of hull response were obtained on all instrumented ships. Records on the EC-2 were good quality throughout the time of chief interest, until passage of the direct shock wave; thereafter, severe mechanical shock motions of the recording equipment occurred because the recording unit platform went beyond the motion anticipated and hit bottom on the supporting springs. However, the vital response information for the EC-2 was obtained.

A few of the records from the DD-474, DD-592, DD-593 and EC-2 are shown on a compressed time scale in order to reveal an overall view of the response to underwater phenomena, in Figures 3.35, 3.36, 3.37, and 3.38. During Shot Umbrella, as shown by these records, the most significant loading phase, insofar as surface ships were concerned, was the direct shock wave. It may be noted that the maximum recorded ship-bottom velocity on the DD-474 was about 8 ft/sec; on DD-592 about 4 ft/sec; on DD-593 about 2 ft/sec; and on EC-2 about 13 ft/sec. The velocities measured over the cross section of the EC-2 hull are shown in Figure 3.39. Note that the maximum recorded side-frame velocity was about 45 ft/sec, which corresponds to the maximum side-frame displacement discussed below. The longitudinal distribution of response along the length of the DD-474 is illustrated in Figure 3.40.

The response upward through the DD-474 as indicated by a few velocity records at positions on the forward fireroom bulkhead is shown in Figure 3.41. Note that maximum response at this bulkhead was about 5 ft/sec at keel and 4 ft/sec at upper-deck levels. However, longer rise times at the upper-deck levels would greatly reduce acceleration and damage effects by as much as a factor of 20 or more.

The vertical displacement of the DD-474 is shown by the records of three gages in Figure

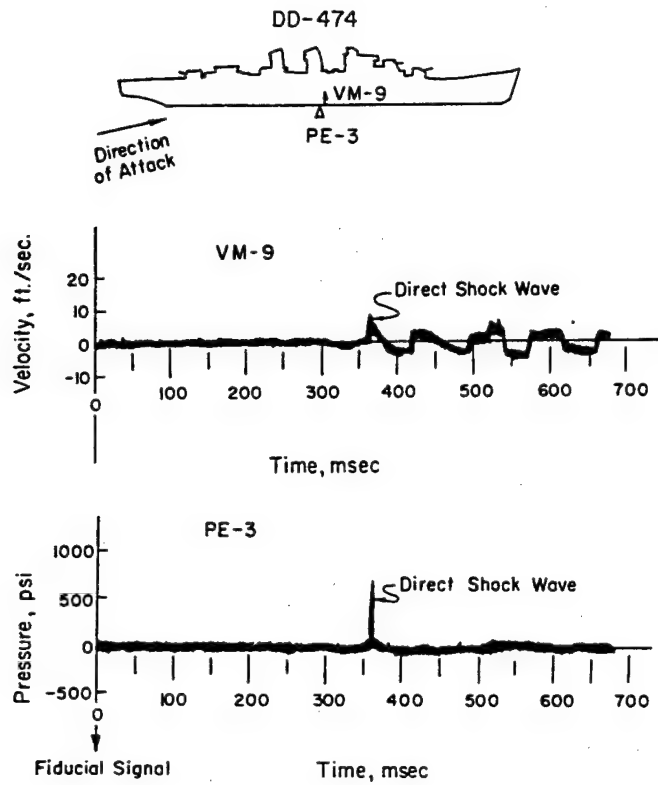


Figure 3.35 Overall underwater phenomena, DD-474, Shot Umbrella.

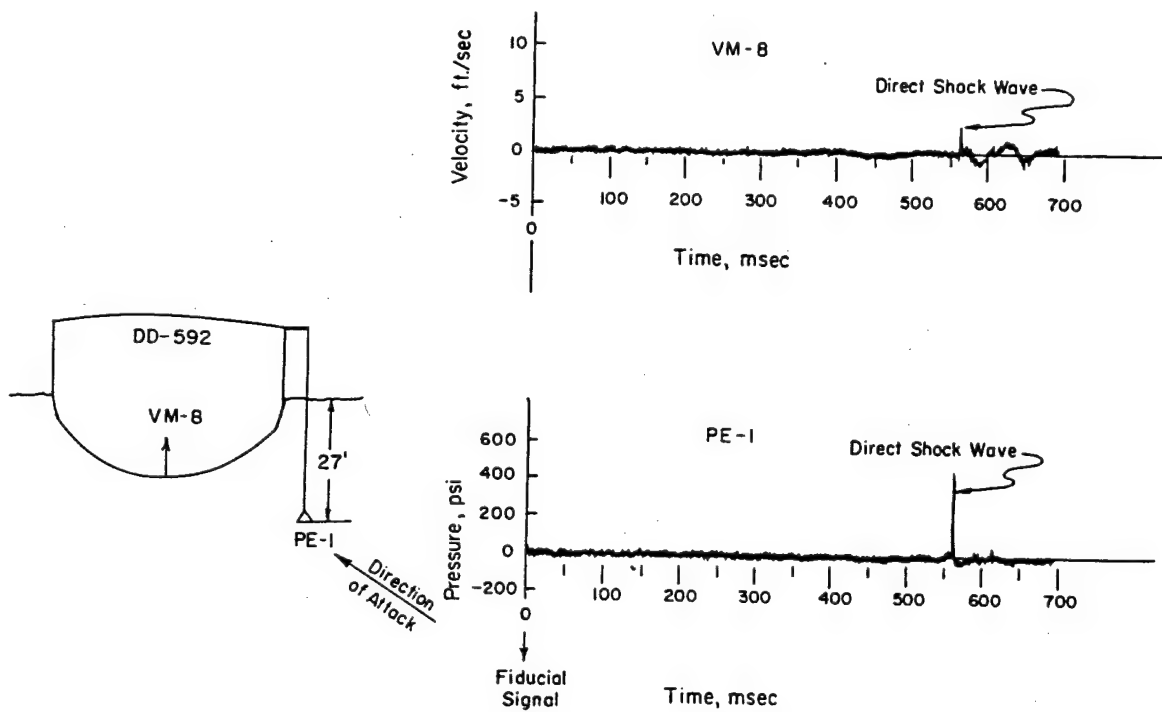


Figure 3.36 Overall pressure phenomena, DD-592, Shot Umbrella.

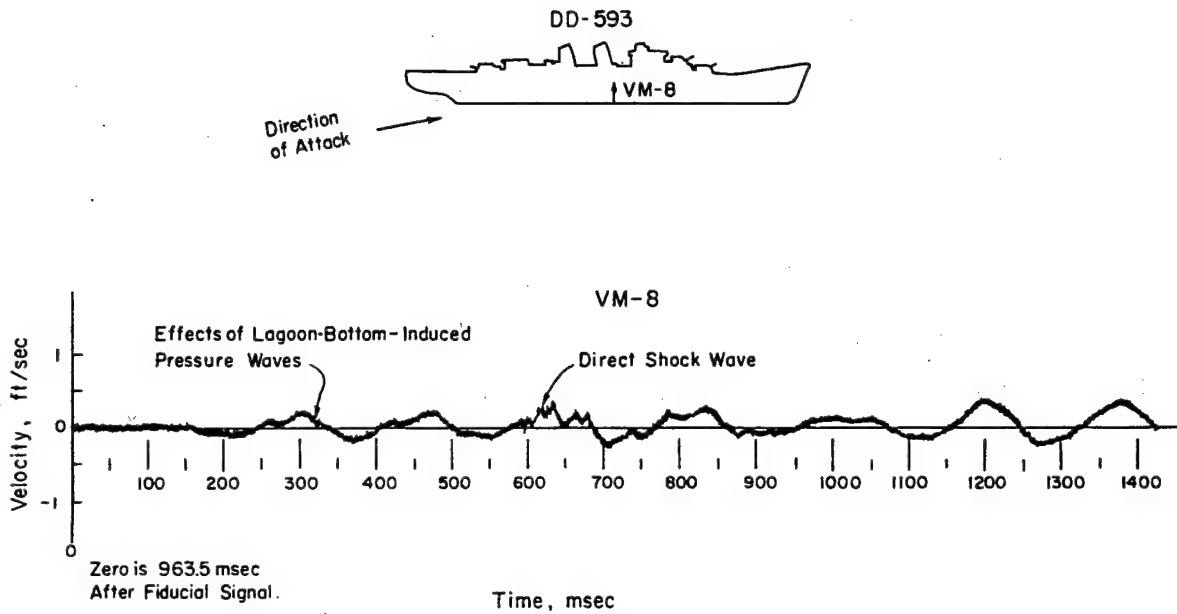


Figure 3.37 Overall pressure phenomena, DD-593, Shot Umbrella.

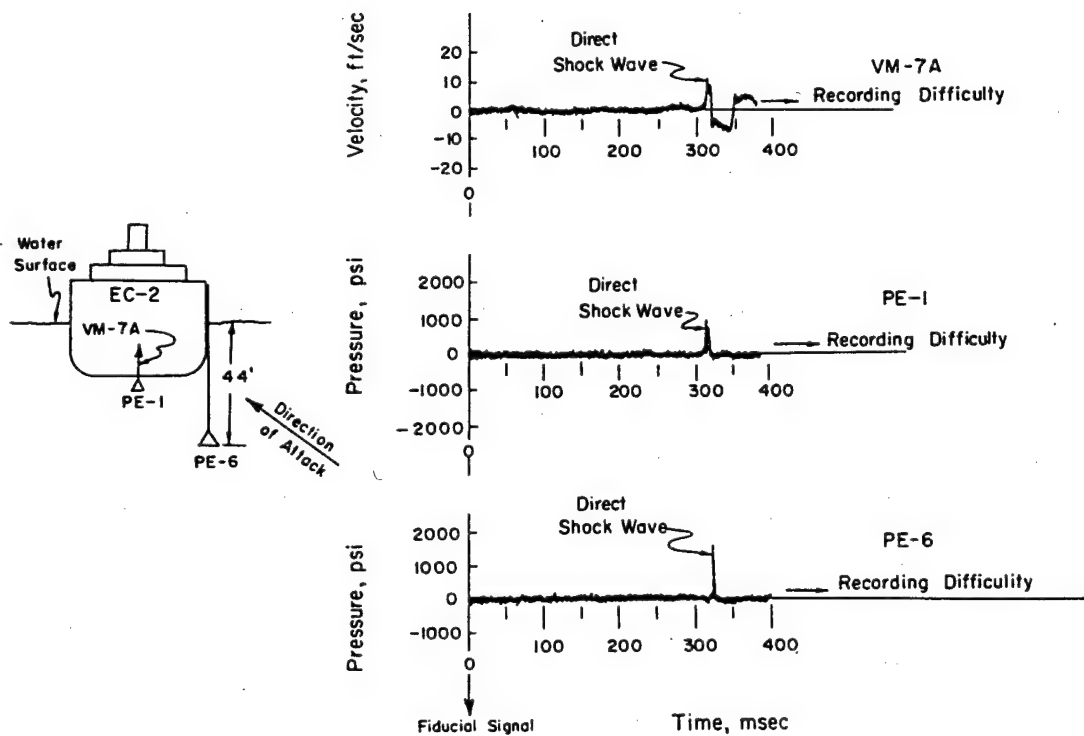


Figure 3.38 Overall underwater phenomena, EC-2, Shot Umbrella.

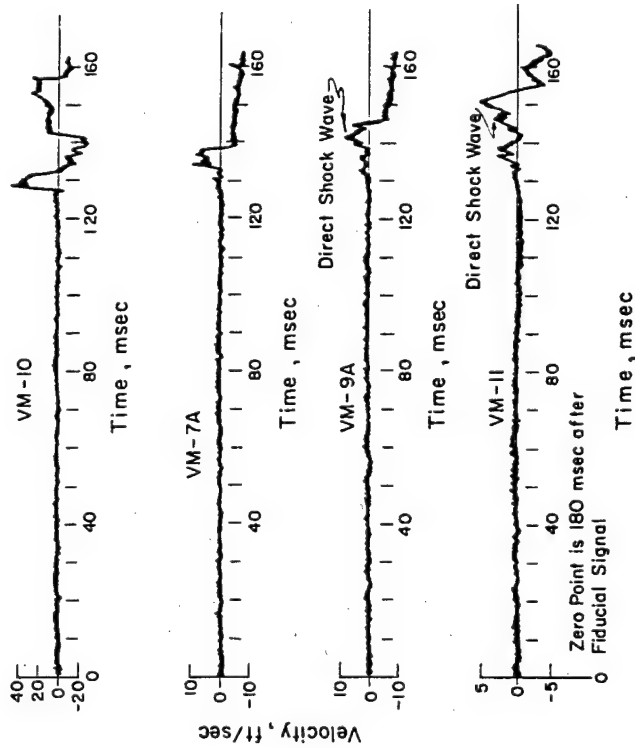
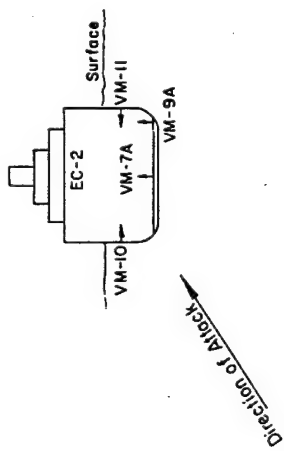


Figure 3.39 Cross-section distribution of initial hull response, EC-2, Shot Umbrella.

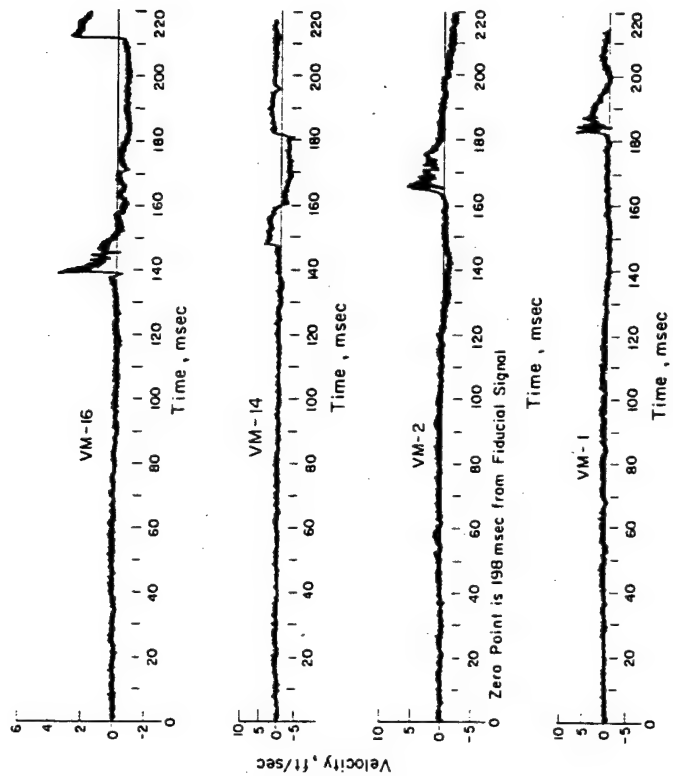
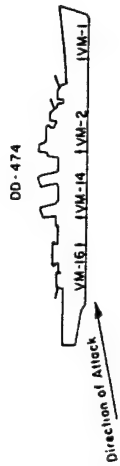


Figure 3.40 Longitudinal distribution of bottom (keel) velocities, DD-474, Shot Umbrella.

3.42, which indicate a maximum of about three inches of whole ship vertical bodily motion due to Shot Umbrella. A maximum vertical bodily motion of the EC-2 of about six inches is indicated in Figure 3.43.

The hull-damage survey of the EC-2 revealed hull damage characterized as light, similar to that found after Shot Wahoo. The maximum transient displacement of approximately  $4\frac{1}{2}$  inches occurred in the hull vertical side frames, with a maximum permanent displacement of about  $1\frac{1}{2}$  inches. In the same side area, maximum permanent hull-plating deformations between the side

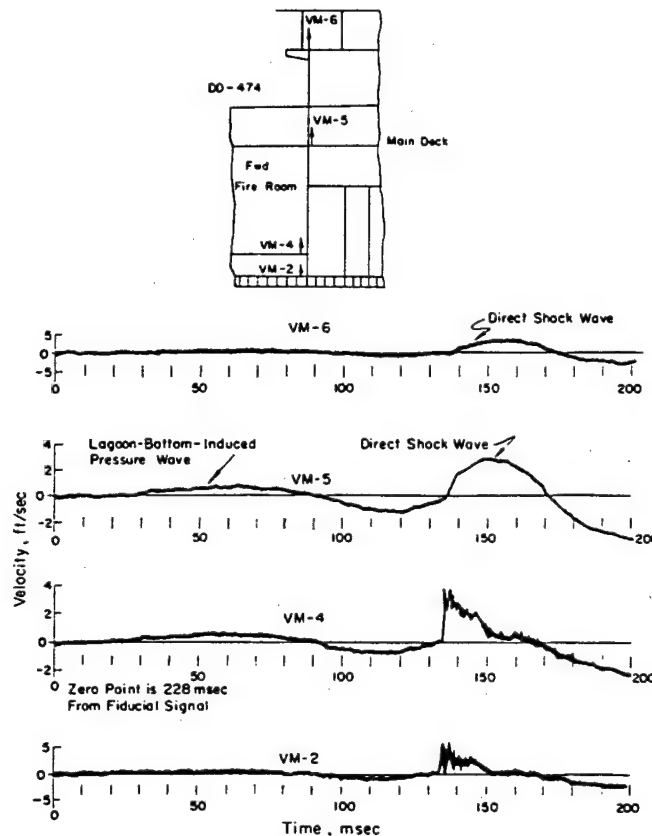


Figure 3.41 Response distribution upward along bulkhead, DD-474, Shot Umbrella.

frames were about  $\frac{3}{4}$  inch. Hairline fracture cracks at various minor locations of the steel hull deck and superstructure were found. The propeller shaft alley tunnel was further seriously distorted to a maximum of about 12 inches. Other damage was essentially the same as that after Shot Wahoo; however, previous damage was accentuated. Diver examination of the hull bottom revealed that most of the hull bottom plating dishes between frames did not exceed  $\frac{1}{2}$  inch; the maximum reported was  $1\frac{1}{2}$  inches in depth. As after Shot Wahoo, minor hull flooding caused by leaks in the hull was controllable by periodic pumping.

An examination of the hull of the DD-474 revealed no hull damage, dishing, or other hull deformation that could be ascribed to Shot Umbrella. However, a slight buckle in the after stack of the DD-474, bent bulwarks around the after-gun tubs, and a slightly buckled mast were produced by a combination of shock and the surface-water wave passage over the stern which faced the detonation. No hull damage occurred on the DD-592 or DD-593.

Conclusions. The hull responses and damages of the EC-2 and the DD-593, DD-592, and

DD-474 were about as expected on Shot Umbrella. However, considerable detailed study and analysis of all data collected is required. The following preliminary conclusions apply to the hull response and damage studies on surface ships in shallow water. It should be understood that Shot Umbrella conditions include yield, shot geometries and to a lesser extent, bottom reflection and thermal-gradient characteristics for these tests.

1. From the standpoint of hull deflection, a safe-delivery range for destroyers of [redacted] feet for Shot Umbrella conditions has been demonstrated. The minimum safe range, from the standpoint of hull deflections, is considerably smaller than this figure.
2. From the standpoint of hull deflection, it can now be estimated that the lethal range for the EC-2 is [redacted] feet under Shot Umbrella conditions.
3. Considerable basic information on hull response as related to free-field pressures and

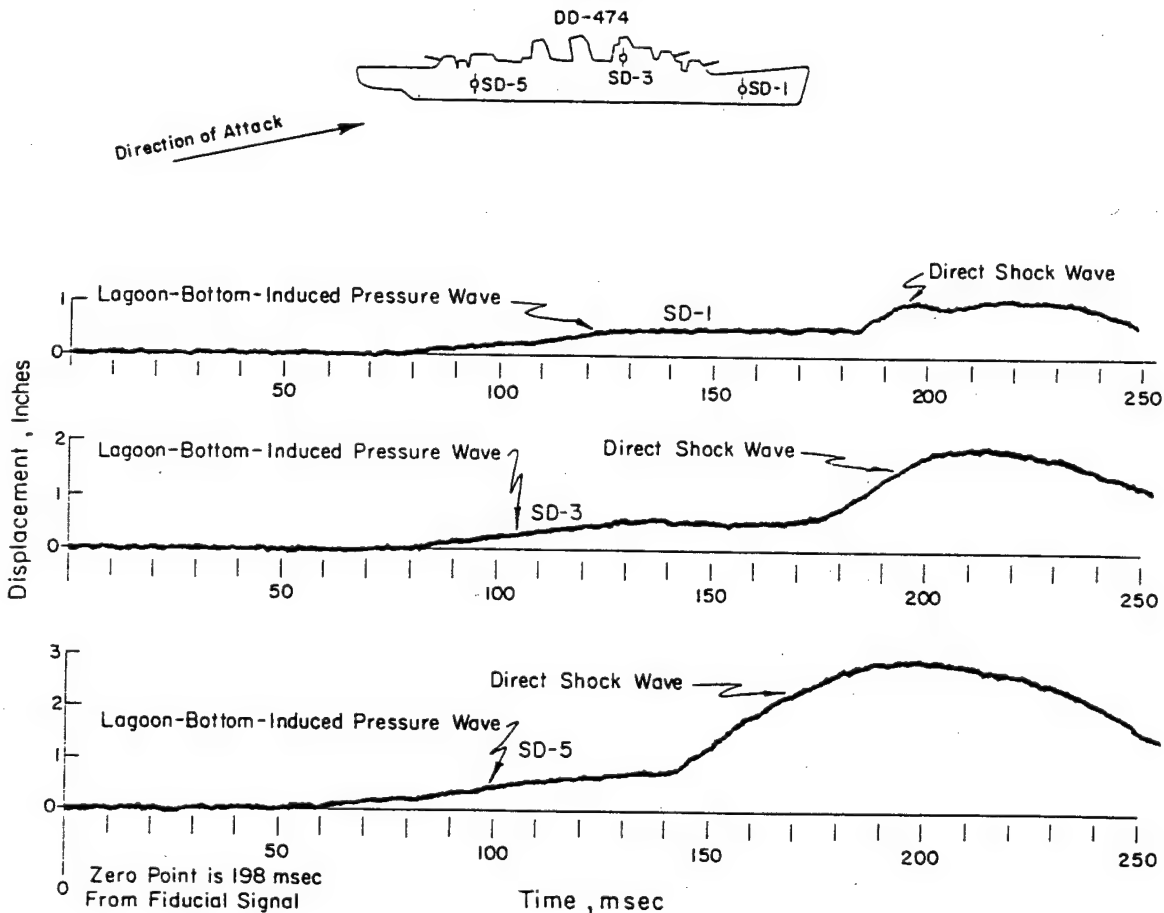


Figure 3.42 Vertical displacements on DD-474, Shot Umbrella.

loading measurements was obtained. This has provided check points for small-scale ship model experiments which confirm developed theories and, upon further analysis, is expected to prove valuable in extrapolating the results of Shot Umbrella to other conditions. Some of the other features of this information are given in the additional conclusions below.

4. During Shot Umbrella the direct-shock wave was the principal loading phase for surface ships within the close ranges of primary interest. Bulk cavitation-reloading effects following the direct shock wave were much smaller than those due to the direct shock wave itself. Vertical



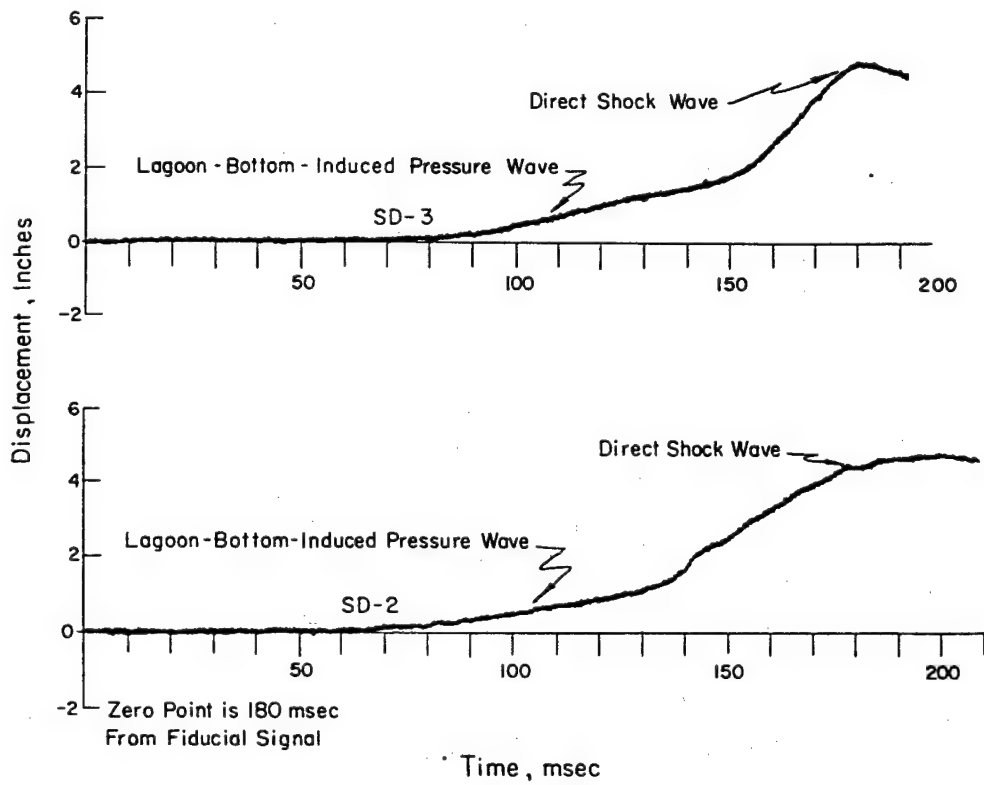
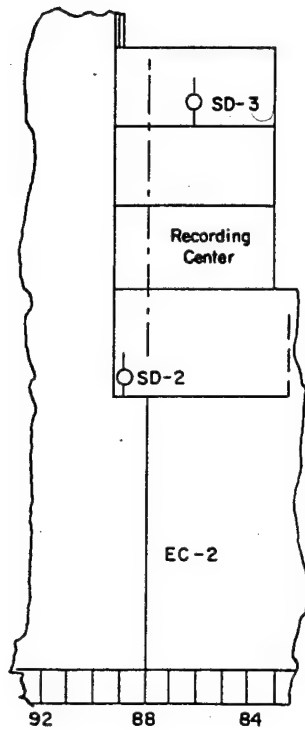


Figure 3.43 Vertical displacements on EC-2, Shot Umbrella.

velocities associated with the lagoon-bottom induced-pressure waves were negligible.

5. Under side-on attack, the bottom vertical and horizontal velocities are not uniform over the length of the ship; despite uniformity of loading, velocity response is critically dependent upon precise location of the structure to which the gage is attached.

6. During Shot Umbrella, vertical velocities measured at the keels of the target ships were considerably higher than corresponding water-particle velocities. The maximum vertical bottom velocities measured were: EC-2, 13 ft/sec; DD-474, 8 ft/sec; DD-592, 4 ft/sec; and DD-593, 2 ft/sec.

7. The severity of the shock motions in a surface ship diminishes considerably from bottom to the upper superstructure decks. The damaging initial accelerations can be reduced by a factor of 20 or more, even though the peak velocities are the same because of the slower rise time at the higher deck levels.

8. The character of the EC-2 hull damage under Shot Umbrella conditions was similar to small scale tests on the EC-2 models. The magnitude of side damage may be predicted, therefore, with an accuracy sufficient for predicting lethal ranges, on the basis of these small-scale tests.

3.4.3 Hull Response Studies of Submarines. Objectives. The principal effort of the submarine hull-response studies on Operation Hardtack was on Shot Umbrella. The effort involved measurement of the loading, strain, deformation, and damage of a submarine-like target, the Squaw-29, and also of the operating submarine, SSK-3. The objectives were to: (1) determine the range for lethal damage to a submarine-like (Squaw) target under attack in shallow water by an antisubmarine nuclear weapon; (2) study the process of hull damage to a submerged target for correlation with observed underwater phenomena and theory, and (3) determine the response of the hull of a submarine in a simulated attack position in shallow water.

Background. As previously discussed in Sections 3.4.1 and 2.4.4, Shot Baker of Operation Crossroads first tested submerged submarines (SS-212 and SS-285 class) exposed to nuclear attacks in shallow water. However, lack of instrumentation on this test made the obtained data questionable and, therefore, unsuitable for extrapolation to other shallow-water geometries. Further, the later Shot Wigwam results regarding submarines exposed in very deep water were not applicable to the shallow-water case. However, the submarine models (Squaws, 4/5 full-scale SS-563 class submarines in cross sectional dimensions) which were utilized in Operation Wigwam tests had been quite useful in determining safe ranges for submarines in very deep water.

On the other hand, the shallow water case was unique in that the close proximity to the burst of both the air-water surface interface and the sea-bottom-reflection boundaries introduced variations so that the prediction of underwater pressure-time histories was very difficult. However, even if the pressure-time history were known, that alone was insufficient to make an estimate of lethal range because of unknowns in plastic response of submarine hulls. Several theoretical methods relating the plastic response of a submarine hull to the short-duration pressure waves had been proposed, and several empirical rules had been suggested. However, none had been satisfactorily verified by experiment, particularly for the shallow-water geometry. As was previously discussed in Section 3.4.1, of the several hypotheses or methods suggested for determining submarine-hull lethality, the excess-impulse method appeared to be the most promising. However, opinions differed on the applicability of the excess-impulse concept, especially with the short duration pulses expected in the shallow-water case.

Thus, there were two difficulties which made theoretical estimates of lethal range of submarines in shallow water uncertain: (1) the variation in underwater pressure versus time was unknown and (2) the theories of plastic response of submarine hulls had not been confirmed.

By placing a submarine-like model (Squaw) target at a range expected to be near-lethal in the

Shot Umbrella geometry, it was expected that the reliability of the lethality-prediction methods could be assessed. Measurements of hull response of the Squaw during Shot Umbrella were also considered desirable to record the progress of the damage process. Correlation with the underwater pressure-time history would cast light on existing theories and serve as a guide for acceptance or rejection.

The operating submarine, SSK-3, was also to be exposed in a simulated attack position on Shot Umbrella, at a range expected to be safe for delivery of an underwater nuclear weapon.

**Procedure.** The Squaw-29 was the only surviving one of three submarine-like (Squaw) targets previously built for the Operation Wigwam test. Design of the Squaw test sections was based on the SS-563-class submarine, built on a 4/5 scale in cross section but of shortened length. The inside diameter of the pressure hull was 14.4 feet; length of pressure hull, 121.5 feet; hull plating, one-inch-high tensile steel with an average yield strength of 60,000 psi; frame spacing 30 inches; length of each test section, 29 feet. Major items of propulsion machinery inside the Squaw were simulated on 4/5 scale by cast-steel weights. These items included the three main engine generators, 11,900 pounds each, and the two simulated motors, 25,000 pounds each.

During Shot Umbrella, the Squaw-29 was submerged at periscope depth, located stern-on at [redacted] foot range from surface zero. Submergence was accomplished by remote-control venting of ballast tanks through hoses connecting the Squaw with associated instrument barge, YFNB-12, located at [redacted] foot range. Weights (clumps) totaling 10 tons were attached to chains hung from the bow and stern of the Squaw. When the weights rested on the lagoon bottom, the Squaw was suspended at the proper depth, with a positive buoyancy of about five tons.

The operational submarine SSK-3, without crew aboard, was located bow-on at [redacted] foot range on Shot Umbrella, also submerged to periscope depth. To more realistically simulate an attack position, two of the four bow torpedo-tube doors were open, one with and one without a torpedo in position. Submergence for test was accomplished by venting ballast tanks, such that when weights (clumps) attached to chains from the bow and stern rested on the lagoon bottom, the SSK-3 was suspended at the proper depth with a positive buoyancy of about 10 tons.

Instrumentation on Squaw-29 was essentially the same as for Operation Wigwam. Deformations of hull plating and stiffeners at typical locations were measured by 24-strain (SR-4) gages and four variable-reluctance-displacement gages. The pressure near the hull, as well as inside the ballast tanks, was measured by 16 piezoelectric-pressure gages. Overall motions of the hull and stiffeners were photographed with nine high-speed motion-picture cameras. The 14 roll, pitch, depth, and flooding gages also recorded those conditions. Figure 3.44 shows principal locations of gages and cameras on the Squaw. In addition, velocity-meter and shock-spectrum-recorder gages were installed for the shipboard machinery and equipment-shock studies. Measurements on the Squaw were recorded on oscillographic and magnetic-tape recorders located on the YFNB barge, after transmission through 850 feet of three special 2<sup>8</sup>/<sub>10</sub>-inch diameter multi-conductor instrument cables from the Squaw to the YFNB-12. The oscillograph recording units on the YFNB barge were protected from radiation by three-inch-thick lead shields; all recording units were located on shock-attenuating spring mountings.

Instrumentation on the SSK-3 hull consisted of seven strain gages and three high-speed cameras, which were identical to those installed for Shot Wahoo, as shown in Figure 3.45. The signals from the gages were recorded on an oscillograph in the submarine.

Operation of all instruments on both targets was triggered by radio-timing signals. The timing signals for the Squaw were transmitted to the YFNB-12. The signals for the SSK-3 were transmitted to an adjacent YC barge and were then relayed by cable to the submarine.

**Results.** Instrumentation functioned well on both the Squaw-29 and the SSK-3 during Shot Umbrella. Squaw hull damage was less than expected; lethal damage to and flooding of the pressure hull did not occur. However, four of the ten external ballast tanks ruptured, and all

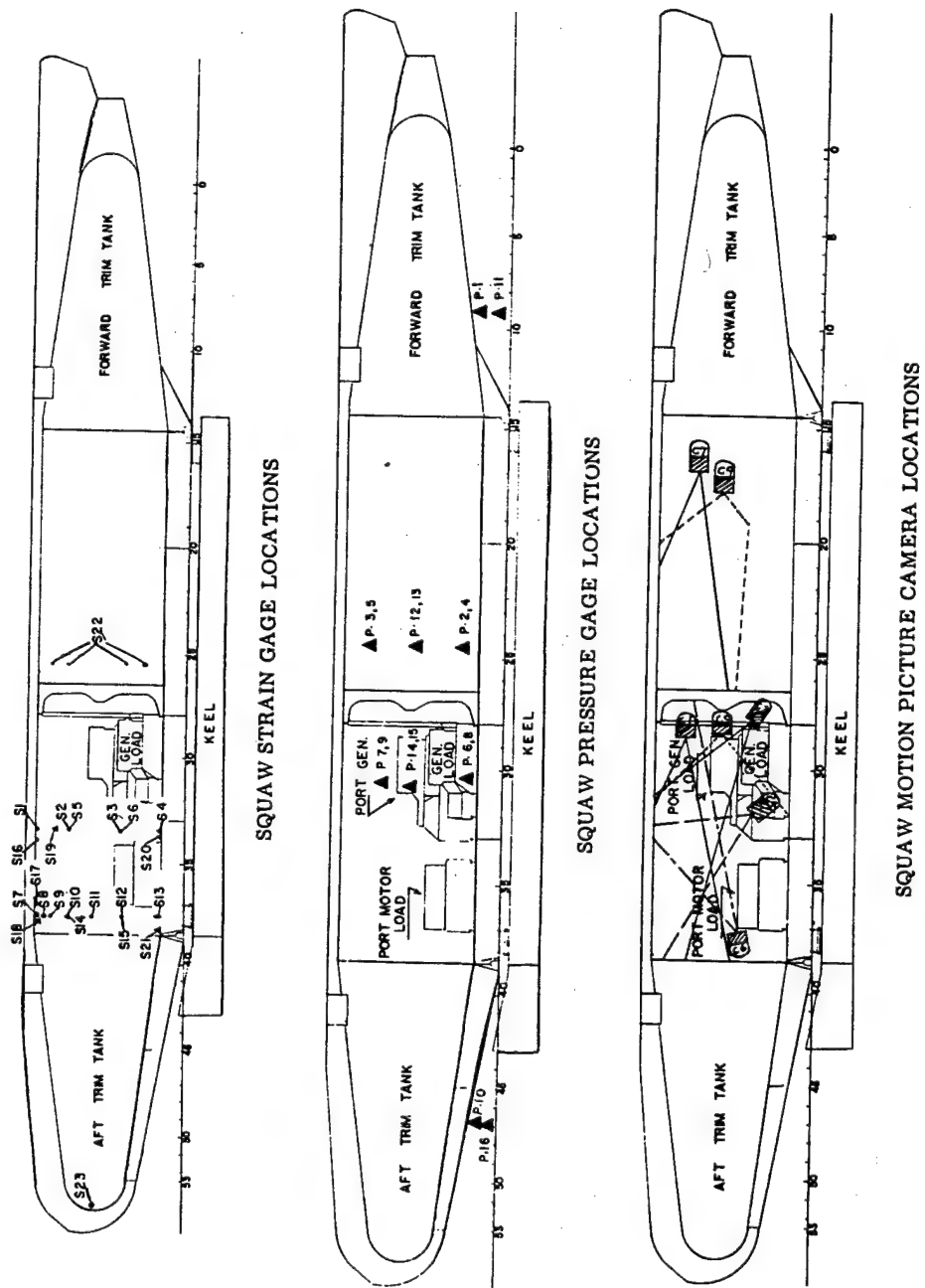
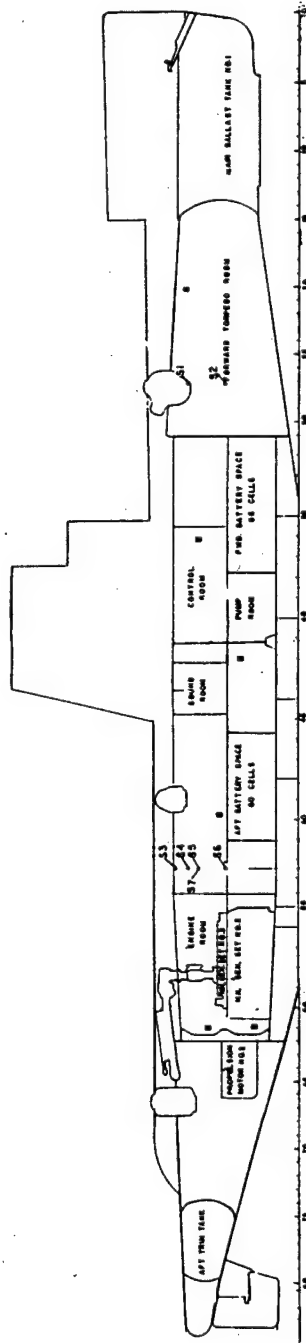


Figure 3.44 Squaw submarine hull instrumentation response.



SSK3 INSTRUMENTATION

Legend

- S— Strain Gage
- — High-Speed Motion Picture Camera

Figure 3.45 SSK-3 instrumentation and hull response.

were seriously dished. This resulted in some loss of buoyancy, and complicated resurfacing the Squaw after the test. Preliminary inspection of the Squaw hull after Shot Umbrella showed a maximum permanent plastic deformation of the hull plating of  $\frac{1}{4}$  inch between frames and one inch local buckling of three internal bulkheads because of hull deformation. As expected, there was no hull damage to the SSK-3 from Shot Umbrella.

Pressures recorded near the Squaw are indicated in Figure 3.46. Records of strain from the reflected shock wave on the Squaw and SSK-3 are shown in Figures 3.47 and 3.48, and the peak values of strain are shown in Tables 3.5 and 3.6.

The peak recorded free-field pressure near the Squaw was about 1,530 psi at [redacted] foot range; the predicted free-field pressure was 1,600 psi at [redacted] foot range. Thus, the actual pressures were slightly less than predicted. Note the positive pressure duration of about 6 msec. The peak pressure measured inside the ballast tanks of the Squaw-29 was 1,300 psi. This was twice the static hull-collapse pressure of 660 psi; after 1 msec this reduced to half of the peak value then increased to a value of about 950 psi for about 5 msec. The duration of that portion of the pressure pulse which exceeds the static collapse pressure was less than 2.5 msec. It is of interest to observe that approximately the same pressure, acting for 10 msec, caused collapse of a similar Squaw during Operation Wigwam. It appears that the pressure loading on the hull was too short to cause failure. One prediction was that an excess impulse of 5 psi-sec was required to collapse a submarine at shallow submergence. The excess impulse in the water near Squaw-29 was only about 1.3 psi-sec.

The maximum strains measured on the SSK-3 hull during Shot Umbrella were well within the non-damage range. The highest dynamic strain recorded was 1,160  $\mu$ in/in, which only approximates the static yield strength.

A subsequent detailed hull survey of Squaw-29 (in dry-dock) was planned, in order to accurately determine the hull deformations. After detailed comparison of data results with results of that survey, it is hoped a further understanding of submarine hull collapse and verification of the submarine hull lethality excess-impulse concept will be possible.

Conclusions. The following are the preliminary conclusions of this submarine hull study on Shot Umbrella. It should be understood that these conclusions apply to Shot Umbrella conditions.

1. The range for moderate hull damage to a 4/5-scale-submarine model, the Squaw, is [redacted] feet under Shot Umbrella conditions. In order to estimate safe or lethal ranges for Shot Umbrella conditions, the pressure field must be known and an adequate theory such as the excess impulse, or another concept correlating the plastic response of a submarine hull to pressure waves of short duration, must be confirmed or developed.
2. The SSK-3, under Umbrella conditions, at [redacted] was shown to be well beyond the minimum safe range for hull damage.
3. Strains as large as 13,000  $\mu$ in/in, which is six times the known yield strain of the plating, may be sustained without rupture in the hull plating of a Squaw. On the basis of Operation Wigwam experience, these strains should have produced much larger hull deformations, and this result will also be further analyzed prior to the final (WT) report.

3.4.4 Shipboard Machinery and Equipment Shock Damage Studies. Objectives. The objectives of the shipboard machinery and equipment shock-damage studies on Shot Umbrella were similar to those on Shot Wahoo, except that their application was to shallow-water geometries. The objectives on Shot Umbrella, therefore, were to: (1) determine safe ranges and moderate damages for delivery of antisubmarine nuclear weapons by destroyers in shallow water, from the standpoint of shock damage to machinery and equipment important to combat capability; (2) determine safe ranges for delivery of antisubmarine nuclear weapons by submarines in shal-

low water, from the standpoint of shock damage to machinery and equipment important to combat capability; and (3) determine the intensity and shock-motion data on ships' machinery, equipment, and foundations for correlation with free-field phenomena, hull loading, and theories so that results of a nuclear test in shallow water could be extrapolated to other burst geometries and ships.

**Background.** The problem of making predictions of shock response and damage to ship-

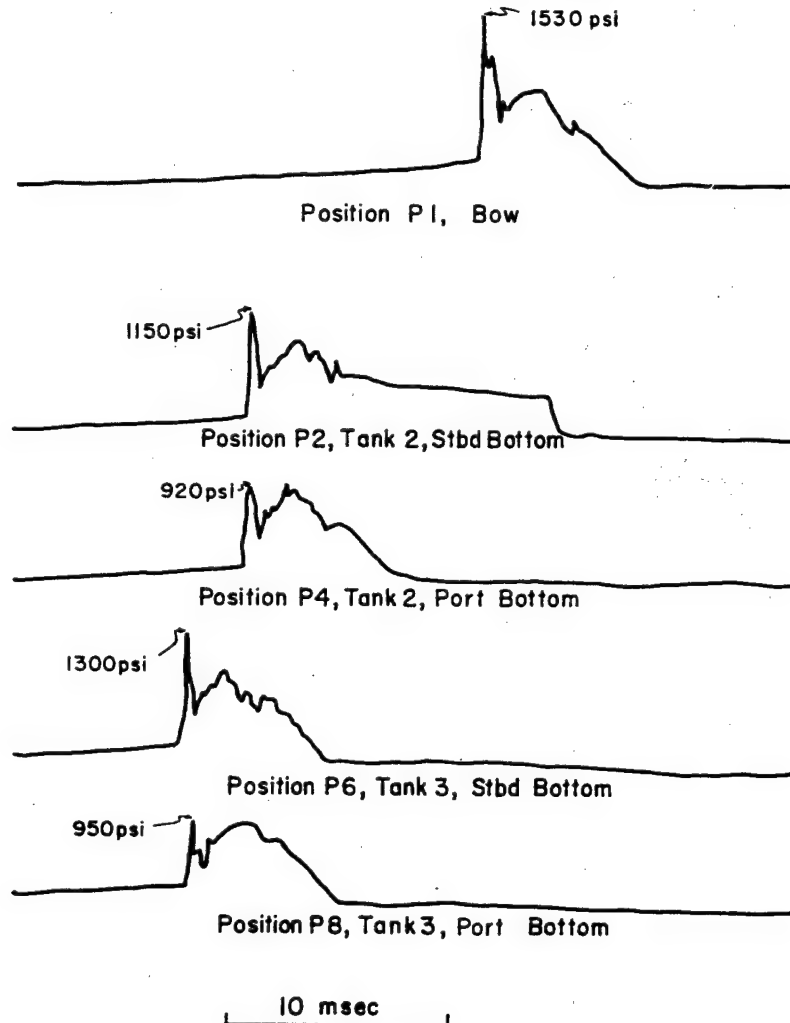


Figure 3.46 Pressures measured under the bow and near the bottom of the ballast tanks in Squaw-29 during Shot Umbrella.

board machinery and equipment from underwater nuclear weapon effects has been previously discussed in Section 2.4.5. The increased difficulty in making such predictions when the ship is in relatively shallow water compared with deep water has been further discussed in Section 3.4.1. The closeness of the burst to both the air-water surface interface and ocean bottom reflection boundaries for the shallow water geometry influences the pressure histories to such an extent as to make theoretical and small-scale explosive treatment quite complex and difficult.

As has been previously discussed, previous underwater nuclear detonations and high-explosive

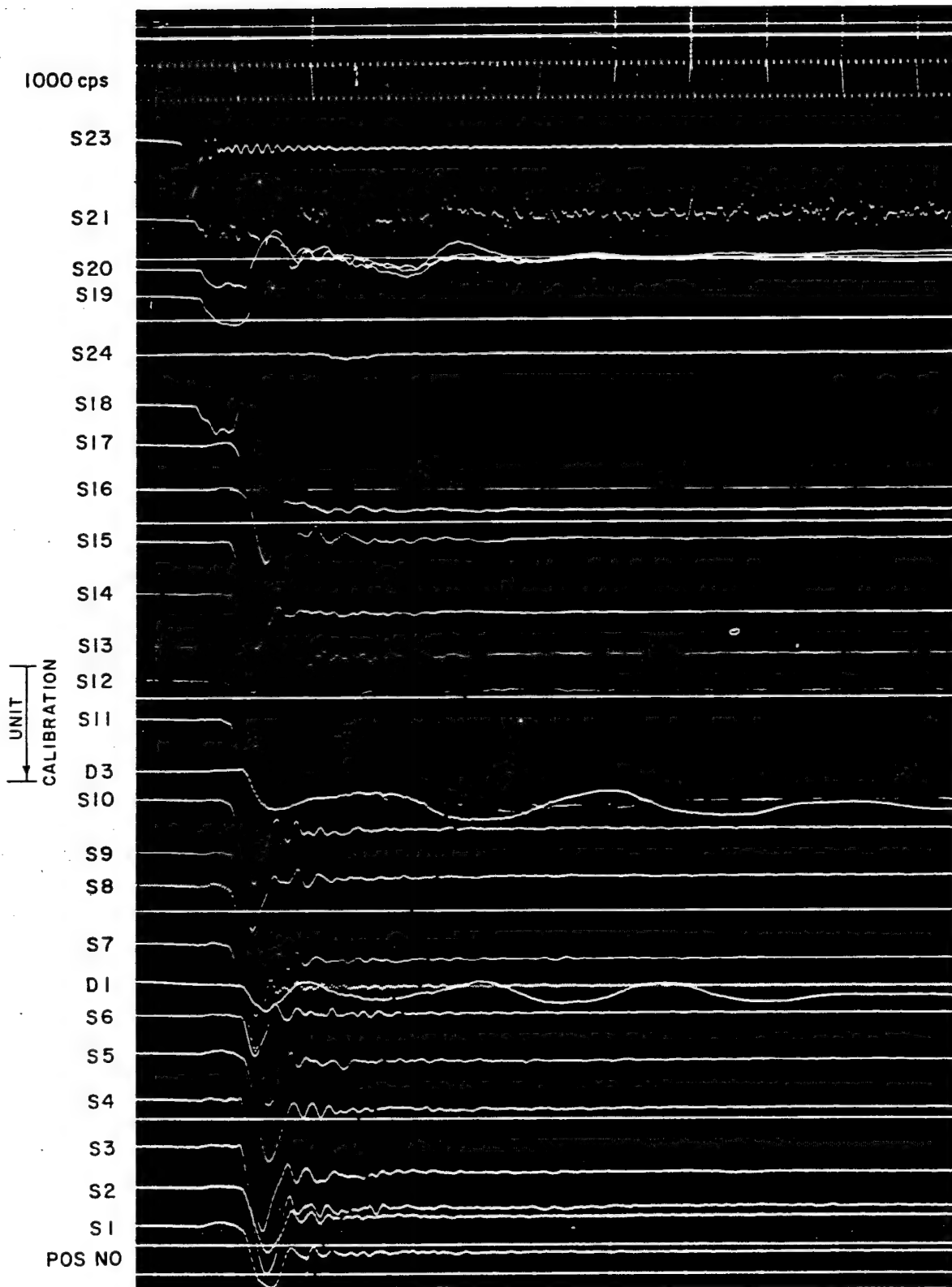


Figure 3.47 Oscillogram of direct shock wave on the Squaw-29 for Shot Umbrella.



tests have left many questions unanswered. Furthermore, existing data with which to correlate a given response from such a nuclear detonation in shallow water, with a given amount of damage, was still lacking. To permit improved shock-hardening design of future ships' machinery and equipment, such response data was urgently required.

It had become clear, therefore, that a full-scale nuclear underwater test in shallow water

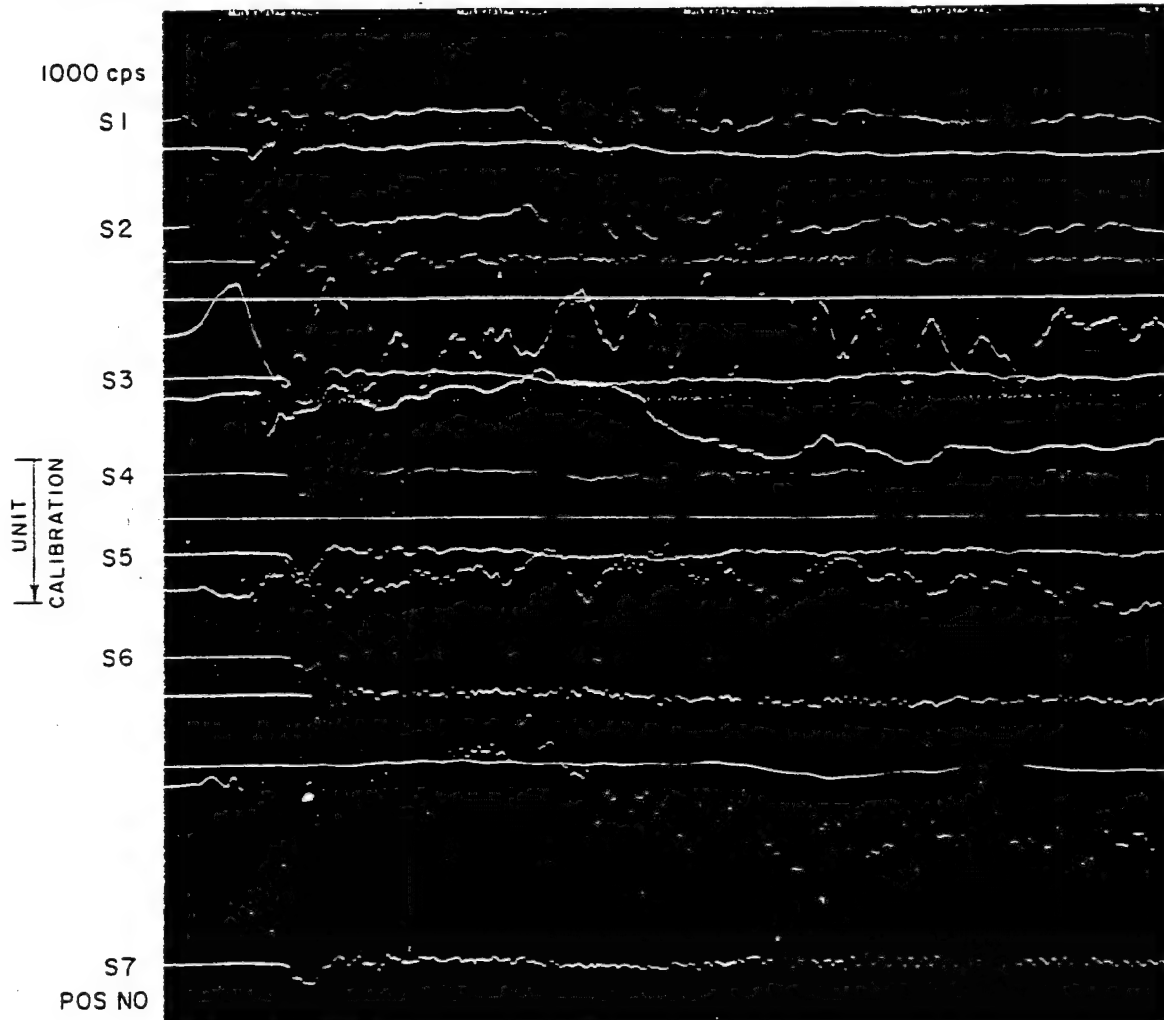


Figure 3.48 Oscillogram of direct shock wave on the USS Bonita (SSK-3) for Shot Umbrella.

was required to gather the necessary data on response and damage to ships' machinery and equipment.

**Procedures.** For the shipboard machinery and equipment shock-damage studies on Shot Umbrella, the same principal four surface target ships and one submarine were exposed as for Shot Wahoo, i. e., the DD-593, DD-592, DD-474, the EC-2 and SSK-3. These ships were, respectively, located stern-on at [redacted] feet, broadside at [redacted] feet, stern-on at [redacted] feet, broadside at [redacted] feet and bow-on at [redacted] feet from surface zero as shown in Figure 3.3 (Umbrella array). In addition, the submarine-like Squaw-29 and its instrument barge, YFNB-12, were included, respectively located stern-on at [redacted] and [redacted] foot range.

The ships' machinery and equipment and the foundations thereof (including hull bottoms, hull frames, decks, and superstructures on the four surface target ships) were relatively highly instrumented with the same gages and gage-recording equipment as had been previously installed for Shot Wahoo. This included a total of 43 high-speed cameras installed in the four surface



TABLE 3.5 STRAINS ON SQUAW-29 FROM SHOT UMBRELLA

Position Number	Direction of Measurement of Strain	Frame Number	Degree from Crown	Strains in mils per inch	
				Maximum	Permanent Set
S1	*	33½	0	3.8	1.6
S2		—	60S	4.7	1.8
S3		—	120S	7.5	3.5
S4		—	180	8.3	4.6
S5		—	60P	5.6	3.0
S6		—	120P	5.5	2.6
S7	*	37½	0	6.9	4.0
S8		—	16P	9.9	6.0
S9		—	32P	10.0	6.6
S10		—	60P	8.7	5.4
S11		—	90P	10.8	7.4
S12		—	120P	11.0	9.0
S13		—	180	5.2	2.4
S14		—	60S	5.2	3.1
S15		—	120S	12.7	9.0
S16	*	34	0	8.1	4.1
S17		37	0	13.0	7.5
S18	†	37½	2P	-6.0	-4.0
S19		33½	32S	-1.7	-0.8
S20		33½	180	-0.9	-0.2
S21		38¼	180	2.0	0.0
S22	*	25½	Av	†	†
S23	‡	54	—	1.7	0.2
S24	§	—	—	0.0	0.0

- \* Circumferential (compression is positive strain).
- † Axial (compression is positive strain).
- ‡ Two gages at right angles (compression is positive strain).
- § Dummy gage on unstrained block.
- ¶ Gage failed before shot.

TABLE 3.6 STRAINS ON THE USS BONITA (SSK-3) FROM SHOT UMBRELLA

Position Number	Location *	Maximum Strain	Equivalent Depth †
		μ in/in	ft
S1	Frame 27 at crown	600	500
S2	Frame 27, 90 deg port	1,160	640
S3	Frame 52½ at crown	360	280
S4	Frame 52½, 26 deg port	350	270
S5	Frame 52½, 45 deg port	390	310
S6	Frame 52½, 90 deg port	200	230
S7	Frame 52½, 90 deg stbd	310	180

- \* All gages measured circumferential strain. Compression is recorded as positive strain.
- † Change in depth of submarine which would produce same static strain as the largest dynamic strain observed. Strain gages were calibrated during deep-dive trials.

ships, the SSK-3, and the Squaw, primarily for the purpose of recording shock damage to machinery and equipment. The same gages and recording equipment were also used on the submarine SSK-3 as had been previously installed for Shot Wahoo. The description of this instrumentation has been included in Section 2.4.3. In general, all shipboard machinery and equipment-response instrumentation installed for Shot Wahoo was also used for Shot Umbrella.

In addition, a total of 16 velocity-meter gages and 16 shock-spectrum-recorder gages were installed on the items of simulated major shipboard machinery and equipment in the Squaw. Seven of the high-speed cameras were installed in the Squaw to measure the shock motions of this equipment, as well as the hull motions thereof, for correlation with the shock velocity-time and shock-spectra data.

**Results.** On all seven ships in the Shot Umbrella array, records of the shock motion versus time were made successfully with all electronic-velocity meters. Timing-signal equipment and zero-time fiducial signals functioned satisfactorily. Good records were obtained on all except six of the 170 shock-spectrum recorders installed. All but one of the 43 high-speed cameras gave satisfactory results, with good quality films. In general, all instrumentation functioned in an excellent manner.

The records of shock versus time obtained from minus two to plus 20 seconds after detonation showed several excitations. However, in all cases, the maximum shock velocity was produced by the direct-shock wave. Minor motions produced by a sea-bottom-induced-pressure wave preceded those from the directly transmitted wave.

Figure 3.49 shows a typical oscillogram record from one of the targets, the response of the direct-shock wave on the EC-2. Tables 3.7 and 3.8 show a tabulation for the EC-2 and DD-474 of the velocities, rise time, and average acceleration for both the initial direct shock and the later motion which occurred after about  $\frac{1}{4}$  second. The tabulations interestingly show the general range of response motions on various items of machinery and foundations. The maximum vertical range of velocity of about 12 ft/sec on the EC-2, 7 ft/sec on the DD-474, 3 ft/sec on the DD-592, and less than 1 ft/sec on the DD-593 compared reasonably well with similar measurements taken for the hull studies.

An example of the shock-spectrum recorder-data, which has been read and reduced, is shown in graphical form in Figure 3.50.

The ship's machinery and equipment of the EC-2, located broadside at 1,600 feet from surface zero, had been previously disabled by Shot Wahoo and this severe damage was increased by Shot Umbrella. This further disabling damage occurred when the casting over the low-pressure cylinder of the main engine broke off. Additional brickwork in the boiler crumpled. Structural damage in the propeller shaft alley was markedly increased.

On the DD-474, stern-on [redacted] feet from surface zero, the ship's machinery and equipment damage could probably be classified as light but closely approaching the moderate-damage range. The bolts attaching the flexure plate that supports the main propulsion turbines and condensers to the ship hull structure were further deformed in both shear and bending. The flexure plate itself began to buckle. Misalignment resulting from these deformations may have seriously damaged the propulsion plant; this will be determined later in a shipyard tear-down inspection. It will be recalled that complete failure of these flexure-plate bolts would drop the turbine into the bilge, and at normal turbine speeds this probably would result in severe damage to the ship. Figure 3.51 shows the vertical velocity records at the bulkhead, at the flexure plate and on the foundations for high-pressure and low-pressure turbine subbases in the forward engine room of the DD-474. The average accelerations were 27, 9 and 6 g, respectively. In addition, the DD-474 ship's master gyrocompass was made inoperable because of failure of support springs. Brick work in three of the four boilers was out of place. The sonar-head motor fell off its supports, preventing operation. Further gun damage, breakage of light bulbs, and shattering of several water closets also resulted.

The shock damage was negligible on the DD-592 and DD-593 at [redacted] and [redacted] feet, respectively.

The shock damage to equipment on the SSK-3 at [redacted] foot range, bow-on, consisted of minor items such as loosened bolts attaching some equipment, the flooding of No. 3 torpedo tube, and

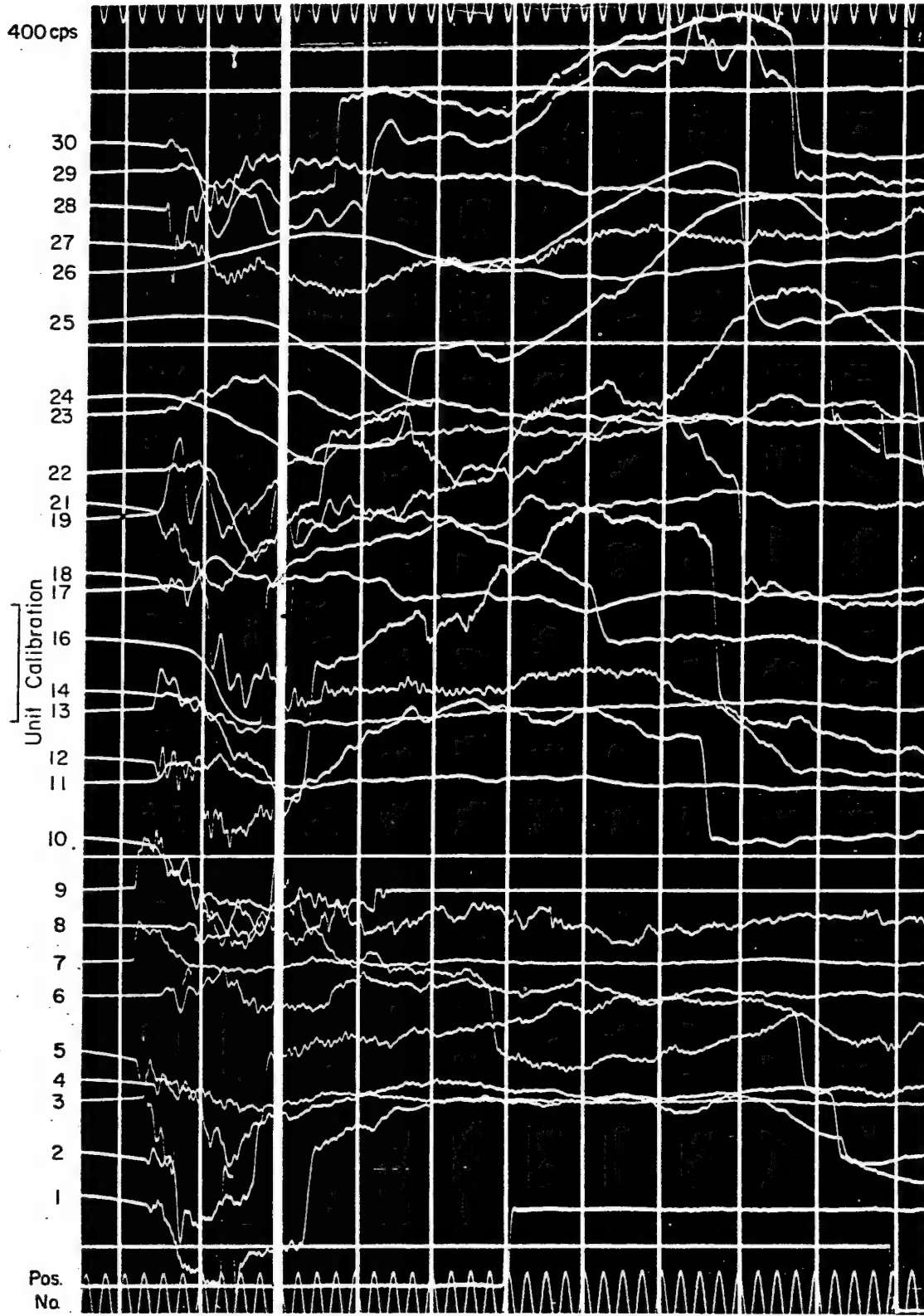


Figure 3.49 Oscillogram of direct shock wave on SS Michael Moran (EC-2) for Shot Umbrella.

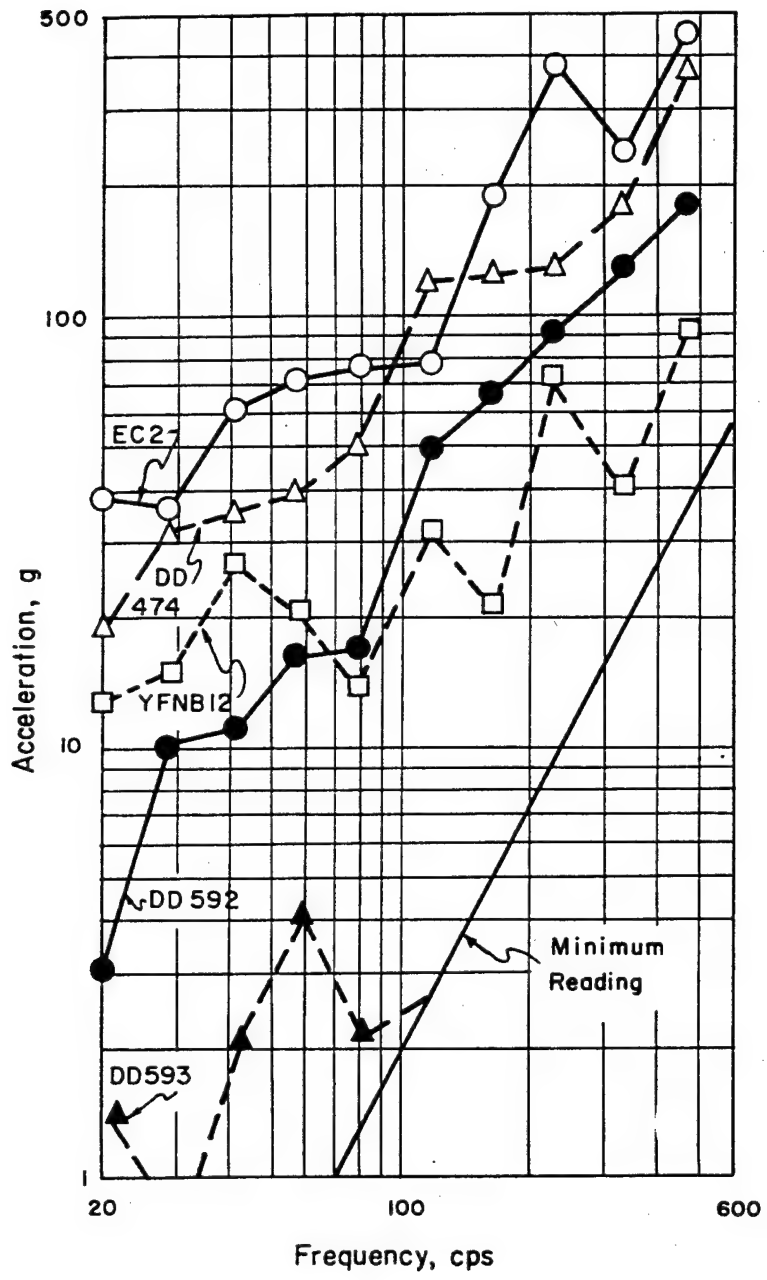


Figure 3.50 Shock spectra obtained near the bottom of a bulkhead on each of the surface targets, Shot Umbrella. Shock spectra are shown for Position 1 on EC-2, Position 17 on each of the three destroyers, and Position 2 on YFNB-12. On DD-593, deflections of the five highest-frequency reeds in the shock-spectrum recorder were all less than the minimum readable value.

some broken fluorescent light tubes. Since any of these items could be rectified within a few minutes, none was disabling.

The Squaw-29, submerged at 50-foot depth, at [redacted] feet from surface zero, stern towards the burst, sustained some simulated equipment damage. The steel weights simulating submarine main engines, generators, and motors had undergone severe response. One of the 24 bolts attaching the one simulated engine-generator failed in tension; the other 23 bolts were loose, many stretched as much as 1/4 inch. In general, all mounting bolts for the simulated equipment on the

TABLE 3.7 VELOCITIES, RISE TIMES, AND AVERAGE ACCELERATIONS ON SS MICHAEL MORAN (EC-2) FROM SHOT UMBRELLA

Position Number	Orientation *	Location	Initial Shock			Later Motion †		
			Peak Velocity	Rise Time	Average Acceleration	Peak Velocity	Rise Time	Average Acceleration
			ft/sec	msec	g	ft/sec	msec	g
1	V	Bottom center Bulkhead 88	5.6	6	31	5.4	48	3
2	V	Bottom center Frame 97	8.6	1	210	4.9	40	4
3	A	Bottom center Frame 97	-6.3	1	-220	1.1	10	3
4	V	Bottom stbd Frame 97	10.7	4	79	5.3	12	13
5	V	Bottom port Frame 97	11.3 †	4 †	97	4.9	40	4
6	A	Low stbd Frame 97	-4.3	6	-25	-4.8	9	-17
7	A	Low port Frame 97	-24.9	1	-1,500	§	§	§
8	A	Higher stbd Frame 97	-8.4	11	-23	-4.8	7	-21
9	A	Higher port Frame 97	-35.3	3	-390	§	§	§
10	V	Subbase main engine	5.3	5	33	5.6	48	4
11	A	Subbase main engine	-2.4	8	-9	0.7	5	4
12	V	Foundation Caterpillar diesel	7.5	4	60	4.7	6	24
13	A	Foundation Caterpillar diesel	-6.7	1	-210	1.7	3	18
14	V	Foundation steam-generators	7.5 †	13 †	18	4.7	13	11
16	V	Top of main engine	7.5 †	7 †	33	4.0	9	14
17	A	Top of main engine	-3.1	3	-32	1.2	9	4
18	V	Caterpillar diesel	9.9	6	48	5.8	13	14
19	A	Caterpillar diesel	-5.0	3	-60	1.4	6	7
21	V	Platform deck Bulkhead 88	5.5	6	27	2.5	11	7
22	V	Platform deck Frame 83	5.5	8	22	5.1	27	6
23	A	Platform deck Frame 83	-3.5	13	-8	-2.7	37	-2
24	V	03 level Frame 89	4.5 †	18 †	8	7.1	46	5
25	V	Wheelhouse	8.1 †	25 †	10	9.7	57	5
26	A	Wheelhouse	-3.6	18	-6	§	§	§
27	V	Steering gear room	2.6	4	18	-1.1	25	-1
28	V	Shaft alley	9.7	1	600	§	§	§
29	V	Foundation operating diesel	5.9	3	61	5.5	37	5
30	V	Operating diesel	4.2	12	11	9.1	48	6

\* Direction of measurement of motion: V, Vertical (motion upward is positive); A, Athwartship (motion to port is positive).

† Occurred about 0.24 second after initial shock motion.

‡ Meter bottomed at the limit of its displacement while velocity was still increasing.

§ Meter damaged after initial shock motion and gave no further record.

SSK-3 were loosened as a result of such stretching action. The YFNB-12, end-on at 2,350 feet, did not receive any equipment or structural damage.

Conclusions. The shipboard machinery and equipment shock damage on the target ships for Shot Umbrella occurred approximately as predicted. In the following conclusions of these studies, it should be understood that they apply to Shot Umbrella conditions:

1. The minimum safe range for delivery of an antisubmarine weapon by destroyers is [redacted] feet for Shot Umbrella conditions. Damage or malfunction of particularly delicate equipment (e. g., some types of electronic equipment) may occur at larger ranges.
2. The range for moderate damage for delivery of an antisubmarine weapon by destroyers is [redacted] feet for Shot Umbrella conditions.
3. The minimum safe range for a submarine is [redacted] for Shot Umbrella

conditions. Damage to particularly delicate equipment may occur at larger ranges.

4. The range for moderate damage to a submarine for Shot Umbrella conditions is from [REDACTED] feet.

5. Shock data defining the intensity and character of shock motions on merchant ships were obtained on an EC-2 at [REDACTED] feet from Shot Umbrella. At this range, complete disablement damage previously received was repeated and considerably increased.

6. Sets of shock motion data were obtained on all ships during Shot Umbrella.

7. Insufficient data still exist for correlating shock motion with damage to ship's equipment.

TABLE 3.8 VELOCITIES, RISE TIMES, AND AVERAGE ACCELERATIONS ON  
USS FULLAM (DD-474) FROM SHOT UMBRELLA

Position Number	Orientation *	Location	Peak Velocity †	Rise Time	Average Acceleration
			ft/sec	msec	g
1	V	Keel Frame 22	5.0	1	250
4	V	Foundation battery control	3.3	1	100
5	V	Battery control	3.5	1	110
6	V	Radio central Bulkhead 72	2.9	16	6
13	V	Keel Frame 99	5.7	1	230
17	V	Keel Bulkhead 110	3.4	3	32
18	L	Keel Frame 109	1.1	1	43
19	V	Flex plate Bulkhead 92½	2.4	1	120
20	V	Foundation reduction gear, fwd	3.1	2	61
21	V	Foundation reduction gear, aft	3.2	5	19
22	V	Foundation turbogenerator, fwd	4.1	12	11
23	A	Foundation turbogenerator, fwd	-1.9	21	-3
24	V	Foundation turbogenerator, aft	3.2	8	13
25	A	Foundation turbogenerator, aft	1.2	1	46
26	V	Reduction gear	4.6	5	30
27	V	Subbase HP turbine	5.6	18	9
28	V	Subbase LP turbine	5.6	27	6
29	V	Subbase turbogenerator	5.0	14	11
31	V	Main deck Bulkhead 110	4.5	12	11
33	V	Main deck Frame 107	3.8	16	8
34	V	Deckhouse top	6.6	18	8
46	V	Foundation 5-in. gun	5.5	3	60
48	V	Steering gear room	5.5	2	110
49	A	Steering gear room	2.0	1	45
50	L	Steering gear room	1.7	12	4
51	V	5-in. gun	7.5	12	19

\* Direction of measurement of motion: V, Vertical (motion upward is positive); A, Athwartship (motion to port is positive); L, Longitudinal (motion forward is positive).

† Values shown are for the initial shock motion. An additional shock motion occurred about 0.19 second after the initial shock but values are not tabulated here. Peak velocities for the additional shock motion were somewhat smaller than for the initial shock and average accelerations were much lower.

The general lack of equipment damage, except on the EC-2, still leaves correlation of response data in the severe-damage range to be resolved.

8. The safe range and the damage for both submarines and surface ships is determined by shock damage to ship's machinery and equipment rather than hull damage, for both Shot Wahoo and Shot Umbrella conditions.

3.4.5 Summary. In summary, it is concluded that on Shot Umbrella, the results obtained



from the projects in Program 3 were generally successful in achieving the main objectives of the program.

The responses and damages to hulls and to ships' machinery and equipment of the surface ships EC-2, DD-593, DD-592 and DD-474 were about as predicted. Response and damage to the submarine target, the SSK-3, was approximately as predicted. Response and damage to the Squaw-29 was somewhat less than predicted. The reason for the latter will be known only after

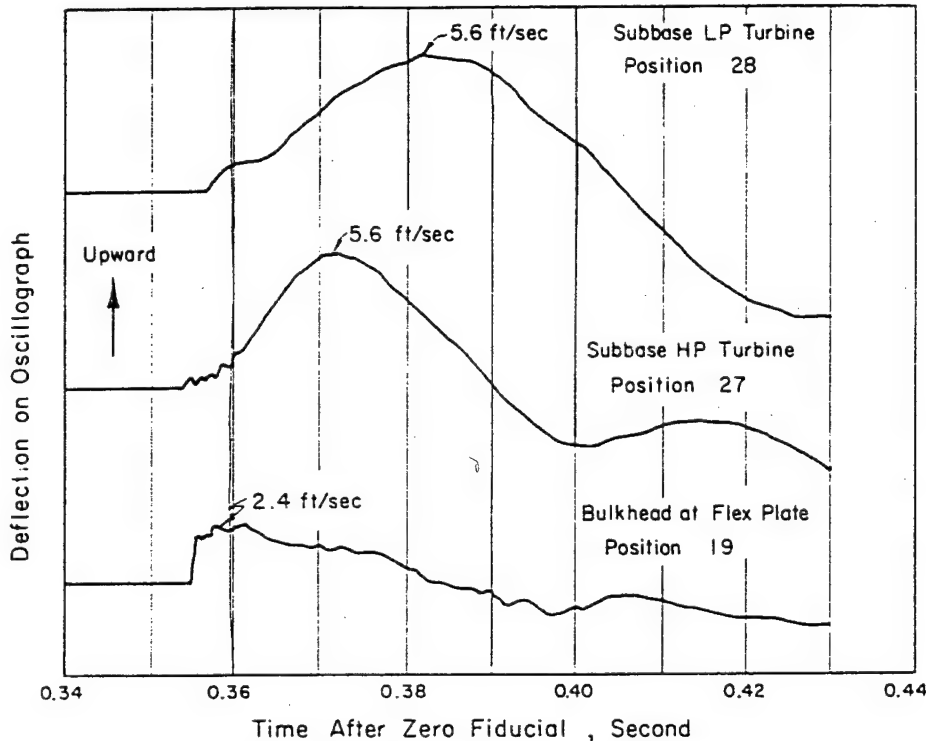


Figure 3.51 Vertical velocities of turbine foundation and subbases in USS Fullam (DD-474), for direct shock wave from Shot Umbrella.

detailed analysis of results. However, it may be due to a greater than estimated hull strength.

The EC-2 merchant ship located broadside (starboard) at [redacted] feet from surface zero sustained light hull damage similar to that previously received on Shot Wahoo, broadside (port). A maximum transient displacement of about four inches in the hull-side frames near the ship's center produced a maximum permanent hull-side-frame displacement of about 1 1/2 inches. Maximum permanent hull-plate dishing between frames was about 3/4 inch. Hair-line fracture cracks at various minor locations on the steel hull deck and superstructure were found. The propeller shaft alley tunnel was further seriously distorted, to a maximum of about 12 inches. As after Shot Wahoo, minor hull flooding, caused by leaks in the hull, was controllable by pumping. In contrast to the light hull damage, the severe disabling damage previously caused by Shot Wahoo to the ship's machinery and equipment of the EC-2 was further increased by Shot Umbrella.

As expected, there was no hull damage to the DD-474, the destroyer closest to surface zero and located stern-to a [redacted] foot range. However, a slight buckle in the after stack of the DD-474 bent bulwarks around the after gun tubs, and a slightly buckled mast was produced by a combination of shock and the surface water-wave passage over the stern. The ship's machinery and equipment damage on the DD-474 could probably be classified as light but closely approaching the moderate-damage range. The flexure-plate bolts which support the foundations to the main turbines were further deformed in both shear and bending. Misalignment between the turbine and propulsion shaft resulting from the bolt deformation was taken up in the coupling. Although the turbine still operated at the normal 400 rpm cruising propeller-shaft speed through and after the shot detonation, an increased machinery noise level indicated that the deformations may have



seriously damaged the propulsion plant. This will be determined later in a shipyard tear-down inspection. Other damage on the DD-474 consisted of ship's master gyrocompass made inoperable; brickwork in three out of four boilers knocked out of place; further five-inch gun damage occurred; and several water closets were shattered.

Hull and machinery shock damage on the other surface target ships on Shot Umbrella was considered negligible.

There was no hull damage of the SSK-3, submerged at a depth [redacted] and located bow-on at [redacted] foot range. Shock damage to equipment consisted of minor items, such as loosened bolts attached to some equipment and flooding of one torpedo tube. None of this shock damage was disabling, and it could have been rectified within a few minutes.

Hull damage to the Squaw-29 was less than expected; lethal damage and flooding of the pressure hull did not occur. However, four of the ten external ballast tanks ruptured. Maximum permanent plastic deformation of the  $\frac{7}{8}$ -inch pressure hull plating was about  $\frac{1}{4}$  inch between frames. Some equipment damage occurred on the Squaw, including tension failure of one  $\frac{7}{8}$ -inch diameter equipment hold-down bolt and up to  $\frac{1}{4}$ -inch stretching of numerous other hold-down bolts, indicating all equipment had undergone severe response.

From the results obtained, there was confirmation that the safe range and damage range for submarine and surface ship targets, under Shot Umbrella conditions, is determined by shock damage to ships' machinery and equipment, rather than by hull damage.

The following other preliminary conclusions drawn from Shot Umbrella data with respect to both hull and shock damage to ships' machinery and equipment are considered significant. It should be understood that these apply to the shallow water Shot Umbrella conditions.

1. From the standpoint of hull deflection, the estimated lethal range for an EC-2 merchant ship is [redacted] feet for Shot Umbrella conditions.
2. The severe or crippling shock-damage range for machinery and equipment of an EC-2 merchant ship is [redacted] feet, under Shot Umbrella conditions.
3. The minimum safe range for repeated delivery of an antisubmarine weapon by destroyers is [redacted] feet for Shot Umbrella conditions. Damage or malfunction of particularly delicate equipment, i. e., electronic equipment, may occur at larger ranges.
4. The minimum safe range for single delivery of an antisubmarine weapon by destroyers, with shipyard availability soon after, is [redacted] feet for Shot Umbrella conditions.
5. The minimum safe range for delivery of an antisubmarine weapon from a submarine is [redacted] for Shot Umbrella conditions. Damage to particularly delicate equipment, i. e., electronic equipment, may occur at ranges [redacted].
6. Considerable basic information on hull response on surface ships as related to free-field pressures and loading measurements was obtained. This has provided check points for small-scale ship model experiments, which, upon further analysis, are expected to prove valuable in extrapolating results of Shot Umbrella to other geometries and ships.
7. From the standpoint of ship damage important to combat capability, the safe range for surface ships likely to delivery nuclear underwater weapons in the foreseeable future is determined by shock damage to equipment, rather than damage to the hull.
8. Further shock testing of both destroyer and submarine types is believed necessary at ranges where more severe damage will occur, in order to provide information required to more adequately shock harden the designs of these types of ships.

### 3.5 NAVAL MINE FIELD CLEARANCE BY ATOMIC UNDERWATER BURSTS

3.5.1 Objective. The objective of this experiment was to determine the ranges at which typical stockpile U. S. Naval bottom mines would be neutralized by a shallow water nuclear burst.

In general, Operation Hardtack offered realistic test parameters for providing field data on the feasibility of clearing bottom mine fields with nuclear weapons, since most bottom mines would normally be planted in [redacted]. The data obtained may be used in conjunction with other experimental data and theory to determine the probable effectiveness of nuclear weapons as a Naval mine countermeasure for all types of underwater mines.

3.5.2 Background. Mines that employ combination-influence mechanisms, delayed-arming devices, variable-ship counts, and anti-sweep devices may present a difficult problem to a mine-sweeping force. Explosive-clearance techniques could be used to destroy such a mine barrier in certain tactical situations, since any type of Naval mine may be neutralized by explosive means in several ways. Simple single-look mine mechanisms may be actuated by explosive shocks; acoustic mines may be actuated by explosions at ranges of several miles; single-and-combination-influence mechanisms may be damaged physically by explosive shock; and sensitive mine detonators may be initiated by near-contact explosions. However, all available data on response of mines to explosives indicate that case rupture is the proper criterion by which to consider a mine destroyed.

The mine characteristics of a typical mine such as the mine [redacted] are presented so as to provide a background for further details about this project. This stockpile mine is an aircraft-laid bottom mine that may be dropped without a parachute from altitudes [redacted]. Specially designed shock mounts within a strong case prevent damage to components when the mine strikes the water. The mine is equipped with an induction-firing mechanism actuated by currents induced in a search coil by the magnetic field of a ship. The mine may be used against [redacted]. This mine is one of the most difficult mines to render inoperative with explosives.

To provide additional background, a brief discussion is presented on the latest additions to the Navy mine arsenal. In the latest designs, there are influence-field detectors and associated firing mechanisms of three types (pressure, acoustic, and magnetic). The mine Mk 52 Mod 1 employs a magnetic-firing mechanism. The Mk 52 Mod 3 uses a combination of two firing mechanisms that respond individually to the magnetic and pressure-influence fields of a vessel. The Mk 52 Mod 6 uses a combination of three firing mechanisms, pressure, and acoustic.

The characteristics of each firing mechanism may be varied over a considerable range by choice of switch settings or plug-in circuits. All modifications of the Mk 52 mine have variable delay-arming times, sterilization times, ship counts, and inter-ship dead period. The total number of possible combinations of operational settings for the Mod 6 is 5,760. This mine is extremely difficult to sweep.

In situations where a nuclear detonation occurs underwater, the shock wave is of much longer duration than the shock wave from conventional mines and depth charges. Damage to mine cases corresponds in static manner to maximum pressure. This criterion is used in "Capabilities of Atomic Weapons," (Reference 15), to obtain curves of range versus yield for underwater mine-field neutralization. Consequently, the following criteria for mine damage were used in selecting mines at each range for Shot Umbrella:

[redacted]

3.5.3 Instrumentation. Two types of instrumentation were used: mechanical peak-pressure gages and mine-operation monitors. The mechanical-pressure gages provided the means by which the peak pressure of a shock wave of known time dependence could be computed from the deformation of a small copper sphere, compressed by a pressure-actuated piston.

The mine-operation monitoring system was designed to be mounted inside the mine in the space normally occupied by the booster and extender. The system was fitted in the booster compartment of the mine. Basically, it was a miniature tape transport that could transport 160 feet of 1/2-inch tape across a six-channel recording head for a period of 14 days. When the mines were planted, a hydrostatic switch was operated by the increase of water pressure with depth. In the case of the Mk 50, this switch simultaneously armed the mine and started the mine-operation monitoring system. All events recorded on the tape could then be related to the time of planting. In the case of mines Mk 39, 52, and 25, Mod 2, the hydrostatic pressure initiated a clock-delay mechanism, which delayed mine arming and recorder initiation for a preset period. The time of arrival could, therefore, be determined with respect to planting time. An indicator was installed in each mine to put a 10-second signal on one of the channels of the tape not used for mine actuations. The indicator was simply a one-shot multivibrator of 10-second period that would be triggered by the pulse emitted by a piezoelectric crystal when the shock wave impinged on the mine case.

The playback system consisted primarily of a tape transport, a time counter, and a readout device. This was installed on Site Elmer. As soon as the recorders were removed from the mines, the tape magazines were removed for processing.

In order to determine the effects of the nuclear detonation upon the mines as a function of distance, the mines were planted in rows at distances of between 1,500 and 8,000 feet from surface zero. The first three rows contained one or more mines of each type. The extent of damage to the mines at each range was determined by visual observation and measurements of deformation upon recovery. The distance of each mine from surface zero was computed from bearings and radar fixes made by means of the navigational equipment aboard the USS Takelma (ATF 113). The distance values are considered to be accurate to  $\pm 20$  yards.

The extent of mechanism damage incurred by each mine type at each range was determined by visual inspection.

After recovery, all mines were given operational tests with standard mine-test sets, in order to determine whether or not all components were functioning normally after the shot.

The operations of 23 mines of various types, planted at various distances, were monitored for a period of time, extending from the time at which the mines were armed to the time of recovery, by means of the system of internal recorders. The types and locations of these instrumented mines are indicated in Figure 3.52.

In order to extrapolate the mine-neutralization data to different weapons, a knowledge of the pressure-time histories at various ranges from Shot Umbrella was desired. In the final report (WT-1641), the pressure-time recordings and ball-crusher-gage data obtained by Project 1.1 will be correlated with that obtained by Project 6.7.

Water depths of all mines laid by the USS Takelma were measured with a fathometer. Data on the bottom characteristics of the Shot Umbrella target area was furnished by Project 1.13. This data will be useful in scaling mine-neutralization ranges for weapons of various nuclear yields in future studies of the mine-clearance problem.

All mines in the first row were completely demolished. The distances and mine types involved in the close-in area are given in Table 3.9. Damage sustained by a Mk 25 Mod 2 at 1,380 feet from surface zero is illustrated in Figure 3.53.

The effects produced by Shot Umbrella at distances greater than 1,600 feet are listed in Table 3.10. The type of damage suffered by Mk 25 Mod 2 mines at 1,980 feet is illustrated in Figure 3.54. These were the only mines in the second row that suffered case damage.

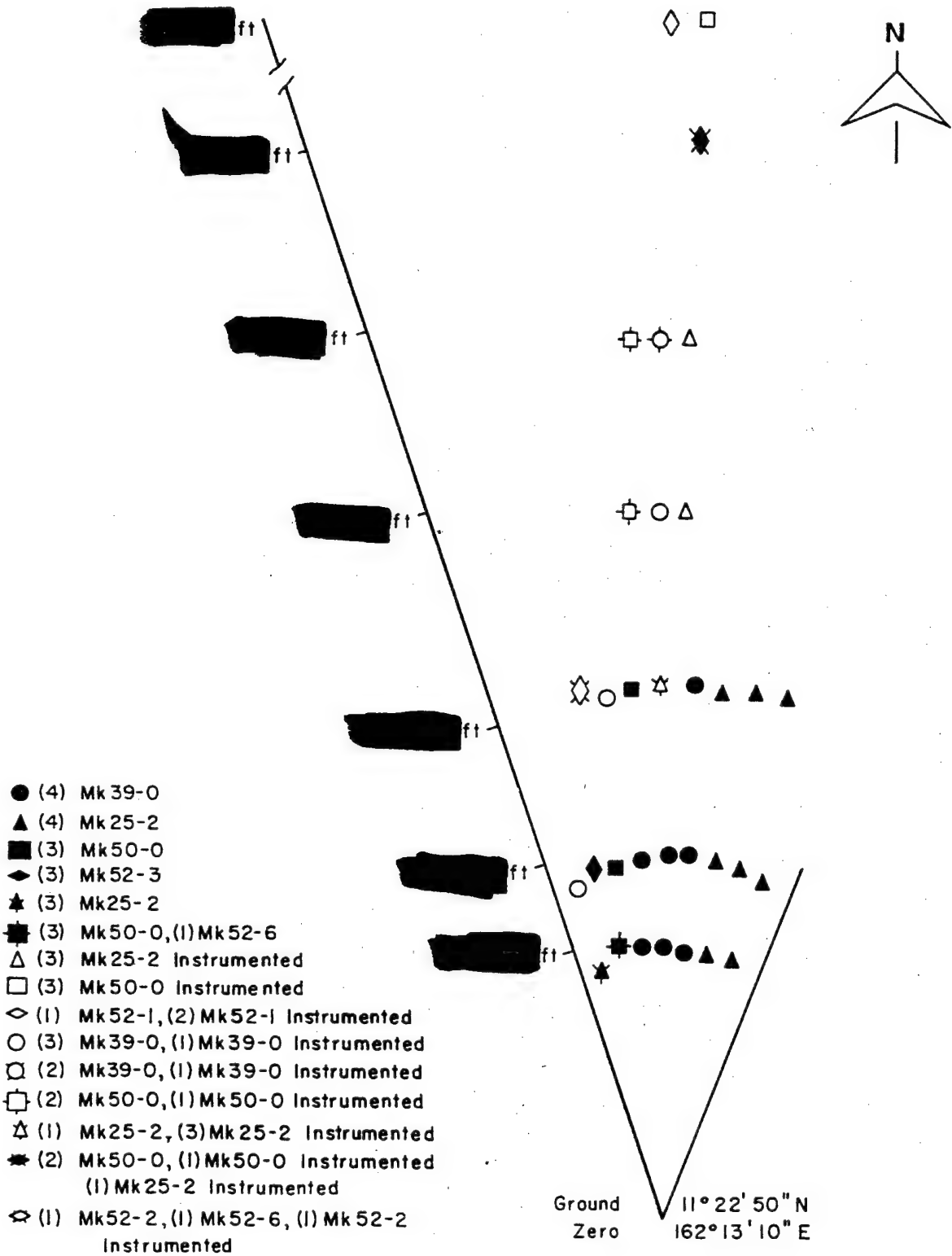


Figure 3.52 Layout of mine field.

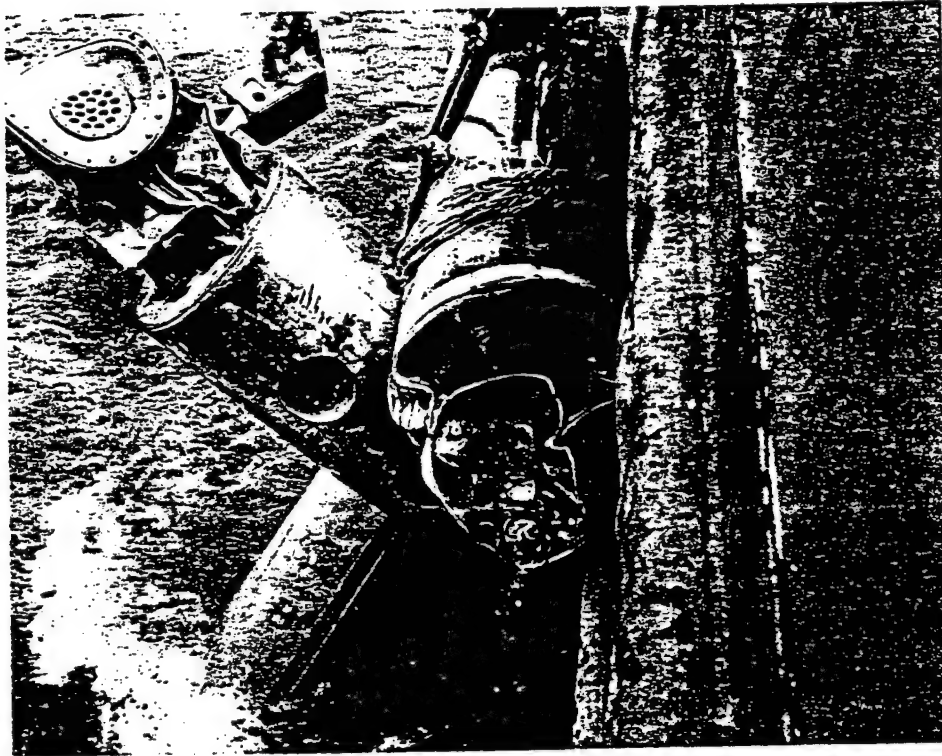


Figure 3.53 Damage to mines Mark 25-2 at [REDACTED]

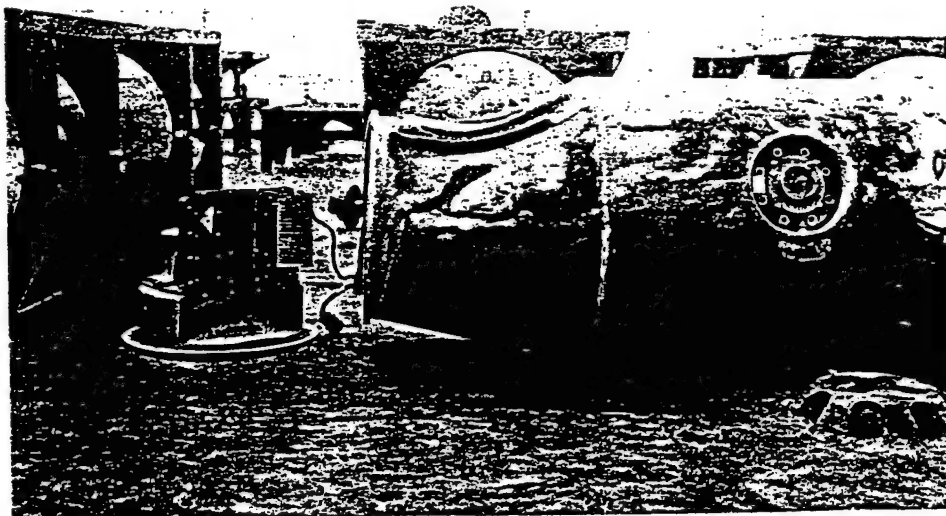


Figure 3.54 Damage to mines Mark 25-2 at [REDACTED]

Pages 182 through 185  
are deleted.

[REDACTED]

the instrumented mines. The cause of the failure of the firing mechanisms M-11 of the two Mk 39 Mod 0 mines and the ACM circuits of the Mk 50 Mod 0 mines is not as yet known.

The mine actuations, by type, that occurred at time of Shot Umbrella are presented in Table 3.11 for mines located from 1,920 feet to 4,000 feet from surface zero. The type of actuations recorded are similar to those that have been recorded in counter-mine tests using high explosives. At the time of the shot, none of the mines fired. The pressure looks which occurred at the time of the shot are assumed to have been caused by closures of the sensitrol relay, SR-9, by shock.

All mechanical-pressure gages were recovered. Eight of the gages did not function. The deformations from the remaining 20 were measured, and the peak pressures were computed. Since the time dependence of the shock waves at various distances from surface zero will not be known until made available by Project 1.1, the peak pressures were computed on the assumption that the time dependence of the shock wave was a simple step function. These values, plotted as a function of distance from surface zero, are presented in Figure 3.55. Since the time constant of the shock wave is expected to be long, the step response approximation is warranted; however, the values in Figure 3.55 should be considered as preliminary.



3.5.4 Feasibility of Wide Area Clearance of Naval Influence Mines by Nuclear Weapons. The overall objective of the project was to determine the feasibility of employing nuclear weapons for wide-area mine clearance by influence means. To accomplish this, the specific objectives of the program were: (1) to measure and record the amplitude, duration, and extent of mine-actuating influences (pressure, acoustic, and magnetic) which may be generated at the sea bottom by the explosion of a low-yield (8 to 13 kt) nuclear weapon in shallow water (approximately 150-foot depth); (2) to determine the reaction of certain instrumented U. S. Naval mines to the influences generated; and (3) to evaluate the effect of influences generated in sweeping single-influence and combination mines.

Project 6.8 was planned on the basis of obtaining data from Shot Umbrella. Data for checkout and calibration purposes was obtained from Shots Wahoo, Yellowwood, and Tobacco. Three LCU instrumentation platforms were located at distances of 8,300, 20,150 and 44,750 feet from surface zero of Shot Umbrella. Figure 3.56 shows the locations of the instrumentation platforms, relative to surface zero, for each of the four shots. Figure 3.57 shows the location of underwater instrumentation with respect to one of the three platforms. Table 3.12 identifies the underwater units and provides code numbers by which results are identified with a specific underwater unit.

3.5.5 Data Requirements. Data was required in order to obtain information on the duration, extent, and characteristics of mine-actuating influences resulting from Shot Umbrella and to determine the reaction of certain instrumented U. S. Naval mines to the influences generated. Instrumentation to obtain the following data was provided:

1. Pressure Measurements: The time-pressure history resulting from the shot. Included were pressure changes due to waves, swells, and the shock wave.
2. Magnetic Measurement: The time history of the magnetic-field changes.
3. Acoustic Measurements: The time history of the sound-pressure level, 2 cps to 40 kc.



TABLE 3.11 CONTINUED

[REDACTED TABLE CONTENTS]

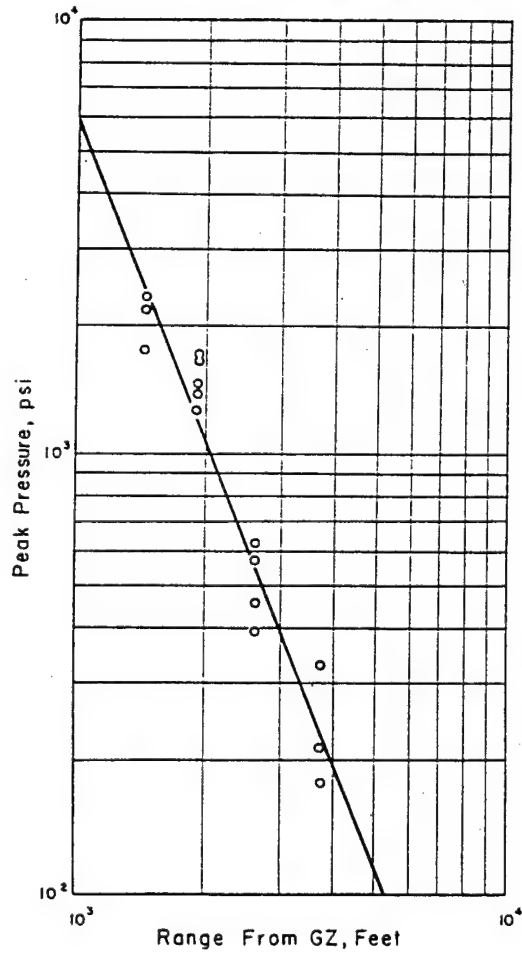


Figure 3.55 Peak pressures computed from mechanical-pressure-gage deformations, assuming step response.



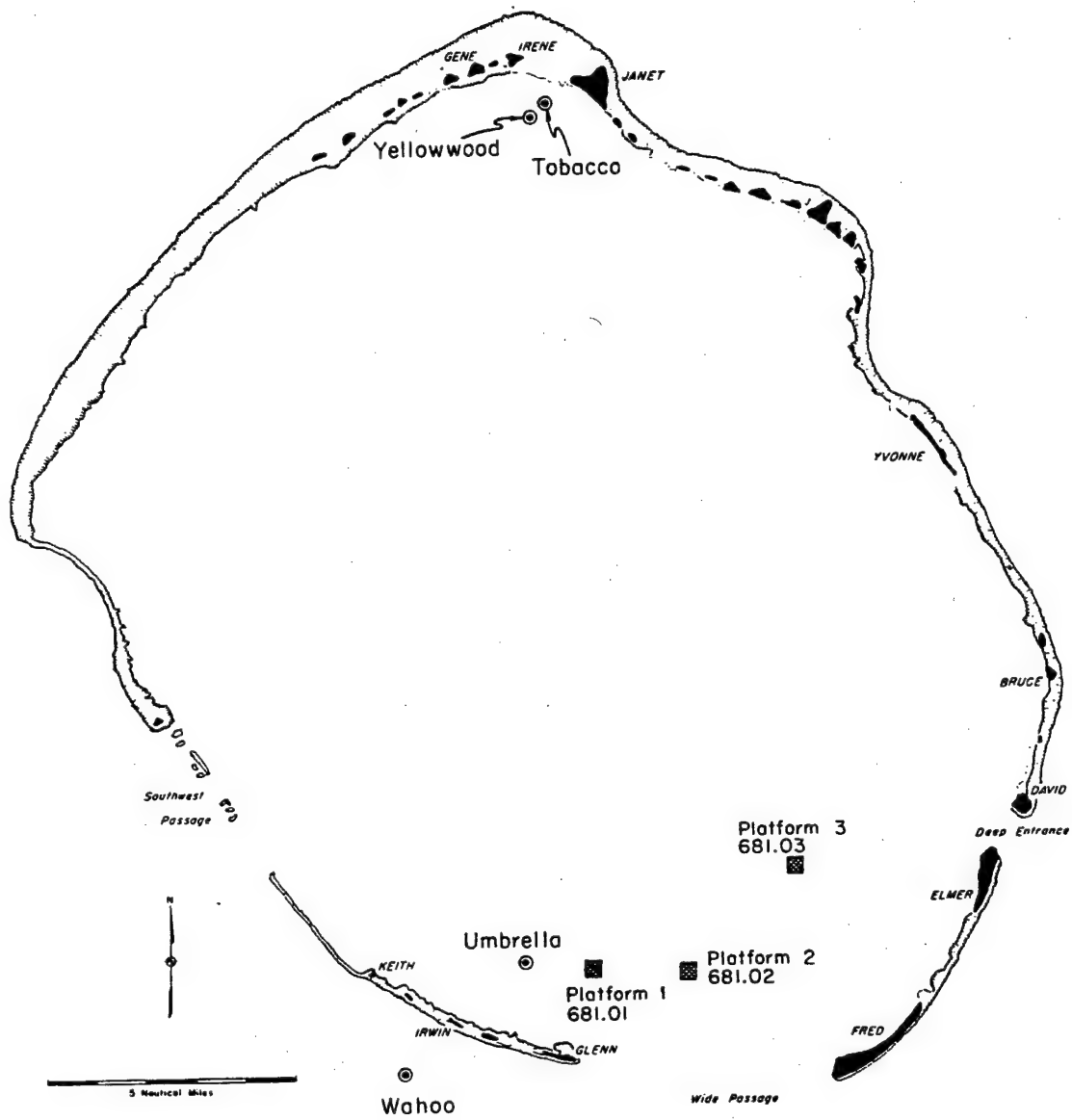


Figure 3.56 Location of instrument platforms relative to surface zero for Shots Umbrella, Wahoo, Yellowwood, and Tobacco.



**LEGEND**

- Mines
- Influence Detectors
- ⊙ Dan Buoy

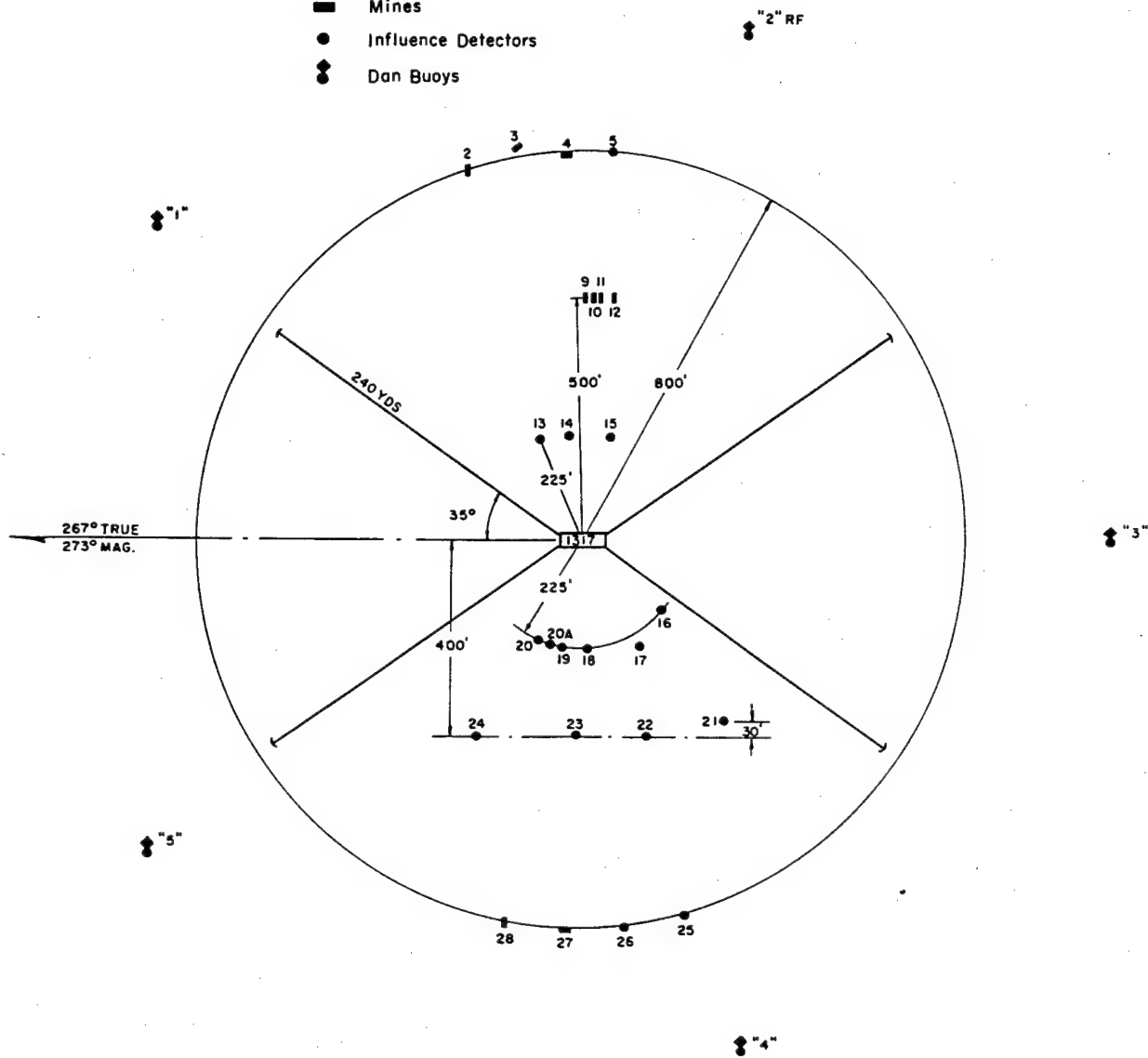


Figure 3.57 Schematic of underwater instrumentation and mines relative to Platform 1 (Station 681.01). For identification of code numbers of underwater units, see Table 3.12.

4. Seismic Measurements: The time history of displacement of the bottom (limited data).
5. Mine Reaction:

Mk 25 Mod 0: looks, fires, and search-coil output.

Mk 25 Mod 2: looks, pressure-switch opening, fires, and search-coil output.

Mk 36 Mod 2: ACM, fires, and plate-voltage rise.

Mk 50 Mod 0: ACM, fires, and plate-voltage rise.

6. Correlation of all influence measurements and mine reactions with respect to time.
- As a typical example of the instrumentation utilized, there follows a detailed description of

TABLE 3.12 ARRAY SPECIFICATIONS FOR PLATFORM 1, STATION 681.01

Item Number *	Mine/Instrument Type	Serial Number	Depth of Water ft	Distance from Platform Center † ft	Bearing from Platform Center ‡ deg true	Orientation of Item § deg magnetic
1	LCU 1317	—	140	—	—	273
2	Mine Mark 25 Mod 0	1M1	145	800	339	000
3	Mine Mark 25 Mod 0	1M3	145	825	347	045
4	Mine Mark 25 Mod 0	1M2	145	790	354	090
5	Total Field Magnetometer	8	145	800	001	—
9	Mine Mark 36 Mod 2	1A1	140	500	357	176
10	Mine Mark 36 Mod 2	1A2	140	500	359	176
11	Mine Mark 50 Mod 0	1A3	140	500	001	176
12	Mine Mark 50 Mod 0	1A4	135	500	004	176
13	½-Inch Tourmaline Gage	130	140	225	334	—
14	½-Inch Tourmaline Gage	134	140	225	349	—
15	½-Inch Tourmaline Gage	128	140	225	010	—
16	Hydrophone BC-50	98	142	225	127	—
17	Hydrophone BC-50	102	142	250	147	—
18	Hydrophone BC-50	104	142	225	173	—
19	Geophone Vertical	453	142	225	—	—
20	Geophone 3-Component	422	142	225	—	273
20A	Geophone 3-Component	490	142	225	193	273
21	Pressure Pickup 0.2-Inch-100-Inch Range	30	140	475	138	273
22	Pressure Pickup 300 Pound	L8V	140	425	158	273
23	Pressure Pickup 0.2-Inch-100-Inch Range	32	140	400	178	273
24	Pressure Pickup 0.2-Inch-100-Inch Range	31	140	460	205	273
25	Total Field Magnetometer	3	143	800	161	000
26	Total Field Magnetometer	5	143	800	170	000
27	Mine Mark 25 Mod 2	1MP2	143	800	179	090
28	Mine Mark 25 Mod 2	1MP1	143	800	188	000
"1"	Dan Buoy Mark 5	—	—	1,100	303	—
"2"	Dan Buoy Mark 5	—	—	1,100	015	—
"3"	Dan Buoy Mark 5	—	—	1,100	087	—
"4"	Dan Buoy Mark 5	—	—	1,100	159	—
"5"	Dan Buoy Mark 5	—	—	1,100	231	—

\* Items correspond to item numbers shown in Figure 3.57.

† Accuracy of distance from platform center is ± 20 feet.

‡ Accuracy of bearing from platform center is ± 1 degree.

§ Accuracy of orientation is ± 3 degrees.

the instrumentation for pressure measurements. (Comparable instrumentation was utilized to obtain acoustic, magnetic, and seismic measurements.) Pressures covering the range from 0.2 inch of water (0.0072 psi), peak to peak, to 2,768 inches of water (100 psi) were recorded in three channels of information. The first channel recorded peak-to-peak pressures from 0.2 to 20 inches of water, and the second channel recorded peak-to-peak pressure from 1 to 100 inches of water. The third channel recorded to 100 psi. The upper frequency cutoff of the high-pressure pickup (100 psi) was approximately 500 cps.

Pressures were recorded as a function of time prior to time zero and for a period of approximately 20 minutes thereafter. The 20-inch and 100-inch pressure signals were detected by an MDL pressure pickup, using a Wiancko  $\pm 10$ -psi gage, Type 1404. The +100-psi pressure signals were detected by an MDL pressure pickup using a Wiancko  $\pm 100$ -psi gage, Type 1404. The pressure pickup containing the  $\pm 10$ -psi gage had been modified by the addition of a low-pass hydraulic filter to prevent damage to the gage during fast rise-time high pressures.

**3.5.6 Playback System.** A block diagram of the pressure instrumentation is shown in Figure 3.58. This system, with the exception of the high-pressure pickup, was duplicated at each station. The MDL pressure-amplifier detector and the MDL pressure pickups were developed at the U. S. Navy Mine Defense Laboratory (formerly U. S. Navy Mine-Countermeasure Station), prior to this project. Information concerning this portion of the pressure system may be obtained from USNMCS Report No. 46 (Reference 16). The 7-channel tape recorder was Ampex Model FR-107. The buffer amplifier used to drive the high-pressure bridge was a push-pull triode circuit with transformer coupling and was identical to the buffer amplifier in the pressure-amplifier detector that drove the low-pressure bridge. The high-pressure bridge was similar to the low-pressure one in the pressure-amplifier detector, but it operated in a balanced condition and used an additional RC network to balance out the reactive component of the current in the bridge. The inputs to the 20-inch and 100-inch cathode followers were connected to the range-switch-voltage divider in the pressure-amplifier detector at the 2-inch and 20-inch points, respectively. The output of each of the cathode followers was fed into a resistive bridge, and the wiper output was fed to the tape recorder. The bucking voltage supply was also fed to this bridge, and, by adjustment of the potentiometer in the bridge circuit, the direct-current bias of each of the cathode followers could be balanced out. The bucking voltage power supplies were simple bridge rectifier types supplied with a floating output of 150 volts dc. By relay action, the pressure-calibration panel operated the calibrate power supply in the pressure-amplifier detector, which in turn produced the calibrate action in both the high-pressure and low-pressure pickups.

An example of a typical monitoring system is that which was used on the Mk 25 Mod 0 mines. A block diagram of the mine-monitoring system is shown in Figure 3.59. (Comparable systems were utilized to monitor Mk 25 Mod 2, Mk 36 Mod 2, and Mk 50 Mod 0 mines.) The mine-control panel remotely controlled power to the firing mechanism and dc amplifier in the mine by means of a relay in the mine. Magnetic signals detected by the search coil produced voltage changes which were fed to the firing mechanism and were also monitored by means of the amplifier. Information on the look and fire reactions of the firing mechanism were monitored by pen recorders. Search-coil voltage was monitored by a frequency-modulation (FM) channel of a tape recorder. A step change magnetic signal was fed from the trailer to the 10-turn coil placed around the search coil for use in calibration of the search-coil voltage monitor and to check operation of the overall system.

The mine-reaction data (looks and fires) were of the go-no-go type, causing a pen deflection for about one second. The search-coil-voltage data was essentially the output of the three pulse-per-second oscillator in the M-11 firing mechanism as seen by the search coil. In the ambient condition, the pulses appeared across the search coil at comparatively low magnitude; when a voltage appeared across the search coil, the pulses showed a change in amplitude. The relative direction of the pulse spikes, both in the ambient-field condition and with search-coil voltage applied, was an indication of direction of search-coil voltage and, hence, of magnetic-field change. The nature of this information is not particularly conducive to interpretation. For this reason, calibration signals of at least six levels from 0.02 milligauss to 5.0 milligauss in both directions were required immediately prior to the shot.

A representative mine idealization and checkout was that performed on the Mk 25 Mod 0 and Mk 25 Mod 2 mines. The preparation of the mines was accomplished with the background (earth's) field vector aligned in the same direction with respect to the mine as it was when planted. (Before idealization, the search coil was removed from the mine and placed at least 50 feet away from the idealizer.) Since mines were planted in each of three orientations, the

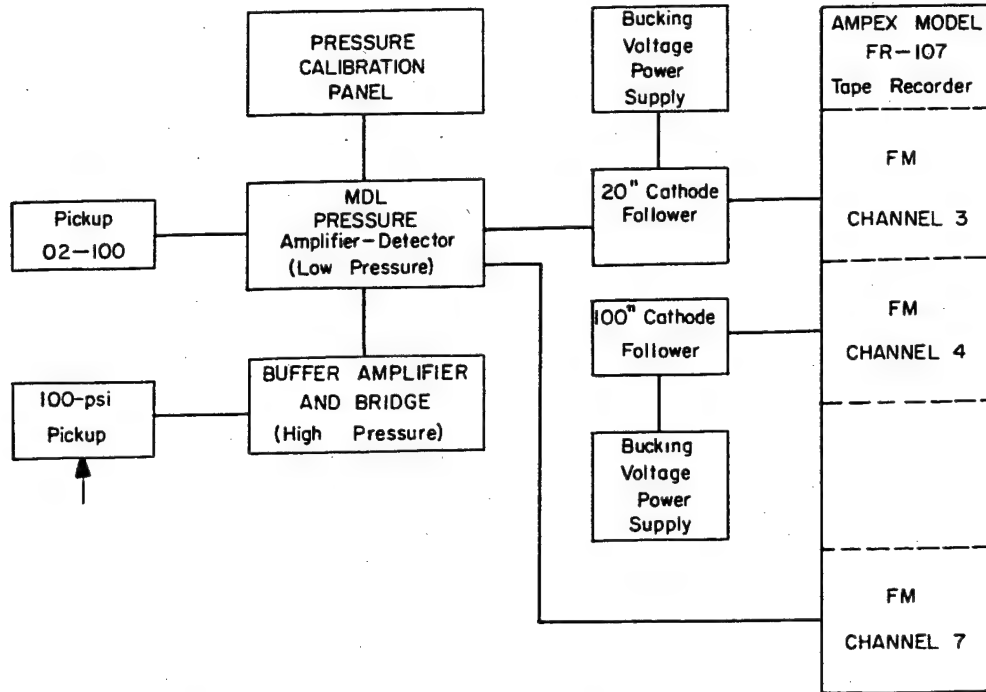


Figure 3.58 Block diagram of pressure measuring system.

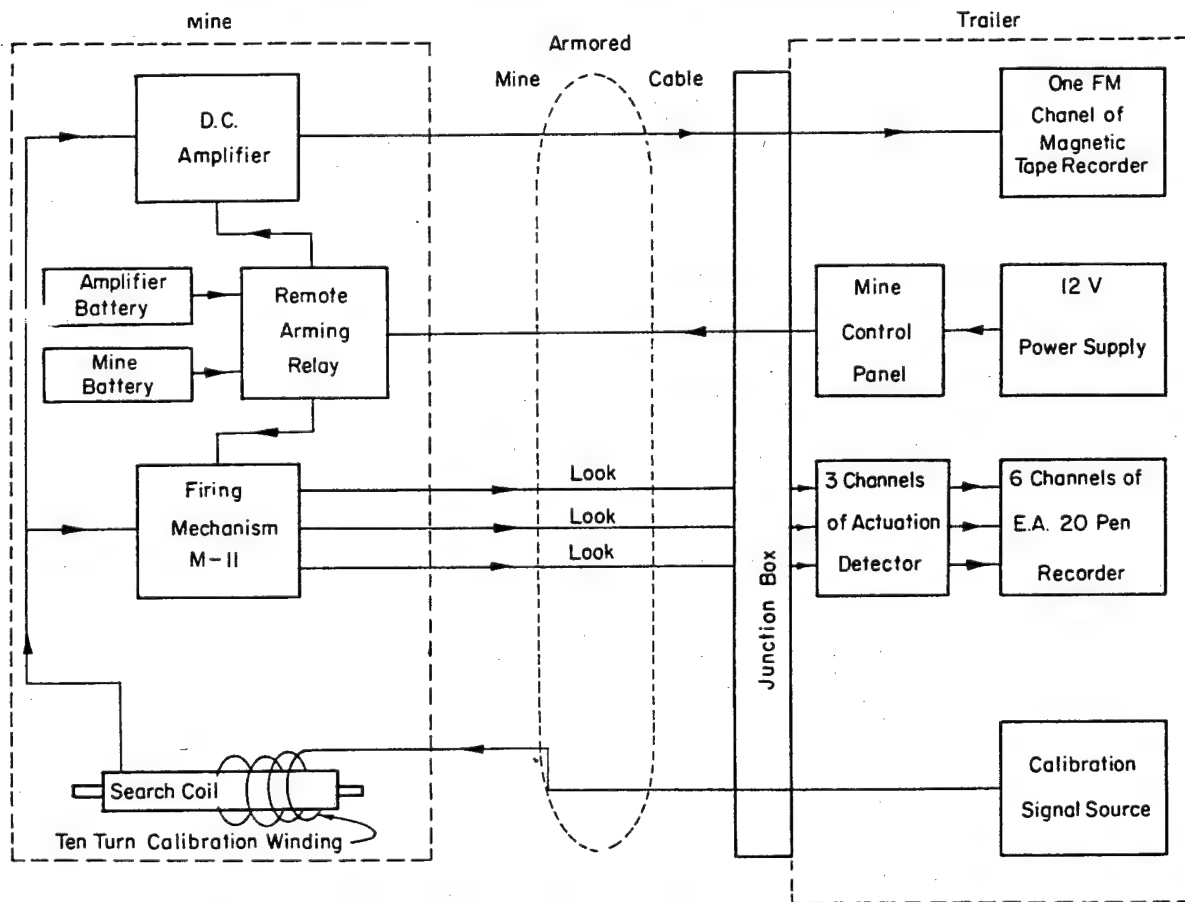


Figure 3.59 Block diagram of monitor system for mine Mark 25 Mod 0.

idealizer was oriented depending on the particular mine being idealized. Idealized mines were handled with care and were stored and repaired, while the specific orientation with respect to the earth's magnetic field was maintained. Preliminary checkout and calibration phases were accomplished with standard mine test sets and special test sets developed specifically for these monitored mines. Spurious magnetic-field changes were minimized during calibration.

The idealizer used (Figure 3.60) consisted of a coil system (with cart and track for moving the mine), a control unit, and a 100-foot cable connecting the two. The control unit operated on 230-volt, three-phase ac and distributed power to both coils of the coil system. The shaking field, a schedule of square pulses whose magnitude decayed with each pulse until the envelope reached essentially zero, was produced by one coil. The schedule was automatic after initiation and was cut off when the schedule was complete, approximately 40 minutes later. A second winding on the coil was available to correct the earth's field if a distorted background field, due to local anomalies, was encountered. Use of the second winding was not required.

The Mk 36 Mod 2 and Mk 50 Mod 0 mines were checked out by means of standard mine-test sets and special-test sets developed for these particular mines. Spurious acoustic background signals during calibration were minimized.

Control of the electronic equipment at each station was derived from a program-control unit actuated by the central-timing system at shot time minus five minutes. The program-control unit provided step-by-step control of the instrumentation, so the tape recorders were started and the influence measuring systems were calibrated prior to time zero. A backup system was provided to start the electronic system at H-5 seconds in the event of failure of the primary control system.

For Shot Umbrella, time zero was obtained by the use of a fiducial marker provided by Edgerton, Germeshausen and Grier (EG&G). On Shots Wahoo, Yellowwood, and Tobacco, the timing system was initiated by the minus-1-second radio signal provided by EG&G. To obtain time relative to time zero for all data, a one-kc signal, interrupted once each second, was superimposed on one channel of each magnetic-tape recorder. A pen deflection synchronized with the magnetic-tape signal was recorded at intervals of one second on each of the 20-pen operational recorders. The time-zero indication was impressed on both the one-kc signal and the pen recorders. The timing pulses were generated by an escapement mechanism that controlled the firing of a thyatron tube, which generated timing pulses that controlled both the magnetic-tape and paper-tape timing indications.

LCU hulls 634, 1123, and 1317 were employed as platforms to mount the trailers housing the monitoring instrumentation. All three installations were similar and had been standardized to the maximum practical extent. Figure 3.61 shows one installation (Platform 1). Padeyes were installed on the deck of each LCU for turnbuckle-pendant tiedown connections. As a further deterrent to movement from shock and for better stability, each set of trailer wheels was placed in steel chocks welded to the deck.

Power for instrumentation for each trailer was supplied by three 5-kw generators. Two were operated on load, with the third in a standby capacity. In case of failure of one of the operating generators, a transfer switch was provided to accomplish a changeover to the third generator. The generators were shock-mounted directly to the deck. Connections to the instrumentation were made through water-tight junction boxes on the outside of each trailer.

The fuel systems for each platform were prefabricated for rapid installation. The diesel oil was fed by gravity, and the gasoline was fed to a Thermo-King air-cooling unit by a separator pump. Each platform was equipped with fire fighting equipment, including P-500 fire pumps. The latter also served as emergency bilge pumps.

A schematic diagram of the underwater instrumentation array planted at Platform 1 is shown in Figure 3.57. Locations of all the arrays, with respect to shot locations, are given in Table 3.13. In order to locate an acceptable sea bottom for positioning the LCU platforms, a fathometer survey was conducted in the vicinity of the desired locations, and divers were employed to check the bottom conditions. Buoys to outline the arrays were planted to prevent craft from sweeping marker-recovery buoys and causing premature actuations of mines. Divers were used to properly position and orient equipment on the bottom. The USS Chanticleer (ASR-7) was

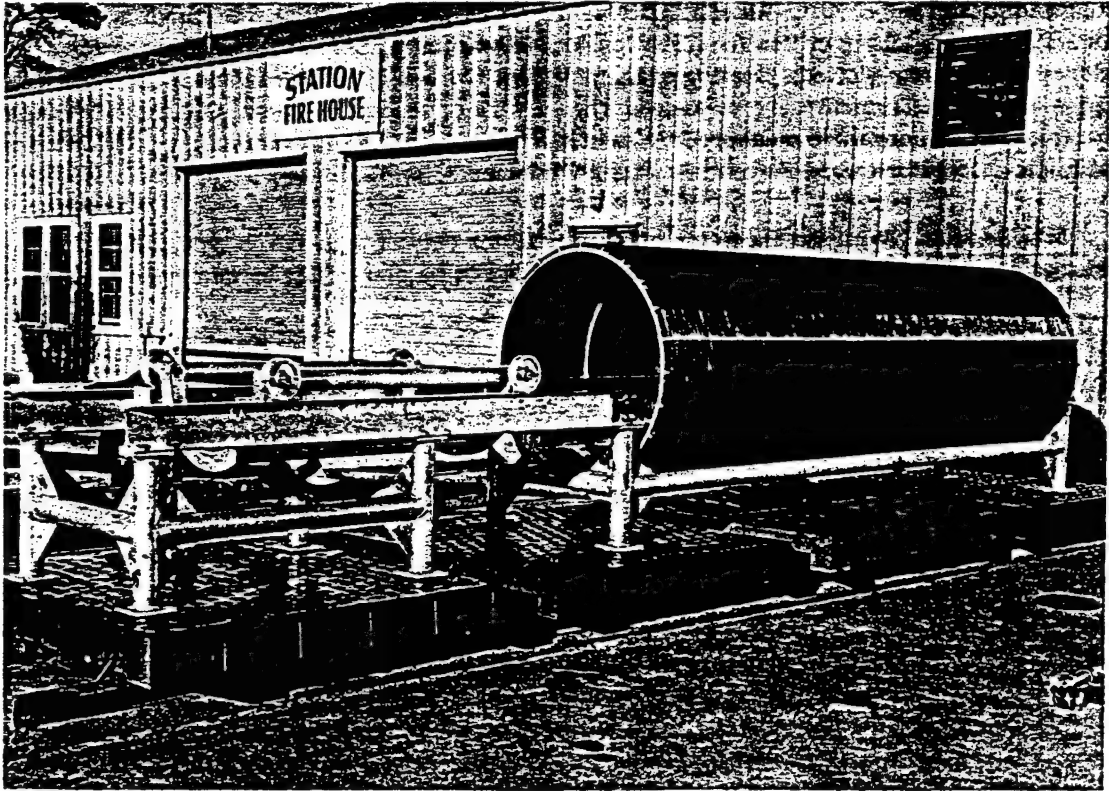


Figure 3.60 Idealizer for magnetic mines.

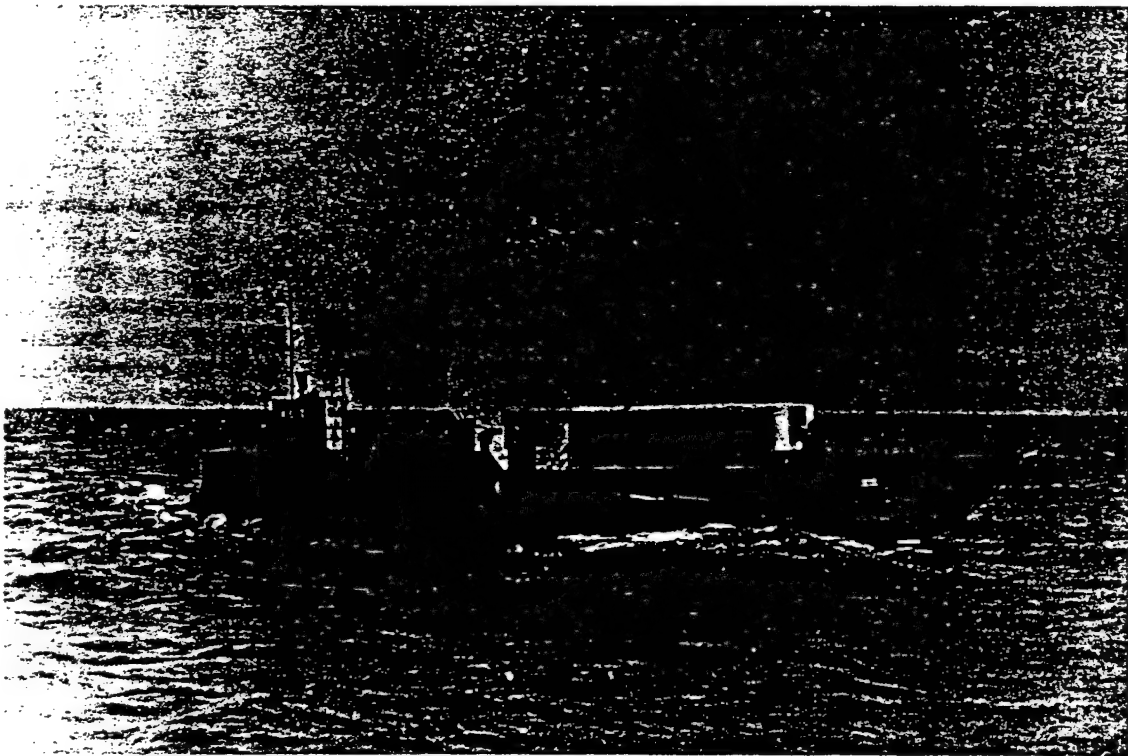


Figure 3.61 View of LCU 1317, Platform 1.

employed for the planting operation, because decompression chambers and diving support, plus lifting facilities, were within its capabilities. An LCM equipped with cable-handling facilities was employed for laying cables from the instruments to the platforms. The location of each underwater unit was plotted, relative to the platform, by use of a pelorus and measuring lines. Depths at each instrument were measured when divers oriented the units. Distances between objects on the bottom were measured by swimmers. Figure 3.62 illustrates a typical mine installation. Detectors were rigged in a similar manner.

**3.5.7 Results.** With the exception of mine reaction data of a go-no-go type, all data must undergo considerable reduction before it is in a form to be pictorially or numerically presented

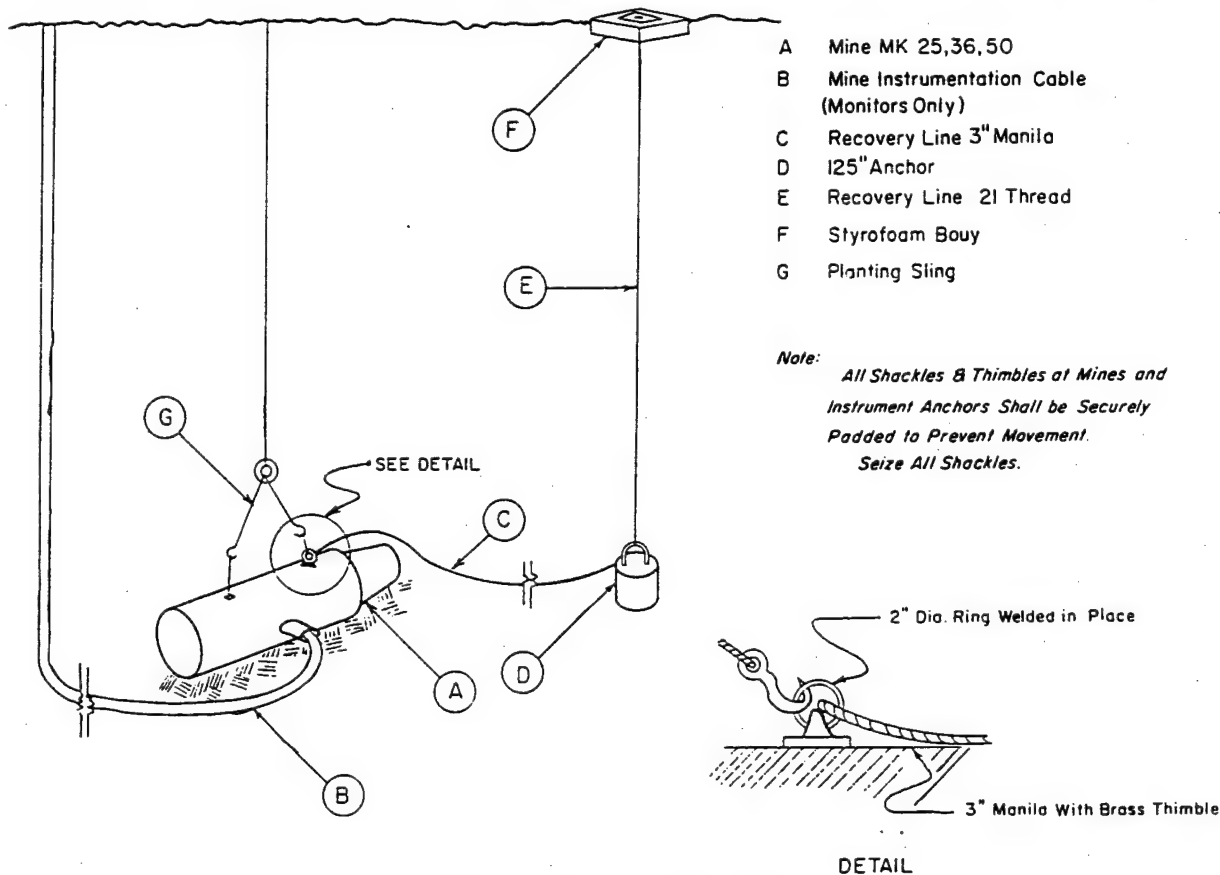


Figure 3.62 Typical mine installation.

or from which any conclusions can be drawn. Significant data reduction could not be accomplished in the field, owing to the lack of facilities and time; therefore, an early comprehensive evaluation of results, i. e., in the field, caused it not to be made, except for mine reaction.

The methods and objectives of the data reduction are, in general, peculiar to the field of mine countermeasures. A considerable portion of the reduction is of a manual nature. The following general methods will be used for reduction of the data:

**Acoustic-Field Measurements.** The data was obtained on magnetic tapes. Overlapping octave band analysis will be made [REDACTED] as a function of time. From this, appropriate plots may be made. The original recording will be played into appropriate simulation equipment to determine ACM's and fires of various types of acoustic mines, if the data shows that this type of analysis proves advantageous.

**Magnetic-Field Measurements.** The output of the total field detectors, as recorded on magnetic tape, will be reproduced for visual scanning on conventional playback equipment. The signal magnitude of any observed signals will be scaled. The time of occurrence of any significant signals will be obtained, and an attempt will be made to correlate these times with



events following the shot (bubble expansion, emergence of plume, shock wave, wave motion, and other effects). Analysis of wave form and probable effect on mines will be performed, as necessary.

**Pressure-Field Measurements.** Data was recorded on magnetic tapes and will be reproduced for analysis on paper tapes. The data will be reduced manually to determine amplitude and other characteristics of the underwater-pressure changes that affect mine counter-

TABLE 3.13 SHOT AND PLATFORM LOCATIONS

Code Name	Coordinates *	Holmes and Narver	Distance of Shots	Distance of Shots	Distance of Shots
		Coordinates	to Platform P-1	to Platform P-2	to Platform P-3
			ft	ft	ft
Wahoo	11° 20' 41"	N 29,000	27,050	37,800	64,800
	162° 10' 45"	E 60,500			
Yellowwood	11° 39' 36.7"	N 143,993	102,300	103,800	87,400
	162° 13' 30.6"	E 78,161			
Tobacco	11° 39' 48"	N 145,140	103,300	104,700	87,700
	162° 13' 47"	E 79,799			
Umbrella	11° 22' 50"	N 42,500	8,300	20,150	44,750
	162° 13' 09.6"	E 76,000			
Platform Code Designation					
P-1 (Station 681.01)	11° 22' 44"	N 41,910			
	162° 14' 32.2"	E 84,274			
P-2 (Station 681.02)	11° 22' 42"	N 41,708			
	162° 16' 31.6"	E 96,147			
P-3 (Station 681.03)	11° 26' 30"	N 64,692			
	162° 19' 40"	E 114,880			

\* The first figure given is north latitude; the second is east longitude.

measures. Mine reactions will be correlated to determine the types of pressure change that caused the mines to fire.

**Monitored Mines.** The monitored magnetic-mine mechanisms gave two channels of information: the go-no-go information obtainable from the record of looks and fires and the search-coil output. As in the case of the magnetometer measurements, an attempt will be made to correlate any looks, actuations, or significant search-coil output with events following the shot. The mine circuit will introduce marked distortion of signal form in the case of search-coil output. An attempt will be made to deduce the original wave shape of the signal (by circuit analysis and simulation techniques) of any significant search coil output recorded.

The acoustic mines will indicate fires and ACM's on a go-no-go basis. Data obtained from monitoring of the plate voltages will be correlated with acoustic measurements to determine the effect of sound-pressure level on the mine mechanism.

The pressure-magnetic mines will provide information on pressure looks obtained. This data will be correlated manually with pressure-field changes recorded.

Data was successfully obtained on about 80 percent of the recording channels. Mine reaction data of a go-no-go type were reduced. The time and facilities required to reduce and evaluate the remaining data in the form necessary for application to mine countermeasures precluded significant data reduction in the field. The following tentative conclusions summarizing results obtained on Shot Umbrella are based on the partial reduction of data:

1. [REDACTED]

2. A detailed study of the influence measurements and mine reaction data obtained from Shot Umbrella will be required to determine the degree of effectiveness of nuclear weapons for use in mine clearance by influence means.



## Chapter 4 SHOT YUCCA

### 4.1 OBJECTIVES

The overall objectives of the very-high-altitude shot were: (1) to determine the effect of extreme altitude on partition of energy in a nuclear explosion and on radii of effects of the various phenomena, and (2) to determine scaling laws for the various effects as a function of altitude and yield.

**4.1.1 Background.** The requirement for knowledge of the effects of nuclear detonations at high altitude on which to base estimates of damage to military targets led to the planning and firing of a high-altitude (36,000 feet) shot during Operation Teapot in 1955. The results obtained from Operation Teapot indicated that there was no appreciable loss of blast energy at this altitude, as predicted, and that Sachs scaling was appropriate for predicting free-air pressures. However, thermal measurements made on aircraft at altitude and by ground stations showed less thermal yield than predicted. At the same time, independent studies of the feasibility of conducting a test at 100,000 feet were made by the Naval Research Laboratory and by the Air Force Special Weapons Center for the Armed Forces Special Weapons Project. These studies were completed in late 1955 and concluded that a test at an altitude approaching 100,000 feet was feasible.

These feasibility studies were analyzed by Headquarters AFSWP and the better parts of each combined into the resultant very-high-altitude program which was designed to carry the nuclear device, with all associated instrumentation, on a dragline suspended from a 128-foot free balloon. See Figure 4.1 for final configuration.

With the approval of the Joint Chiefs of Staff, the Chief, AFSWP, proceeded with the establishment of a weapon-effects program. A foremost goal in this endeavor was to bring the greatest capability to bear on the overall objectives of the program. Thus, the program was pursued by the combined efforts of two Navy laboratories (NRL and NRDL), two research and development centers of ARDC (AFCRC and AFSWC) and two AEC contractors (Sandia Corporation and EG&G). The resultant program was finally approved by the Secretary of Defense on 27 December 1956 for a total sum not to exceed \$3,660,000.

The program as established was as follows:

<u>Project</u>	<u>Agency</u>	<u>Objectives</u>
1.10	AFCRC	Blast
2.7 *	USNRL	Nuclear
8.2 *	AFCRC	Thermal
8.3 *	EG&G	Photography
8.4 *	USNRDL	Thermal spectrum
8.5	BuAer	Infrared
9.2a	Sandia Corp.	Detonation
9.2b	AFCRC	Balloon Carrier
9.2c	AFCRC-AFSWC	Aircraft Modification

\* Included support for very-high-altitude program.

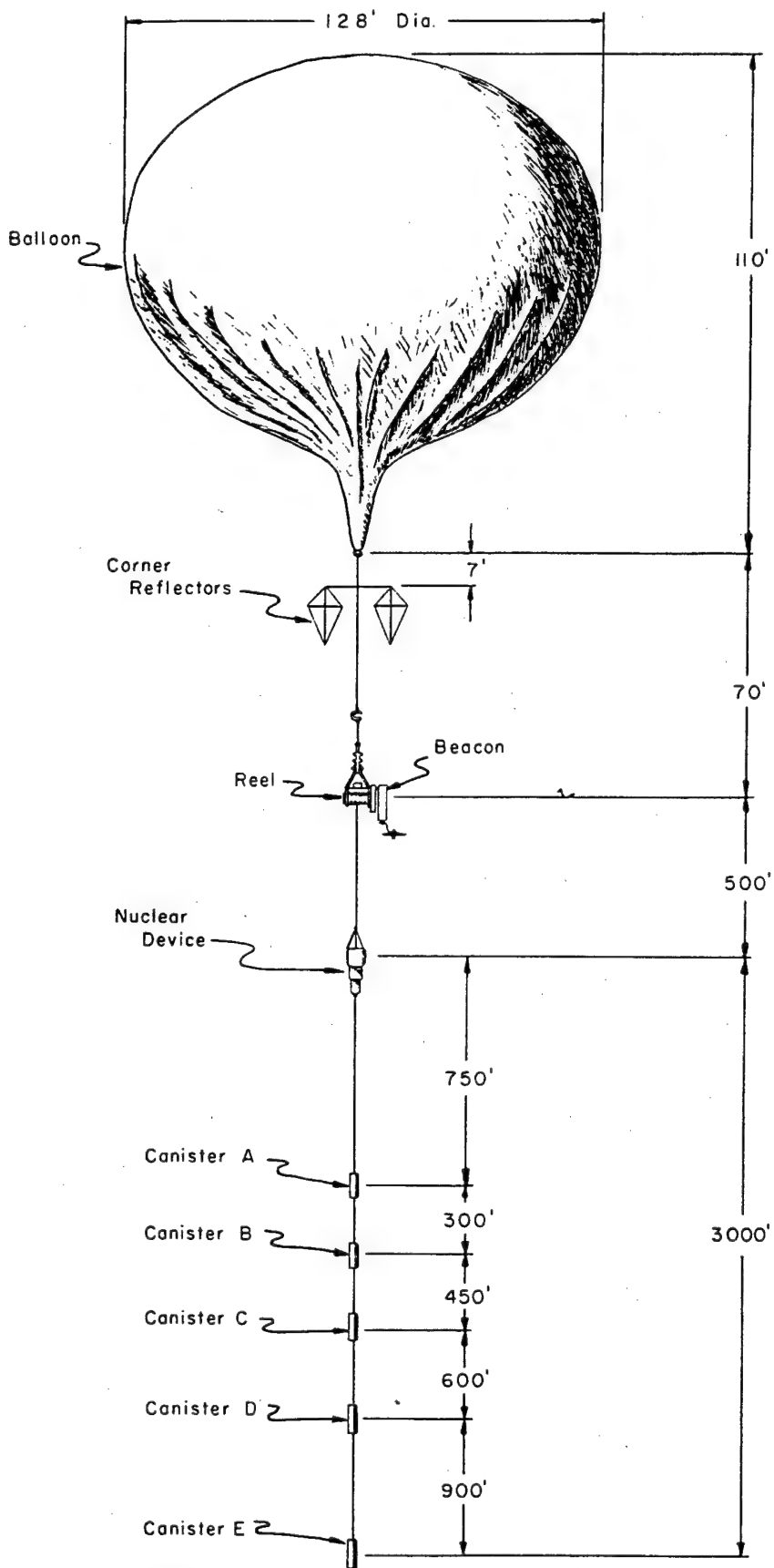


Figure 4.1 Yucca in-flight configuration.

4.1.2 Operation. Upon assignment of responsibility to AFCRC for perfection of the balloon carrier system, an extensive balloon-testing program was initiated to provide for 62 to 90 test flights at a total cost of \$1,069,500. Throughout the program, a total of 86 balloons were expended in perfecting the system. The result was a reliable balloon carrier and canister-deployment system.

The Sandia Corporation, under Project 9.2a, accepted responsibility for supplying the nuclear device, together with its detonation system. Extensive flight-testing plans were prepared for the proof-testing of 14 dummy Pandora systems. Throughout the program prior to Shot Yucca, a total of 13 dummy weapons were expended.

Responsibility of contracting for necessary aircraft modifications (Project 9.2a) was accepted by AFCRC and performed by the Air Modification Corporation. The RB-36's were maintained and flown by AFSWC.

Agencies responsible for effects measurements initiated work on their technical projects to provide for canister and aircraft instrumentation for a readiness date of 15 April 1958.

4.1.3 Results. The Yucca nuclear device was successfully armed and fired by radio command from the USS Boxer at 1440 on 28 April 1958. At time of detonation, the device was at a floating pressure altitude of 85,000 feet at coordinates 12° 27' N and 163° 01.5' E. All radio commands to the device during the entire flight of three and a quarter hours operated to perfection.

The balloon-carrier system (Project 9.2b) fulfilled all project objectives by successfully carrying the nuclear device and associated instrumentation to a measured radar altitude of 85,500 feet.

The modifications to the two RB-36's, as performed by the Air Modification Corporation, (Project 9.2c) proved to be adequate for the instrumentation associated with Projects 8.2, 8.3 and 8.4.

Due to failure of Project 1.10's command transmitter on board the ship, no data of any significance was received by Canister Projects 1.10, 8.2 and 2.7.

The results of Aircraft Projects 8.2, 8.3, 8.4 and 8.5 will be reported elsewhere.

4.1.4 Summary and Conclusion. Support Projects 9.2a, 9.2b and 9.2c were accomplished satisfactorily. The extensive proof testing of the device by Project 9.2a and balloon testing by Project 9.2b provided a high degree of reliability. The aircraft carrier proved to be an effective means for creating the necessary wind conditions for launching such a balloon system.

Based on the results obtained by all projects, it must be concluded that Shot Yucca was only partially successful in meeting the original objectives of the program. The capability of the balloon system to reliably carry a nuclear device to altitude, deploy the five canisters, and accomplish the required 500-foot separation of equipment was clearly demonstrated. Likewise, the superb effectiveness of the arming and firing system was established.

Due to failure of the canister command system at H - 2 1/2 minutes, no canister data was obtained via the telemetering link.

The results obtained by instrumentation on board the B-36 aircraft were successful in meeting the objectives of the projects concerned. The extent to which this information can be applied to meet the requirements for close-in data has yet to be determined; however, it is believed that the fireball photography (Project 8.3) and total thermal-intensity versus time (Project 8.2), with correction for attenuation, may provide a partial answer. The thermal-spectrum data obtained by Projects 8.2 and 8.4 at distant ranges may also provide needed information.

## 4.2 BLAST MEASUREMENTS

4.2.1 Objectives. The objective of the blast program on Shot Yucca was to make measurements which would describe the blast wave from a shot at high altitude. Specific objectives were to determine the energy partition (the fraction of total yield going into blast), and whether or not a type of Sachs scaling could be used to correlate high-altitude-blast data. Measurements

were to include time of arrival (from which peak overpressure can be calculated), and overpressure as a function of time.

**4.2.2 Background.** Air-blast measurements were made by arrays of parachute-borne canisters on Operations Jangle, Snapper, Ivy, Upshot-Knothole, Teapot, and Redwing. In order to minimize development time and cost, it was decided to use the same type of pressure and telemetering systems as the basis for the type of system needed for Shot Yucca.

It was felt that the most feasible method of obtaining measurements from a free-balloon shot would be to suspend a number of instrumented canisters at various distances below the device. From the pressure-measurement standpoint, a blast line long enough to establish the shape of the pressure-distance curve was needed. The instrumentation configuration decided upon was an array of five canisters at distances of 750, 1,050, 1,500, 2,100, and 3,000 feet below the device, forming an approximately exponential series.

On Teapot Shot 10 (fired at 36,000 feet), data from two canisters at ranges of 640 and 720 feet were lost because of a brief black-out of the telemetering signals, which was believed to have been due to ionization of the air by prompt radiation. This experience indicated that radiation effects at the altitude at which Shot Yucca was to be detonated might be severe. It was, therefore, decided that the Yucca instrumentation should have a data-storage system to prevent loss of data by telemetering black-out.

**4.2.3 Theory.** Overpressure and time of arrival data measured on Teapot 10 (36,000-foot height of burst) correlated well with the 1 kt free-air curve (Figures 2 and 3, TM 23-200) when multiplied by Sachs scaling factors for overpressure distance, and time:

$$S_p = \frac{1013}{P_0} \quad \text{(pressure scaling factor)} \quad (4.1)$$

$$S_d = \left(\frac{P_0}{1013}\right)^{1/3} \left(\frac{1}{W}\right)^{1/3} \quad \text{(distance scaling factor)} \quad (4.2)$$

$$S_t = \left(\frac{T_0 + 273}{288}\right)^{1/2} \left(\frac{P_0}{1013}\right)^{1/3} \left(\frac{1}{W}\right)^{1/3} \quad \text{(time scaling factor)} \quad (4.3)$$

Where:  $P_0$  = ambient pressure, mb  
 $W$  = device yield, kt  
 $T_0$  = ambient temperature, C

The success of these equations in correlating pressure data is primarily dependent on the energy partition being the same for all shots for which pressures are to be correlated. It has been found that about 35 percent of a device's energy is released as thermal radiation, and about 45 percent goes into blast. The Sachs scaling factors will apply as long as these percentages remain essentially constant. It was expected, however, that the energy partition from a shot at high altitude would be different than at sea level, and that a smaller amount of energy would go into the blast wave. The reason for the change in energy partition is that a significant amount of thermal radiation should be emitted before the shock wave leaves the fireball. Most of this radiation would normally be absorbed near the shock wave and be converted to blast energy.

It was hoped that Sachs scaling would still apply if the change in energy partition were taken into account. That is, if an effective blast yield (less than the total yield) were used in Equation 4.2 and 4.3 instead of the total yield normally used.

Dr. F. H. Shelton has given an approximate theoretical treatment of the dependence on altitude of the effective blast yield. He assumes the stage of appreciable radiation-hydrodynamic coupling to extend to the time at which the temperature at the shock front is about 3,000 K, and that

the thermal radiation emitted prior to this time is lost energy as far as contribution of energy to the blast wave is concerned. On this basis he arrives at an expression for the effective blast yield:

$$\ln\left(\frac{W_h}{W}\right) = \left(\frac{P_0}{P_h} - 1\right) \ln(1 - \alpha) \quad (4.4)$$

Where:  $W_h$  = effective blast yield at altitude  $h$   
 $W$  = total yield  
 $P_0$  = ambient density at sea level  
 $P_h$  = ambient density at altitude  $h$   
 $\alpha$  = fraction of total yield which is emitted prior to the time the fireball temperature decreases to 3,000 K

Flow conditions around a gage in a blast wave result in deviation of the observed pressures from actual free-stream conditions. Although it is possible to make wind tunnel or shock-tube calibrations to account for these deviations, it was believed that peak overpressures calculated from time of arrival of the blast wave (using the Rankine-Hugoniot equations), would be more reliable. The general type of equation used is:

$$U = C_0 \left(1 + \frac{6P}{7P_0}\right)^{1/2} \quad (4.5)$$

Where:  $U$  = shock wave velocity  
 $C_0$  = ambient sound velocity  
 $P_0$  = ambient pressure  
 $P$  = air blast overpressure

The shock velocity,  $U$ , was to be the primary measurement, and would be determined from the arrival times of the blast wave and the known distances between canisters. From the pressure data obtained, a value of  $W_h$  can be determined to check the validity of Equation 4.4, and provide a basis for scaling  $W_h$  to higher and lower altitudes.

**4.2.4 Instrumentation.** Instrumentation included pressure transducers in all canisters, plus Project 8.2 thermal phototubes in three canisters, and a Project 2.7 nuclear-radiation detector in one canister. Additional equipment included batteries, electronic components, a telemetering transmitter, a tape recorder, and a command receiver. Figure 4.2 shows a canister instrumented with pressure transducer and thermal photocells.

**Pressure Transducer System.** Predicted pressures varied from 6.3 psi at 750 feet to 0.24 psi at 3,000 feet. Northam absolute-pressure transducers having ranges of 10, 5, 2, 1, and 0.5 psi were used to modulate a 14.5 kc subcarrier oscillator.

The predicted pressures are relatively low in terms of sea-level phenomena, but represent strong shocks at an ambient pressure of 0.2 psi. For this reason, scaled models of the canisters were calibrated at high Mach number conditions in a wind tunnel at Wright Air Development Center. No calibration was needed for the determination of arrival times.

**Telemetering System.** A standard Bendix TXV-13, 2-watt FM/FM telemetering system similar to the systems used for pressure measurements on Operations Ivy, Jangle, Snapper, Upshot-Knothole, Teapot, and Redwing was used in all canisters. Each canister operated on a discrete frequency between 247.50 Mc and 256.25 Mc. Subcarrier frequencies of 7.35, 10.5, 14.5, 40, and 70 kc were used to transmit overpressure, thermal, and nuclear data, a standard

frequency for time reference, and zero time. The transmitter would continuously retransmit data stored in the tape recording system.

**Command System.** The command receiver consisted of five vibrating reed relays, each of which was activated by a specific frequency. The functions performed by each relay of the command system are shown in Table 4.1. The last command disabled the power-off command circuit so that the impact of the blast wave would not accidentally activate the tone C relay and turn off the canister power.

**Data Storage System.** A complete description of the tape-recording system used is

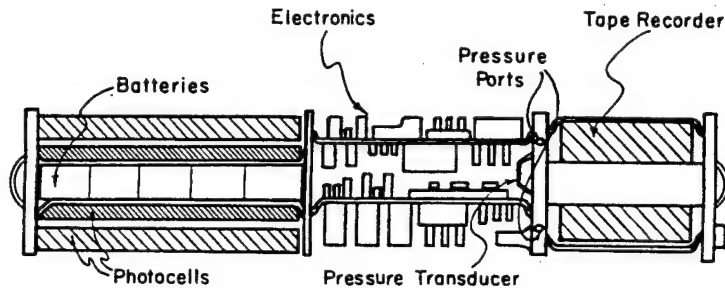


Figure 4.2 Canister with pressure transducer.

given in the Project 8.2 ITR. Only a brief summary of the pressure data-recording functions will be given here.

The recorder had two separate recording systems, one providing six channels for thermal data, and the other providing three channels for overpressure, zero time, and timing frequency data. The overpressure system was designed to record for 2½ seconds, and then play the three channels back into the telemetering transmitter continuously.

**Acoustic Charge System.** In order to calculate pressure from time of arrival data, the distance of the gage must be known. The nylon dragline, by which the canisters were sus-

TABLE 4.1 COMMAND TONES AND TONE FUNCTIONS

Tone	Tone Frequency cps	Time of Initiation	Function
A	288.5	H-7 min	Turned on transmitter and miniature tape recorder electronics. Also closed NRL power circuit in Canister 5.
B	306.7	H-2 min and H-9 sec	Closed microphone circuit and fired acoustic charges.
C	326.0	—	Capable of turning off canister power.
D	346.0	H-10 sec	Turned on tape recorder motors and locked tone C out of operation on Canisters 1, 2, 3, and 4.
E	368.5	H-2 sec	Fired the NRL rocket in Canister 5 and simultaneously cut the No. 5 command receiver out of operation.

ended, stretched under load, and some means was needed to determine the actual configuration of the canisters at zero time. Two approaches were taken. First, a stretch calibration was made, giving the percent elongation as a function of time. Second, Canister 5 had two ½-pound high-explosive charges which were to be dropped and detonated shortly before zero time. A

microphone in the bottom of each canister could register the arrival of the acoustic wave and transmit the pulse to the ground station via the 10.5 subcarrier. The separation could then be determined, using the arrival times observed and the acoustic velocity calculated from air-temperature data.

**Telemetry Receiving and Recording.** The receiving-station trailer located aboard the USS Boxer contained seven Clarke receivers, five of which were tuned to the canister transmitter frequencies, one of which was tuned to a frequency of the Sandia Pandora system, and one of which was a spare. Outputs from each receiver were recorded on a seven-channel Ampex 800 tape recorder. The command transmitter was located in the same trailer and radiated approximately 70 watts on a frequency of 42.138 Mc. All tones were manually initiated from the trailer.

**4.2.5 Results.** At about H - 2.5 minutes, a sudden drop in power-supply voltage and subsequent current surge activated the protective circuit breakers, disabling the command trans-

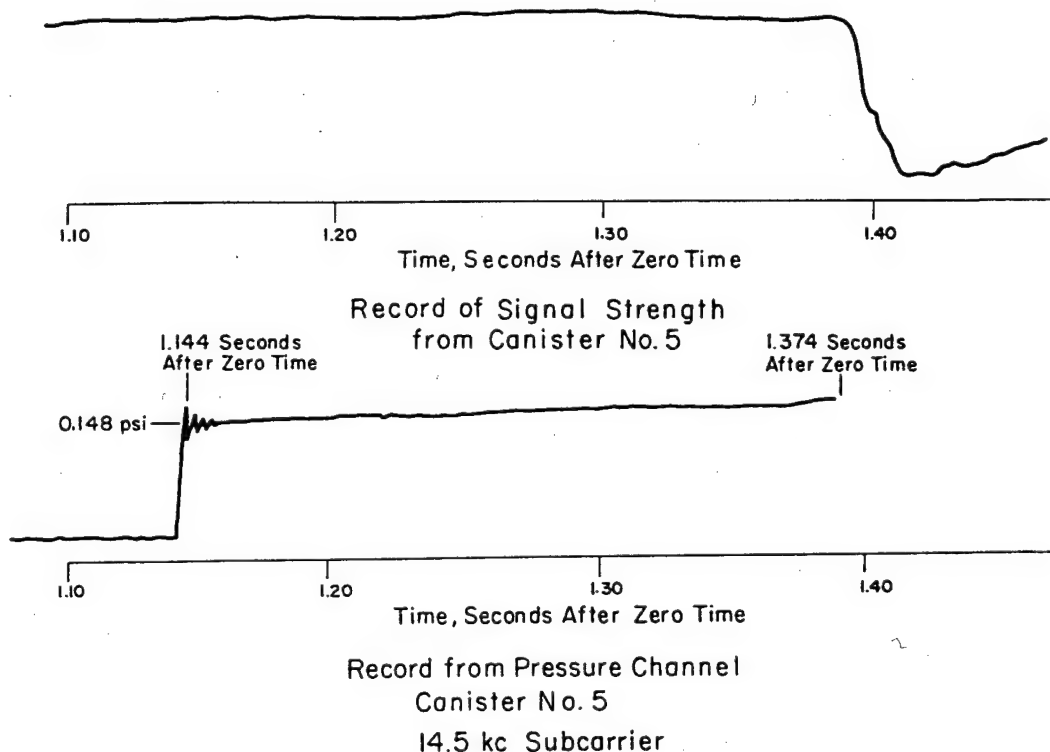


Figure 4.3 Trace of direct telemetering, Canister 5.

mitter. For operational reasons, a delay could not be granted, and commands B, D, and E shown in Table 4.1 were never sent. The result was that the acoustic charges were not fired, the tape recorders were not turned on, and the command receiver was not disabled.

The ionization blackout at zero time reduced the signal from all canisters below a detectable level. The subsequent behavior of the signals from the canisters was as follows:

**Canister 1:** No signal was detected at any time. Instrumentation is presumed to have been damaged by radiation or inactivated by the shock-sensitive command relays.

**Canister 2:** Signal reached a detectable level at about 3.2 seconds, reaching approximately preshot level at about 4.65 seconds. Data presumably would have been recovered if the recorder had been in operation.

**Canister 3:** A barely detectable signal began to be received at about 1.05 seconds. Signal strength was small and variable, never reaching the level required for subcarrier discrimination. It is believed that the antenna was damaged beyond the point of effective operation.

Canister 4: This canister had not responded to the power-on command. An attempt was being made to turn on power when the transmitter was inactivated.

Canister 5: Range was calculated to be 3,049 feet, based on the known stretch characteristics of the nylon line, and a free-fall distance of 21 feet. Detectable signal recovery began at 0.09 second, reached limiting value, and then began decreasing at 1.34 seconds. Subcarrier discrimination began at 0.19 second, and was lost at 1.37 seconds.

A trace of the directly telemetered record is shown in Figure 4.3.

It is immediately apparent that the wave form shown is not a typical pressure pulse, since there is no decay following the initial rise. It is conceivable that the non-decaying wave shape could have been caused by a changing orientation of the canister, but it is more probable that the signal was spurious, and was caused by malfunction of some circuit component.

Calculation of an effective blast yield using the arrival time, 1.144 seconds, results in a value of about 3.5 kt, considerably higher than the total yield of the device. Wind-tunnel gage calibrations are not yet available, but from previous experience it is believed that the calibration factor can hardly amount to more than a factor of 1.5. The effective blast yield calculated from the observed pressure trace, 0.148 psi, is 0.5 kt. Using a gage-correction factor of 1.5, the calculated yield is 0.96 kt.

Results of fireball photography (from one film) indicate that the Shot Yucca fireball radius versus time values plot within a few percent of Shot Osage and the TM 23-200 curve, when scaled according to the usual density factors. Nothing conclusive is proved, but the indication is that there were no anomalies or unexpected events connected with the early history of the fireball during which hydrodynamic motions are initiated.

On the basis of the mutual inconsistency between the magnitude and arrival time of the apparent pressure pulse, it is apparent either that Sachs scaling does not apply at the altitude of Shot Yucca, or that the record was spurious.

It must be concluded that the one record recovered was spurious, and that no real data was obtained.

#### 4.3 NUCLEAR MEASUREMENTS

One of the projects of the Nuclear Radiation and Effects Program was devoted to making measurements of the prompt nuclear radiation from Shot Yucca. The measurements which were to have been made by this project (Project 2.7) included neutron-flux measurements by means of a time-of-flight technique and integrated gamma-dose measurements.

4.3.1 Objectives. The objectives of Project 2.7 were to measure the neutron spectrum and total gamma-ray flux produced by the detonation of a nuclear device of low yield (approximately 2 kt) at an altitude of about 90,000 feet.

4.3.2 Background and Theory. Neutron flux and gamma-dose measurements at altitude were made by means of instrumentation in canisters dropped from aircraft for a weapon detonated at an altitude of 36,600 feet MSL during Operation Teapot (Reference 17). The neutron-flux measurements were accomplished through use of threshold fission and activation detectors, while gamma-dose measurements were made with film pack, DT/60, silver-phosphate glass, and chemical dosimeters. This type of instrumentation was satisfactory in this application as the canisters could be recovered after falling to the desert floor. Because of the altitude proposed for Shot Yucca and the inherent difficulty in recovering instruments from the open sea, the recovered canister technique was not suitable for use on Shot Yucca, and an instrumentation system which permitted data telemetering was required.

Neutron spectrum measurements by a time-of-flight method had been made as early as Oper-



ation Greenhouse (Reference 18). Measurements of this type can give good energy-spectrum data, provided the geometry is good (neutrons scattered into the detector are excluded or negligible) and if the time duration of neutron production is short compared to the mean time-of-flight of the neutrons. Since at Shot Yucca altitude the air density was approximately one percent of the air density at sea level, and the range to the detectors was small, the time-of-flight method was feasible for the measurement of the energy-spectrum of the bomb-generated neutrons.

A further problem presented itself in the consideration of the telemetering of the data obtained. In the initial stages of the project, it was planned to use a real time or instantaneous telemeter link; however, there were indications from other test measurements that an electromagnetic-blackout condition could exist in the vicinity of the burst point for some time after detonation. Since the theory of this phenomena was inadequate for the calculation of the attenuation period for Shot Yucca conditions, preliminary measurements for one frequency range (X-band) and for one distance were made during Operation Redwing (Reference 19). Further attenuation measurements were made at Operation Plumbbob to enlarge the available data and to field-test telemetering techniques (Reference 20). These measurements indicated that a real time link was not feasible for any reasonable frequency or transmitter power, and the project instrumentation was, therefore, designed to incorporate a data-storage and delayed-transmission capability.

4.3.3 Experimental Plan. The project instrumentation was built to fit into a pressurized aluminum container 22 inches high and  $8\frac{1}{4}$  inches in diameter, which comprised the upper half of Canister 5. Control of the instrumentation operations and of the data telemetering was to be accomplished with equipment mounted in the lower portion of the canister. This equipment served both Projects 2.7 and 1.10. At the time of burst, the canister was suspended below the device at a distance of 2,750 feet, or an altitude of 82,250 feet.

Basically, the neutron time-of-flight instrumentation consisted of an  $\text{Li}^6\text{I}$  scintillator photodiode detector and a similar detector composed of normal  $\text{LiI}$  used to provide information for gamma-ray-response correction. The neutron measurement extended to +120 msec. The gamma-ray dose measurements were to have been made with two types of instrumentation. A  $\text{CsI}$  scintillation detector, whose output was integrated for the first 10  $\mu\text{sec}$  after burst, provided gamma-dose information for very early time. The second detector consisted of a  $\text{KBr}$  crystal whose darkening as a function of time was to provide gamma-dose data to 120 msec after zero.

The outputs of the various detectors were electronically encoded and recorded on a magnetic tape recorder for 120 msec. At this time the recorder was programmed to reduce its speed to  $\frac{1}{16}$  of the recording speed and continuously play back the data throughout the period of the canister fall. The recorder output modulated a 70-kc voltage-controlled oscillator used in a standard frequency modulated telemetering system. The telemetering signal was to have been received and recorded at a ground-receiver trailer located on the flight deck of the USS Boxer.

4.3.4 Results and Discussion. Due to failure of the command transmitter, which was to have activated the project instrumentation, the system was in an unarmed condition at time of detonation. The failure of the command transmitter at -2.5 minutes resulted in the instrumentation not being switched and locked into the playback mode. Although data was probably recorded, the data was erased on the next transit of the recorder tape loop according to the normal operational sequence of the system in its unarmed ready state. Even if the command system had functioned properly, only 6 percent of the recorded data would have been transmitted, due to the failure of the canister telemetering transmitter at +2.5 seconds. A 42-second period was required for a complete transmission of the recorded data.

4.3.5 Conclusions. Since the attempted measurements were unsuccessful, no conclusions on the neutron and gamma phenomena could be made. From all indications, the project detector-recorder instrumentation performed satisfactorily. If an event similar to Shot Yucca were to be conducted at some future date, a preliminary ground-test of the instrumentation in a nuclear-radiation environment would be considered advisable.

#### 4.4 THERMAL RADIATION MEASUREMENTS

4.4.1 Introduction. Thermal radiation measurements on Shot Yucca were made by four projects in Program 8. These were:

1. Project 8.2, Wide Band Spectroscopy, by the Air Force Cambridge Research Center (AFCRC).
2. Project 8.3, Fireball Photography, by Edgerton, Germeshausen, and Grier (EG&G).
3. Project 8.4, Early Time Streak Spectroscopy, by the U. S. Naval Radiological Defense Laboratory (NRDL).
4. Project 8.5, Infrared Spectroscopy and Fireball Measurements, by the Bureau of Aeronautics of the U. S. Navy (BuAer).

4.4.2 Background. Early in the rocket and guided-missile programs of the military services, the potentialities of nuclear devices as air-defense weapons against enemy aircraft and missiles was realized, and the development planning of the services in these fields provided for a number of varying types of rockets and missiles, each equipped with nuclear warheads and each designed to meet the needs of the developing service in accomplishing its part in the mission of air defense. Throughout the research and development stages of these weapons, many theories have developed as to effects from nuclear weapons which would be useful for air-defense purposes, and as to the ranges of these effects. Most of these theories are based on sound physical principles, yet both scientists and the military must, of necessity, tend toward the conservative in the acceptance of new theories and new methods without some proof of their validity. The weapons are in existence today and are taking their places in the air defense system of the United States. The need to know, based on something more substantial than theory, the capabilities and limitations of these weapons is pressing. In some way, through testing, these theories must be validated in order that the users of these weapons may know the nature of their weapons and have confidence in them.

4.4.3 Methods. For Shot Yucca, seven stations were instrumented with thermal-measuring devices. Two of these were RB-36 aircraft, one was a P2V aircraft, one was the USS Boxer, and the remaining three were canisters carried by the balloon on a dragline at approximate distances of 1,050, 1,500, and 2,100 feet below the nuclear device (Figure 4.1).

4.4.4 Instrumentation. The RB-36 aircraft carried essentially three types of instrumentation, wide-band spectral units for measuring irradiance as a function of time (Project 8.2); Fastax and slitless streak-camera equipment for determining the fireball radius as a function of time, and other camera equipment for documenting the general phenomenology of the detonation (Project 8.3); and a high-speed streak spectrograph for determining the characteristics of the early time spectra (Project 8.4).

The wide-band spectral units were slit and prism-type devices utilizing masks for sharp cut-off and photomultiplier units as sensors. These units measured in the bands 2,000 to 2,500 Å, 2,500 to 3,950 Å, 3,950 to 5,000 Å, and 5,000 to 10,000 Å. In addition, a bolometer was used to measure the irradiance as a function of time of the entire spectrum.

The streak cameras were operated without slits in order to draw the envelope of the expanding fireball. At a nominal film speed of 20 ft/sec, the streak camera can resolve a few μsec and with a six-inch lens its spatial resolution is a few meters. The Fastax is a high-speed, conventional, shuttered-type motion-picture camera.

The high-speed streak spectrograph was a specially constructed instrument utilizing a Hilger small quartz spectrograph having a flat field at the focal plane and a high-speed film-drive system developed by NRDL. This instrument spread the spectrum from 1,850 to 8,000 Å, over approximately 8.5 cm, giving estimated practical wave-length resolutions of about 1 Å at the short wave-length end of the spectrum.

The P2V aircraft (Project 8.5) carried two types of instrumentation, both designed for measurements in the infrared. These were a Perkin-Elmer rapid-scan monochromator and an AN/AAS-4(XA-2) infrared electronic camera.

The Perkin-Elmer monochromator utilized a sodium-chloride prism to spread the spectrum,

and a zinc-doped germanium crystal at liquid helium temperature as a receiver. The instrument was preset to automatically scan the region 2 to 12 microns at a rate of 90 spectra per second.

The AN/AAS-4 (XA-2) was a standard infrared mapper which was modified to replace the lead telluride cell with a zinc-doped germanium crystal for much higher sensitivity capabilities, and to place wide-band filters in five of the six optical systems.

The three canister stations on the balloon dragline carried instrumentation similar to the wide-band spectral instruments carried by the two RB-36's, except that phototubes were used as sensors. The data was to be recorded on specially developed tape recorders which would then automatically switch over to a playback mode and transmit the data by way of a telemetering link to a receiving station aboard the USS Boxer.

Also aboard the USS Boxer was the seventh station mounted on the Mk 25 radar antenna. This consisted of a slitless streak camera, a 70-mm motion-picture camera, and a gun-sight-aiming-point (GSAP) camera aimed at the burst, and a GSAP camera aimed at the zenith. Since the Mk 25 was used to track the balloon array and provide data to the Air Operations Center - Combat Intelligence Center (AOC-CIC), the cameras were continuously aimed at the device.

4.4.5 Positioning Methods. The instrumentation in the RB-36 aircraft was aimed at 90 degrees to the axis of the aircraft, and at a previously calculated position angle, or angle of elevation, which was determined from the positioning requirements. These were that the two aircraft be positioned at 12 nautical miles horizontal range from the device at zero time, and at 40,000 and 39,000 feet true altitude. Since the instrumentation aim was fixed with respect to the aircraft, it was necessary, therefore, to aim the aircraft. To assist in doing this, the two RB-36's were provided with E-4 fire-control radar systems, and a radar beacon was mounted on the dragline to aid the E-4 systems in tracking.

As a backup to the E-4 system, in the event some unforeseen difficulty with equipment might occur, the CIC system aboard the USS Boxer with AOC controllers was utilized. This required some preplanned techniques for two principal reasons:

1. Data from the Mk-25 radar, which tracked the device, could not be piped into the scopes of the CIC, and
2. The data on the PPI scopes of the CIC is presented only as slant range and azimuth. Because of the latter, the distance between the device and the aircraft as it appeared on the scope was meaningless. These problems were solved in the following manner:
  - a. An altitude-slant range-horizontal range chart was prepared.
  - b. Slant range altitude and azimuth readings to the device from the Mk-25 radar were made at specified intervals and communicated to the CIC.
  - c. In the CIC, the chart operator entered the slant range and altitude of the device, projected this point to the altitude of the aircraft, and read a new slant range. This new slant range and the azimuth were then plotted on the scope with a wax pencil. The distance measured on the scope between the projection of the device and the aircraft was then approximately the horizontal distance between them with very little error (Figure 4.4).

d. By projecting ahead on his scope the plots of the projected device position, the controller could predict the projected position of the device at zero time with reasonable accuracy.

Another problem that had to be considered and preplanned was how to handle a deviation of the balloon-stabilized altitude from that planned on. Of a similar nature was the question of what to do if one of the aircraft were forced, for operational reasons, to fly at an altitude lower than that planned on. These eventualities were covered by preplanned adjustments in altitude and range. For the purposes of working out these problems, a balloon altitude of 90,000 feet was assumed, and aircraft altitudes were assumed to be 40,000 and 39,000 feet. The instruments were then oriented at position angles dictated by this geometry. Conversion charts were then worked out for the E-4 operators in terms of altitude and slant-range changes, and for the AOC-CIC controllers in terms of altitude and horizontal-range changes. For a high balloon a range change was planned, since it was not desirable to try to take the aircraft higher. For a low balloon it

was planned that the aircraft would operate at lower altitudes, so as to maintain the respective 50,000- and 51,000-foot separation in altitude between the balloon and the aircraft and, thereby, to maintain the correct geometry for the fixed position angle of the instrumentation. If this was not possible, due to cloud conditions, then as much adjustment as possible would be made in altitude and the remainder in range. An aircraft flying low, which might result from operational necessity, such as loss of an engine, presented the same problem as a high balloon and was to be handled in the same manner.

With this type of preplanning, it was possible to cover almost any conceivable situation within the capabilities of all elements of the system, including the aircraft, the balloon, the instruments, the radars, and even to some extent, the weather.

Since the E-4 radars read slant range from aircraft to device, and since the AOC-CIC system

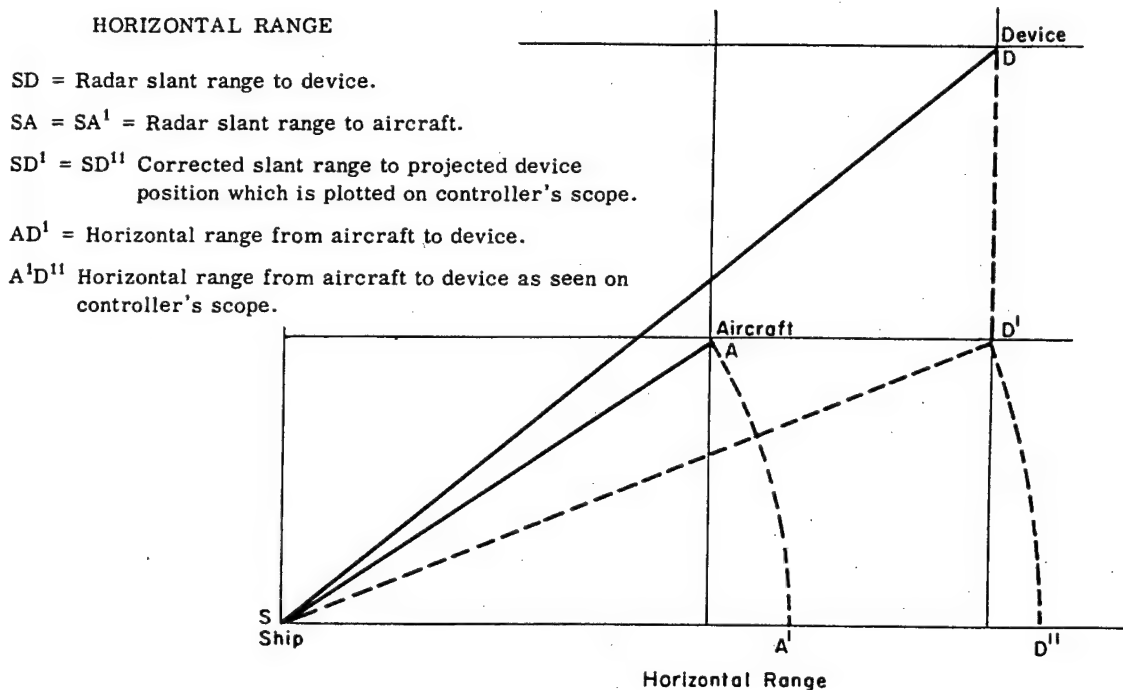


Figure 4.4 Positioning technique used by AOC-CIC.

used a common reference horizontal plane for all three elements, aircraft AOC-CIC and device, and since distances were short, problems due to curvature of the earth were negligible.

The P2V was positioned by the AOC-CIC on the USS Boxer. Since one of its instruments, the mapper, had an extremely large field of view and the other, the monochromator, was adjustable in position angle by the operator, the problems of the RB-36's, resulting from small field of view instruments and fixed position angles, were not encountered by the P2V.

**4.4.6 Results.** The instrumentation on the RB-36's was successful in obtaining data. While one streak camera jammed, and not all of the wide-band spectral units recorded data, the mission of these aircraft was completely successful. This was the result of duplication of instruments and variation of sensitivity settings to cover a large range of possible values. Both NRDL streak spectrographs, one on each aircraft, performed excellently.

A sample of data obtained in each band by the wide-band spectral instruments and a sample of the data obtained by the bolometer are shown in Figures 4.5 through 4.9. Table 4.2 gives measurements at critical data points for these curves. For more complete preliminary data, see ITR 1648-1.

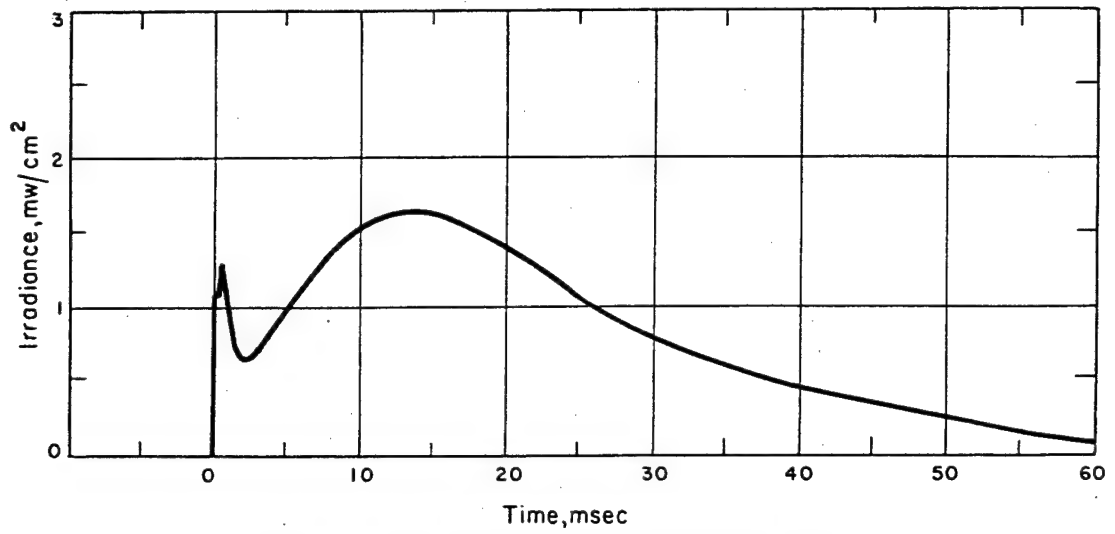


Figure 4.5 Shot Yucca thermal pulse from FUV No. 77,  
2,000 to 2,500 Å, Project 8.2, AFCRC.

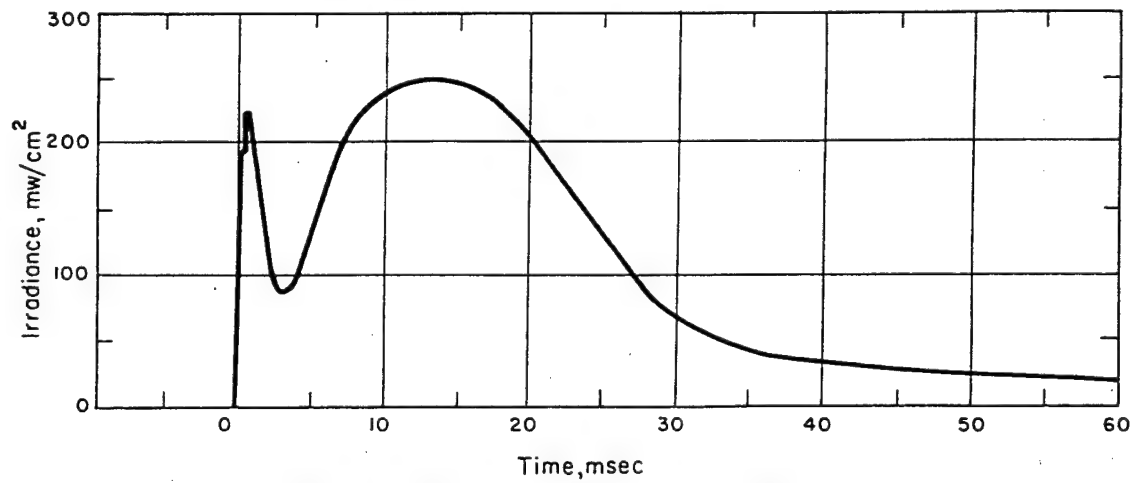


Figure 4.6 Shot Yucca thermal pulse from NUV No. 14,  
2,500 to 3,950 Å, Project 8.2, AFCRC.

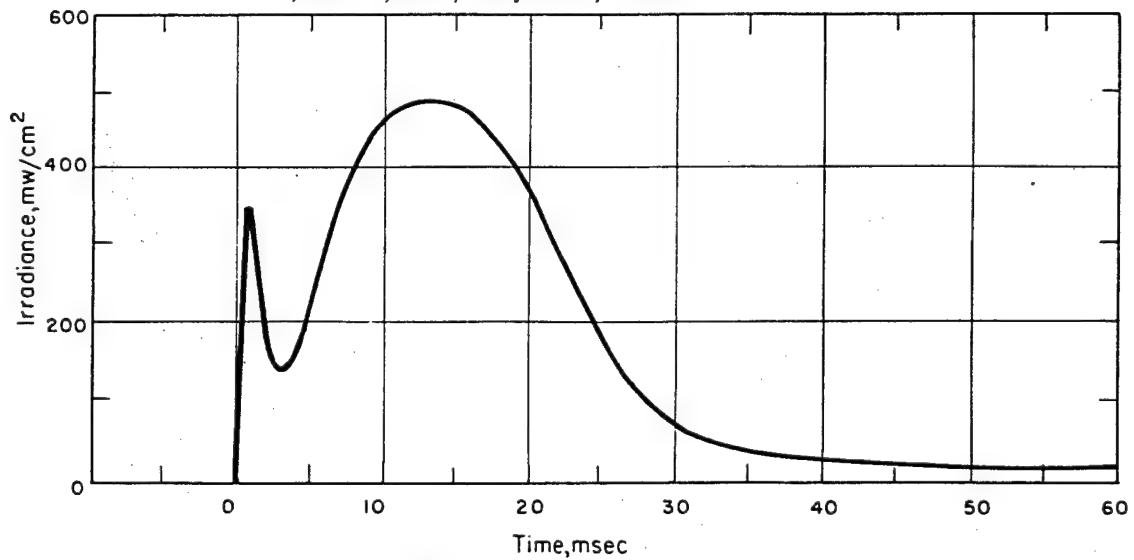


Figure 4.7 Shot Yucca thermal pulse from VIS No. 27,  
3,950 to 5,000 Å, Project 8.2, AFCRC.



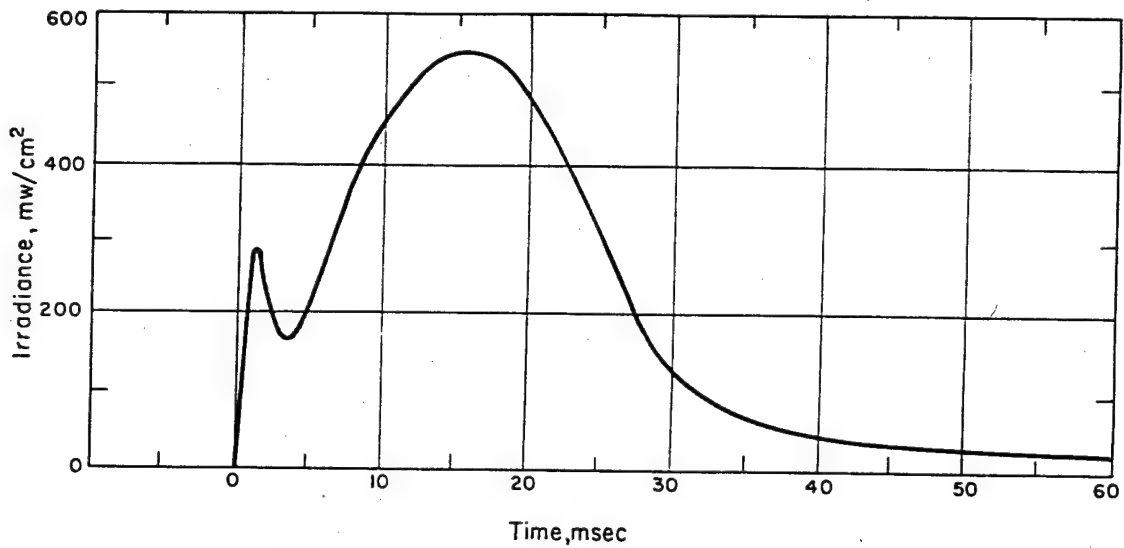


Figure 4.8 Shot Yucca thermal pulse from IR No. 44, 5,000 to 10,000 Å, Project 8.2, AFCRC.

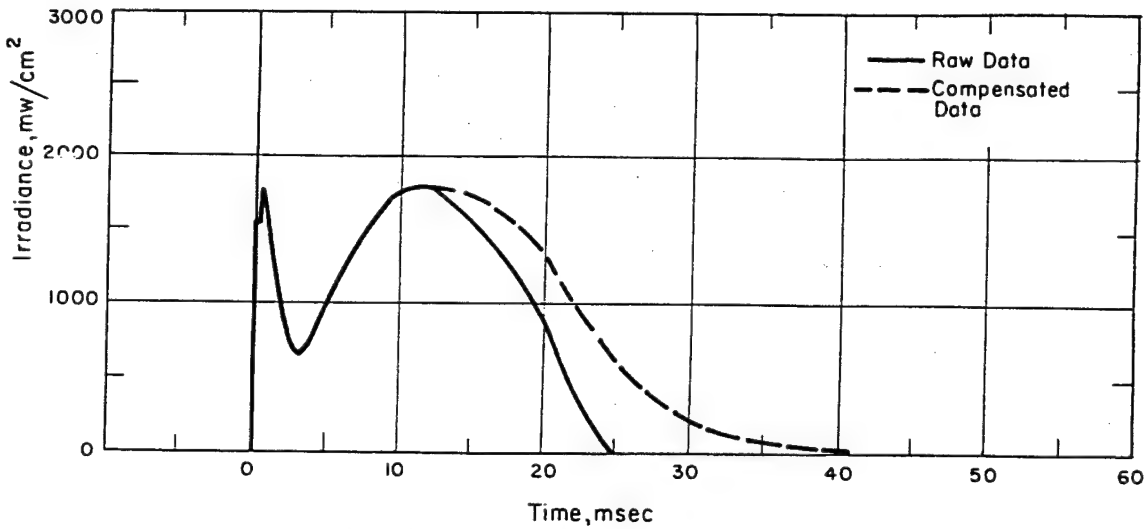


Figure 4.9 Shot Yucca thermal pulse from the bolometer (A/C 15750), Project 8.2, AFCRC.

TABLE 4.2 IRRADIANCE DATA FROM SHOT YUCCA

Aircraft used were R3-36 No. 15748 and RB-36 No. 15750.

Wave Length Range	First Maximum			Minimum		Second Maximum			
	Time	A/C 748	A/C 750	Time	A/C 748	A/C 750	Time	A/C 748	A/C 750
	msec	w/cm <sup>2</sup>	w/cm <sup>2</sup>	msec	w/cm <sup>2</sup>	w/cm <sup>2</sup>	msec	w/cm <sup>2</sup>	w/cm <sup>2</sup>
2,000 to 2,500 Å	0.67	0.0014	0.0005	2.8	0.0006	0.0002	12	0.0018	0.0005
2,500 to 3,950 Å	0.67	0.21	0.21	3.1	0.052	0.079	13	0.14	0.23
3,950 to 5,000 Å	0.65	0.32	0.39	2.8	0.12	0.14	13	0.43	0.50
5,000 to 10,000 Å	0.78	0.29	0.34	2.9	0.16	0.18	15	0.55	0.61
Bolometer	0.63	—	1.8	3.2	—	0.62	12.5	—	1.8

A plot of the fireball radius-versus-time from the various cameras in RB-36 No. 750 is shown in Figure 4.10.

A plot of temperature and brightness versus time, which was worked out by the J-10 division of LASL from densitometry measurements on one film record and from sensitometric data furnished by Project 8.3 (EG&G), is shown in Figure 4.11. For more complete data, see ITR 1649-1.

The records obtained by Project 8.4 streak spectrographs were excellent; however, they were of such a nature that they were not reproducible and they require extensive and detailed analysis in order to obtain quantitative results. The initial qualitative results reported by the project officer in ITR 1650-1 are as follows:

"The principal features of the bomb light spectra are as follows. During the first approximately 100  $\mu$ sec after zero time, a very definite discrete absorption spectrum is observed. The intensity of the underlying continuum appears to then decrease to a minimum at about 350  $\mu$ sec and then to rise again to a maximum at about 550  $\mu$ sec. This is then followed by another decrease in intensity to a minimum at about 2 msec (this appears to correspond to the usual thermal pulse minimum).

"During the period after the first 100  $\mu$ sec and up to the minimum at about 2 msec the spectrum appears to be essentially continuous with little or no discrete structure. As the intensity begins to rise beyond the minimum at 2 msec there is a marked appearance of discrete absorption which continues to just beyond the maximum at 13 msec. The discrete absorption structure then disappears and is replaced by discrete emission lines or bands which persist for the remainder of the bomb pulse.

"In both films the spectrum appears to have a sharp cutoff at about 3,000  $\text{\AA}$ . This is apparent during the maxima in the spectra. On the other hand, the spectrum apparently extends beyond 7,000  $\text{\AA}$  in the long wave-length region without noticeably decreasing in intensity."

On the P2V aircraft, the infrared mapper did not function properly and no data were obtained. The monochromator operated well, obtaining data intermittently. This is believed due to aircraft motion causing the fireball to move out of the field of view. Not all channels of data could be examined; however, those that were examined appeared to be saturated even at a fairly long time after zero time. The data could not be reduced in the field and, hence, do not appear in this report.

No data were obtained from the wide-band spectral instruments in the canisters. Approximately 2.5 minutes before zero time, a power surge in the command system aboard the USS Boxer caused the command transmitter to go off the air. The power system relays were, therefore, not locked in and the recorders had not been started. Almost all of the thermal instrumentation in the canisters consisted of new development items and, consequently, many difficulties were encountered during the planning phase, all adding up to delivery delays. As a result, it was not possible to conduct a complete system test prior to arriving in the field. After arriving in the field, all components checked out satisfactorily; however, when assembled into the system it was determined that the AM (thermal) side of the recorder was in serious trouble with induced radio frequency, which was modulated by almost any movement or vibration of parts producing large noise signals. From tests and analysis it was determined that the induced radio frequency was due to the antenna design, wherein the skin of the canister was utilized as a ground plane, or, effectively, as the long side of an unbalanced dipole. Similar difficulties had been previously encountered on test flights with the command receiver, and were cleared up by modifying the receiver. It was also determined that the radio-frequency noise was not recorded, but appeared to be introduced into the high-gain playback amplifier during the playback phase. The most that could be done in the field was to filter and bypass appropriate parts of the amplifier circuitry, and to add additional shielding to the extent possible. This resulted in a tremendous reduction in the noise level, but not sufficient reduction to insure proper operation. However, since the system would repeat its transmission of data hundreds of times during the descent of the canisters, it was possible that some noise-free transmissions might get through; only one would be required to obtain the data.

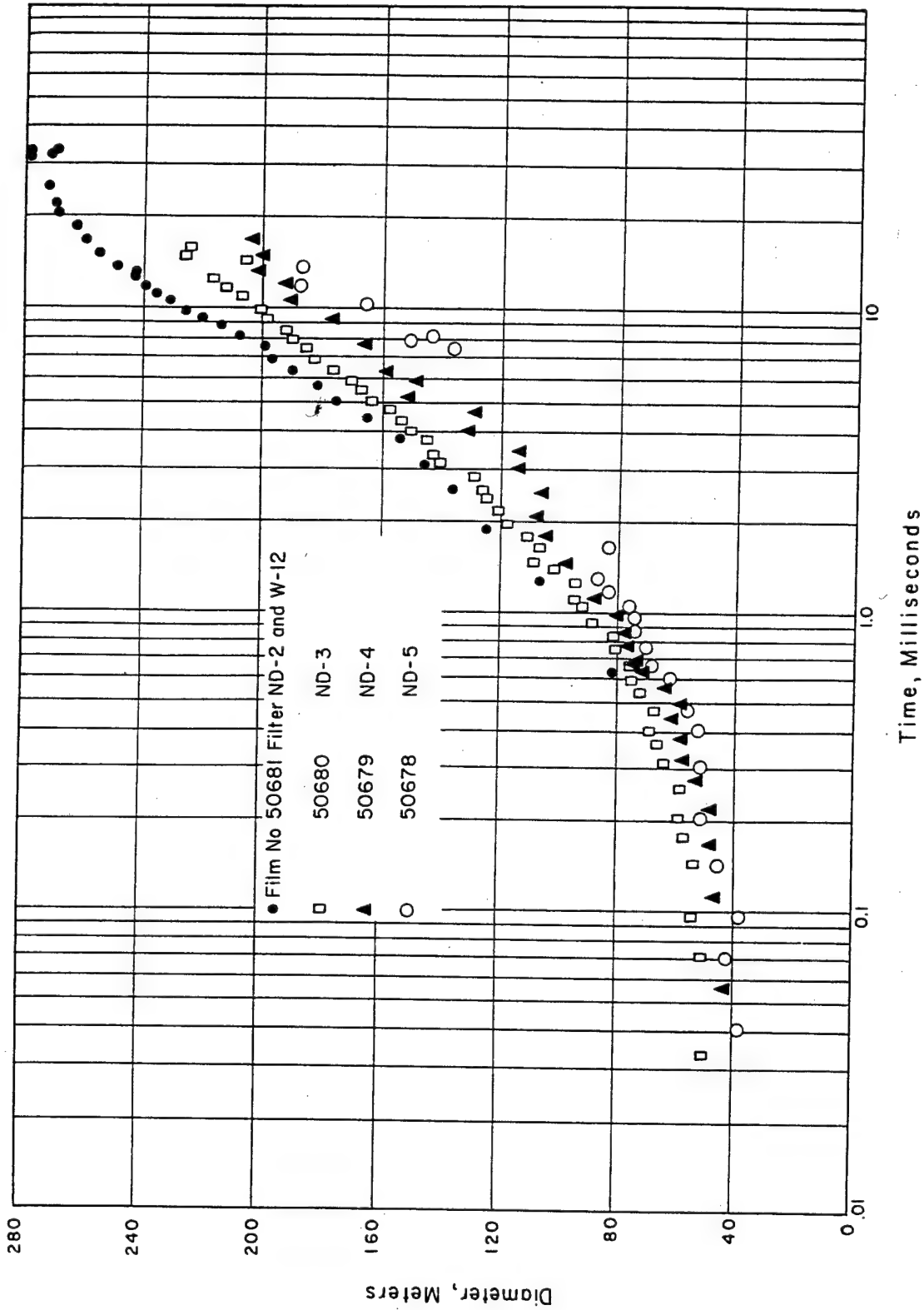


Figure 4.10 Shot Yucca fireball versus time, Project 8.3, EG&G.



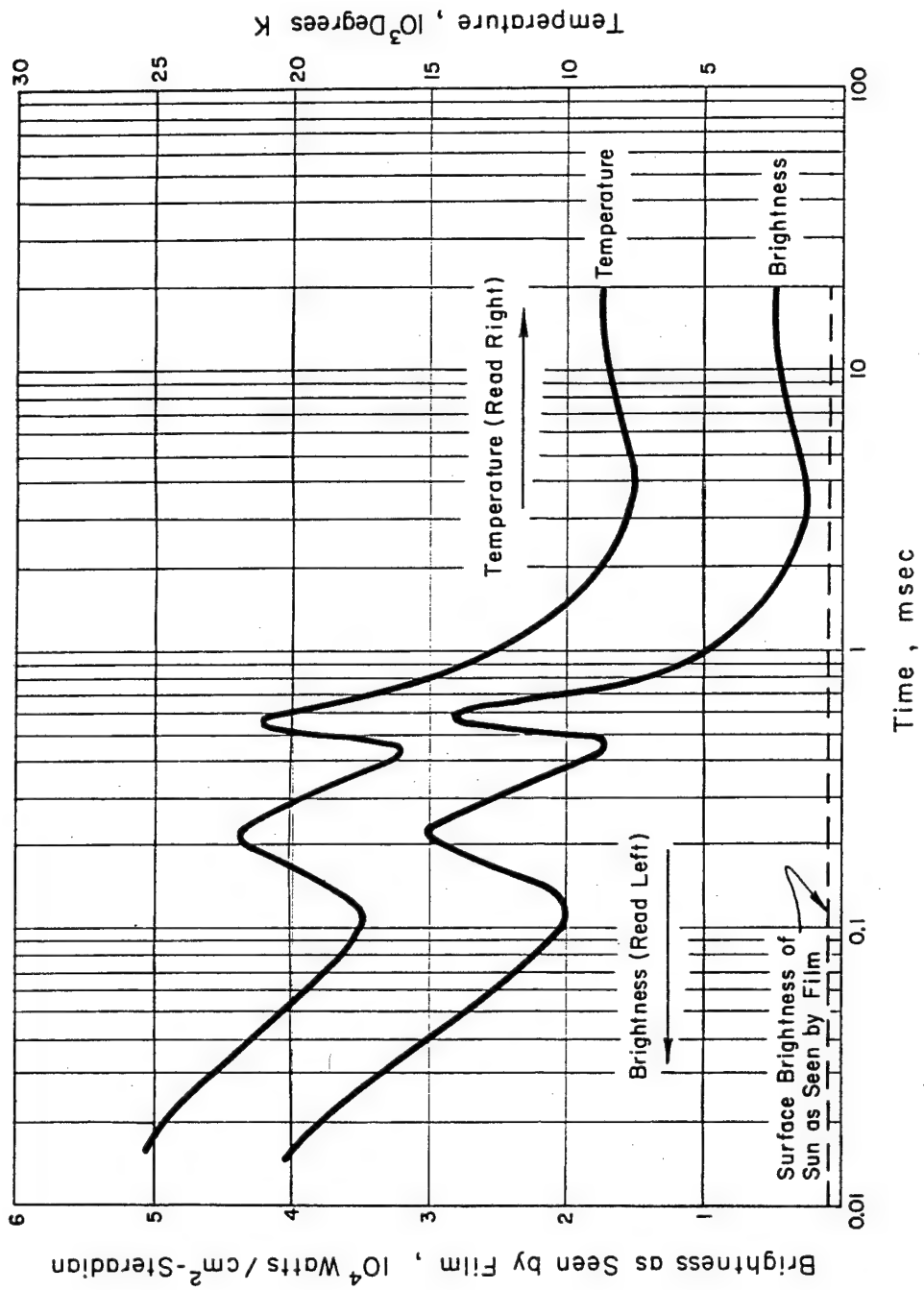


Figure 4.11 Shot Yucca temperature and brightness, Project 8.3, EG&G.

On shot day, the E-4 radar system in RB-36 No. 750 was operational and was utilized to position the aircraft. The E-4 system on RB-36 No. 748 failed during the mission and this aircraft was positioned by the AOC-CIC. The particular E-4 systems provided proved to be unreliable and were a constant maintenance problem. The beacons provided for use with the E-4 were never successfully operated for sufficient time to carry out a mission. Apparently they had temperature troubles at altitude and froze up. The E-4's were never successfully locked on either a beacon or the reflector, so that they tracked in the automatic mode.

The AOC-CIC positioned the P2V successfully and stood by as a backup for positioning the RB-36's. When the E-4 on aircraft No. 748 failed, the AOC-CIC took over and successfully positioned the aircraft.

Zero-time geometry of the various elements in the array is presented in Table 4.3. The ITR's

TABLE 4.3 SHOT YUCCA GEOMETRY

Reported Data:

<u>Device Altitude</u> ft	<u>Source</u>
82,500	Arowagram
85,250	Mk-25 Radar
85,000	Sandia Corp. Pressure Transducer, uncorrected

<u>Data</u>	<u>Aircraft 750</u>	<u>Aircraft 748</u>	<u>P2V</u>	<u>Source</u>
Aircraft altitude, true	37,000 ft	36,000 ft	—	Aircraft logs
Bearing, balloon to aircraft, true	276 deg	202 deg	243.5 deg	Air Operation Center and aircraft logs
Aircraft heading, magnetic	355 deg	293 deg	—	Aircraft logs
Aircraft heading, true	002 deg	290 deg	—	Aircraft logs
Slant range, aircraft to reflector	14.5 naut mi	—	—	E-4 Radar
Slant range, aircraft to balloon	—	14 naut mi	—	Aircraft log
Slant range, aircraft to device	80,659 ft	85,709 ft	—	Air Operation Center
	85,817 ft	—	—	E-4 Radar
	—	85,120 ft	—	Aircraft log
Horizontal range, aircraft to device	10.7 naut mi	11.6 naut mi	16 naut mi	Air Operation Center

Considered Best Values:

Device altitude: 84,683 ft

<u>Data</u>	<u>Aircraft 750</u>	<u>Aircraft 748</u>
Aircraft altitude, true	37,000 ft	36,000 ft
Bearing, balloon to aircraft, true	276 deg	202 deg
Aircraft heading, true	002 deg	290 deg
Slant range, aircraft to device	85,817 ft	85,415 ft

will show figures which differ from these in some respects; however, they represent the best information available to the projects at the time of writing. The data presented in Table 4.3 are taken from the records sent in by the various elements, and represent the best information on the geometry of the array. The information included was compiled as follows:

1. The altitude of the device reported by the Mk-25 radar was accepted as the best value; correction for curvature of the earth was determined to be negligible, and a correction of 567

feet was applied for the difference in altitude between the reflector and device.

2. Slant ranges were computed using the reported horizontal and slant ranges, corrected device altitude, and reported aircraft altitudes. Wherever, in the process of computation, a value could be computed using two different trigonometric functions, it was computed both ways and the average taken as the correct value.

3. The slant ranges for Aircraft No. 748 computed from values given by two different sources are in fair agreement, and an average value is taken as the best value.

4. The slant ranges for Aircraft No. 750 computed from values given by two different sources do not agree by approximately 6,000 feet; therefore both values are given. If the E-4 radar was properly tuned and adjusted, then the value obtained by it and corrected should be the best value of all values given for either aircraft. However, the fact that the AOC and another source agree so well on the data for Aircraft No. 748, while the AOC and the E-4 radar do not agree so well on the data for Aircraft No. 750, may lend doubt as to the accuracy of the E-4 data.

No further information is anticipated which will change these data.

4.4.7 Conclusions. The conclusions reached after analysis of the preliminary Shot Yucca data are tentative conclusions only, and are based on an analysis of the Shot Yucca data only.

1. The principal noticeable effect of altitude on thermal phenomena from nuclear weapons is a shortening of the time base on which certain events take place.

2. This shortening of the time base results in making the detonation appear time-wise, like one only a fraction of its actual yield.

3. The apparent yield scales as the relative density to the two-thirds power.

4. The time base scales as the relative density to the one-third power.

5. The radius of the fireball at time to the normal second maximum scales inversely as the relative density to the one-sixth power.

6. There is no conclusive evidence that the partition of energy into thermal energy varies with altitude.

## *Chapter 5*

# *SHOTS TEAK and ORANGE*

### 5.1 BACKGROUND AND OBJECTIVES

Shots Teak and Orange were scheduled to be fired from Bikini Atoll and to detonate megaton-range warheads at 250,000 and 125,000 feet, respectively. Prior to Operation Hardtack, the only two shots fired at altitude were a 3-kt detonation at approximately 36,000 feet over Yucca Flat (Operation Teapot, 1955) and a 1.7-kt detonation at approximately 19,000 feet over Yucca Flat (Operation Plumbbob, 1957). As can be seen, both were of small yield and at relatively low altitudes. Specific objectives and backgrounds of each project are discussed in detail in following sections of this chapter. However, Shots Teak and Orange were authorized as a part of the continuing effort to understand high-altitude phenomena and to derive scaling laws therefrom. Highest priority was assigned in the areas of nuclear heating for antiICBM applications, partition of energy with consequent effects, effectiveness of detection systems, and ionospheric effects.

5.1.1 Operations. Only the operations of the missile carriers themselves are discussed in this section. Project operations, procedures, and instrumentation are to be found in following sections.

As previously stated, launch sites were originally planned for Site How, Bikini Atoll for April and May of 1958. Valid considerations of the possibility of retinal burns to the 8,000 natives within a line of sight of the bursts dictated the move of these launch sites to a more remote area, population-wise. The decision to move came after all major construction had been completed and after most personnel and equipment were in place at Bikini Atoll. The problems and cost of the move and new construction at the selected alternate site, Johnston Island, will not be enumerated. It is sufficient to say that the move was successfully made and the carriers and associated equipment were ready for firing on schedule.

Due primarily to lack of real estate, rather than through inability of the projects to make a rapid change of location, some projects had to be dropped, but some others were added. The space available on Johnston Island can be seen in Figure 5.1.

The Army Ballistic Missile Agency (ABMA) was assigned the mission of providing the carriers, two Redstone missiles, for the megaton-range warheads, (Figure 5.2). Surface zero for Shot Teak was planned at a horizontal distance of approximately 5.4 nautical miles at 180 degrees true from the launcher at an altitude of 250,000 feet and Shot Orange at a horizontal distance of 21 miles at 180 degrees at an altitude of 125,000 feet. Four instrument carriers (pods) were to be carried externally and ejected from each missile during the powered phase of trajectory so as to be in predetermined positions at burst time (Figure 5.3). Instrumentation was provided by scientific projects, and detailed discussions of the pods and results are to be found in other sections of this chapter.

A detailed description of the missile is not appropriate for this publication. Essentially, they were tactical Redstones with slightly modified guidance systems. They were tracked in flight by the standard combination DOVAP and Beat-Beat (Doppler tracking systems). Pod locations were calculated on the basis of known missile velocity and acceleration at ejection, as obtained from DOVAP, and accurate ejection times obtained from telemetering records. Arming and firing

functions were performed by a self-contained adaption kit developed by the Long Range Applications Laboratory of Picatinny Arsenal.

**5.1.2 Results.** For Shot Teak, missile lift-off occurred at 2347:14.99 LST on 31 July. As planned, this lift-off time was used as zero time for the master timing system. Burst occurred at 2350:05.597 LST. Because the missile did not program properly, the burst point was not

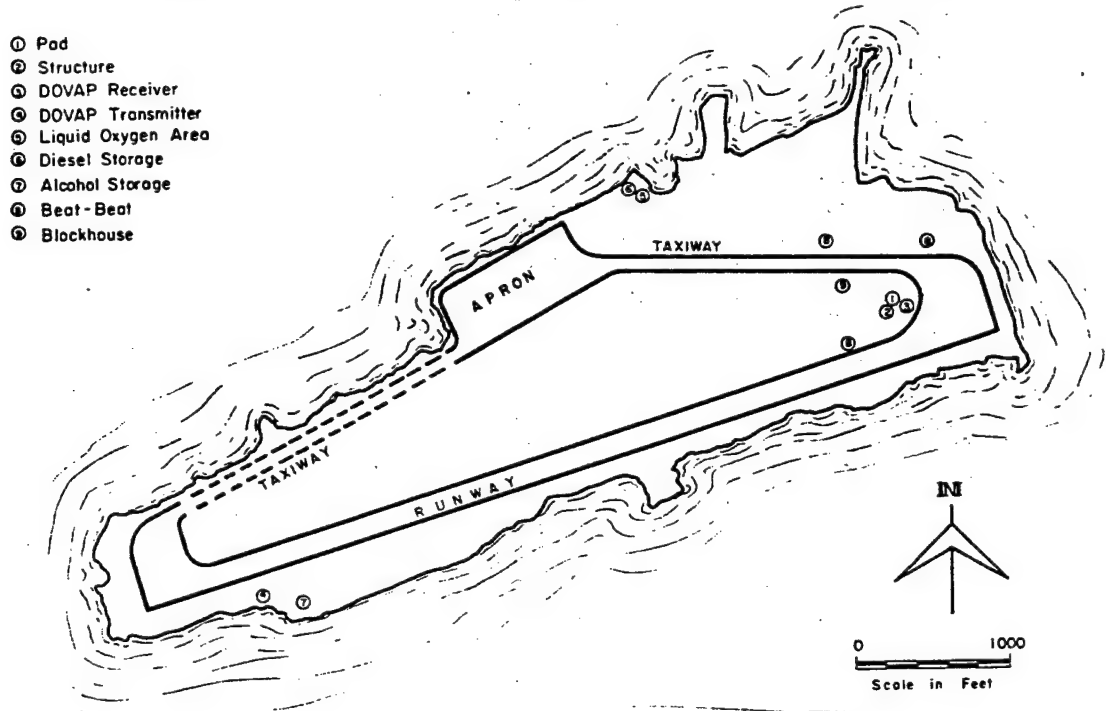


Figure 5.1 Johnston Island layout.

where expected. The missile followed a vertical trajectory and the burst altitude was approximately 250,000 feet.

For Shot Orange, the missile programmed about as expected. The burst altitude was approximately 140,000 feet. Lift-off was at 2327:34.498 LST, and burst at 2330:08.607 LST, on 11 August.

## 5.2 PRESSURE MEASUREMENTS FOR HIGH-ALTITUDE BURSTS

**5.2.1 Objective.** The objective of this phase of Project 1.7 was to obtain surface and near-surface air-blast and pressure-time measurements from the very-high-altitude detonations, Shots Teak and Orange.

**5.2.2 Background.** Prior to Shots Teak and Orange, there were two high-altitude shots where surface and near-surface pressure measurements were made. These events, Shot 10, the high altitude shot of Operation Teapot, and Shot John of Operation Plumbob, were detonated at altitudes of 36,645 feet and 19,110 feet, respectively. Both were well below the burst altitudes of the Teak and Orange detonations.

Data from the high-altitude shot were fitted to a 1-kt free-air curve by applying the modified Sachs scaling laws. Data from Shot John were reduced to the curve by applying the standard Sachs scaling laws. The deviations in these data prevented their scaling similarly; this, coupled

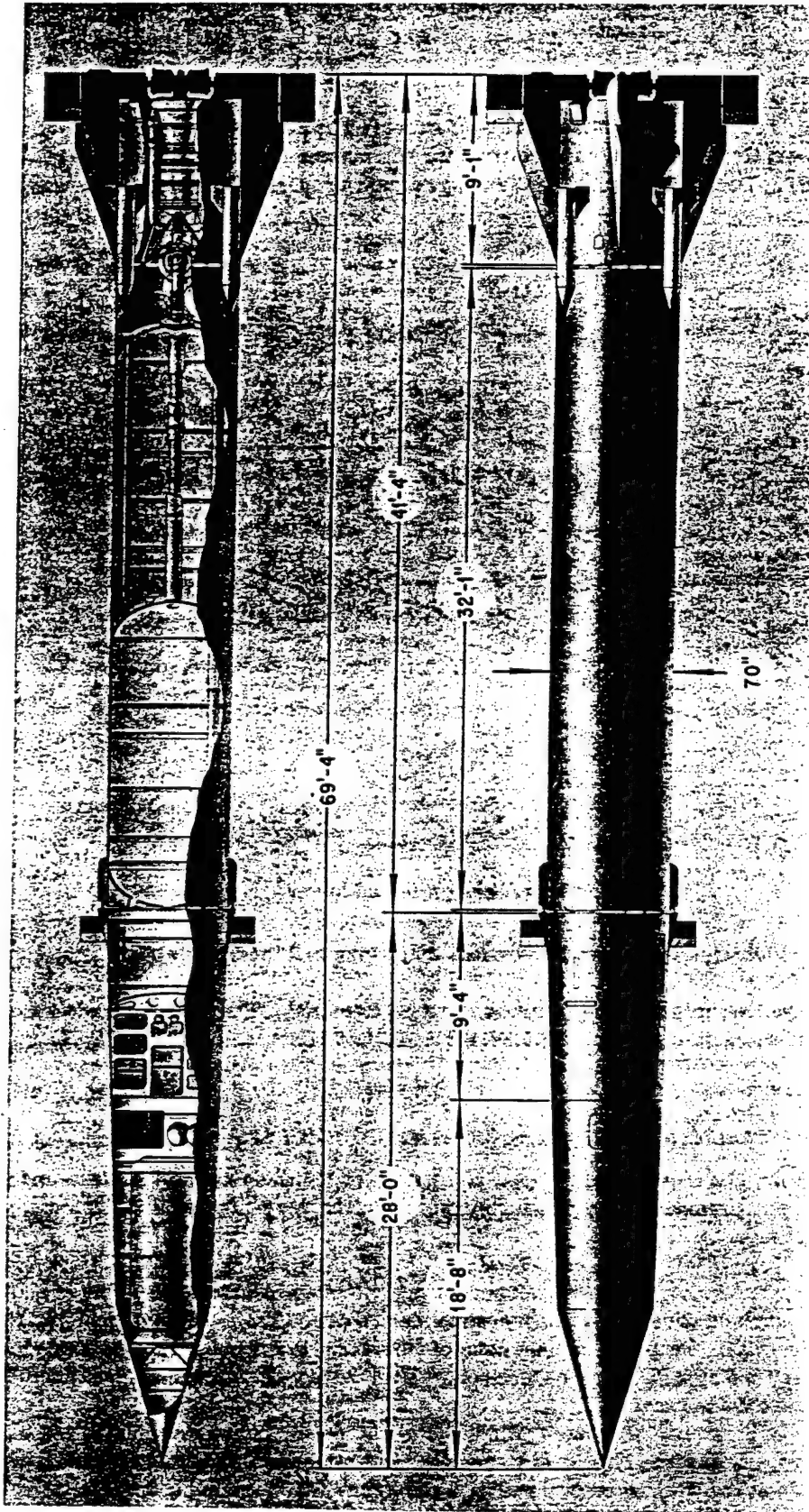


Figure 5.2 Redstone missile.

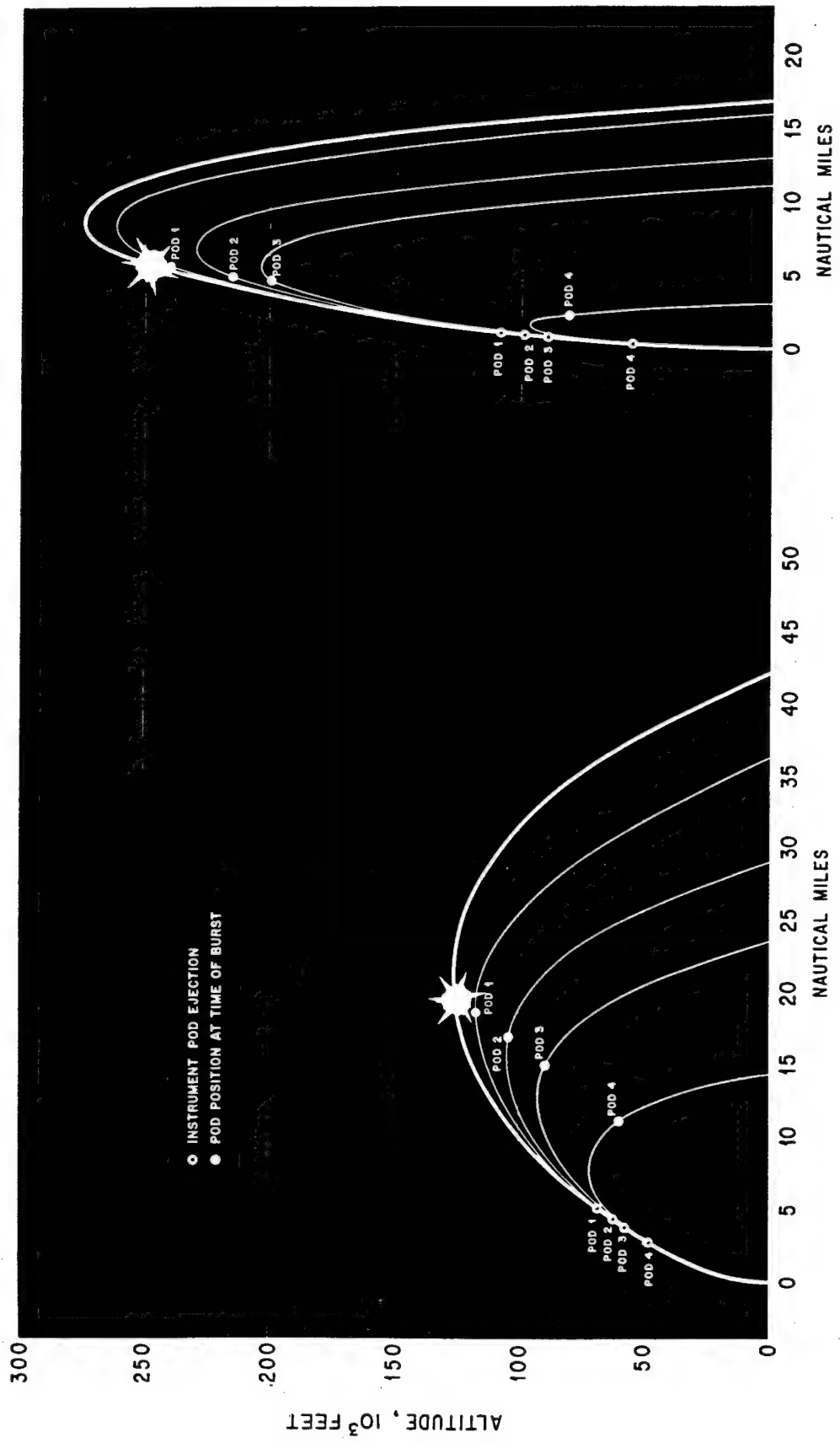


Figure 5.3 Planned Redstone missile trajectories: Shot Orange, left and Shot Teak, right.

with the altitude differential among high-altitude Shots John, Teak, and Orange made the prediction of blast pressures from very-high-altitude detonations quite uncertain.

5.2.3 Method of Experimentation. Three types of end instruments, or gages, were used to obtain the desired air-blast measurements. Two were of the self-recording variety and the third was an electronic gage. The original plan of using only self-recording gages was changed because of the apparent discrepancies in the results obtained from them during a number of the shots at Eniwetok. Upon return of the project personnel to the Ballistic Research Laboratories (BRL) after the initial Eniwetok participation, the electronic recording systems were assembled. The following sections present a short description of these gages and recording systems.

Self-Recording Instruments. The BRL self-recording pressure-time ( $P_t$ ) gage, a self-contained unit designed to give a scratch record of the pressure-time variations in air-blast shock waves, consisted of a pressure-sensing capsule comprised of two nested metal diaphragms. An increase in outside pressure entering through a small inlet hole caused expansion of the diaphragms; a light, osmium-tipped stylus soldered to the center of the free diaphragm recorded the diaphragm deflection as a  $\frac{1}{2}$ -mil scratch on a rotating, aluminum-coated glass disk. Constant rotational speed was assured by using a chronometrically-governed dc motor as the recording-blank drive. The 3-rpm motors used during Shots Teak and Orange permitted time resolution of records to 2 msec. Initiation of the motor was obtained by relay closures from the timing signals.

The BRL very-low-pressure (VLP) gage employed the same recording principle as the  $P_t$  instrument. The difference in design was primarily in the use of a single diaphragm in the VLP, thus permitting greater sensitivity.

An accessory delay box was used with these self-recording gages. The limited running times of the VLP and  $P_t$  gages made it necessary to insert a hold interval between shot time and blast arrival. This interval was highly dependent upon the distance from the burst point to recording station. An ideal setting of this no-run interval would initiate the gage several seconds prior to blast arrival and, hence, ensure the complete recording of the long-duration pressure-time phenomenon. The delay box was started by a timing signal and served to furnish relay closure (or initiation) for all self-recording instruments at a station.

Electronic Recording Instruments. In the electronic recording system, Satham strain-type pressure transducers were employed (Figure 5.4). This gage had three fundamental components: a diaphragm, a Wheatstone bridge, and a temperature-compensating device. One of the resistive elements of the bridge was connected to the diaphragm. Pressure variations of the latter thus influenced the bridge balance. Eight Satham transducers were used: four with a range of 0 to 0.1 psi, the other four 0 to 0.5 psi. All gages were capable of withstanding 3.5-psi peak overpressure.

In order to record the output of the transducers just described, a graphic, electric-pen recording system was used. The fundamental components of the system, dc amplifiers, magnetic pen recorders, and recorder power supplies, were products of the Brush Instruments Corporation. Associated parts, sequence timers, junction boxes, relays, and tuning-fork circuits, were designed and constructed at BRL. System power was supplied by two 24-volt dc-ac converters driven by four 12-volt batteries. A photograph of the recording equipment is shown in Figure 5.5.

5.2.4 Field Layout of Equipment. For both Shot Teak and Shot Orange, three land and two shipboard stations were utilized. Two of the land stations (one on Johnston Island, Station 172.01, and the other on Sand Island, Station 172.02) were considered primary stations because the electronic backup systems were used. A 34-foot tower was erected at each of these stations and was instrumented at the top and bottom for free-air and surface-pressure measurements, respectively. Each instrument cluster consisted of two Satham gages, a  $P_t$  gage, and a VLP gage. The electronic equipment for the Satham gages was housed at the base of the tower in a wooden box measuring 3 by 6 by 10 feet. Each shelter was covered with aluminum to provide protection against thermal radiation.

The third land station (on Johnston Island, Station 172.03) was located about midway between





Figure 5.4 Statham pressure gage.

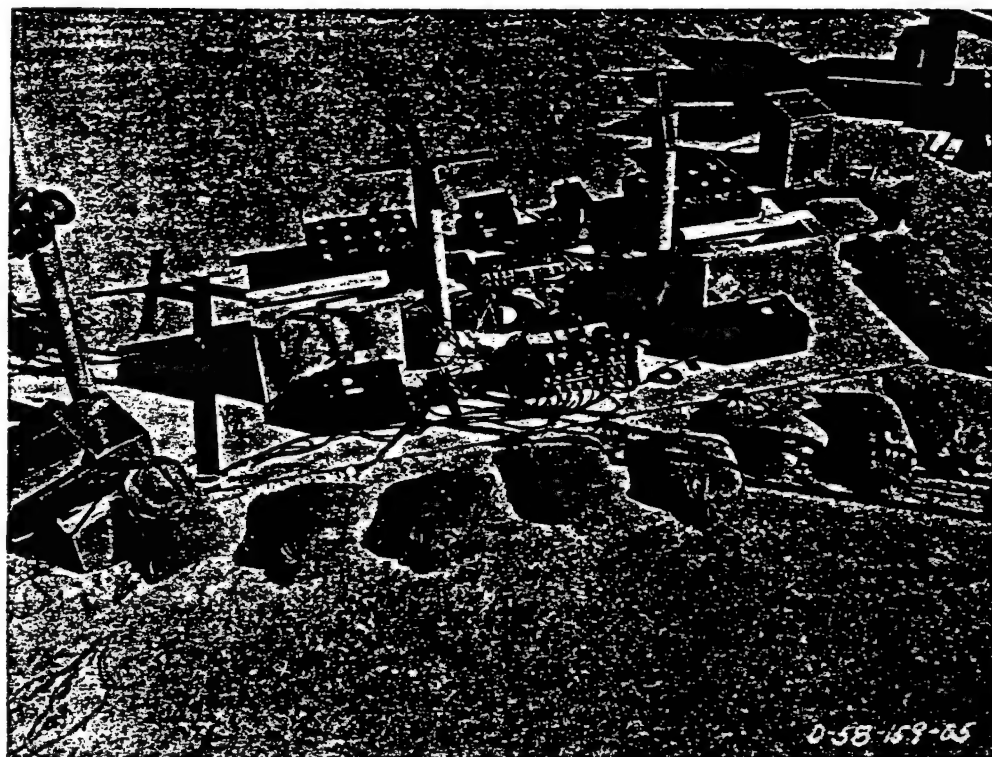


Figure 5.5 Field layout of electronic recording system.



the two tower stations and employed a  $P_t$  and a VLP gage for Shot Teak, and two  $P_t$  gages for Shot Orange. Figures 5.6 and 5.7 are photographs of a tower station.

The two shipboard stations employed VLP gages only. For Shot Teak, there were two gages aboard the USS Boxer and one aboard the USS Lansing. For Shot Orange, there was one gage on each ship. The positions of these ships at blast arrival time and the location of the ground stations are shown in Figures 5.8 and 5.9. All gages except the ground-level  $P_t$  gages were positioned side-on to the incident blast wave.

**5.2.5 Results.** The data obtained during Shot Teak are listed in Table 5.1. The results do not show complete pressure-time curves on the self-recording land gages. All self-recording gages, except those aboard ship, were set up to initiate at  $H + 3.41$  minutes. This starting time was based on BRL predictions. Blast arrival occurred on Johnston Island at 3.16 minutes; hence, the gages were not running when the blast wave reached the instruments. The blast wave arrived approximately 15 seconds prior to gage initiation, and according to the shipboard stations, where the complete phenomena were recorded, the blast was 5 seconds into the negative phase when the gage disks began to register the pressure-time history.

The characteristic of the gage was such that peak-pressure values were recorded even when the gage was not running. Thus, peak pressure and the majority of the negative phase were obtained. The records show as a function of time the preshot baseline, the deflection resulting from blast arrival, and the negative deflection. All gages, except one VLP at the ground station 172.03 (the station nearest the launch point), operated as programmed. At this site the recording needle left the reproducing disk when the diaphragm was excited and did not return.

All shipboard stations functioned normally, and good records were obtained. Five of the eight electronic channels functioned as programmed; however, results were not considered to be good. It appeared that the atmospheric-vent plugs, which serve to equalize the gage-pressure diaphragm in the event of ambient-pressure changes, too rapidly adjusted the pressure differential and, hence, affected the accurate measurement of positive and negative duration. Two of the three channels failed completely because of excessive baseline drift. The third channel failed because of a poor contact on an amplifier input plug.

During Shot Orange the blast wave was strongly attenuated, probably as a result of reflection from cloud interfaces. The data from the land and ship stations are shown in Table 5.2. Photographs of representative pressure-time curves are shown in Figures 5.10 and 5.11.

Six of the eight electronic gages functioned as programmed; however, one of the records was questionable. Four of the six VLP gages gave pressure-time records. Two gages recorded peak pressure only. Five of the six  $P_t$  gages yielded pressure-time records. For reasons not yet determined, one  $P_t$  gage produced no record. Arrival time was measured at the two shipboard stations and at the Johnston Island electronic station.

**5.2.6 Discussion.** The blast-arrival times and positive-phase durations are shown in Table 5.3. The times listed for Stations 172.01 and 172.02 were obtained from the electronic-gage records, which had a zero-time fiducial from a blue box and a 50-cycle timing marker. The arrival time at Station 172.03 was obtained by adding the preselected time delay to the interval between drive-motor start and disk record. At the sea stations, stop watches recorded the time interval between the voice-announced shot time and shock arrival.

Figure 5.12 shows the arrival time as a function of slant range. The upper point on this graph represents the measurement (from Shot Orange) made on the USS Boxer and indicates an excessively long arrival time. At this location, observers stated that the pressure wave manifested itself by a dull rumble rather than a distinct shock. Pressure-time measurements showed a slow-rise character and, hence, substantiated the observations. It appeared that excessive cloud formations between the burst point and the station caused multiple shock-wave reflections that increased the path length of the wave to some indeterminate value.

The positive-phase duration is plotted as a function of slant range in Figure 5.13. Again the upper point (data from the USS Boxer) depicts an extremely long value of this phase of the

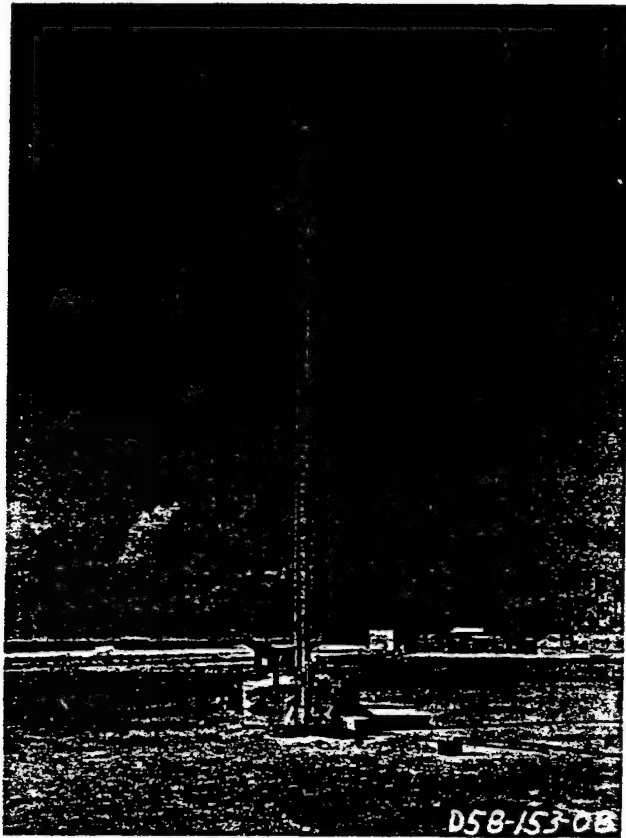


Figure 5.6 Tower station.

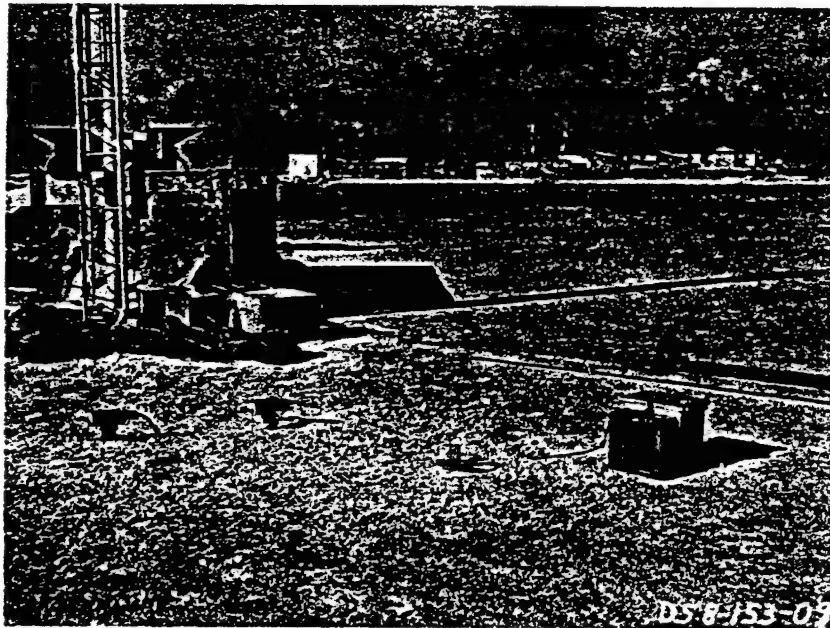


Figure 5.7 Base of tower station.

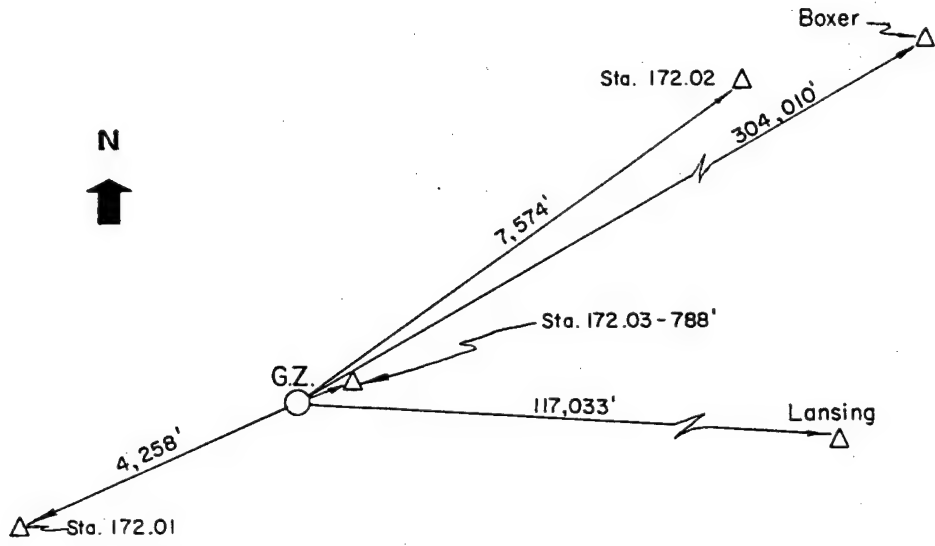


Figure 5.8 After-the-fact station layout for Shot Teak.

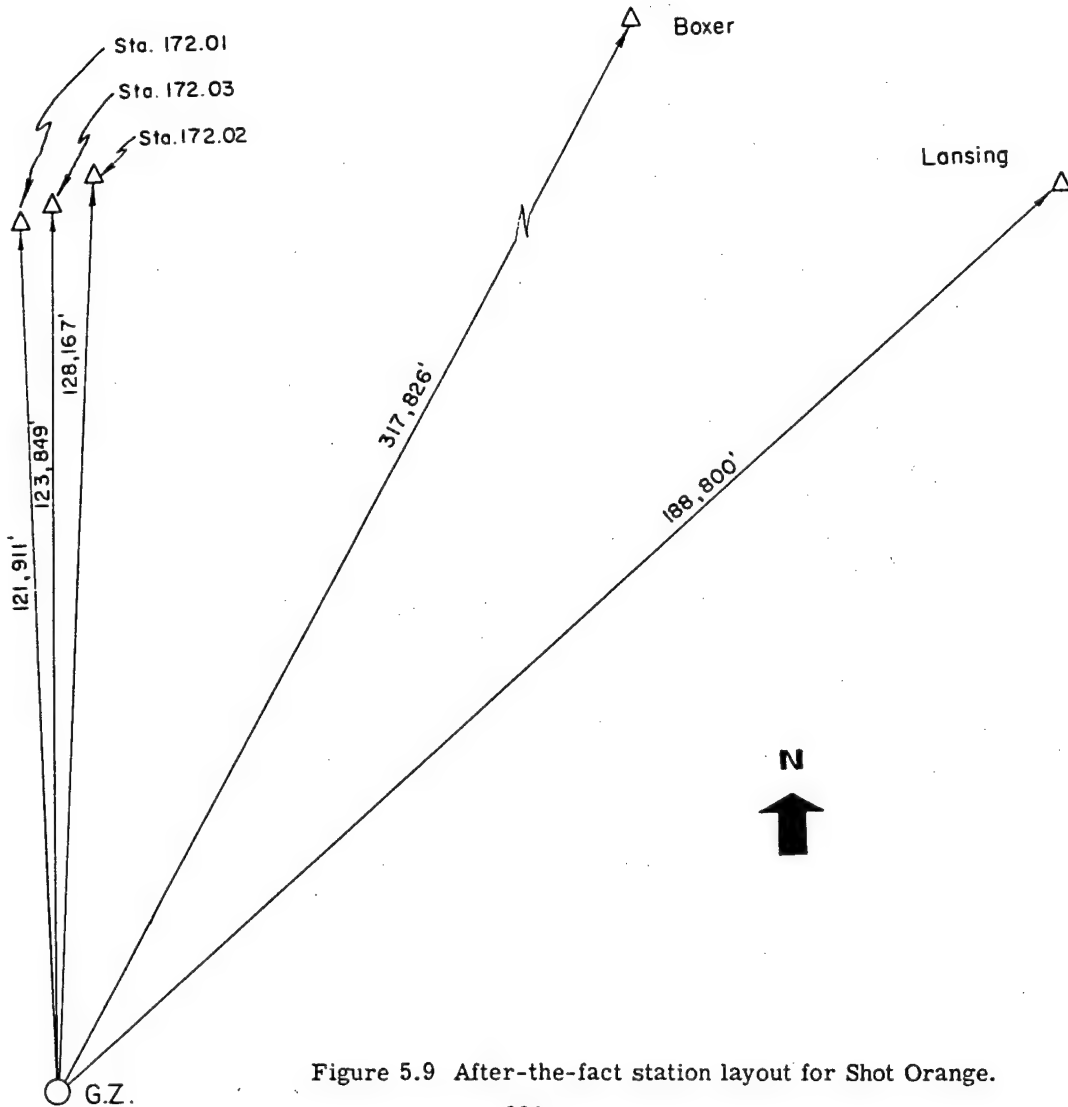


Figure 5.9 After-the-fact station layout for Shot Orange.

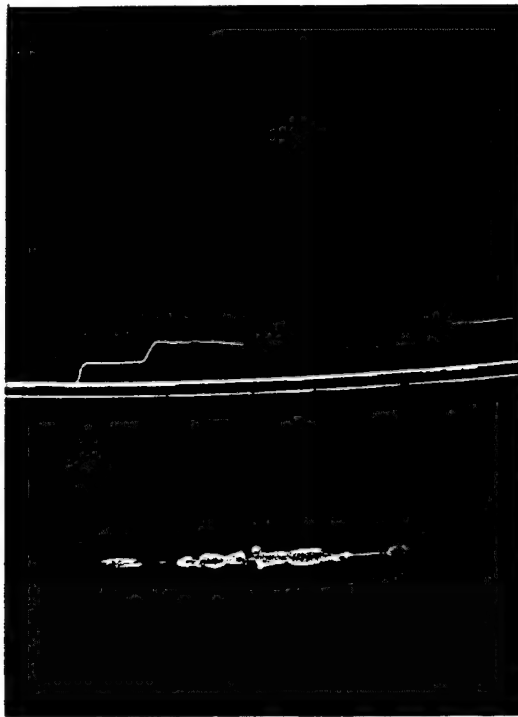


Figure 5.10 Overpressure time record from Station 172.02, 34-foot tower, Shot Orange.

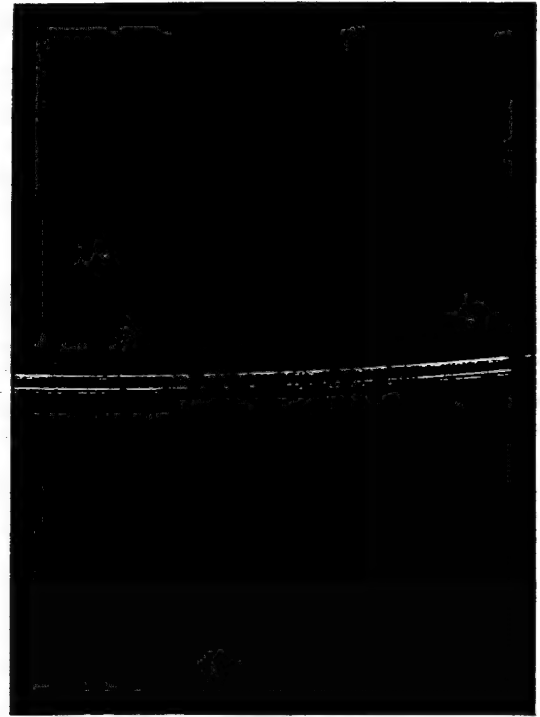


Figure 5.11 Overpressure time record from Station 172.02, ground level, Shot Orange.

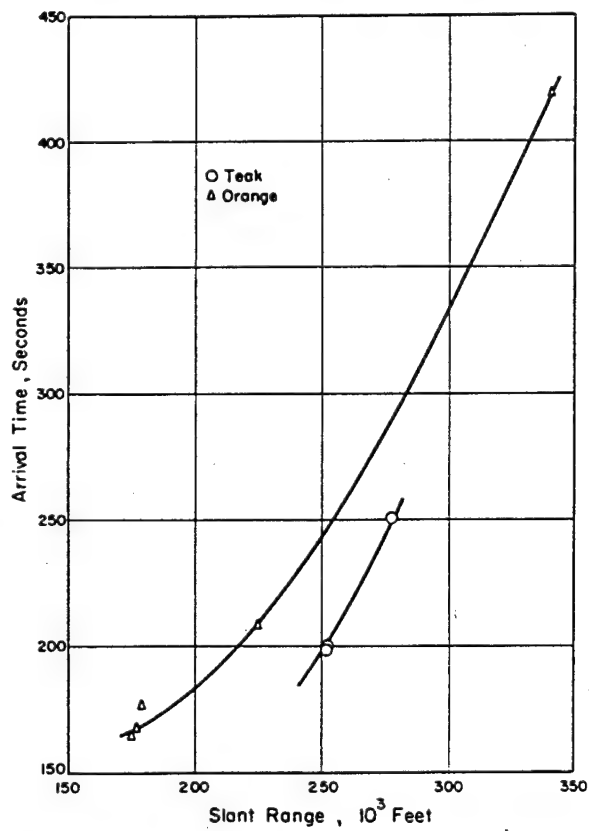


Figure 5.12 Arrival time versus slant range for Teak and Orange.

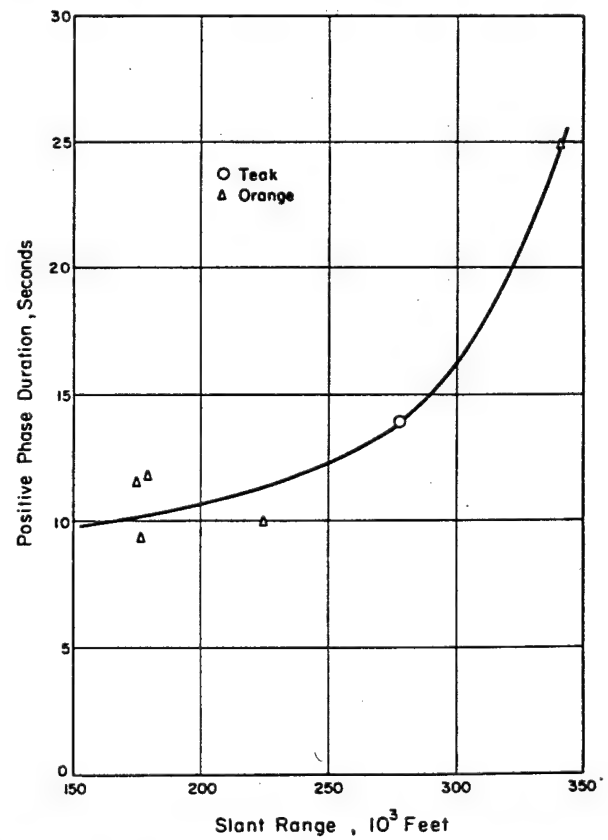


Figure 5.13 Positive phase duration versus slant range for Teak and Orange.

TABLE 5.1 OVERPRESSURE MEASUREMENTS, SHOT TEAK

Station	Position	Ground Range	Slant Range	Gage Type	P <sub>1</sub>	P <sub>2</sub>	P <sub>4</sub>	Maximum
					Ground Level Overpressure	Incident Overpressure	Reflected Pressure	Negative Pressure
		ft	ft			psi	psi	psi
172.01	34-ft tower	4,258	252,036	Electronic-Statham	—	0.080	0.120	—
				Electronic-Statham	—	0.035	0.075	—
				VLP	—	—	0.085	0.035
				P <sub>t</sub>	—	—	0.100	0.051
172.01	Ground	4,258	252,036	Electronic-Statham	0.108	—	—	—
				Electronic-Statham	0.086	—	—	—
				VLP	0.122	—	—	0.030
				P <sub>t</sub>	0.110	—	—	—
172.02	34-ft tower	7,574	252,114	Electronic-Statham	—	0.062	0.084	—
				Electronic-Statham	—	—	—	—
				VLP	—	—	0.081	0.034
				P <sub>t</sub>	—	—	0.085	—
172.02	Ground	7,574	252,114	Electronic-Statham	—	—	—	—
				Electronic-Statham	—	—	—	—
				VLP	0.110	—	—	0.040
				P <sub>t</sub>	0.110	—	—	—
172.03	Ground	788	252,001	VLP	—	—	—	—
				P <sub>t</sub>	0.126	—	—	0.045
USS Lansing	Fantail	117,033	277,850	VLP	0.095	—	—	0.037
USS Boxer	Flight Deck	304,010	394,875	VLP	0.045	—	—	0.015
				VLP	0.060	—	—	0.020

TABLE 5.2 OVERPRESSURE MEASUREMENTS, SHOT ORANGE

Station	Position	Ground Range	Slant Range	Gage Type	P <sub>1</sub>	P <sub>2</sub>	P <sub>4</sub>	Maximum
					Ground Level Overpressure	Incident Overpressure	Reflected Pressure	Negative Pressure
		ft	ft			psi	psi	psi
172.01	34-ft tower	121,911	174,933	Electronic-Statham	—	0.084	0.180	—
				Electronic-Statham	—	0.110	0.210	—
				VLP	—	0.100	0.200	0.060
				P <sub>t</sub>	—	0.100	0.206	0.065
172.01	Ground	—	—	Electronic-Statham	0.200	—	—	—
				Electronic-Statham	0.190	—	—	—
				VLP	0.170	—	—	—
				P <sub>t</sub>	—	—	—	—
172.02	34-ft tower	128,167	179,200	Electronic-Statham	—	—	—	—
				Electronic-Statham	—	—	—	—
				VLP	—	—	0.183	—
				P <sub>t</sub>	—	0.105	0.205	0.080
172.02	Ground	—	—	Electronic-Statham	0.172	—	—	—
				Electronic-Statham	—	—	—	—
				VLP	0.170	—	—	0.060
				P <sub>t</sub>	0.210	—	—	0.080
172.03	Ground	123,849	176,319	P <sub>t</sub>	0.190	—	—	0.080
				P <sub>t</sub>	—	—	—	—
USS Lansing	Fantail	188,800	225,000	VLP	0.160	—	—	0.020
USS Boxer	Flight Deck	317,826	341,706	VLP	0.055	—	—	0.015

pressure-time history. The multiple reflections, indicated by the travel time of the wave, could conceivably redistribute the blast-wave energy and cause an increase in the positive-phase duration.

Figure 5.14 shows the surface-level overpressures at the slant-range distances for both shots. Each point is an average of the pressure at a station.

**5.2.7 Conclusions.** The pressure values measured at the surface and near-surface were considerably lower than were predicted for Shots Teak and Orange. Assuming a 3.8-Mt yield for

TABLE 5.3 TABULATION OF ARRIVAL TIMES AND POSITIVE-PHASE DURATIONS, SHOTS TEAK AND ORANGE

Station	Shot Teak			Shot Orange		
	Slant Range	Arrival Time	Positive-Phase Duration	Slant Range	Arrival Time	Positive-Phase Duration
	ft	sec	sec	ft	sec	sec
172.01	252,036	197	—	174,993	165.3	11.5
172.02	252,114	199	—	179,200	177.5	11.7
172.03	252,001	—	—	176,319	167.0	9.3
USS Lansing	277,850	250	13.9	225,000	208.0	10.0
USS Boxer	394,875	—	9.0+	341,706	419.6	25.0

both shots, the pressure measurements indicated a blast efficiency of only 10 to 15 percent at these altitudes in comparison to the standard efficiency of 45 to 50 percent for surface or near-surface detonations. These percentages, based on the modified Sachs scaling laws, indicate

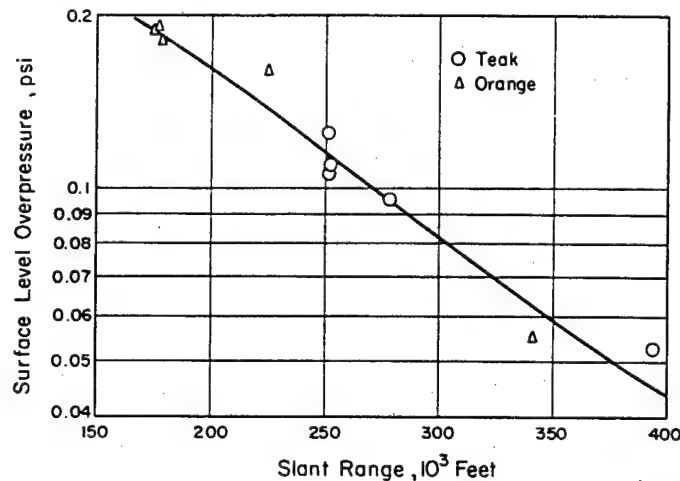


Figure 5.14 Surface level overpressures versus slant range for Teak and Orange.

quite a reduction in blast efficiency for high-altitude detonations. Lack of verified scaling procedures for these very-high altitudes preclude the possibility of drawing firm conclusions at this time.

### 5.3 NEUTRON FLUX FROM VERY-HIGH-ALTITUDE BURSTS

**5.3.1 Objectives.** The general purpose of Project 2.6 was to provide data on neutron flux (primarily 14-Mev neutrons) versus range from missile-borne megaton-range detonations at very-high altitudes. Instrumented pods were to be ejected from the missile during the thrust period; ejection times were planned to place the pods at preselected distances from the detonation. Specific objectives were as follows:

1. Data was sought from which a neutron spectrum could be constructed, i. e., the total flux, peak flux intensity, and rise time of the 14.2-Mev neutron group in Pods 2 and 3 (see Figures 5.15 and 5.16 for positioning information of all pods).
2. The integral of the prompt-gamma rays prior to 14.2-Mev-neutron arrival was to be measured in all pods.
3. Measurement of the gamma-ray flux versus time was required using multiple detectors with different sensitivity ratios for neutrons and gamma rays.
4. Gamma rays on a coarse time scale were sought and were to be measured by means of an integrator that provided a pulse rate proportional to the gamma-dose rate for a long time compared to the prompt-radiation interval.
5. The same type of measurement planned for Pods 2 and 3 was also planned for Pod 4. It was necessary, however, to provide for a different interpretation of the neutron flux versus time, since 14-Mev neutrons can be scattered into the detectors at times corresponding to the time-of-flight of lower energy neutrons. Plastic scintillator detectors were to be used to provide dose information in the period following the 14-Mev group arrival.

**5.3.2 Background.** Although only a small part of the energy of a megaton-range detonation appears as nuclear radiation, the low-atmospheric density at very-high altitudes permits both gamma rays and neutrons to penetrate great distances into the atmosphere. The effects of the 14.2-Mev neutron flux will be substantial at altitudes now accessible to manned aircraft. Although theoretical estimates have been made of these effects, it was necessary to make measurements to provide check points and to give confidence to the calculations.

The predictions and calculations of effects of a weapon detonated at high altitude had indicated that lethal ranges for radiation effects would be larger than those for shock and blast.

The neutron measurements during the HA shot were made with threshold and activation detectors. Film, glass, and chemical dosimeters measured gamma-ray dose. These detectors were recovered from parachute-borne canisters dropped by the delivery aircraft.

Shock and blast information during the HA shot was telemetered. There were indications that the ionization produced in the air by the nuclear and thermal radiation absorbed the telemetered signal from the closest canister for a substantial period.

During Operation Redwing, Project 6.6 produced a measurement of radio attenuation versus time at 1- $\mu$ sec resolution along a radial path chosen to give a convenient value of attenuation. The assumption that the peak attenuation is independent of electron removal rates (equivalent to a supposition that electron mean life is long compared to the alpha phase) made the calculation for station placement possible. The ionization cleanup was rapid and indicated a mean life for the electron of less than about 1.6  $\mu$ sec.

Project 2.7 was established during Operation Plumbbob to field-test detector and telemetered equipment and to seek parameters that would permit extrapolation of essentially sea-level attenuation data to high altitude. Using this data and the best available information from Los Alamos Scientific Laboratory (LASL), the calculation of the mean life of the electron at sea level gives



a value probably not greater than 50 shakes, nor less than 5 shakes. The mean life of the electron at 250,000-foot altitude (if one assumes an inverse scaling with density) is about  $2.7 \times 10^4$  times as large as the mean life at sea level. The attachment rate goes down with density; that is, the mean-life time at altitude is the reciprocal of the density ratio times the mean life at sea level.

Because the blackout period will exceed 1 msec for the most optimistic case and because the electron density cannot be predicted with confidence by theory, it becomes necessary to store information for a time longer than the pessimistic estimate of the blackout period. Data storage methods put strict limits on the band width of information that can be handled. Electronic and electromechanical delay lines do not provide sufficient delay.

Time-of-flight measurements can be interpreted and converted to neutron-energy spectrum data, if the characteristics of the device as a neutron source are known. During Operation Plumbbob, it was observed that the neutron sensitivity of gamma-ray fluors was sufficient to present the neutron spectrum riding on the tail of the prompt gamma-ray signal. This tail was produced by gamma rays from inelastic neutron scattering, neutron capture, and gamma-ray decay from the fission fragments. The gamma-ray level at a time after detonation (chosen long compared to the alpha phase, e. g., at 14-Mev neutron time of arrival) depended on the relative magnitude of contributions from the several processes. Fission fragment decay was considered negligible at the short times concerned. This consideration was equivalent to the assumption that there were no half lives shorter than milliseconds and that the  $1/t^{1/2}$  statistical decay approximated the gamma rays from fission fragment decay in this time regime. It was assumed that the gamma rays produced by neutron reactions in the bomb components appeared mostly in the prompt-gamma-ray pulse. This assumption was equivalent to the consideration that all the gamma rays came from neutron interactions and that no gamma rays were emitted in the fission process (particle emission competed effectively with gamma-ray emission if energetically possible). Many microseconds after the alpha phase, the gamma rays came predominantly from neutron interactions in the air. The gamma-ray contribution from this source should have decreased with the density so that during Shot Teak the level should have been about  $10^{-4}$  of the level observed during Operation Plumbbob. During Shot Orange it should have been about  $10^{-2}$  of this value. Since the Teak and Orange pods were to be at distances large compared to the ranges during Operation Plumbbob, the neutron time of arrival was later, and neutrons arrived at the detectors when the gamma-ray flux was down another two orders of magnitude, i. e.,  $10^{-4}$  to  $10^{-6}$ , of the level observed during Operation Plumbbob.

The long delay required by the blackout period necessitated the use of a memory unit. Considerations of weight and space economy resulted in the choice of a magnetic tape recorder to provide the delay. The intrinsic rise-time limitations of tape recorders and standard telemetry techniques placed a severe limitation on the information band width that could be handled. The use of subcarrier oscillators (i. e., an FM/FM system) permitted response from dc up to about 2,000 cycles. The high-frequency response requirements were derived from the rise time of the 14.2-Mev neutron-flux pulse at the detectors.

The energy distribution of the (d, t) neutrons had been calculated by LASL and NRL. On the basis of reaction temperature alone, it was shown that the 14-Mev neutron-energy-spectrum-half width was given by  $\Delta E = 5.59 \sqrt{kt}$ , where  $t$  is the absolute temperature and  $k$  is Boltzmann's constant. The energy dependence of the cross section of the (d, t) reaction was not considered in this development. However, it was a good approximation in the energy range of interest. A calculation of the half width in time at a station  $10^6$  cm (about 30,000 feet) away gave 16  $\mu$ sec for a  $kt$  value of 200 kev and an assumed Maxwell-Boltzmann distribution. The rise time was smaller, but comparable to this figure. Minimum rise time computed by other means was expected to be about 8 msec. Circuitry having an intrinsic rise time of 3  $\mu$ sec reproduced this rise time with only a small phase delay. The circuitry required a high-frequency cutoff at 100 kc or above.

The magnetic tape recorder design provided for this upper frequency limit.

**5.3.3 Method of Experimentation.** The Redstone missile launched from Johnston Island carried aloft the device and the instrumentation (in 3 pods for each shot and ejected ballistically at pre-determined ranges). Figures 5.15 and 5.16 show the planned positions of the missile and of the pods at time of burst. The error in actual position was expected to be within 10 percent, while postshot determination of position was expected to be within  $\pm 3$  percent. Table 5.4 (based on Figures 5.15 and 5.16) gives the values of predicted slant range and altitude for the missile and the pods. These values were derived from planned trajectory data furnished by ABMA.

Eleven pods were supplied, three for Shot Teak, three for Shot Orange, and five spares. Two

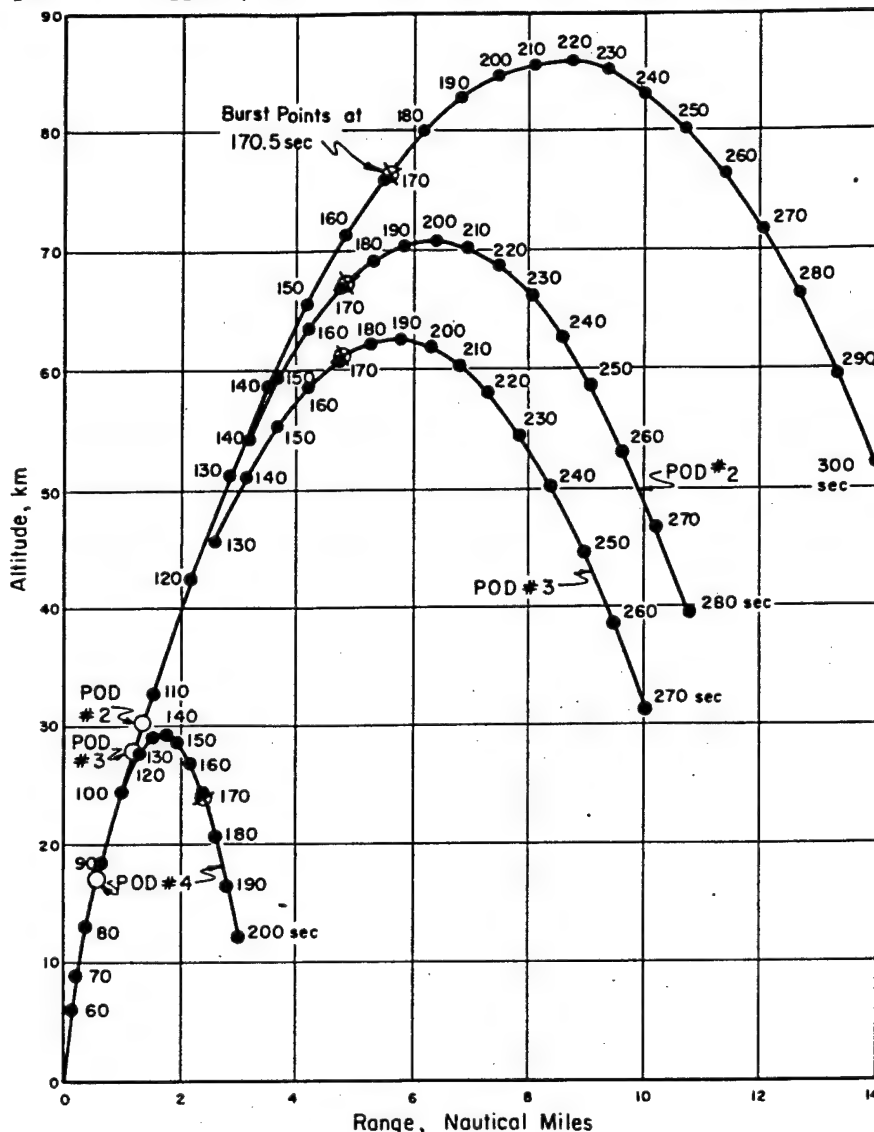


Figure 5.15 Missile and pod trajectories for Shot Teak.

of the latter were not completely instrumented, but were prepared so that they could be adapted for either far or near application by completion of instrumentation installation in the field. For both Shot Teak and Shot Orange, Pods 2 and 3 (referred to as near pods) were similar except for time constants. Pods 4 (far pods) had similar circuitry during both shots, but were used differently because of the interference by back-scattered neutrons and late-gamma rays from neutron interactions in the lower atmosphere.

239

The instrumentation in the pods consisted of detectors, tape recorders, commutator, telemetering transmitter, and electronic circuits to handle the signals. Mechanical commutation was required to transmit the eight channels of magnetic tape information in sequence. Electronic commutation was required in order to record the portions of the signal for which each detector was designed. The types of detectors and the measurements for which they were used follow: (1) plastic scintillators, fast-fusion neutrons; (2)  $\text{Li}^6\text{I}$  scintillators, slower fission neutrons;

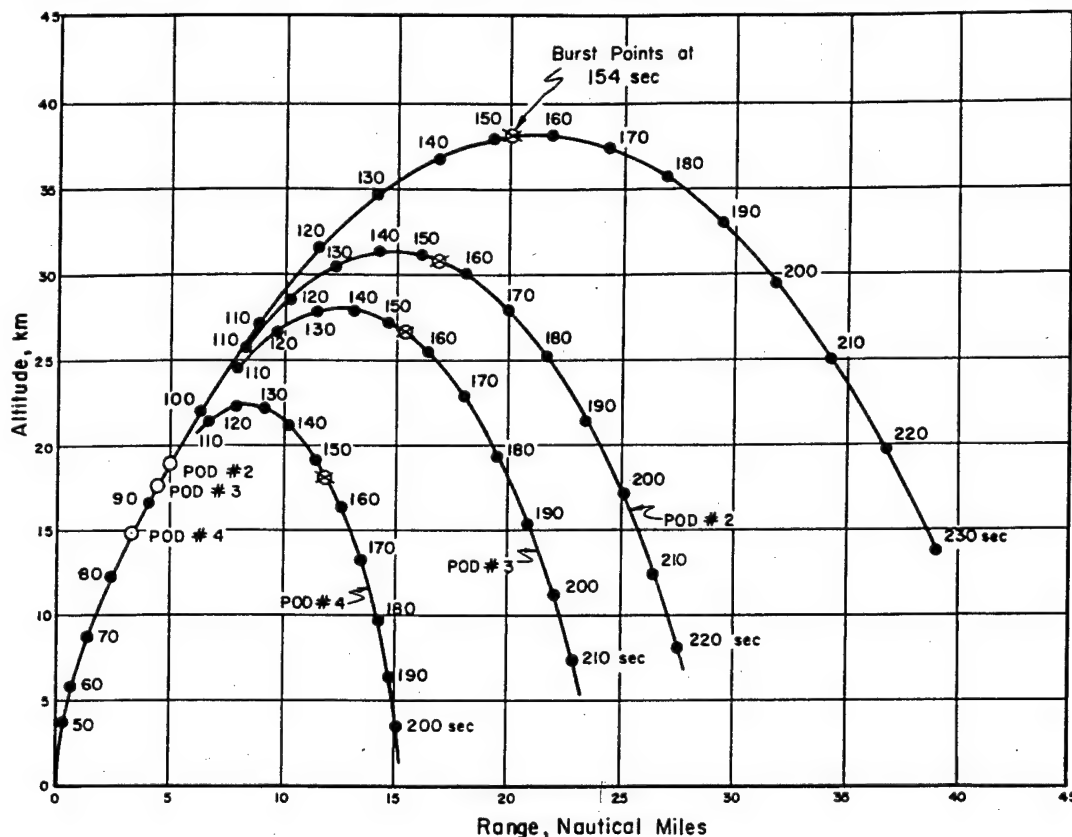


Figure 5.16 Missile and pod trajectories for Shot Orange.

(3) normal  $\text{LiI}$  scintillators of low-neutron sensitivity, background gamma rays; (4)  $\text{CsI}$  scintillators, prompt-gamma-ray integral; (5)  $\text{KBr}$ , integrated gamma-ray dose; and (6) nonscintillator blanks, any interfering effects (e. g., electromagnetic disturbances or gamma-ray influences) on the photodiodes themselves.

The detector outputs were electronically encoded, commutated, and recorded on a magnetic-tape recorder. The latter was programmed to record for 120 msec after the prompt-gamma-ray pulse and to switch repeatedly to a playback condition to telemeter the recorded information. The recorder output contained on its eight tracks: (1) FM subcarrier (VCO) calibration, (2) FM subcarrier (VCO) information, (3) current pulse-controlled oscillator (PCO) information, and (4) direct records of signal currents. The recorder output frequency modulated the transmitter. A real-time PCO was used as an integrator to measure the long-term-dose accumulation. This signal, in turn, amplitude-modulated the transmitter. A telemetry station in the missile-control bunker received and recorded the signals from the pods.

5.3.4 Reliability of Data. The inclusion of the far pod positions complicated the instrumentation, because atmospheric scattering of neutrons made time-of-flight analysis meaningless. Thus, data requirements fall into two groups: (a) those resulting from the original proposal for near stations, Pods 2 and 3, and (b) those for the far stations, Pods 4. For the former, the objective re-

TABLE 5.4 TRAJECTORY DATA

Shot	Horizontal Range	Altitude		Slant Range	Slant Range
	from Launch Point	km	ft	to Burst	to Burst
	naut mi	km	ft	km	ft
Teak					
Missile	5.52	76.36	250,525	—	—
Pod 2	4.78	66.98	219,750	9.48	31,100
Pod 3	4.74	60.93	199,900	15.50	50,850
Pod 4	2.40	24.08	79,000	52.62	172,640
Orange					
Missile	20.30	38.26	125,525	—	—
Pod 2	16.88	30.97	101,607	9.69	31,790
Pod 3	15.41	26.69	87,560	14.71	48,260
Pod 4	11.92	18.12	59,450	25.46	83,530

mained to measure the neutron-energy spectrum by time-of-flight measurement. The difficulties to overcome involved sensitivities and dynamic range of the instruments. The prompt-gamma-ray signal swamped all detectors, except the one designed to integrate the prompt-gamma rays. The sensitivities were set to provide a signal above the middle of the range in order to give reading accuracy. This requirement made it imperative that good estimates of expected fluxes be formulated, or that the number of channels be multiplied by three or four, or that some compression system be used. The number of channels required to provide adequate dynamic range was too large for the pod volume. Compression of the signal was obtained by use of a logarithmic load on the detectors. Rather precise estimates of expected signal were still required in order to use the system in its best range. The logarithmic load resistor (Log R) set 15 percent as the probable error in the interpretation of detector currents. The calibration of detectors contained about the same uncertainty. The absorption and scattering of neutrons in the associated apparatus gave an uncertainty of about 10 percent. The indecision in the location of the pods gave about a 10 percent uncertainty in the energy assignment to the time axis. Thus, the spectrum data had a 25 percent probable error in amplitude with a  $\pm 10$  percent error in energy assignment. The probable error in the measurement of integrated gamma-ray dose was about  $\pm 25$  percent, and because of inherent difficulties in the calibration of the integrating process it depended on detector calibrations in the same way as the neutron-flux measurements. The far pods were subject to such uncertainties in the relation between time of arrival and neutron energy that no plans were made for time-of-flight analysis of the whole spectrum. Since the time of arrival for most of the 14-Mev group was free from scattered neutrons, this group could be measured and analyzed. For later arrivals, only measurements equivalent to dose were made because high-energy neutrons that were scattered reached the detectors late and simultaneously with lower energy neutrons. Data from the far pods had a probable error of about  $\pm 50$  percent for all quantities measured.

5.3.5 Results. During Shot Teak the missile did not program as planned. Consequently, the slant ranges from burst point to the pods were different from those predicted (see Table 5.5).

The internal time sequence in the pods was designed for the predicted values  $\pm 10$  percent. The changes in slant ranges for Shot Teak Pods 3 and 4 were easily accommodated, but the variation for Pod 2 brought the 14.2-Mev neutron arrival time near the front end of the pedestal, and analysis of data from Pod 2 was complicated by this range discrepancy.

During Shot Orange the missile programmed properly, but did not show the design acceleration. As a consequence, the pods were ejected at slightly later times than those planned. How-

TABLE 5.5 PREDICTED AND ESTIMATED ACTUAL SLANT RANGES TO PODS

Pod	Slant Range	Slant Range, Actual
	Predicted	(Estimate of ABMA)
	km	km
Teak 2	9.48 $\pm$ 0.9	8.25 $\pm$ 0.3
Teak 3	15.50 $\pm$ 1.5	14.35 $\pm$ 0.3
Teak 4	52.62 $\pm$ 5	50.15 $\pm$ 0.3

ever, the slant ranges were within the range accommodated by the internal programming of the pods.

Table 5.6 gives the preliminary estimate of channel performance. The symbols in the columns have the following meaning:

DA = data analyzed (preliminary treatment)

D = data collected

NA = not analyzed, data uncertain

F = channel failed

Since only the most rudimentary facilities for data reduction could be brought to the field, those data channels in which the data resisted reduction were not analyzed. The RDB subcarrier (VCO)

TABLE 5.6 PRELIMINARY ESTIMATES OF POD PERFORMANCES

DA, data analyzed (preliminary treatment); D, data collected; NA, not analyzed, data uncertain; F, channel failed.

Pod Number	1 Csl		2A Pilot-B		2B Pilot-B	3 Li <sup>3</sup>		3 Pilot-B (6)	4 Li <sup>1</sup>	4 Pilot-B (1)	5 Blank
	Integral Timing		14.2-Mev Neutrons	Time History		14.2-Mev Neutrons	Time History				
Teak 2	NA	DA	NA	DA	NA	NA	DA	—	DA	—	DA
Teak 3	NA	DA	D	DA	NA	NA	DA	—	DA	—	DA
Teak 4	NA	DA	—	—	NA	—	—	DA	—	DA	DA
Orange 2	NA	DA	D	DA	NA	NA	DA	—	DA	—	DA
Orange 3	NA	F	F	F	F	F	F	—	F	—	F
Orange 4	NA	DA	D	DA	NA	—	—	DA	—	DA	DA

channels were susceptible to noise interference and interchannel cross talk. It was necessary to play these channels back many times, through carefully adjusted discriminators, in order to extract the data from the magnetic-tape records. The field-data extraction and reduction was delayed until more refined techniques could be applied at NRL.

Data were extracted from some of the PCO channels by direct methods. The magnetic-tape record was played back at its lowest speed and the recording oscillograph was run at its highest paper speed. These PCO data were then presented as a train of pulses on a time scale. The information desired, the PCO pulse repetition rates versus time, were obtained by counting pulses.

Data on the 14.2-Mev neutron flux appeared during the pedestal period and were to be found in

the PCO tape track. The time scale involved for the 14.2-Mev group was short compared to the time scale for the PCO record. The pedestal was not resolved for Pods 2 at either shot because both the oscillograph paper and galvanometer response speeds were too small. In Pods 3 and 4 the same difficulty occurred, but to a lesser degree. The analysis of the 14.2-Mev data required oscilloscope-camera methods and film processing facilities not available in the field.

Figure 5.17 is a composite of the gamma-ray dose of Shot Teak Pod 3C. The data were derived from the calibrated blank, the LiI, and Pilot B detectors. The ordinate is  $r/\mu\text{sec}$  and the abscissa is time in msec.

Figure 5.18 is the neutron-flux data taken from the  $\text{Li}^6\text{I}$  detector in Shot Teak Pod 3. Cor-

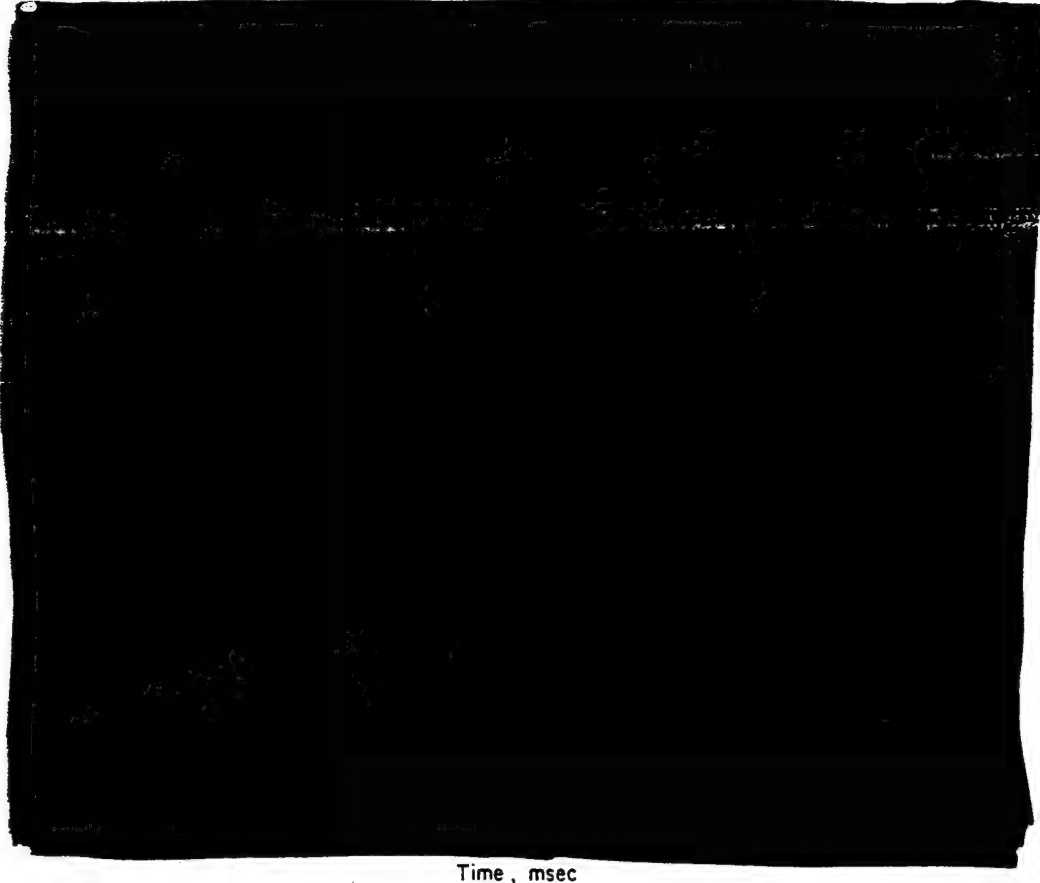


Figure 5.17 Pod 3C dose rate, Shot Teak.

rections for gamma sensitivity have been made.

Figure 5.19 is a composite of the data on gamma rays versus time in Shot Orange Pod 2 taken from the LiI, blank, and Pilot B detectors.

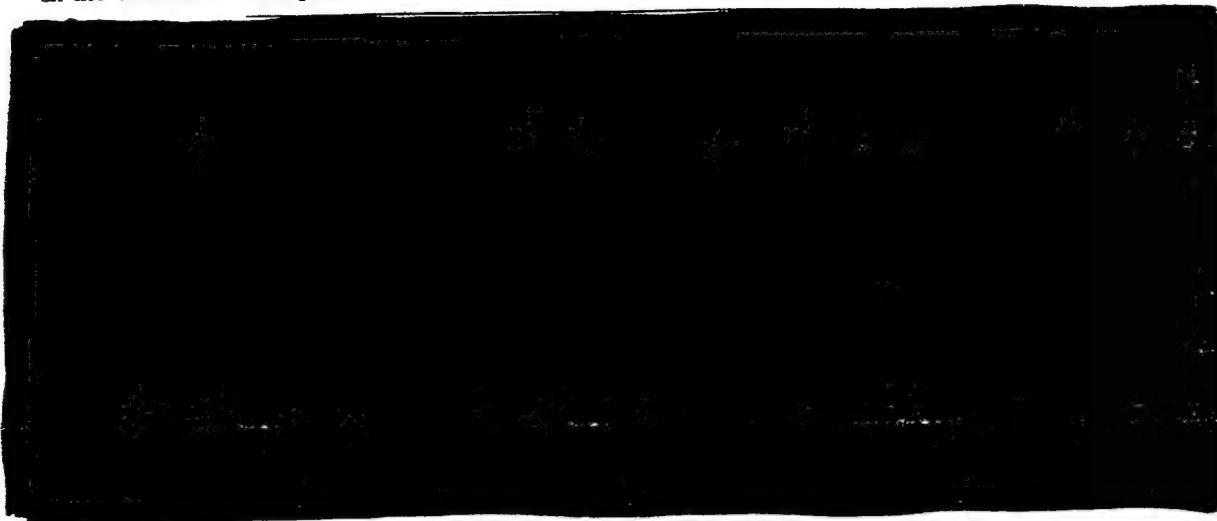
Figure 5.20 gives the neutron-flux data derived from the corrected detector currents from the  $\text{Li}^6\text{I}$  detector of Shot Orange Pod 2.

Figure 5.21 is the total dose versus time data derived from the Pilot B detectors in Shot Orange Pod 4.

The attenuation data observed are tabulated in Table 5.7. The blackout time given is the

time from burst to the time that the signal first recovers to a 10-decibel signal-to-noise ratio. Pod positions are based on preliminary trajectory information.

5.3.6 Summary. The data presented under Results represent only a portion of that available in the records. Two pods at each shot yielded relatively good data. Shot Teak Pods 3 and 4



Neutron Energy, Mev

Figure 5.18 Pod 3 neutron flux 14.35 km, Shot Teak.

yielded information that could be analyzed in the field; only the Pod 3 data were graphed. The Pod 4 data departed from expected detector currents in an inconsistent way. It was suspected that either a personnel coding error was made during pod calibration, or a circuit failure in the pod during flight confused the detector currents. In any event, the Pod 4 dose-rate data was inconsistent and was not included. Shot Teak Pod 2 gave signals and seemed to operate, but fur-

TABLE 5.7 ATTENUATION DATA

ther laboratory analysis of the data will be required to explain the observed detector currents. At first glance, it appeared that there was a partial failure in the complete system. Shot Orange Pod 3 apparently failed to follow its internal-timing sequence. The signal showed that all channels operated, but did not send detector signals. The Shot Orange Pods 2 and 4 operated and provided analyzable PCO information.

The gamma-ray dose rate (Figure 5.17) was measured during the period in which gamma rays from inelastic reactions of neutrons with the air and the weapon case were expected to interfere with the neutron measurements. The gamma-ray fluxes represented were large. They were in the expected range, however; all the gamma-ray detectors in the pod yielded the same results. The gamma-ray correction applied to the neutron detectors was less than half the total detector current in the range reported.

The neutron-flux data (Figure 5.18)



[REDACTED]

The gamma-ray dose rate (Figure 5.19) showed the expected shape for the time interval 1 to 10 msec. The ratio of intensity between Pod 2 at Shot Orange and Pod 3 at Shot Teak was in the right range, i. e.,  $(5/3)^2 \approx 3$ .

The neutron-flux data (Figure 5.20) also showed the humps. [REDACTED]

[REDACTED]

In Pods 4 for both shots, the data available by preliminary analysis consisted of dose informa-



Figure 5.21 Pod 4 dose rate, Shot Orange.

tion in the period out to 10 msec. For Shot Orange Pod 4 the gamma-ray-dose rate at 5 msec was about  $1/100$  of the rate at Shot Orange Pod 2. This ratio was made up of two factors, the inverse square (about  $1/10$ ) and the exponential absorption (about  $1/10$ ).

5.3.7 Conclusions and Recommendations. The objectives were accomplished insofar as the data could be reduced in the field.

Gamma-ray measurements were consistent from pod to pod. The neutron fluxes were approximately as calculated, but were a little low at some stations, as judged by the relation of the observed detector currents to those expected. [REDACTED]



[REDACTED]

The use of instrumentation riding along with the weapon vehicle presented distinct advantages over independently placed instrumentation, since part of any error in placement of the weapon cancels out for the pods. The cleanness of high-altitude detonations and the possibility of strong military requirements for high-altitude deployment of weapons lead to the recommendation that instrumentation for time-resolved measurements of nuclear radiation at high altitude be developed further.

#### 5.4 CHORIORETINAL BURN STUDIES

5.4.1 Objective. The primary objective of Project 4.1 (Effects on Eyes from Exposure to Very-High-Altitude Bursts) was to determine the extent of chorioretinal damage caused by exposure to a high-altitude, high-yield nuclear detonation and to relate experimental results to theory and laboratory calculations.

5.4.2 Background. For many years the clinical phenomenon of retinal damage caused by the radiant energy of the sun has been known and numerous cases have been documented. Most of these cases have occurred when humans watched solar eclipses without eye protection, and thus this type of retinal lesion has become known as eclipse blindness. Since the fireball of a nuclear detonation attains temperatures comparable to that of the sun, the predicted thermal-energy release is of sufficient magnitude to cause concern about retinal damage in humans who view nuclear detonations without proper protection. Hence, a series of studies was begun to evaluate this hazard.

During Operation Upshot-Knothole (1953), chorioretinal burns were produced in the eyes of rabbits at distances up to 42.5 miles from ground zero. At this operation also, in four instances, retinal burns were accidentally produced in humans at two to ten miles distance. The burns resulted in permanent scotomata in these individuals. During Operation Redwing (1956), chorioretinal burns were produced in the eyes of rabbits and small primates at distances of 2.7 to 8.1 nautical miles. Some of these burns were produced even though the eye was protected by filters.

The lesions in the above experiments, as well as those produced in eclipse blindness, resulted from the same spectral components of electromagnetic radiation, mainly, the visible portion and infrared. In general, the differences in degrees of retinal damage resulted from variance of the rate of energy delivery per unit area. Since eclipse blindness is sustained through a markedly contracted pupil, which limits the amount of radiant energy delivered to the retina, this damage can occur only through protracted exposure. Other factors of importance are the low rate of delivery of the radiant energy from the sun and the ability of the retina to dissipate the heat by conduction. In cases of nuclear detonations, however, a large portion of the thermal energy may be delivered to the retina before the protective-blink reflex becomes operative. In addition, this exposure may occur at night when the pupil admits approximately 10 times the energy that a contracted pupil does in the same time interval. This is a function of relative pupillary areas.

During Operation Redwing, animals exposed to megaton-yield detonations at sites where the total thermal radiation was of the order of 0.8 to 1.0 cal/cm<sup>2</sup> did not receive chorioretinal burns; whereas animals exposed to detonations of much lower yield (therefore, higher rate of energy delivery), at sites where the total thermal radiation was as low as 0.13 cal/cm<sup>2</sup>, did receive burns.

**5.4.3 Theory.** The optical system of the eye acts as a focusing device which results in an image, on the retina, of the fireball of a nuclear detonation. Because of this focusing effect, the intensity of thermal radiation on the retina is much greater than the intensity incident upon the eye. Theoretically, neglecting attenuation by air and other media, the thermal-intensity incident upon the eye will be inversely proportional to the square of the distance from the fireball. The area of the fireball image on the retina, however, is also inversely proportional to the square of the distance to the fireball. This results in an intensity of thermal radiation on the retina which is independent of the distance from the fireball. The inference, then, is that if a fireball is capable of producing chorioretinal damage, it is capable of producing chorioretinal damage at great distances. The only difference caused by increasing the distance is that the burn will cover a smaller area. That this is not true is due primarily to the attenuation by intervening media (air, water vapor, dust, etc.).

There is, however, another factor which must be considered, and that is the chorioretinal damage produced is dependent on the rate of delivery of energy as well as total energy delivered. If the rate of delivery of the energy to the retina is below the rate at which the energy can be dis-

TABLE 5.8 POSITIONING OF RABBITS AND THERMAL RECORDING DEVICES FOR SHOTS TEAK AND ORANGE

Teak	Shot		Horizontal Distance from Ground Zero naut mi	Slant Range from Burst naut mi	Angle of Elevation deg	Azimuth from Johnston Island deg True	Altitude of Station	Number of Animals Exposed
	Orange							
Johnston Island	—		0	41	83	0	Surface	5
—	USS Boxer		70	73	15	030	Surface	8
USS DeHaven	—		75	79	28	020	Surface	11
—	USS Epperson		85	88	10	020	Surface	8
—	USS DeHaven		140	141	7	020	Surface	8
USS Cogswell	—		150	155	15	020	Surface	12
USS Hitchiti	—		305	307	5	060	Surface	12
B-36 (Bigamy)	—		70	79	27	060	31,000 ft	4
B-36 (Goldenrod)	—		70	79	27	060	30,000 ft	4
C-97 (Excelsior)	—		305	307	5	060	15,000 ft	8
—	C-97 (Excelsior)		225	226	3	060	15,000 ft	8
Total								88

sipated by the retina, then there will be no damage. In addition, the total time of exposure must be considered. The normal blink reflex of about 300 msec in rabbits and 50 to 150 msec in man will limit exposure to that period of time. Only that radiation received before the blink reflex becomes operative, rather than the total thermal radiation, is of importance in causing chorioretinal damage.

Reduced attenuation, higher irradiance, and higher total thermal output during the first few msec can result in chorioretinal damage from a high-altitude burst at distances and for yields which would present no problem for surface or low-altitude bursts.

**5.4.4 Procedure.** The experimental plan required positioning of rabbits and thermal recording devices operated by Project 8.1 at exposure stations both on the surface of the earth and in the air at various distances from the burst (Table 5.8). Animals were secured with one eye exposed to the burst, and photographs, using GSAP cameras, taken to assure that the eye was open at shot time (Tables 5.9, 5.10, 5.11, 5.12). A photograph also was taken at shot time at each station to determine cloud cover.

Following exposure, each rabbit received an ophthalmoscopic examination, the retina was photographed, and selected animals were sacrificed and their eyes enucleated and preserved for further gross and microscopic pathologic study at the School of Aviation Medicine, USAF. Additional rabbits were returned to the School of Aviation Medicine for long-term follow-up.

5.4.5 Instrumentation. Specially designed holding boxes were used so that the head of the animal would be immobilized for exposure and photography. For the ground- and ship-exposure

TABLE 5.9 CLOUD COVER, SHOT TEAK

Station	Degree of Cloud Cover	Line of Sight to Detonation
Johnston Island	Clear	Unobstructed
DD DeHaven	Strato-cumulus	Unobstructed
DD Cogswell	Strato-cumulus	Unobstructed
USS Hitchiti	Strato-cumulus	Obstructed
B-36, No. 1	Clear	Unobstructed
B-36, No. 2	Clear	Unobstructed
C-97	Clear	Unobstructed

stations, wooden "A" frames with racks were constructed. These frames could be positioned either upright or horizontally to correct for different angles of incidence. Racks, which accommodated four rabbits, were designed to fit the radio compartment blisters of the two B-36's.

Sixty-four pigmented rabbits of both sexes, weighing between 4 1/2 and 7 1/2 pounds, were se-

TABLE 5.10 CONDITION OF RABBITS' EYES AT EXPOSURE TIME, SHOT TEAK

Number of Animals	Station	Condition of Eye
5	Johnston Island	Open
11	DD DeHaven	Open
12	DD Cogswell	Open
12	USS Hitchiti	Open
4	B-36, No. 1	Open
4	B-36, No. 2	Open
8	C-97	Open

lected for study. Each animal was numbered by tattoo, and the right ear marked for ease of identification. Each animal was baselined with ophthalmoscopy, and retinal photographs obtained with the Zeiss-Contax retinal camera.

After Shot Teak, all exposed rabbits were returned to Johnston Island or Hickam AFB where the exposed eyes were examined.

In addition, postexposure-retinal photographs were taken, using atropine sulfate, 1/2-percent solution, for pupillary dilatation. Sedation, when necessary, was accomplished with sodium pentathol or thiorazine.

After Shot Orange, these procedures were re-accomplished on the contralateral eye and selected animals were sacrificed, and the eyeballs enucleated.

5.4.6 Results and Conclusions. The very-high-altitude nuclear explosion is particularly effective in producing chorioretinal burns because of the rapid rate at which the essentially single-phase power pulse delivers thermal energy, and the relatively low atmospheric attenuation encountered. A 3.8-Mt detonation at 250,000 feet (Shot Teak) delivers approximately 90 percent of its thermal component during the first 100 msec of the explosion. Consequently, with a blink-reflex time of 250 to 350 msec for the rabbit and 100 to 150 msec for man, all of the radiant

TABLE 5.11 CLOUD COVER, SHOT ORANGE

Station	Degree of Cloud Cover	Line of Sight to Detonation
USS Boxer	Strato-cumulus	Obstructed
DDE Epperson	Strato-cumulus	Unobstructed
DD DeHaven	Strato-cumulus	Obstructed
C-97	Clear	Unobstructed

dosage from a very-high-altitude burst is received by the retina before the eye can be protected by blinking. This is in contrast to low-altitude detonations of the same size where the power pulse is markedly biphasic and comparatively much slower in its over-all delivery of its thermal component.

Minimal chorioretinal burns (0.1 mm or less in diameter) can be produced on the surface at distances closely approaching 300 naut mi from relative ground zero from a 3.8-Mt nuclear det-

TABLE 5.12 CONDITION OF RABBITS' EYES AT EXPOSURE TIME, SHOT ORANGE

Number of Animals	Station	Condition of Eye
8	USS Boxer	Open
8	DDE Epperson	Open
8	DD DeHaven	Open
8	C-97	Open

onation at 250,000-foot altitude. Comparable lesions would be experienced at somewhat greater distances where the exposure position is at altitude and subject to less atmospheric attenuation. For a 3.8-Mt weapon detonated at 125,000 feet (Shot Orange), the critical surface distance for the production of minimal lesions more nearly approaches 225 naut mi, with correspondingly greater distances at altitude.

Chorioretinal lesions were produced in all animals at all of the stations with line-of-sight transmission. Calculated and measured radiant dosages were correlated on Shot Teak, but cloud cover precluded this possibility on Shot Orange. The information from Shot Teak, however, was most useful in predicting the occurrence of lesions for stations that did have line-of-sight transmission on Shot Orange. The physical data obtained with appropriate scaling factors permitted the determination of reasonable exclusion radii for various yield weapons at various altitudes.

The lesions received at all exposure stations within 160 naut mi were of sufficient size and severity to result in permanent retinal damage with severe loss in visual acuity, i. e., 20/200 providing the lesion had occurred on the macula of the human (Table 5.13). For burns (which

involve the rods and cones immediately beneath and adjacent to the lesion) produced at other positions on the retina, the visual loss would be a scotoma and/or a segmented visual field defect.

Minimal lesions of variable severity were encountered at the most distant air stations. Although assessment at this time is premature, it appears that at least several of these lesions eventually may regress to insignificance. Irreversible lesions, because of their small size, would result in visual impairment in man only if the burn included the macula. During the period of inflammation, transient loss of visual acuity could vary from 20/40 to 20/200, depending upon the position of the injury.

Burn diameter consistently correlated with distance from relative ground zero, i. e., progressively smaller lesions were encountered at increasing distance from the burst. Typical burns

TABLE 5.13 ESTIMATED THERMAL INTENSITIES AT VARIOUS EXPOSURE STATIONS

Station	Horizontal Distance from Ground Zero	Slant Range from Burst Point	Estimated Thermal Intensity at Station	Diameter of Retinal Image	Estimated Thermal Energy at Retina
	naut mi	naut mi	cal/cm <sup>2</sup>	mm	cal/cm <sup>2</sup>
<b>Shot Teak</b>					
Johnston Island	0	41	1.2	0.98	28
DD DeHaven	75	79	0.23	0.64	23
DD Cogswell	150	155	0.05	0.35	17
USS Hitchiti	305	307	0.005	0.19	7
B-36, No. 1	70	79	0.35	0.72	31
B-36, No. 2	70	79	0.35	0.72	31
C-97	305	307	0.016	0.19	19*
<b>Shot Orange</b>					
USS Boxer	70	73	0.25	0.42	56
Destroyer 1	85	88	0.15	0.36	50
Destroyer 2	140	141	0.035	0.23	31
C-97	225	226	0.011	0.14	46*

\* Assumes 85 pct transmission through aircraft plexiglass windows.

were round to oval in shape, generally pearl-gray or blanched in color, and frequently characterized by hemorrhagic centers. Lesions were elevated and often circumscribed by an orange halo concentric with a blanched zone terminating in a yellow periphery. Postirradiation follow-up will include sequential ophthalmoscopic examination, retinal photography, and histopathology.

No double or dumbbell-shaped lesions were observed. These burns are normally associated with movement of the eye during exposure where thermal delivery is sufficiently protracted, as in the case of high-yield weapons detonated at sea level or low altitude. The absence of this type of lesion in the present case attests to the extremely high rate of thermal energy of the very-high-altitude explosion.

## 5.5 ELECTROMAGNETIC ATTENUATION STUDIES

**5.5.1 Background.** The lack of knowledge of the effects and the effectiveness of nuclear detonations occurring at high altitudes, prior to Operation Hardtack, gave rise to urgent service requirements to obtain information.

The electromagnetic-effects program was designed to determine the effects of very-high-altitude bursts on electronic systems in order to ascertain possible defenses against ballistic missiles. In particular, it was desired to obtain information needed to determine the performance of missile-guidance systems, missile-detection systems and communication links. Also, any observations useful in detecting foreign high-altitude shots were desired.

**5.5.2 Objectives.** Specific objectives in this program were: (1) to investigate the nature of radar echoes from the fireball produced by very-high-altitude nuclear detonations; (2) to investigate the ionization and associated effects created in the high atmosphere by a very-high-altitude nuclear detonation; (3) to determine the effects of very-high-altitude nuclear detonations on pulsed electromagnetic transmission in the S and L bands; (4) to obtain attenuation of electromagnetic energy passing through the ionized cloud at 450 Mc; and (5) to obtain qualitative data through radarscope photography of the reflection coefficient of the cloud at 425, 675, and 9,375 Mc.

**5.5.3 Experimental Plan.** To accomplish these objectives, observations of the following effects were made:

1. Attenuation of radio frequency signals. Two distinct types of attenuation measurements were made: (a) measurement of attenuation over a known path for frequencies of 240 and 450 Mc and (b) measurement of total ionospheric absorption. The first measurement was made with the propagation paths shown in Figure 5.22. These paths were all in the vicinity of the burst. Total ionospheric absorption was measured by monitoring the cosmic noise background. Measurements

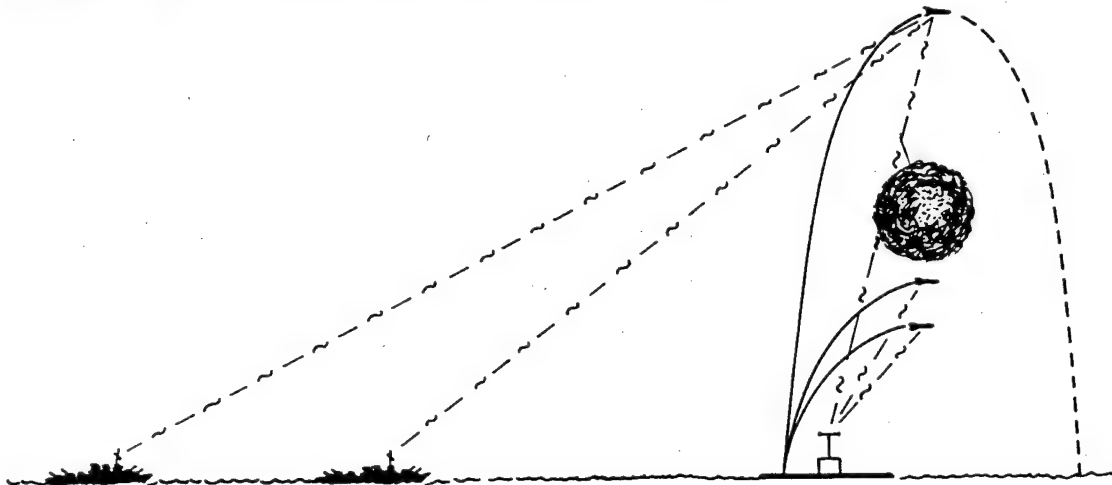


Figure 5.22 Array for ionospheric absorption measurements.

at 30, 60, and 120 Mc were made with stations located at Johnston Island and at distances of 500 and 715 naut mi.

2. Radar reflections (or echoes). Studies of radar reflections were made over a frequency range of 11 to 10,000 Mc using a variety of service equipments and specially constructed sets. Figure 5.23 shows the general placement of these various types of instruments.

3. Noise emission. The presence of any noise was expected to be seen on most of the equipment already planned for use in the 10-to-1,000-Mc frequency range. Additional instruments were provided to especially look for noise at the frequencies 32, 113, 10,000, and 35,000 Mc.

4. Ionospheric conditions and related communication disturbances. Ionospheric conditions were monitored, using ionospheric recorders, which looked at reflected pulses in the frequency range 1 to 25 Mc. One station was located at Johnston Island and a second station was placed in a C-97 aircraft whose mobility was to be used to determine the extent of the ionospheric effects. To supplement the usual subjective observations of existing communication links, special monitoring receivers were located at Johnston and Oahu. The Johnston Island receivers monitored transmissions from Oahu on 9, 15, and 20 Mc, and the Oahu receivers monitored transmissions from Kwajalein, Christmas Island, and Guam on 17, 19, and 22 Mc, respectively. Receivers on the C-97 aircraft monitored the three Oahu frequencies.

5.5.4 Results. Shot Teak. The immediate effect of Shot Teak was

The boundaries of these regions were not determined.

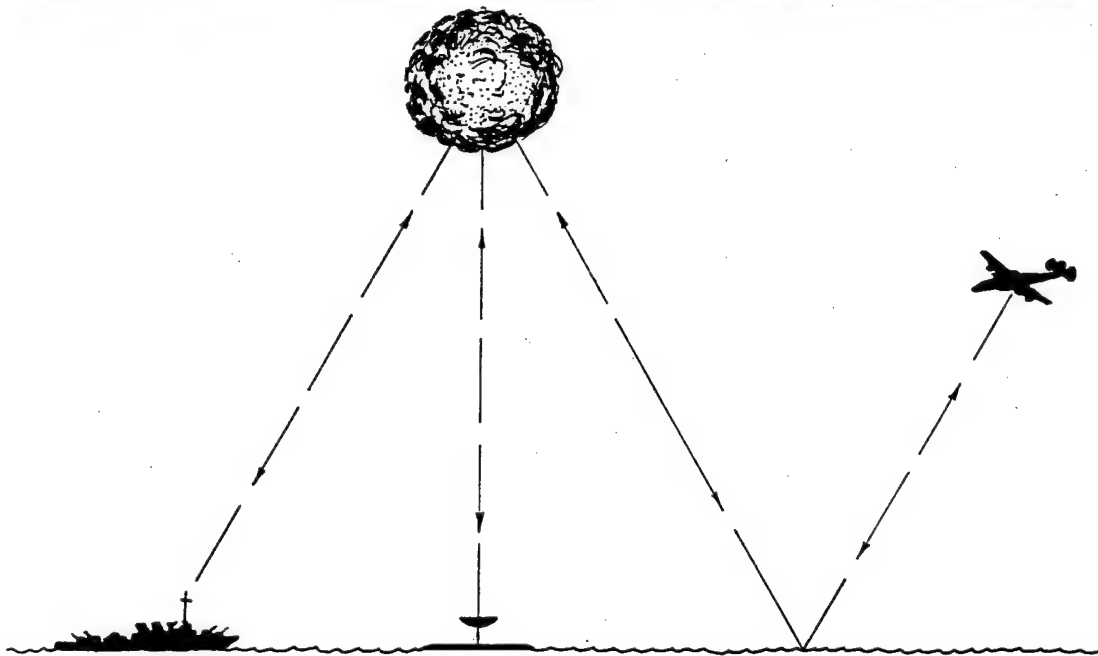
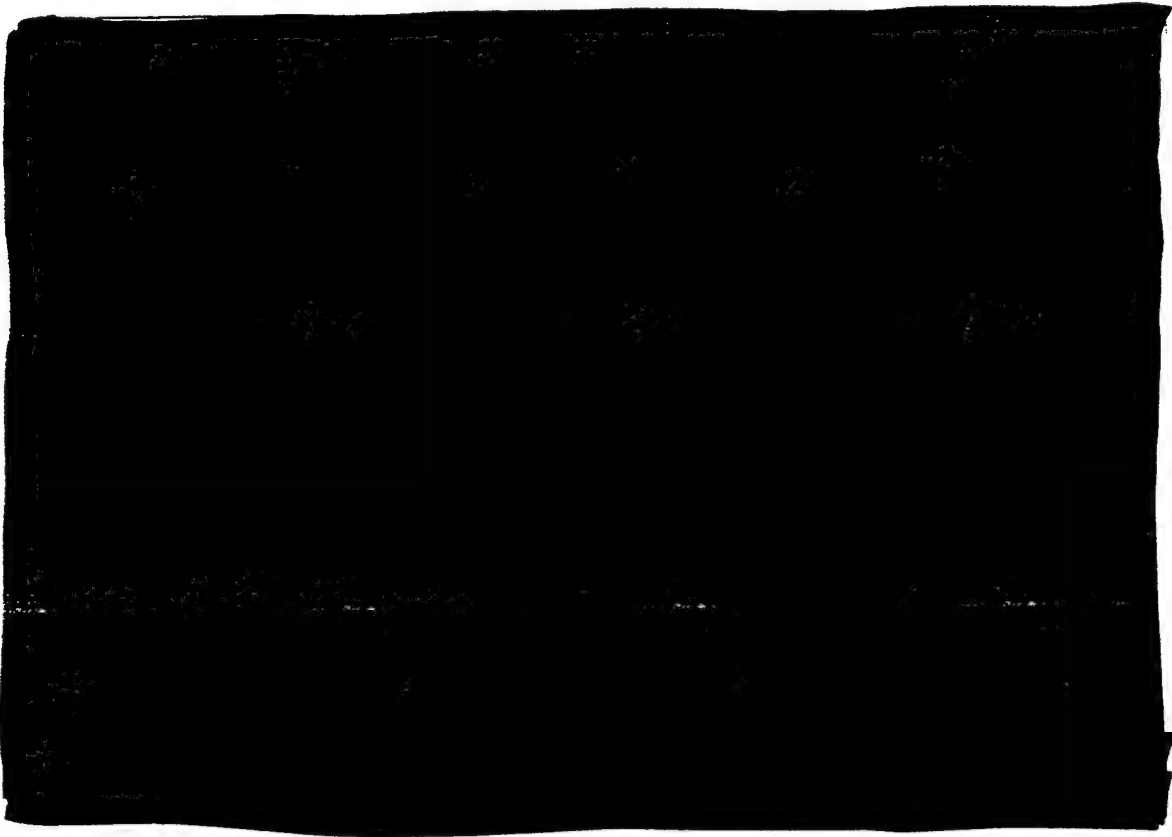


Figure 5.23 Array for radar reflection measurements.



Time

Figure 5.24 Typical communication circuit input versus time records.

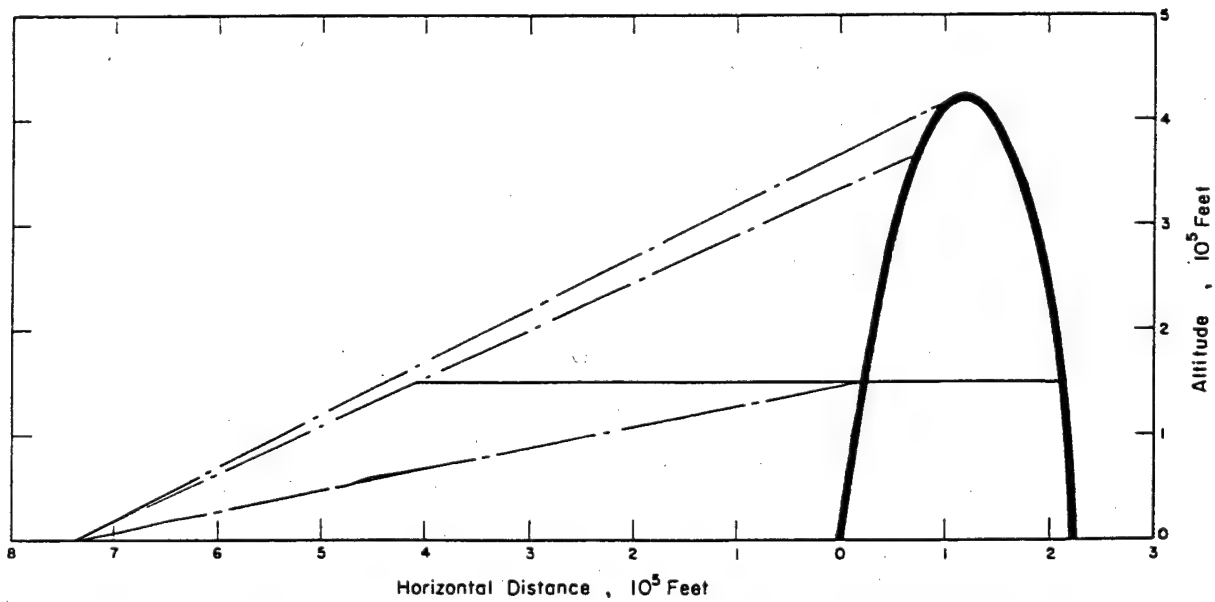
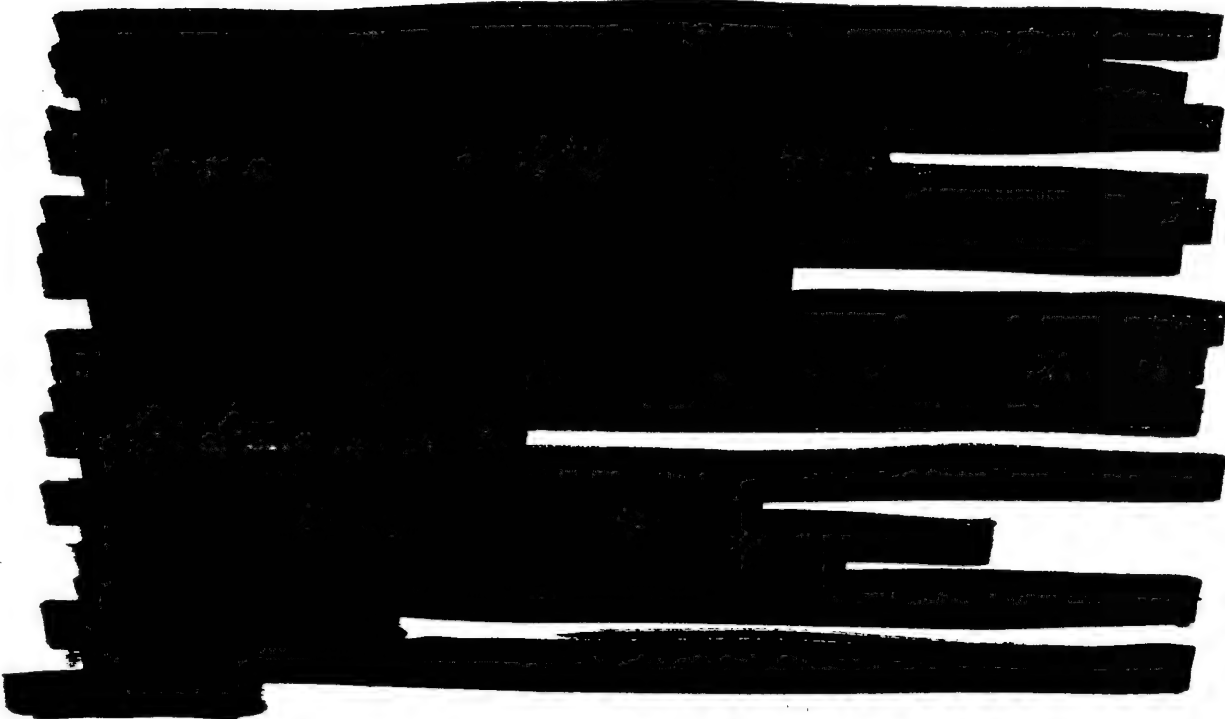


Figure 5.25 Typical rocket trajectory for determining Shot Orange attenuation region.







## 5.6 THERMAL RADIATION MEASUREMENTS

5.6.1 Introduction. The projects which made thermal measurements on Shots Teak and Orange were the same as those which participated on Shot Yucca and are described in Section 4.4. The aircraft-borne instrumentation of Projects 8.2, 8.3, 8.4, and 8.5 was essentially unchanged. The instrumentation measured three general aspects of the thermal phenomena: irradiance, both total and in broad spectral bands between 2,000 Å and 120,000 Å; spectral distribution of the bomb light; and the size of the visible and infrared fireball. The positions of the aircraft, relative to the Teak and Orange bursts, are shown in Table 5.14.

5.6.2 Background. Thermal-radiation characteristics of nuclear devices have been the subject of extensive studies in the past, and it is felt that most aspects of thermal phenomena are reasonably well understood. Two previous shots (Teapot 10 and Hardtack Yucca) have provided some information about the effect of altitude on various phenomena. It was generally agreed that the phenomena produced by Shots Teak and Orange would be different by orders of magnitude, but there was considerable uncertainty as to what the magnitudes would be. In order to understand the significance of the measurements made on Shots Teak and Orange, it will be useful to describe the thermal history of a sea-level burst.

1. The first observable effect of a nuclear detonation appears before the shock wave breaks the bomb case. Prompt-gamma radiation ionizes and excites atmospheric nitrogen producing the Teller light emission bands between 3,000 Å and 5,000 Å.
2. The next phase of the detonation is called radiative expansion. During this phase, the surrounding air is rapidly heated by radiation transfer before hydrodynamic motion is initiated.
3. When the temperature has dropped to about 300,000 K, transfer of energy by hydrodynamic motion becomes more rapid than radiation transfer, and a strong shock wave advances ahead of the radiation front. Hydrodynamic coupling begins to convert radiant energy to blast-wave energy.

The shock front radiates at the temperature of the shock-heated air. The rate of growth of the fireball is approximately described by:

$$D = C \left( \frac{W}{\rho} \right)^{0.2} t^{0.4} \quad (5.1)$$

Where: D = diameter of the (spherical) shock front

C = a constant (assuming that the internal energy bounded by the shock front, and  $\gamma$ , the ratio of specific heats, is constant)

$\rho$  = ambient air density

t = time at which the diameter is D

This equation is based on a Taylor point-source solution, and is called  $\phi^5$  scaling.

4. When the temperature of the shock-heated air drops below 5,000 K, significant amounts of  $\text{NO}_2$  are formed. Since  $\text{NO}_2$  absorbs most of the visible spectrum, comparatively little radiation penetrates beyond the shock front, and the thermal minimum occurs. About 1 percent of the total

TABLE 5.14 POSITIONS OF AIRCRAFT FOR SHOTS TEAK AND ORANGE

	Shot Teak		Shot Orange	
	B-36's	P2V	B-36's	P2V
	ft	ft	ft	ft
Slant Ranges	480,000	396,000	436,000	396,000
Altitudes	30,000	22,000	30,000	30,000

thermal energy has been radiated up to this time. A few milliseconds have elapsed since the beginning of the detonation.

5. The temperature of the shock front continues to drop as it expands, and again becomes transparent to visible radiation. The radiant power of the fireball again reaches a maximum (greater than the first) and subsequently radiates about 35 percent of the bomb's energy in a visible pulse lasting several seconds.

The general effect of decreased ambient air density (at high altitudes) was expected to influence fireball phenomena in at least three ways. First, the hydrodynamic coupling mechanism by which the air-blast wave is generated will change in such a way that less energy will appear as air blast, and more will remain in the form of thermal radiation. Second, the molecules responsible for absorption of thermal energy, particularly  $\text{NO}_2$  and  $\text{HNO}_3$ , will be produced in smaller quantities, again increasing the proportion of thermal energy. Third, and most important, the increased mean-free path for nuclear and thermal radiation will result in the deposition of large amounts of energy in the atmosphere at large distances from the detonation.

Several studies were made which permitted at least qualitative predictions of effects from Shots Teak and Orange. In general, these indicated that the growth of the fireball would involve considerably different mechanisms than those described above.

Hydrodynamic coupling at 250,000 feet was expected to begin at times as late as a second and also to be quite weak. If so, most of the energy of the bomb would be deposited by gamma and thermal X-rays at long ranges from the bomb. Deposition of energy would excite, dissociate, and ionize the molecules of the atmosphere, and the subsequent behavior of the atmosphere would determine the nature of the visible phenomena. It is to be expected, then, that the thermal

radiation from Shot Teak would appear to be a single fast pulse (having little or no evidence of the usual minimum) consisting mostly of discrete emissions of the atmosphere, rather than the usual black-body emission.

Hydrodynamic transport of energy is important at 125,000 feet, although probably not as effective as it is at sea level. It was difficult to predict the nature of Shot Orange, since it was expected to have characteristics of both sea level and high-altitude bursts.

5.6.3 Instrumentation. Since the nature and magnitudes of the thermal phenomena could not be accurately predicted, extensive instrumentation was required to provide wide dynamic range, provide sufficient backup to assure a high degree of success, and cover the spectral region of interest.

The thermal instrumentation was carried in the three aircraft used on Shot Yucca. The positions of the aircraft at H hour for Shots Teak and Orange are shown in Table 5.14.

5.6.4 Results. The thermal program was almost completely successful on both Shot Teak and Shot Orange. All projects obtained complete sets of data, except for infrared spectrometer data on Shot Teak.

The thermal measurements made on Shots Teak and Orange require extensive analysis before a complete picture can be presented. However, the data available give a reasonably good indication of the nature of some phenomena.

Photography. Figures 5.26 and 5.27 show high-speed photographs of the Shots Teak and Orange fireballs. It should be pointed out that the word fireball means the extent of the early visible effects and has a different significance from the sea-level case. It is seen that the top of the Shot Teak fireball is hazy and indistinct, while the bottom is sharp and well defined. This effect is undoubtedly caused by the fact that the difference in density at the top of the fireball is less than that at the bottom, by a factor of four. The vertical streak through the Shot Orange fireball is probably the beginning of the aurora caused by electrons oriented by the geomagnetic field ionizing the nitrogen of the air.

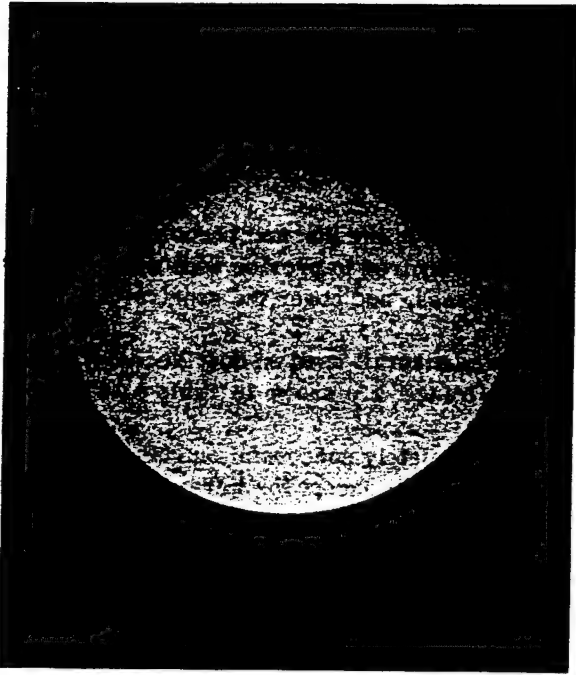
Streak photographs of Project 8.3 are shown in Figures 5.28 and 5.29. These represent the envelope of the expanding fireball as a function of time, the time scale being horizontal.

Three regions of different intensity can be seen in the streak photographs of Shot Teak. The diameters of all three are plotted in Figure 5.30, along with the diameter which would be predicted by scaling a sea-level fireball to 250,000 feet. The earliest data show that the outer edge of the Shot Teak fireball has expanded with an average velocity of  $5 \times 10^9$  cm/sec for the first 100  $\mu$ sec, a speed corresponding to one sixth the speed of light. The diameter at the end of ten msec is more than ten miles. Comparison with the radius which would be predicted on the basis of the usual hydrodynamic scaling procedure (Equation 5.1) clearly shows that the mechanisms which produced the visible phenomena on Shot Teak are greatly different from those which produce a fireball at lower altitudes. It is expected that analysis of the photographs and other records will eventually confirm some of the theories which were proposed to describe high-altitude phenomena.

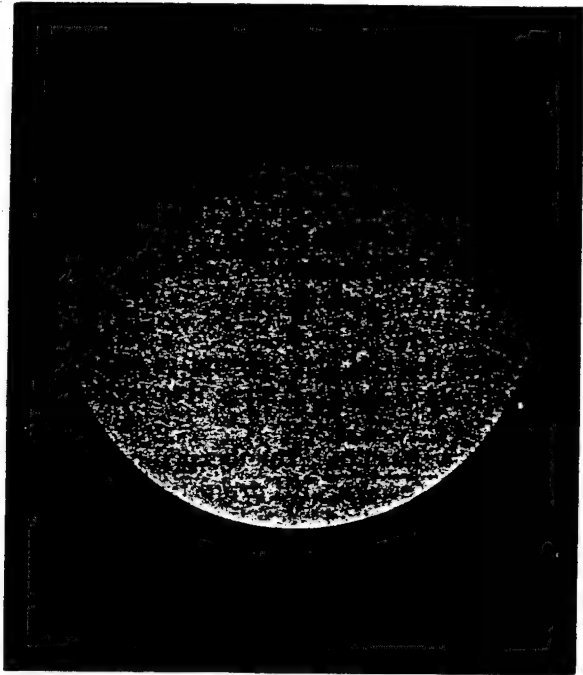
Thermal Intensity. Figures 5.31 through 5.40 show the intensity versus time records obtained in the specified spectral regions, plus the bolometer records, which record all thermal radiation. For comparison, a typical thermal pulse of a 3.8-Mt air burst is included (Figure 5.41). The short thermal duration shown by the bolometers is a characteristic of the instrument; the actual thermal durations are given more accurately by the photocells. No immediate comparison of thermal deposition rate (watts/cm<sup>2</sup>) for sea level versus high altitude shots can be given, but it can be pointed out that the total energy in the Shot Teak and Shot Orange pulses is at least as great as the energy in the sea-level pulse and is delivered in less than a second.

The thermal pulses from Shot Teak show no evidence of the usual minimum and second maxi-

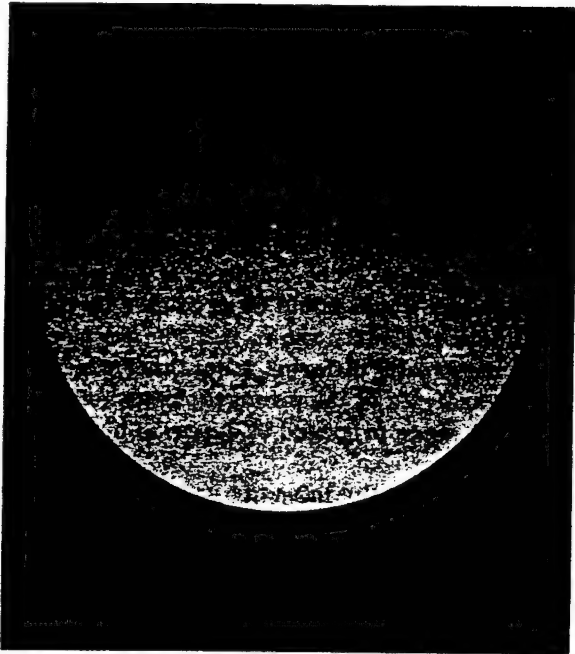
(Text continued on Page 261)



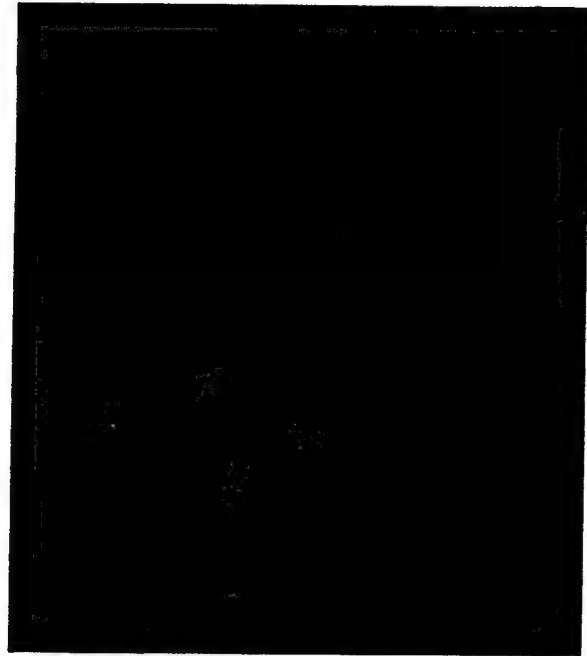
0.58 msec



1.16 msec



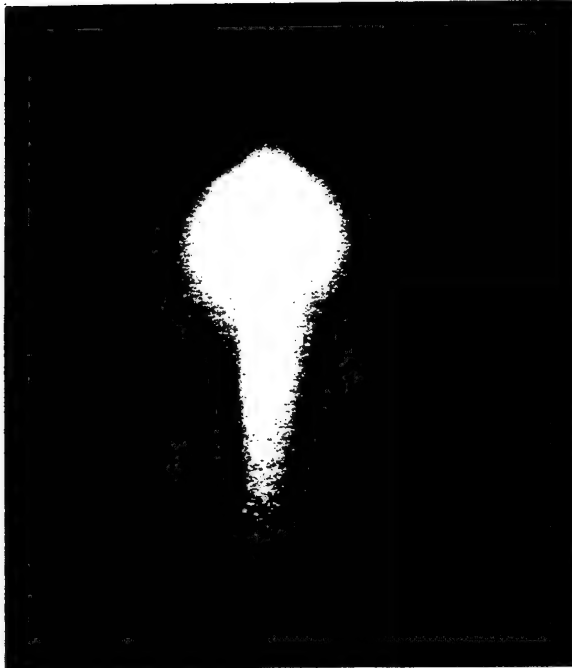
9.28 msec



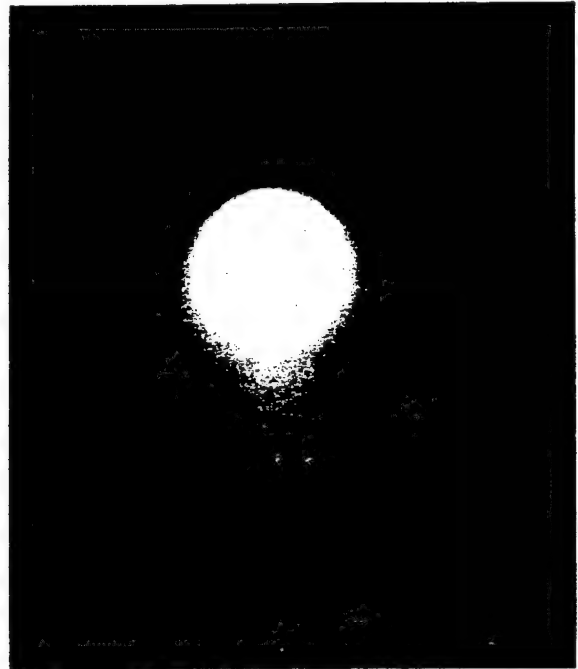
105 msec

Figure 5.26 Shot Teak fireball.

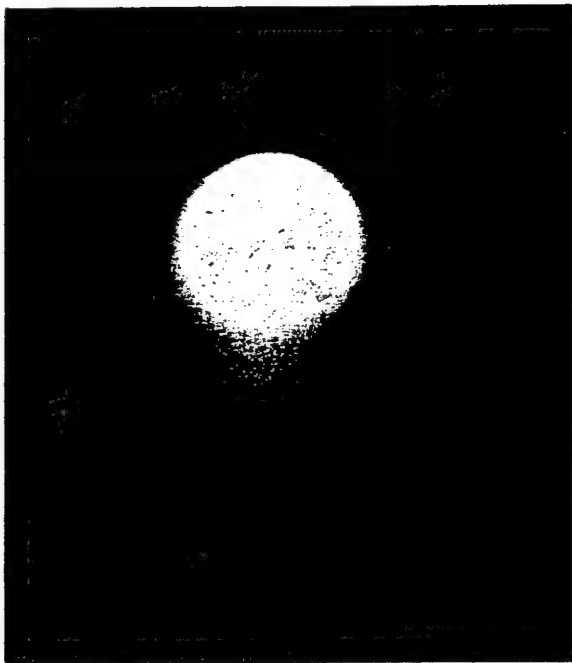




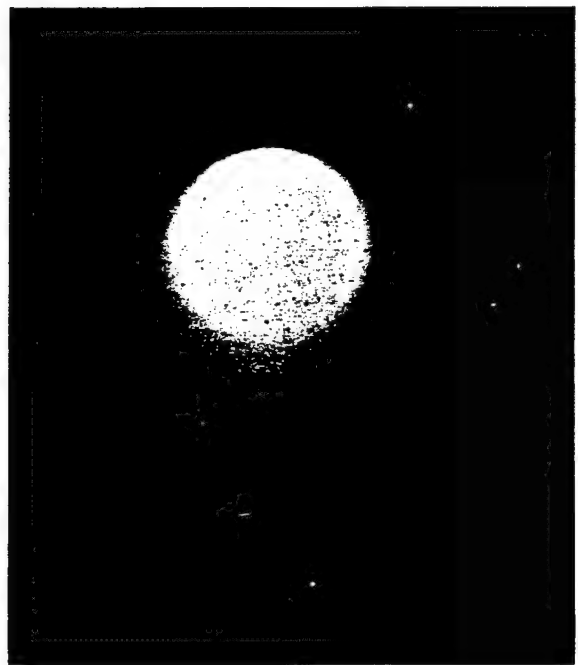
0.43 msec



9.86 msec



100.2 msec



300.2 msec

Figure 5.27 Shot Orange fireball.

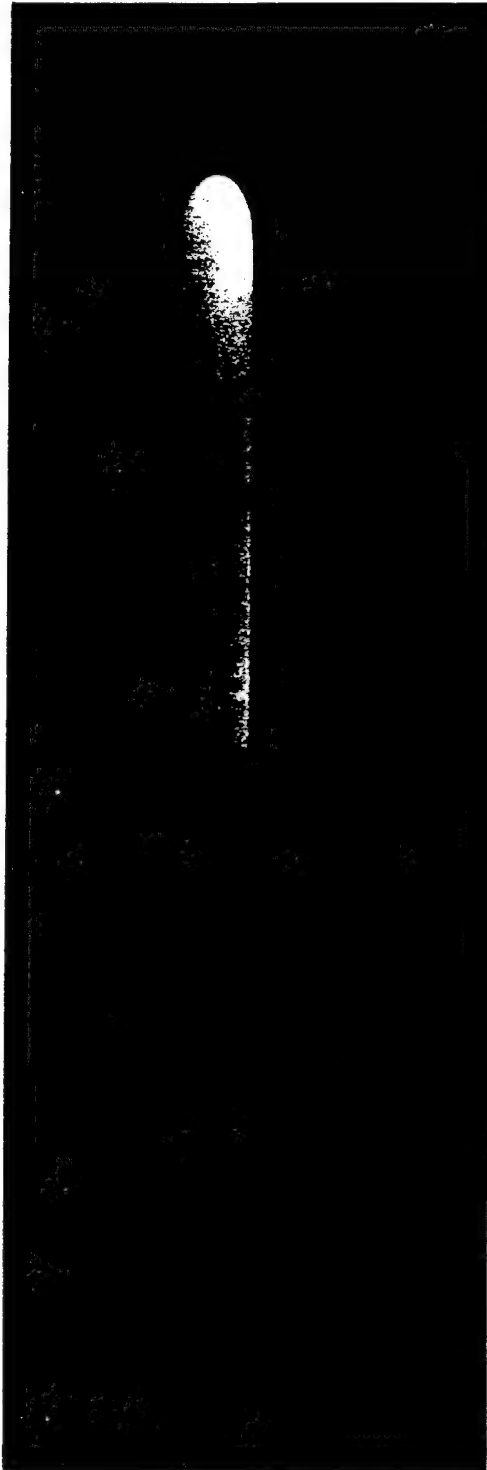
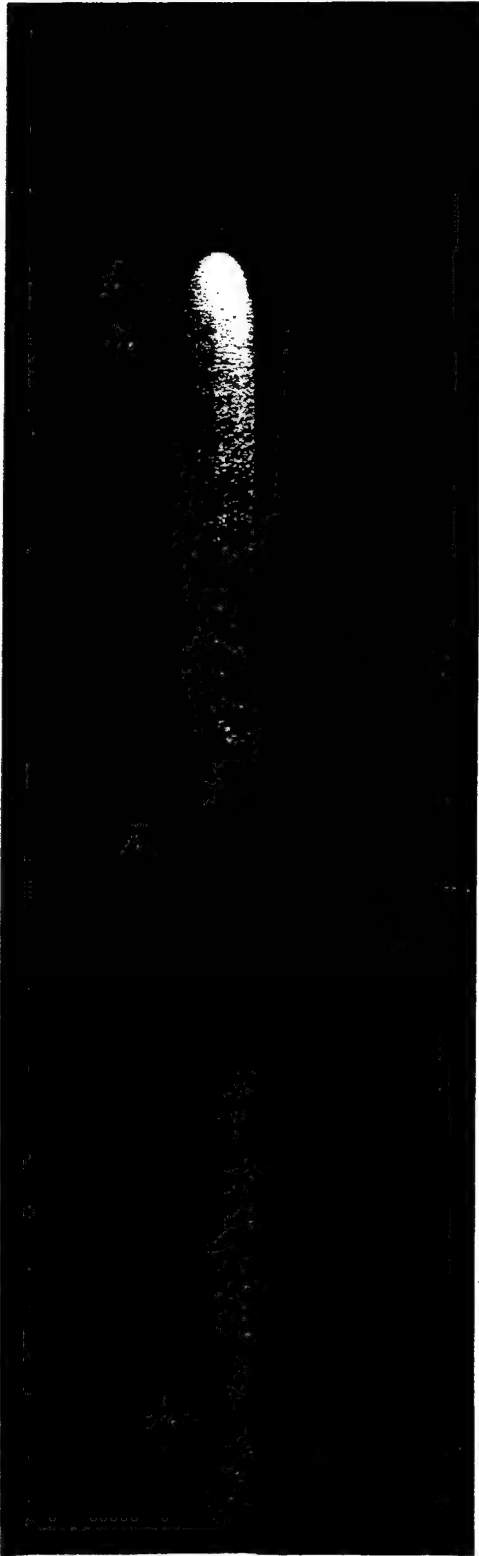


Figure 5.28 Streak records, Shot Teak.

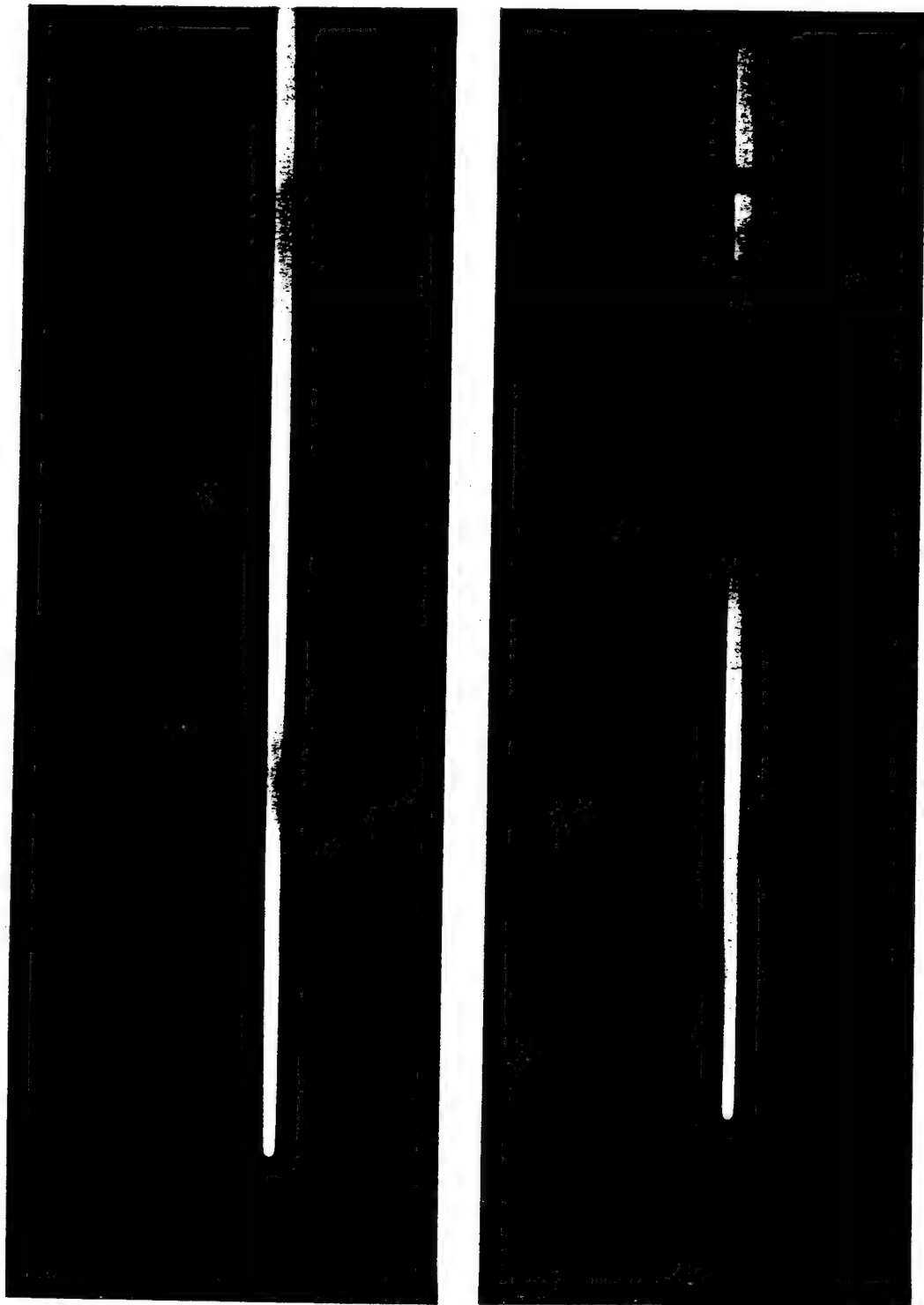


Figure 5.29 Streak records, Shot Orange.



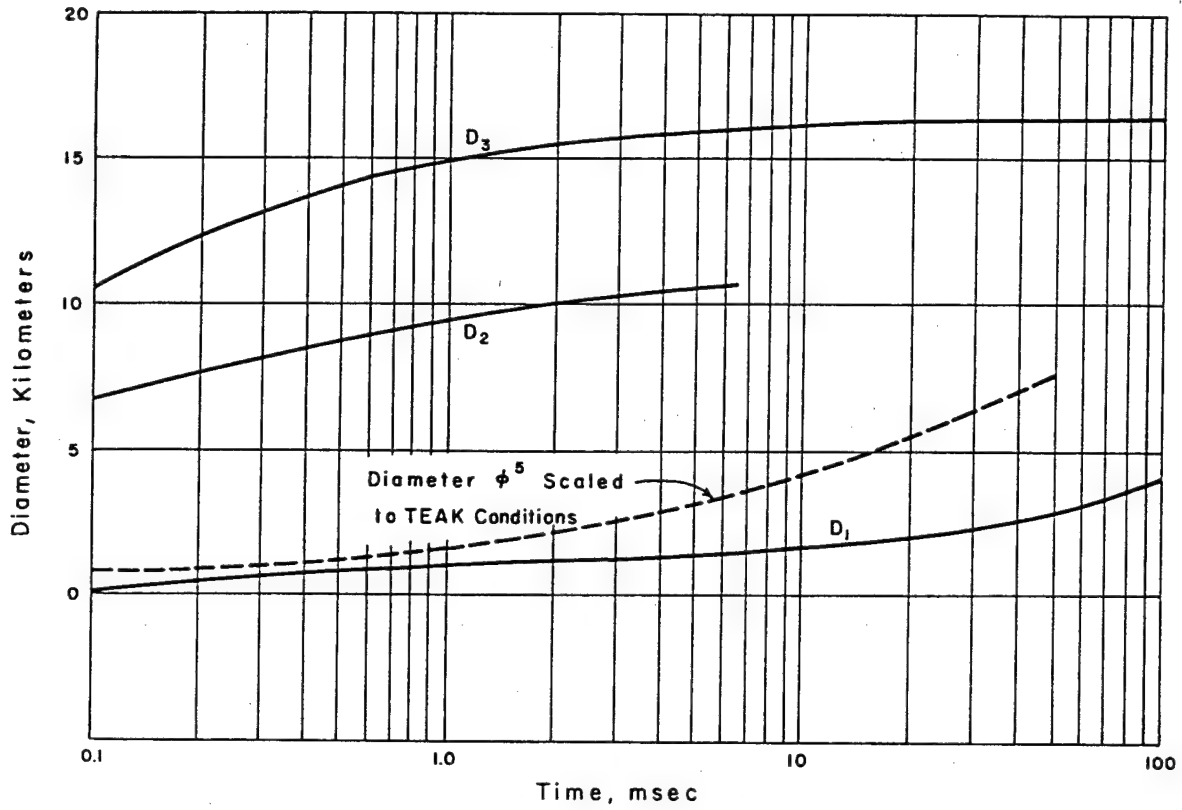


Figure 5.30 Shot Teak diameter-time data.

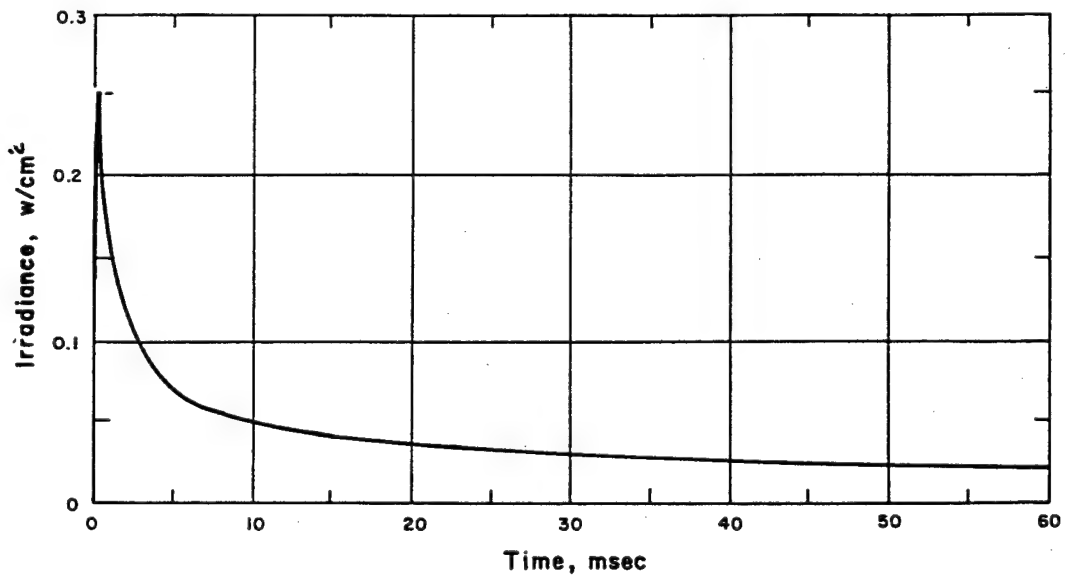


Figure 5.31 Shot Teak thermal pulse from FUV No. 57 (far-ultraviolet), 2,000 to 2,500 Å.



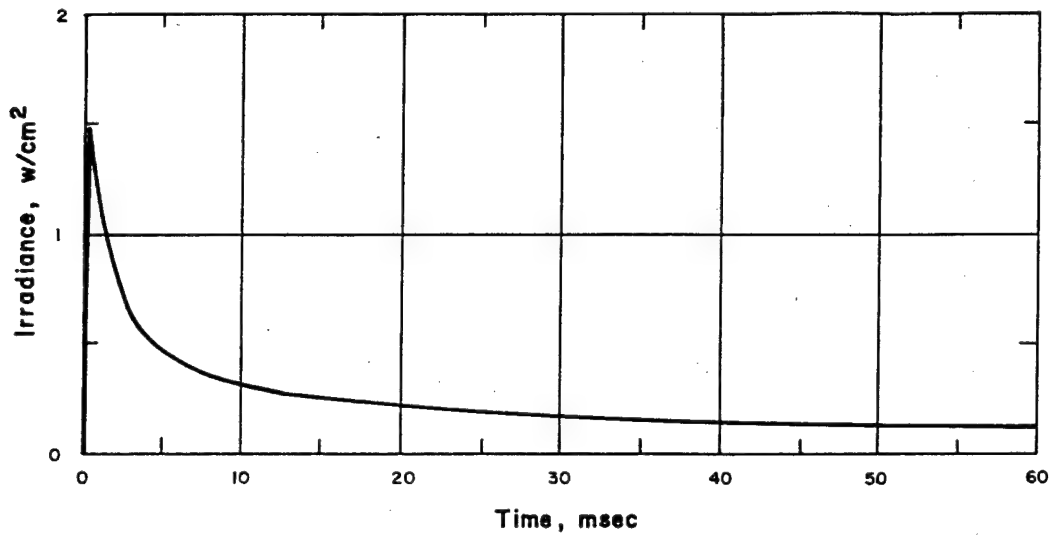


Figure 5.32 Shot Teak thermal pulse from NUV No. 78(d) (near-ultraviolet), 2,500 to 3,950 Å.

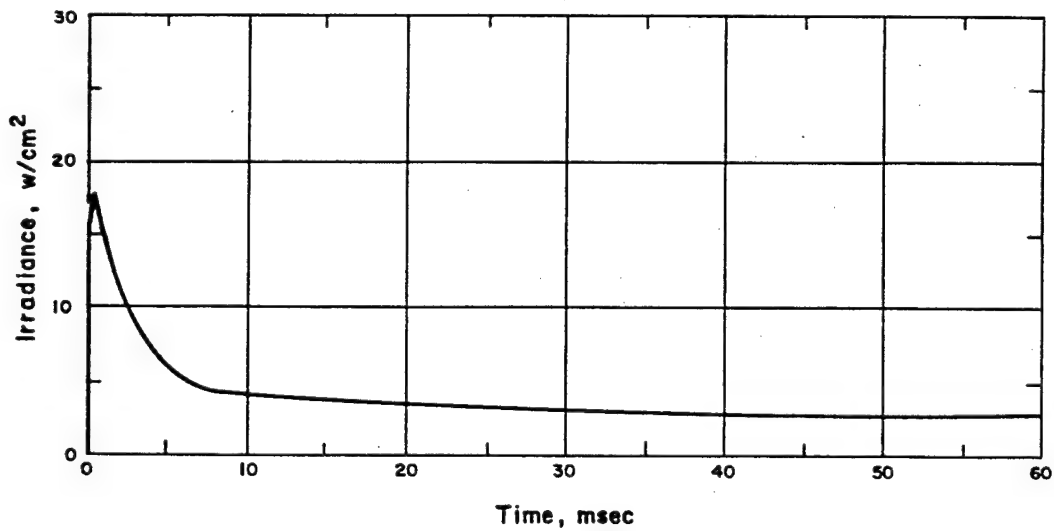


Figure 5.33 Shot Teak thermal pulse from VIS No. 23 (visible), 3,950 to 5,000 Å.

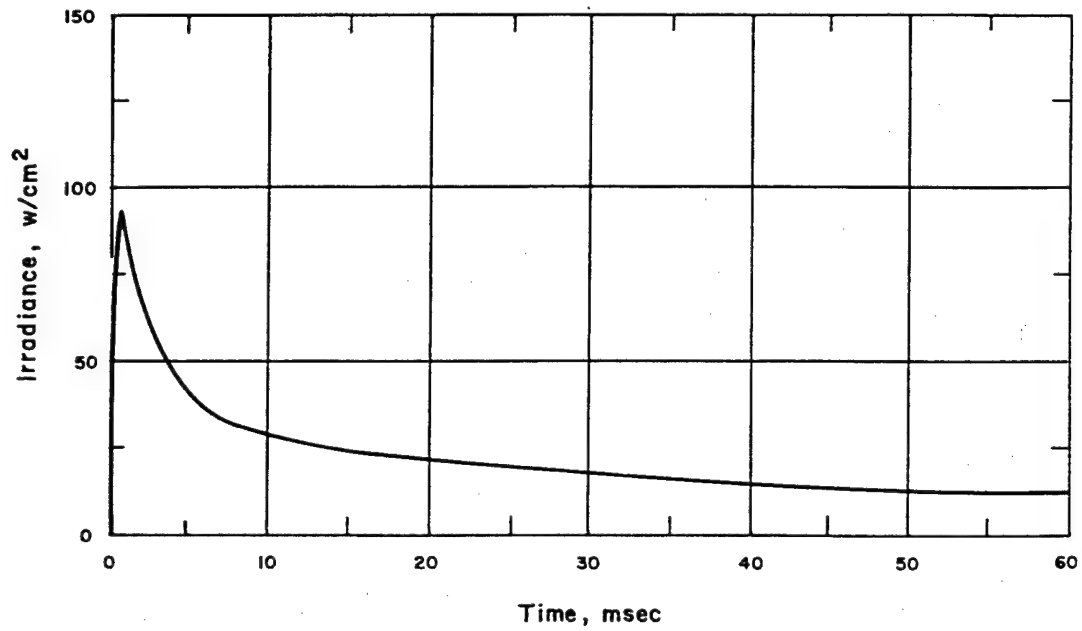


Figure 5.34 Shot Teak thermal pulse from IR No. 48 (infrared), 5,000 to 10,000 Å.

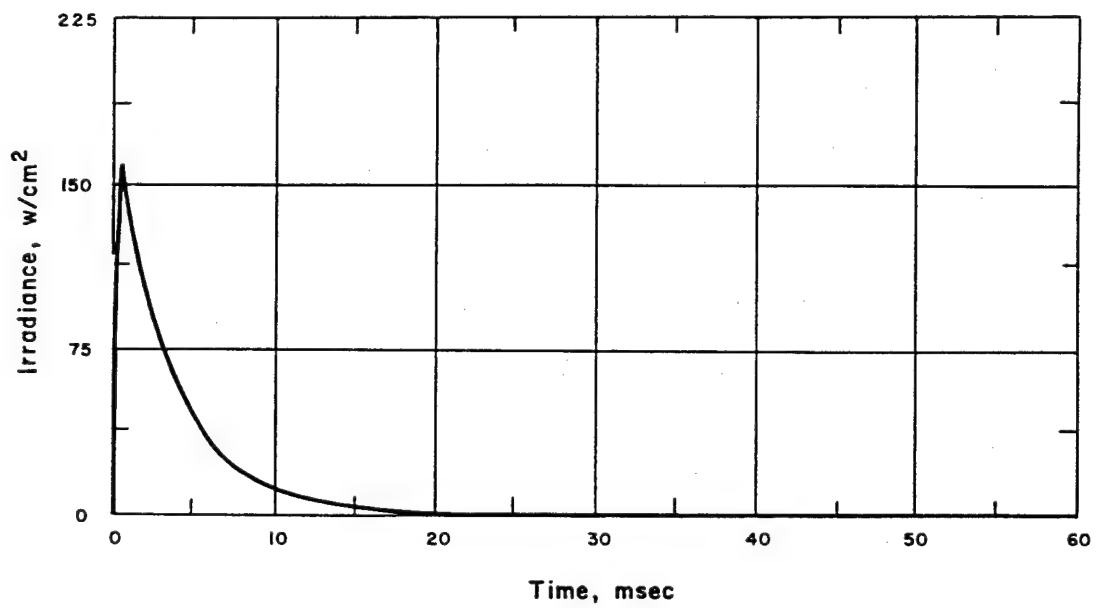


Figure 5.35 Shot Teak thermal pulse from Bolometer No. 2.

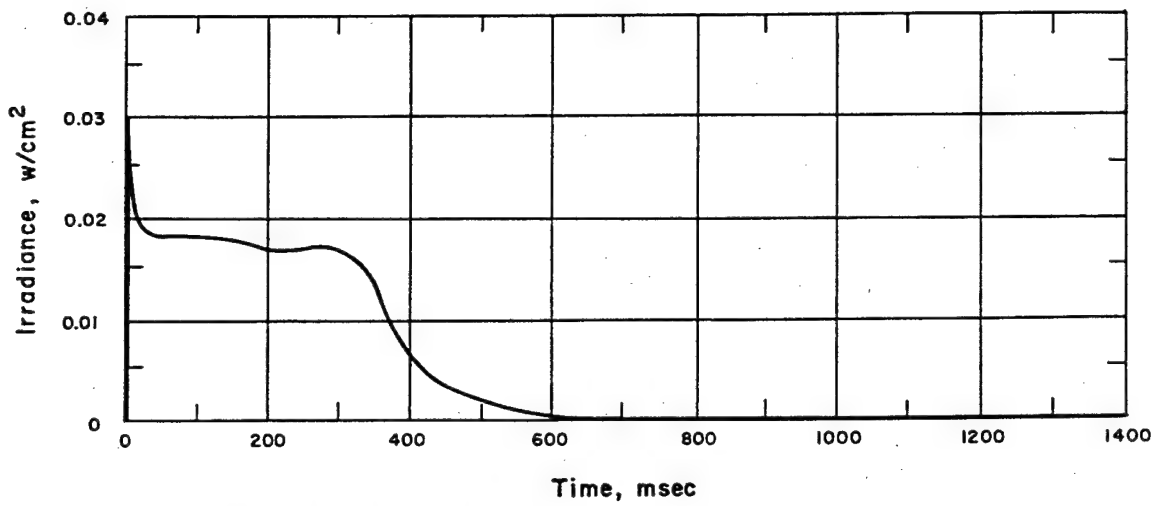


Figure 5.36 Shot Orange thermal pulse from FUV No. 57, 2,000 to 2,500 Å.

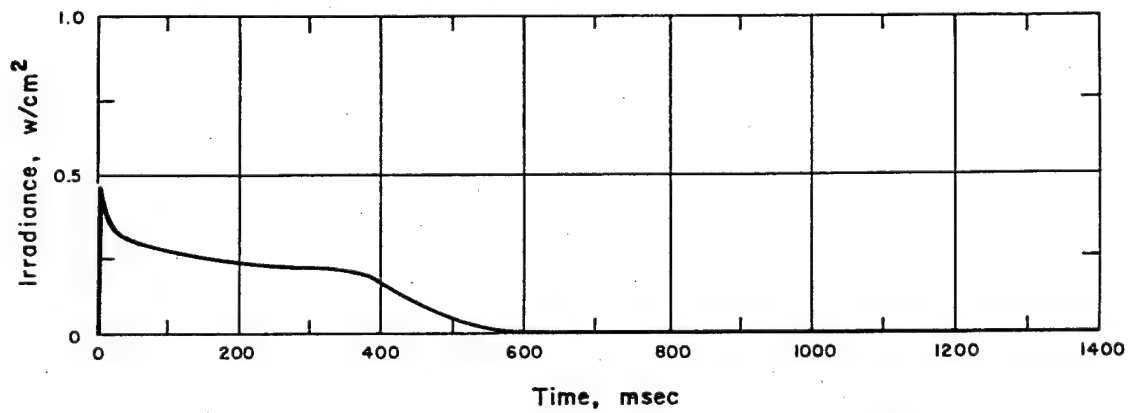


Figure 5.37 Shot Orange thermal pulse from NUV No. 78(d), 2,500 to 3,950 Å.

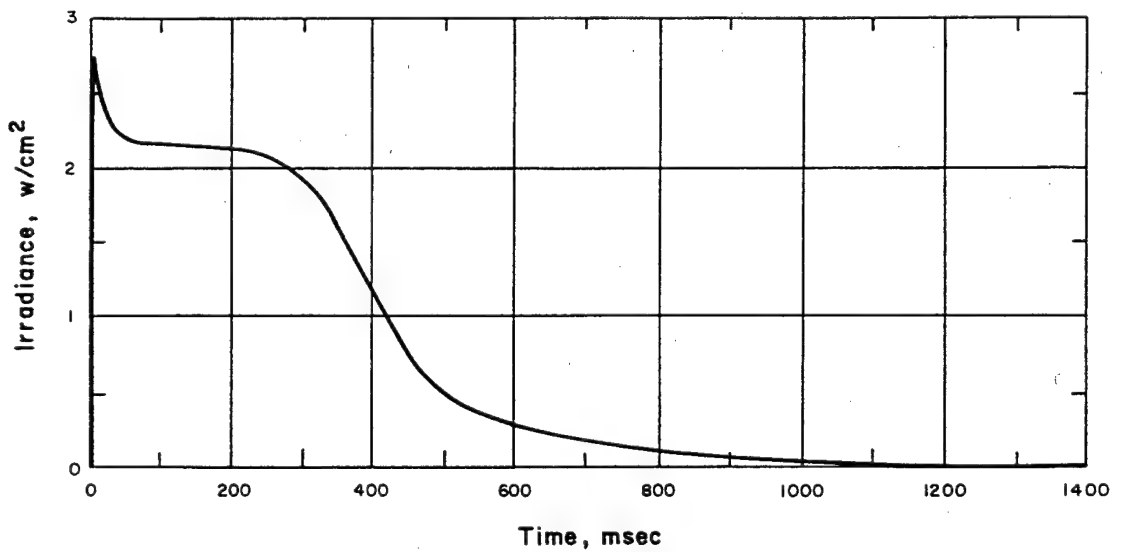


Figure 5.38 Shot Orange thermal pulse from VIS No. 31, 3,950 to 5,000 Å.

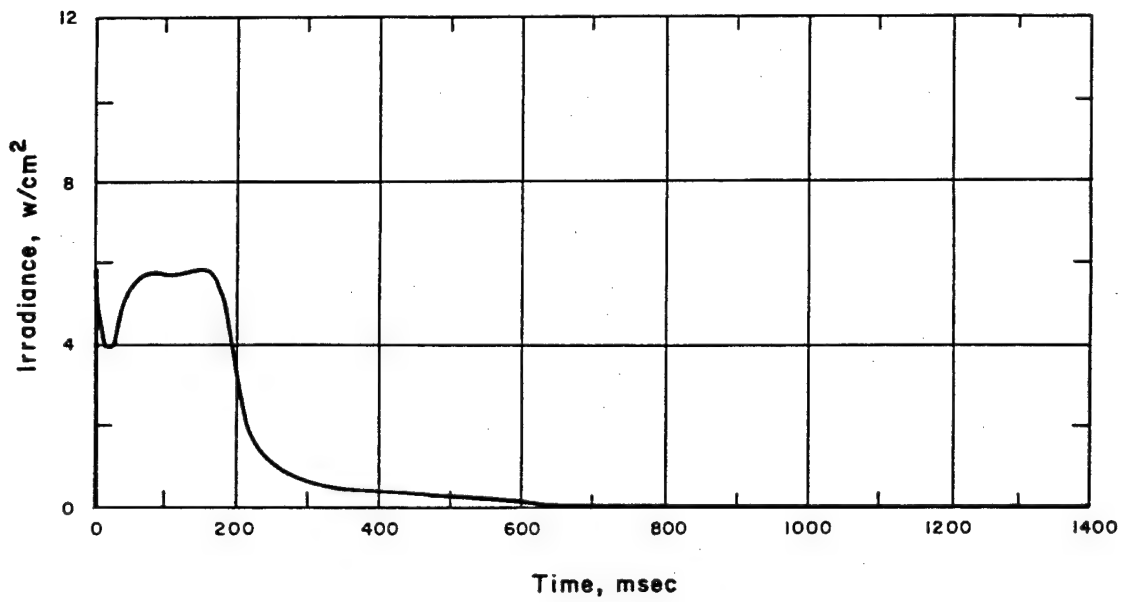


Figure 5.39 Shot Orange thermal pulse from IR No. 16, 5,000 to 10,000 Å.

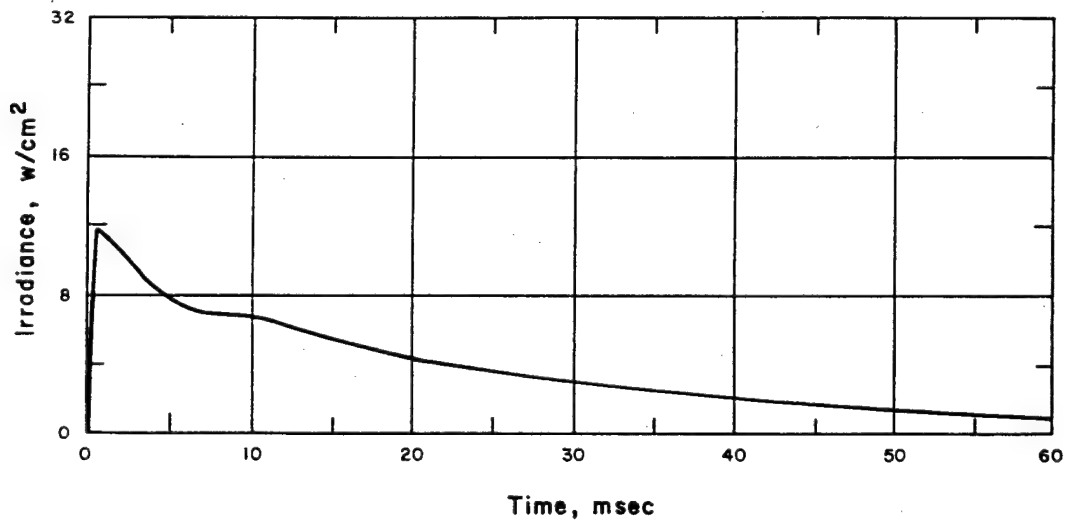


Figure 5.40 Shot Orange thermal pulse from Bolometer No. 2.

mum, again confirming that unusual mechanisms affect the disposition of energy from high altitude shots.

The Shot Orange records show a longer thermal duration than Shot Teak records. There is a thermal minimum in the infrared region and a plateau lasting about 300 msec in the visible and ultraviolet bands. Although Shot Orange indicates evidence of mechanisms common to low-altitude bursts, the total thermal duration is still less than a second.

Infrared. The only data on infrared radiation (20,000 Å to 120,000 Å) from Shot Teak was provided by the infrared mapping device, a modified AN/AAS-4 (XA-2). A positioning error

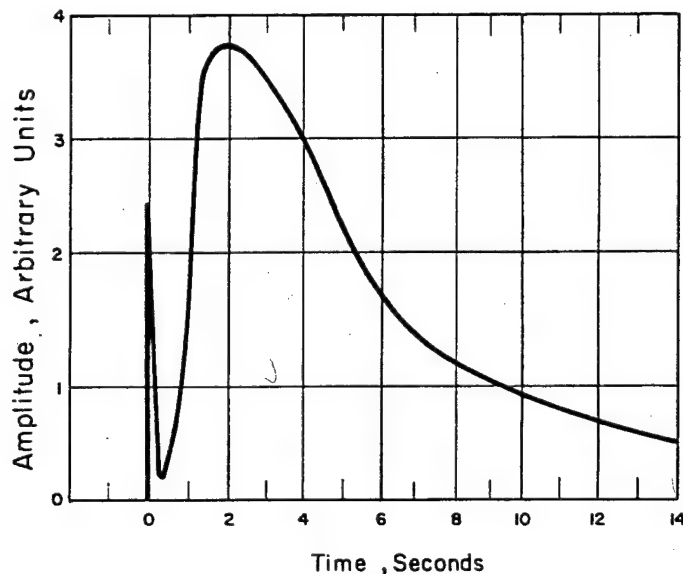


Figure 5.41 Approximate thermal pulse, 3.8 Mt air burst.

placed the Shot Teak fireball outside the field of view of the monochromator. Because of the relatively slow sweep-repetition rate of the mapping device (one complete sweep every 1.3 seconds), the first observation of the Shot Teak fireball was made 1.025 seconds after detonation. The results are shown in Figure 5.42.

Although the observations were made at relatively late times, the maximum diameter of the infrared fireball was almost 200,000 feet.

The next scan, 2.325 seconds after Shot Teak detonation, recorded no observable infrared emission.

Successful measurements were made on Shot Orange with both the infrared mapping device and the monochromator. The mapping device recorded infrared emission for 18 seconds. Results of the first scan are shown in Figure 5.43. It is seen that the extent of infrared emission (average diameter about 120,000 feet) is considerably larger than the visible fireball (about 20,000 feet diameter).

The spectral data from the monochromator are shown in Figure 5.44. Further calibration of the equipment is necessary before absolute values of infrared intensity can be reported.

Thermal Spectra. Spectral structure of the Shot Teak and Shot Orange thermal pulses was determined from the photographic records shown in Figures 5.45 and 5.46. The vertical dimension represents wave length. Shot Teak records show intense Teller light in the first few  $\mu$ sec, consisting primarily of emission bands of the first positive system of  $N_2$  and a few bands of  $N_2^+$  and the second positive system of  $N_2$ . After the Teller light, the bomb light appeared to

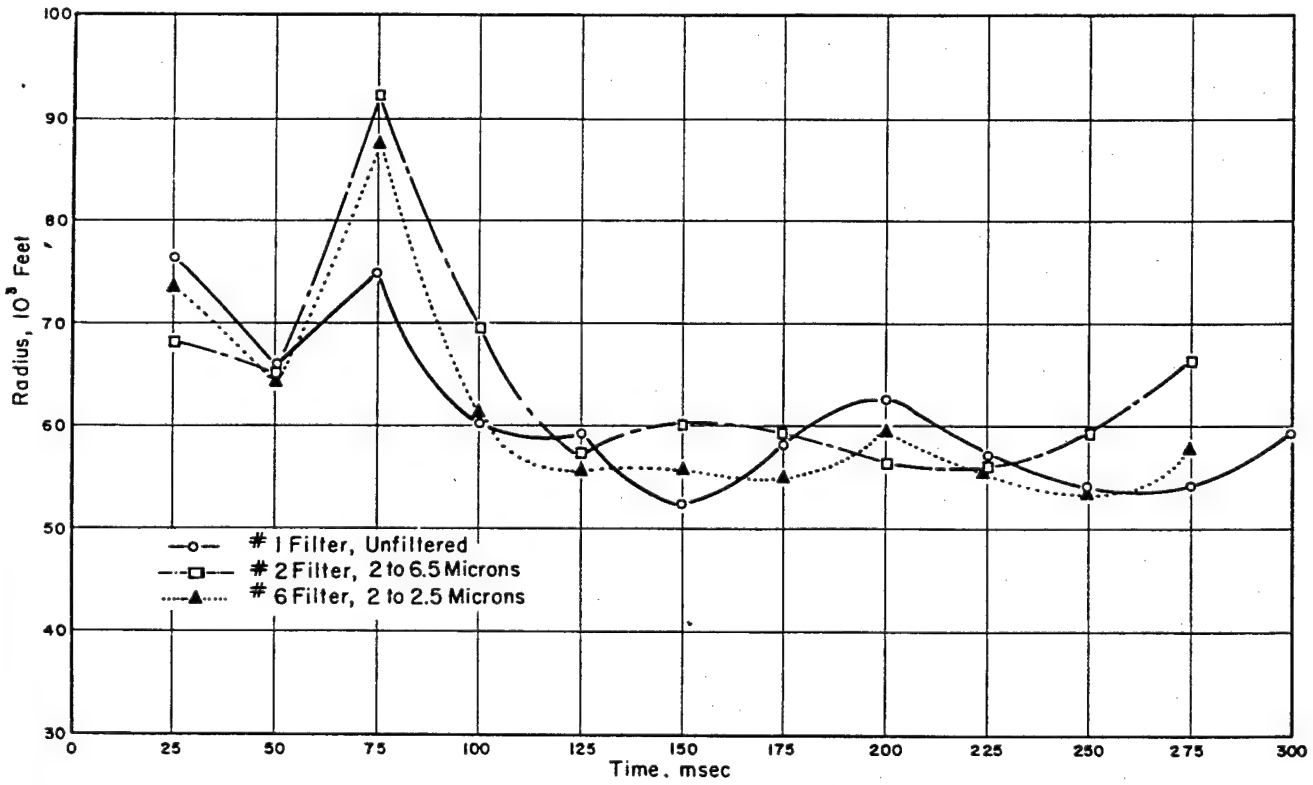
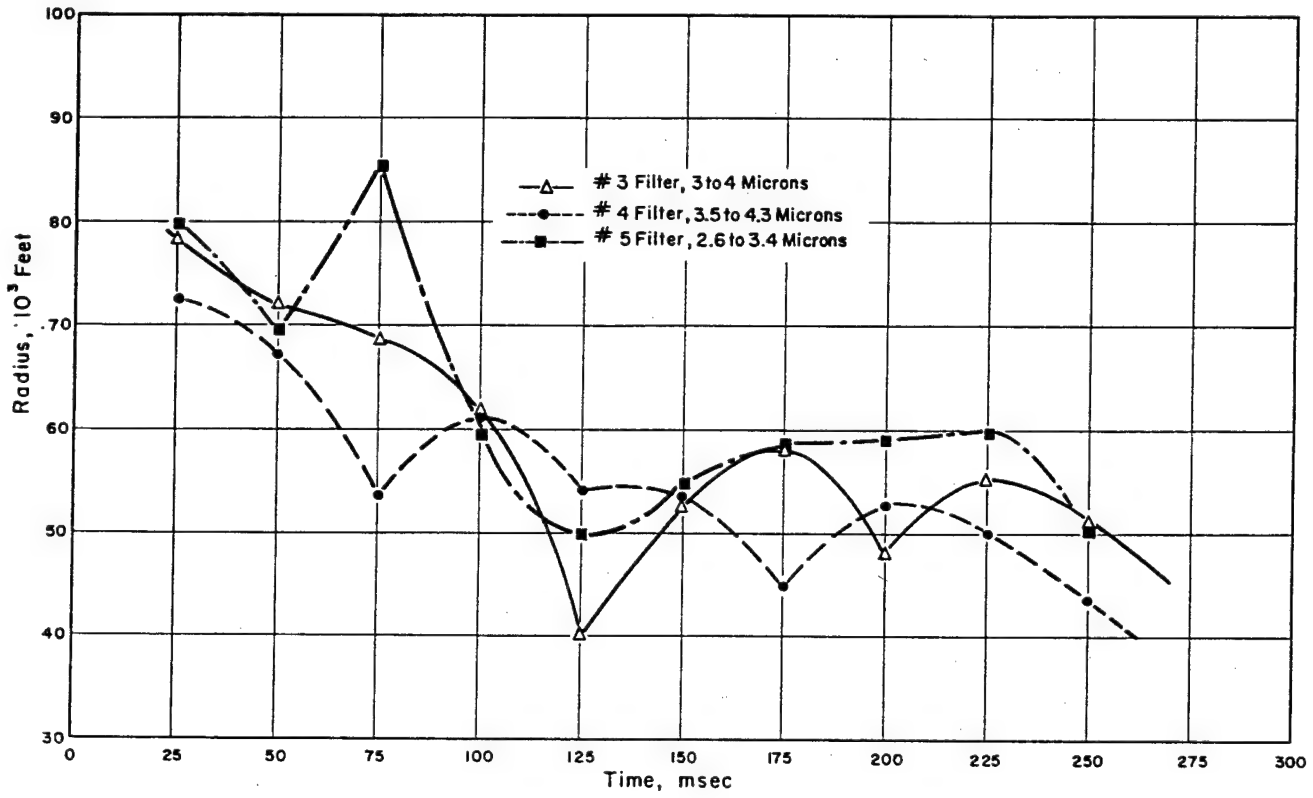


Figure 5.42 Fireball radius versus time, Shot Teak. (Add 1 second for true time.)

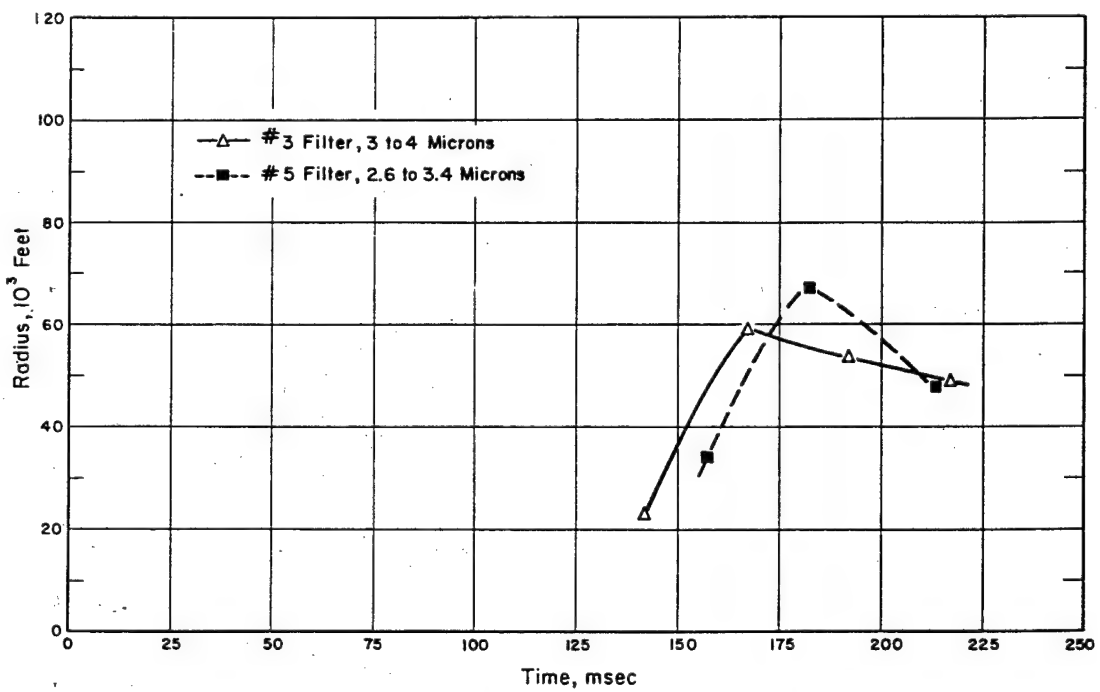
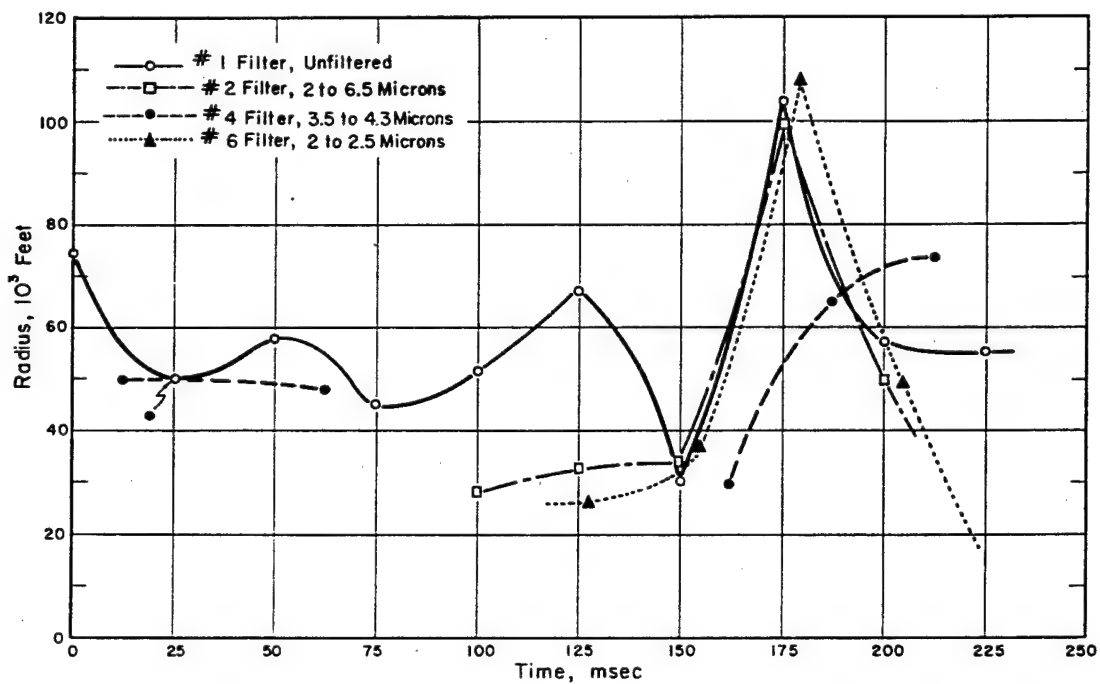


Figure 5.43 Fireball radius versus time, Shot Orange.

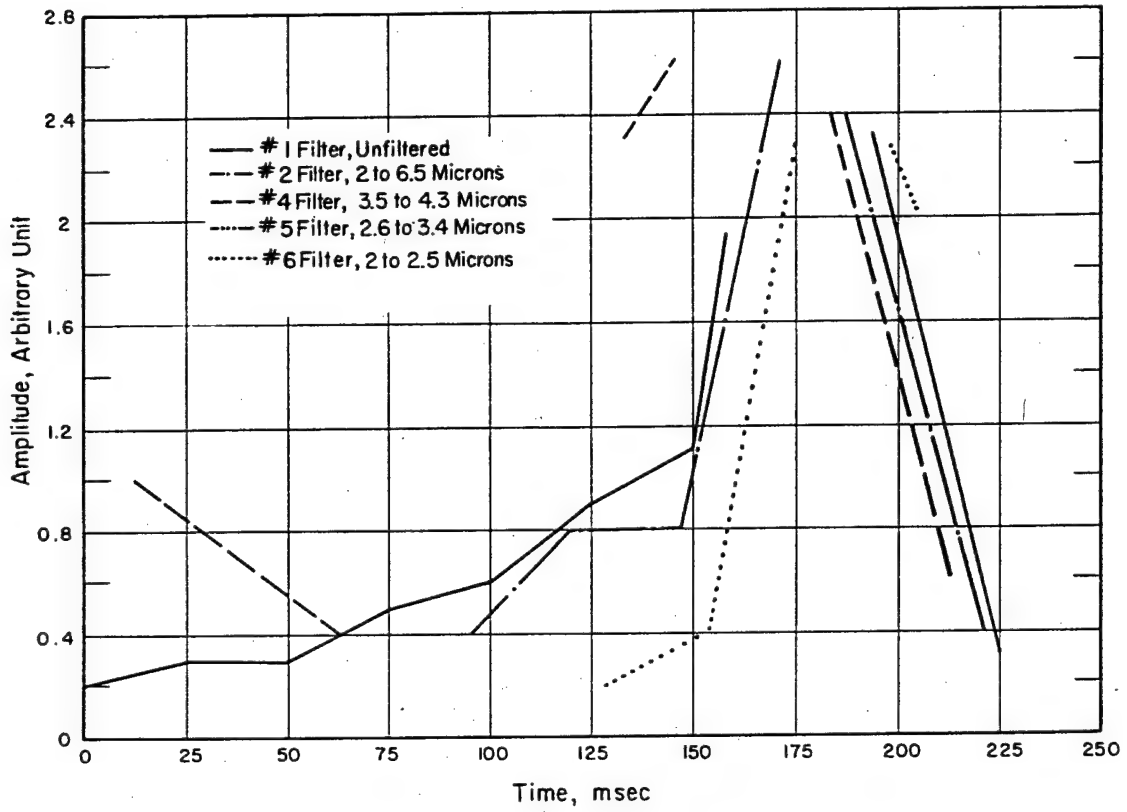


Figure 5.44 Spectral irradiance versus time, Shot Orange.

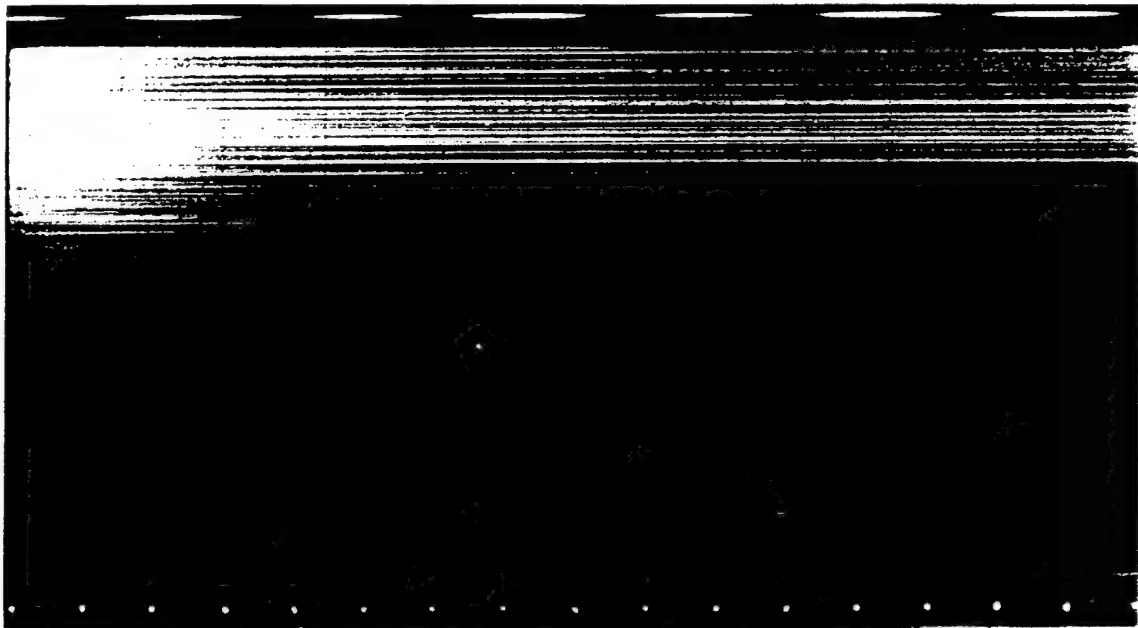


Figure 5.45 Streak spectra of Shot Teak. Zero time at the left.



consist mainly of intense emissions from  $N_2$ ,  $N_2^+$ , and  $O_2^+$ . Almost negligible emission continuum was observed, indicating that the fireball was not radiating like a black body. The absence of an emission continuum would preclude observation of any absorption bands which might have been present.

Bomb light spectra from Shot Orange was much different from that of Shot Teak. Teller

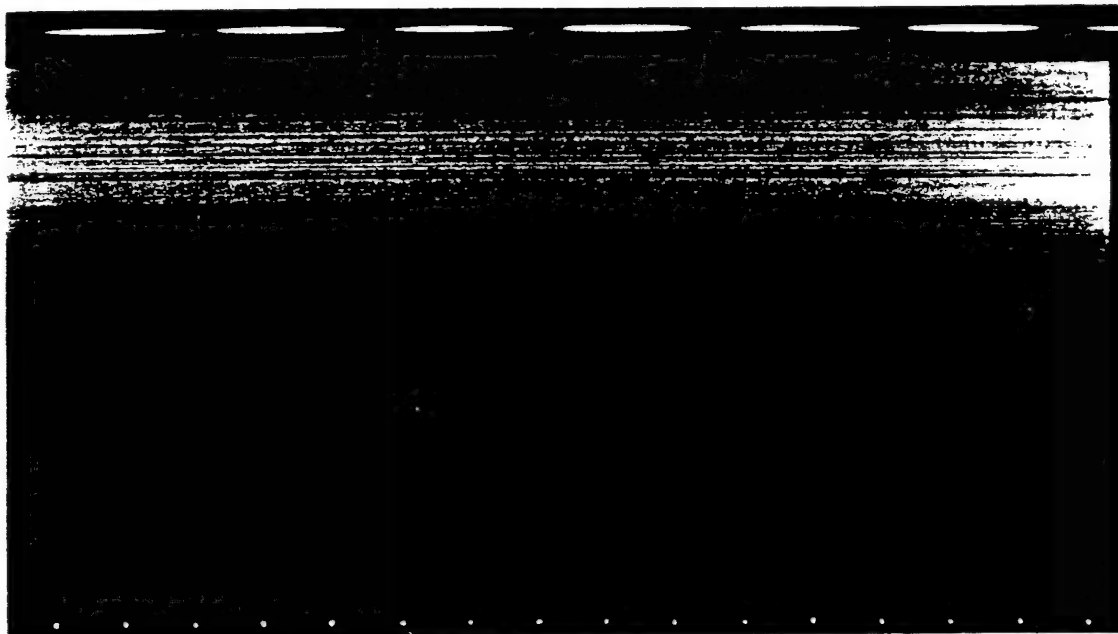


Figure 5.46 Streak spectra of Shot Orange. Zero time at the left.

light was again observed, but it consisted only of the second positive system of  $N_2$  and a few bands of  $N_2^+$ . A strong emission continuum was observed throughout the thermal pulse. Absorption bands due to  $N_2^+$ ,  $O_3$  and other constituents were observed.

## 5.7 DESTRUCTIVE EFFECTS OF VERY-HIGH-ALTITUDE DETONATIONS

**5.7.1 Objectives.** Project 8.6 directed its efforts toward assessment of the destructive effects specifically associated with nuclear bursts at very-high altitudes by participating in Shots Teak and Orange. Particular emphasis was placed on X-ray effects. An instrumented pod was affixed to the Redstone and was ejected from the missile prior to burnout so as to be in close proximity to the device at burst time. The specific objectives were as follows:

1. Measurements of the effect of X-rays were attempted on a variety of structural materials. These measurements were made to evaluate the impulsive loadings to be expected on ballistic-missile structures and also on flimsy structures characteristic of decoys. It was also hoped that measurements of the absolute intensity and the spectral distribution of the X-rays could be made. Measurement of X-ray effects were restricted to Shot Teak (altitude, 250,000 feet), since the mean-free path of this radiation was too short to reach an appreciable distance in Shot Orange (altitude, 125,000 feet).

2. For both Shots Teak and Orange, theory predicted a rather long (several seconds) thermal pulse following the high-intensity, short-duration first pulse. The long thermal pulse might have been capable of melting an appreciable quantity of metal. Measurements of the character-

istics of this long pulse were, therefore, attempted.

3. Shot Orange, at 125,000 feet, was expected to furnish a measureable blast effect at distances of 8,000 feet. Measurements of the static and dynamic pressure at this range were, therefore, attempted. In addition to the conventional blast effect, the vaporization of the missile wall resulted in a blow-off pressure that was predicted to be larger than the blast overpressure at 125,000 feet. Instruments were, therefore, designed to independently measure both the blast and blow-off overpressures.

4. For both Shot Teak and Shot Orange, the neutron mean-free path had been calculated to be extremely long so that neutron measurements were made during both events. The absolute flux and the energy spectrum were of interest to vulnerability studies; hence, both of these quantities were measured. Since low-energy neutrons (less than 1 ev) are not emitted from a burst at this altitude, an attempt was made to measure the albedo effect of these neutrons.

When these neutrons reached the earth's atmosphere at approximately 100,000 feet, however, they were thermalized to less than 1-ev energy, and a certain fraction of them were reflected to the pod. A measurement of the neutron flux below 1 ev, therefore, gave a measure of the thermal-neutron albedo.

5. The experiment was designed so that all of the instrumentation was simple in concept. If there were any effects of a nuclear burst at high altitude which had not been predicted, it was hoped that the effect on the pod instrumentation, and on the pod itself, would be measurable. Recovery of the pod was essential to a determination of any new effects and for substantiating or disproving old theories on the nature of very-high-altitude detonations.

5.7.2 Background. Above 250,000 feet, two radiations, neutron and X-ray, may be used to nullify the ICBM attack. The neutrons may destroy the effectiveness of the nuclear warhead by melting the fissionable material (with the aid of the bonus energy due to neutron-induced fission). The X-rays, on the other hand, may induce a structural failure of the missile. This structural failure is caused by the following sequence of events: (1) The X-rays penetrate the missile wall for a short distance. (2) The energy dissipated within the thin outer layer by the X-rays, as they are absorbed, serves to raise this layer to an extremely high temperature and pressure. (3) The pressure is sufficiently high to cause the thin layer of metal vapor to expand explosively, imparting a large impulse to the wall. (4) The wall is forced inward at high velocity and may fail if the yield point of the material is surpassed.

The two applications of this X-ray impulse are to the destruction of ICBM re-entry bodies, and to the destruction of the accompanying swarm of decoys. The particular interest of X-rays with respect to the latter is that there may be an extremely large destructive range (of the order of ten miles) within which a whole swarm of decoys could be destroyed.

Below about 60,000-foot altitude, the fireball of a nuclear detonation has a temperature-time history similar to that of a sea-level detonation. The high-temperature environment is capable of vaporizing enough metal to be considered an effective threat to ICBM re-entry bodies. If the re-entry body is constructed of an organic material such as plastic, however, the thermal effects of a blast will almost certainly be negligible. This fact has emerged from the field experiments during Operations Redwing and Plumbbob. In this case, the most-important lethal effect to a blast-resistant re-entry body would be the melting of the fissionable material by the neutron flux from the defensive weapon.

Associated with the rapid vaporization rate of materials in a high-temperature fireball is a concentration of energy at the surface of the ablating wall. This concentration of energy leads to a pressure in excess of the isothermal-sphere pressure. Efforts have been made during sea-

level tests to detect this so-called blow-off pressure, but no clear-cut measurements have been made. For altitudes very-much above 125,000 feet, the isothermal sphere cools rapidly; hence, the blow-off pressure does not exist for a long-enough time to cause static loading. The blow-off effect is analogous to the X-ray impulse; the major difference between the two phenomena is that the X-rays instantaneously penetrate a finite thickness, while the thermal flux must penetrate the vapor barrier by a diffusion process.

Following the thermal X-ray pulse of energy and the subsequent radiative-transport phase, there remains a relatively low temperature fireball of large radius. The fireball persisted for times of about 5 seconds for Shot Orange and 20 seconds for Shot Teak. A ballistic missile moving with a velocity of 6 km/sec would have spent about  $2\frac{1}{2}$  seconds in the Shot Orange fireball and 5 seconds in the Shot Teak fireball. These times are sufficiently long to cause appreciable melting of a metallic wall. The energy required to melt a given thickness of most metals is less than  $\frac{1}{10}$  the energy required to vaporize the same thickness. Thus, the late, persistent fireball of a very-high-altitude detonation would be an effective agent in destroying a metal-walled ballistic missile. This late fireball was predicted to contain about 25 to 50 percent of the total yield of the weapon.

The absorption length in air of thermal X-rays emitted by a nuclear weapon is too short for X-rays to be of tactical importance below a 250,000-foot altitude. Since an ICBM kill above this altitude would be desirable, it is not felt that this fact is a severe limitation to the utilization of X-rays for a structural kill. [REDACTED]

There are two basic phenomena which must be understood before the X-ray impulse may be calculated: first, the emission of thermal X-radiation by the nuclear device itself and, second, the conversion of the X-ray energy to mechanical impulse at the wall of the missile. No exact calculation existed before Shot Teak of the emission of thermal X-rays from the Shot Teak device. [REDACTED]

At the range of the WADC pod (approximately 21,000 feet below the burst), the LASL calculation [REDACTED]

The larger prediction would be expected to produce appreciable mechanical effects, and the structural loading on the pod was predicted to cause structural damage for certain orientations of the pod axis with respect to the burst point.

5.7.3 Method of Experimentation. A conical nose was employed in order to provide the proper aerodynamic characteristics for the pod while being carried by the Redstone and during the period immediately after its ejection from the missile. The conical nose, however, had the disadvantage of offering no surface upon which instruments could be located directly facing the detonation. Therefore, a system was used whereby some few seconds after ejection of the pod, the conical nose was separated from the main instrument-bearing body by an explosive disconnect. After separation of the nose cone, the pod presented a flat surface on which were situated instruments for measuring the effects of a nuclear detonation. During the pod's descent, the flat front surface provided a large aerodynamic drag and reduced the velocity of the falling pod. A two-

stage-parachute system slowed water entry to preclude hydrodynamic-impact damage. Upon water entry, the tail section was jettisoned by the action of an explosive device initiated by a salt-water-activated battery. Devices to facilitate location and recovery of the floating portion were thus exposed. These devices included radio transmitters, flashing light, and sea dye.

The instrument casting (canister) which was located behind the nose cone was designed to house all the necessary instrumentation and to withstand the impulse loads due to the X-radiation. The instrumentation was designed to fit holes tapped to take devices of a cylindrical configuration. Figure 5.47 shows the machined canister.

When X-rays impinge upon a material, they are absorbed before penetrating an appreciable thickness. For a sufficiently intense X-ray pulse, this material will be vaporized and, hence, will expand into surrounding space. This mass motion will impart a momentum to the unvaporized material. The nature of the experiment required that a permanent record of the momentum be made. This was done by using the available momentum to permanently deform a metal. The device used consisted of a piston coated on one end with the material to be exposed to the X-ray pulse. The other end was a 60-degree conical section. The point of this piston was allowed to impinge upon a copper anvil. When the X-rays vaporized the material on the face of the piston, the latter gained all the resulting momentum and was driven into the anvil. The depth to which the piston penetrated the copper was a function of the kinetic energy of the piston. An attempt to lengthen the impulse time was made by attaching the material to be studied to a linen-filled phenolic, which was in turn fixed to the piston. The effect of the phenolic was to act as a bumper to slow the shock wave by multiple reflections. The overall effect of this pulse-lengthening technique was to cause the piston to move into the copper anvil with uniform velocity.

The selection of materials to be used on the faces of the pistons was determined by the mass-absorption coefficient of the material and its thermodynamic properties. The test materials selected were: lead, gold, zinc, aluminum, carbon, and phenolic plastic. At least one of each of these various materials was exposed to the burst from the instrument casting; only lead and zinc were exposed around the periphery.

Four different types of impulse-measuring devices were used in this experiment. Figure 5.48 is a photograph of the simplest of these devices, the single piston. The threaded body of this device screwed into the instrument casting. Wherever possible, the impulse-measuring instruments were designed so that the anvils retracted after the X-ray-impulse measurement.

Three different-sensitivity calorimeters were used to measure the total X-ray intensity incident on the pod. A small lead or copper foil was irradiated by the X-rays through a pin hole. The space between the pin hole and foil was filled with plastic, beryllium, or copper foam. The effect of the foam was two-fold; it acted as a window through which X-rays, and not thermal radiation, could pass, and it provided the thermal insulation necessary to isolate the foil from its environment. The rear of the foil was painted with four temperature-sensitive paints, which recorded the peak temperature of the foil.

The melting of a thin film of metal by the X-rays was used as a method of determining the orientation of the pod with respect to the burst. A small cylinder of styrene was coated with a thin film of carbon. The X-rays were allowed to pass into the styrene through a pinhole. The effect was to leave a spot on the carbon coating. The orientation of the styrene cylinder with respect to the axis of the pod was determined by having the pinhole slightly off the axis of the cylinder. The orientation of this hole with respect to some fixed reference on the instrument casting face was then carefully measured. A determination of the orientation of the axis of the pod was then a simple geometry problem.

The neutron-measuring apparatus consisted of five threshold-detecting foils. The foils were provided by the Army Chemical Warfare Laboratory. The gold foils used to determine the number of thermal neutrons at the pod were mounted as close to the face of the front casting as possible. An unshielded foil was placed at the rear of the calorimeter with the carbon window,

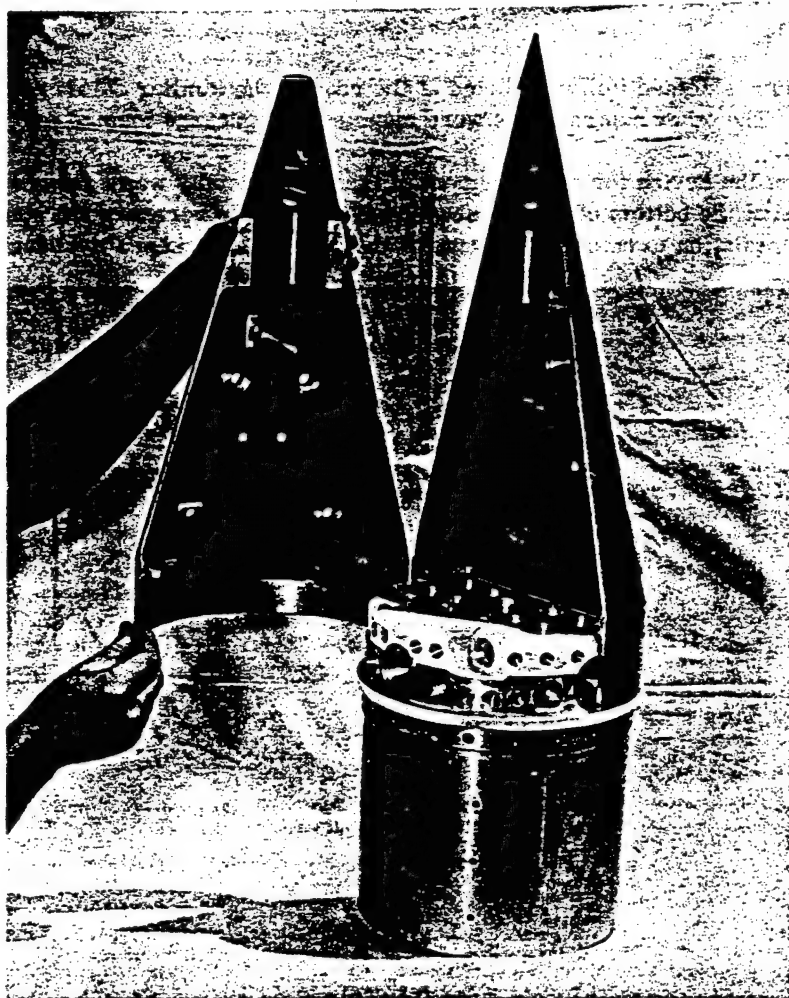


Figure 5.47 Nose cone and instrument canister.

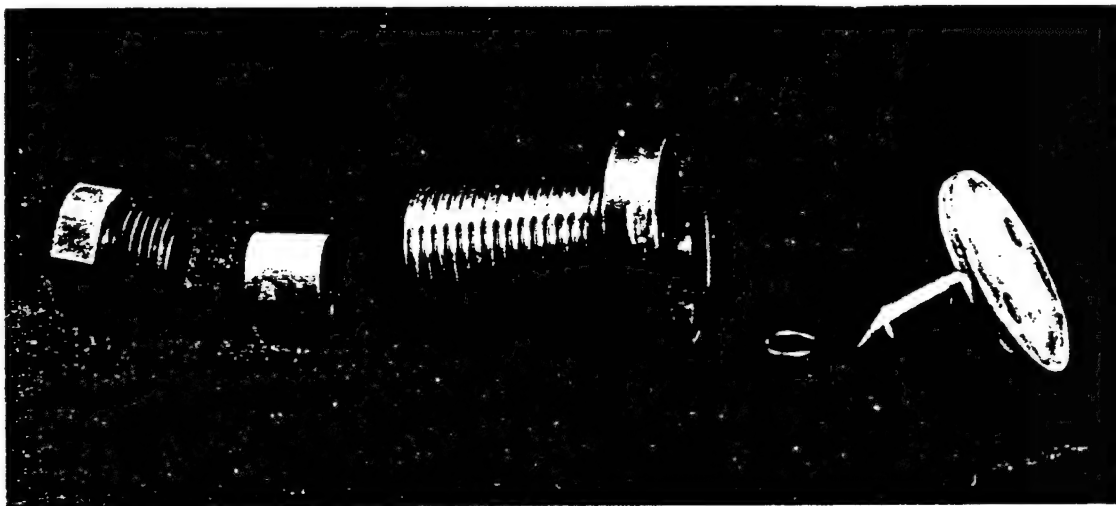


Figure 5.48 Photograph of single piston device.

while a cadmium-shielded foil was placed at the rear of the similar calorimeter with the beryllium window. The other neutron foils were mounted in a package foamed into a space near the tail of the pod.

The heart of the device for measurement of thermal intensity was a thin copper disk, which was positioned at the bottom of a cone-shaped cavity. At the vertex of the cone was a small hole to permit the radiation to enter. The front of the disk was blackened to absorb all radiations in-

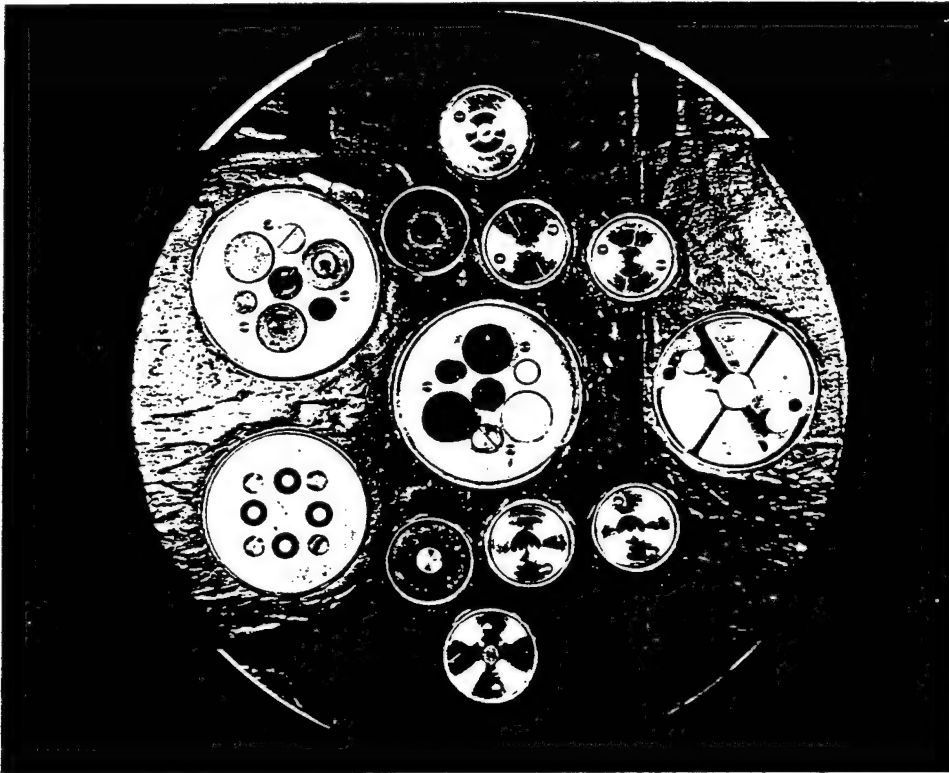


Figure 5.49 Front face of instrument casting (Shot Teak).

cident on it, and the back surface was dotted with an array of temperature-sensitive paints. As the radiation entered the small hole and heated the copper, the paints melted, one by one, thereby indicating the maximum temperature to which the disk rose. The information could then be used to find the time duration and intensity of the thermal pulse.

Ablation measurements were made by exposing the face of a cylindrical test specimen to the fireball and observing how much of the material was ablated. The materials studied were: iron, zinc, copper, magnesium, aluminum, carbon, bakelite, and polystyrene.

Figure 5.49 is a photograph of the front face of the casting after all of the instrumentation had been installed. Scribe lines are visible on most of the devices, as well as on the casting itself. These lines were used to determine the orientation of the various devices before and after the burst. Figure 5.50 is a photograph of the instrument casting from the side. It illustrates the installation of the calorimeters and single-piston devices. Figure 5.51 shows the installation of the thermal-intensity device.

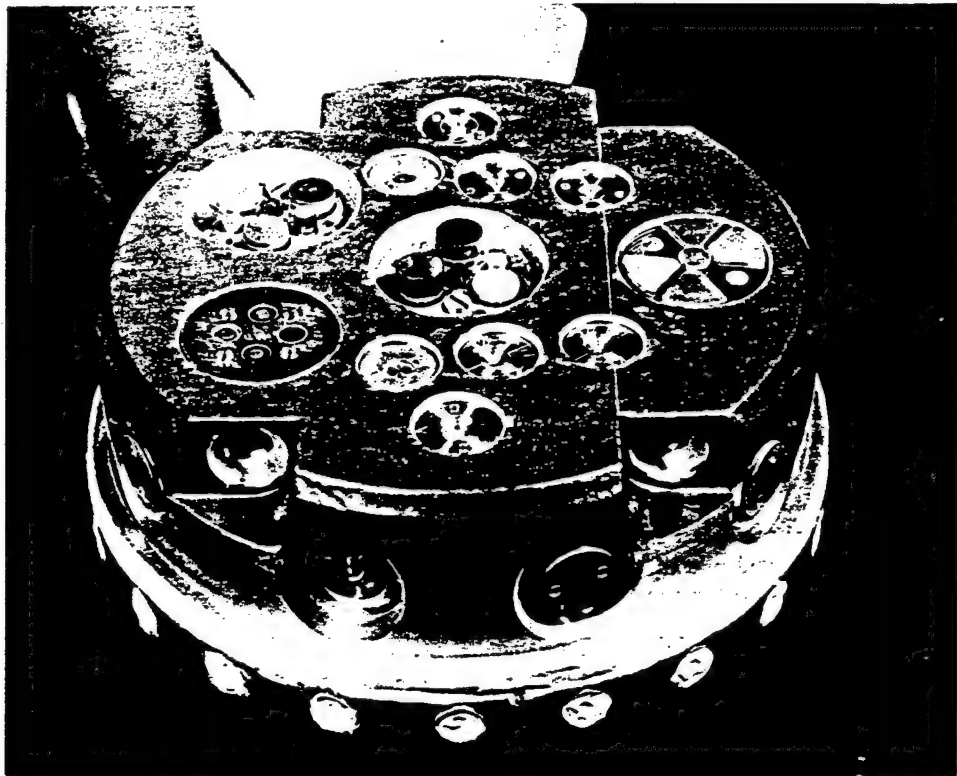


Figure 5.50 Side view of instrument casting (Shot Teak).

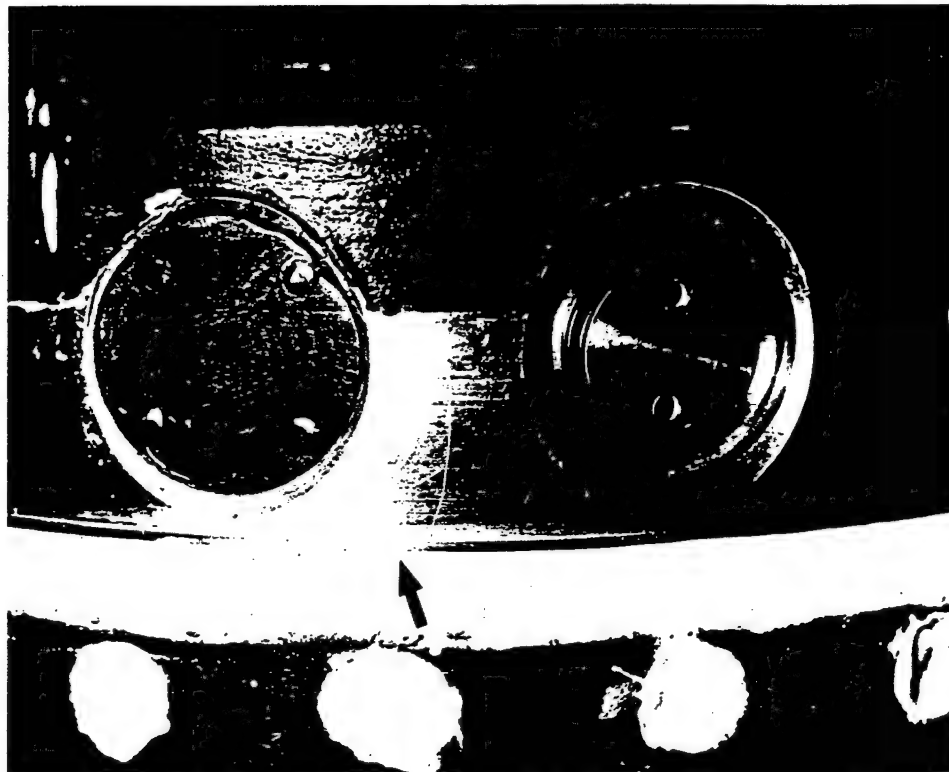
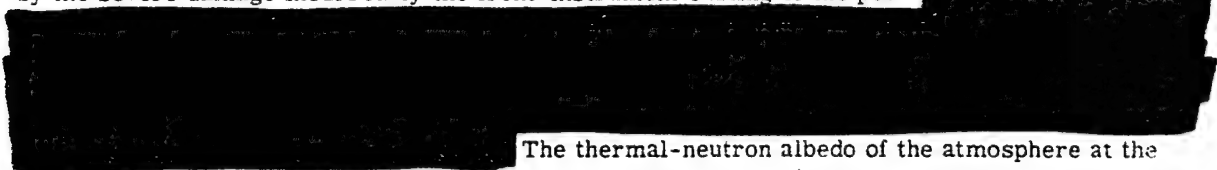


Figure 5.51 Installation of thermal-intensity device.



5.7.4 Results. The Shot Teak pod was recovered about four hours after the detonation. There appeared to be large thermal X-ray-induced mechanical impulses of even greater intensity than had been predicted. These impulses were capable of producing structural failures as evidenced by the severe damage incurred by the front-instrument casting of the pod.



The thermal-neutron albedo of the atmosphere at the high-burst altitude was appreciable. The neutron foils were recovered in sufficient time to allow all of them to be counted. Table 5.15 summarizes the preliminary results of the neutron-intensity measurements. The long thermal pulse (of the order of 100-200 cal/cm<sup>2</sup>) may have been sufficiently intense to cause some effects on a thermally-vulnerable missile.

The environment to which the Shot Orange pod was exposed was far more severe than that of the Shot Teak pod. The use of a finned pod (a requirement placed on the project for aerodynamic

TABLE 5.15 NEUTRON INTENSITY MEASUREMENTS

Activated Material	Nuclear Interaction	Range of Neutron Energies Detected	Half Life	Measured	Predicted
				Neutron Intensity	Neutron Intensity *
				n/cm <sup>2</sup>	n/cm <sup>2</sup>
Gold (Au <sup>197</sup> ) (Cadmium difference)	n, γ	0 to 1 ev	2.7 days	[REDACTED]	[REDACTED]
Neptunium (Np <sup>237</sup> )	n, f	0.75 to 15 Mev	t <sup>-1.7</sup> (t in hours)	[REDACTED]	[REDACTED]
Uranium (U <sup>238</sup> )	n, f	1.5 to 15 Mev	t <sup>-1.7</sup> (t in hours)	[REDACTED]	[REDACTED]
Sulphur (S <sup>32</sup> )	n, p	3 to 15 Mev	14.3 days	[REDACTED]	[REDACTED]
Zirconium (Zr <sup>90</sup> )	n, 2n	12 to 15 Mev	78 hours	[REDACTED]	[REDACTED]

\* The predicted neutron intensity (at a slant range of 23,000 feet) does not include any albedo effects.

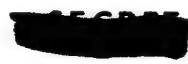
reasons) rendered the pod particularly vulnerable to moderate-blast loads. The centrifugal forces on the ends of the pod were predicted to be of the order of 500 g for a time of approximately 20 seconds. The parachute-ejection system and all other mechanical parts were designed to withstand this load. The Shot Orange pod sank either because of damage suffered during the blast, or all of the various devices to facilitate location and recovery were sufficiently damaged by the blast to be inoperative. Despite an all-night and a 10-hour daylight search by various air and surface components, the Shot Orange pod was not recovered.

5.7.5 Conclusions. Any important conclusions relative to the specific objectives of ICBM-material vulnerability from the effects of a very-high-altitude nuclear detonation must await thorough analyses of the recovered instrumentation. The results of these analyses will be presented in the Project 8.6 final report (Reference 21).

#### 5.8 TEMPERATURE, DENSITY, AND PRESSURE OF THE UPPER ATMOSPHERE DURING A VERY-HIGH-ALTITUDE NUCLEAR DETONATION

5.8.1 Objectives. The objectives of Project 9.1d were to measure the density of the upper atmosphere between 200,000 and 300,000 feet MSL and from this basic measurement to calculate the temperature and pressure.

5.8.2 Background. This project was undertaken to provide basic data on the properties of the atmosphere in the region between 200,000 and 300,000 feet. Such information would support





data obtained in experiments established for evaluating weapon effectiveness. Though experimenters have conducted similar tests in geophysical research to obtain information on the properties of the atmosphere at high altitudes, this was the first time the problem was approached in connection with a nuclear detonation.

5.8.3 Experimental Plan. The technique employed was to measure the drag acceleration of a sphere as it fell to earth when released from a rocket vehicle at an extreme altitude. The sphere contained the air-borne instrumentation consisting of a transit-time accelerometer, a telemetering transmitter and subcarrier oscillator, and a DPN-19 radar transponder.

The transit-time accelerometer was an instrument designed to measure the difference be-

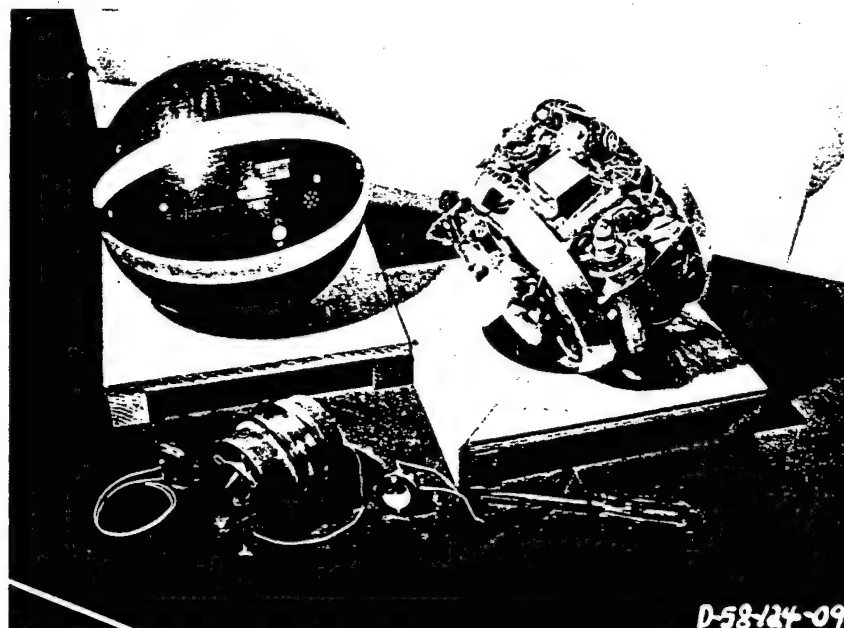


Figure 5.52 Complete sphere assembly.

tween the acceleration of gravity and the acceleration of the body in which the instrument is mounted. Data from this device was presented as a time interval, proportional to the acceleration difference, which was a function of the average air density over the time interval measured. The accelerometer consisted of a reference body, called the bobbin, and a contact ring. The latter was rigidly attached to the sphere and, hence, was the body upon which the drag force acted. The bobbin contained an electromechanical caging mechanism, which positioned the bobbin a known distance from the contact ring, released the bobbin once it was in place, and recaged the bobbin after it struck the contact ring. The sphere telemetry system transmitted the time interval between the release of the bobbin and its contact with the contact ring. The accelerometer operation commenced shortly after sphere ejection and continued throughout the flight.

A plastic cover housed the complete sphere assembly; a plated configuration on the outside of this cover served as the telemetering antenna. An O-ring seal retained bobbin-exhaust pressure inside the sphere, and the pressure was periodically vented by a differential valve. External power for ground operation of the telemetering transmitter and radar beacon was applied through flush-mounted pins. Figure 5.52 shows the bobbin, the sphere assembly, and the plastic cover.

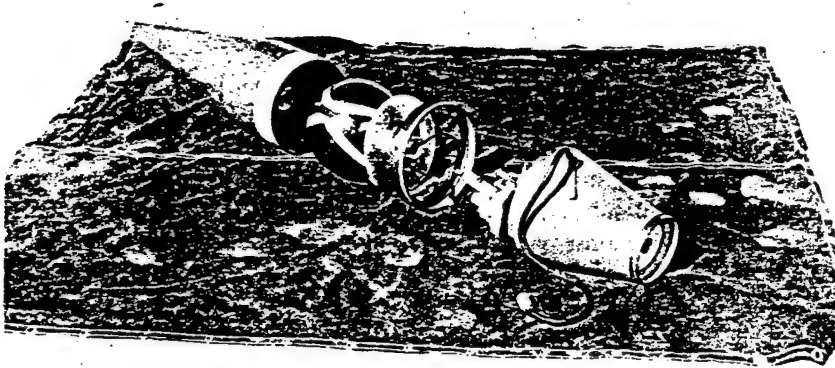


Figure 5.53 Head assembly, exploded view. The frangible blow-off ring is attached to the nose cone and is followed in sequence by the sphere, the pressure plate, the blasting-cap manifold, the programmer, and the aft-body section containing the ballast and external power cable.

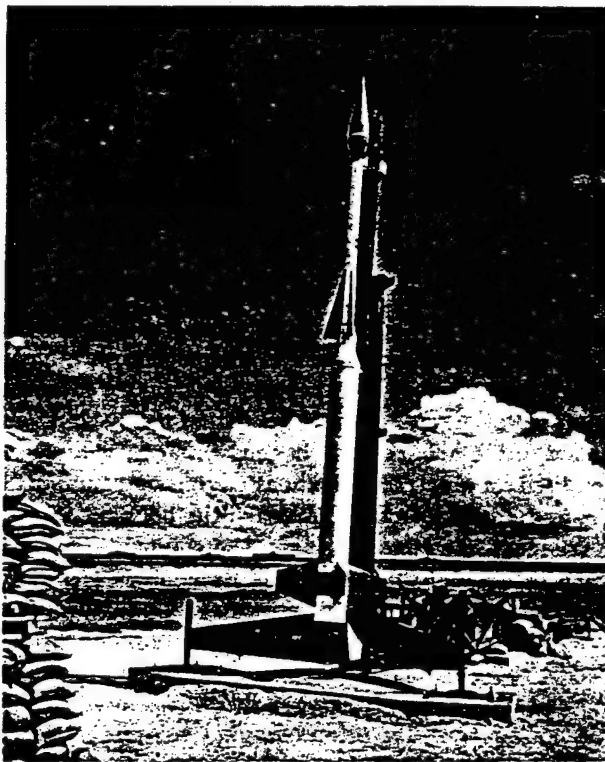


Figure 5.54 Aspen vehicle in firing position.

A Nike-Asp (Aspen) two-stage vehicle was used to fire the sphere into the atmosphere. The first stage was a standard Nike booster employing the four-fin configuration used by the NACA. The second stage was an Asp atmospheric-sounding rocket originally developed by Cooper Development Corporation for use during Operation Redwing. The head assembly (Figure 5.53) contained the sphere, programmer, ejection mechanism, and ballast. The Aspen rocket was fired from a modified Nike launcher. First-stage ignition was provided by a hard-wire system from the firing bunker to the Nike booster. At launch, acceleration started the programmer which fired the Asp and ejected the sphere (at 175,000 feet). Density measurements then began. Figure 5.54 shows the Aspen vehicle in firing position.

The tracking radar was an MSQ-1A system located on Sand Island, about 8,000 feet from the launch site. A Boeing data recorder photographed angles of elevation and azimuth, range, and time as generated by the radar. A telemetry ground station contained receiving and data-recording equipment. The telemetry system provided accelerometer-transit time versus flight-time information. The modulated telemetry carrier from the receiver was registered on magnetic tape. An oscillograph and a 16-mm data camera recorded the output from the discriminator.

Data reduction would have consisted of reading applicable film or oscillograph records and was to have been carried out by students at the University of Hawaii. The radar data would have been card punched and processed through an IBM 650 computer to give altitude and total velocity as a function of flight time. The telemetry data, the total velocity, and a stored table of drag coefficients as a function of Mach and Reynolds numbers would then have been used to compute density, pressure, and temperature. The method may be summarized as: (1) measure the drag acceleration; (2) use the drag equation for a sphere to obtain the density; (3) integrate, using the hydrostatic equation of state to obtain the pressure; and/or (4) integrate, using the hydrostatic equation of state and the universal gas law to obtain the temperature.

5.8.4 Results. Four soundings were made, all of which were unsuccessful. Firing of subsequent rounds was cancelled.

5.8.5 Conclusions. The Nike-Asp, instrumented-sphere system requires further development to prove its suitability for obtaining high-altitude atmospheric data. The DPN-19 radar beacon was unreliable for its application to the falling-sphere technique of measuring this data. The type potassium-hydroxide batteries used were not reliable and were difficult to service. The sphere packaging did not provide easy access for servicing of components. Excessive time was expended in preparing the sphere for flight. The two second-stage-ignition failures which occurred were attributed to either mishandling of the rocket or programmer malfunction and did not indicate any characteristic trouble which might provide an approach to a solution of the problem.

5.8.6 Recommendations. Further refinement of the sphere system should be accomplished, and adequate developmental tests of the entire system should be completed, prior to any further field participations.

## Chapter 6

# BLAST and SHOCK

### 6.1 INTRODUCTION

The Armed Forces have a requirement for design of facilities which would survive near a nuclear burst. Data considered necessary to fulfill this requirement include an accurate definition of the environment in which structures and their contents must survive, a knowledge of the response of the structures to the environment, and a knowledge of the response of the contents of the structure. Five projects of Program 1 had the objective of providing the free-field blast and shock conditions near a nuclear detonation. Experiments were conducted to measure and analyze crater dimensions; air-blast pressures; and ground-shock pressures, accelerations, shock spectra, and displacement.

Many studies have been made of blast and shock parameters on past operations, and particularly on Operation Plumbbob. Operation Hardtack projects were designed to extend the available data to include the effect of three important values: soil type, long-duration blast waves (from high-yield devices), and higher pressures than previously studies. The effect of high (Mt range) yields, and the associated long duration air-blast waves can be determined only in the EPG, because of yield restrictions in effect at NTS.

The specific objectives to be fulfilled by each project are listed below:

1. Project 1.4 had the objective of measuring the physical dimensions of craters produced by Operation Hardtack shots, and of measuring the residual ground displacement outside the crater.

2. Project 1.7 had the following objectives: (a) to measure overpressure and dynamic pressure versus time as a function of ground range in the high-pressure region; (b) to provide free-field input data and instrumentation support for other projects in Programs 1 and 3.

3. Project 1.8 had the objective of measuring ground motion (acceleration and relative displacement) as a function of depth, range, and yield.

4. Project 1.9 had the objective of determining the following factors: (a) attenuation of soil pressure above and below the water table; (b) the effect of air-blast-wave duration on pressures transmitted through the soil; (c) the effect of flexibility on the pressure transmitted to a structure; (d) the ratio of horizontal to vertical underground pressures.

5. Project 1.12 had the objective of determining the surface level shock spectra (displacement, velocity, and acceleration) as a function of distance and yield.

The physical location of the project instrumentation was critical in several respects. First, a land mass of considerable size was needed to provide sufficient space to accommodate the desired instrumentation layout. A blast line several thousand feet long was needed for Project 1.7; Project 1.8 required space to drill twelve holes 100 feet deep; and Project 1.9 needed two trenches over 100 feet long. Second, it was necessary to participate on two shots, one in the kiloton range to compare with Shot Priscilla of Operation Plumbbob, and one in the megaton range to allow a study of the effect of the resulting longer positive-phase duration blast wave. The choice of shot participation was quickly narrowed to Shots Koa and Cactus, having predicted yields of 2 Mt and 15 kt, located on Sites Gene and Yvonne. Although the zero height of burst was representative of many probable applications, it represented a variable, since little previous data was available for this type of burst.

Figures 6.1 and 6.2 show the final locations of the project instrumentation stations.

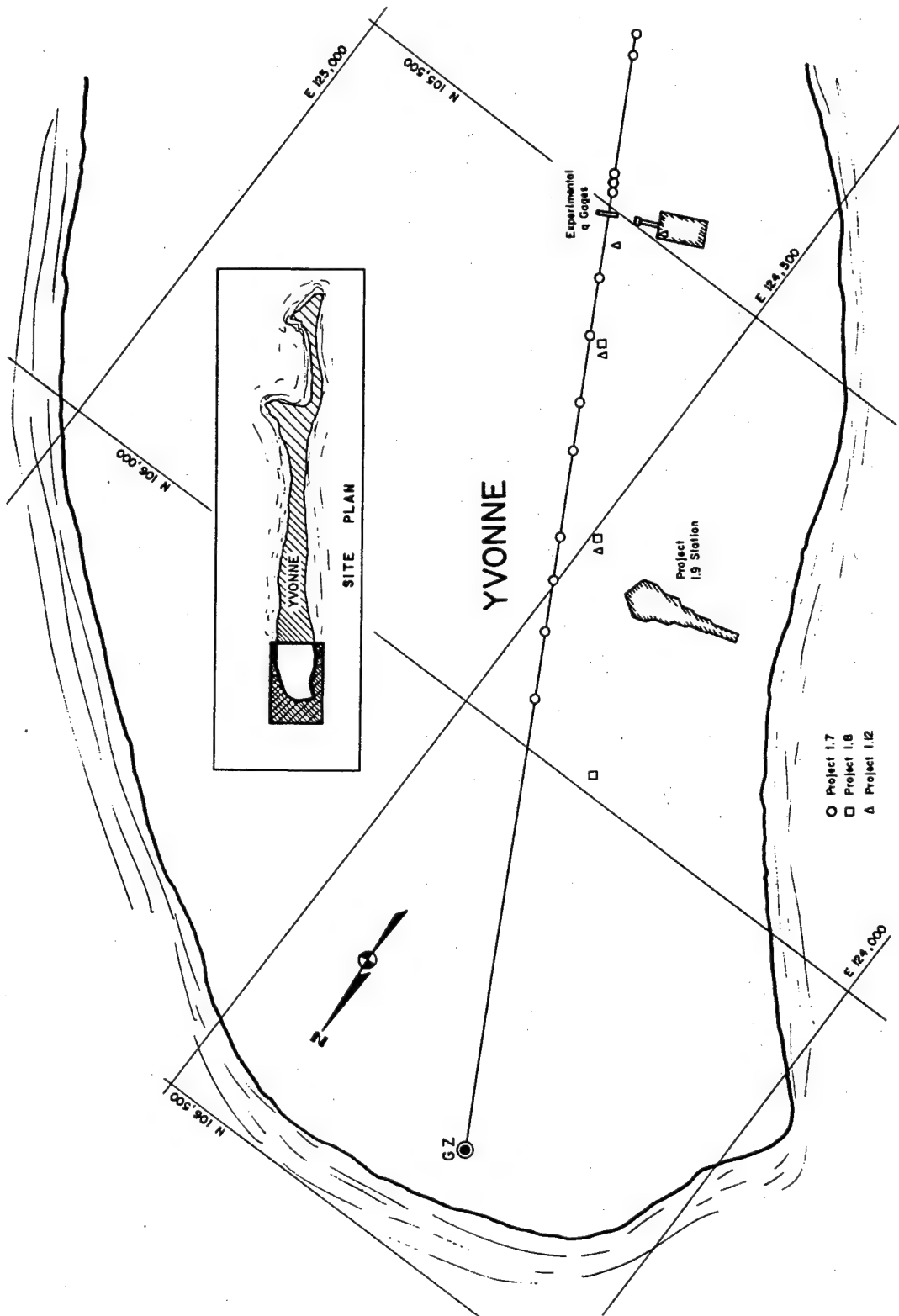


Figure 6.1 Instrumentation location, Shot Cactus.

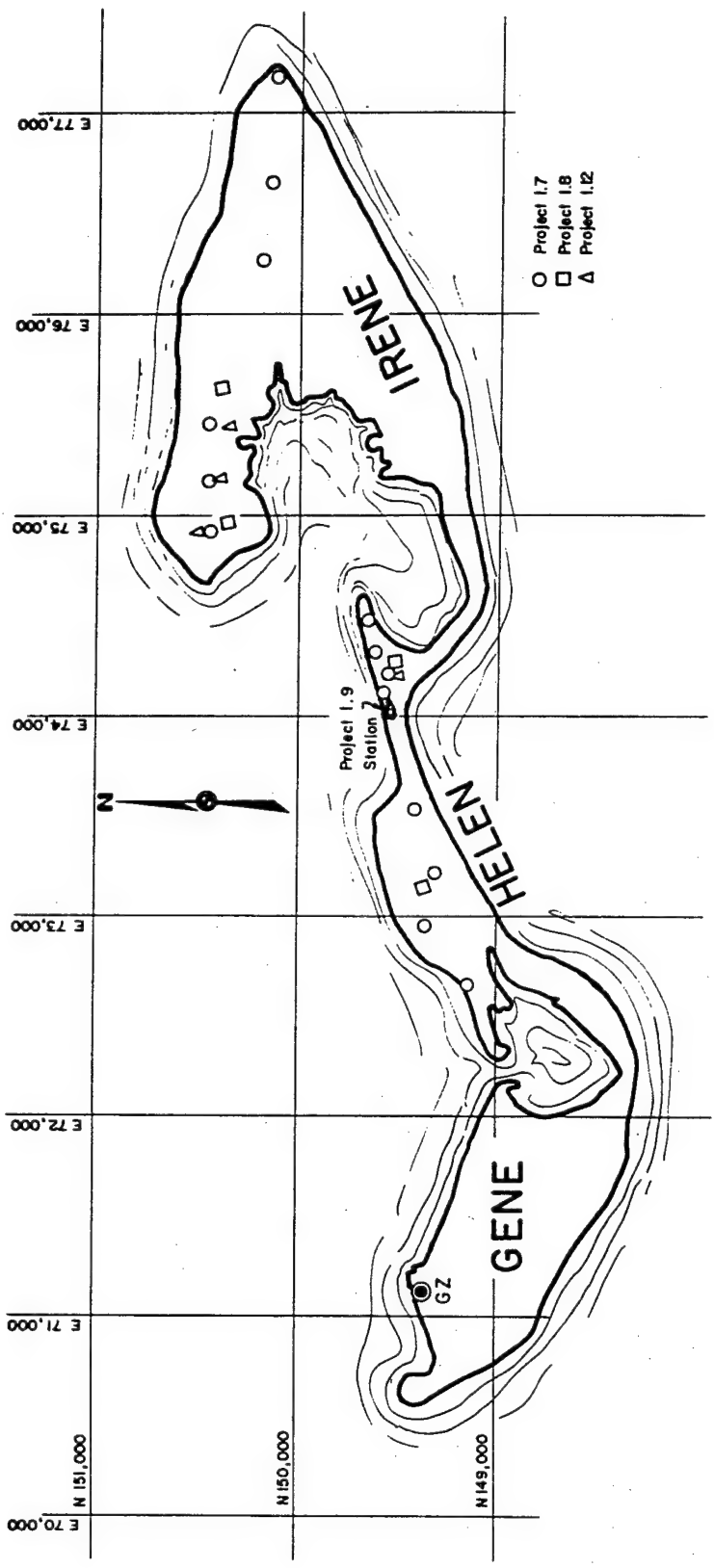


Figure 6.2 Instrumentation location, Shot Koa.

## 6.2 CRATER MEASUREMENTS

Cratering effects of nuclear devices were investigated during Operations Greenhouse, Buster-Jangle, Ivy, Castle, Teapot and Redwing. Measurements consisted essentially of preshot and postshot surveys, and the radius and depth data obtained was used to establish an empirical prediction method. Three crater-effect shots were made at NTS: Jangle U, Jangle S, and Teapot Ess. Data from these shots, plus extensive high-explosive cratering studies (such as Operation Mole), were the basis for the TM 23-200 sandy-soil curves for crater radius and depth versus height of burst (Reference 15, Figures 2.20 through 2.26b). Data from craters at the EPG were observed to form a curve of the same general shape as the sandy-soil curve, and, therefore, the EPG craters were incorporated into the prediction method by means of multiplication factors to be used with values from the sandy-soil curve. A typical factor indicated that craters formed in saturated coral and washed by waves are twice as large in diameter as a crater at the NTS produced by a device of the same yield.

Knowledge of surface bursts is important since the surface burst appears to be the most probable tactical condition for producing craters. It is apparent from Figures 6.9 and 6.10 that considerable scatter exists in the near-surface burst data from previous EPG operations. Additional data were needed to confirm the tentative curves and scaling factors used to describe EPG craters.

All crater data were obtained by means of preshot and postshot surveys. Three surveying methods were used: stereographic aerial photography, rod and transit surveys, and fathometer and lead-line soundings.

Aerial photography was provided through Program 9, and was accomplished using an RB-50 aircraft equipped with a T-11 gyro-stabilized aerial camera. Aerial surveys were made of Shots Koa and Cactus, (Figures 6.5 through 6.8).

Rod and transit surveys were made of the land areas around Shots Koa and Cactus, along the radii shown in Figures 6.3 and 6.4. Lead-line surveys were made where it was necessary to extend the radii over parts of the reef which were covered with water. In addition, a number of concrete gage pads, pipeline supports, etc., were surveyed out to several crater radii to determine residual ground displacement.

Fathometer surveys were made of barge Shots Oak, Holly, Magnolia, Butternut and Yellowwood as part of the normal operations of Holmes and Narver, and the results were made available to Project 1.4.

Preshot and postshot aerial photographs and topographic surveys of Shots Koa and Cactus are shown in Figures 6.3 through 6.8. Scaled data are plotted with previous data in Figures 6.9 and 6.10. The most apparent feature of the results was that the crater from Shot Koa had the largest scaled radius (by a factor of 15 percent) ever measured. It is interesting to note that Shot Seminole, which had the next largest scaled radius, and Shot Koa were detonated inside almost identical water tanks, each containing about a million pounds of water. It is believed that the water shielding changed the energy partition and increased the energy coupling to the ground.

The Shot Cactus crater compared well with the TM 23-200 sandy-soil curve when the environmental factors (Figure 2.20, Reference 15) are applied. The scaled radius is divided by the 1.5 factor given for unwashed craters in saturated soil, and divided by 0.9, because the Site Yvonne soil structure is more rocklike than the Nevada soil upon which the sandy-soil curve was based, but not as hard as granite or sandstone, for which TM 23-200 gives a factor of 0.8.

## 6.3 AIR BLAST

Air-blast measurements of some kind have been made during every operation since Trinity, and the data accumulated probably represents the most extensive documentation of a single phenomenon available in the effects field. Nevertheless, certain areas exist in which data is needed

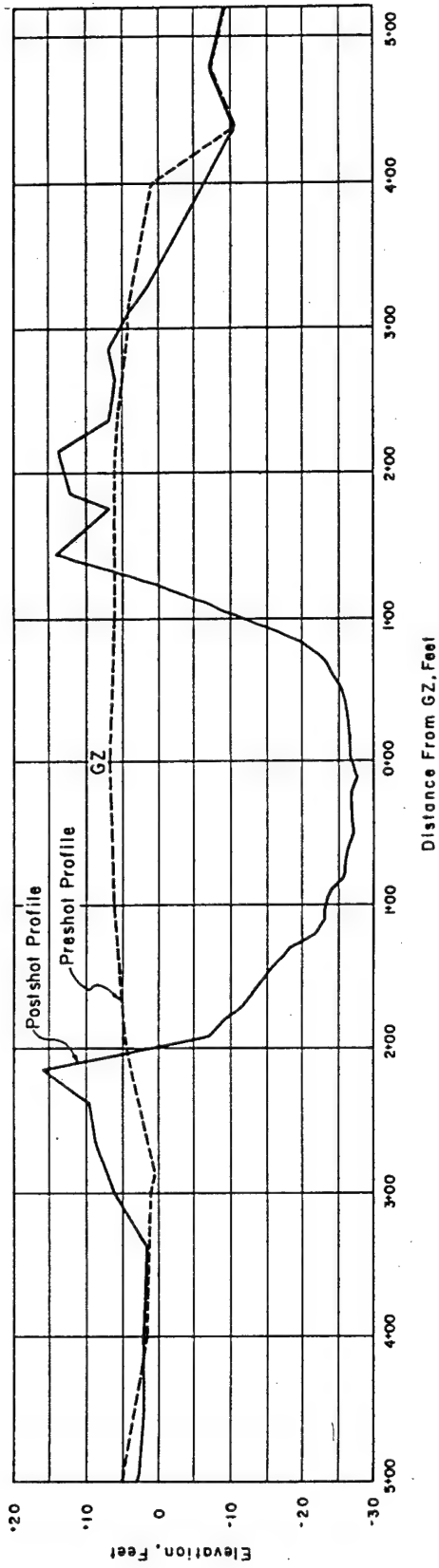


Figure 6.3 Cactus: Preshot and postshot surveys.

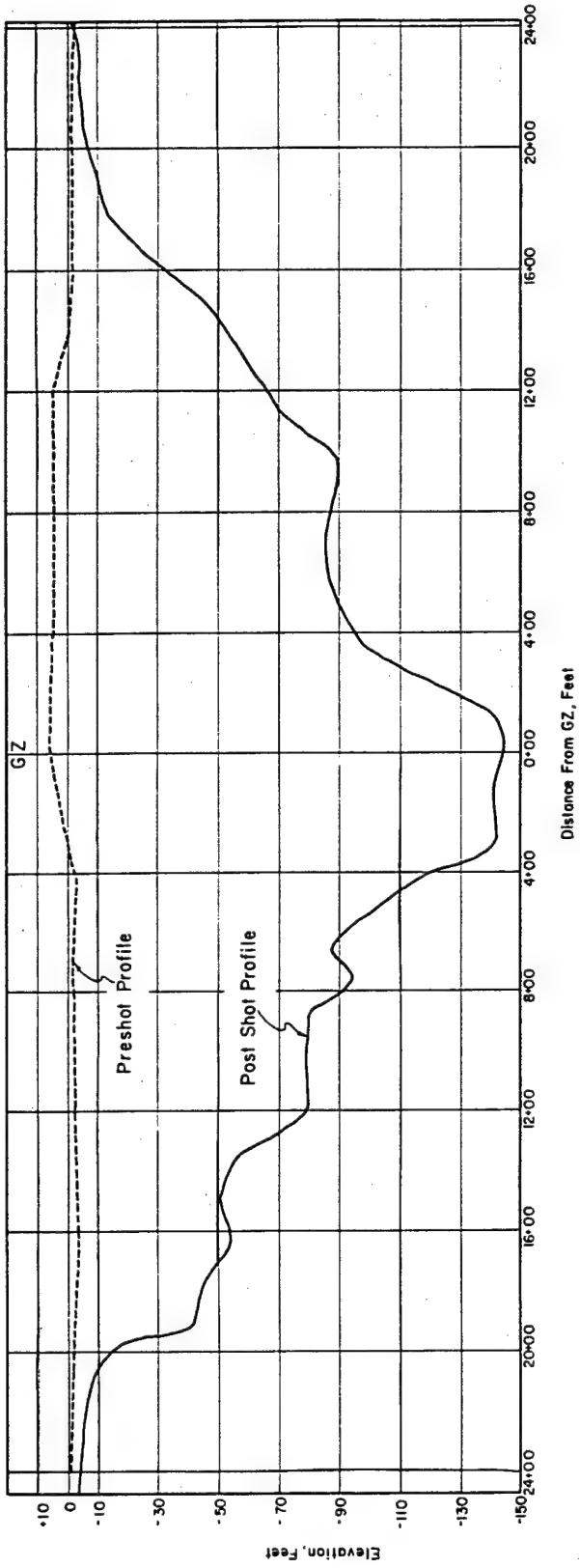


Figure 6.4 Koa: Preshot and postshot surveys.



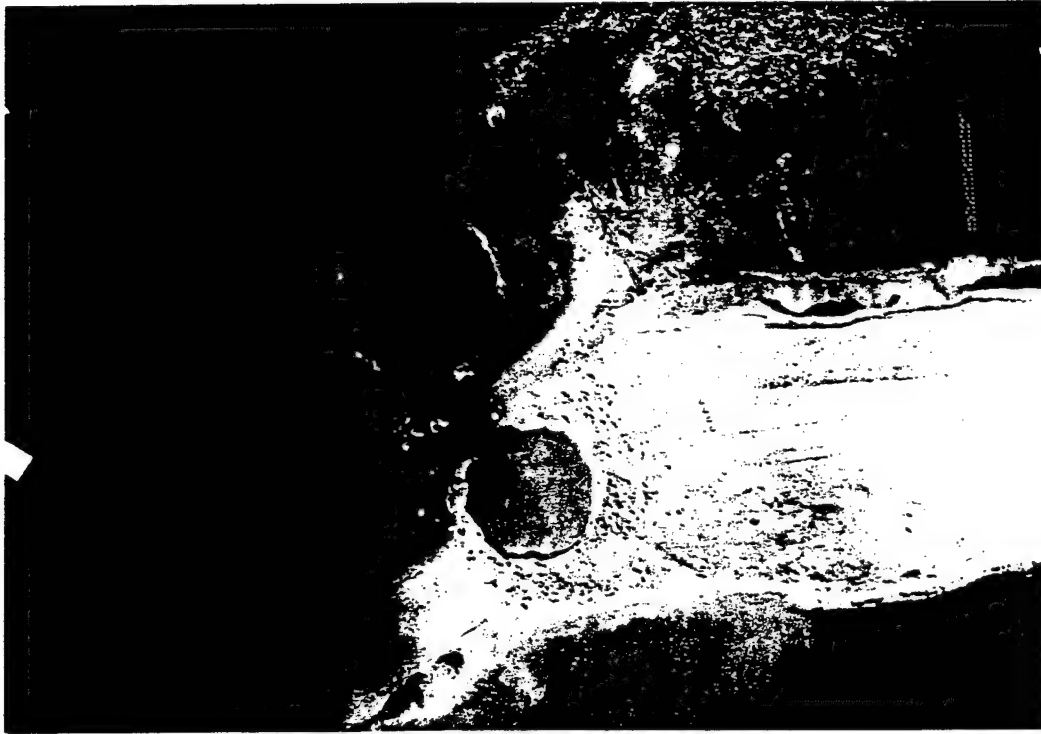


Figure 6.5 Cactus preshot aerial photograph.



Figure 6.6 Cactus postshot aerial photograph.

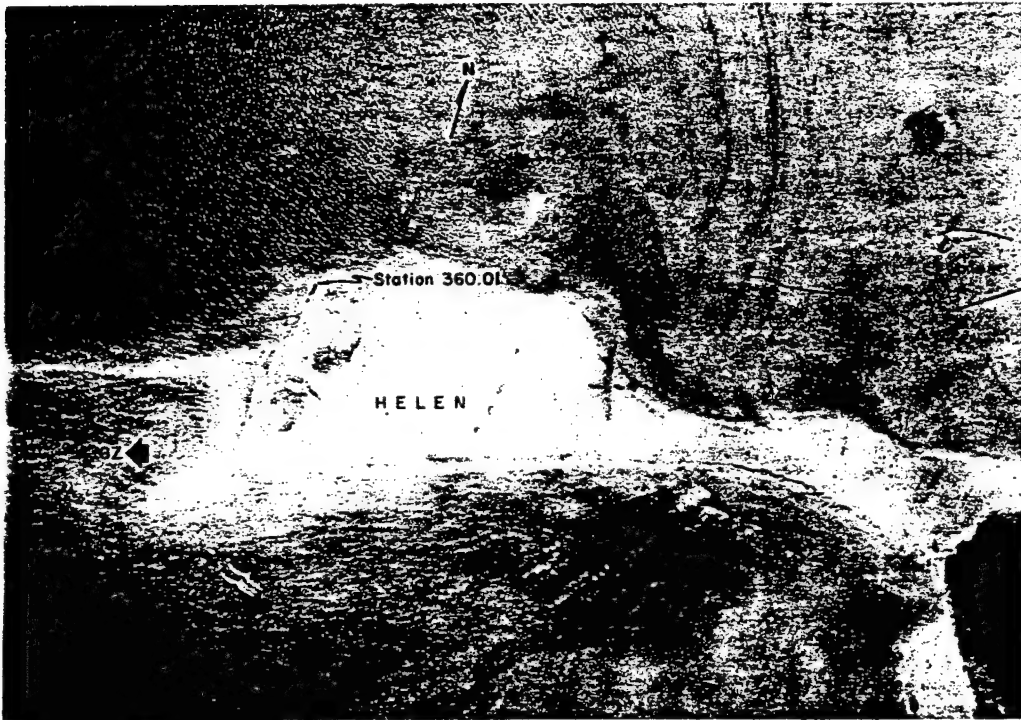


Figure 6.7 Koa preshot aerial photograph.

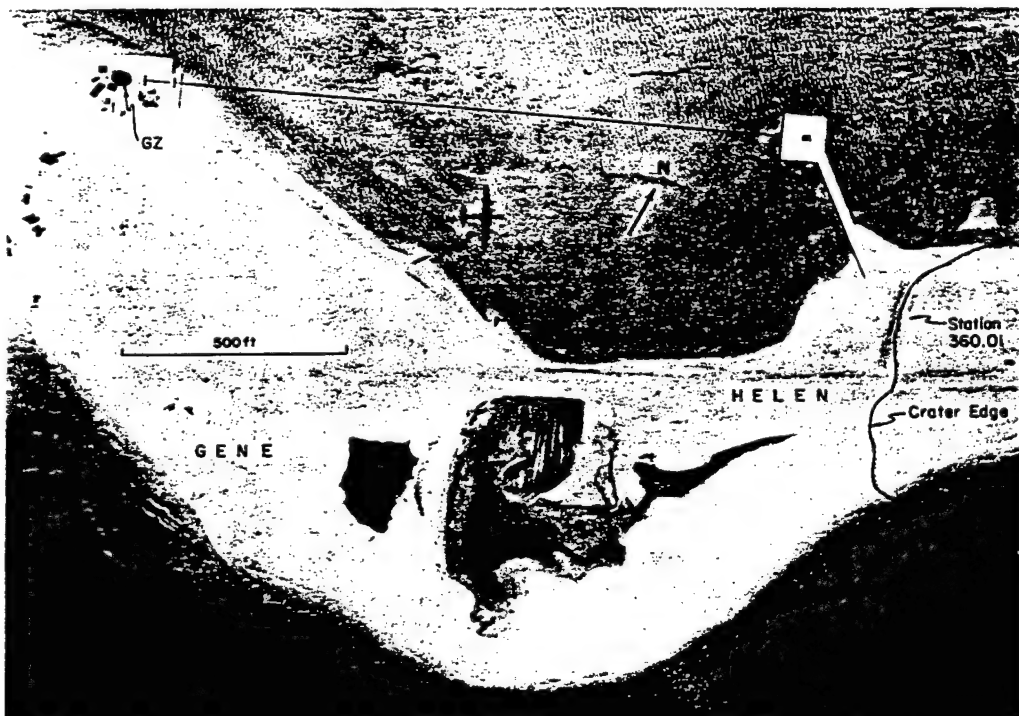


Figure 6.8 Koa postshot aerial photograph.

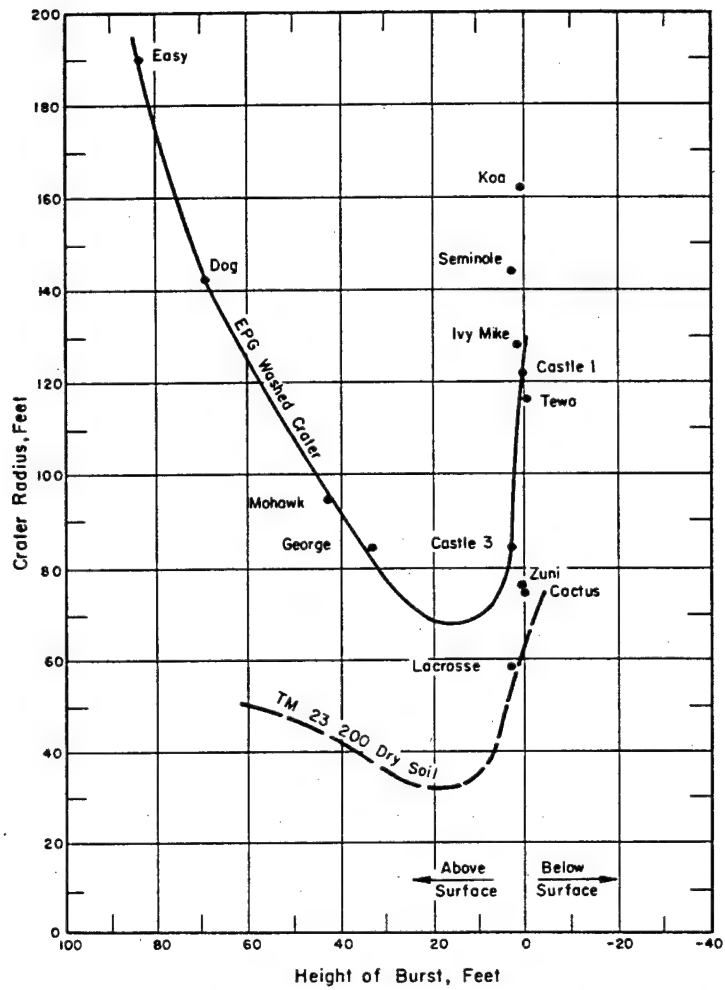


Figure 6.9 Crater radius versus height of burst, scaled to 1 kt.

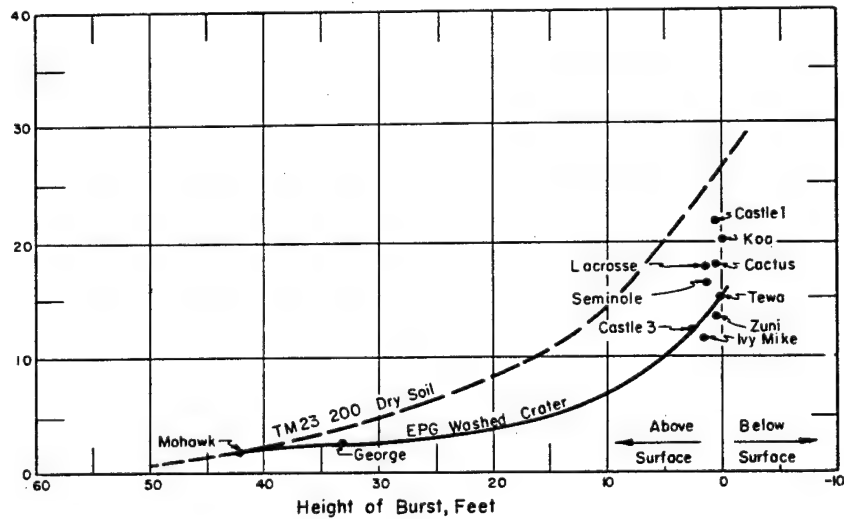


Figure 6.10 Crater depth versus height of burst, scaled to 1 kt.

to verify theoretical studies, extrapolation techniques, and prediction methods. Of primary interest at the moment is the region of pressures up to 1,000 psi, and particularly those produced by surface bursts.

Pressures from a surface burst ideally would appear to have been produced by a burst twice as large as the actual yield, based on a free-air prediction method. The reason, of course, is that all the energy from a surface burst appears in a hemisphere (assuming an ideally reflecting surface), rather than in a sphere as for the free-air case. Strictly speaking, it would seem that the 2W correlation should apply regardless of reflection-factor considerations, since the 2W assumption is incorporated into the hydrodynamic calculations used to determine the yield of thermonuclear devices. Nonetheless, it has been found in past operations that pressure data correlate better if the free-air curve for 1 kt is scaled to 1.6 to 1.8 kt, rather than the ideal value of 2 kt. It is current practice to use the TM 23-200 free-air curve (Figure 2.3, Reference 15) scaled to 1.6 kt to correlate pressures from a surface burst.

There is some doubt as to the probability of precursor formation from surface bursts. A precursor was observed on Shot LaCrosse, (37.8 kt), Operation Redwing, but it was believed that this case represented about the lowest yield which could be expected to form a precursor under surface-burst conditions. Shot Zuni of Operation Redwing (3.53 Mt) produced a clearly defined precursor, but Operation Castle Shot 6 (1.7 Mt) did not. It was hoped that Shots Koa (1.3 Mt) and Cactus (18 kt) would give further data on precursor phenomena from surface bursts.

Results of a study of the very-low-pressure region (less than 1 psi) carried out at the NTS indicated that there are atmospheric inhomogeneities such as thermal inversions which often result in large prediction errors. It was desired to conduct a similar study in the more homogeneous atmospheric conditions of the EPG to determine whether pressures at long ranges could be accurately predicted under any circumstances. The data are useful not only as input for blast-sensitive military targets (such as blimps) but also as an aid to predictions needed during the test series.

The blast line layouts for Shots Koa and Cactus are shown in Figures 6.1 and 6.2. For Shot Koa, 30 overpressure (Pt) gages and 4 dynamic-pressure (q) gages were used at 18 stations covering the range of predicted pressures from 1,000 psi (at 1,550 feet) to 30 psi (at 6,023 feet).

The Shot Cactus blast line used 25 Pt gages and 5 q gages at 19 stations extending from predicted pressures of 400 psi (at 470 feet) to 1 psi at 7,860 feet.

The Pt gages and q gages used in the blast lines were the standard BRL self-recording gages used on several previous operations. Free-field support was simplified by the fact that four of the projects being supported, 1.9, 1.12, 3.2 and 3.6, were located essentially on the blast line, and pressure gages supporting these projects comprised a considerable part of the blast line itself. Because of financial considerations, Project 3.2 experimental structures were used as recording stations on both shots.

An objective added in the field was the evaluation of several types of dynamic-pressure gages to determine the response of each type to dust loading (the momentum flux of dust particles measured). To fulfill this objective, self-recording and electronic versions of the Sandia Greg gage, Sandia Snob gage, the standard pitot-static q gage, an electronic SRI supersonic total-head gage and a BRL self-recording total head (gooseneck) gage were installed side by side on the blast line 980 feet from Shot Cactus ground zero. After Shot Cactus, the four self-recording gages were installed on Site Irene, 6,023 feet from Shot Koa ground zero.

The Greg gage was designed to measure a large percentage of the total-momentum flux (dynamic pressure) of the dust as well as of the air in a dust-laden blast wave, while the Snob was designed to minimize the dust loading measured. The other gages presumably measured all of the air-dynamic pressure plus some unknown fraction of the dust momentum. It was hoped that the Greg and Snob gages would permit an analysis of the dust momentum, from which the dust response of the other gages would be evaluated.

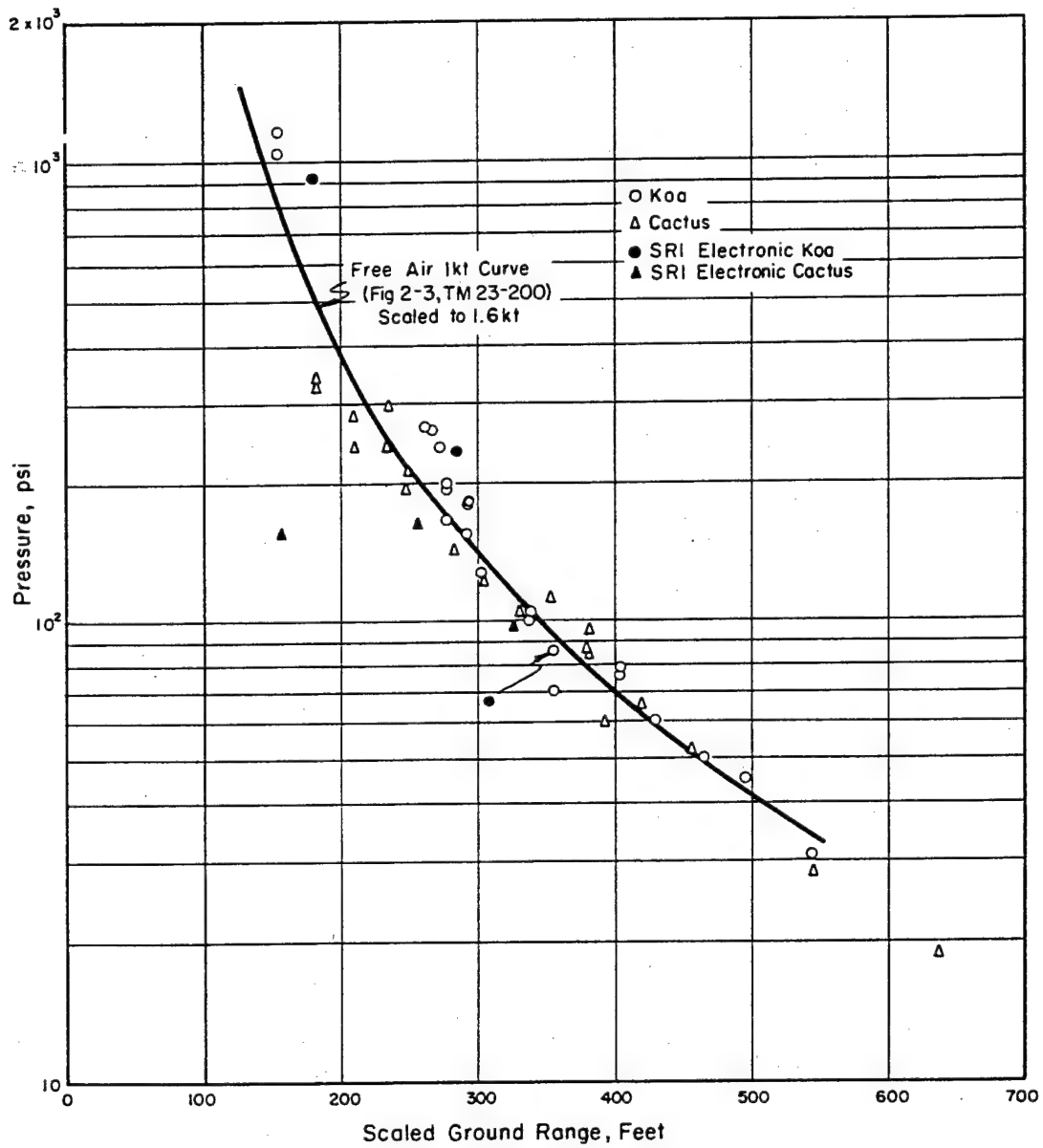


Figure 6.11 Scaled pt data, Shots Cactus and Koa, with free-air 1 kt curve (from TM 23-200) scaled to 1.6 kt.

About 90 percent of the Pt gages used on the Shot Koa and Shot Cactus blast lines were recovered, and produced readable records. Good records were obtained from about half of the Shot Cactus gages. The remainder had poor records or peak pressures only. Twenty-six of the 30 gages used on Shot Koa were recovered, of which 15 had good records, 9 had poor records, and 2 had no record. In addition to the blast line data, Project 1.8 had three electronic gages on each shot. Overpressure data scaled to 1 kt, using modified Sachs scaling, are compared with the 1 kt

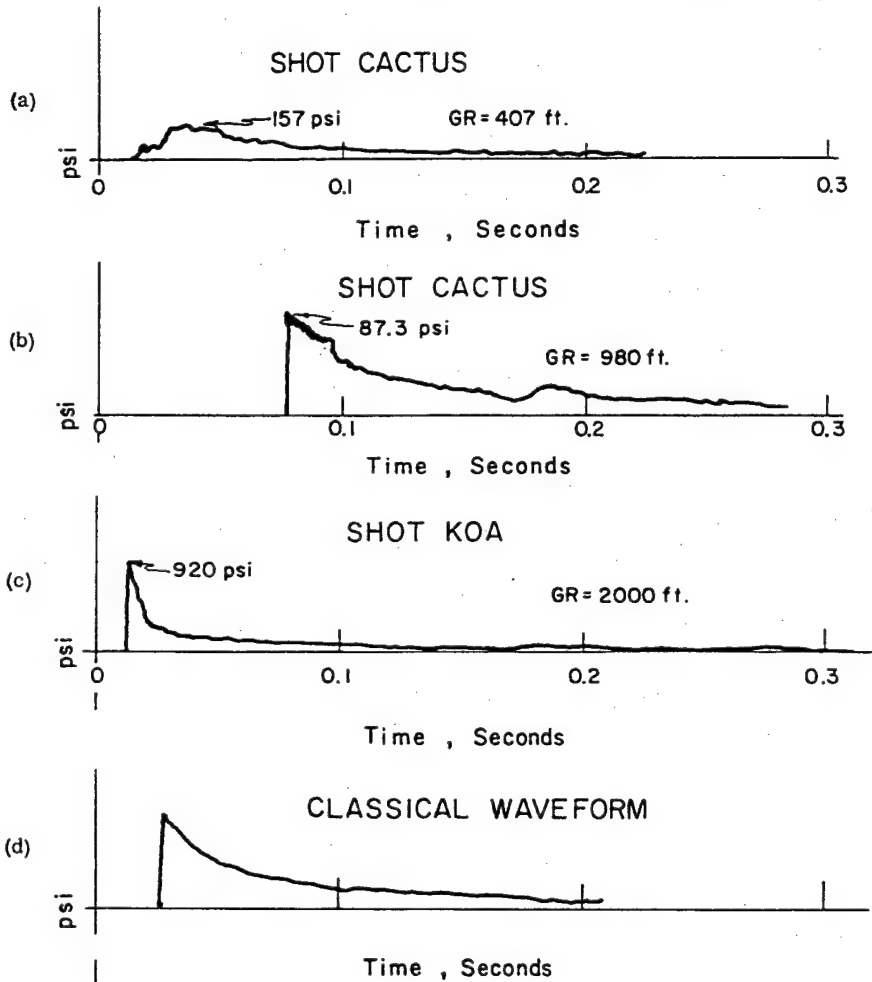


Figure 6.12 Pt wave forms.

free-air curve from TM 23-200 (Figure 2.3 of Reference 15) scaled to 1.6 kt in Figure 6.11. The values represented are preliminary readings; the expected accuracy is  $\pm 10$  percent.

The wave forms shown in Figure 6.12 have sharp initial rises, indicating that neither shot produced a precursor. The one exception was the record from the electronic gage 407 feet from Shot Cactus ground zero shown in Figure 6.12(a). Predicted pressure was 600 psi, actual pressure was 157 psi, with a severely disturbed wave form. Another apparent anomaly was noted on Shot Cactus. All gages on Shot Cactus between 450 and 980 feet show the type of wave form shown in Figure 6.12(b), a sharp rise, slower than normal decay for 50 to 100 msec, followed by a rapid decay and finally, normal decay. At ranges greater than 980 feet, all wave forms are classic as shown in Figure 6.12(d). The three closest stations on Shot Koa recorded wave forms similar to Figure 6.12(c). Wave forms were classic at greater ranges.

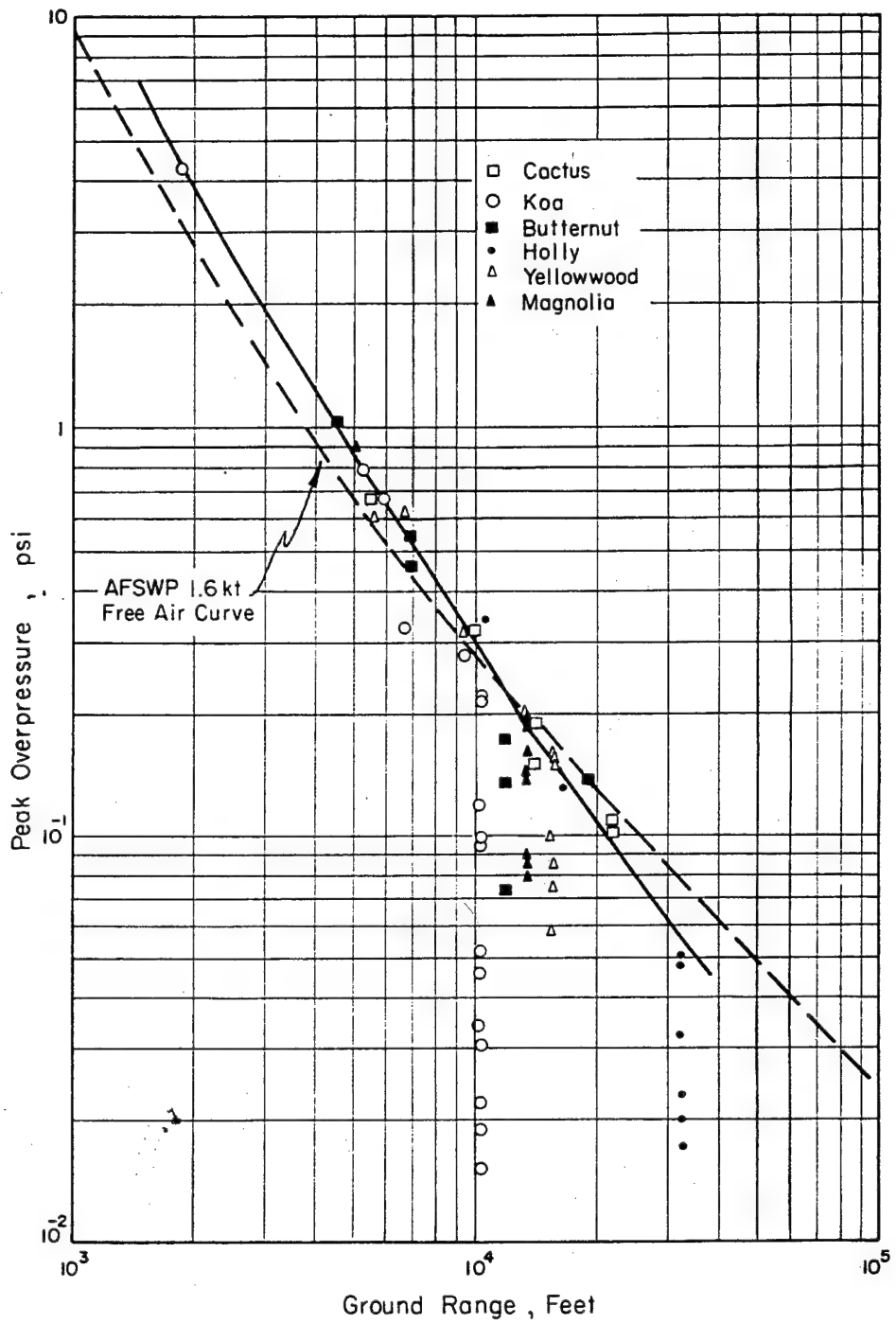


Figure 6.13 Scaled VLP data.

It should be pointed out that there appeared to be a significant difference between the scaled values of peak overpressure from Shot Koa and those from Shot Cactus. Both sets of data generally agree with the TM 23-200 free-air curve scaled to 1.6 kt, the usual correlation for surface bursts. However, most of the Shot Koa data above 100 psi fall above the 1.6-kt curve, while the Cactus data generally fall below. Of the 15 Shot Koa values above 100 psi, 11 deviate from the 1.6-kt curve by more than 10 percent, and all of these are above the curve. Seven Cactus points deviate by more than 10 percent, and 6 of these are below the curve. This trend was not expected, since past experience indicated that Shot Koa might produce a precursor. No explanation of the apparent anomalies can be offered at the moment.

The results of the dynamic pressure-gage evaluation were inconclusive. Of the eight gages tested on Shot Cactus, five produced records, but only two were considered good. Peak readings from the good records were 120 psi for the electronic pitot-static gage, and 137 psi for the electronic Snob gage. These results are surprising, since the Snob gage, which registers none of the dust momentum, was expected to give the lowest reading of any of the gages. The three records which were recovered from the self-recording gages on Shot Cactus show severe acceleration effects and are not expected to be of much value. Two of the four self-recording q gages on Shot Koa produced readable records. Peak values were 17.6 psi from the Snob gage, and 47.2 from the pitot-static gage.

A total of 82 overpressure measurements, 63 of which were successful, were attempted in the very-low-pressure region. The scaled data is compared with the 1.6-kt curve in Figure 6.13.

#### 6.4 GROUND MOTION

A theoretical model of ground motion caused by a nuclear detonation is far from complete. Approaches have been taken which describe the effects of an ideal blast wave on earth models of certain characteristics, but no theory has so far been able to account for all of the effects which influence data obtained in test operations. Measurements of earth accelerations at relatively low pressures were made during Operations Buster-Jangle, Tumbler-Snapper, Upshot-Knothole, Ivy and Castle. About the only consistent trend noted was that the vertical maxima corresponded time-wise with the arrival of the air-blast wave over the gages. Extensive acceleration data, covering a wide range of depths and incident overpressures, was obtained during Operation Plumbbob, but analysis of these data is not complete.

Studies have been made of transmission of ground pressures in Operations Buster-Jangle, Upshot-Knothole, and Plumbbob. The principal difficulty encountered was the interpretation of the data, because there was considerable uncertainty in the relation between the true-earth pressure and the values measured as earth pressure. Types of instrumentation have included Carlson stress cells, oil-filled bags and flexible-aluminum diaphragms. The use of drums with aluminum diaphragms in place of drumheads, Project 1.7, Operation Plumbbob (Reference 22), was the most recent development, but Operation Plumbbob results have not been fully analyzed.

Some of the variables influencing ground-shock phenomena whose effects have not been adequately defined include soil characteristics, such as the elastic constants, moisture content, and dissipative properties; refraction properties of inhomogeneous media; positive-phase duration of the air-blast wave; and height of burst, particularly air bursts compared to surface bursts. The experiments conducted during Operation Hardtack were designed to provide information on these variables, and to extend the limit of knowledge of basic-effects phenomena into higher pressure regions than previously investigated.

**6.4.1 Accelerations.** To fulfill the objectives of measuring ground acceleration and displacement, a total of 54 gages were installed, 27 for Shot Cactus, and 27 for Shot Koa. Gage locations are shown in Table 6.1. The locations of the stations, at predicted pressure levels of 600



psi, 200 psi, and 100 psi, are shown in Figures 6.1 and 6.2. The results of the stations at 100 and 200 psi were to be compared with similar measurements made during Operation Plumbbob; the 600-psi station was installed to extend the available data to higher pressure regions.

Standard Wiancko variable-reluctance accelerometers were used. Horizontal and vertical accelerometer pairs were installed in special waterproof canisters designed for underground placement.

Of the 27 acceleration channels on each shot, 22 from Shot Cactus and 21 from Shot Koa produced good records. Peak values from Shots Koa and Cactus are plotted and compared with predictions in Figures 6.14 and 6.15, respectively. Some typical wave forms are shown in Figure 6.16.

Predictions of vertical accelerations shown in Figures 6.14 and 6.15 were based on the assumption of classic air-blast wave forms and the attenuation of acceleration with depth deter-

TABLE 6.1 GAGE LOCATIONS FOR EACH PROJECT 1.8 STATION

Depth	Accelerometer		
	Horizontal and Vertical	Displacement	Overpressure
ft			
0	◇	◇	◇
10	◇	—	—
30	◇	◇	—
50	◇	◇	—
100	◇	◇	—

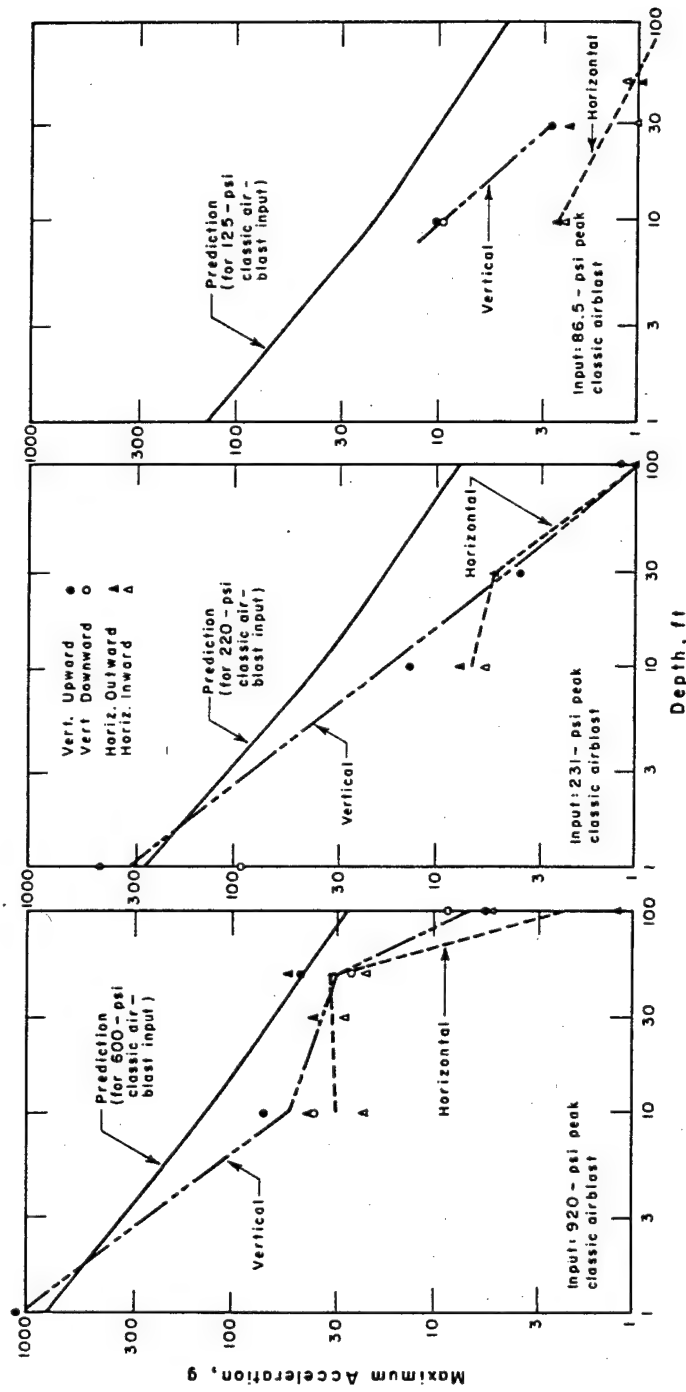
mined from several air bursts at NTS. Predictions for horizontal accelerations were not made, but it has been observed that horizontal accelerations do not exceed  $\frac{1}{2}$  to  $\frac{1}{3}$  of the vertical values.

In two cases, the predicted input conditions were not fulfilled, these two being the 600-psi stations for Shots Koa and Cactus. Both stations had an electronic Pt gage at the ground surface directly over the accelerometers. The record from Shot Koa showed a steep rise to a peak of 920 psi, while the record from Shot Cactus, at essentially the same scaled range, showed a slow rise to a peak of 157 psi. No mechanical or electronic malfunction was known to have affected either gage, and there is no obvious reason to discount either value.

Peak vertical accelerations at the surface agreed with predictions within a factor of two, but peak vertical accelerations at depths below the surface, in general, fell below predicted values by a factor of two to four. The general indication was that attenuation of vertical acceleration with depth is greater in EPG soil than in Nevada soil.

Horizontal-peak values, on the other hand, were considerably larger than expected, equal to, or greater than, vertical values. The high horizontal-peak values and the complex wave forms indicate that a significant amount of energy was transmitted by refraction and reflection, in addition to the normally dominant shock produced by the air-blast wave.

Probably the most significant feature of the acceleration records was their complexity, compared to a typical record obtained from Operation Plumbbob, Figure 6.16. Normally, it would be expected that the peak accelerations would correspond to the arrival of the air-blast wave over the gage. At the two most distant stations (predicted 200 psi and 100 psi) on both Shot Koa and Shot Cactus, the records indicate that mechanisms other than the induced shock produced by the air-blast wave had considerable effect on the accelerations. Some records show considerable motion well before blast-wave arrival, and others show the greatest accelerations occurring well after blast-wave arrival. In addition, records from both shots show random high-frequency,

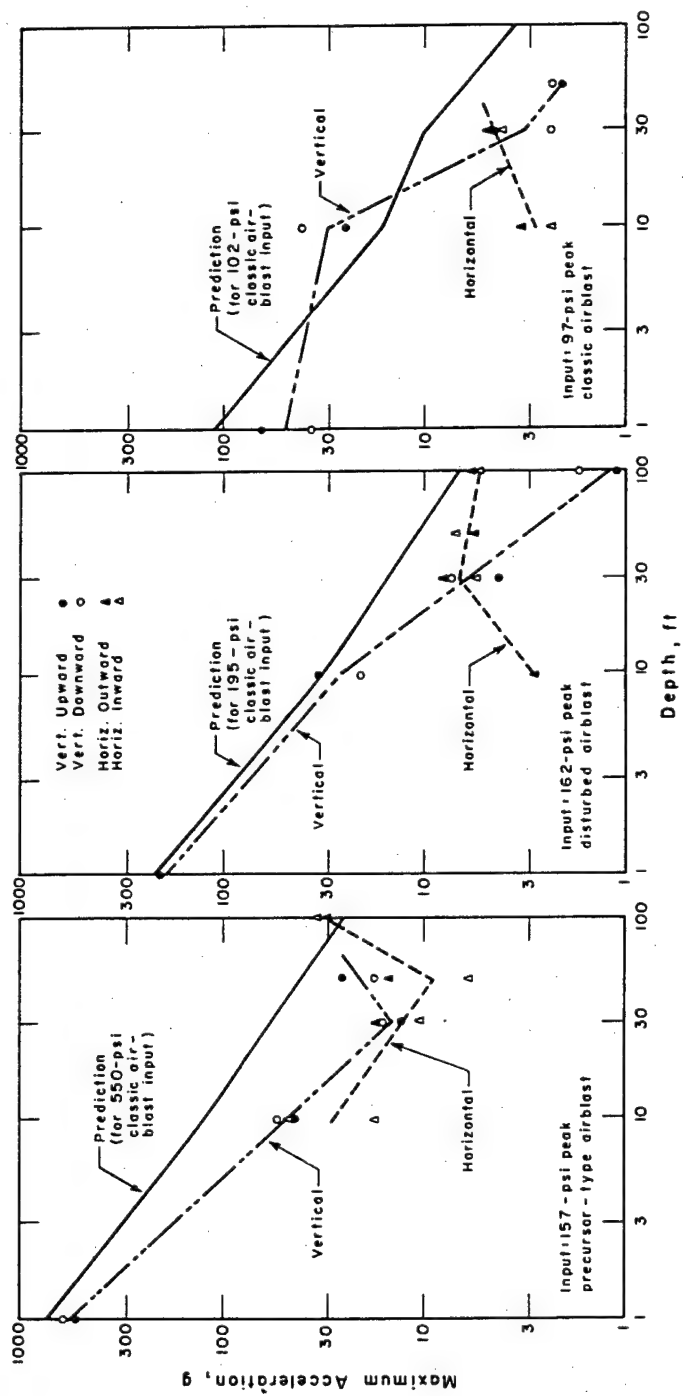


Sta. 13 (3950 - ft GR)

Sta. 12 (3144 - ft GR)

Sta. 11 (2000 - ft GR)

Figure 6.14 Maximum slap acceleration versus depth, Shot Koa.



Sta. 3 (840-ft GR)

Sta. 2 (650-ft GR)

Sta. 1 (407-ft GR)

Figure 6.15 Maximum slap acceleration versus depth, Shot Cactus.

high-amplitude pulses arriving at late times, which appear to travel upward toward the ground surface.

**6.4.2 Displacement.** The displacement gages were a modification of those used by Sandia Corporation in Operation Teapot Project 1.5. The gages consisted essentially of a buried anchor and a rotating drum at the ground surface. The two were connected by a piano wire, which was

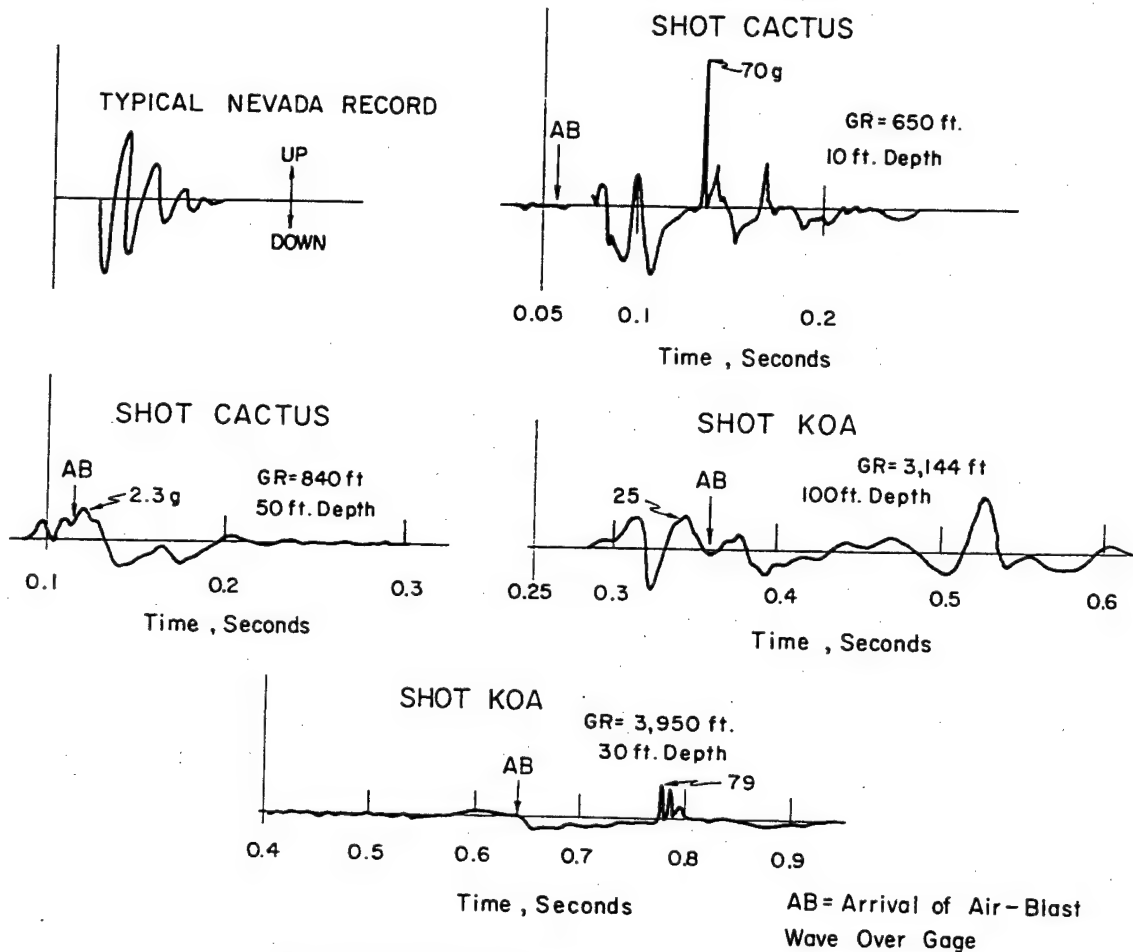


Figure 6.16 Typical acceleration records.

attached to the anchor at one end and wound around the drum at the other. A displacement of the surface with respect to the anchor was measured by recording the rotation of the drum.

One of the six displacement gages on Shot Cactus produced a record, and four of the six on Shot Koa produced records. The record from Shot Cactus, shown in Figure 6.17, indicates that there was a rapid initial downward movement of the ground surface with respect to the anchor 50 feet deep, followed by a rebound to an upward displacement of 0.82 inch, and a residual displacement of 0.2 inch. The four records from Shot Koa were recorded from the two farthest stations. Figure 6.14 shows the record from the 50-foot-deep anchor from the most distant station; the other records are similar. None of the Shot Koa records show the rebound observed on Shot Cactus. The difference in the two records may well be due to the longer-duration blast wave from Shot Koa, but there is reason to believe that the unconsolidated and inelastic soil on

Sites Helen and Irene may also have affected the Shot Koa results. The displacements observed were considerably smaller than those measured at NTS, where a vertical displacement on the order of a foot was measured at the 270-psi level.

**6.4.3 Soil Pressure.** The devices used to measure soil pressures were 43 steel drums, two feet long and two feet in diameter, each having a flexible aluminum diaphragm on one end. The drum type of instrument was chosen in the belief that the size and shape would be a reasonably good model of an underground structure. Diaphragms of three different thicknesses (0.5, 0.125 and 0.063 inch) were used to simulate structures of different flexibilities.

Twenty of the 43 drums were used on Shot Koa, and 23 were used on Shot Cactus. The drums were buried at depths from the surface down to 20 feet, as shown in Figure 6.18. On both shots, stations were located at a predicted pressure level of about 250 psi.

All of the drums have been recovered and the pressures calculated from the measured dia-

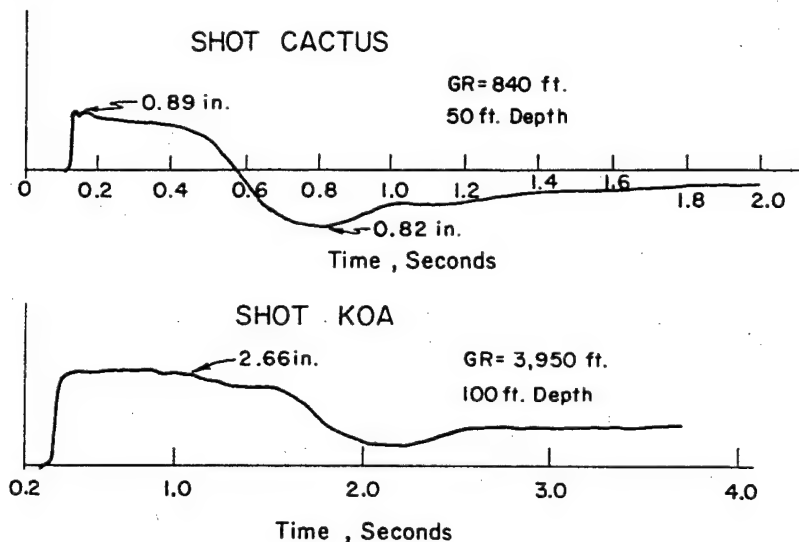


Figure 6.17 Displacement records.

phragm deflections are plotted in Figures 6.19 and 6.20. The points with arrows pointing upward indicate that the diaphragms ruptured, or (for the 0.5-inch diaphragms) were not calibrated above the pressure indicated. The most obvious trend was that the pressure decreased with depth for a few feet, but increased at depths greater than about eight feet. On Shot Cactus, the pressure reached about the surface level value at a depth of twenty feet. The Shot Koa results were similar, but at depths greater than eight feet, the half-inch diaphragms indicated pressures greater than 500 psi, twice the incident air overpressure.

In almost every case, the two thinner (most flexible) diaphragms showed lower pressures than the thickest (most rigid) diaphragms. This is to be expected on the basis of a soil phenomenon called arching, and was previously observed during Operation Plumbbob. It is seen that an increase in flexibility up to a point resulted in a decrease in pressure felt by an object.

The pressures on the horizontal drums below the water table were about equal to the vertical pressure at corresponding depths, indicating that a state of hydrostatic stress existed. The horizontal drum at a depth of one foot on Shot Cactus showed a pressure which indicated that the

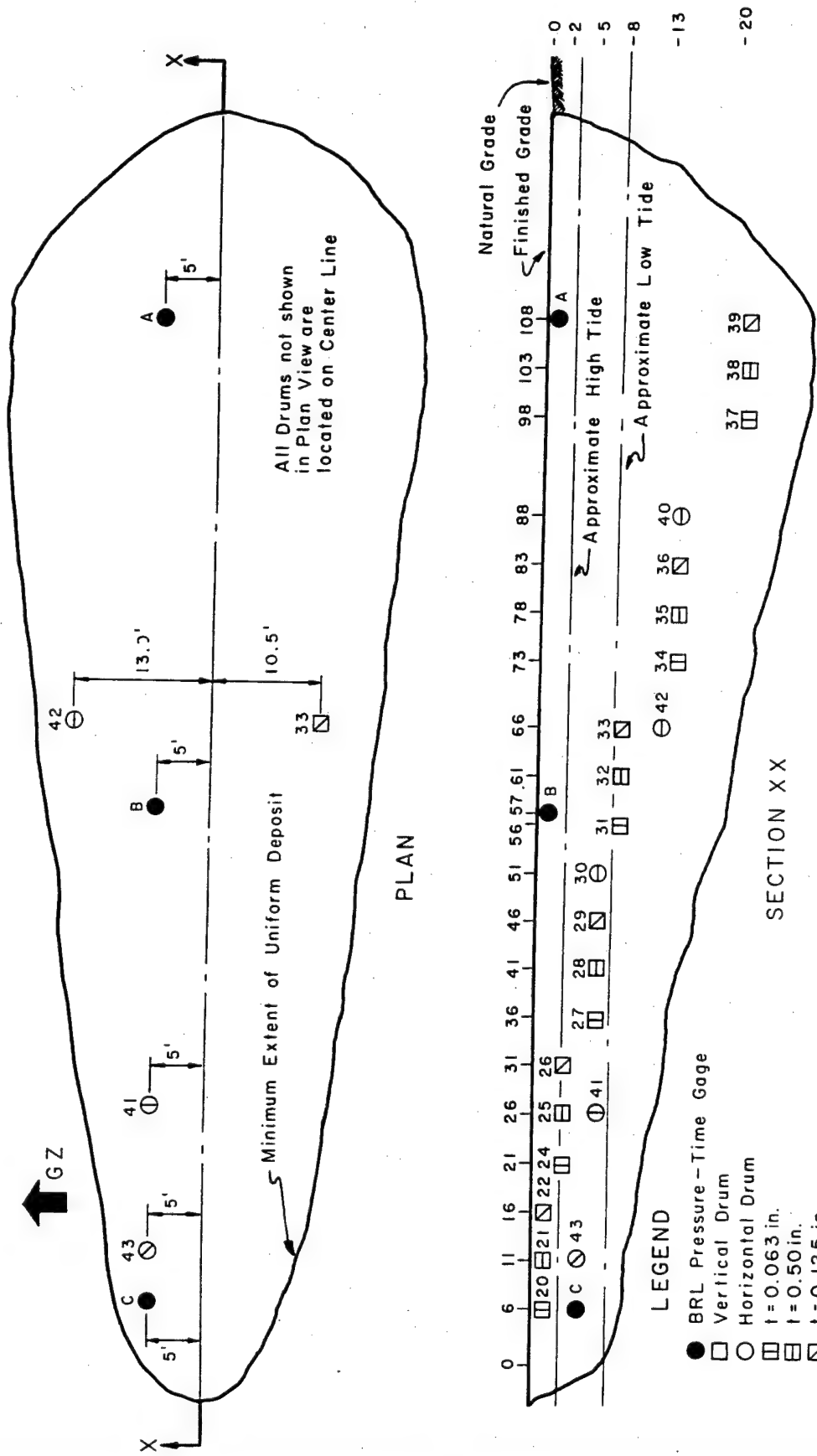


Figure 6.18 Drum layout for Shot Cactus.

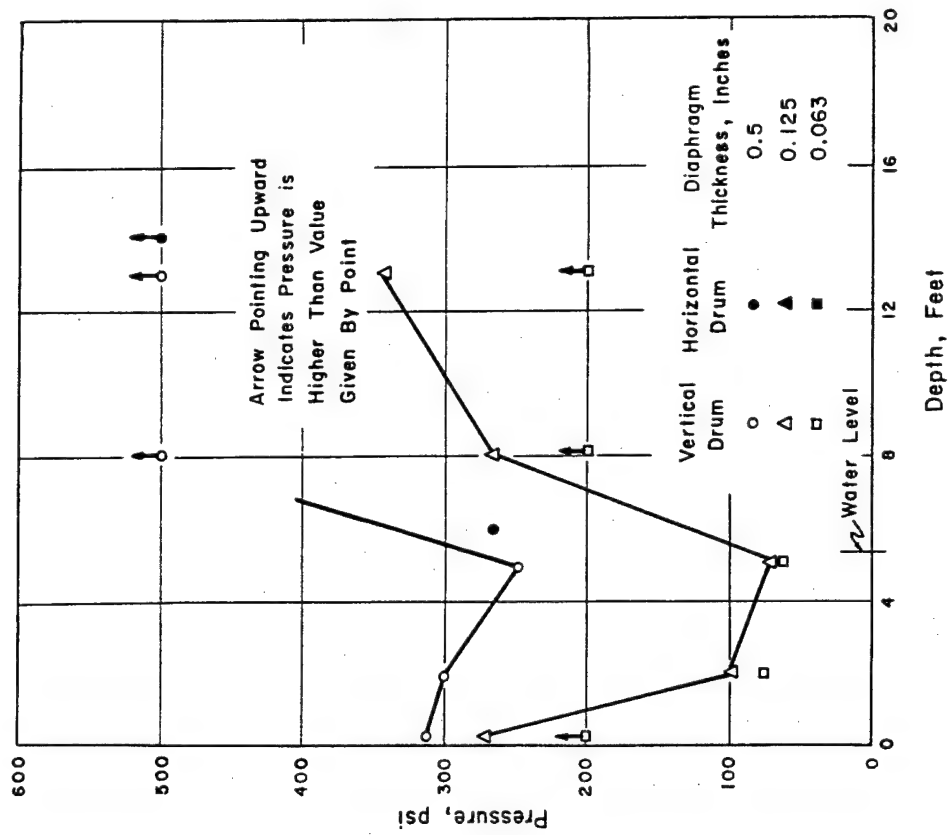


Figure 6.19 Underground pressures, Shot Cactus.

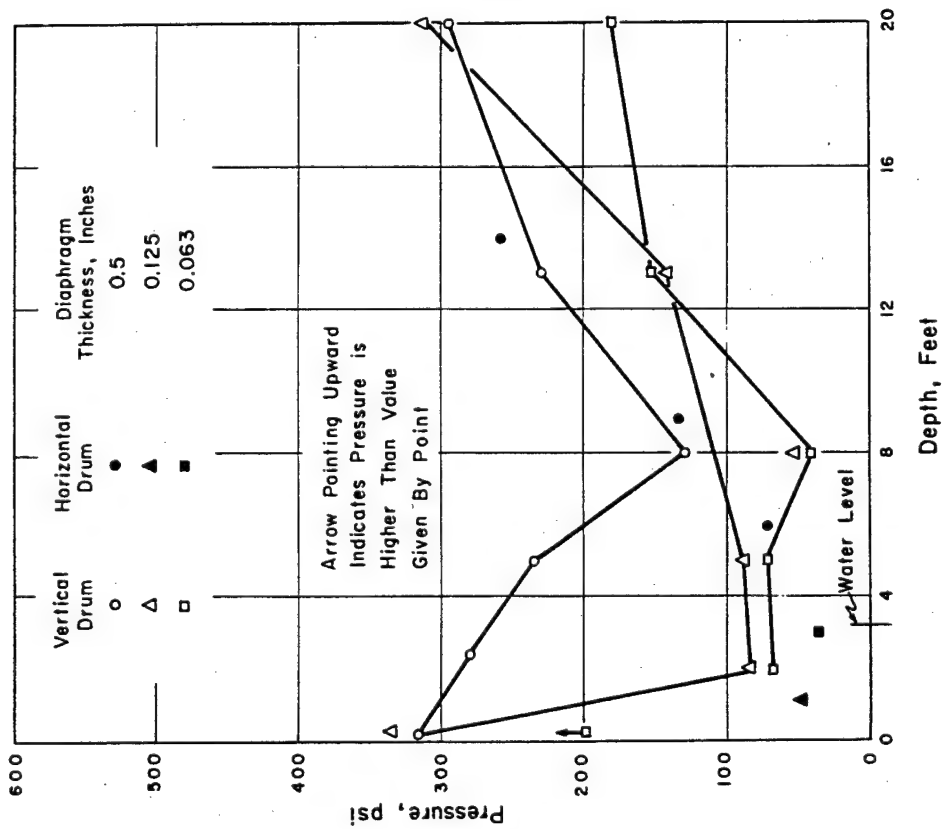


Figure 6.20 Underground pressures, Shot Koa.

horizontal pressure above the water table was considerably less than the vertical pressure at the same depth.

The most surprising result of the underground pressure experiment was the very-high pressure measured at depths below eight feet on Shot Koa. It is apparent that a considerable amount of pressure can be transmitted directly through the soil, in addition to the pressure induced by the air-blast wave. Since no unusual pressures were observed on Shot Cactus at the same scaled range, it is most likely that the Shot Koa results were primarily influenced by soil factors, and possibly by the coupling mechanism mentioned in Section 6.2.

**6.4.4 Shock Spectra.** Spectra of the ground shock produced by nuclear effects were first measured directly in Operation Plumbbob, Project 1.9 (Reference 23). Instrumentation consisted of self-recording reed gages, a type long used for analysis of vibrations in many industrial applications. The gages were essentially masses on the end of cantilever springs, each spring-mass system having a specified resonant frequency. The spring-mass systems (called reeds) respond to corresponding frequency components of the ground-shock input.

Two types of gages are shown in Figures 6.21 and 6.22. The gage shown in Figure 6.21 is similar to those used during Operation Plumbbob. There are ten reeds in each gage, having fundamental frequencies of 3, 10, 20, 40, 80, 120, 160, 200, 250 and 300 cps. The gage shown in Figure 6.22 is a low-frequency gage developed for use on a megaton shot of Operation Hardtack. It has three masses, spring loaded in opposite directions. The fundamental frequencies were 3, 6, and 10 cps. The low-frequency gage has a much larger dynamic range than the standard gage, and can be used at higher pressure levels. Twenty-three standard gages and ten low-frequency gages were used. Position of gages according to shot and pressure level are shown in Figures 6.1 and 6.2, and listed below:

<u>Predicted Pressure</u>	<u>200 psi</u>	<u>120 psi</u>	<u>100 psi</u>
Shot Koa: Standard gage	2, 2*	2, 2*	6
Low-frequency gage		2, 2*	6
Shot Cactus: Standard gage	2	3	2, 2*

\* Gages were anchored to the floor slab of Project 3.2 experimental structures.

At each station there were gages in both horizontal and vertical orientations. In all cases, the gages were buried with their tops flush with the ground surface.

Peak displacements of the masses were measured. The peak displacements are described by:

$$q_{\max}(\omega, \epsilon) = D = \max_{\tau > 0} \left| \frac{1}{\omega} \int_0^{\tau} a(t) \exp - \omega \epsilon (t - \tau) \sin \omega d\tau \right|$$

Where:  $q_{\max}(\omega, \epsilon)$  = maximum displacement of gage mass  
 $\omega$  = resonant frequency of spring mass system  
 $\epsilon$  = ratio of damping to critical viscous damping  
 $a(t)$  = shock acceleration input to gage

The velocity spectrum is defined as  $V = D\omega$  and the acceleration spectrum as  $A = D\omega^2$ . It should be immediately pointed out that the values given for displacement, velocity, and acceleration are factors of the particular reed gage, and not of ground motion.



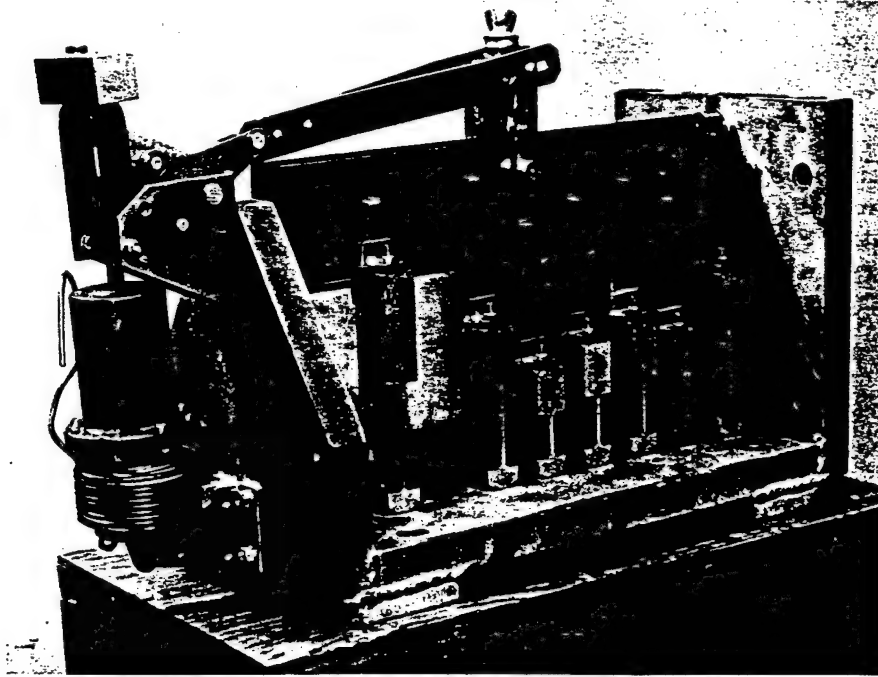


Figure 6.21 Self-recording reed gage.

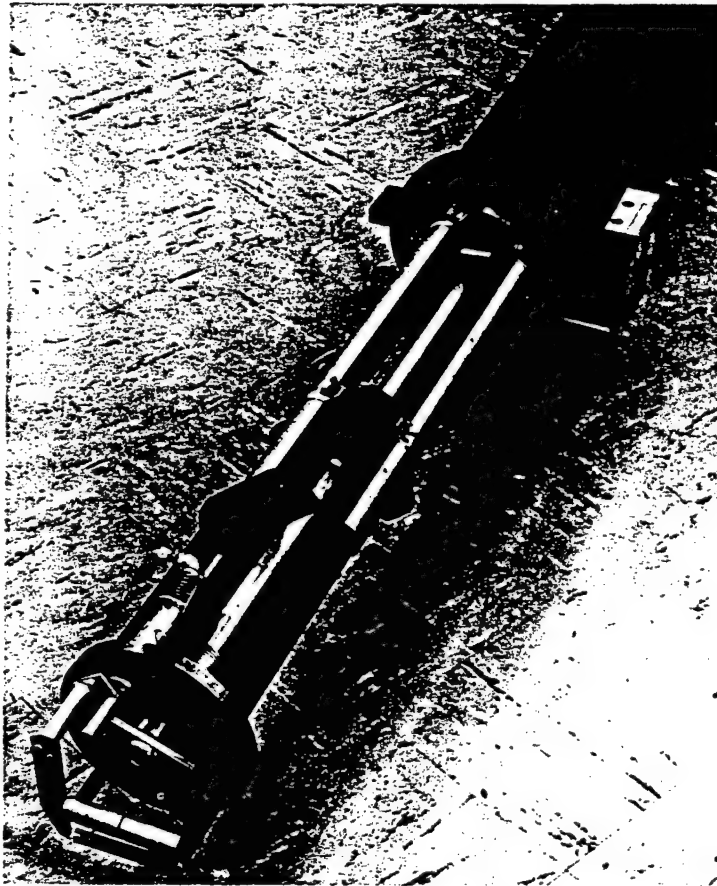


Figure 6.22 Low-frequency self-recording gage.

6.4.5 Results. Although shock spectra are somewhat abstract quantities, they are of real and important value to structural designers. Spectrum analysis of acceleration-time ground-shock records have been made, and appear to agree reasonably well with the shock spectra data from Operation Plumbbob, particularly in the higher frequencies. Difficulties exist, however, in analyzing acceleration-time records for low-frequency components (which are of the greatest interest), especially since most types of accelerations have somewhat limited frequency response.

Of the 33 gages, 25 were recovered. The remaining eight were in collapsed structures or in areas where radiation levels did not permit entry; these will be recovered when working conditions permit. Records were obtained from all of the 25 gages available. The most significant results which can be presented are comparisons between the responses measured on Shots Koa and Cactus in the EPG, and the EPG shots versus shots at NTS.

1. Shot Koa produced greater vertical response at low frequencies (twice as high at 3 cps) than Shot Cactus. Vertical response on Shot Koa was lower than Shot Cactus from 10 to 50 cps, and about the same above 50 cps. Horizontal response was lower than vertical response at all frequencies below 200 cps on Shot Koa. On Shot Cactus, the horizontal and vertical responses were about equal.

2. The vertical response at low frequencies was lower (by one fourth) on Shot Cactus than from Nevada shots. Low-frequency response from Shot Koa was about the same as the Nevada shots; high-frequency response was several times greater from both EPG shots than from Nevada shots.

## Chapter 7

# NUCLEAR RADIATION

### 7.1 GENERAL

Only two Program 2 projects participated in shots not previously discussed. These were Project 2.4, which made measurements of neutron flux from two large-yield detonations, and Project 2.8, which collected fallout samples from radioactive clouds produced by large-yield detonations fired under different environmental situations. Since the objectives and participations of these projects were entirely independent, they are discussed separately.

### 7.2 NEUTRON FLUX FROM LARGE-YIELD BURSTS

7.2.1 Objectives of Project 2.4. The objectives of this project were to measure neutron flux and dose as a function of distance for two megaton-range nuclear detonations and to make neutron flux and dose measurements as required by other Department of Defense (DOD) projects.

7.2.2 Background and Theory. The determination of the number and energy of neutrons in the external environment of a detonated device is of prime importance in the field of weapon effects. External-neutron-flux measurements have been made on almost all nuclear weapons tests since Operation Sandstone. However, neutron flux measurements from megaton-yield weapons had not been entirely successful prior to Operation Hardtack. Measurement of neutron flux and dose from megaton-yield devices had been attempted during Operations Castle and Redwing, but because of various operational problems encountered, the experiments yielded little or no data of value. Project 2.4 was, therefore, an attempt to make measurements to supplement previous data where incomplete and to obtain close-in measurements where no data were available.

Neutron measurements were made by the Hurst fission-foil method. This method involved the use of small quantities of detector elements that were activated through nuclear transformation involving neutron capture or fission. The method has been used on many tests with excellent results. In the laboratory, using cyclotron and reactor facilities, the dose measurements obtained with the foil method have been found to agree well with measurements made with the Hurst proportional counter.

In making neutron measurements over water a new complication was encountered, since it became necessary to evaluate the neutron albedo of an infinite air-water interface plane. Once this effect has been evaluated, the experimental results obtained by this project will have to be interpreted accordingly. This problem is presently being studied at the National Bureau of Standards, using high-speed computer techniques.

7.2.3 Experimental Method. Participation. As stated in the objectives, the project was to have made neutron measurements for two megaton-range nuclear detonations. To satisfy this requirement, the project participated during Shots Yellowwood and Walnut. Shot Yellowwood, which had a predicted yield of 2.5 Mt, was a barge shot which gave an actual yield of 319 kt. Shot Walnut was also a barge shot and had a design yield of 1.7 Mt. The actual yield is presently quoted as having been 1.5 Mt. The surface zero point was identical for both shots, the location being west of Site Janet.

**Operations.** The neutron-detector systems were installed on 25 buoys anchored on a non-radial line extending from 900 yards to 4,100 yards from surface zero. Figure 7.1 shows the general station layout for both shots. The buoy which was used consisted of a mine case, to which a tripod steel-pipe tower had been attached. The detectors were exposed on a short cable attached to the tripod tower. Each buoy was fastened by a cable line to a 400-pound concrete anchor, which in turn was connected to a main anchor cable lying on the lagoon floor and

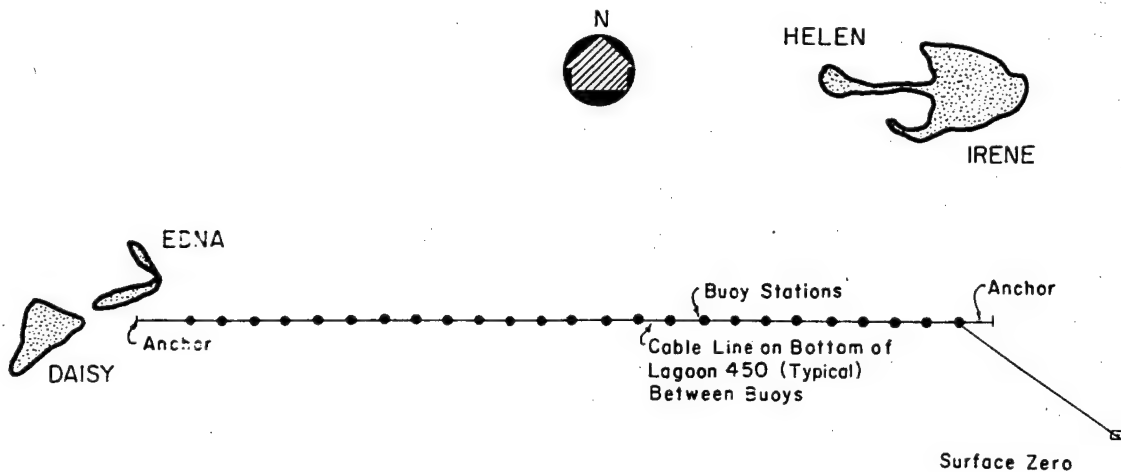


Figure 7.1 Station layout, Project 2.4, Shots Yellowwood and Walnut.

extending the full length of the array. This main cable assisted in anchoring the floats and facilitated recovery of floats that had been sunk. In the recovery of sunken buoys a recovery vessel picked up the main cable at a floating buoy and followed it to the anchor of a sunken buoy, from which it was a simple matter to recover the sunken buoy. Figure 7.2 depicts a typical portion of the station array, showing buoys, anchors, and the main cable.

Recovery was accomplished through use of a crane mounted in an LCU. Floats were picked out of the water, and the short cable, to which the detectors were attached, was removed from the tripod. Sunken buoys were raised in the manner described in the preceding paragraph, and the detectors detached in the usual fashion.

**Instrumentation.** Each detector system consisted of seven detector foils: gold, cadmium-shielded gold, plutonium, neptunium, uranium, sulfur, and zirconium. The use of these detectors permitted the documentation of the neutron spectrum in broad energy bands from zero energy to 14 Mev. The essentially thermal neutron flux was measured by means of two gold foils, one shielded by cadmium and the other unshielded. The cadmium-shielded foil gave a measure of the neutron flux above 0.3 ev, while the bare foil gave a measure of the total neutron flux. Subtraction of the two fluxes yielded the neutron flux below the 0.3 ev energy. In both cases, the reaction of interest was  $Au^{197}(n, \gamma) Au^{198}$ .

Intermediate-energy neutrons (3.7 kev to 3 Mev) were measured by means of plutonium, neptunium, and uranium foils. These three materials fission when bombarded with neutrons having energies in excess of certain threshold values. Because plutonium has a fission cross section extending down into the thermal range, an artificial cross section was produced by shielding the foils with elemental boron. This cross section had an effective threshold at 3.7 kev, an arbitrary point determined by the thickness and density of the boron shield. For this particular application the thickness was 2 cm, and the density was 1.13 gm/cm<sup>3</sup>. The other two materials, neptunium

and uranium, fission only with fast neutrons but were included with the plutonium in the boron shield for convenience.  $\text{Np}^{237}$  and  $\text{U}^{238}$  have effective thresholds of 0.75 Mev and 1.5 Mev, respectively.

Neutrons in the 3-Mev to 12-Mev range were measured by sulfur pellets, the reaction of interest being  $\text{S}^{32}(\text{n}, \text{p}) \text{P}^{32}$ . Very-fast neutrons (above 12 Mev) were measured by means of zirconium foils. The reactions of interest were  $\text{Zr}^{90}(\text{n}, 2\text{n}) \text{Zr}^{89}$  and  $\text{Zr}^{89} - \text{Y}^{89} + \text{e}^+$ . The positron-

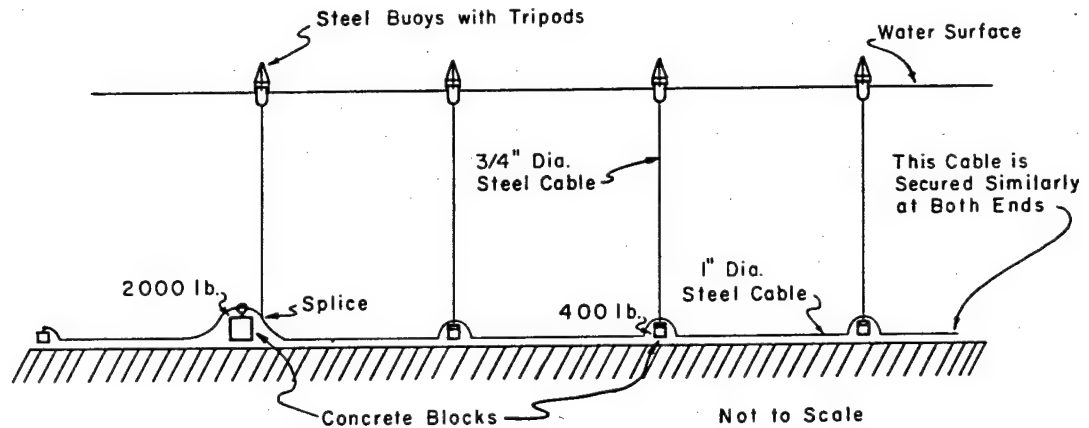


Figure 7.2 Station array with ground cable and anchors.

decay scheme permitted the activity of interest to be separated from the other activities present.

For exposure, the individual detector foils were enclosed in steel containers for protection against both detonation and normal environmental effects.

Special counting trailers were used to measure the resultant activities of the exposed samples. These trailers incorporated the counting equipment necessary to measure the various activities produced in the different foils. All foils had been calibrated at LASL before the test operation. Neutron flux was calculated directly from the measured activity of the detectors, while the neutron dose was calculated from the flux values using the single-collision theory of dose contribution per neutron (Reference 24).

**7.2.4 Results and Discussion.** Since the results of neutron measurements made in support of other projects are covered in the sections pertaining to those projects, they will not be presented here. This section will be devoted to a discussion of the results obtained in the measurements made on Shots Yellowwood and Walnut.

**Neutron Flux.** Results of neutron-flux measurements are presented in Figure 7.3 for Shot Yellowwood and Figure 7.4 for Shot Walnut. The curves show the neutron flux, as determined from the various foils, times the slant distance squared versus the slant distance. As seen from these curves, the data obtained was somewhat limited. Complete spectral coverage was not obtained at all stations, nor did all stations produce data. These failures are attributed to a number of causes. First, the late recovery of the detectors, made necessary because of early radiological conditions, allowed the activity from the fission samples at the more distant stations to decay to such an extent that accurate counting was no longer possible. Second, some of the close-in stations were lost because of missile or blast effects. Third, other close-in stations were damaged by shock, and some individual detectors were missing. In addition, on Shot Walnut, a large number of the detector holders were damaged by shock, thereby allowing contaminated sea water to enter the holder. In cases where the contaminated water permeated the detector material, it became necessary to distinguish the neutron-produced activity from that introduced by the contaminated sea water. Although it is believed that the method used to separate the activities was effective, further work will be required before complete confidence can be placed in the sulfur results.

Examination of the flux curves revealed that the slopes were not all the same for these shots,

which could imply the parallel-line, constant-spectrum concept proposed for kiloton devices (Reference 25) may not be valid for these weapons. Because the detectors used during Operation Hardtack were not on a line radial to the device and because various amounts of shielding inherent in the weapon configuration could have been interposed between the actual sources of neutrons and the detectors, the flux spectrum measured at one angle from the device should not necessarily be exactly the same as that measured from another angle. Thus, the implied change in spectrum with distance may be real or could be the result of asymmetry of the weapon. When more complete information is obtained concerning the actual weapon configuration, an attempt will be made to correlate this with the measured flux.

Neutron Dose. Neutron dose was calculated from flux data using the single-collision theory of dose contribution per neutron mentioned in "Instrumentation", in this Chapter. Plots of the neutron dose versus slant distance are presented in Figure 7.5 and Figure 7.6. Expected neutron dose from fission weapons of the same yields as calculated from TM 23-200 (Reference 15) are plotted on the figures, together with the actual results. For these calculations, a relative air density of 1.0 was assumed, and a water-surface correction factor of 0.7 was used, as given in the reference. An RBE (relative biological effectiveness) of 1.3 was used to convert the dose in rem as given in the reference to a dose in rep so that comparison could be made with shot results. It is seen that the Shot Yellowwood dose is lower than the predicted value and the Shot Walnut dose is lower than prediction. Since TM 23-200 states that for the predicted dose may be high the agreement of the measured values with prediction is considered good.

7.2.5 Conclusions. Although the neutron flux and dose measurements made on Shots Yellowwood and Walnut were limited in many respects, the dose results show good agreement with predicted values of neutron dose.

Changes in the accepted value of the over-water correction factor and the assumed RBE could possibly result in closer agreement. Better data would have been obtained, were it not for the long-recovery time of the instrumentation dictated by rad-safe considerations. The buoy system of placing neutron-detecting instrumentation proved effective in areas with overpressures less than 90 psi, and with minor modifications the system could be made effective in areas of higher overpressures.

### 7.3 AIRCRAFT AND ROCKET FALLOUT SAMPLING

7.3.1 Objectives of Project 2.8. The general objective of this project was to estimate, by collection and analyses of cloud samples, the relative contribution of certain radio-nuclides to both local and world-wide fallout arising from megaton-range land- and water-surface detonations.

Specific objectives were to: (1) obtain airborne particulate and gas samples by rocket- and aircraft-sampling techniques; (2) determine radio-nuclide distributions among particle groups that differ according to falling rates and that may be defined as the major contributors to local and world-wide fallout; (3) attempt to determine an early time radio-nuclide and particle space distribution with respect to the upper and lower halves of the cloud and radially outward from the axis of the cloud in a vertical plane passing through ground zero; and (4) estimate the extent of separation of fallout particles from gaseous-fission products by fission measurements on gas and particulate samples of the cloud collected near the top of the cloud and on particulate samples collected near the surface of the earth.

7.3.2 Background and Theory. Because of the number of large-scale nuclear tests being conducted, it has become important to know the hazards connected with the fallout from such bursts. It is well recognized that a substantial fraction of radioactive-fission products from a nuclear detonation are borne by the atmosphere to be deposited in various parts of the world and that these fission products are, to a large extent, harmful to the biological environment of man, if accumulation becomes excessive.

conditions, it was hoped that the effect of shot environment on fallout distribution could be determined. Much information was needed to assist in extrapolation to varying shot conditions or yields through an increased understanding of the formulation, composition, and transport of fallout.

7.3.3 Experimental Method. Shot Participation. The project initially planned to participate during Shots Koa, a megaton-range land-surface burst, and Walnut, a megaton-range water-surface burst. However, because of indicated contamination of Shot Koa samples by debris from a Bikini detonation, Shot Fir, the project participation was later extended to include Shot Oak, a 9.4 Mt burst fired over the lagoon reef in approximately 15 feet of water. Although this alternate shot did not provide a true land-surface environment, it had been found from results from Shot Tewa of Operation Redwing that a burst of this size in shallow water was representative of a land-surface burst.

Operations. The project was organized into three distinct efforts: (1) Rocket Sampling, wherein direct measurement of the distribution of various radio-nuclides was planned by analysis of samples obtained at early times from the cloud by rocket-borne samplers, (2) High-Altitude Aircraft Sampling, wherein collection of samples was planned for altitudes near the top of the cloud or in strata that had separated from the rest of the cloud, and (3) Low-Altitude Aircraft Sampling, wherein collection of samples was planned at altitudes of 1,000 feet, along a predicted height line corresponding to an altitude of approximately 55,000 feet.

The sampling head of the rocket was so designed that separation of particles according to size would occur before filtration. The particles were roughly divided into two groups: those having falling velocities greater and less than about 3 in/sec, which corresponded, respectively, to particles having diameters greater and smaller than 25 microns. This falling velocity was chosen because it corresponded to the critical size separation of particles contributing to local and world-wide fallout. Particles falling at a rate greater than about 3 in/sec would arrive at the earth's surface within 3,000 miles of the burst point, thus ensuring their deposition in the Pacific Ocean. It was planned that rockets be fired in pairs at various radial distances in a vertical plane passing through ground zero. One rocket from each pair was to collect a sample from the base to the top of the cloud, while the other was to collect a sample from some intermediate point (at or near the tropopause) to the top. By examination of the relative amounts of large and small particles, and their associated activities, in the upper and lower halves of the cloud at increasing distances from the burst point, an evaluation could be made of the particles that would contribute to local and world-wide fallout.

High-altitude collections were made by B-57D's. The altitudes chosen for sampling corresponded to parts of the cloud that would not receive additional fallout from other sections of the cloud. The aircraft were to take gas samples, from which particulate matter was removed and retained, and also gross-particulate samples. The gas samples would be analyzed for  $Kr^{88}$ , while the particulate samples would be analyzed for various fission-product radio-nuclides. The  $Kr^{88}$  served as a basis for determining the maximum number of fissions in world-wide fallout, while the particulate analysis would determine which of the fission-product radio-nuclides were being enhanced or depleted at increasing distances from the burst point and, hence, which of these radio-nuclides were contributing to world-wide or local fallout.

Low-altitude particulate collections were made by WB-50's. From an analysis of past operations, it was found that the typical wind structures at EPG led to the isolation of a height line corresponding to an altitude of about 55,000 feet along the eastern periphery of the fallout pattern as a result of the usual reversal of wind direction at this altitude. Since the low-altitude samples were to be taken along a height line corresponding to the altitude at which the high-altitude samples were taken, it was a simple matter to perform high-altitude sampling at the altitude at which reversal of the wind direction occurred and to perform the low-altitude sampling by flying to the west until activity was encountered. This would be the eastern edge of the fallout pattern and would correspond to the reversal altitude height line. By sampling at increasing distances from the burst point, it would be possible to determine the particle-size



distribution for various distances from surface zero, since particle-size separation, due to natural fallout processes, would occur during deposition. Also, confirmation of the local fallout data from rocket sampling could be obtained, and correlation could be made with the enrichment and depletion effects as observed from high-altitude sampling, thus giving further information on the contribution of total debris to both local and world-wide fallout.

**Instrumentation.** The rocket-borne cloud sampler consisted of an air-sampling nose section mounted on a two-stage, 20-foot rocket. The nose section consisted basically of an orifice, a diffuser section, and a collecting filter. The orifice was designed to open and close by electronic timing at specified times. Particles entering the orifice would be decelerated in the diffuser section and subjected to forces normal to the axis of the rocket. These forces would separate the particles according to their size, with the larger particles remaining near the centerline, while the smaller particles were forced outward. The design of the diffuser section was such that particles would be resolved into sizes greater or less than 25 microns in diameter, which corresponds to the critical falling velocities greater or smaller than 3 in/sec. After resolution of the particles according to size, a filter collected and retained the particulate while allowing the gases to pass through to exhaust ports at the rear of the nose section.

The speed of the rocket during sampling was designed to be about Mach 2. After completion of the sampling, electronic equipment closed the sampler orifice, disconnected the sampler from the propulsion unit, and ejected a system of parachutes designed to first slow the unit from supersonic speeds and then to lower the unit back to earth at a slow rate of descent. At launch time, a homing beacon was activated to facilitate recovery of the sampler units from the ocean.

Figure 7.7 shows the complete sampling rocket on a launcher. Part A is the primary motor, Part B the sustainer motor, Part C the parachute compartment, Part D the electronics compartment, and Part E the sampler nose section.

Aircraft-borne cloud samplers were of three types. Two of the types were mounted in pairs on the B-57D aircraft used for high-altitude sampling. The third type was mounted on the WB-50 aircraft used for low-altitude sampling. The first type, a gross-particulate sampler, was mounted on the forward part of wing-tip tanks on the B57D. It consisted of an intake orifice, the opening of which was controlled by a butterfly valve, and a 24-inch filter screen near the rear of the sampler. The second type, a coincident gas-particulate sampler, was also mounted on the B-57's. In these, air was drawn through a desiccant section and then through a filter section, after which it was pumped to storage tanks. The third type sampler, used in the low-altitude sampling, was attached to the fuselage of a WB-50 aircraft and consisted of an AFOAT-1 standard E-1 filter unit. The filter unit was sealed, except during sampling, by doors ahead of and behind the filter screen.

**Data Requirements.** There were ten specific radio-nuclides to be collected during sampling operations. Those of concern to world-wide fallout were  $\text{Sr}^{90}$ ,  $\text{Cs}^{137}$ , and  $\text{I}^{131}$ . Those which could supply correlative information in the case of fractionation were  $\text{Mo}^{99}$ ,  $\text{U}^{237}$ ,  $\text{Ce}^{144}$ ,  $\text{Eu}^{156}$ ,  $\text{Y}^{91}$ ,  $\text{Sr}^{89}$ , and  $\text{Cs}^{136}$ . It was desired that complete radiochemical data for the above ten nuclides be obtained by all three sampling techniques, in addition to determining the amount of each in the two size groups (greater or less than 25 microns) as collected by the rocket samplers. An additional nuclide that was collected was  $\text{Kr}^{88}$  in the gas samples of the B-57D aircraft for reasons listed under "Operations", in this Chapter.

**7.3.4 Results and Discussion.** Shot Koa was fired on Site Gene at 0630, 13 May 1958. Weather conditions were good for all types of sampling. It was planned to fire 18 rockets into the cloud after cloud stabilization. However, the firing line to six of the rockets failed on D-1, and could not be repaired before the shot. The other 12 rockets failed to fire because of electrical deficiencies in the launch-programming circuitry. Therefore, no rocket sampling was accomplished during Shot Koa. High-altitude sampling by B-57D aircraft yielded five particulate samples collected from 3 1/2 to 28 hours after shot time. Only two gas samples were obtained because the compressor motors were inoperative during the last three sampling runs. Low-altitude sampling was accomplished by WB-50 aircraft along the 55,000 to 60,000-foot-height lines at two-hour intervals from



H+4 to H+12 hours. One sampling mission was accomplished at H+6 hours along the 45,000-foot-height line. All aircraft sampling was successful where fallout was encountered, yielding sample sizes representing  $10^{14}$  to  $10^{15}$  fissions.

Preliminary analysis of the samples at continental laboratories indicated that many of the samples collected after Shot Koa were probably contaminated by debris from Shot Fir, a 1.5 Mt detonation fired on Bikini Atoll the day before Shot Koa.

Shot Walnut was fired at 0630 on 15 June from a barge located near Site Janet. Weather con-

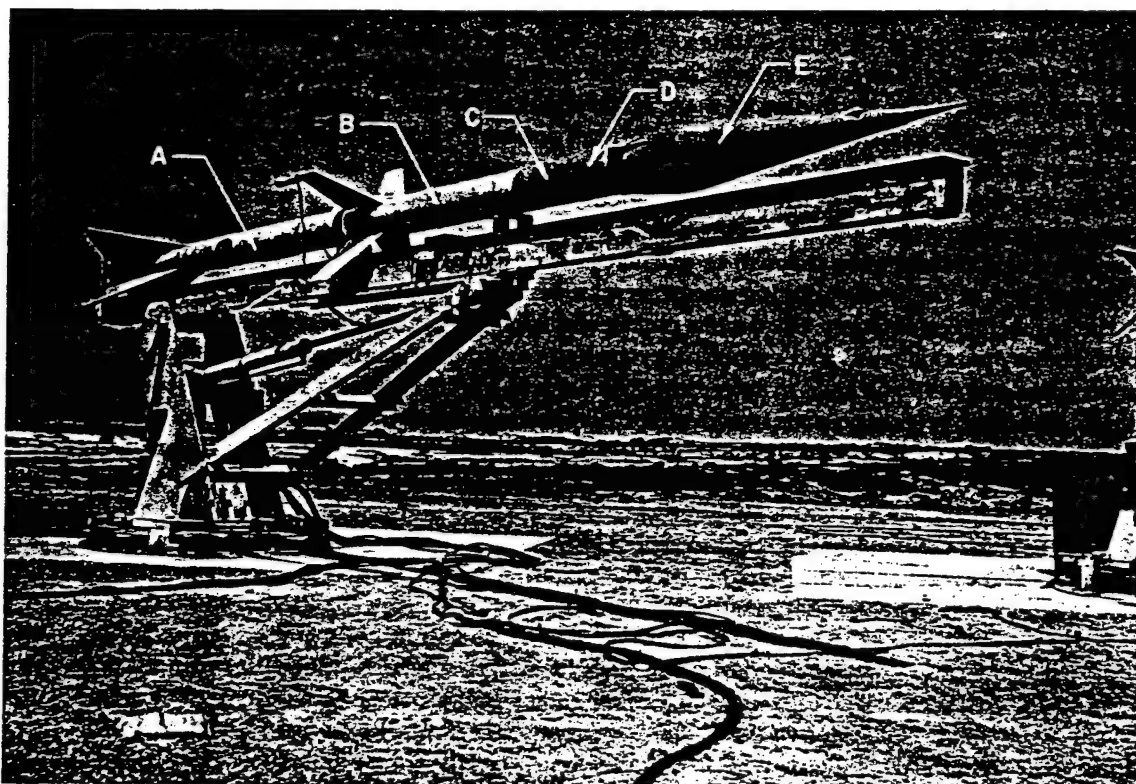


Figure 7.7 Air-sampling rocket.

ditions were favorable for rocket and high-altitude sampling, but the wind structure indicated that height-line sampling might not provide good samples because of the overlap of particles originating at 40,000 to 55,000 feet. It was planned to launch a total of ten rockets into the cloud. However, four of the rockets failed to launch because of difficulties with firing circuits. Of the six rockets launched, only two of the nose cones were recovered, while the other four were lost. Samples from the two recovered nose cones were contaminated by sea water which had somehow leaked into the chambers. The presence of the water significantly reduced the value of the samples. High-altitude sampling by B-57D aircraft yielded six particulate and six gas samples collected from 1 1/2 hours to 26 hours after shot time. Low-altitude sampling by WB-50 aircraft was accomplished despite the possibility that it might be ineffective. Three low-altitude missions yielded samples collected from 4 to 13 hours after shot time. Sample sizes from all high-altitude and the first two low-altitude missions represented  $10^{14}$  to  $10^{15}$  fissions, while the third low-altitude mission yielded sample sizes representing  $10^{12}$  fissions.

Shot Oak was fired at 0730 on 29 June from an LCU anchored over the reef four miles south of Site Alice in about 15 feet of water. Project participation in Shot Oak was considered necessary because of the uncertainty of data obtained from Shot Koa. Rocket sampling was not accomplished during Shot Oak. The rocket-sampling portion of the project was discontinued after Shot Walnut because it became apparent that the various technical difficulties encountered during prior participations and special nose cone tests could not be corrected with the limited facilities available at the EPG. Weather conditions during Shot Oak were favorable for high-altitude aircraft

sampling, but the wind structure indicated that height-line sampling might not be effective because of the overlap of particles originating at 55,000 feet with those originating at lower altitudes.

High-altitude sampling yielded five particulate and five gas samples collected from 2 to 26 hours after detonation. Height-line sampling by WB-50 aircraft was accomplished despite the possibility that the results might be inconclusive. Five height-line sampling missions yielded

TABLE 7.1 SUMMARY OF AIRCRAFT SAMPLES

Shot	B-57 Collections			1,000 Foot WB-50 Collections			
	Time	Altitude	Approximate Number of Fissions	Time	Bearing	Distance	Approximate Number of Fissions
	H+hr	ft		H+hr	deg	miles	
Koa	3.5	60,600	10 <sup>14</sup>	4	054	28	10 <sup>13</sup>
	6	56,000	10 <sup>14</sup>	6	051	59	10 <sup>14</sup>
	8	60,300	10 <sup>14</sup>	8	061	88	10 <sup>14</sup>
	11	60,300	10 <sup>14</sup>	10	057	109	10 <sup>14</sup>
	28	60,300	10 <sup>14</sup>	12	052	131	10 <sup>15</sup>
	—	—	—	6	020	42	10 <sup>15</sup>
Walnut	1.5	56,500	10 <sup>15</sup>	4	320	40	10 <sup>14</sup>
	3.25	56,500	10 <sup>15</sup>	10	283	142	10 <sup>15</sup>
	6	56,500	10 <sup>15</sup>	13	278	151	10 <sup>12</sup>
	9	56,500	10 <sup>15</sup>	—	—	—	—
	12	56,500	10 <sup>15</sup>	—	—	—	—
	24	58,000	10 <sup>15</sup>	—	—	—	—
Oak	2	56,300	10 <sup>16</sup>	4	310	65	10 <sup>14</sup>
	6	56,300	10 <sup>15</sup>	6	307	93	10 <sup>14</sup>
	9	56,300	10 <sup>15</sup>	8	303	125	10 <sup>14</sup>
	12	56,300	10 <sup>15</sup>	10	300	160	10 <sup>15</sup>
	26	55,400	10 <sup>14</sup>	12	299	187	10 <sup>15</sup>

samples collected from 4 to 12 hours after shot time. All samples collected during Shot Oak represented 10<sup>14</sup> to 10<sup>15</sup> fissions.

Table 7.1 provides a summary of all aircraft samples taken by the project during this operation.

Since analysis of the collected samples is presently in progress, no discussion of the data is feasible at this time. Technical data will be available after analysis of the samples taken has been completed.

**7.3.5 Conclusions.** Sampling of fallout by B-57D and WB-50 aircraft was successful. Adequate samples were obtained by these two means to provide sufficient data to meet the general objective of the project. There is evidence that the Shot Koa samples may have been contaminated by debris from Shot Fir. After detailed analysis of the samples obtained, results will be presented in the final report of the project. At that time it will be determined which of the project's specific objectives were fulfilled.

Rocket-sampling was not successful because the rocket samplers had not reached a stage of development necessary to permit attainment of the objectives planned for them.

It appears at present that good results will be obtained concerning radio-nuclide distributions among particle groups that differ according to falling rates. Also, good estimates should be obtained concerning the extent of separation of fallout particles from gaseous-fission products at both high and low altitudes. Determinations of early-time radio-nuclide and particle-space distribution with respect to the upper and lower halves of the cloud at various radial distances in a vertical plane will not be achieved because of the failure of the rocket-sampling portion of the project.

## *Chapter 8*

# *STRUCTURES and EQUIPMENT*

### 8.1 OBJECTIVE

The objective of Program 3 was to provide information on the effects of nuclear bursts on ship structures and equipment and on various land structures, under certain conditions that have not been heretofore investigated. The effects on ships and their equipment have been discussed in Chapters 2 and 3.

In the land-structures program, various earth-confined flexible arches were tested to determine the effect of long- and short-duration air blast. Deep reinforced-concrete slabs were tested to determine their behavior under blast loading in the high-overpressure region. Incidental information, by inspection of existing structures for past tests in the EPG, was documented and will be analyzed.

### 8.2 BACKGROUND (LAND STRUCTURES)

Previous full-scale nuclear effects tests in Operations Redwing, Teapot, Castle, Upshot-Knothole, Greenhouse and Buster-Jangle had collected a considerable amount of structures-loading-and-response data from air blast and ground-shock effects, primarily in the low and moderate overpressure ranges up to about 15 psi. During Operation Plumbbob, loading-and-response data were successfully obtained from the various types of above- and below-ground protective structures in the moderate- and high-overpressure regions up to about 190 psi, resulting from a 36.6-kt air burst.

Planning for Operation Hardtack indicated available surface shots with yields in the Mt range as well as the kt range, with suitable, though quite limited, land areas available for locating structures and associated free-field measurements by Program 1, in the high-overpressure regions up to about 600 psi. After due consideration of the various planning factors (e.g., island location which determined construction costs, limited available land area, choice of shots with predicted yields and planned readiness dates, scheduled shots in vicinity which would affect construction and/or recovery) the land structures program was concentrated on Shot Koa (1.3 Mt) and Shot Cactus (18 kt), both land-surface shots. In addition to the effort on these two shots, damage to numerous existing structures in the Eniwetok and Bikini Atolls was documented to add to the general knowledge and assist future planning and design of structures to resist the effects of nuclear devices.

### 8.3 RESPONSE OF EARTH-CONFINED FLEXIBLE ARCH-SHELL STRUCTURES IN HIGH-PRESSURE REGION

8.3.1 Objectives. The objective of Project 3.2 was to determine failure criteria of underground corrugated-steel arches under long-duration, high-pressure loads.

To satisfy this objective, taking into account soils and topographical conditions at the EPG, it was decided to (1) make an empirical determination of the response of three prefabricated, corrugated-steel, flexible-arch structures confined within non-drag-sensitive earthwork configurations of coral sand and subjected to long-duration-blast loading from a megaton-range detona-

tion, and (2) determine the effects of short-duration-blast loading on a similar structure and environment.

A collateral objective was to determine the radiation-shielding effectiveness of such structures with a minimum cover of five feet of coral sand.

8.3.2 Background. Above-ground, prefabricated-metal, flexible arch-shell structures, 25 feet in span and with various earth configurations were tested during Operations Upshot-Knothole and Teapot at overpressures up to 30 psi. Thereby, the existence and effect of significant dynamic pressure and damage from asymmetrical loading on this type structure, with a drag-sensitive earth cover, was documented.

During Operation Plumbbob, data on this type structure was extended into the 100-psi-peak overpressure region. Three of the same type flexible metal arches (two of which were reinforced by the addition of ribs) were tested in a semiburied configuration that satisfactorily eliminated asymmetrical loading of the arches from dynamic pressures such as had previously occurred on the similar above-ground structures. The Operation Plumbbob test configuration consisted of a semiburied structure whose volume of cut was approximately equal to the volume of fill so as to obtain maximum blast protection at a minimum cost, while maintaining a 5-foot depth of earth cover at the crown. The standard unstrengthened-arch structure withstood 56-psi peak overpressure (short duration) without significant damage. A rib-strengthened structure withstood a 100-psi peak overpressure (short duration) without significant damage.

The current structures-hardening requirements of the DOD extended beyond the information provided by the previous Operation Plumbbob tests. Thus, this Operation Hardtack project was devised to test the flexible-arch structure, in the 75-to-200-psi-overpressure region, under megaton yields, and to test a larger span with thicker shell in order to obtain information concerning maximum resistance and usability of such commercially available structures.

The planning philosophy for the four flexible-arch structures tested in Operation Hardtack was as follows:

1. Structure 3.2a was included to correlate the effects of the NTS with the soil effects of the EPG.
2. Structure 3.2b was included to correlate the effects of a long-duration loading with the effects of short-duration loading of Structure 3.2a.
3. Structure 3.2c was included to determine an upper limit of structural capability.
4. Structure 3.2d was included as a pioneer experiment involving a large span, flexible arch, within a non-drag-sensitive earthwork which was subjected to long-duration loading.

Because of the high water table at the EPG (within three to six feet of ground surface), it was impractical to construct the semiburied structure configuration such as tested on Operation Plumbbob. Therefore, to accommodate the overall requirements of Project 3.2 within the practical limits of topography and small available land areas at the EPG, it was necessary to construct large dimension non-drag-sensitive earthworks to confine the structures (Figure 8.1). These earthworks were designed to give maximum structural support to the confined-arch shells, and thus simulate, in effect, the Operation Plumbbob earth-configuration structures. The ground-zero sides of the earthworks were highly-compacted, massive-coral-sand shields intended to protect the arch shells from dynamic pressures to essentially the same degree as though they had been placed beneath the ground surface. Smaller, but similarly highly-compacted coral-sand masses were used for the parts of the earthworks on the sides away from ground zero.

8.3.3 Structure Description and Construction. The three small, flexible-arch structures (3.2a, 3.2b, and 3.2c) were basically Navy stock ammunition storage magazines, arch-type, 25-foot span, 48-foot length, bolted, 10-gage corrugated-steel sheets as shown in Figure 8.2. The end walls consisted of eight-gage corrugated-steel sheets, reinforced by a steel-rod tie-back, and concrete dead-man anchorage arrangement. The one large flexible arch (Structure 3.2d) was a specially fabricated, bolted, one-gage corrugated-steel-arch 38-foot span, 40 feet in length; both endwalls of the 3.2d structure were of bolted, shaped, three-gage steel panels.

These endwalls were also reinforced by steel tie-rod and concrete anchorages as shown in Figure 8.3. The test-access entrance for each structure consisted of a horizontal four-foot-diameter circular tunnel of corrugated eight-gage steel rigidly attached to one end wall and extending outward 30 feet from the structure. The access to this tunnel from the ground surface was through a circular opening equipped with a dome-shaped steel ( $\frac{3}{8}$ -inch thick) hatch which served as a blast door.

The concrete footings for the three 25-foot span arches (Structures 3.2a, 3.2b, 3.2c) were one-foot wide and one-foot-six-inches deep; the footing was one-foot-six-inches wide for the 38-foot-span arch (Structure 3.2d). Figures 8.4 and 8.5 show the earth-cover configuration and

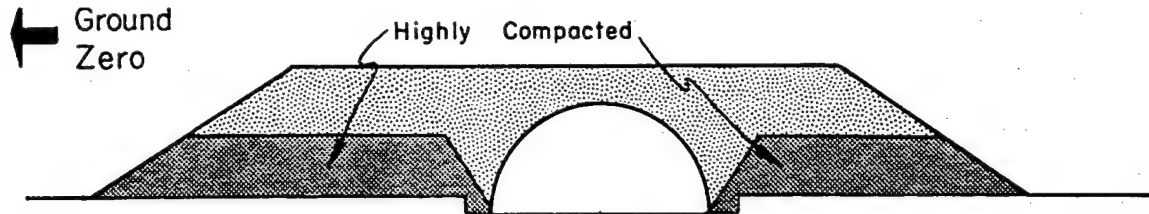


Figure 8.1 Typical non-drag-sensitive earthwork configuration.

the relations of the structure to the existing ground surface. The tops of footing and floor slab were placed one foot above the water-table level, which resulted in floor-slab elevations of  $1\frac{1}{2}$ -to-5 feet below existing ground surface. In each of the structures, a four-inch-thick floor slab was separated from the footings by a one-half-inch space filled with premolded asphalt-impregnated fiber board.

After erection of the corrugated-steel arches, a confining non-drag-sensitive earthwork configuration was formed about the structures as shown in Figure 8.6. These earthworks were formed with the coral sand from the same island sites. Most of the earthwork material was placed in one-foot lifts by carryall scrapers. Compaction was accomplished by spraying sea water, and by passes with D8 bulldozers. The coral sand close to the sides, ends, and atop the structures (five feet of cover at crown of each structure) was placed with clamshell cranes in approximately 3-foot lifts, and each layer of soil was sprayed with sea water to accomplish necessary consolidation.

None of the four arch structures contained any additional supporting members. No partitions or mechanical equipment were in any of the structures, inasmuch as the primary objectives of the project were limited to structural systems only. Timber stagings were used to support instrumentation, but these were placed so as not to interfere with any responses of the structure below failure deformation ranges.

8.3.4 Instrumentation. The purpose of the structural instrumentation was to measure the following:

1. Interior pressure versus time. Two self-recording BRL-type gages were used per structure.
2. External overpressure versus time. Two self-recording BRL-type gages were used per structure.
3. Acceleration of floor slab versus time. One self-recording and fifteen electronic accelerometers were installed in the four structures by Ballistic Research Laboratories (BRL), Stanford Research Institute (SRI), and the Naval Civil Engineering Laboratory (NCEL). All except two instruments measured the vertical component of acceleration.
4. Deflections of arches. Scratch-type deflection gages were placed at 10 positions in each structure. In addition, self-recording drum-type deflection gages were placed in five positions in each structure subjected to long-duration loadings from Shot Koa to give a deflection-versus-time record.
5. Dynamic pressure versus time. Electronic and self-recording drag-pressure gages

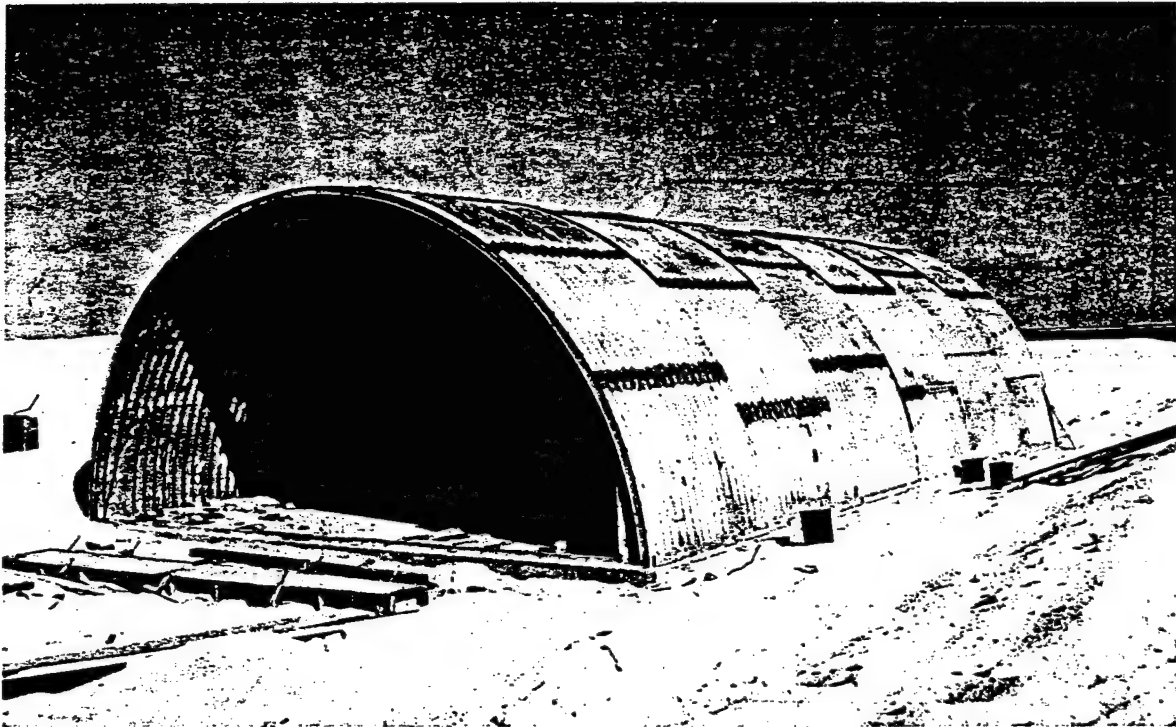


Figure 8.2 One of the 25-foot-span arch shells.

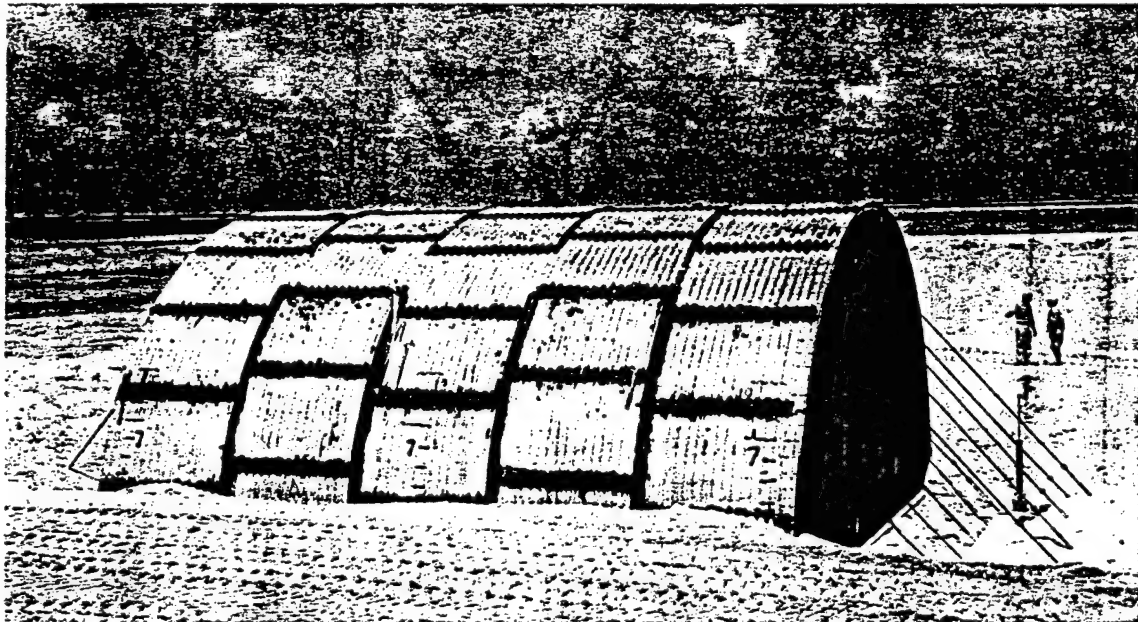


Figure 8.3 Structure 3.2d, endwall reinforcing by steel tie-rods and concrete deadman anchorage.



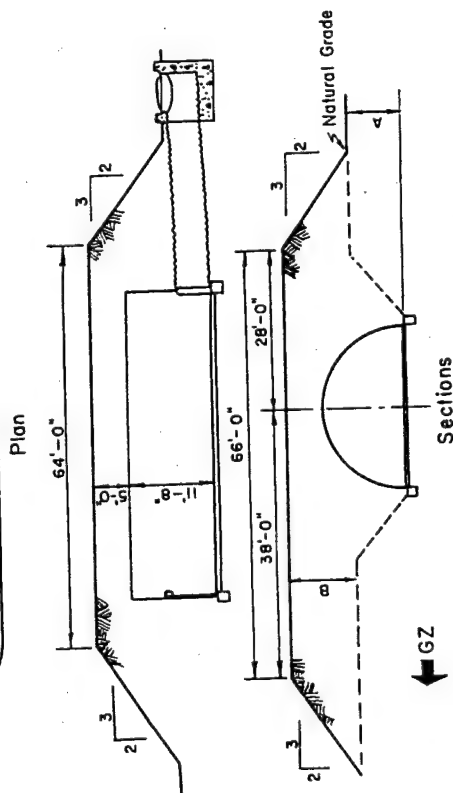
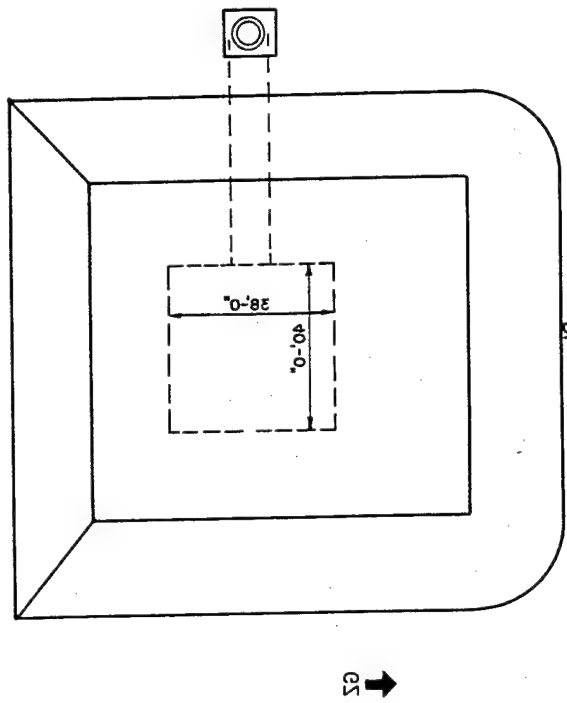


Figure 8.4 Earth configuration, 25-foot-span structure; for 3.2a, A = 5.0 feet, B = 12 feet; for 3.2b, A = 3.0 feet, B = 14 feet; and for 3.2c, A = 1.5 feet, B = 15.5 feet.

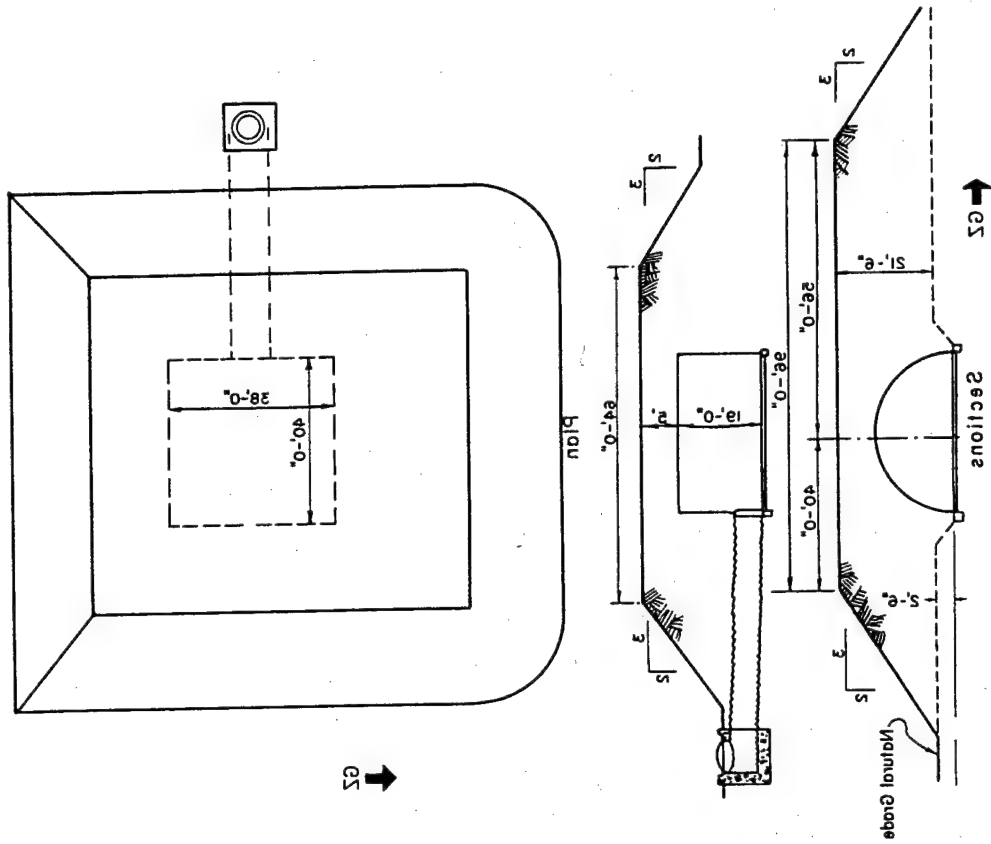


Figure 8.5 Earth configuration, 38-foot-span structure.

were installed by BRL at the natural grade adjacent to each structure.

Gamma- and neutron-radiation shielding effectiveness was measured with chemical dosimeters provided by the U. S. Air Force School of Aviation Medicine, and gamma film badges provided by TU-6 of TG-7.1.

**8.3.5 Results.** Table 8.1 includes a summary of important blast and structural considerations, together with certain results that were obtained by remote instrumentation. A description of the postshot condition of each structure is presented below.

Structure 3.2a. Figure 8.7 shows the condition of Structure 3.2a after a partial excavation.

TABLE 8.1 SUMMARY OF STRUCTURAL RESULTS

NYA, data not yet available.

	3.2a	3.2b	3.2c	3.2d
Span of structure, ft	25	25	25	38
Gage of steel arch sections	10	10	10	1
Gage of endwalls	8	8	8	3
Earth over crown of structure, ft	5	5	5	5
Code name of shot	Cactus	Koa	Koa	Koa
Site of device	Yvonne	Gene	Gene	Gene
Site of structure	Yvonne	Irene	Helen	Irene
Yield predicted	13 to 17 kt	1.25 to 2.25 Mt	1.25 to 2.25 Mt	1.25 to 2.25 Mt
Approximate yield reported	18 kt	1.3 Mt	1.3 Mt	1.3 Mt
Distance from ground zero, ft	980	4,470	3,200	3,950
Overpressure predicted, psi	75 *	75 *	200 †	100 †
Overpressure measured, psi	90	78	180	100
Duration positive phase, sec	0.40	1.6	1.2	1.52
Arrival time, sec	0.14	0.85	0.2	0.5
Dynamic pressure, psi	NYA	NYA	NYA	NYA
Maximum internal pressure, psi	2.5	NYA	NYA	NYA
Maximum vertical acceleration of floor slab, g ‡	+7.8 -3.5	NYA	NYA	NYA
Maximum horizontal acceleration of floor slab, g §	+4.2 -1.85	NYA	NYA	NYA
General postshot conditions	Collapse on side away from ground zero	Complete collapse (symmetrical)	Complete collapse (symmetrical)	Complete collapse (symmetrical)

\* On basis of 15 kt.

† On basis of 1.5 Mt.

‡ + indicates upward acceleration; - indicates downward acceleration.

§ + indicates direction away from ground zero; - indicates direction toward ground zero.

tion to permit safe recovery of data. Scratch-gage records indicated that the initial translation of the arch shell was almost directly downward at the crown for a distance of eight to nine inches, while points at 45 degrees on both sides of the arch moved almost downward four to five inches. After these initial deflections, the records show random traces which apparently occurred during the structural collapse, and while one of the instrument-supporting stages was being severely damaged. The collapse of the structure on the side away from ground zero was apparently initiated by bearing failure of the shell plates at bolt holes of the horizontal bolted seam, approximately five feet above the floor level on the collapsed side of the structure.

The fact that the initial response was nearly symmetrical and that the failure occurred on the side away from ground zero indicates that the earthwork configuration minimized the effects-



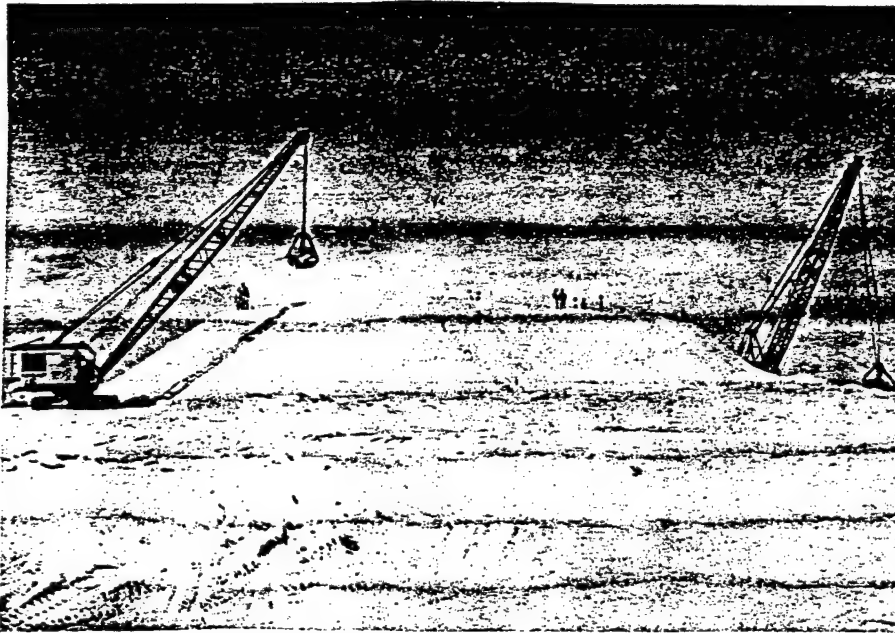


Figure 8.6 Completion of earthwork construction, Structure 3.2b.



Figure 8.7 Postshot view of horizontal plate joint in Structure 3.2a. Note bearing failure of metal adjacent to bolt holes, caused by compressive forces transmitted along arch shell.

asymmetrical loading due to dynamic pressure. The footing on the ground-zero side had moved downward 3 1/2 inches relative to the floor slab. The footing on the side away from ground zero was covered with folded portions of the steel-arch shell, and relative elevations of the slab and footing were not determined. It should be noted that a hard-cemented-sand layer was located approximately two feet below the bottom of the footing for this structure.

Structure 3.2b. Complete and apparently symmetrical collapse of the arch shell occurred and a large quantity of sand entered the structure when the excessive deformation pulled the shell clear of the end wall. Figure 8.8 shows the postshot condition of the two ends of the structure. No data or equipment could be retrieved from within the structure until complete uncovering of the structure when radiation levels from other test events permit. All results were based upon exterior visual inspection of the structure. At both ends the arch shell had deformed in a peaked shape, approximately symmetrical about the crown.

Structure 3.2c. The arch shell collapsed completely, and entry into the structure to re-

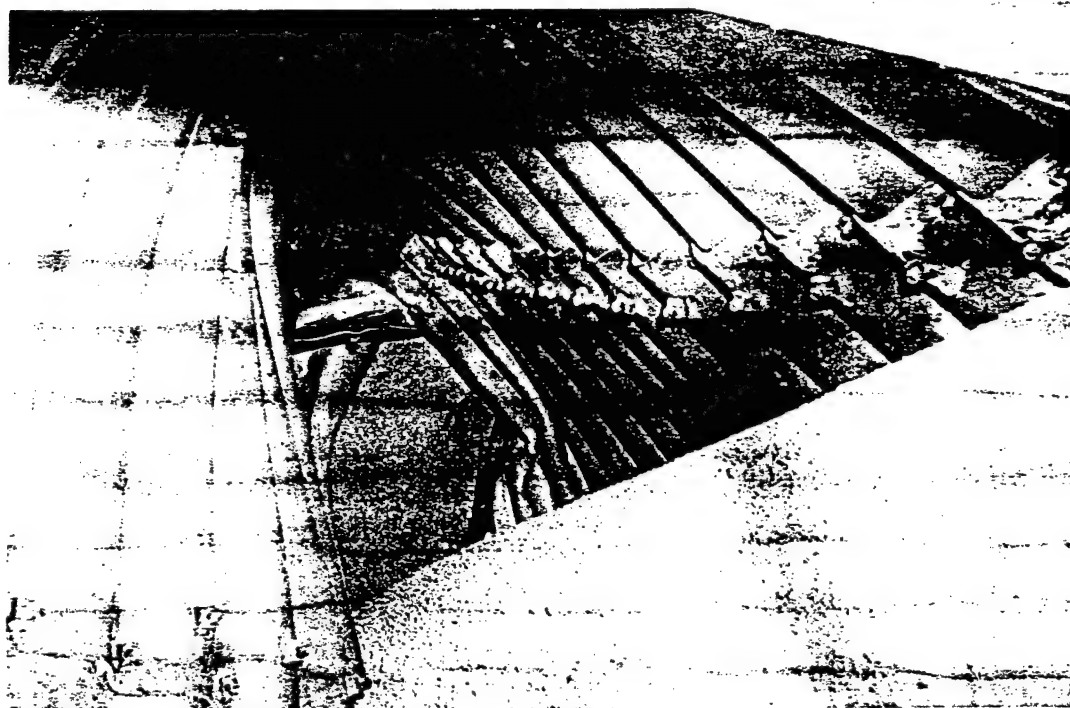


Figure 8.8 Structure 3.2b, postshot. Closeup immediately inside access-end edge of arch shell. Clearance between sand and shell near center of photograph is approximately 2 feet. Ground zero was at right.

cover data and records was not possible until complete uncovering of the structure. Figure 8.9 shows the 12 inches of mud covering the floor slab, and the crown of the structure deflected close to the floor slab. The water apparently entered at the ends of the structure during the wave which resulted when the shot inundated the area.

Structure 3.2d. Figures 8.10, 8.11 and 8.12 show the posttest collapsed condition of the structure. The arch shell near the crown had been formed into an approximately symmetrical hyperbolic-like arch shape becoming narrower near the center of the structure. The sand apparently entered the structure after the excessive deformation pulled the shell away from the end walls. No data or equipment has yet been recovered except for the center scratch-gage measuring deflections at the crown. This gage indicated a downward vertical movement of approximately 19 inches before collapse of the shell and subsequent random scratch traces.

General Discussion. An earthwork, confined-steel-arch shell virtually identical to

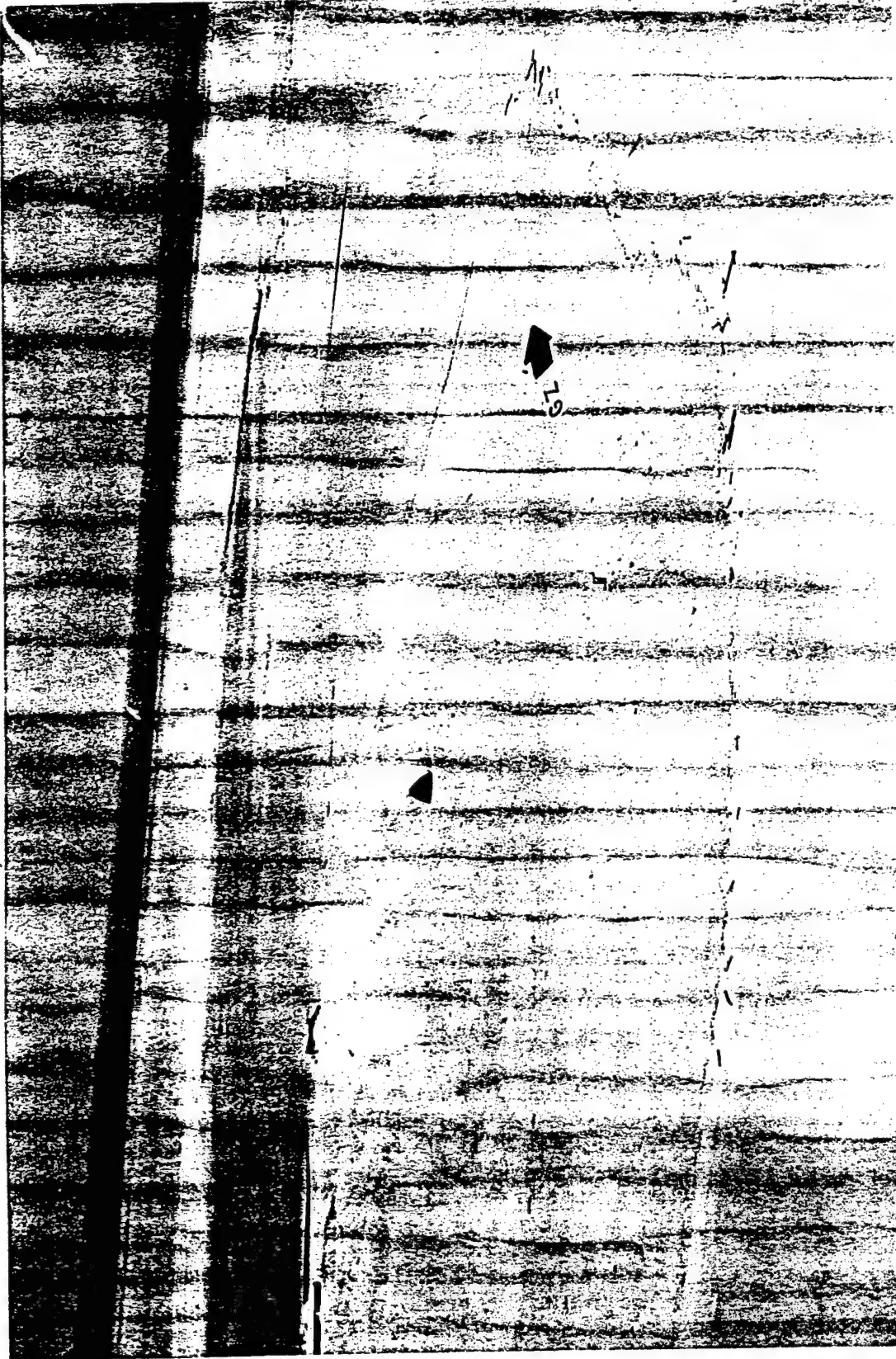


Figure 8.9 Aerial view Structure 3.2d, postshot.





Figure 8.10 Structure 3.2d, postshot. Closed-end shell edge visible. Ground zero was at left. Note 2-foot sag in shell of deformed structure.

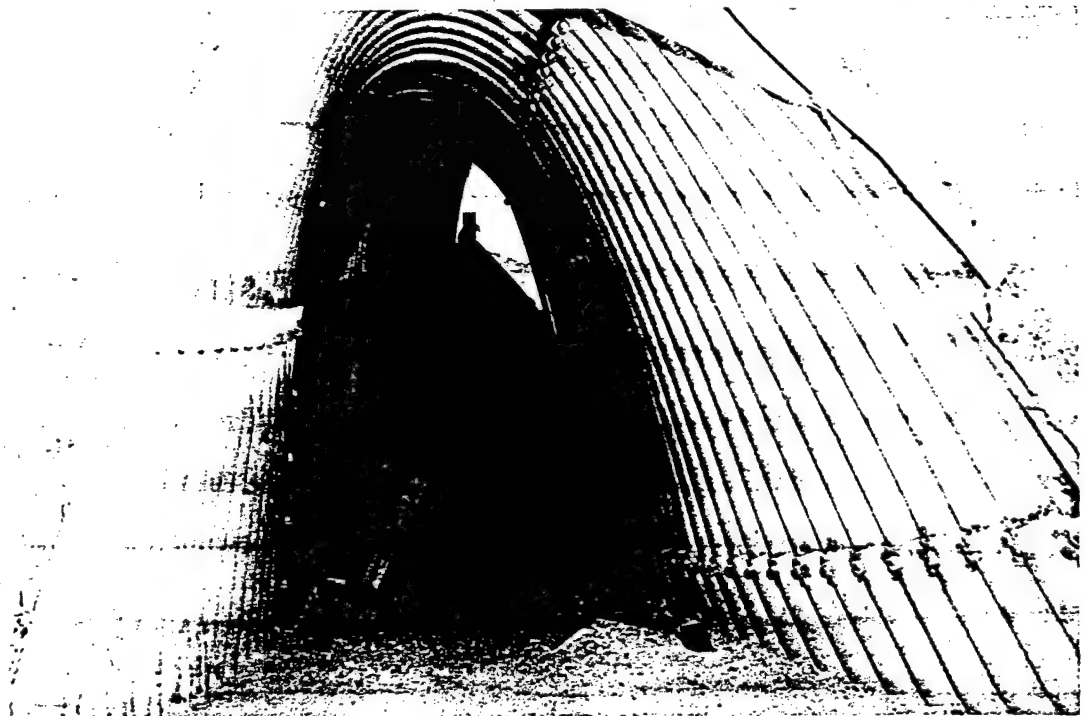


Figure 8.11 Structure 3.2d, postshot. Closed-end shell edge with structure deformed symmetrically about crown. Narrowest part shown was 8 feet above sand and 3 feet wide. Ground zero was at left. Photograph was made at downward angle of 30 degrees.

Structures 3.2a, 3.2b, and 3.2c successfully sustained short-duration peak-overpressure loading of 56 psi from a kiloton-range detonation at 700 feet altitude in Operation Plumbbob. The collapse of Structure 3.2a under short-duration loading of 90 psi, when compared with the survival of a similar structure under short-duration loading of 56 psi during Operation Plumbbob, seems to indicate the upper survival limit of such type structure is bracketed between 56 and 90 psi for short-duration loadings.

Data and equipment recording the initial responses and other structural measurements of structures 3.2b, 3.2c, and 3.2d were not recovered immediately because of high-radiation levels

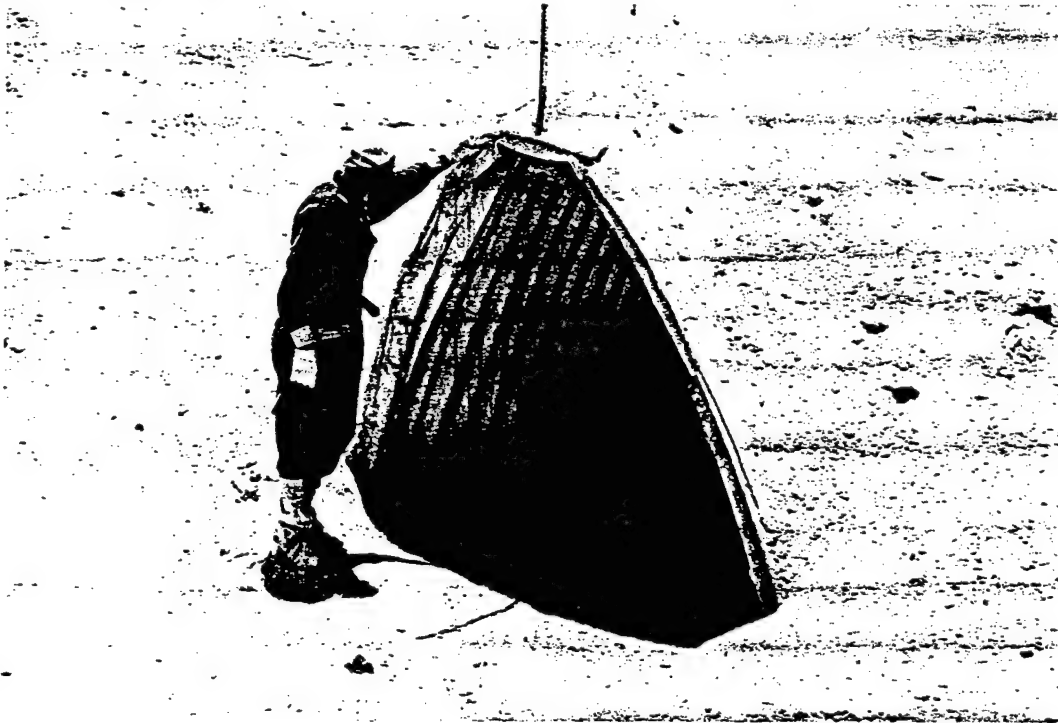


Figure 8.12 Structure 3.2d, postshot. Closed-end shell edge at crown.

which prevented removal of the earth covering and earth inside the structures. Data recovery will be accomplished when radiation levels permit.

The mode of collapse in Structure 3.2a, which apparently began with bearing failures of certain shell plates along a horizontal bolted joint, indicates that strengthening of such joints by using a greater number of bolts might increase the efficiency of the structure.

It should be noted that no direct comparison of structural loading and response of flexible-arch shells can be made between the structures of Operation Plumbbob and similar structures of Operation Hardtack, because of the collapse of the correlating structure, 3.2a, under overpressures higher than anticipated. It should be recognized that the response of flexible-arch structures is dependent upon many soil characteristics which differ according to site location. However, little general knowledge is available concerning the effects of these various environmental conditions, such as the dynamic-bearing capacities of foundation material, the dynamic load-transmission strength, and arching characteristics of soil, and ground-motion characteristics of various soils.

A collateral objective, the determination of radiation-shielding effectiveness of the structures tested, was not satisfied because the ruptures of the steel-arch shells and resulting large sand infiltration prevented valid results from being obtained.

8.3.6 Conclusions. On the basis of preliminary studies of the results of these experiments, it can be stated that:

1. A Navy-stock, 25-foot span, 10-gage, corrugated-steel-arch shell in a non-drag-sensitive confining earthwork of coral sand collapsed on the side away from ground zero when subjected to 90-psi peak overpressure from a surface burst of 18 kt. The collapse was apparently initiated by bearing failure of the shell plates at a bolted horizontal seam, approximately five feet above floor level on the collapsed side of the structure.

2. A Navy-stock, 25-foot span, 10-gage, corrugated-steel-arch structure in a non-drag-sensitive confining earthwork of coral sand collapsed completely when subjected to 80-psi peak overpressure from a 1.3-Mt surface burst.

3. A specially fabricated, 38-foot span, one-gage, corrugated-steel-arch shell in a non-drag-sensitive confining earthwork of coral sand completely collapsed when subjected to 100-psi peak overpressure from a 1.3-Mt surface burst.

4. A Navy-stock, 25-foot span, 10-gage, corrugated-steel-arch shell in a non-drag-sensitive confining earthwork of coral sand completely collapsed when subjected to 180-psi-peak overpressure from a 1.3-Mt surface burst.

The upper limits of survival for all structures tested in this project was less than the overpressures experienced.

Data recovery for this project has not been completed, due to high radiation levels. Therefore, complete or firm conclusions regarding the results are premature. As of the date of this writing no direct comparative analyses could be made that would tend to invalidate the recommendations of Operation Plumbbob Project 3.3 (Reference 26).

#### 8.4 BEHAVIOR OF DEEP REINFORCED-CONCRETE SLABS IN HIGH-PRESSURE REGIONS

8.4.1 Objectives. The original objective of Project 3.6 was to determine the behavior of deep (thick) reinforced-concrete slabs in the overpressure region of 200 to 1,000 psi. and, thereby, to provide a basis for establishing design criteria for massive reinforced-concrete structures under blast loading. The upper limit of overpressure was subsequently reduced to 600 psi to avoid the possibility of losing the slabs in the crater formed by the surface test shot. The term deep is intended to include slabs having depth-to-span ratios from 0.15 to 0.78. It is expected that for slabs of these latter proportions, shear or diagonal tension will prove to be the most significant strength parameter.

8.4.2 Background. A large amount of information on the static strength of concrete beams and slabs has been accumulated during the last several decades by extensive theoretical studies and thousands of laboratory tests. Very few of the previous tests have involved dynamic loadings of reinforced-concrete beams and slabs. Those that have been subjected to dynamic loads were designed for relatively low-loading intensities which resulted in beams and slabs of normal proportions in common use under static-design procedures. Under high-dynamic loadings (hundreds of psi) which protective structures must resist, the normal proportions of beams and slabs must be severely altered to depth-to-span ratios as high as 0.3 to 0.4. Experimental studies for slabs of such proportions have been few and, under dynamic loads, virtually nonexistent.

Information has been urgently needed for the design of doors and covers for entrance ways into underground protective structures, especially structures to be designed and built as a part of our retaliatory installations. The doors of such structures may have to be power operated. In such cases, the weight of the door is important and must be kept to a practical minimum, consistent with requirements for blast and radiation protection.

Ultimate strength design criteria are available for beams or one-way slabs of normal proportions under statically applied loads. Extrapolation of these criteria to deep sections could lead to serious errors, particularly in regard to shear strength since such criteria have developed empirically. Ultimate strength-design criteria for two-way slabs have not been well estab-





lished even for slabs of normal proportions under static loads. Therefore, the design of two-way slabs for dynamic loads has required an even more conservative approach than that for one-way slabs, and has resulted in poor economy. In summary, current design specifications are inadequate for reliable, economical, use for dynamically-loaded slabs of the depths required.

The three modes of failure for both one-way and two-way slabs are flexure, pure shear, and diagonal tension. The following known parameters influence the strength of reinforced-concrete slabs under static loads in each of the modes of failure: concrete strength, steel strength, depth of slab, percentage of tensile reinforcement, percentage of compression reinforcement, and percentage of shear reinforcement. Under dynamic loads the slab strength is also influenced by the ductility factor, natural period of vibration, and load duration. The expected effective load duration (at least 0.10 second) from a device yield in the megaton range is long, relative to the natural period of vibration of the slabs (approximately 0.005 second). The assumption of infinite load duration can therefore be made, thereby simplifying the design computations. The errors introduced by this assumption are considered small in comparison to other uncertainties. For this test project, theoretical design criteria were developed in terms of the above parameters for the loads required to produce failure in each of the three specified modes: flexure, pure shear, and diagonal tension.

8.4.3 Structure Description and Construction. The span lengths and overpressure levels of the slabs tested were chosen with due consideration for field construction and financial limitations. It was originally conceived that both 6-foot and 20-foot-span slabs would be tested, but financial limits restricted the tests to the shorter spans. All slabs were designed with clear span between supports of 6.0 feet, and with their top surfaces flush with ground level so that only the overpressure would act on them.

An extensive instrumentation program was not included because of the gross lack of data concerning dynamic diagonal tension strength. Therefore, information gained from the tests depended primarily upon the differences between the slabs which failed, and those which did not.

The test specimens consisted of 30 one-way and 10 two-way reinforced-concrete slabs. The test specimens were located on Site Helen for Shot Koa. The 10 two-way slabs and 15 one-way slabs were located at the predicted 600-psi overpressure level, and the remaining 15 one-way slabs or beams were located at the predicted 175-psi overpressure level. The 10 two-way slabs had five different effective depths from 10 to 30 inches, with variations in flexural steel and web reinforcement to change the strength at common depths. The one-way slabs were similarly divided into five different effective depths at each location, 20 to 56 inches at the predicted 600-psi level, and 11 to 31 inches at the 175-psi level. Figures 8.13 and 8.14 show details of the test specimens and supporting structures. The slabs were proportioned so that a departure from the predicted overpressure levels of as much as  $\pm 50$  percent would still give results which would yield valuable information.

For better concrete control, all slabs were precast at a site in California and shipped to the EPG. Test cylinders for each slab were provided for determining the 28-day concrete strength, and also concrete strength on shot day. Results of the 28-day strengths which were received after all slabs had been delivered to the EPG indicated that the strengths exceeded the 4,500-psi upper limit of the specified concrete strength by 15 to 20 percent. However, the upward revision of predicted yield for Shot Koa indicated the probability of higher overpressures at both project locations, so this higher-than-specified concrete strength was not considered a totally undesirable feature in the test.

8.4.4 Instrumentation. The minimum data considered necessary for success of this project included the free-field overpressure at each location, and the maximum deflection and mode of failure for each damaged test specimen. Because of the lack of knowledge concerning the rela-

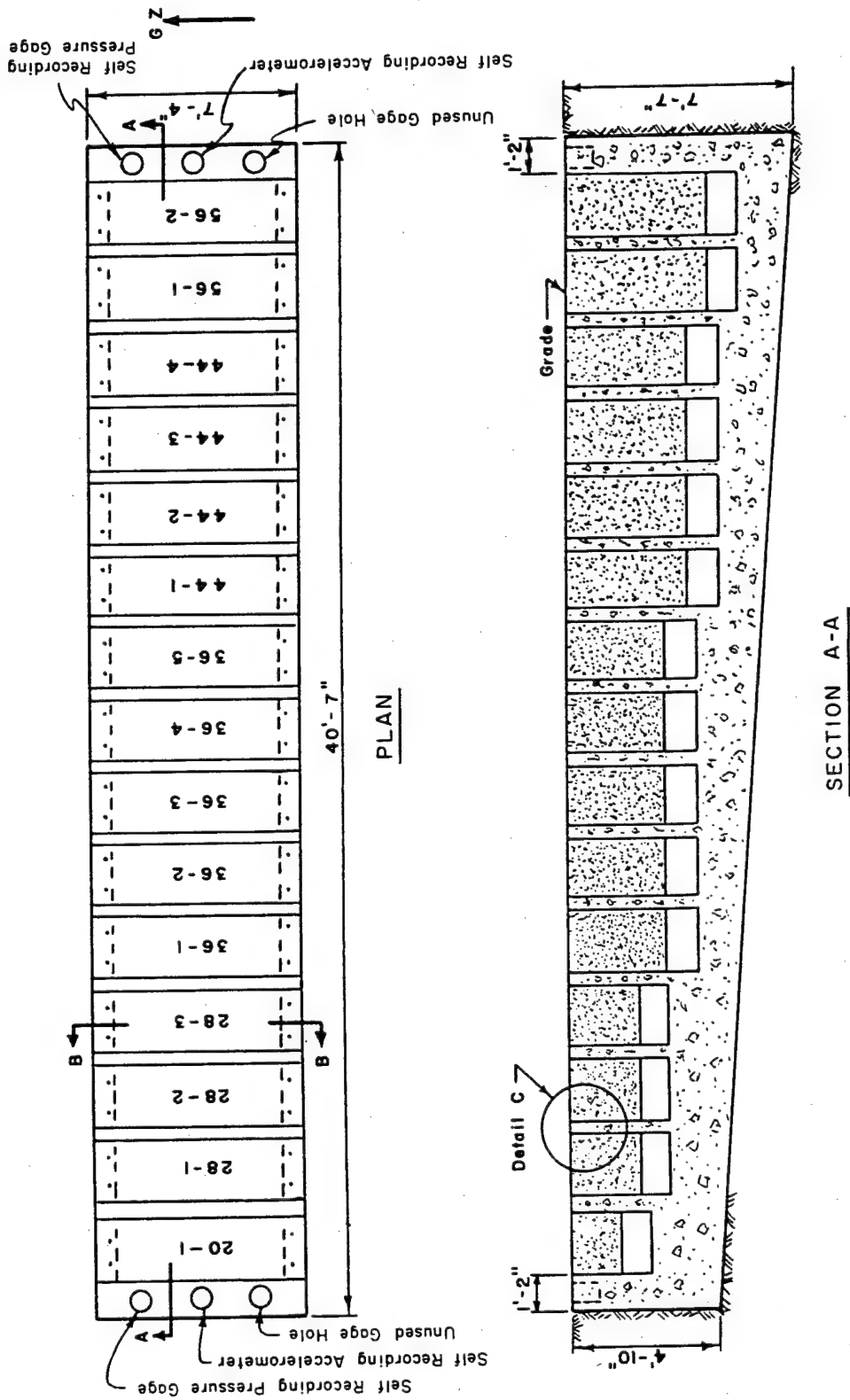


Figure 8.13 One-way slab supports at the 600-psi location.



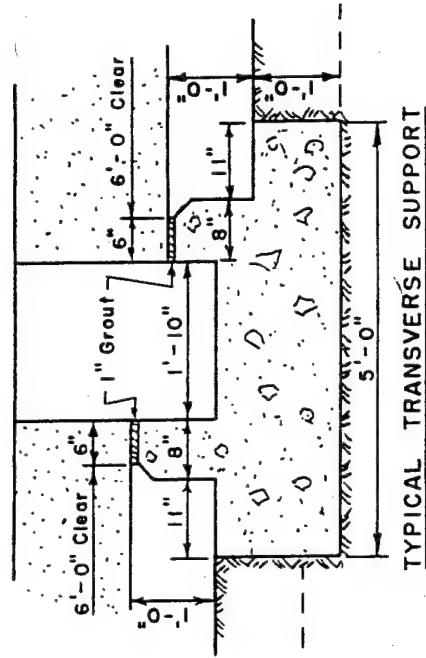
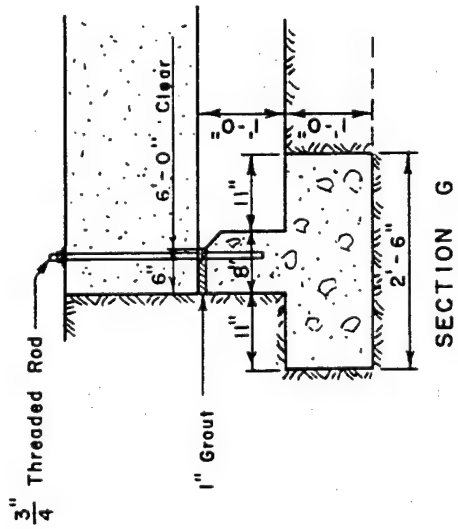
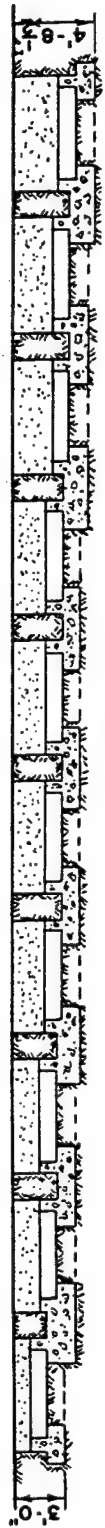
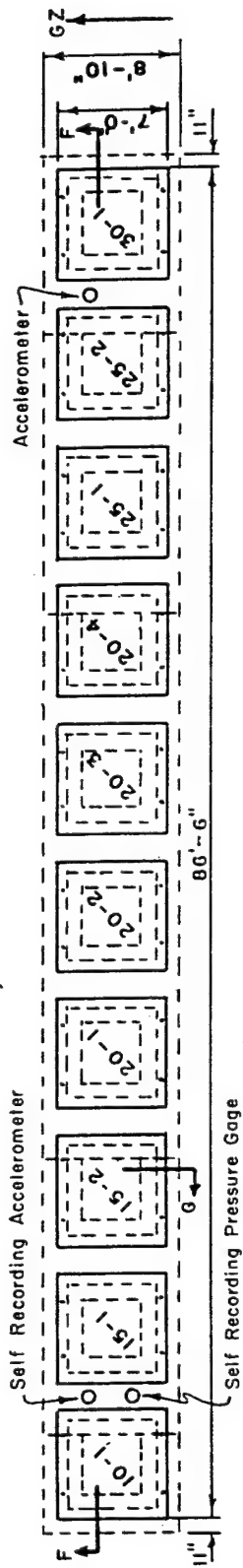


Figure 8.14 Two-way slab support.

tive significance of the several strength parameters, the minimal instrumentation system was intended primarily to define the relative significance of the strength parameters, flexure, pure shear, and diagonal tension.

Overpressures were measured at each of the two locations by BRL self-recording pressure-time gages mounted on the supporting structures. In addition, two BRL self-recording acceler-

TABLE 8.2 PEAK SURFACE OVERPRESSURES

Range	Predicted Peak Overpressure *	Measured Peak Overpressure
ft	psi	psi
1,830	400 to 800	1,110
3,100	125 to 225	190

\* Based on variation in predicted yields of from 1.0 to 2.0 Mt.

ometers were mounted on each supporting structure to record the accelerations. It was expected that information obtained from the accelerometers would be of limited value insofar as the analysis and interpretation of data for this project was concerned; however, the records were expected to yield additional and much-needed data on the magnitude of accelerations which the structures experienced.

The response of each slab to the applied loading was to be determined by deflection measurements of the top of each slab and by visual inspection of the slabs after removal from the supporting structure. Five steel bolts were equally spaced along the centerline of the top surface of each slab to define the deflected shape. Additional bolts were placed on the diagonals of the two-way slabs.

**8.4.5 Results.** The free-field measurements consisted of surface overpressure measured by BRL self-recording gages. Some of the gages exceeded their calibrated ranges; however, extrapolation from the existing calibration yielded the reasonably reliable peak pressure recorded in Table 8.2.

The canisters housing the self-recording accelerometers did not prove to be water-tight; therefore, no acceleration and records were obtained.

High posttest radiation levels at both slab locations limited the amount of data recovered, and detailed data recovery is scheduled for a period several months after the test. Visual inspection of the surface of the one-way slabs or beams at the 1,830-foot range indicates the following response: (1) a deflection of approximately  $\frac{1}{2}$  inch, and general cracking at the center of the top surface of the weakest slab; (2) all other deflections less than  $\frac{1}{4}$  inch; and (3) cracks in the top surface only on four other test specimens at this overpressure level. Visual inspection of the two-way slabs indicated no cracking on the surface, and a maximum deflection of approximately  $\frac{1}{8}$  inch on one specimen. One two-way slab was missing and several were tilted and buried, indicating a failure of the supporting structure. This location was within 10 feet of the edge of the crater resulting from the shot and, therefore, subjected to severe ground movements. A general subsidence of the slab stations and surrounding ground area of about five or six feet was noted. Figure 8.15 is a view of the general posttest condition of the 1,830-foot-range slabs.

The one-way slabs at the 3,100-foot range were not inspected because of a covering of approximately one foot of dense material and the high-radiation level which prevented removal. Therefore, no data is yet available on the posttest condition of these slabs.

Reference to Table 8.2 indicates that the pressure measured at the 1,830-foot-range location was significantly higher than the predicted values and should have produced failures in most of these test specimens. As previously indicated, the average 28-day concrete strength was above the specified strength. The average strength at shot day exceeded the design assumption of 4,000 psi by 55 percent. These high concrete strengths increased the strengths of the test specimens, but they did not entirely account for the comparatively small amount of damage sustained by the slabs.

Preliminary free-field air-blast results indicate an overpressure-decay rate greater than assumed, so as to give effective durations of only about  $\frac{1}{3}$  to  $\frac{1}{2}$  of the assumed values. Another

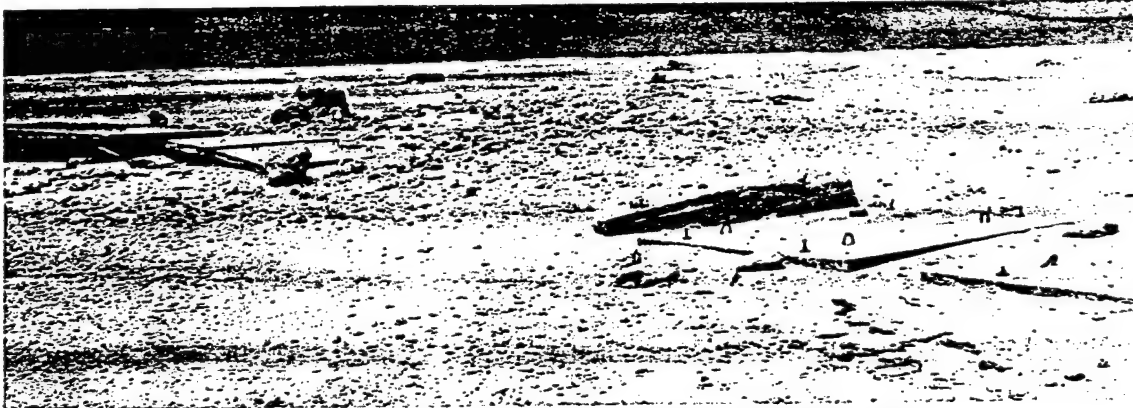


Figure 8.15 Posttest view of two-way slabs at range of 1,830 feet, looking away from ground zero, depicting the evidence of foundation failure.

factor was that the predicted slab strengths were obtained by extending empirical data beyond their previous range of application. Further discussion is not warranted until completion of data recovery and analytical studies of the test results.

**8.4.6 Conclusions.** No firm conclusions can be drawn from the limited amount of data currently available. It appears, however, that the resistance of slabs, particularly in diagonal tension, to high-blast pressures is considerably higher than was expected. Even though preliminary results indicate only relatively minor damage to the slabs, it is believed that when fully evaluated, this information should be sufficient to form the basis for more reliable criteria than is now available for the design of reinforced-concrete slabs to resist high-intensity blast loads.

## 8.5 DAMAGE TO EXISTING EPG STRUCTURES

**8.5.1 Objective.** The objective of Project 3.7 was to record and evaluate damage from blast, radiation, and water waves to pre-existent and new structures at the EPG by preshot and post-shot examinations and measurements.

**8.5.2 Background.** Many structures have been built in prior tests at EPG for the purpose of housing scientific instruments in extreme environments. Damage to these structures was reported, but their exposure to nuclear effects was only incidental to their function, and the opportunity to gain useful information from their behavior was not fully exploited. In addition, a number of test structures still existed in an undamaged or partially-damaged condition. This project was planned to observe those structures, which were subjected to loadings and effects

of interest, in order to amplify and supplement existing design criteria with minimal additional effort.

General damage surveys in published reports have been limited to three shots and have not discussed overall damage-distance relationships. In addition to published reports, Holmes and Narver, Inc. (H&N) had made damage observations and had taken numerous photographs of scientific stations during the preceding EPG operations. These postshot damage reports were given limited distribution to the AEC, LASL, and LRL as a basis for modifying existing scientific stations and designing new stations for future operations. The H&N reports were reviewed, and a tabulated summary of all previous miscellaneous damage observations was included in the Project 3.7 ITR.

8.5.3 Procedures. The objective required the project to adequately document structural damage from most of the Operation Hardtack events at Bikini and Eniwetok.

Instrumentation consisted of 11 self-recording air-overpressure gages, and 6 self-recording accelerometers which were furnished, calibrated, and read by BRL. These gages were located near or inside the structures expected to exhibit responses of interest to the project. Standard dosimeter film packets were located in many of the structures for determining radiation-shielding effectiveness. In addition to a large photographic effort of preshot and postshot pictures, the project performed several level surveys to determine loss of earth cover from water-wave action.

8.5.4 Results and Discussion. Operation Hardtack data points were plotted on the air-overpressure curve compiled from data from previous EPG operations as shown in Figure 8.16. The plotted points agreed closely with the prediction curve and established a high level of confidence for the predicted overpressure values where overpressures were not actually measured.

Limited Operation Hardtack acceleration data was available, and only a few points were plotted on the acceleration-prediction curve compiled from Operation Plumbbob data as shown in Figure 8.17. The data is not sufficient to determine the overall reliability of results obtained from using the curve; however, it appears that a reasonable value can be obtained.

The limited number of radiation measurements made within structures was not sufficient to form firm conclusions. However, the predicted values by use of the concept of the path of least resistance gave closer correlation with film-badge readings than did the values from least-slant-distance computations.

Damage to certain common facilities and installations such as camp sites, generators, and storage tanks had been observed and reported in several previous operations. For these items the previous damage data, as well as that obtained during Operation Hardtack, were studied for the purpose of determining damage-distance relationships. Where possible, the damage was compared with the curves of TM 23-200 (Reference 15).

The damage-distance relationships shown in Figure 8.18 are for the typical light-wood-frame camp-site buildings, and represent the results of observations of damage made in Operations Ivy, Castle, Redwing and Hardtack. Distances shown for severe damage are those for which the probability of the damage occurring is 50 percent, the 2.0-psi level. The spread of the data in the severe damage range supports the methods of obtaining 10-percent and 90-percent probability given in TM 23-200. The moderate damage level (1.0-psi) was determined by using the distance for a weapon of four times the desired yield as in TM 23-200. The light damage curve (0.75-psi) is intended to represent the upper limit of nuisance damage and the threshold of light damage. The severe damage curve (50 percent probability) for wood-frame buildings, one- or two-story house type, as given in TM 23-200, is also shown on Figure 8.18.

A 21,000-gallon bolted-steel water tank directly exposed to 6.5 and 7.0-psi of air overpressure received light damage. The roof was dished in and there was a small amount of buckling above the level of liquid in the tank. In addition, it was noted that there was no damage to the exterior

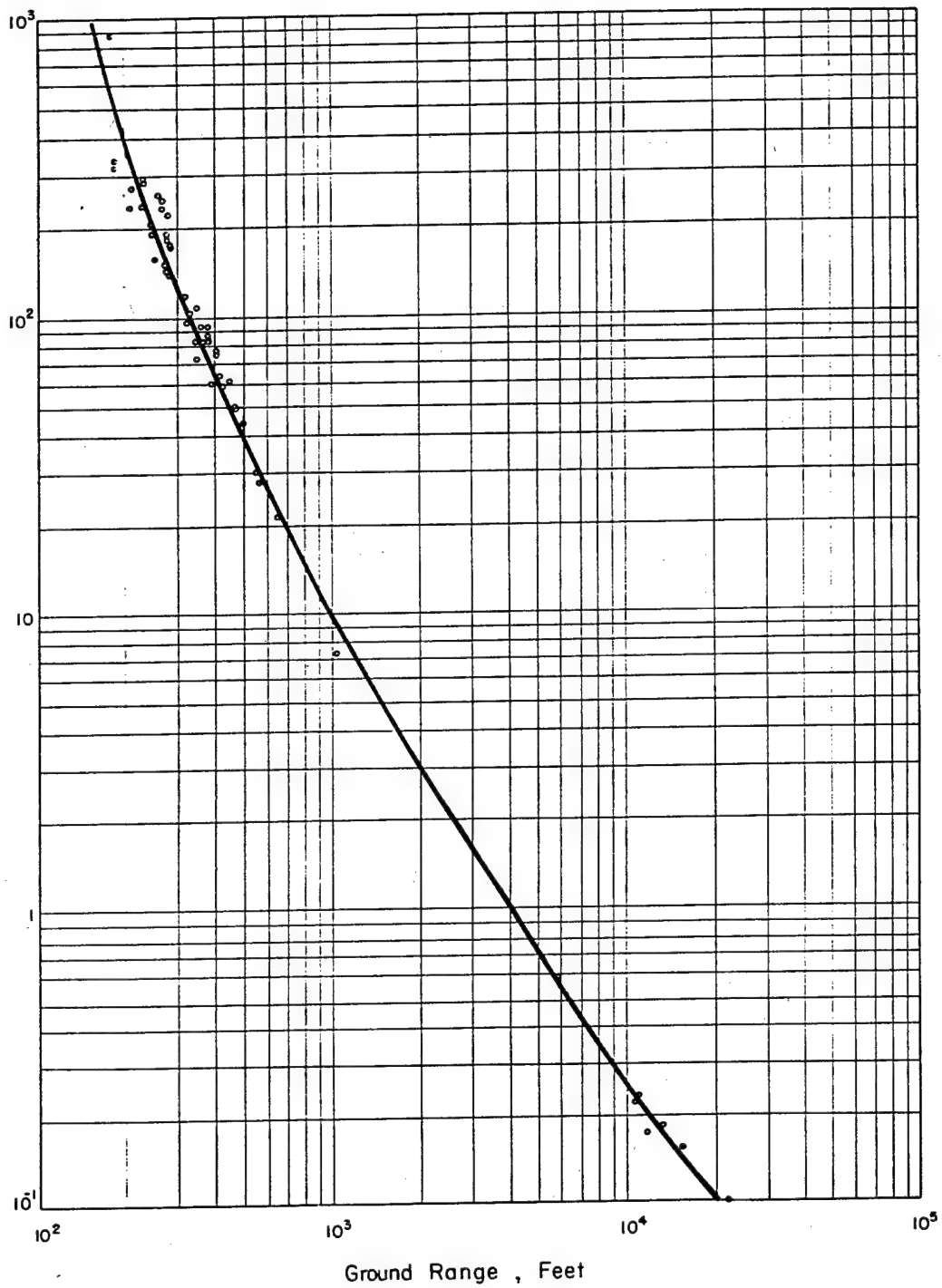


Figure 5.16 Peak air overpressure for a 1-kt surface burst, with observed points.

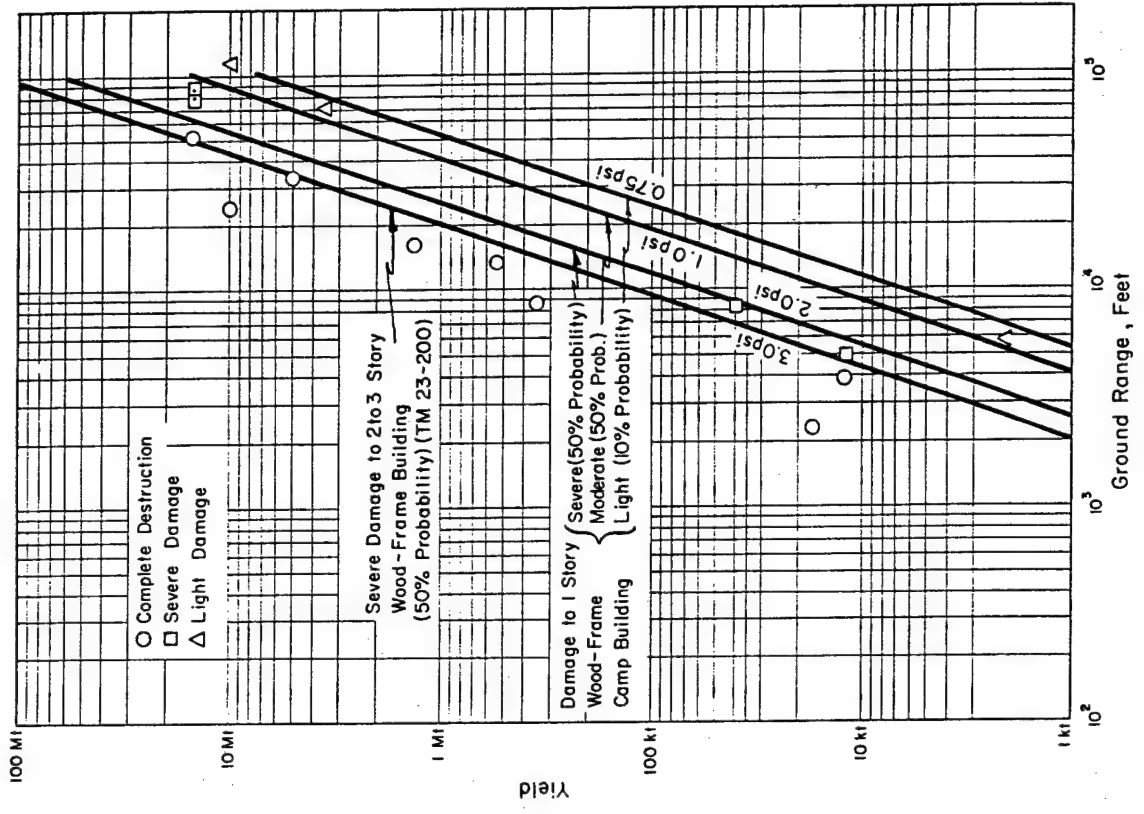


Figure 8.17 Reduced vertical ground acceleration 10 feet below ground surface for a 1-kt surface burst, with observed points.

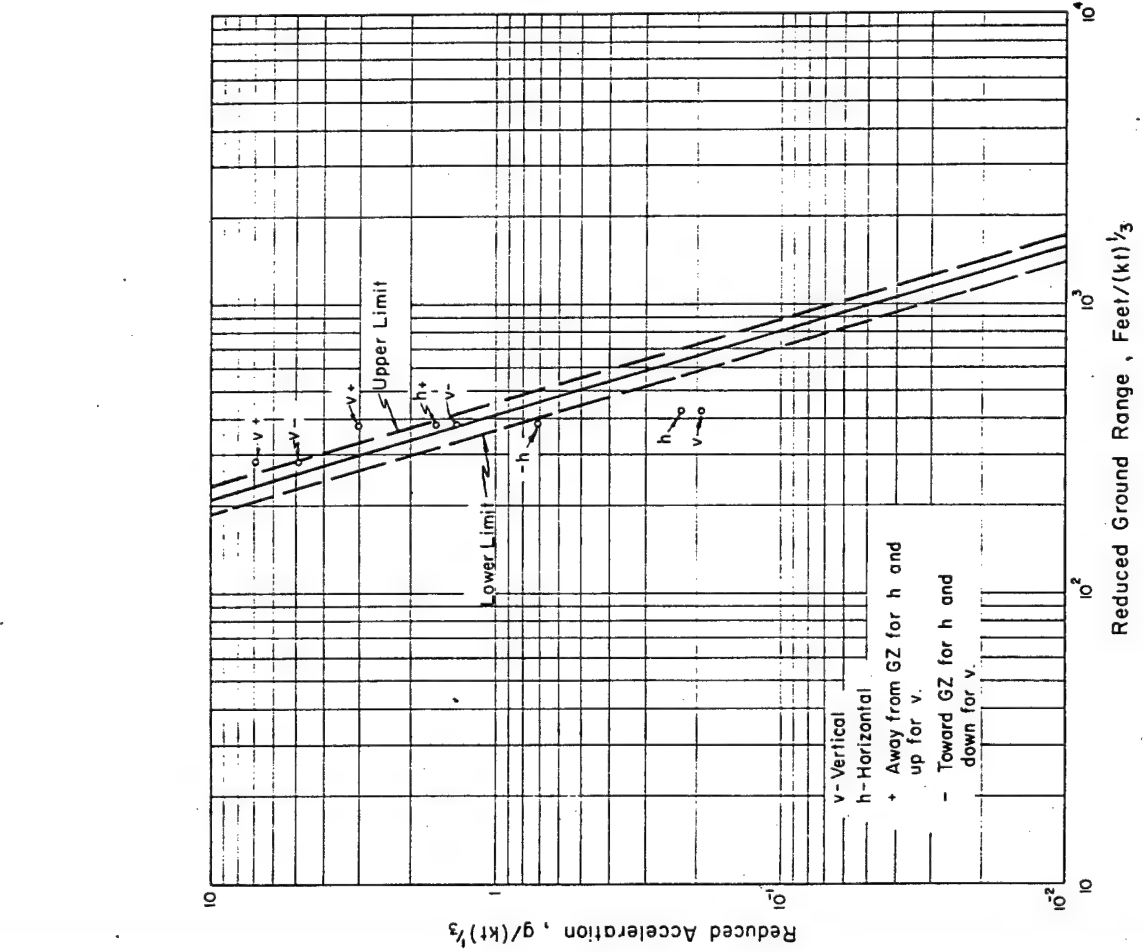


Figure 8.18 Damage to wood-frame camp structures for a surface burst.

connecting piping. Similar tanks exposed in previous operations confirm the observation that these smaller tanks are considerably less vulnerable to damage at a given pressure level than large oil storage tanks. Preliminary examination of the data indicate that light damage is to be expected between air overpressure of 3 and 10 psi.

All heavily reinforced concrete structures, buried, mounded over, or above ground performed satisfactorily without exhibiting any indication of structural failure. One of the buried structures was exposed to an air overpressure of 450 psi.

Blast-generated water waves were instrumental in removing considerable quantities of loose material from earth mounds and earth berms. Observations during this, and past operations, indicate that close-in structures surviving the effect of air blast will undoubtedly survive the force of water waves.

Generators, located some distance behind an earth-mounded structure and exposed to an overpressure of 35 psi, suffered severe damage. However, of particular interest was the striking evidence of the protection afforded objects sheltered from the air blast by an obstruction. The fully sheltered generator located within a distance equal to the height of the mound moved only two feet and was virtually undamaged, whereas the least sheltered generator was thrown 60 feet, and suffered severe damage.

8.5.5 Conclusions. The objective of recording and evaluating damage from air blast, radiation, and blast-generated water waves was attained. The following tentative conclusions are made from a preliminary review of the data:

1. The peak air-overpressure curve, Figure 8.16, is reliable for scaled overpressures from 0.1 to 340 psi.
2. The peak ground-acceleration curve, Figure 8.17, gives reasonable predictions of floor-slab accelerations. However, the overall reliability of the curve was not verified, inasmuch as limited data was obtained.
3. Radiation levels inside several structures were adequately predicted by using the path-of-least-resistance concept while the least-slant-distance concept did not give realistic values.
4. Light wood-frame structures (camp buildings) suffered severe damage from air overpressures ranging from 1.4 to 3.0 psi.
5. Bolted-steel ground-surface storage tanks (20,000 to 30,000 gallon capacity), full of water, suffered only light damage from overpressures less than 10 psi.
6. Heavily reinforced concrete above-ground structures, earth mounded and having five- to six-foot-thick walls, can survive air overpressures up to 450 psi without damage.
7. Objects located close behind earth mounds within a distance approximately equal to the height of the mound receive considerable protection from dynamic pressures at overpressures up to 35 psi.
8. Exposed standard two-inch and four-inch water pipes, including standard rising stem valves, survived pressures up to 8 psi without sign of damage.

8.6 Summary. It is concluded that the results from the projects involved in the land structures phase of Program 3, Operation Hardtack, were successful in achieving their objectives and have contributed a significant amount of information on the effects of nuclear bursts on various land structures under conditions that have not been investigated heretofore.

The upper limits of survival of the three 25-foot spans and the 38-foot span underground corrugated-steel-arch structures are less than the overpressures experienced. These were: 90 psi from kt yield; 80 and 180 psi from Mt yield on the 25-foot spans; 100 psi from Mt yield on 38-foot span. Because of incomplete data recovery, due to high-radiation levels, firm conclusions cannot be drawn at this time. However, comparison with the Operation Plumbbob Project 3.3 structures is expected to permit an estimate of the upper limit of survival of such

337

structures under Mt-yield conditions. As of this date, no direct comparative analyses could be made that would tend to invalidate the recommendations of Operation Plumbbob Project 3.3 regarding such structures under kt-yield conditions. The deep reinforced-concrete slabs tested in the high overpressure sustained generally less damage than expected. Preliminary results indicate that the resistance of the slabs, particularly in diagonal tension, is considerably higher than was expected. Damage to miscellaneous structures at EPG was successfully documented and the information obtained will add to the current knowledge of effects on structures from blast forces, radiation, and water waves resulting from nuclear explosions.



## *Chapter 9*

# *EFFECTS on AIRCRAFT STRUCTURES*

### 9.1 BACKGROUND AND THEORY

Definition of nuclear weapon safe-delivery criteria is a basic objective in all studies of effects on aircraft structures. Nuclear weapon delivery by manned aircraft is often limited by weapon blast and thermal effects on the delivery aircraft and nuclear-radiation exposure of the crew. Analytical methods have been developed for the prediction of these weapon-effect inputs and for the response of the aircraft to these inputs. Data from previous tests have been used to verify and correct these analyses. The data indicates that blast inputs and the skin-temperature rise resulting from thermal inputs can be analyzed and predicted with relatively good accuracy. Prediction of aircraft structural response to the blast and the predictions of thermal inputs have less reliability, however. For planned-delivery tactics where margins of safety may be critical, additional testing was required during Operation Hardtack to establish safe and efficient weapon-delivery criteria. As a by-product of testing to establish weapon safe-delivery limitations, experimental data were also obtained to correct and refine analytical methods with general application to the delivery problem and for utilization in the design of new aircraft.

The crushing effects of overpressure, the transitory effects on lift due to particle velocity in the shock wave, and the short-duration loading caused by pressure imbalance during shock-wave diffraction are important blast inputs in determining aircraft structural loads. All these effects can be defined in terms of overpressure, making this a fundamental measurement in all aircraft-effect projects. Overpressure predictions during Operation Hardtack were based upon a combination of the analytically derived M-problem curve and data published by Haskell-Brubaker as used by the Air Force project (Reference 27), or a curve extracted from "Capabilities of Atomic Weapons" (Reference 15) in the case of Navy projects. The two curves were, for practical purposes, nearly identical. Both curves were established in terms of a 1-kt burst in a homogeneous sea-level atmosphere, necessitating scaling to the yield and prevailing atmospheric conditions. Modified alpha scaling was used by the Air Force project; modified Sachs scaling by the Navy projects.

Prediction of aircraft-structural responses were derived from theoretical analyses and experimental data by the engineering staffs of the aircraft manufacturers concerned. The analyses utilized standardized methods and techniques with heavy reliance upon machine computations. Diffraction loading was included in the dynamic analyses of the A4D and FJ-4 responses because of the very short structural-response times for these aircraft. Diffraction loading was also assumed in the response predictions for the B-52 tail loads. Analysis of Operation Redwing B-52 tail-load data indicated a lack of correlation which was attributed to diffraction effects. Factors were derived from the Operation Redwing data and utilized in initial predictions of the effects on the tail surfaces for the Operation Hardtack participations. No diffraction was accounted for in the B-52 wing analysis, due to the relatively slow response time of this structure, which, it was assumed, precluded any reaction from this type of loading.

Thermal-input predictions were based upon the methods of Chapman and Seavey by the Air Force project (Reference 28), and upon a Bureau of Aeronautics method by the two Navy projects. Thermal-response predictions were developed by the contractors concerned, based upon service specifications. Nuclear-input predictions were based upon the methods and curves contained in

AFSWP Report Number 1100, "Nuclear Radiation Handbook" (Reference 29).

## 9.2 OBJECTIVES

The overall objective of the Aircraft Structures Program was to obtain data from which to determine the delivery capability of the participating aircraft and upon which to base modifications and refinements of prediction methods which would be applicable to these and similar aircraft types.

In particular, structural responses of the B-52 to side loads were studied in order to verify or correct the analysis used in predicting side-load response. This analysis was basic to the problem of defining the capability of the aircraft for multiple-weapon delivery where blast and thermal loads would be received from weapons delivered by other aircraft in a multiple attack.

The two A4D-1 aircraft and two FJ-4 aircraft had, as project objectives, the measurement of effects inputs and structural responses to these inputs. This data will be correlated with that obtained from Operation Plumbbob in order to correct or verify theoretical analyses to be used in the definition of capabilities for delivering Class D weapons.

## 9.3 PROCEDURE

Procedures resembled those of past operations. To insure safety, positions were chosen on the basis of the highest yield that could be expected. Positions in space and tracking information were obtained through radar-guidance systems, MSQ-1A, and the aircraft's bombing and navigation system for the B-52, and M-33 gun-laying radar for the A4D and FJ-4 projects. All systems gave excellent results.

## 9.4 RESULTS

The range of azimuth angles planned for the Project 5.1 participations is indicated in Figure 9.1. These planned positions, although not realized exactly, were approached closely enough to obtain the desired data. In addition to the azimuth angles illustrated, a range of elevation angles from 10.0 degrees to 51.8 degrees was obtained. In general, the more remote the position from ground zero, the lower the elevation angle.

Overpressure measurements, scaled to one kiloton, sea-level, homogeneous-atmosphere conditions, were found to be approximately ten percent conservative. This is illustrated in Figure 9.2, where overpressure and shock-arrival data from all three projects have been reduced and summarized on a common basis to permit comparison.

Significant responses to overpressure existed in the flaps, body frames, fin, and stabilizer. Preliminary observations indicate the flap was more critical, due to bumper loads caused by overpressure, than was the basic airplane. Field analysis of the body response was not performed, due to the complexity of the problem. Preliminary fin- and stabilizer-overpressure response caused by diffraction loading was included in the loads resulting from the material velocity, due to the difficulty in separating the two types of load in the field.

Neither the engine nacelles or the external wing-fuel tanks were found to be critically loaded by blast effects.

Field correlation of test data indicated that the analytical value for bending moment at Wing Station 1178 was a reliable guide to the capability of the wing. Approximately 73 percent limit-allowable load was reached at this station. Stabilizer-load data indicated the pre-Hardtack correlation factors, which included corrections for assumptions of effective area, downwash, and the influence of diffraction loading, were appreciably below the measured values obtained for some orientations. Fin data also indicated this same underpredicting, due to the factors used.

TABLE 9.1 PEAK RESPONSES OF STABILIZER AND FIN, PROJECT 5.1

Calculated loads are based upon material velocities computed from measured overpressures.

Shot	Stabilizer Station 300				Fin Station 291			
	Shear	Moment	Torsion	Load Ratio *	Shear	Moment	Torsion	Load Ratio *
	10 <sup>3</sup> lb	10 <sup>6</sup> in-lb	10 <sup>5</sup> in-lb		10 <sup>3</sup> lb	10 <sup>6</sup> in-lb	10 <sup>6</sup> in-lb	
Fir								
Calculated	7.06	0.337	0.110	0.44	9.72	0.634	0.150	0.56
Measured	4.78	0.352	0.170	0.47	6.40	0.533	0.346	0.55
Koa †								
Calculated	3.73	0.182	0.060	0.24	11.1	0.721	0.168	0.63
Measured	3.51	0.176	0.211	0.36	6.56	0.554	0.287	0.52
Rose ‡								
Calculated	4.47	0.211	0.121	0.28	3.97	0.246	0.105	0.23
Measured	2.91	0.273	0.084	0.36	1.42	0.136	0.114	0.16
Maple †								
Calculated	5.72	0.275	0.151	0.37	7.09	0.571	0.309	0.55
Measured	5.45	0.329	0.293	0.50	7.84	0.672	0.415	0.67
Walnut ‡								
Calculated	6.77	0.624	0.194	0.82	7.42	0.590	0.386	0.61
Measured	6.81	0.792	0.200	1.03	6.81	0.536	0.384	0.59
Redwood †								
Calculated	13.64	0.641	0.374	0.86	—	—	—	—
Measured	9.50	0.634	0.413	0.86	§	§	§	§
Elder †								
Calculated	5.09	0.760	0.241	1.00	10.63	0.858	0.534	0.87
Measured	5.99	0.423	0.489	0.72	10.50	0.998	0.545	0.94
Oak †								
Calculated	3.97	0.198	0.224	0.40	9.02	0.724	0.388	0.77
Measured	4.52	0.289	0.296	0.47	9.72	0.804	0.490	0.80
Cedar †								
Calculated	10.57	0.647	0.411	0.88	9.10	0.656	0.494	0.76
Measured	9.55	0.715	0.469	0.98	8.75	0.729	0.559	0.88
Dogwood ‡								
Calculated	5.95	0.606	0.239	0.80	6.45	0.626	0.408	0.63
Measured	6.96	0.605	0.138	0.79	5.62	0.540	0.386	0.56

\* Load ratio = gust load/limit allowable load.

† Right hand stabilizer.

‡ Left hand stabilizer.

§ Zero response, symmetrical exposure.

TABLE 9.2 THERMAL INPUT AND RESPONSE DATA, PROJECT 5.1

Shot	Direct Irradiance		Indirect Radiant Exposure 160 deg Field of View Horizontal	Temperature Rise *				Convective Cooling Calorimeter Measured
	90 deg Field of View			Body Station 1151		Stabilizer BL 120		
	Irradiance	Time to Second Maximum		Calculated †	Measured	Calculated †	Measured	
	cal/cm <sup>2</sup> -sec	sec	cal/cm <sup>2</sup>	F	F	F	F	F
Walnut	3.96	1.25	8.60 (12.6) ‡	316	167	286	171	201
Redwood	6.56	0.73	8.48 (12.3) ‡	367	197	345	191	208

\* Temperatures shown for black-painted surfaces, absorptivity 0.90.

† Calculated values based upon measured input.

‡ Numbers in parentheses ( ) are calculated based upon measured yield.

Table 9.1 summarizes the significant stabilizer and fin data, which are the most critical surfaces from the gust standpoint.

Thermal inputs and responses on the B-52 were generally of very-low magnitude, except for Shots Redwood and Walnut. From the data of these two shots, the predicted-thermal input was found to be conservative. Temperature rises resulting from the thermal input were 60 percent or less of those calculated from the measured-thermal input. In addition, the measurement obtained from the shielded convective-cooling calorimeter was substantially below the calculated value. Table 9.2 illustrates the principal thermal data obtained.

The range of overpressures and elevation angles investigated by Project 5.2 is illustrated in

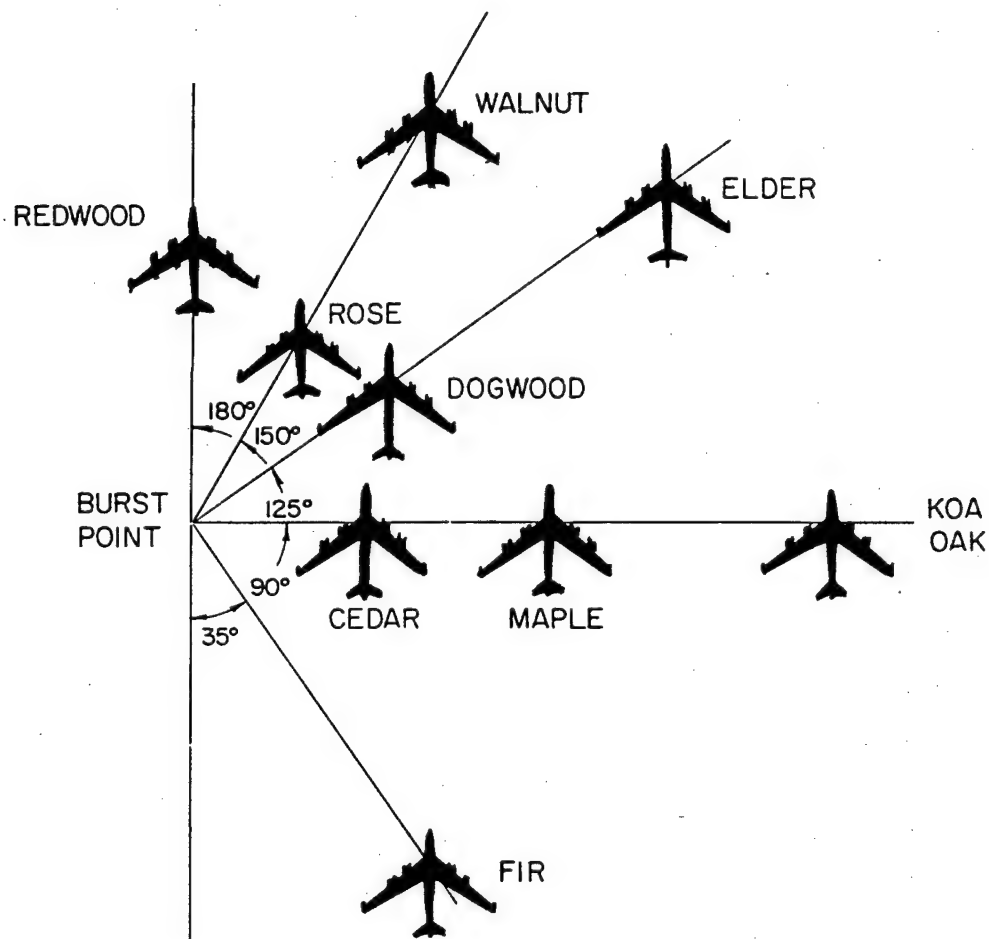


Figure 9.1 Location of the B-52 for each shot participation.

Figure 9.3. It was found that there was a consistent overprediction of overpressures as illustrated in Figure 9.2. As can be seen from the same figure, however, time-of-shock-arrival correlation was excellent. Generally speaking, the A4D structural-response correlation confirmed the analysis with a slight conservatism existing as shown in Figure 9.4.

In general, measured direct-radiant exposure indicated a conservatism when compared with calculated values, but with considerable scatter in the data. The correlation of measured and theoretically-calculated temperature rise reflected these facts as shown in Figures 9.5 and 9.6.

It can be seen in Figure 9.7, however, that if the measured-vertical component of radiant exposure was used in the temperature-rise calculations, much better correlation was obtained, although scatter still existed. This indicated that although radiant exposure predictions were conservative, the temperature-response predictions were relatively quite reliable.

Calculated overpressures for Project 5.3 were also consistently too high as shown in Figure 9.2. Time-of-shock-arrival correlation was good, however. Table 9.3 summarizes the blast

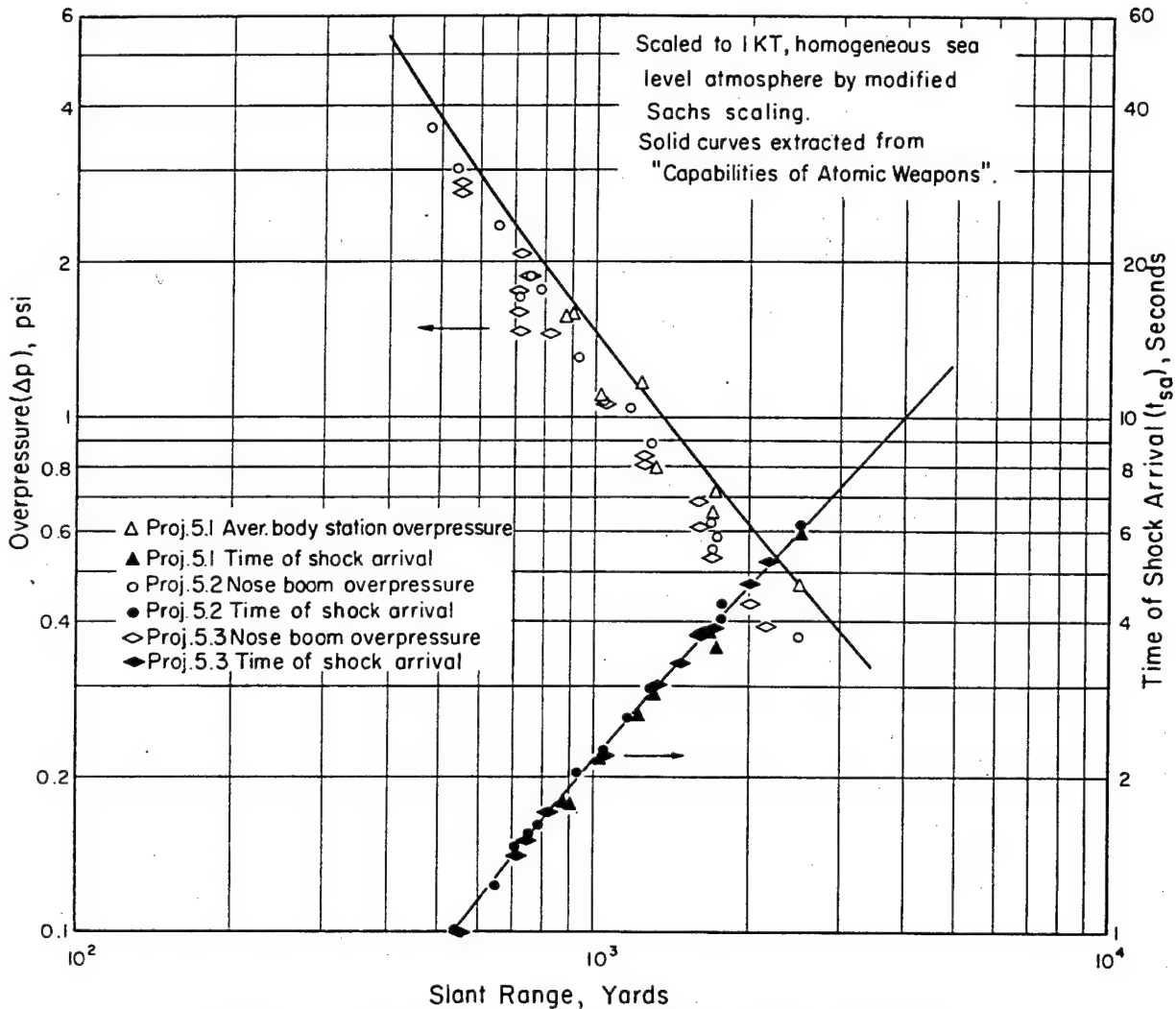


Figure 9.2 Overpressure and time-of-shock-arrival correlation.

input and corresponding dynamic-response data for the aircraft, both predicted and measured. Typical variations of bending-moment stress and of normal-load factor with time, taken from the oscillograph records, are illustrated in Figures 9.8 and 9.9.

Of particular interest with respect to the structural analysis were the results of a wing-pressure survey utilizing data obtained from several series of chordwise-pressure pickups. This measurement technique appears to have promise in surveying the transitory effects during shock-front passage. In particular, it permits an examination of the increment of loading contributed by the diffraction pulse; a study of the gust effects under controlled conditions of aircraft angle of attack

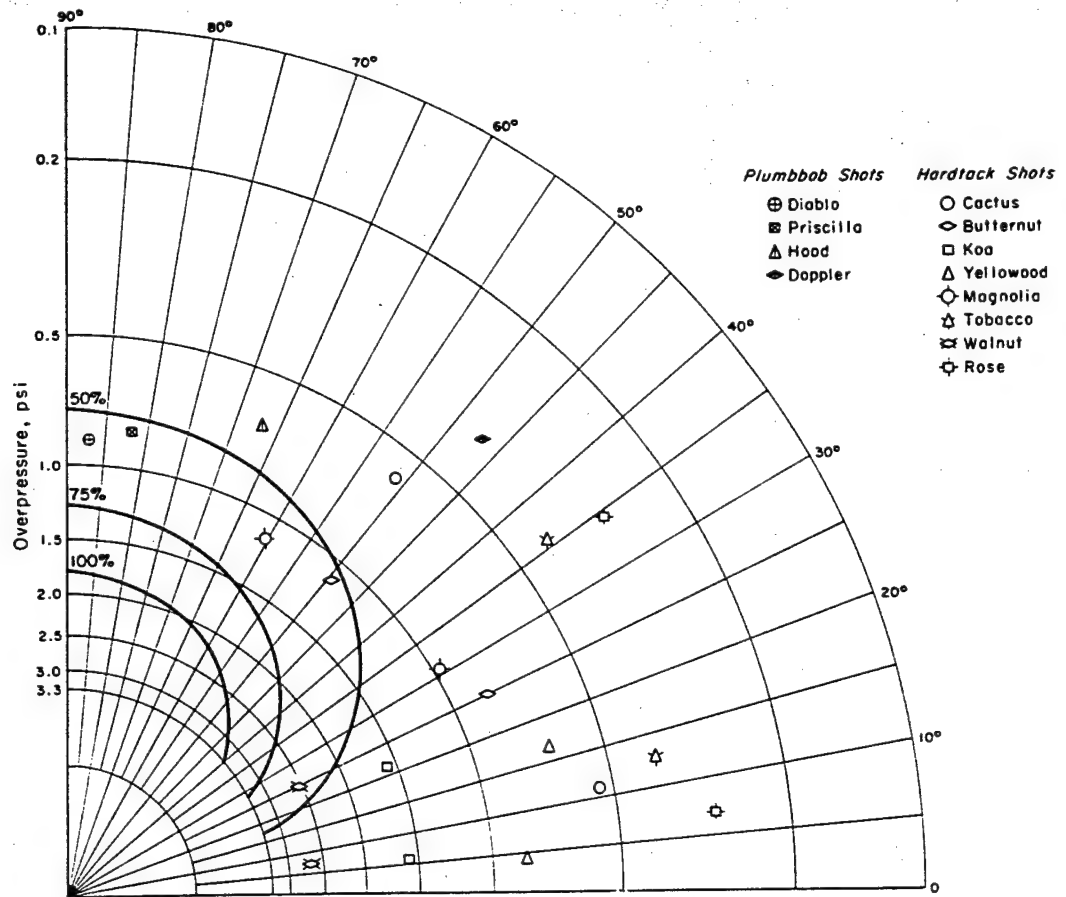


Figure 9.3 Orientation angle and overpressure coverage. Percent lines are percent of design limit bending moment at 600 ft/sec.

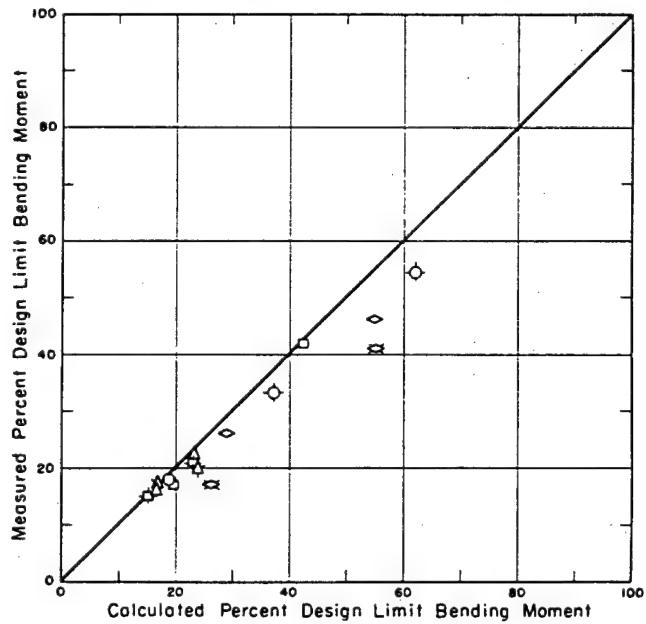


Figure 9.4 Correlation of measured and calculated percent design limit bending moment.

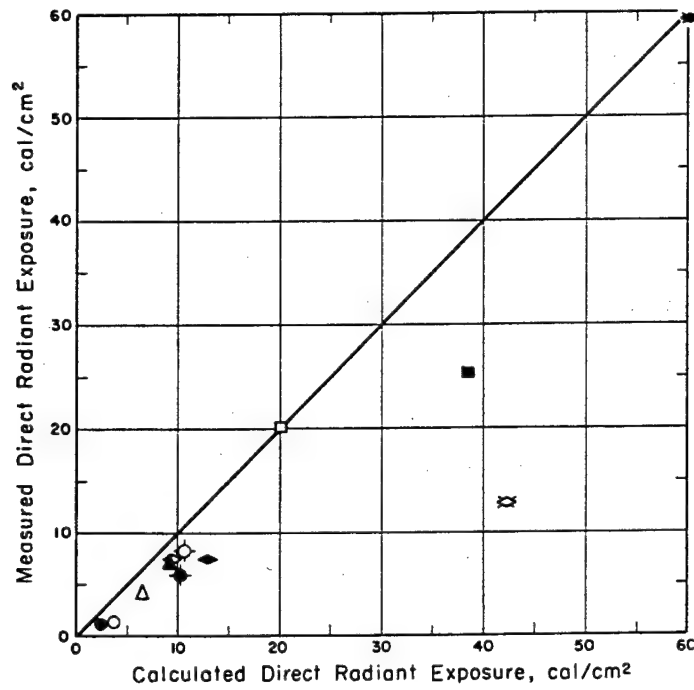


Figure 9.5 Correlation of measured and calculated direct radiant exposure.

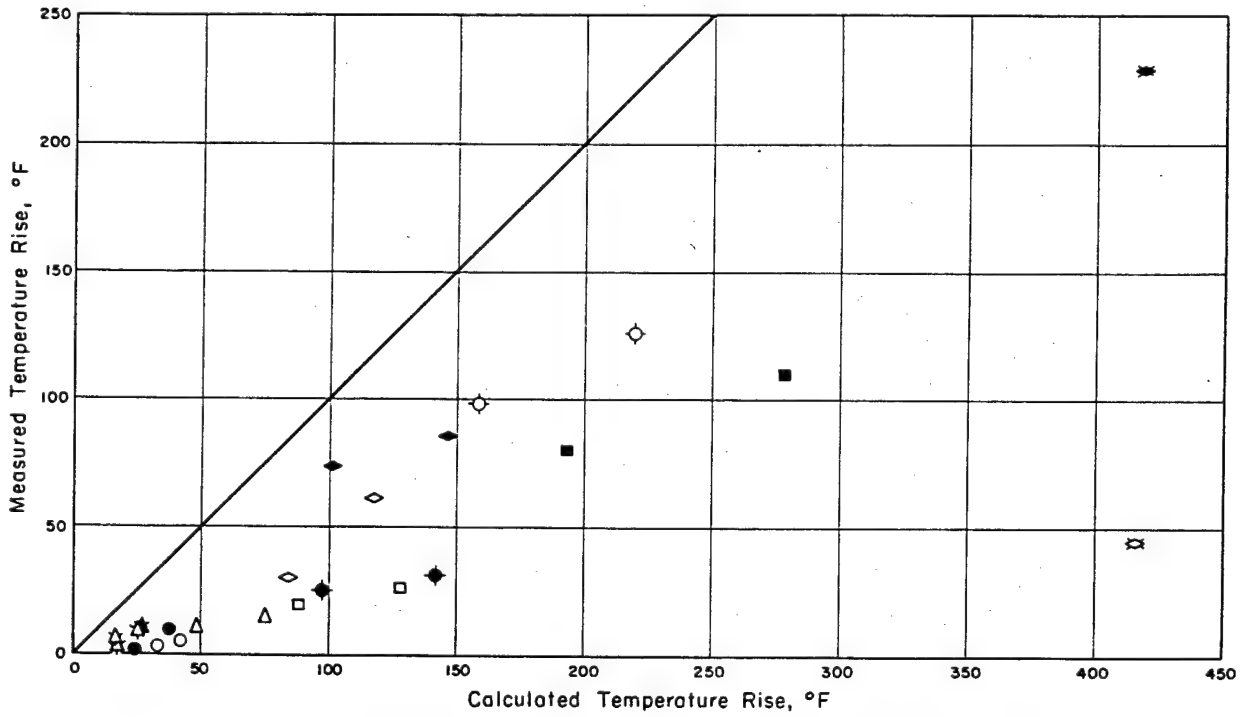


Figure 9.6 Correlation of measured and calculated temperature rise.

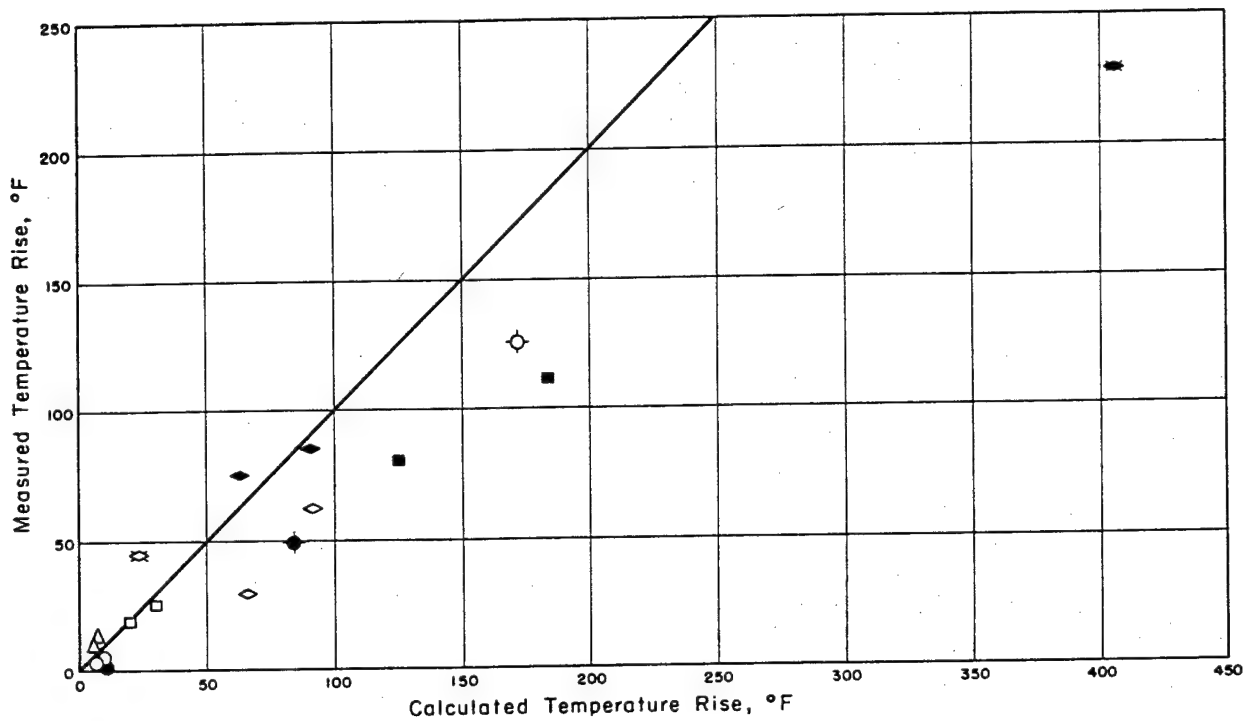


Figure 9.7 Correlation of measured and actual temperature rise using the measured vertical component of the radiant exposure ( $Q_N$ ).

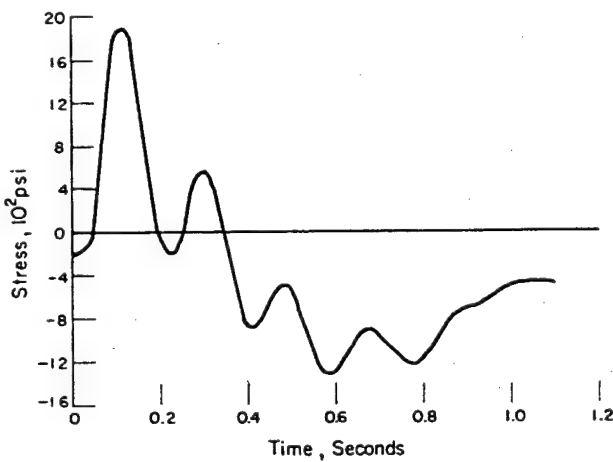


Figure 9.8 Measured variation of bending-moment stress at right-wing Station 17.5 for FJ-4 139467; Shot Koa.

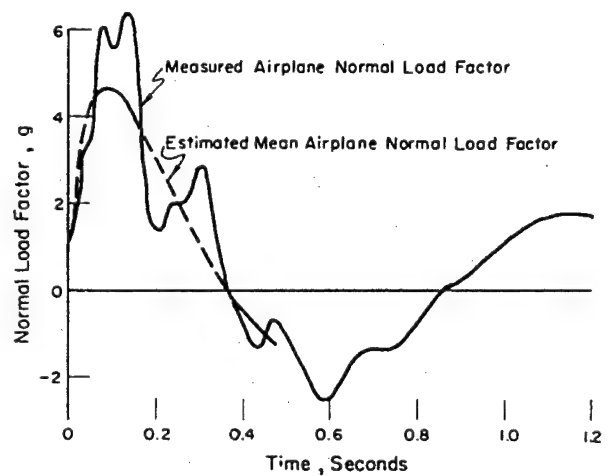


Figure 9.9 Measured normal load factor near the airplane center of gravity for FJ-4 139310; Shot Butternut.



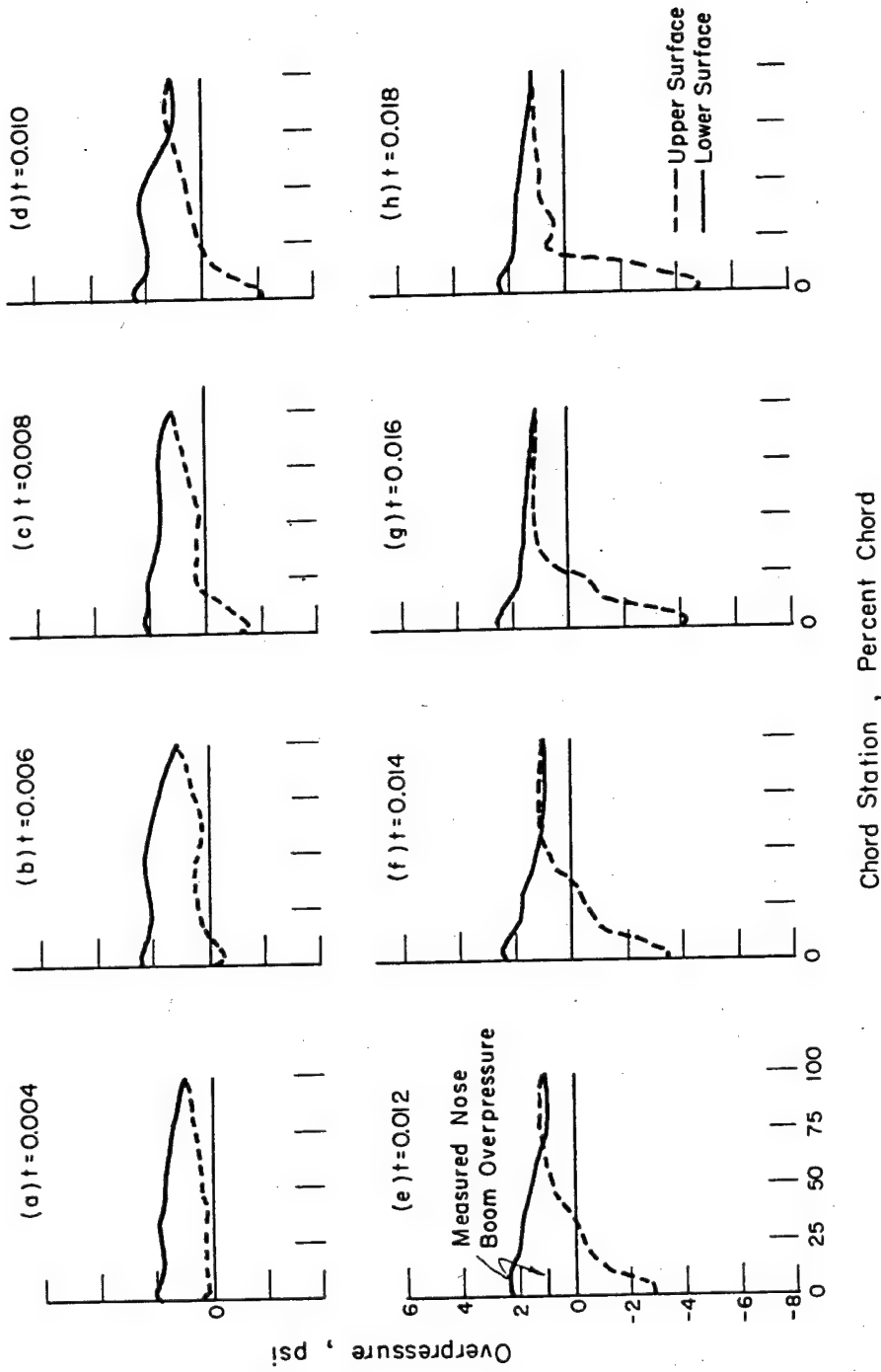


Figure 9.10 Chordwise overpressure distribution at 0.002-second intervals following shock arrival at the tail at Wing Station 175.75 for FJ-4 139310; Shot Butternut.

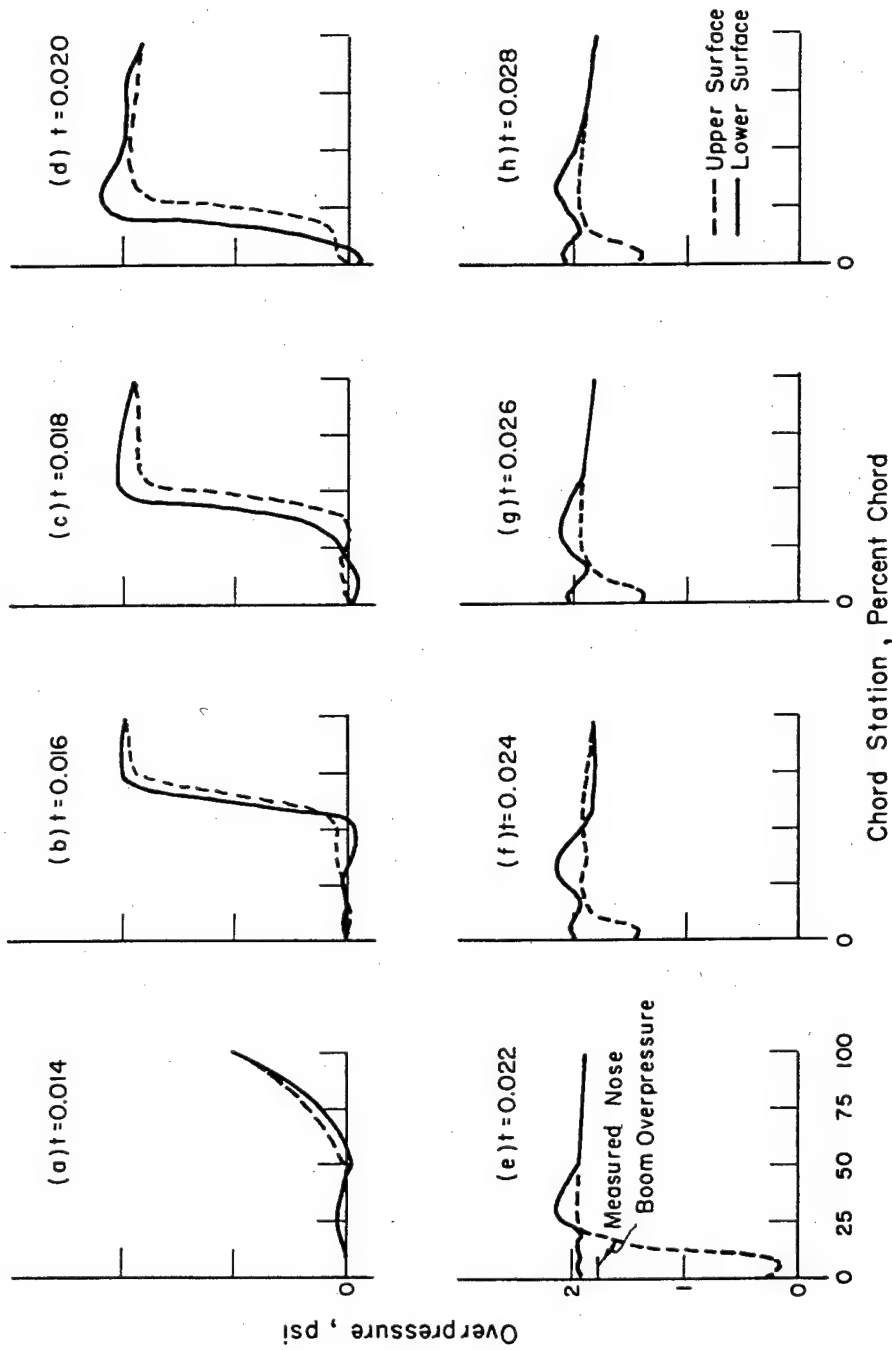


Figure 9.11 Chordwise overpressure distribution at 0.002-second intervals following shock arrival at the tail at Wing Station 175.75 for FJ-4 139467; Shot Koa.

and gust-incident angle; and the obtaining of more complete data to confirm the structural analysis by progressing from the measured-overpressure input resulting from the shock wave, to measured-aerodynamic reaction resulting from this overpressure, and, hence, to the measured-dynamic response of the structure. The pressure-survey results were typical of the data received in both Projects 5.2 and 5.3. Representative plots of this data are shown in Figures 9.10 and 9.11. The first illustrates the pressure distribution for a high-angle-of-incident shock in which the aircraft is nearly over the burst at time of shock arrival. It can be clearly seen that the incremental pres-

TABLE 9.3 MEASURED AND CALCULATED VALUES OF OVERPRESSURE AND TIME OF SHOCK ARRIVAL

Shot	Overpressure			Time of Shock Arrival	
	Measured		Calculated †	Measured	Calculated †
	Nose Boom	Fuselage			
	psi	psi	psi	sec	sec
Cactus *	0.59	0.68	0.71	12.48	11.89
Cactus †	0.62	0.68	0.76	10.66	10.31
Butternut *	0.77	0.98	1.00	14.05	13.95
Butternut †	0.99	1.07	1.40	9.83	8.96
Koa *	1.81	2.19	1.93	19.81	19.27
Koa †	1.09	1.16	1.23	24.96	23.70
Yellowwood *	0.63	0.77	0.77	30.66	30.17
Yellowwood †	0.54	0.57	0.64	31.61	30.71
Magnolia *	1.16	1.42	1.50	8.14	7.69
Magnolia †	1.05	1.06	1.34	9.56	8.96
Tobacco *	0.35	0.43	0.49	13.93	13.82
Tobacco †	0.32	0.36	0.45	16.10	15.77
Rose *	0.34	0.41	0.48	17.66	17.26
Rose †	0.39	0.41	0.51	14.55	13.90
Walnut *	2.50	3.06	2.80	15.18	14.17
Walnut †	1.91	1.95	2.25	16.97	15.54

\* Aircraft 139467. † Aircraft 139310. ‡ Calculated overpressure and time of shock arrival based on preliminary postshot yield, actual aircraft position, and existing atmospheric conditions.

sure on the top surface, due to blast effect, is less than that on the bottom until after diffraction takes place. At this time, approximately 15 msec after the onset of shock arrival, the flow over the wing recovers and a characteristic distribution of steady flow is then maintained. The second figure illustrates the condition typical of a low-angle-of-incident shock in which the increase in pressure, due to the overtaking shock, can be seen progressing across the wing, from trailing edge to leading edge. As can also be seen, the pressure differential between top and bottom surfaces exists over a very small portion of the chord at any one time interval. In Figures 9.12 and 9.13, the chordwise-static pressures have been integrated. The peak in section lift due to the diffraction pulse can be clearly seen, as well as the difference in relative magnitude of incremental lift for the two shot conditions.

Radiant exposure was consistently overpredicted by Project 5.3 during the tests, and as a consequence, calculated maximum temperatures based upon these predictions were greater than measured. However, correlation of maximum temperature based on measured radiant exposure

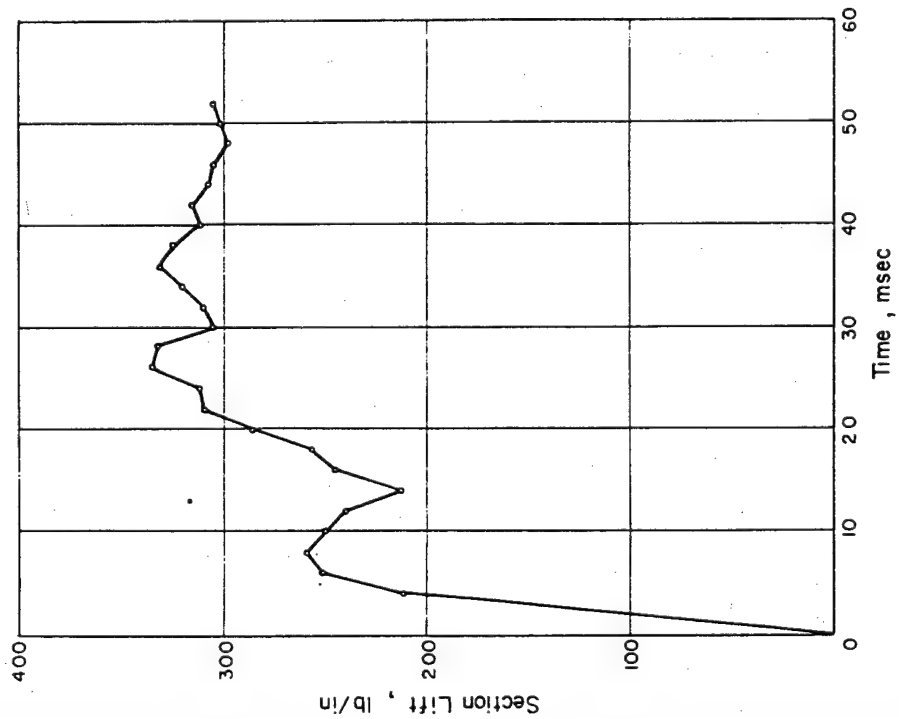


Figure 9.12 Incremental section lift, following shock arrival at the tail, at Wing Station 175.75 for FJ-4 139310; Shot Butternut.

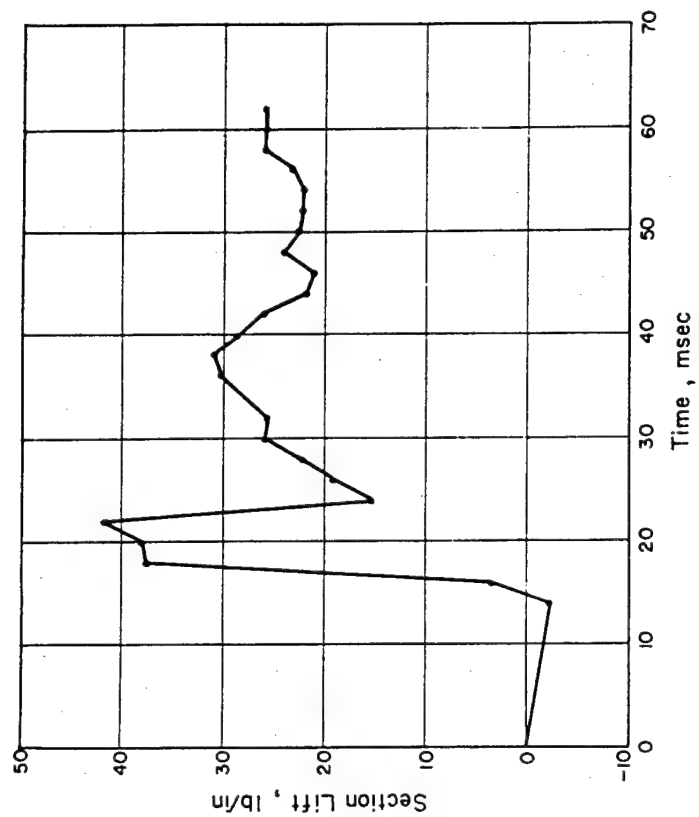


Figure 9.13 Incremental section lift, following shock arrival at the tail, at Wing Station 175.75 for FJ-4 139467; Shot Koa.

TABLE 9.4 MEASURED AND CALCULATED VALUES OF MAXIMUM TEMPERATURE RISE

All temperature measurements given in °F. Data from Shots Tobacco and Rose not significant.

Shot	Fuselage	Fuselage	Fuselage	Fuselage	Wing	Wing	Aileron	Elevator	Flap
	Station 210	Station 250	Station 331	Station 389.375	Station 170	Station 222	Honeycomb Face Plate	Honeycomb Face Plate	Honeycomb Face Plate
Cactus †									
Calculated §	28.0	—	35.1	—	—	—	35.6	33.2	—
Calculated ¶	8.8	—	11.0	—	—	—	11.2	10.5	—
Measured	7.0	††	6.5	††	††	††	9.0	5.5	††
Butternut *									
Calculated §	45.2	—	56.4	79.4	—	—	54.1	47.4	—
Calculated ¶	28.3	—	35.3	49.4	—	—	34.0	29.7	—
Measured	22.0	††	29.0	34.0	††	††	25.0	28.5	††
Butternut †									
Calculated §	51.3	—	64.1	—	—	—	55.8	51.2	—
Calculated ¶	27.4	—	34.2	—	—	—	29.9	27.4	—
Measured	19.6	††	17.0	††	††	††	28.5	18.0	††
Koa *									
Calculated §	46.8	47.7	58.1	81.7	—	—	52.2	46.5	—
Calculated ¶	12.6	12.8	15.5	21.9	—	—	13.8	12.3	—
Measured	14.0	22.0	23.0	34.2	††	††	16.5	17.5	††
Koa †									
Calculated §	97.1	98.7	—	169.0	135.0	76.2	104.9	95.3	105.7
Calculated ¶	58.6	59.5	—	102.1	81.0	45.6	62.0	56.4	62.5
Calculated **	61.0	60.0	—	90.0	—	—	60.2	57.5	61.0
Measured	44.0	60.0	††	108.0	83.0	43.0	53.6	54.5	62.5
Yellowwood †									
Calculated §	32.1	32.6	39.2	55.6	45.0	24.8	44.4	38.5	44.8
Calculated ¶	33.1	33.5	41.2	57.8	45.7	25.9	37.3	33.0	37.5
Measured	23.0	41.0	43.5	61.5	46.0	23.5	25.7	33.0	35.7
Magnolia *									
Calculated §	45.9	46.3	57.2	80.3	—	—	57.0	53.0	—
Calculated ¶	24.6	24.8	30.5	42.9	—	—	29.4	27.0	—
Measured	18.5	††	36.5	40.0	††	††	27.5	29.0	††
Magnolia †									
Calculated §	75.9	76.6	94.8	133.0	102.2	59.8	94.4	87.4	95.2
Calculated ¶	47.5	48.1	59.5	83.8	65.1	37.6	58.7	53.6	58.8
Measured	38.0	50.0	58.0	93.0	81.0	40.0	45.5	56.0	60.0
Walnut *									
Calculated §	‡	‡	‡	‡	‡	‡	‡	‡	‡
Calculated ¶	‡	‡	‡	‡	‡	‡	‡	‡	‡
Measured	‡	‡	‡	‡	‡	‡	‡	‡	‡
Walnut †									
Calculated §	‡	‡	‡	‡	‡	‡	‡	‡	‡
Calculated ¶	‡	‡	‡	‡	‡	‡	‡	‡	‡
Measured	143.0	219.0	235.0	498.0	256.0	142.0	173.0	190.5	171.1

\* Aircraft 139467. † Aircraft 139310. ‡ Data not available. § Computed using calculated normal radiant exposure from Table 3.4, ITR 1636. ¶ Computed using measured normal radiant exposure from Table 3.4, ITR 1636. \*\* Obtained from temperature-time histories computed using measured normal irradiance from Table 3.4, ITR 1636. †† Data not recorded.

normal to the flight path was good. These correlations are indicated in Table 9.4.

## 9.5 CONCLUSIONS AND RECOMMENDATIONS

It was concluded that the participation of the B-52D successfully accomplished the objective of the project. Sufficient data was collected to substantiate a correlation between measured and analytical responses. Overpressure diffraction loading was noted to be significant on fin and stabilizer. It was recommended that revisions should be made to inboard wing flaps, ECM radome, and bomb-bay doors to increase overpressure capability to that of the basic aircraft.

It was concluded that the objectives of the A4D project were met and the data obtained, and when combined with that from Operation Plumbbob, will permit a definition of the delivery capability of the airplane. The method of predicting dynamic response was effective, although correlation of wing response time histories can be improved in the final analysis through the use of modes and frequencies that pertain to the actual distribution of fuel. Wing chordwise pressure-distribution data was obtained which will assist in the analysis of overpressure propagation and the buildup in lift over the wing. Thermal radiant exposure was, in general, predicted conservatively. In this connection, assumed attenuation, correction for fireball orientation, and the scattered radiation phenomena require further study. Given the measured radiant exposure in space, methods for computing temperature rise were satisfactory.

It was concluded that data obtained by the FJ-4 project from yields up to one and one half megatons was compatible with that obtained from Operation Plumbbob. From the two operations, blast and thermal inputs, and structural responses to these inputs were obtained over a sufficiently wide range of yields and incidence angles to permit subsequent definition of the Class D delivery capability of the FJ-4 models. The theoretical dynamic-response analysis was verified within the range of test conditions. A discernible diffraction pulse was detected from the wing-pressure surveys. These surveys also appeared to confirm the basic assumptions made in the dynamic-response analysis. Radiant exposure-prediction methods were conservative. However, the predictions of maximum temperature rise gave good correlation when based upon measured radiant exposure. The predictions of delivery capability presently in force may be restrictive as a result of the overprediction of radiant exposure.

## *Chapter 10*

# *TEST of SERVICE EQUIPMENT and MATERIALS*

### 10.1 OBJECTIVES

This phase of Operation Hardtack included three projects whose objectives were to determine the ionospheric effects of nuclear detonations, and to determine the effects of nuclear radiation on certain selected energized electronic-fuze components, and on an energized Corporal fuze system.

### 10.2 BACKGROUND

The United States Army has a high-priority requirement for an electronic system usable on a nuclear battlefield to determine nuclear-burst data from friendly, as well as from enemy detonations. The ionospheric experiments were designed to increase available knowledge in three areas: (1) technical information for use in approximating, by electronic means, the location of the burst point of a nuclear device; (2) information to aid in refining the analysis of electromagnetic-pulse wave form pertaining to its possible correlation to nuclear-burst data of military value (height of burst, range, yield and type of device); and (3) experimental data which would be of assistance in the determination of extent and amount of disruption to radio communication from a nuclear detonation.

The Army considered essential the evaluation of the vulnerability of ordnance electronic-fuze items in stockpile to nuclear detonations, particularly from nuclear-radiation effects. Also, it was necessary to determine the effect of nuclear radiation upon the functioning characteristics of a typical captive guided-missile fuze system. Accordingly, an experiment was designed and conducted in an effort to obtain this information considered essential in the research and development program on fuzes for bombs, rockets, mortar projectiles, mines and missiles.

### 10.3 WAVE FORM OF ELECTROMAGNETIC PULSE FROM NUCLEAR DETONATIONS

The objective was to obtain and analyze the wave form of the electromagnetic (EM) pulse resulting from nuclear detonations. In particular, broad-band measurements were made from 0 to 10 Mc at ranges up to 460 miles.

Previous measurements of the EM pulse were made during Operations Crossroads, Sandstone, Greenhouse, Buster-Jangle, Tumbler-Snapper, Ivy, Upshot-Knothole, Castle, Teapot, and Redwing. The equipment used for these measurements ranged from narrow-band tuned receivers to broad-band untuned receivers. The antennas used with these receivers varied from simple probes to specially designed discons. Equipment similar to that used by Operation Hardtack Project 6.4 had been used during Operation Castle. In general, the EM-pulse energy was found to be predominantly in the low frequencies (approximately 10 to 20 kc), with measurable components at frequencies as high as 300 Mc. The duration of the EM pulse was found to be approximately 50  $\mu$ sec, with an initial rise time as short as 10  $\mu$ sec.

Experiments during Operations Teapot and Plumbbob demonstrated the feasibility of locating the point of detonation of a nuclear device. Also, analysis of available wave-form data has in-

licated a possible correlation between wave-form parameters and nuclear-burst information, such as height of burst, range, yield, and type of nuclear device. Based upon this possible correlation and other pertinent information, the Army has formulated a tactical requirement for a system (known as Pin Point) to determine various burst parameters that pertain to both friendly and enemy nuclear detonations.

The data pulses were recorded with Dumont Type 298 and Type 321 cameras at five different time bases, 0.2, 0.25, 1, 2, and 10  $\mu\text{sec/cm}$ . There were two scopes per sweep range to provide a safety factor. The total number of scopes used was six. Tektronix Types 517 and 545 were used for the two fastest time bases: namely, 0.2 and 0.25  $\mu\text{sec/cm}$ . The other four scopes were Hewlett-Packard Type 150. Two laboratory-built cathode-follower receivers were used to match the two probe antennas (12 inches, and 1 meter long, respectively) to the 50-ohm cable.

Two stations were used: Kusaie, 460 miles from Bikini and 420 miles from Eniwetok; and Wotho, 100 miles from Bikini and 240 miles from Eniwetok. At Kusaie, the site was located just off the beach on the north shore of the island. The site at Wotho, located on the northwestern shore of the island, was similar to the one at Kusaie. The sites consisted of three S44G demountable shelters. The equipment was housed in one of the shelters; the other two were used for office and darkroom space. Each antenna used had its own ground plane, made of galvanized chicken wire. The ground planes were installed on or near the ground, just above the water line. The remote antenna and ground plane were located behind the shelters at a distance of about 500 feet from the local ground plane.

The data required was the exact wave form of the EM pulse out to 100  $\mu\text{sec}$ , with an expanded view of the initial rise. Since the main objective of this experiment was to obtain the overall wave form, rather than to examine the wave form for kilomegacycle components, equipment commensurate with the objective was chosen. The best scope available within the range of interest was the Tektronix 517. Since the band width of the cathode follower was better than that of the 517, the latter was the limiting piece of equipment. Accordingly, frequency components above 60 Mc were not detected.

The reliability of the recorded pulse was such that the time axis was accurate to within 0.05 percent, while the voltage axis was accurate to within 3 percent.

The data was recorded on Kodak Tri-X film which was developed in Ilford Microphen fine-grain developer for about 12 minutes at 72 F. These films were then enlarged to 8-by-10-inch size and printed on glossy paper.

Correlation of the data was performed by arranging the various wave form and shot parameters in tabular form.

Selected photographs of the actual pulse wave forms are shown in Figures 10.1 through 10.9. The shot name, yield, range, and calibration data are included on the photographs. Table 10.1 summarizes the wave form and shot parameters. Discussion of the data obtained on several shots follows.

Shot Yucca (see Figures 10.1 and 10.2). No data was recorded at Wotho for this shot because of technical photographic problems. Several camera shutters did not open. Trace intensity was, in general, too low for proper recording. Also, field strength at Kusaie indicated that deflection at Wotho would have been some five times the scope limits.

All scopes at Kusaie triggered, and the signal was recorded. The wave form was radically different from that expected. The initial pulse was positive, instead of the usual negative. The signal consisted mostly of high frequencies of the order of 4 Mc, instead of the primary lower-frequency component normally received (Figures 10.1 and 10.2). The fact that Shot Yucca was a very-high-altitude shot may have provided a more favorable propagation path for the higher frequencies that were recorded.

Shot Cactus (see Figures 10.3, 10.4 and 10.5). The signal from this shot was received and recorded at Wotho. A secondary positive spike appeared in the signal, even though a single-



stage nuclear device was used (Figure 10.4). The wide band width and large dynamic range of the system permitted recording of the high-frequency initial spike at the 240-mile range.

Shot Cactus did not trigger the Kusaie scopes, which were set for a trigger level of 0.5 volts/meter.

Shot Fir (see Figures 10.6 and 10.7). This shot triggered all scopes at Wotho.

[REDACTED] Note also the small positive signal occurring immediately before the main negative spike.

No scopes were triggered at Kusaie. Field strength was not up to the predicted value. Prominence of the higher frequencies in the initial pulse may have been responsible for the lack of trigger, since the higher-frequency components tend to be greatly attenuated at the 450-mile range.

Shot Nutmeg (see Figures 10.8 and 10.9). At Wotho, all scopes triggered and wave forms were recorded (Figure 10.8).

[REDACTED] A small positive spike was noted on the Shot Nutmeg wave form, as on Shot Fir. The range was 100 miles for each of these shots. Peak negative-field strength was greater than predicted at both Kusaie and Wotho. Local shielding, consisting of two walls of lead-loaded paraffin, perpendicular to each other, could have produced a corner-reflector effect. This could have produced greater field strength, especially at the higher frequencies.

At Kusaie, all scopes were triggered by interference at minus one half second. Consequently, no data was recorded other than on the Tektronix 517, which did not require resetting of the trigger.

Data presented in Table 10.1 indicate the following correlations and conclusions: (1) The presence of a second stage in a thermonuclear weapon can be detected within certain range and system-band-width limitations. (2) Correlations of first and second crossover points with total yield, noted in previously recorded wave forms, are supported by these measurements. (3) The correlation of negative-field strength with yield is also supported by these measurements.

[REDACTED]

(4) In order to obtain wave forms with good correlations on all of the above items, system band-width should be at least 15 Mc. (5) The different wave form recorded from Shot Yucca indicates that high-altitude bursts can be differentiated from surface bursts. (6) The prediction method used (based on Operation Redwing final report data), is valid at ranges up to 250 miles, provided both shielding and [REDACTED] are taken into consideration.

#### 10.4 EFFECTS OF NUCLEAR DETONATIONS ON THE IONOSPHERE

This project originally had as its prime objective the determination of the effects of high-altitude large-yield nuclear detonations on the ionosphere, and on signals propagated via the ionosphere. After Shots Teak and Orange were rescheduled, no suitable station locations could be found for relocation of the project equipment, so this project objective was changed. The new objective was to increase the recorded knowledge about ionospheric effects of large-yield surface detonations.

This project was divided into two elements: Wake Island, the northern station, and Kusaie,

TABLE 10.1 WAVE FORM AND SHOT PARAMETERS

Shot	Yield kt	Number of Stages	Peak Negative		Plateau Negative		Initial Rise Time $\mu$ sec	Time to First Cross- Negative Peak over Time $\mu$ sec		Time to First Cross- Second Cross- over Time $\mu$ sec		Time to Second Stage Field Strength $\mu$ sec		Predicted Field Strength v/m
			Range miles	Field Strength v/m	Range miles	Field Strength v/m		Time to First Cross- over Time $\mu$ sec	Time to Second Cross- over Time $\mu$ sec	Time to Second Stage Field Strength $\mu$ sec	Time to Second Stage Field Strength $\mu$ sec			
Cactus Fir	17	Single	240	1.7	0.92								1.6	
	1,360	Two	100	6.4	2.6								5.2	
Butternut	82	Two	240	2.8	1.3								1.8	
	1,370	Two	240	1.2	—								2.2	
Koa	5.75	Single	240	1.2	0.82								1.4	
Holly	22.5	Two	100	8.0	2.9								4.0	
KUSAIE DATA:*														
Yucca	2.0	Single	440	0.45	—								0.7	
Cactus	17	Single	460	—	—								0.8	
Fir	1,360	Two	440	—	—								1.2	
Butternut	82	Two	460	0.33	—								0.9	
Koa	1,370	Two	460	0.28	—								1.2	
Holly	5.75	Single	460	0.18	—								0.7	
Nutmeg	22.5	Two	440	0.54	—								0.9	

WOTHIO DATA:

KUSAIE DATA:\*

\* Note: Kusaie data has been tentatively omitted from the correlations due to the effect discussed in Section 3.4, ITR-1638.

TABLE 10.2 FIRST DISTURBANCE ABOVE KUSAIE, SHOT FIR

Shot Fir was detonated at 0450 hours, L time;  $h'F2$ ,  $f_oF2$ , and  $f_xF2$  are standard symbols indicating, respectively, the virtual height and the ordinary and extraordinary critical frequencies of the F2 layer.

Time After Shot minutes	First Disturbance		Regular Layer	
	Apparent Height km	Frequency Range Mc	$h'F2$ km	$f_oF2$ Mc
27	—*	—*	230	—
36	370	6.5 to 7.2	230	5.8
37.25	350	5.3 to 8.3	240	5.5
38	340	5.6 to 7.7	240	—†
39.25	315	5.0 to 7.9	240	—
40	300	5.0 to 7.0	230	—

\* Disturbance not yet visible in ionogram.

† The effect has now apparently arrived overhead; the two traces have joined, obliterating the regular-layer critical frequencies. Actually, the segment associated with the disturbance now determines the critical frequencies.

the southern station. Each station included a modified C-4 ionosphere recorder normally used for vertical-incidence soundings. Originally, it was planned to connect the recorder at Kusaie to an auxiliary rhombic antenna for simultaneous transmission toward Wake, and to connect the recorder at Wake to a similar rhombic antenna for reception of the signals from Kusaie. If synchronization of the two recorders had been effected, data could have been obtained for radio signals obliquely incident to the ionosphere. However, synchronization was not possible, due to equipment malfunction. Experimental operations were thereafter concentrated on normal vertical procedure of a 15-second logarithmic sweep from 1 to 25 Mc. Pulses of 50- $\mu$ sec duration were transmitted at the rate of 60 pulses per second. The Model C-4 ionosphere recorder is an instrument which measures and records the virtual heights and critical frequencies of the various ionospheric layers. Briefly, its operation is as follows. It: (1) transmits radio-frequency pulses ranging from 1 to 25 Mc; (2) receives these pulses after reflection from the ionosphere; (3) displays them as oscilloscope traces; (4) photographs these traces automatically. On the face of the oscilloscope is presented the virtual height of reflection plotted against the frequency of the signal. Height markers were used for each 100-km interval, and frequency markers were used for each megacycle.

The Wake ionosonde was operated continuously from Shot Yucca plus 5 minutes to plus 70 minutes, then routinely (five times an hour) for the next 18 hours. The Kusaie ionosonde was operated continuously during Shots Yucca, Fir, Butternut, and Koa, starting at H - 1 hour (except for radio-silence periods), until about H + 6 hours.

The results obtained at the southern project site for Shot Fir are outlined next. At about H + 35 minutes, an additional segment began to appear in the recorded trace. As the effect termed the "first disturbance" observed at the same site after seven shots of Operation Redwing, this disturbance occurred above the critical frequency of the F layer. It moved downward in height as shown in Table 10.2. Thus, it fitted the former interpretation of an approaching region of increased-ion density viewed obliquely. Further confirmation was indicated by the appearance of an additional trace 240 to 250 km above the descending segment, as had occurred during the seven Operation Redwing shots. This was interpreted as a signal refracted vertically groundward by the disturbed portion of the F region, thence reflected upward from the earth's surface, and back to the recorder over the same path.

A "second disturbance" was also observed with an appearance similar to the Operation Redwing records. It could not be determined precisely when it was overhead, but it was seen moving lower in height at H + 54 and H + 55 minutes (385 km to 370 km). It was probably overhead at about H + 1 hour.

The conclusions drawn from this experiment are as follows: in agreement with results of Operation Redwing, the energy responsible for the first disturbance in the ionosphere above Kusaie was propagated with a mean velocity of 20 km/min. Also corroborating previous results, the second disturbance resulted from energy propagated with a mean velocity of about 13 km/min. The first effect has been postulated as due to a compressional wave, and the second to a hydro-magnetic wave. The fact that the first effect was seen approaching but not receding is indicative of the shape of the ion-density variation associated with the disturbance.

#### 10.5 EFFECTS OF NUCLEAR RADIATION ON ELECTRONIC FUZE COMPONENTS AND MATERIALS

The objectives of this experiment were: (1) to expose electronic-component parts and materials used in ordnance electronic-fuze circuitry to the same radiation environment that would be experienced by the various fuzes when they are tactically operated or stored in the vicinity of a nuclear detonation; (2) to perform measurements on these component parts and materials before, during, and after a detonation; and (3) to evaluate the behavior of an operating, captive,

typical, guided-missile-fuze system (Corporal) when exposed to the same radiation environment as the individual electronic component parts.

The Army has agencies which are engaged in research and development on fuzes for bombs, rockets, mortar projectiles, land mines, and missiles. It was considered essential that the vulnerability of stockpiles of such items, and their component parts, to a nuclear detonation be evaluated. In addition, it was of utmost importance to determine the vulnerability of an operating guided- or ballistic-missile-fuze system. If several such missiles containing nuclear warheads are simultaneously proceeding toward targets which are in close proximity to one another, and one functions at its target while the others are still in flight, it must be determined whether the remaining missiles will prefire, become duds, or be unaffected.

The electronic-component parts to be tested were placed in special test circuits designed to emphasize the property to be measured. The signals were fed into a magnetic tape recorder which recorded the performance of the components during the detonation. In addition, the circuit check points of a T-3008 proximity-fuze system were monitored, and any departure of the signal levels from their normal values was recorded on the tape. The general scheme was to place the recorder system and measuring circuits (Figures 10.10 and 10.11) in a deep pit where they would not be appreciably affected by the detonation. The pods containing the components (Figures 10.12 and 10.13) which were to be tested, and the fuze system, were placed at the top of the pit. Cables were used to electrically connect the components, or fuze, to the measuring circuits at the bottom of the pit. Each component recorder had the capability of recording 28 channels of information on a single tape. Thus, 26 component properties were measured at each recorder station. The remaining two channels were used to measure the cable properties, and to provide a phase reference for the capacitor measurements. Fourteen channels of a separate recorder were used to monitor the fuze.

In view of the many different component parts to be tested and the limited number of recorder channels available, it was decided to measure a sample of three for each property. To provide some insurance against a complete loss of data on a particular property, one sample of each component was to be measured in each of three shots, rather than three samples in one shot. This scheme had the additional advantage that all the circuitry was identical in each component recorder, thus making the recorders interchangeable.

To obtain a trend in the radiation-damage data, it was planned to expose the component parts to three levels of neutron dosage:  $10^{12}$ ,  $10^{13}$ , and  $10^{14}$  n/cm<sup>2</sup>.

Two fuze systems were made available for this experiment. It was originally planned to expose the two systems to two neutron-flux levels in each of two shots. The loss of one fuze in the first participation allowed the use of only a single system thereafter.

The shots participated in were Nutmeg, Maple, Hickory, and Juniper.

To attain the desired dosages, three stations (630.01, 630.02, and 630.03) were constructed on Site Tare (Figure 10.14) and two stations were constructed on Site Fox (630.04 and 630.05) (Figure 10.15). Stations 630.01 and 630.03 were dual stations which had the capability of enclosing both a component-part test recorder and a fuze-system test recorder. Stations 630.02, 630.04, and 630.05 were single stations in which only a component-test recorder could be placed.

In Shot Nutmeg, all three stations on Site Tare were used to obtain the three levels of neutron dosage for the test components and two levels of dosage,  $10^{14}$  and  $10^{12}$  n/cm<sup>2</sup>, for the fuze systems. Stations 630.04 and 630.05 were utilized during Shot Maple to expose the electric component parts to  $10^{14}$  and  $10^{13}$  n/cm<sup>2</sup>. Stations 630.01 and 630.02 were used during Shot Hickory to obtain a neutron dose of  $10^{13}$  n/cm<sup>2</sup> for one component-recorder system and one fuze-recorder system, and  $10^{12}$  n/cm<sup>2</sup> for a second component-recorder system. The final participation was during Shot Juniper. On this shot, Stations 630.01, 630.02, and 630.03 were used to expose three component-recorder systems to  $10^{14}$ ,  $10^{13}$ , and  $10^{12}$  n/cm<sup>2</sup>.

There were a certain number of tests which did not require a documented history during the

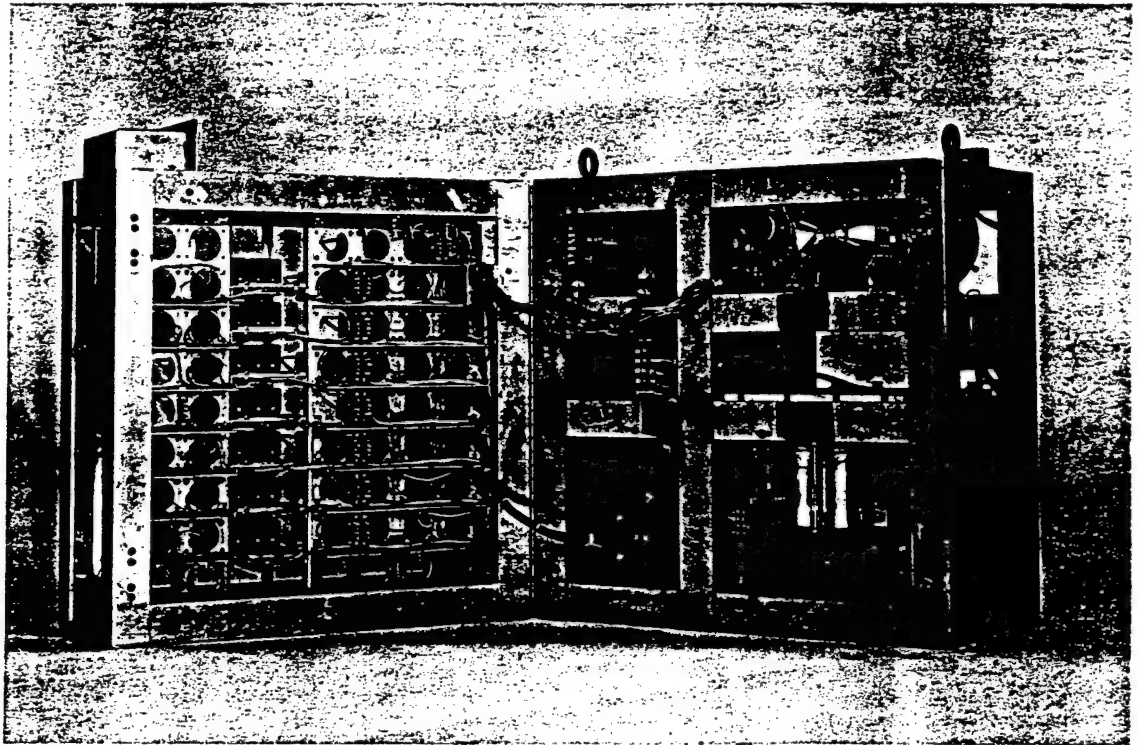


Figure 10.10 Component magnetic recorder, showing electronic and power decks open for servicing.

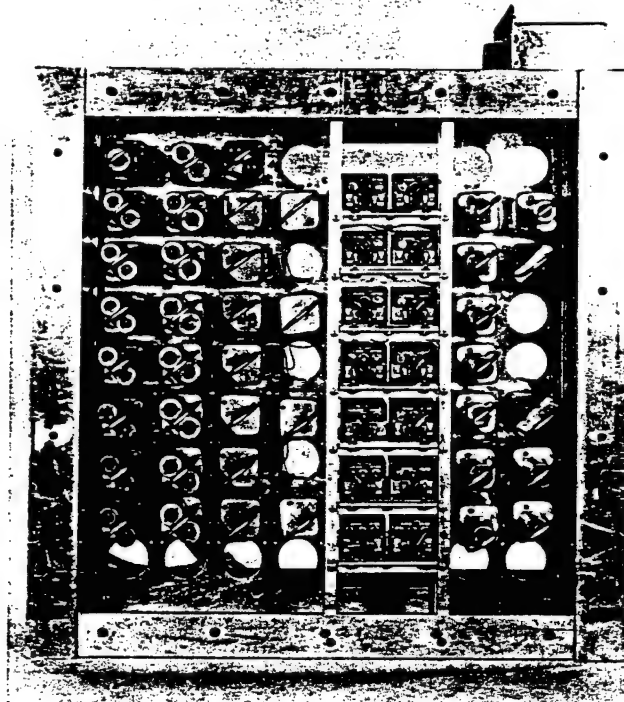


Figure 10.11 Component magnetic recorder, showing plug-in circuit elements.

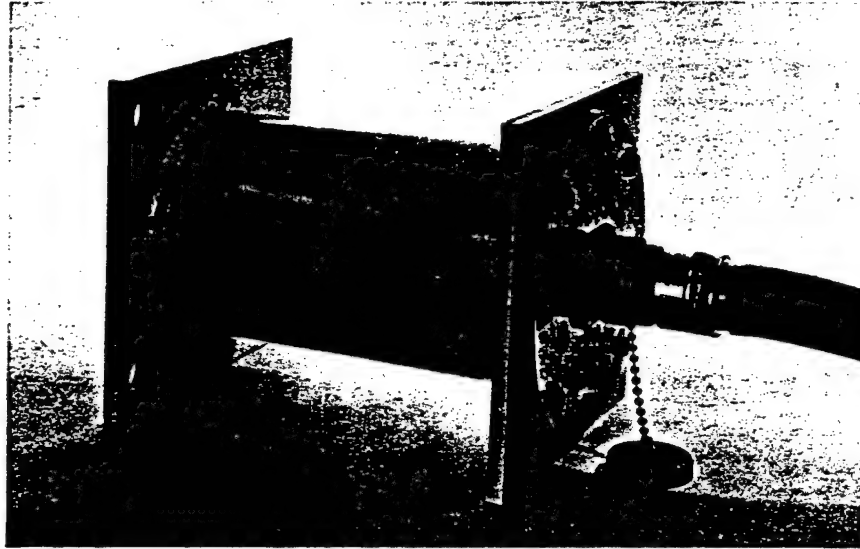


Figure 10.12 Exposure pod for dynamic test of components.

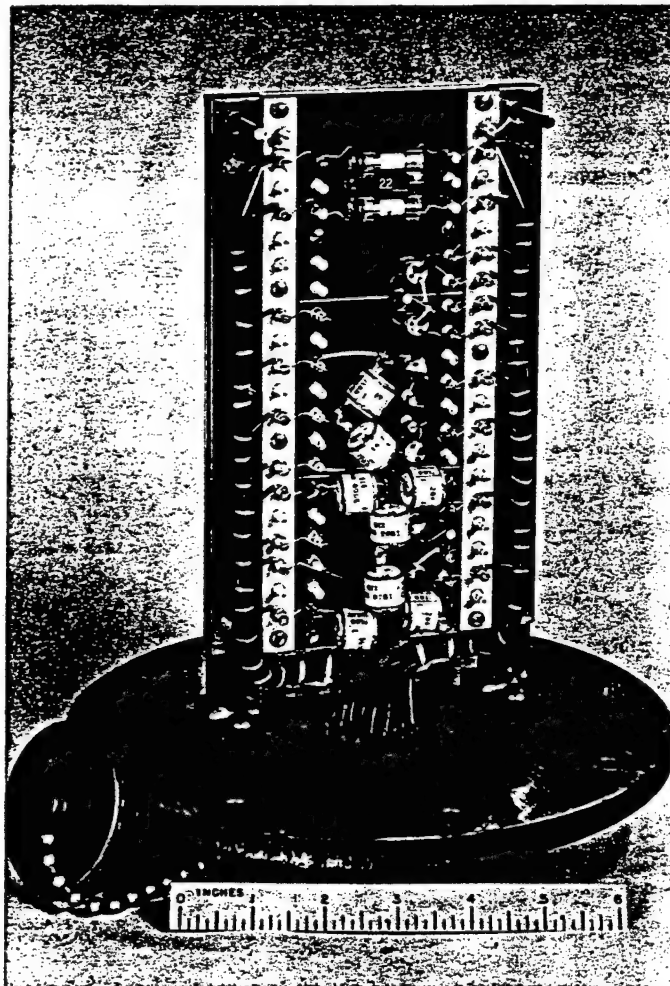


Figure 10.13 Interior of exposure pod, showing method of mounting components for test.

detonation, but only some means of determining, by subsequent examination, whether or not a component temporarily failed. Such tests were designated as flag tests. These tests were performed during Shot Maple. The flag-test circuit consisted of a battery, the component to be measured, and an excess-current-detecting device, all connected in series. The excess-current-detecting device was a simulator squib or a solid state switch.

A simulator squib is designed to give a visual indication if more than a minimum amount of

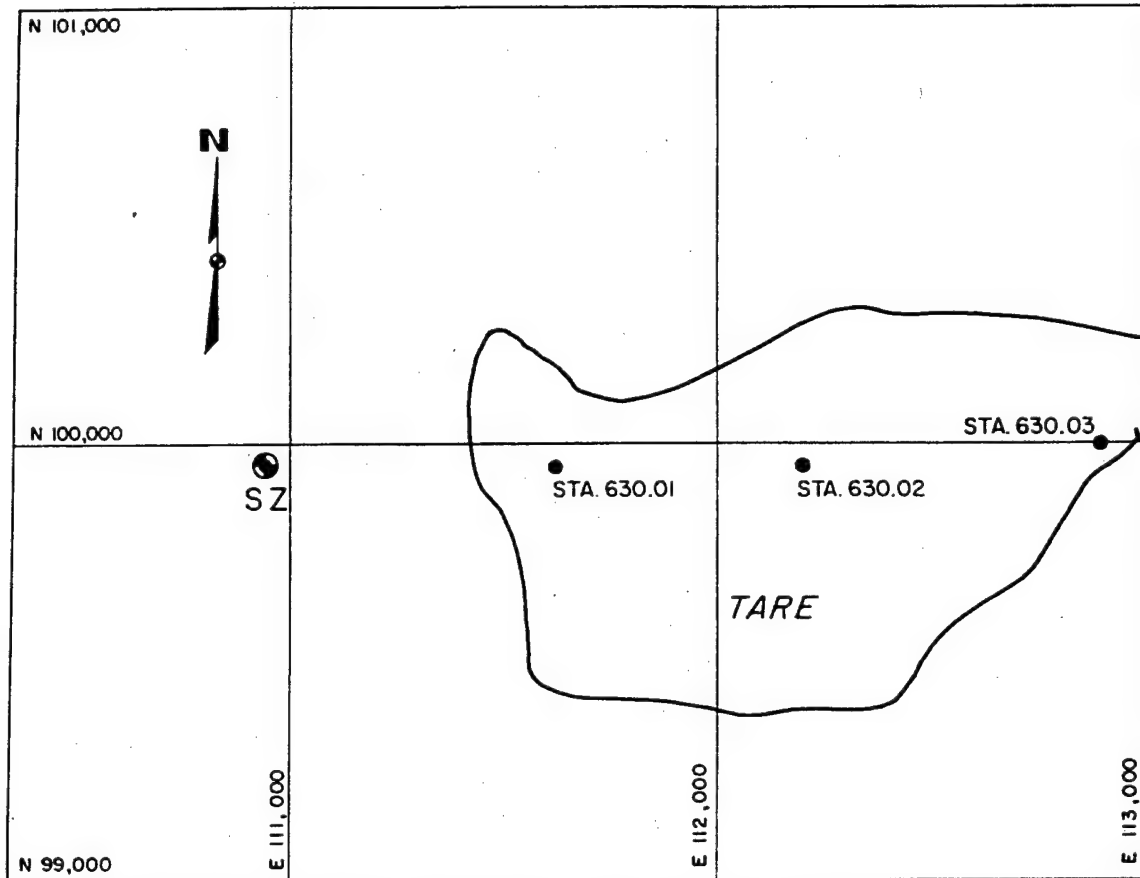


Figure 10.14 Station map, Site Tare.

electrical energy is expended within it. The lowest amount of energy that would fire the squibs used in this test was about 200 ergs. To expend this amount of energy in the squib, the component would have to undergo a tremendous change in impedance. For this reason, the squibs were used only in the flag tests on trigger tubes, and sufficed to determine whether or not the tube fired.

The choice of component parts to be tested was governed by the extent of their use in the T-3008 fuze system, the probability of their being susceptible to the effects of the detonation, the economics of the project, and the effect that their failure would have on overall fuze performance.

Dynamic tests were made on a surface-barrier transistor (2N128), a silicon-switching transistor (2N496), and a germanium transistor which is being considered for use as a power converter (2N316). The vacuum tubes on which dynamic data were taken were the 5702WA and 6943 pentodes and the 5718 triode. The solid-state diodes tested were a Zener diode, a diffused-junction diode, and a mixer diode. Dynamic data was taken on wire-wound, metal-film, and

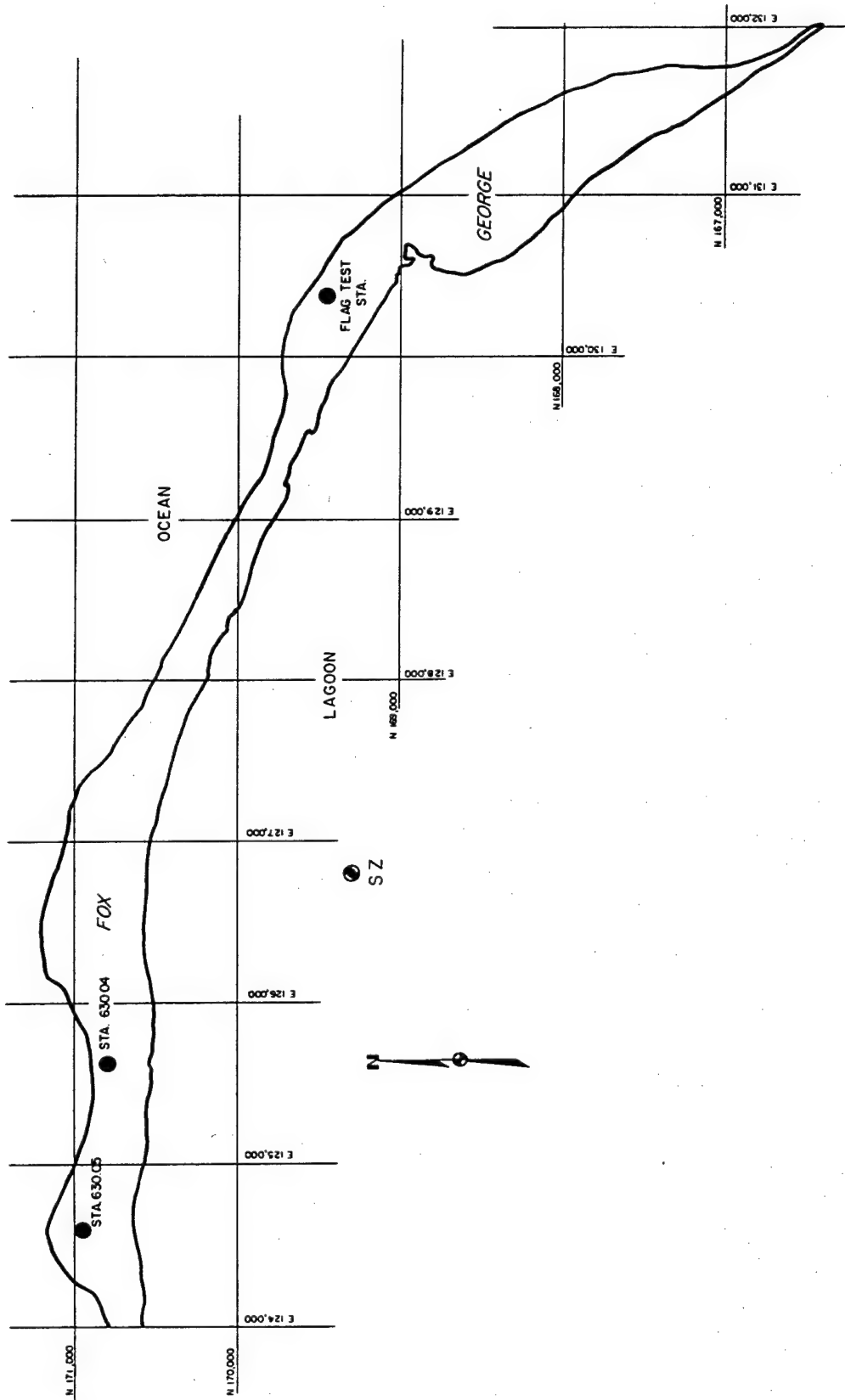


Figure 10.15 Station map, Site Fox.



carbon-composition resistors. The capacitors dynamically tested were mylar, mica, paper, ceramic, and tantalum electrolytic. An epoxy-encapsulating resin was also examined.

Flag tests were made on tantalum capacitors and some trigger tubes, such as the 5643 hot-cathode tetrode, the QF-391, and QF-848 cold-cathode tetrodes, and the NE-2 diode.

The XD1C and XD4C were of particular interest because of their mine-fuze application. One of the specific objectives of this experiment was to find electronic components which would reliably discharge a firing capacitor at zero time. These two diodes were particularly investigated for this application.

The design of the instrumentation stations was similar to that used in Project 6.2, Operation Plumbbob. Each station consisted of a concrete-lined pit of square cross section. The recording equipment and associated circuitry were suspended by springs attached to crossbeams near the bottom of the pit. Sandbags or concrete plugs were used to fill the region between the recorder and the top of the pit. The boxes containing the components or the fuze system were placed at the top of the pit and connected, by shielded cables, to the recorder system.

Three stations were constructed on Site Tare: 630.01 at 725 feet from ground zero, 630.02 at 1,250 feet from ground zero, and 630.03 at 2,000 feet from ground zero. In addition, two stations were constructed on Site Fox: 630.04 at 1,875 feet from ground zero, and 630.05 at 2,700 feet from ground zero.

Stations 630.01 and 630.03 were constructed as dual stations so that both a component recorder and a fuze-system recorder could be placed in the same station. The rest of the stations were single stations.

Neutron dosimetry was provided by Project 2.4. The dosimetry was accomplished by the use of threshold detectors. The particular detectors used were sulfur, gold, neptunium, plutonium, and uranium.

Gamma dosimetry was accomplished by the use of film badges supplied by Project 2.3 and TU-7.1.6.

The data required was the change in operating parameters of the fuze system and the various component parts as a function of time and as a function of radiation level. It was anticipated that this data would appear on the magnetic tapes. The data for the flag tests was obtained by examination of the current detectors.

In summary, the components tested included: transistors, electron tubes, solid-state diodes, resistors, capacitors, and an epoxy-encapsulating resin. These items were exposed to neutron doses ranging from  $10^{12}$  to  $10^{14}$  n/cm<sup>2</sup> and gamma doses ranging from  $10^4$  r to greater than  $10^5$  r. The experimental results indicated some noteworthy changes:

1. It was found that some transistor parameters underwent transient changes which were greater than 84 times their initial value, without receiving permanent damage.
2. Vacuum tubes exhibited changes in plate current of up to 120 percent for periods of 200  $\mu$ sec after a detonation. Gas diodes, when biased as much as 70 percent of their firing voltage, reliably fired at distances up to 4,500 feet from ground zero in a detonation of 20-kiloton yield.
3. The reverse resistance of a silicon-diffused-junction diode fell to less than one tenth of its normal value.
4. Resistors exhibited decreases in resistance which ranged from 10 to greater than 20 percent for periods of a millisecond.
5. All the capacitors tested showed increases in capacitance and dissipation factors which ranged from zero to 13 percent for periods of 10 msec.

In addition, the Corporal fuze system exhibited transient disturbances which indicated a strong possibility of firing when it was exposed to a neutron dose as low as  $10^{12}$  n/cm<sup>2</sup> and a gamma dose as low as  $10^4$  r. This occurred at a distance of 2,000 feet from a detonation of approximately 20 kilotons.

At this stage of data analysis, it may be concluded that almost all electronic-component parts

may suffer deleterious effects, which cannot be detected by a simple measurement, before and after exposure to a nuclear detonation. In some instances, the transient disturbances are of such duration that ordnance-electronic circuitry can be made immune to them. It is particularly important to note the duration, as well as the magnitude, of these effects before rejecting a particular fuze component. These results indicate that caution should be observed when utilizing radiation-damage data which has been acquired in many reactor studies. Many of these transients would not be observed in tests, other than full-scale nuclear detonations.

It may be further concluded that almost all electronic component parts which were examined showed some degree of transient susceptibility which, in general, was directly dependent upon the degree of exposure.

The data obtained on a number of diodes showed conclusively that they may be reliably employed to discharge a firing capacitor at the time of a nuclear detonation. This application would be highly desirable for use in multi-influence land mines.

The effects of a nuclear detonation on the Corporal fuze system caused sufficient deviation from normal behavior to make its operation in a nuclear environment highly suspect. A more detailed analysis will have to be made in the laboratory to determine its exact vulnerability.

## *Chapter 11*

# *THERMAL RADIATION*

### 11.1 INTRODUCTION

The principal effort of the thermal program on Operation Hardtack was directed toward documentation of the thermal-radiation characteristics of the three high-altitude detonations, Shots Yucca, Teak, and Orange. Results obtained from Shot Yucca are reported in Chapter 4 of this report, and results obtained from Shots Teak and Orange are included in Chapter 5.

The remaining thermal-program experiments on Operation Hardtack consisted of experiments to extend the knowledge of effects on materials from megaton-range yields with the objectives of validating laboratory procedures, extending the testing of a skin simulant for use in laboratory experiments to the megaton range, obtaining infrared spectral data from surface bursts for correlation with high-altitude bursts, and extending the knowledge previously obtained on the mechanisms of material ablation from specimens inside the fireball.

### 11.2 EFFECTS ON MATERIALS AND SKIN-SIMULANT EXPERIMENTS

Project 8.1 from the naval Material Laboratory conducted the experiments. The work done on Operation Hardtack was an extension of similar work done on Operation Plumbbob.

The effects of thermal radiation on materials are known to be functions of rate-of-energy delivery and time-history-of-energy delivery, as well as of the total energy delivered. On Operation Plumbbob, experiments were conducted on relatively small-yield weapons whose time histories of energy delivery were fairly short; therefore, any given total amount of thermal energy was delivered in less time that it would have been from larger-yield weapons. On Operation Hardtack, similar experiments were conducted to extend the data into the longer time-history region of larger-yield weapons.

Three shots were initially selected to provide a reasonably well-spaced coverage of the range of yields from approximately 100 kt to 10 Mt. These were Shots Elder, Yellowwood, and Poplar.

Later, Shot Elder was indefinitely postponed and there was no other shot of suitable yield scheduled in an area for which the project stations would be suitably located. Subsequently, Shot Yellowwood was fired at a lower-than-designed yield. The result was that only partial data was obtained on a shot of the order of yield planned for Shot Elder.

It was then planned to participate on Shot Walnut which would be suitably located and which would provide an intermediate test point between Shots Yellowwood and Poplar. Good results were obtained on Shot Walnut.

Prior to the detonation of Shot Walnut, Shot Poplar was indefinitely postponed. There were no other shots of suitable yield available on a time scale which would permit participation since the project was committed to participation on Shots Teak and Orange.

### 11.3 INSTRUMENTATION

Instrumentation was similar to that used on Operation Plumbbob, consisting of approximately 30 skin-simulant specimens in various configurations, including bare and blackened control specimens, and samples clothed with materials in contact, and with spaced fabrics. In addition, various size apertures were utilized to study the effect of exposure area. Time-temperature

histories of the specimens were recorded; maximum temperature provided a criterion for determining the severity of burn which would be received by animate skin.

Recording radiometers and calorimeters were used at the stations in order that the total energy, and time history of energy delivered, might be known. Motion picture cameras were used to view the burst and the specimens in order that cloud obscuration effects and smoking and flaming of the specimens might be taken into account in data analysis.

#### 11.4 RESULTS

Although complete data were not obtained on Shot Yellowwood, and the energies received were not as high as would be desirable for correlation purposes, nevertheless, data obtained will serve a useful purpose.

The maximum temperature rises measured by the skin-simulant specimens on Shot Yellowwood are listed in Table 11.1. There was no evidence of scorch, char, or ignition of fabrics. The thermal exposure measured at the station was  $3.2 \text{ cal/cm}^2$  as opposed to the  $20 \text{ cal/cm}^2$  planned for. The irradiance maximum was  $2.6 \text{ cal/cm}^2\text{-sec}$  and occurred at 0.62 second. The irradiance history was essentially that of the normalized thermal pulse.

The differences, in percent, between the laboratory-predicted temperatures and the field-measured temperatures for Shot Yellowwood are given in Table 11.1 as percent of predicted temperature.

The temperature histories of the bare and blackened simulants for Shot Yellowwood, normalized on the maximum temperatures, are shown in Figure 11.1. Those for the fabrics in contact are shown in Figures 11.2 and 11.3.

Comparison of the laboratory-predicted simulant temperatures with those obtained in the field on Shot Yellowwood showed a non-linearity, which was unexpected, in the field temperatures between results from high and low-radiant exposures.

While the average differences between field and laboratory-predicted simulant temperatures on Shot Yellowwood were not large, there were, individually, some large discrepancies which did not leave a clear comparison picture.

Differences in spectral characteristics between laboratory and field source on Shot Yellowwood were indicated by results obtained from the hot-wet fabric assemblies. The values obtained in the field were significantly lower than those predicted. A rough calculation of the apparent fireball temperature based on irradiance measurements when used to determine new predicted values resulted in predictions comparable to the values measured.

In general, laboratory predictions and analyses were normally in the simulant temperature range of interest in burn studies, i. e., 15 to 30 C. A comparison of the temperatures resulting from Shot Yellowwood which were out of this range resulted in a comparison outside the optimum region of interest.

Relatively lower temperatures for 9-mm apertures were correctly predicted, indicating that laboratory methods for evaluating exposure areas are valid.

The maximum temperature rises measured by the skin-simulant specimens on Shot Walnut are listed in Table 11.2. Many of the uniforms were charred, and all of the dark-gray uniform assemblies which were spaced away from the simulant were consumed either by flame or glow. The hot-wet spaced uniform assemblies did not ignite, but were severely charred and appeared to have been on the threshold of ignition. The thermal exposure measured at the station was  $14.8 \text{ cal/cm}^2$ . The irradiance maximum was  $6.5 \text{ cal/cm}^2\text{-sec}$  and occurred at 1.17 seconds. The irradiance history was essentially that of the normalized thermal pulse.

The differences, in percent, between the laboratory-predicted temperatures and the field-measured temperatures for Shot Walnut are given in Table 11.2 as percent of predicted temperature.

Normalized temperature histories for Shot Walnut are not presented in this report since

there was insufficient time in the field, because of Shot Teak and Shot Orange preparations, to reduce these data.

A non-linearity in simulant temperatures between results from high- and low-radiant exposures similar to that obtained on Shot Yellowwood appeared on Shot Walnut. As a result, it is

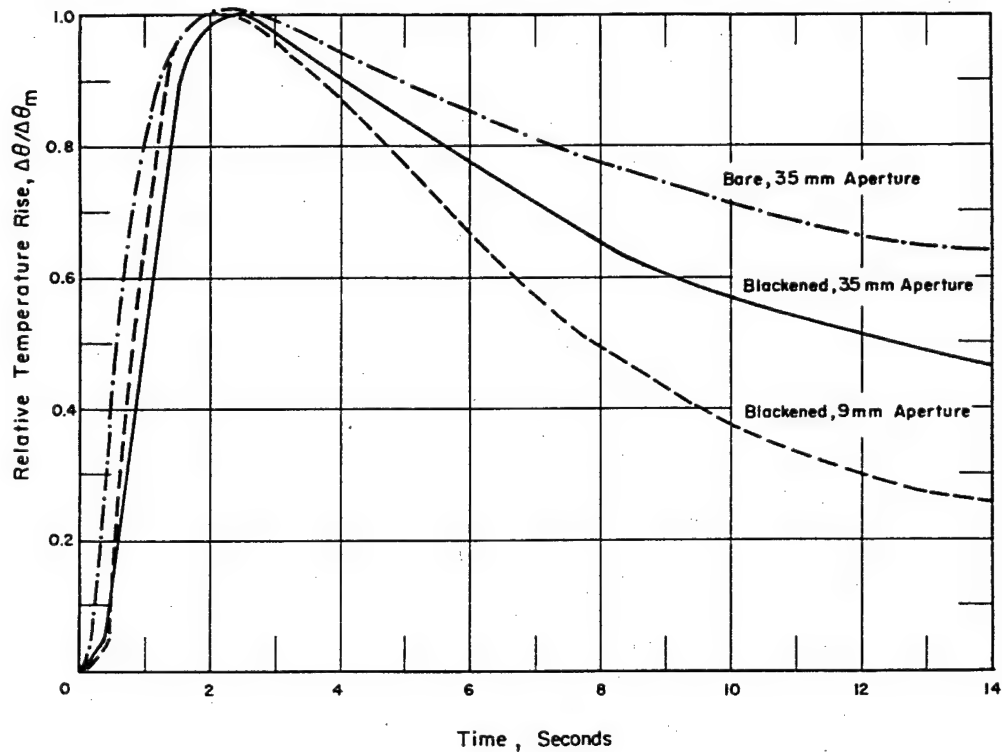


Figure 11.1 Temperature histories of the NML simulant bare and blackened.

suspected that the attenuation screens had a slightly higher transmission than was measured in the laboratory.

Hot-wet uniform assemblies again gave significantly lower simulant temperatures on Shot Walnut than predicted, again indicating the possibility of a different fireball spectrum than anticipated.

Lower simulant temperatures for the 9-mm aperture contact-assembly temperatures were again correctly predicted on Shot Walnut, thus further validating the laboratory evaluation of exposure-area effect.

Bare, unblackened, and blackened simulant temperatures on Shot Walnut agreed reasonably well with laboratory predictions.

The dark-gray sateen uniforms spaced away from the simulants ignited, causing higher temperatures than were experienced in similar situations on Operation Plumbbob. This was probably a result of the greater distance at which a given radiant exposure was obtained on larger yield detonations. The shock wave, therefore, arrived at a later time, thus permitting the ignition to proceed further before being extinguished (Reference 13).

It is interesting to note that the effect of a weaker shock at a given thermal exposure level discussed in Reference 13 was probably also demonstrated on Shot Walnut. The gray spaced assembly with a 35-mm aperture had a flame, or glow, which apparently survived the shock

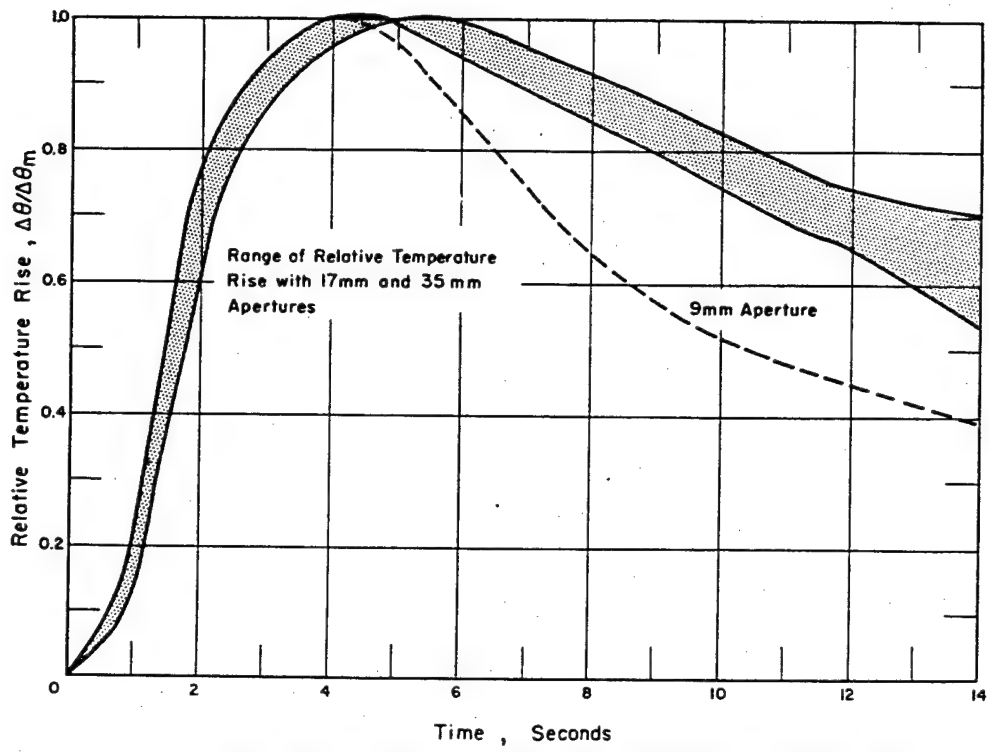


Figure 11.2 Temperature histories of the NML simulant in contact with the

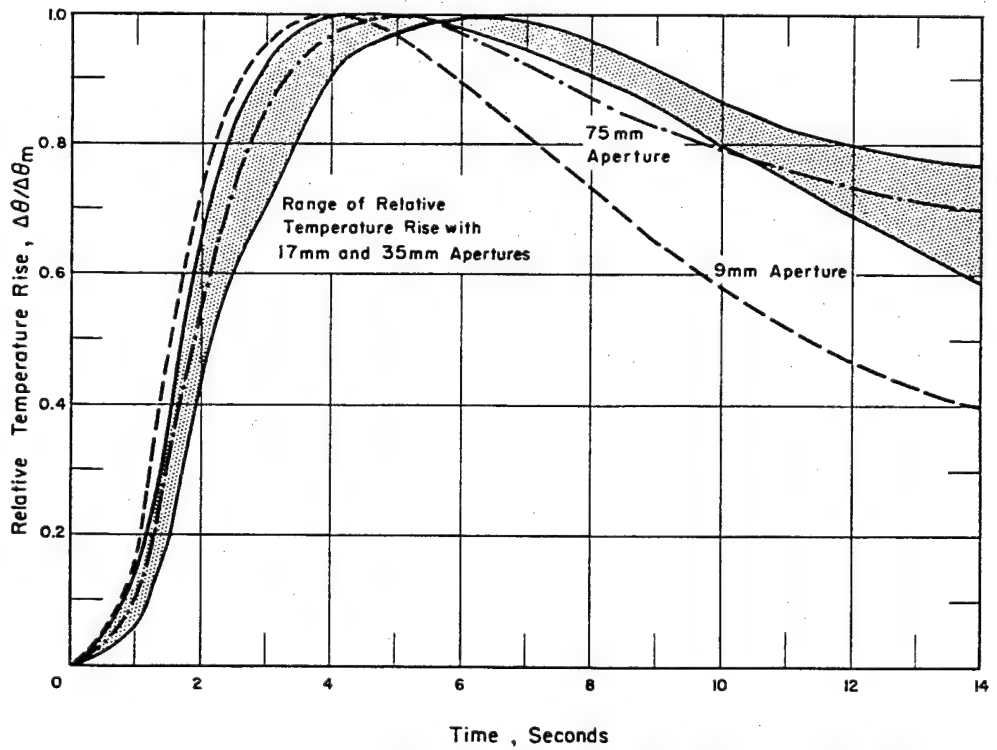


Figure 11.3 Temperature histories of the NML simulant in contact with the gray uniform assembly.

TABLE 11.1 MAXIMUM TEMPERATURE RISE OF THE SKIN SIMULANTS,  
SHOT YELLOWWOOD

Specimen (Skin simulant covering)	Aperture Diameter cm	Maximum Temperature Rise		Difference pet
		Laboratory C	Field C	
Uncovered	35*	11.0	10.0	-9
Blackening	9*	14.9	17.3	+16
	35*	14.9	18.0	+21
Poplin and sheeting in contact	9*	6.1	6.2	+1.5
	17*	7.1	7.2	+1.5
	17*	7.1	6.8	-4.0
	35*	7.1	6.4	+10
	35*	7.1	6.8	-4.0
	75*	7.1	2.6	---
	17	14.8	11.9	-20
	35	14.8	9.1	-38
Gray sateen and sheeting in contact	9*	6.2	5.8	-6.5
	17*	7.3	10.2	---
	17*	7.3	8.3	+14
	35*	7.3	8.4	+15
	35*	7.3	8.2	+5.5
	75*	7.3	8.6	+18
	9	13.0	12.2	-6
	17	15.2	13.2	-13
Poplin and sheeting spaced 5 mm	17	15.2	16.3	+7.5
	35	15.2	14.4	-5.5
	17	3.0	2.0	---
Gray sateen and sheeting spaced 5 mm	17	3.6	2.6	---
	35	3.6	2.6	---
	75	3.6	2.6	---
Gray sateen and sheeting spaced 5 mm	9	3.0	1.3	---
	17	3.6	1.2	---
	35	3.6	3.0	---
	75	3.6	2.5	---

\* Exposed with a 0.48 attenuating screen.

TABLE 11.2 MAXIMUM TEMPERATURE RISE OF THE SKIN SIMULANTS,  
SHOT WALNUT

Specimen (Skin simulant covering)	Aperture Diameter cm	Maximum Temperature Rise		Difference pet
		Laboratory C	Field C	
Uncovered	35*	39.6	38.7	-2
Blackening	9*	59.0	61.1	+3.5
	35*	59.0	60.8	+3.0
Poplin and sheeting in contact	9*	26.1	23.4	-10
	17*	30.7	26.6	-13
	17*	30.7	27.3	-11
	35*	30.7	30.3	-1
	35*	30.7	27.3	-11
	75*	30.7	28.9	-6
	17	64.0	52.0	-18
	35	64.0	55.9	-13
Gray sateen and sheeting in contact	35	64.0	44.5	-30.5
	9*	27.1	27.2	+0.4
	17*	31.9	35.5	+11
	17*	31.9	32.4	+1.5
	35*	31.9	34.8	+9
	35*	31.9	31.8	-0.3
	75*	31.9	32.7	+2.5
	9	56.5	47.7	-15.5
Poplin and sheeting spaced 5 mm	17	66.5	57.8	-13
	17	66.5	60.3	-9
	35	66.5	61.4	-7.5
Gray sateen and sheeting spaced 5 mm	17	8	5.2	---
	17	30	11.7	---
	75	>30	13.1	---
Gray sateen and sheeting spaced 5 mm	9	20	47.5	---
	17	30	49.7	---
	35	>30	89	---
	75	>30	42.1	---

\* Exposed with a 0.48 attenuating screen.

arrival and resulted in an exceptionally high-temperature rise in the simulant.

### 11.5 INFRARED CORRELATION MEASUREMENTS

The P2V aircraft of Project 8.5, which made infrared measurements on Shots Yucca, Teak, and Orange (Chapter 4), also participated on Shots Butternut and Koa. On these shots, it made instrumentation checks and obtained data for correlation of a surface detonation with high-altitude shots.

On Shot Butternut the monochromator failed to function properly, but the mapper functioned satisfactorily. On Shot Koa both instruments operated well. A sample of the Shot Koa data which was reduced in the field follows:

1. Mapper Device: Signals were obtained at the following times: 0.286, 1.32, 2.76, and 3.96 seconds. The bands covered are shown in the table below:

Time sec	Wave-Length Region, microns						Diam. ft	Height ft
	2 to 2.54	2.6 to 3.35	3.05 to 3.92	3.34 to 4.34	2 to 6	2 to 12		
0.286						◇	11,000	1,000
1.32	◇				◇	◇	13,000	2,300
2.76	◇			◇	◇	◇◇	11,000	4,000
3.96	◇◇	◇◇	◇◇	◇◇◇	◇◇◇	◇◇◇	17,000	8,000

It should be noted that the diameters correspond to the estimated magnitude in the 2-to-12-micron region and are given in feet. For the narrow bands the diameters are smaller. The multiple number of ◇'s corresponds to the vertical extent of the fireball, since the sweep through one cycle of bands corresponds to approximately three degrees in the vertical plane.

2. Monochromator: The monochromator provides detailed spectral data from 2 to 12 microns. RF noise and other extraneous line surges will obscure detailed information, unless filtered out by narrow-passband filters. The available playback system permitted only the examination of one channel of six. The results obtained can be summarized as follows:

- a. Infrared irradiance first appeared at about 2.0 seconds after time zero.
- b. The peak was reached at about 29 seconds and was still evident at 55 seconds. The late time was a limitation in available time for write-out of data with the write-out system used.
- c. The maximum signal at 29 seconds for 2 microns was about 2 volts and, at 55 seconds about 0.75 volt. At the longer wave lengths the signal was correspondingly lower, similar to a black-body curve. Further, the spectra showed characteristics of a black body in absorption with H<sub>2</sub>O and CO<sub>2</sub>.

### 11.6 MATERIAL ABLATION AND NEUTRON STUDIES

These experiments were carried out on Shot Cactus by Project 8.6, Wright Air Development Center (WADC). Two ablation study specimens with temperature-measuring thermocouples embedded at various depths were mounted on a tower so as to be inside the fireball. The thermocouples measured the temperature of the material in their immediate vicinity and recorded it as a function of time on tape recorders inside the specimens. By noting the time and temperature at which the thermocouples ceased to record, it was hoped to learn something of the rate of ablation of material.

In addition, the project attempted the measurement of the speed of sound within the fireball as a means of determining temperature. A long, rigid, pipe specimen containing at each end a



recorder and transducers was used to record the arrival of weak shocks produced by explosive charges set off at various times after time zero.

Both ablation-study specimens and the speed-of-sound specimens were recovered and shipped back to the laboratory for analysis. No results are available at this time.

Two neutron-study specimens containing samples of materials to be used in the Shot Teak and Shot Orange pods were placed near ground zero in order to study possible neutron degradation of these materials. Neither specimen had been recovered when this report was written.

## Chapter 12

# SHOTS QUINCE and FIG

### 12.1 INTRODUCTION

Shot Fig was the surface detonation of a newly developed, subkiloton-yield (10 to 30 tons) device on Site Yvonne, Eniwetok Atoll. The device was detonated on 18 August 1958. The program of effects measurements consisted of a crater survey, blast, thermal, radiation, and fallout effects, including a series of measurements taken from 100 to approximately 1,500 feet by suspension from a balloon over ground zero.

12.1.1 Objectives. The use of small-yield nuclear weapons by ground troops and by low-flying aircraft will offer possibilities that have not been explored. In order to develop tactics for delivery, much more knowledge was needed regarding the radiological, thermal, and blast effects of such weapons.

To achieve this general primary objective the following specific objectives were established: (1) measurement of the air-blast parameters as a function of time and distance; (2) definition of the characteristics of the radiological environment; (3) measurement of the thermal flux; and (4) determination of the fallout pattern.

It was considered that the minimum objectives of the test would be met if the device gave a yield of five tons and the contours of militarily significant fallout could be defined.

12.1.2 Background. With increased knowledge of the mechanics and means of triggering nuclear devices, it became possible to build a small device that could probably be hand carried. This idea, when fully developed, might allow the infantryman to carry a bazooka-type rocket launcher into the battlefield as an antitank weapon. Or, the launcher might be mounted on a light vehicle for rapid movement on the battlefield. The range (of 2,000 to 4,000 yards) of such a rocket would add much to the present antitank-weapon ranges. In addition, such a low-yield nuclear device might be adaptable to small air-launched weapons.

Prior to Operation Hardtack there had been no study of the effects of subkiloton nuclear devices. Scaling laws become questionable when extended to this low range, without actual confirmation. Therefore, it was decided to conduct the necessary test in the latter part of Operation Hardtack.

In view of the urgency of the situation and the need for speedy action to get the test into Operation Hardtack, which was nearing completion, the general content of the test had already been decided upon by Chief, AFSWP, the Department of the Army, and the AEC's Division of Military Application. The project agencies, project numbers and project objectives are shown in Table 12.1.

12.1.3 Planning and Operations. On 18 June 1958, a preliminary planning conference was held at the University of California Radiation Laboratory (UCRL), Livermore, California. This meeting was attended by representatives from Chief, AFSWP, UCRL, Sandia Corporation, and TU-7.1.3.

It was first planned to conduct the test at Bikini Atoll on the Sugar-Tare complex. When plans

were almost complete for this site and personnel were moving in, certain shot scheduling and radiological conditions dictated that a change of site be made to Eniwetok Atoll, Site Yvonne.

Accordingly, plans were laid, preparations made, and a shot date of 28 July was established for Shot Quince.

Delays in delivery of the Quince device caused postponement of shot date until 5 August, with a primary shot time of 1000, EPG time.

On 5 August, during final preparations, trouble was encountered in the checkout of the device,

TABLE 12.1 SUBKILOTON YIELD NUCLEAR DEVICE, SHOTS QUINCE AND FIG

Project Number	Project Agency and Project Officer	Objective	Funds
1.4 (Extended)	Engineering Research and Development Laboratory (ERDL), A. W. Patteson	Crater measurement	\$5,744
1.7 (Extended)	Ballistic Research Laboratories (BRL) Daniel P. Le Fevre	Air blast parameters as a function of time and distance	\$27,274
2.4 (Extended)	Chemical Warfare Laboratory (CWL) David L. Rigotti	Neutron flux spectrum and dose versus range	\$55,260
2.9	Chemical Warfare Laboratory (CWL) Manfred Morgenthau	Initial gamma dose versus range	\$92,362
2.10	Chemical Warfare Laboratory (CWL) Manfred Morgenthau	Radiation intensities in contaminated areas	\$127,185
2.11	Chemical Warfare Laboratory (CWL) David L. Rigotti	Neutron, thermal and gamma measurement up to 1,500 ft, (Balloon)	\$87,395
8.7	Chemical Warfare Laboratory (CWL) J. J. Mahoney	Thermal flux versus distance	\$69,142
34.8	Sandia Corporation (SC) R. E. Butler	Fallout measurements	\$9,769
34.9	Sandia Corporation (SC) H. G. Sweeney	Cloud photography	\$2,931
34.10	Sandia Corporation (SC) D. G. Palmer	Wind measurements	\$6,838

and the decision was made to postpone the shot until 6 August.

At daylight, 6 August, the balloon of Project 2.11 was observed to be damaged and slowly descending. A new balloon was taken to the site, prepared, inflated, and positioned. This factor, plus troubles that UCRL and Sandia Corporation were having with device checkout, and poor wind conditions caused delays until Shot Quince was eventually fired at 1415, 6 August.

Shot Quince did not function as a nuclear device. None of the project instrumentation was disturbed. There was alpha contamination around and downwind from ground zero. Thus, only minor preparations and time checks were necessary for Shot Fig. The problem was one of waiting for delivery of the device.

On 13 August the Fig device arrived, final preparations were begun, and a primary shot time of 1000 on 15 August was established.

On 15 August there was general rain and poor wind direction which caused postponement until

16 August. The rainy season and fluctuating wind directions led to daily postponement until Shot Fig was eventually detonated at 1600 on 18 August 1958.

## 12.2 BLAST MEASUREMENTS

12.2.1 Objectives. The primary objective of the Quince-Fig phase of Project 1.7 activities was to obtain measurements of the variations of air blast-pressure time with distance from a very-low-yield (10 to 30 ton, predicted) surface-positioned nuclear detonation. The measurements were intended to determine the applicability of existing nuclear scaling laws to very-low-yield nuclear weapons.

12.2.2 Background. Much air-blast data, particularly overpressure time, has been gathered from kiloton- and megaton-range detonations under varied conditions. The state of knowledge for predicting overpressure as a function of time for these ranges of device yield is considered to be reasonably good.

However, air-blast data is limited for very-low-yield bursts. Data have been obtained from a 0.3-kiloton device on Operation Redwing and a 0.1-kiloton device on Operation Plumbbob. For these two detonations, precursor wave forms were not present. In general, under similar burst conditions, precursor wave forms would be present for kiloton- and megaton-range detonations. In the absence of precursor formations, classical-type shock waves were obtained from the very-low-yield bursts, and the overpressure and dynamic pressure corresponded to the Rankine-Hugoniot relation within experimental accuracy. With the formation of a precursor, the Rankine-Hugoniot relation between overpressure and dynamic pressure would cease to be valid.

A fractional-kiloton nuclear device is to be incorporated into the Battle Group Atomic Delivery System, under development by Army Ordnance. Nuclear-effects data for this size device were lacking. The effects parameters of interest were air blast, ground shock, craters, thermal radiation, initial and induced radiation, and fallout. It was planned to conduct the fractional-kiloton test at NTS, where overall conditions would yield more favorable results. Because of the short element of time for implementing the program and other factors, such as availability of personnel and logistics, it was deemed more desirable to conduct the test at the EPG as a part of Operation Hardtack. Under these circumstances, only a minimal program for effects data was possible. Part of the minimal program was to obtain air-blast data on Shot Quince and subsequently on Shot Fig. Although it was felt that air-blast parameters could be predicted for the fractional-kiloton device with reasonable accuracy, further corroboration was required.

12.2.3 Instrumentation. A total of 36 conventional self-recording pressure-time (pt) gages and dynamic-pressure-time (q) gages were used to instrument the blast-line stations. All gages were initiated by a minus-five-second-timing signal supplied from a central distribution station. In order to avoid complete loss of data due to damage to the timing-signal wire between the source and the gages, a number of separate relays were used. Only four gages were activated by any one relay, and these gages were located at different ground distances from surface zero.

As indicated in Figure 12.1, several gages were employed at most positions. This multiplicity of gages was necessary to insure obtaining data, regardless of the yield of the device. For example, at a ground range of 70 feet from surface zero, four gages were installed, each containing a pressure capsule of different recording range (0 to 1,000 psi, 0 to 800 psi, 0 to 400 psi, and 0 to 100 psi). This gage variation assured obtaining satisfactory data for any yield from 1 to 100 tons.

The normal recording speed of the pressure-time gage is three rpm. However, in order to realize the maximum resolution of the expected brief pressure-time history, some of the gages

at most positions were equipped with higher-speed-drive motors giving a recording speed of 10 rpm.

To instrument the blast line, 28 pressure-time and 8 dynamic-pressure gages were used. These gages were installed at 10 gage positions, ranging from 40 feet to 700 feet from surface zero. The type and number of gages at each position, as well as the general configuration of the blast-line layout, is shown in Figure 12.1.

It has been found that overpressure measurements obtained from a surface burst scale favor-

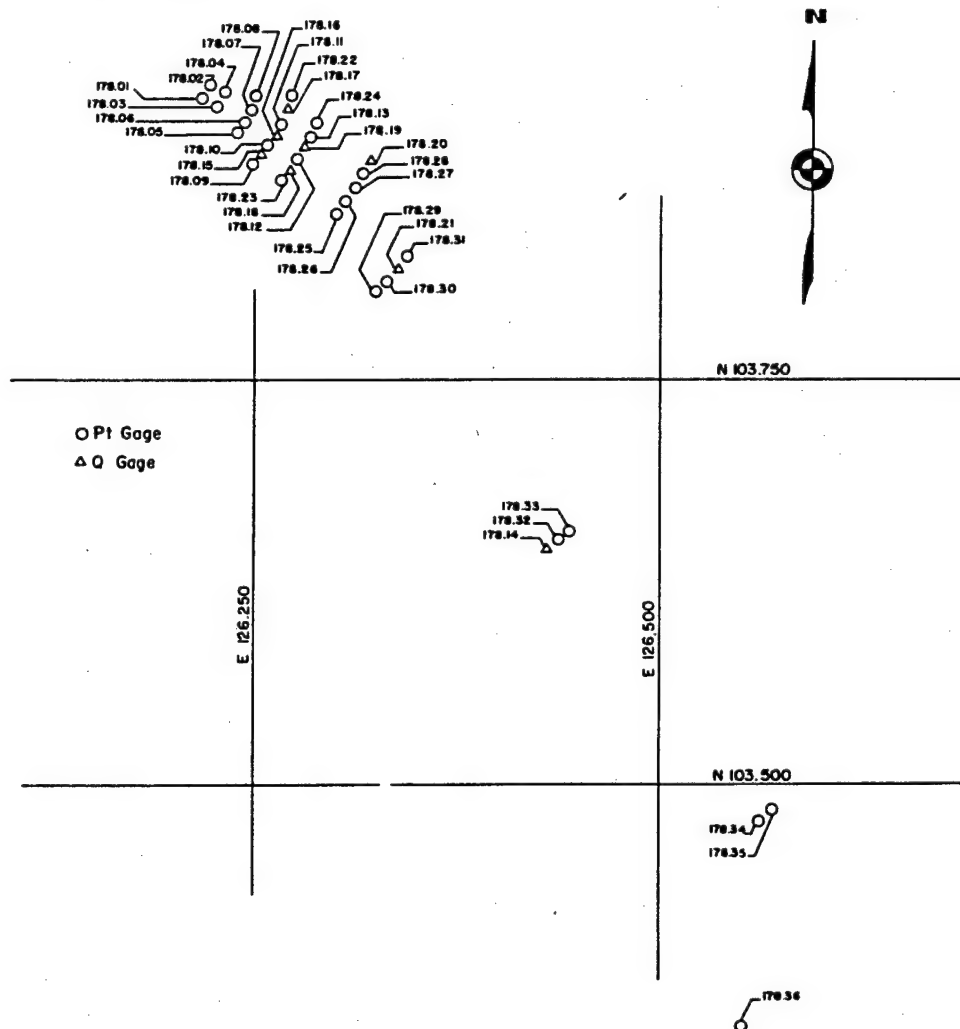
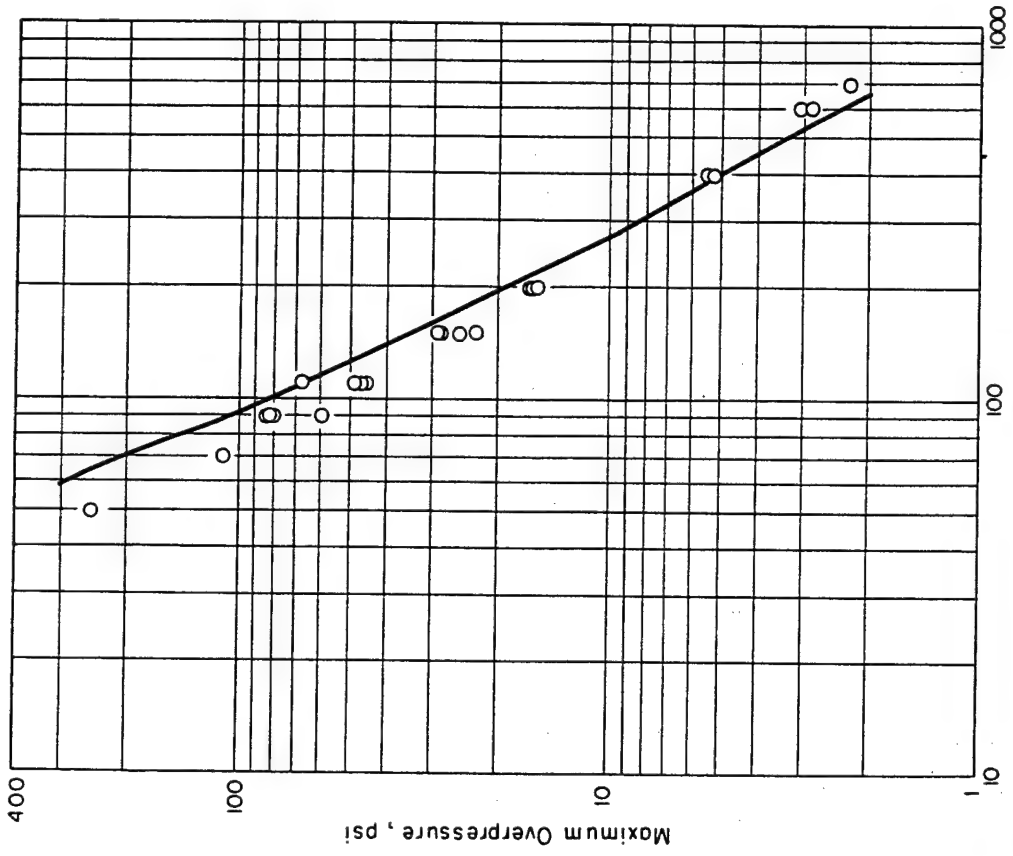


Figure 12.1 Blast line layout for Shots Quince and Fig, Site Yvonne.

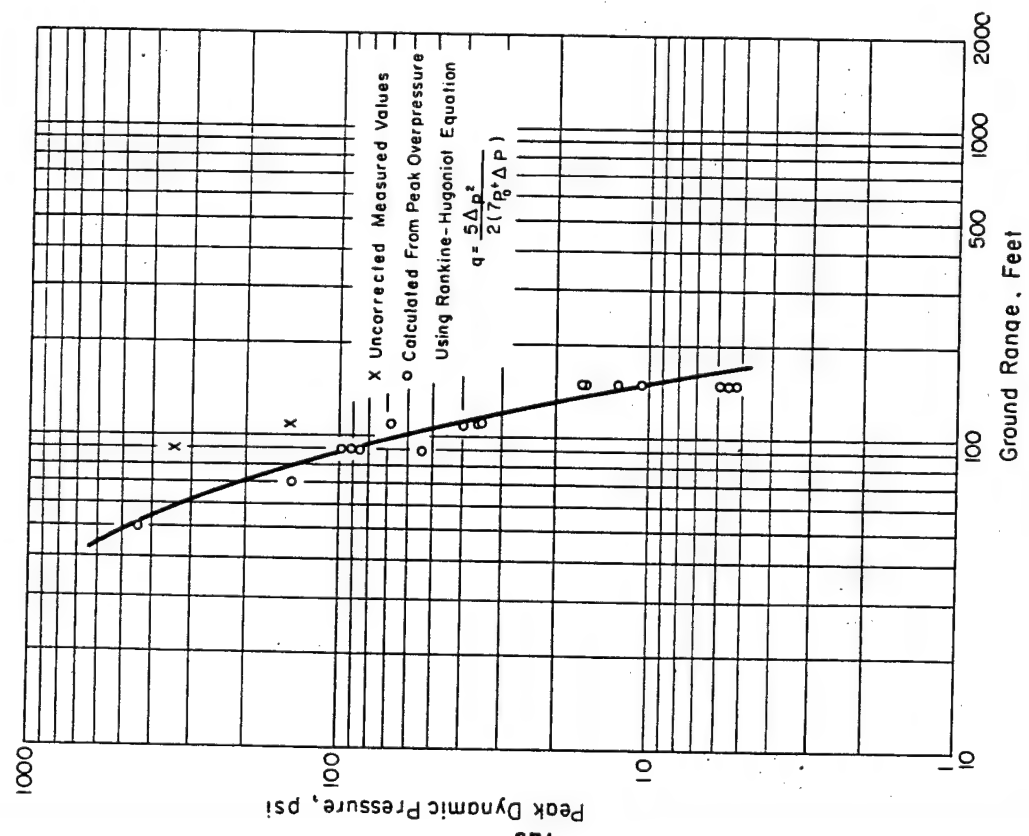
ably as 1.6 times the yield of a free-air burst. This method was used to determine the positions of the pressure-time gages. The dynamic-pressure-time gages were located at varying positions along the blast line, according to data collected by BRL and Sandia Corporation during Operation Redwing.

**12.2.4 Results. Shot Quince.** The non-nuclear detonation of Shot Quince resulted in blast pressures far below the minimums predicted for the nuclear detonation. In spite of this, data was obtained on 20 of the 28 pressure-time gages and seven of the eight dynamic-pressure



Ground Range, Feet

Figure 12.3 Comparison of Fig overpressure data with the 1-kt free-air overpressure curve scaled to 1.6 kt and then to 21.5 tons.



Ground Range, Feet

Figure 12.2 Peak dynamic pressure versus ground range, Shot Fig.

gages. Failure to record wave form at six stations was primarily due to capsule ranges too high for response to the relatively weak pressure wave. Thus, the pressures recorded were from one to five percent of the capsules' rated-pressure capability and resulted in extremely small deflections.

Shot Fig. All of the 36 gages functioned as programmed; however, results were obtained from only 22 of the 28 pressure-time gages and two of the eight dynamic-pressure gages. The pressure-time records of two stations (178.04 and 178.08) were considered questionable since

TABLE 12.2 RESULTS OF PRESSURE-TIME GAGES, SHOT FIG

Station Number	Ground Range	Maximum Overpressure	Arrival Time	Positive Duration	Remarks
	ft	psi	sec	sec	
178.01	40	—	—	—	Record lost
178.02	40	—	—	—	Record lost
178.03	50	—	0.155	—	No record
178.04	50	251.0	0.152	—	No record
178.05	70	—	0.167	—	No record
178.06	70	—	—	—	No record
178.07	70	—	0.156	—	No record
178.08	70	110.0	—	—	Poor record
178.09	90	84.3	0.183	0.034	Poor record
178.10	90	86.4	—	0.050	Good record
178.11	90	81.3	1.163	—	Poor record
178.22	90	59.5	—	0.037	Good record
178.12	110	68.0	0.133	0.057	Good record
178.13	110	49.4	0.032	0.049	Fair record
178.23	110	45.9	0.192	0.040	Fair record
178.24	110	46.3	0.009	0.053	Good record
178.25	150	23.1	0.198	0.058	Poor record
178.26	150	29.7	0.043	0.054	Good record
178.27	150	29.3	0.202	0.047	Good record
178.28	150	25.6	0.065	0.056	Good record
178.29	200	16.4	0.104	0.053	Good record
178.30	200	16.8	—	0.052	Good record
178.31	200	15.9	—	0.053	Fair record
178.32	395	5.5	0.221	0.081	Good record
178.33	395	5.3	0.315	0.083	Good record
178.34	605	2.9	0.362	0.096	Good record
178.35	605	3.1	—	—	Poor record
178.36	700	2.3	0.526	0.102	Good record

chipping of the glass-recording disks partially obscured the records. Failure to obtain records at the remaining six stations was the result, primarily, of severe ground acceleration which caused the glass-recording disks to shatter. The fragments were assembled and analyzed. Four of the shattered records indicated partial, but unreadable, records. The remaining two records were too badly shattered to be pieced together. The two dynamic-pressure records were considered, at best, only peak-pressure data. The remaining six dynamic-pressure gages appeared to function as programmed; however, there was no indication of any response to a pressure wave although the same gages had previously recorded the very-low pressures associated with Shot Quince.

The pressure-time-gage data is shown in Table 12.2, while the dynamic-pressure-gage results are listed in Table 12.3.

12.2.5 Discussion. Shot Quince. As the shot did not produce any nuclear yield and the pressures recorded represented only the high-explosive component, no discussion of Shot Quince will be included in this summary.

Shot Fig. The maximum overpressure data as shown in Figure 12.2 indicate a good rela-

TABLE 12.3 RESULTS OF DYNAMIC-PRESSURE GAGES, SHOT FIG

Station Number	Distance from	Total Pressure	Static	Static	Arrival Time	Positive Total	Duration Static	Remarks
	Ground Zero		Overpressure (at 3 feet)	Overpressure (ground baffle)				
	ft	psi	psi	psi	sec	sec	sec	
178.15	90	414	—	72	—	—	—	Peak pressure only
178.16	90	—	—	72	—	—	—	No record
178.17	90	—	—	72	—	—	—	No record
178.18	110	197	63.7	48	—	—	—	Peak pressure only
178.19	110	—	—	48	—	—	—	Bad record
178.20	150	—	—	27.4	—	—	—	Bad record
178.21	200	—	—	16.7	—	—	—	Bad record
178.14	395	—	—	5.4	—	—	—	Bad record

tionship of the recorded pressure with ground range. An eyeball curve was drawn through the data points. All failures to obtain reliable data occurred at the close-in stations (40 to 70 feet from surface zero). The shattered glass disks at these ranges indicated a severe shock loading about the gages. Between the ranges of 70 feet and 90 feet from surface zero, the records were chipped, but the data was read and considered to be questionable. From a ground range from 90 feet out, the condition of the records was considered to be good.

At the time of the initial reading of the records, a yield value within reasonable limits had not been given. Thus, the plotted values of the recorded pressures were compared to a scaled-down curve for a nuclear burst of 21.5-ton yield (Figure 12.3).

It cannot be determined at this time why the dynamic-pressure gages failed to record the presence of the shock wave.

Laboratory analysis of these data will be necessary before arrival times and positive-phase durations can be presented.

12.2.6 Conclusions. Data from Shot Fig show that the blast phenomena from a very-low-yield nuclear device appear to scale reasonably well. Any reason or reasons for the slight deviations from the established cube-root-scaling law cannot be explained at this time.

### 12.3 CRATER MEASUREMENT

Project 1.4 was assigned the mission of measuring the size of the crater produced by the surface detonation of a very-low-yield detonation. To make these measurements more realistic, 100 tons of soil from the NTS were transported to the EPG and placed below surface zero to about 90 percent of its natural density of 116 lbs/ft<sup>3</sup>, as discussed in Section 12.4.2. It is believed that the crater was completely contained in this soil.

The depth was 9.7 feet below grade, with a 3.6-foot lip above grade. At the time of measurement, D + 3 days, there was evidence of earth slides which resulted from severe rains which occurred after the detonation. The crater was briefly observed on D + 1 day,



prior to the slides. Based upon this observation and the measurements made later, it is estimated that the original crater was 1 to 2 feet deeper and 4 to 6 feet smaller in diameter, from lip to lip, immediately following the detonation.

## 12.4 NUCLEAR RADIATION

12.4.1 Introduction. The Program 2 participation on the very-low-yield detonations included seven projects. Program 2 participated on both Shots Quince and Fig. Shot Quince produced no nuclear yield, so with the exception of alpha-contamination measurements, no results are reported. Instrumentation, in general, was identical for both shots.

A device of the Shot Fig design, with a yield of about 20 tons, could have several military applications. Its possible employment in close support of tactical troops, however, required that detailed effects information, particularly on radiation, be obtained. Three basic questions determining the tactical doctrines of weapon employment would be entirely or partially answered when complete knowledge of radiation patterns, both immediate and residual, was obtained. These questions were: (1) What enemy casualties could be expected from the burst; (2) What time and space would be denied to either enemy or friendly troops; and (3) What was the safe-delivery range for a close-support-type launcher. Four specific objectives were established in an attempt to obtain the required answers. These included documentation of: (1) neutron flux in a three-dimensional pattern, (2) gamma dose in a three-dimensional pattern, (3) residual-gamma radiation, and (4) fallout contamination.

No device specifically designed to give a very-low yield had been previously detonated. Scaling laws had come from much larger yields and would not necessarily have been valid in predicting the radiation hazards from very-low-yield detonations. Due to the proposed test suspension, participation by Program 2 on these developmental shots was highly desirable. Conditions were somewhat unsuitable, however, because of lack of land areas on which to establish instrument stations. It was necessary in some cases to adjust instrument lines along directions where land area was available or to utilize floating stations in the lagoon.

12.4.2 Operations and Instrumentation. Project 2.4 established two surface neutron-flux lines for Shot Fig. One line ran along an azimuth of 143 degrees, [REDACTED] and the other along an azimuth of 233 degrees. The 143-degree line was entirely on land, and the threshold detectors (gold, cadmium-shielded gold, boron-shielded  $\text{Pu}^{239}$ ,  $\text{Np}^{237}$ ,  $\text{U}^{238}$ , and  $\text{S}^{32}$ ) were placed on sandbags and connected to a  $\frac{3}{4}$ -inch-wire rope to facilitate recovery. The other line consisted of two stations on land, and six stations on buoys anchored in the lagoon. The same detection system was used. The detectors on buoys were connected to a cable lying on the lagoon floor to allow recovery if the buoy sank. Recovery was made after the shot, and induced activities in the exposed detectors were measured in a mobile laboratory at Site Elmer. Both pretest and posttest detector calibrations were accomplished at LASL, utilizing the thermal column of the water-boiler reactor and the Cockraft-Walton accelerator as neutron sources. The neutron flux was calculated from the activity level of the exposed detectors at H + 10 hours by multiplying this value by a calibration number.

For the detection of gamma radiation, Project 2.9 installed 55 instrument stations. Eight stations were along the 233-degree line of Project 2.4; seven were suspended from a balloon anchored near ground zero; 36 were placed on stakes on available land sites, extending generally northwest and southeast from ground zero; and the remaining four were Emmett devices placed northwest of ground zero. The Emmett device was essentially a conveyor belt of film badges, each of which was exposed in turn from an underground shield and returned thereto. Basic instrumentation at all stations was the film badge, with a total range from 0.3 to 50,000 r. They were installed several days prior to the shot and recovered at approximately H + 24 hours. The

exposed film badges, as well as specially-exposed calibration badges, were immediately returned to the U. S. Army Signal Research and Development Laboratory for development and interpretation. The basic Emmett device did not have a fast-enough-time resolution to differentiate among the various initial-gamma pulses of a subkiloton device. It was, therefore, modified so that each badge was exposed for one minute, allowing for measurement of initial, induced, and fallout radiation in time increments of one minute. Three additional badges were located on the conveyor belt above ground. One film was exposed from 0 to 3 seconds, another from 0 to 15 seconds, and a third from 0 to 30 seconds.

At the total-dose gamma stations, film badges were placed in NBS holders, which were, in turn, placed in electrical condulets for blast and thermal protection.

In close association with the neutron-flux and gamma measurements, Project 2.11 lofted a polyethylene General Mills Aerocap balloon from which an instrument line was suspended. The line was located approximately 100 yards downwind from the zero point. Neutron-threshold detectors and gamma-measuring film badges were suspended from this line. It was planned to include thermistor calorimeters on the line for thermal measurements.

The gamma and neutron detectors were placed at seven air stations, ranging from 100 feet to 1,180 feet above ground. Each station consisted of a four-foot length of wire rope, attached to a ring on the main cable by means of a halyard snap. Recovery of the detectors consisted merely of detaching this short wire rope from the main cable. The thermal detectors were to be attached directly to the balloon cable, with hard wire connections from the detectors to the recorders located in an instrument shelter.

Project 2.10 instrumentation consisted of helicopter-to-ground survey instruments, fallout collectors, a crater-survey instrument, air samplers, gas-flow proportional-alpha counters, and AN/PDR-39 gamma-survey meters.

The helicopter-to-ground-survey instrument consisted of a radiation detector, described in detail in ITR 1319 (Reference 30), mounted in a probe which, in turn, was mounted in a tripod. The entire assembly was so rigged that it could be lowered from a helicopter. When the tripod rested on the ground, the probe was exactly three feet above the surface. Readings could be taken in the helicopter. In actual operation the readings were taken over pre-marked points and over well-defined geographical locations. The initial survey was begun at about H + 20 minutes. Additional surveys were made at H + 17 and H + 24 hours.

Two types of fallout collectors were used by Project 2.10. Five open-close gross-fallout collectors and 57 open-type, expendable, bucket collectors were placed in the array described below. The open-close collector consisted of a metal-support framework and a conical liner with a door covering the opening. The liner had a circular opening approximately two feet in diameter. In the bottom of the cone was a stainless-steel filter, four inches in diameter, covering a small hole leading to a polyethylene bottle. The door opened and closed with a sliding action and was activated by the minus-one-second timing signal. The door closed automatically after a specified collection time. The door was opened manually on recovery, and a cover was put on the cone liner. After the hose to the polyethylene bottle was disconnected, the cone liner and the bottle were removed from the gross collector and transported to the laboratory.

The open-type collectors were polyethylene pails, 16 inches deep, each with a 13-inch diameter opening and polyethylene cover to prevent spilling during transportation after recovery. Covers were removed manually before the shot.

One open-close collector was at 300-foot range on an azimuth of 270 degrees, and four were at 600-foot range on azimuths of 150, 165, 300 and 330 degrees. The open-type collectors were placed in a polar coordinate-grid system at 15-degree intervals at ranges of from 200 to 600 feet from ground zero. Other buckets were placed on barges at ranges of 2,100 to 7,600 feet. During recovery, readings were taken three feet above ground with an AN/PDR-39 survey meter. The buckets were sealed and returned to the laboratory, where they were monitored in a fixed

geometry. The fallout was then removed and the total weight and activity determined.

The crater-survey instrument consisted of a detector probe of the same type as used in the helicopter-to-ground aerial-survey instrument which had been modified to record the radiation intensity on a Brown recorder. The probe was housed in a fiberglass cylinder to prevent breaking. It was placed on the ground 375 feet from ground zero at an azimuth of 317 degrees. A cable extended from the probe toward ground zero, made an arc 80 feet from and around ground zero, and thence ran 600 feet to a winch and the recorder. At H + 5 minutes, the winch was to pull the probe toward, and into, the crater where it was to automatically record the radiation intensity for 24 hours.

Five air samplers were used to measure alpha concentration in the air. These samplers consisted of 24-volt dc motors, manufactured by the Electrolux Corporation. They ran at 10,300 rpm and drew approximately 6 ft<sup>3</sup>/min of air through a No. 6 Chemical Corps filter paper. The sampling area was 15.5 in<sup>2</sup>.

Two Model PAC-3G gas-flow proportional-alpha counters were used for surface monitoring. The sensitive window area had a density of 0.85 mg/cm<sup>2</sup> and an area of 61 cm<sup>2</sup>. The maximum reading of the instrument was 100,000 cpm, but the range could be increased by covering a part of the sensitive area. Readings were taken at 54 surveyed points over broom-finish concrete surfaces, typical of urban sidewalks.

Ground-gamma surveys were made with AN/PDR-39 survey meters. The meters were held three feet above the surface during measurements.

A project closely related to 2.10 was 2.14a/34.8, "Fallout Contamination From Small Yield Weapons." Associated with this project were 2.14b/34.9, "Dimensions of Nuclear Cloud from a Very-Low-Yield Burst," and 2.14c/34.10, "Special Meteorological Measurements for Very-Low-Yield Fallout Studies." These latter two projects were in support of 2.14a/34.8 and are mentioned only to point out that to analyze any fallout pattern and to draw conclusions as to what might follow a similar detonation under different weather conditions, the size, height and shape of the cloud and the exact wind pattern from the surface to the altitude of the top of the cloud must be accurately known.

Coral soil is neither physically nor chemically similar to widely occurring soils. For this reason, and the fact that most fallout data for relatively low yields had come from bursts on and over Nevada soil, 130 tons of NTS soil were transported to the EPG. This soil was compacted to about 90 percent of its natural density of 116 lbs/ft<sup>3</sup> in a conical excavation 30 feet wide and 8 feet deep at ground zero. It was estimated that the entire crater would be contained in this volume.

Sample collection was hampered by lack of ground area, with a large part of the fallout pattern expected to occur over water. The 2.14a/34.8 instrumentation was located at 146 surveyed points, comprising one rectangular and one radial grid system. Two remote-area-monitoring systems (RAMS) were used in this experiment. One system of 10 units was installed on Site Yvonne and one of 6 units on a YCU barge in the lagoon. Each remote unit consisted of a Neher-White-type ionization chamber and a remotely operated check source, all mounted in a waterproof housing. Each remote station was hard wired to a central control station. Two sleds with a remote detector were to be pulled into the crater at H + 10 minutes. Gamma-dose rates were measured by monitors using Jordan Model AGB-500B-SR and AN/PDR-T1B portable meters. Readings were taken at all 46 land stations at a height of 30 inches above ground. Similar readings were also taken aboard five barge stations in the lagoon. Coral soil was spread on the barge decks to simulate the effects of soil irregularities on measured dose rates. Three types of barges were utilized. They were the YCU, YC, and sectional barge, with dimensions 60 by 200, 32 by 100, and 30 by 60 feet, respectively. A correction factor was necessary for readings taken on the center of the barges because of the reduced area of surface contamination. Divisions by factors of 0.52, 0.38, and 0.35, respectively, were used for the three types of barges.

High volume (50 cfm) air samplers were also installed on the barges. Each sampler used a 4-inch-diameter Type BM-2133 filter and had an intake air speed of about 8 knots. They were aligned to face into the wind.

Sticky-pan fallout collectors, 8-by-10-inch flat metal trays covered with an alkyd-resin toluene solution, were mounted on 2-foot-square baffle plates. These pans were placed on the barges, at 32 shore stations, on 87 lagoon stations mounted on buoys, and at eight stations on the reef upwind of ground zero. Clusters of these pans were established at selected stations for two separate determinations. One was for purely statistical reasons and the other to determine weathering effect, with some pans being collected early and others in the same cluster at a later time. Except for those designated for late recovery, the sticky pans were collected as soon as possible after the shot by helicopter, water taxi, LCM, DUKW, jeep, and weapons carrier. They were brought to the established counting tent and counted in a fixed geometry.

Since an elaborate array was not possible because of lack of sufficient land area, the array was so arranged on land and in the lagoon that, for success, the wind had to be from along the prevailing wind direction  $\pm 10$  degrees and with a velocity of 20 knots or less.

12.4.3 Results and Discussion. Shot Quince. Because of the absence of nuclear yield on Shot Quince, the stated objectives of the program were not realized. However, Project 2.10 conducted an alpha survey of the area contaminated by the plutonium throwout, as well as obtaining air samples from H-hour to H + 19 hours.

An area of approximately 20 yards in diameter around ground zero was found to be highly contaminated. Outside this area the alpha contamination was spotty, with pieces of plutonium causing some hot spots in the downwind area. The highest concentration was 1,400,000 counts per minute, or  $3,300 \mu\text{g}/\text{m}^2$ , at a station located 150 feet from ground zero.

Air samples showed alpha concentrations of between 0.1 and 966 dis/min- $\text{m}^3$  at stations located 300 feet from ground zero. Sampling at these stations began at H + 1 hour and continued for approximately 18 hours.

Shot Fig. Shot Fig was a surface shot with a nuclear yield of 21.7 tons and was fired at Site Yvonne. All projects participating in this event obtained useful data.

Neutron dose was obtained from the neutron-flux measurements made by Projects 2.4a and 2.11. The dose was calculated from the flux values through the use of the single-collision theory of dose contribution per neutron. Neutron-dose values obtained from Shot Fig are presented in Table 12.4.

[REDACTED] This phenomena of increased neutron dose with altitude has been previously observed (Reference 31).

To permit direct comparison of the measurements from the two surface lines, buoy-station data from the water line has been corrected to equivalent land readings by division by 0.7 as suggested in TM 23-200 (Reference 15).

[REDACTED]

Total gamma-dose measurements were made by Projects 2.9 and 2.11. Also, Emmett devices used by Project 2.9 gave some indication of the times at which the gamma dose was received. Gamma doses as received by the various lines of instrumentation, as well as a prediction curve based on TM 23-200, are plotted as a function of distance in Figure 12.5. This figure shows that the readings over water are practically the same as those at the corresponding land stations, while the readings at the balloon stations are higher. Doses as recorded by the Emmett devices

show good agreement with adjacent film-badge stations and indicate that essentially all of the 24-hour gamma dose was received within the first 30 seconds after detonation. No variation of dose with time, to indicate fallout arrival, was recorded. This was to be expected, since the instruments were not in the primary fallout area.

A radiological survey of the residual radiation was performed by Project 2.10. Surveys were

TABLE 12.4 NEUTRON DOSE, SHOT FIG

Station Number	Slant Range yds	Dose rep
Land Line:		
241.10	30	$1.32 \times 10^5$
241.01	100	$9.92 \times 10^3$
241.02	200	$1.49 \times 10^3$
241.03	300	$3.72 \times 10^2$
241.04	400	$1.56 \times 10^2$
241.05	500	$6.29 \times 10^1$
241.06	600	$3.22 \times 10^1$
241.07	700	*
Water Line:		
242.01	30	$6.36 \times 10^4$
242.02	100	$4.83 \times 10^3$
242.03	247	$6.9 \times 10^2$ †
242.04	311	$2.24 \times 10^2$ †
242.05	444	$8.33 \times 10^1$ †
242.06	603	$2.27 \times 10^1$ †
242.07	816	*
Balloon Line:		
1	121	$6.65 \times 10^3$
2	133	$5.79 \times 10^3$
3	173	$2.90 \times 10^3$
4	227	$1.66 \times 10^3$
5	283	$7.69 \times 10^2$
6	347	$3.53 \times 10^2$
7	410	‡

\* Below level of detection by threshold system, approximately 10 rep.

† Corrected to Equivalent Land Values by division of water dose by 0.7 as suggested in TM 23-200.

‡ Detectors lost.

accomplished by helicopter probe and ground-party survey crews. The project found that at H + 1 hour, the 200 r/hr dose rate contour had a downwind dimension of approximately 120 yards and a crosswind dimension of 50 yards, while the 100 r/hr dose rate contour dimensions were approximately 160 yards downwind and 40 yards crosswind. Readings in the near vicinity of the crater were greater than 10,000 r/hr at H + 30 minutes.

The crater survey instrument, which was located 375 feet from ground zero at the time of detonation, recorded the initial-gamma pulse off scale, greater than 10,000 r/hr, for approximately seven seconds. Because of fouling of the cable that was to tow the probe into the crater,

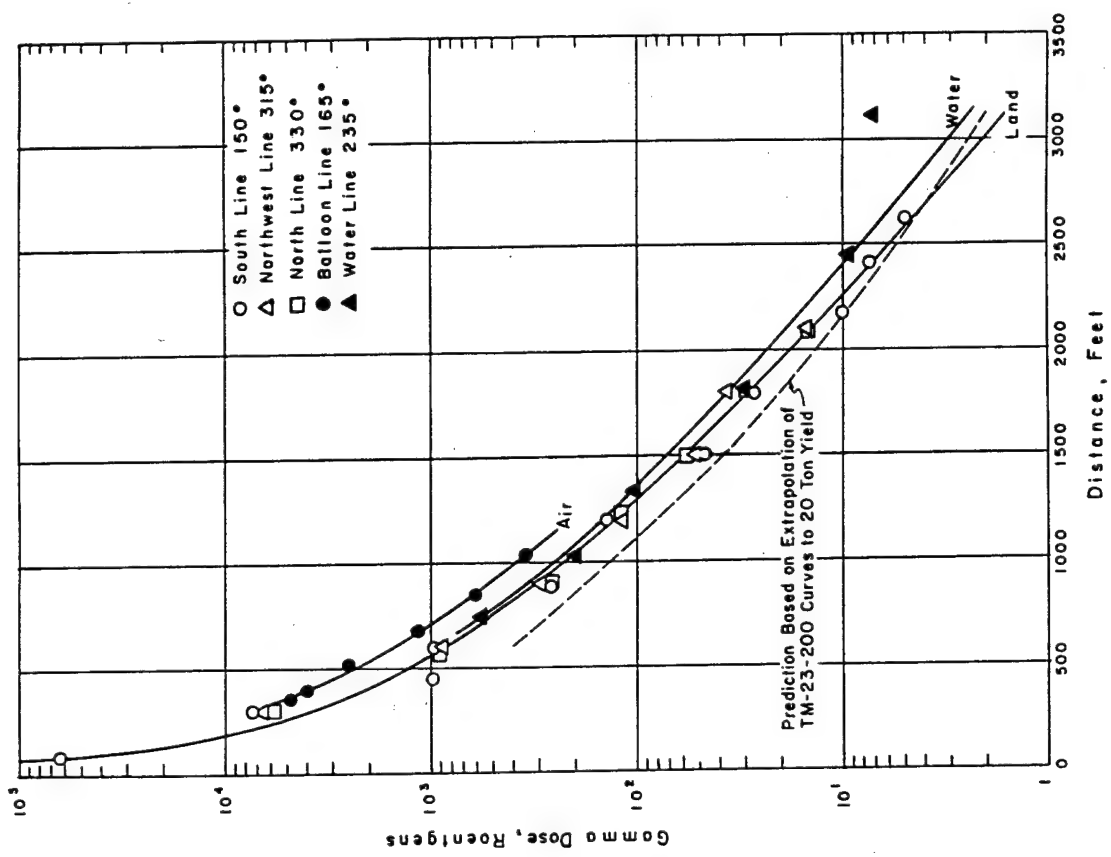


Figure 12.5 Gamma doses versus distance.

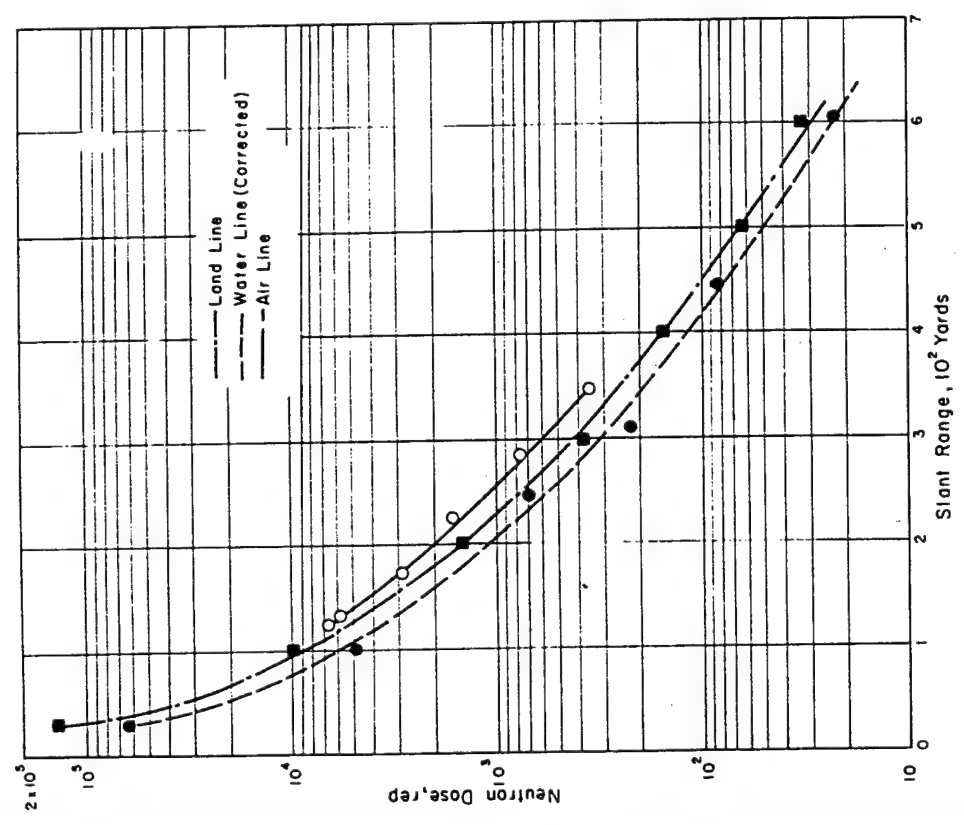


Figure 12.4 Neutron dose, Shot Fig.

wind speeds for the first ten minutes after Shot Fig ranged from 15 to 16 knots and the direction varied from 264 to 277 degrees. These wind characteristics were ideal for fallout sampling by Projects 2.10 and 2.14a/34.8.

12.4.4 Conclusions. Shot Quince. Plutonium throwout from a device of this nature from which no nuclear yield is realized presents a hazard from alpha contamination in an area 20 yards in diameter around ground zero. There will also be further hazards in the downwind direction.

Shot Fig.



Practically all of the 24-hour gamma dose received in nonfallout areas is received in the first 30 seconds after detonation. All gamma doses were higher than those predicted by TM 23-200.

The crater and lip formed from a surface burst of the Shot Fig type will have a residual activity of greater than 10,000 r/hr at H + 30 minutes. The resultant residual-gamma field will be limited in extent for meteorological conditions identical to those of Shot Fig, with the 100 r/hr contour extending only 40 yards crosswind and 160 yards downwind at H + 1 hour.

The fallout decayed according to  $t^{-1.35}$  from H + 1 to H + 3 hours and at  $t^{-0.94}$  between H + 3 and H + 24 hours.

Cloud dimensions after stabilization were well within the range of accuracy of the predictions from TM 23-200. Better cloud-dimension data could have been obtained at a test site where the available land area allowed better positioning of camera stations.

Based on meteorological measurements after Shot Fig, fallout-collection instrumentation was ideally located for collection of samples.

## 12.5 THERMAL RADIATION FROM A VERY-LOW-YIELD BURST

One objective of this experiment was to determine the thermal radiant-exposure versus distance from ground zero for a very-low-yield burst and to compare these values with the theoretical results obtained from existing thermal scaling laws.

12.5.1 Objectives. Specifically, the objectives were to measure the thermal radiant exposure and thermal irradiance at various distances from ground zero for Shots Quince and Fig to: (1) accumulate basic thermal data for fractional-kiloton weapons for which data was not previously available; (2) check the existing thermal-scaling laws and to modify and extend them to include device yields equal to those of Shots Quince and Fig; (3) measure radiant exposure and irradiance for ground stations in order to examine the existing scaling laws; and (4) compare the values of radiant exposure at ground stations as determined by three different types of measurement instruments.

12.5.2 Background. Thermal radiation has been measured by various agencies during nearly all previous nuclear tests, but thermal radiation has not been measured for nuclear devices of



the low-yield values expected from Shots Quince and Fig. Measurement of the thermal-radiation values for such devices was necessary from both a theoretical and practical military standpoint, unless reliance was placed in extensive extrapolation from previous larger-yield values.

12.5.3 Instrumentation. There were nine ground-instrument stations ranging in distance from 150 feet to 900 feet from ground zero.

Three types of instruments were used to measure thermal radiant exposure. These were

TABLE 12.5 GROUND STATION INSTRUMENTATION

Station Number	Ground Zero Distance	Instrumentation	
	ft		
872.01	150	CWL	
872.02	175	CWL	
872.03	200	CWL	
872.04	250	CWL	
872.05	350	CWL	NML
872.06	450	CWL	NML
870.01	450	NRDL	
872.07	600	CWL	NML
872.08	750	CWL	NML
870.02	900	NRDL	

the Chemical Warfare Laboratory thermistor calorimeter, the Naval Radiological Defense Laboratory disk calorimeter, and Naval Material Laboratory thermal-radiant-exposure meter. These instruments were installed as shown in Table 12.5.

12.5.4 Chemical Warfare Laboratory Instrumentation. This instrument was essentially a bead-type thermistor, embedded in one end of a solid silver cylinder. Radiation incident on the other end of the cylinder resulted in a temperature rise of the cylinder and embedded thermistor. The thermistor, a semiconductor, composed of oxides of manganese, nickel, and cobalt, had a coefficient of electrical resistance of -3.9 percent/C at 25 C. The particular thermistor used in this test was the VECO-32A11. A change in electrical resistance caused a variation in the current at the recording milliammeter. The silver cylinder was insulated by Teflon, and the entire assembly was mounted in a hermetically-sealed-brass housing fitted with a hemispherical pyrex window. The complete unit was 2.5 inches in diameter and 6.5 inches long.

Due to the crash program involved in preparing for this test, only a cursory calibration of the instrument was made. However, it was designed to be an absolute instrument so that no calibration would be required. Results obtained during Operation Redwing indicated that calibration of the thermistor calorimeter against other instruments, assumed to be standards, was of little value. Accordingly, the radiant exposures were calculated for Shots Quince and Fig without reference to secondary calibration standards. If necessity indicates, calibration will be made prior to the final report, and the results will be contained therein.

The basic equation involved for the thermistor calorimeter is:

$$H = mst$$

where H is the radiant exposure in calories per square centimeter; m is the mass, in grams,



of the silver cylinder;  $s$  is the specific heat of silver; and  $t$  is the temperature rise of the silver cylinder due to incident thermal radiation.

The value for  $M$  was obtained by weighing the silver cylinder to within 0.1 gram, which is to three significant figures. The hole in the silver cylinder in which the thermistor was pasted was 0.1 inch in diameter and 0.25 inch deep. Elementary arithmetic and direct experimental weighing showed that at the worst, an error of only two percent could be introduced by considering the hole empty or full of silver or glass. For simplicity and with negligible loss of accuracy, the weight of the cylinder with the hole empty was used.

The value  $s$  is the specific heat of silver, 0.056 cgs units.

The value  $t$  is the temperature rise in the silver cylinder, obtained by subtracting the initial temperature from the final temperature of the thermistor (and silver cylinder) as read from the recording milliammeter. Each thermistor used was previously calibrated for electrical resistance in ohms versus temperature, by immersing the thermistors in a water bath and measuring the resistance directly, using a Wheatstone bridge.

The only correction required in the calculation was a four-to-six-percent correction to be added to the temperature difference to account for a cooling loss. This was done in each case from the actual experimentally-recorded trace for the nuclear shot. Since the cooling loss was small, only four to six percent in approximately six seconds, errors in determining this small cooling rate were of little consequence.

A factor of eight percent was added to the calculated radiant-exposure values to account for the absorption loss of the thermal radiation incident through the pyrex-glass hemisphere of the calorimeter.

12.5.5 Naval Radiological Defense Laboratory Instrumentation. As the yields of Shots Quince and Fig were unpredictable, the thermal sensors were selected to measure thermal energies from yield ranges of 0.01 to 0.1 kiloton. The thermal sensors used were: NRDL Mk6F calorimeters, with a sensitivity of 0 to 10 (cal/cm<sup>2</sup>)/mv; and NRDL 20-junction calorimeters, with a sensitivity of 0 to 0.02 (cal/cm<sup>2</sup>)/mv.

The measurement of luminous flux was made with Weston photronic cells, Type RRV, used in conjunction with neutral-density filters.

Sixteen-millimeter gun-sight-aiming-point (GSAP) cameras were included in the instrumentation for the purpose of instrument orientation with ground zero and fireball studies.

The signals from the thermal and photronic sensors were registered by Heiland oscillographic recorders, on Kodak microfilm film running at a speed of 24 in/sec.

The instrumentation was located at two stations at 450 feet and 900 feet from ground zero. At each station there were eight calorimeters, four photronic cells, and two 16-mm cameras. These sensing instruments were mounted in a pod atop a 10-foot tower and oriented to face ground zero. The tower was attached to an NRDL underground shelter which contained the recording oscillograph, junction box, and 24-volt battery power supply.

All thermal instruments were calibrated at NRDL prior to the operation by exposure to a Mitchell high-intensity thermal radiation source. Several series of calibration runs were made prior to shipment of the instruments to the EPG. The calibration procedure is to be repeated upon the return of the instruments to NRDL.

The electrical calibrations were accomplished by introducing standard mv signals in series with the final field circuits on the night before the shot. The photronic cells were calibrated by the use of a laboratory-calibrated Weston photometer and a 500-watt projection lamp used as a source. The light source was placed at ten different distances from the instrumentation and the photometer sensor. The light levels corresponding to the different distances were recorded on the Heiland oscillograph, and the corresponding reading of the photometer was taken. This calibration procedure was repeated on D + 2 for postshot calibration.

12.5.6 Naval Material Laboratory Instrumentation. This instrument consisted of several Tempilstik pellets in contact with a blackened copper plate. The commercially available Tempilstik pellets melt at different temperatures. If the initial (ambient) temperature is known, the radiation exposure can be determined. After the shot, the instruments were returned to NML for reduction of data which was not available at the time of this report.

12.5.7 Results. CWL Measurements. The radiant exposures measured by the thermistor calorimeters during Shot Fig are given in Table 12.6. These results are the actual

TABLE 12.6 RADIANT EXPOSURE DATA

Station Number	Ground Zero Range	Radiant Exposure	Remarks
	ft	cal/cm <sup>2</sup>	
CWL Ground Stations			
872.01	150	11.1	
872.02	175	10.8	
872.03	200	6.9	
872.04	250	5.8	
872.05	350	1.6	
872.06	450	1.6	
872.07	600	1.4	
872.08	750	No Data	Recorder Malfunction
NRDL Ground Stations			
870.01	450	1.42	Average
870.02	900	0.28	Average
NML Ground Stations			
872.05	350	*	
872.06	450	—	
872.07	600	—	
872.08	750	—	

\* Data to be included in final report.

values of radiant exposure at three feet above ground at the stations. No correction was made for atmospheric attenuation.

NRDL Measurements. The radiant exposure measured by the NRDL instruments was:

Station Number	Ground Zero Range	Radiant Exposure (cal/cm <sup>2</sup> )
870.01	450 feet	1.42
870.02	900 feet	0.28

The reduction of the thermal data was exceedingly difficult, since there was no timing correlation. This abnormality was caused by the timing lights not being intense enough to expose the microfilm running at 24 in/sec. It was, therefore, necessary to assume that the film

speed was constant throughout the measurement. Until some method of time correlation can be found, it will not be possible to reduce this data to a better accuracy than is reported here.

There was no luminosity data presented, inasmuch as all the photronic-cell traces deflected off scale. This fact indicated a very high luminous flux. It is possible that an exhaustive laboratory analysis of the photronic cell data will yield useful information about the total-luminous flux, as a function of time and the peak illuminance.

The 16-mm cameras were installed primarily to orient the stations. However, a study of the images will be made and any significant thermal findings will be reported in the final report.

NML Measurements. No results are available for the NML thermal instruments, as the instruments were sent to NML for reading and calibration. These results will be reported in the final report.

12.5.8 Conclusions. The CWL thermistor-instrument data for distances of 150 feet to 450 feet and the NRDL disk-calorimeter data at 450 feet and 900 feet fit the same experimental curve. This experimental data closely parallels the curves obtained from existing scaling laws for yields of 0.02 and 0.03 kt.

## Chapter 13

# NEVADA TEST SITE PHASE

Prior to the completion of the Pacific Phase of Operation Hardtack it was decided to conduct a continental series of nuclear tests at NTS. The primary consideration leading to this series was the Presidential decree of a nuclear test suspension effective 31 October 1958. Many devices, planned for testing at a later date, were to be fired during this phase.

In August, DCS/WET, Field Command, was informed by the Chief, AFSWP, that some DOD participation was planned. This participation was a relatively small effort compared with normal test series. The prime participation was on the very-low-yield shots, Hamilton and Humboldt, with scattered projects operating on other shots as noted in the following sections of this chapter. (See Table 13.1 for shot participation.)

Although considerable data had been collected on very-low-yield detonations on Shots Quince and Fig in the EPG, [REDACTED] offered an opportunity to supplement this information and to obtain data on effects on biological specimens. This low-yield event was originally labeled Shot Grizzly and scheduled for 25 September. Much of the test equipment was in the EPG. Where feasible, priority air transportation was arranged. By the 25th of September, most instrumentation was on hand. However, due to developmental problems, the shot, the name of which had been changed to Hamilton, was rescheduled for 12 October. This allowed more time for project preparation.

When Shot Hamilton, detonated on a 50-foot wooden tower on Frenchman Flat, gave a yield of about one ton, a second detonation was scheduled. This shot, Humboldt, fired from a 25-foot wooden tower in Area 3, gave a yield of approximately 5.2 tons. The DOD effort was organized, with some modifications, as for a full-scale continental test. (See Figure 13.1.) Shot-yield information, environmental data and meteorological data are listed in this report.

### 13.1 NUCLEAR RADIATION AND EFFECTS

13.1.1 Introduction. Program 2 participation in the NTS phase of Operation Hardtack was directed toward the documentation of nuclear radiation from very-low-yield bursts. In the present concept of tactical employment of nuclear weapons, fractional kiloton weapons are assuming a role of increasing importance. Of primary importance in evaluating weapons of low yield was the determination of the nature and radial extent of militarily-important-biological effects. To meet this requirement, a biomedical experiment (Project 4.2) was included. It was the prime mission of Program 2 to support this experiment through documentation of the neutron and gamma doses to which the biological specimens were exposed.

During the initial stages of preparation, the program consisted of a single project, Project 2.12. This, in turn, was made up of three separate experimental efforts designated as Sub-Projects 2.12a, 2.12b, and 2.12c. Subsequently, Sub-Project 2.12d was approved on a minimal-cost and noninterference basis to measure total thermal exposures. A new project, Project 2.13, was also approved to obtain specific nuclear-radiation data required in Air Force studies relating to air-to-air delivery of very-low-yield weapons. As finally organized, the project consisted of two numbered projects, one of which was made up of four sub-projects, as follows:

Project 2.12 (Chemical Warfare Laboratories)

Project 2.12a Neutron-Flux and Dose Measurements

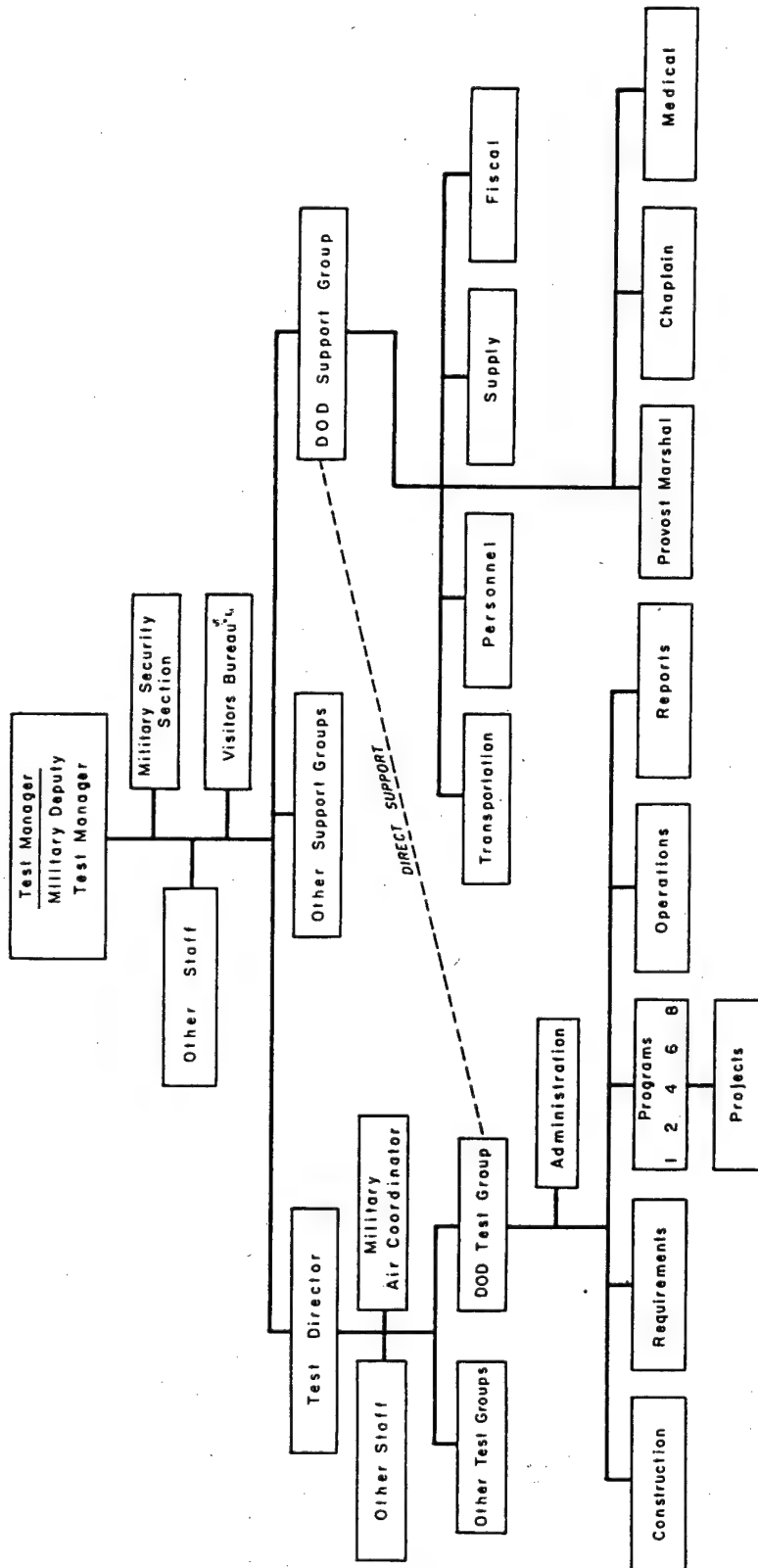


Figure 13.1 DOD organization, NTS phase of Operation Hardtack.

- Project 2.12b Gamma-Dose Measurements
- Project 2.12c Induced-Activity Measurements
- Project 2.12d Total Thermal-Exposure Measurements
- Project 2.13 (Air Force Special Weapons Center).  
Nuclear Radiation Measurements on Low-Yield Weapons.

13.1.2 Objectives. The primary objective of the program was to provide neutron and gamma-dose measurements (2.12a, 2.12b) in support of the biomedical Project 4.2. All other objectives were subordinate to this principal mission and were approved on a noninterference basis. These

TABLE 13.1 PROJECT PARTICIPATION, NEVADA PHASE  
One-point safety test shots not included.

Project	SHOT																		
	Eddy	Mora	Tamalpais	Quay	Lea	Hamilton	Logan	Dona Ana	Rio Arriba	Socorro	Wrangell	Rushmore	Sanford	De Baca	Evans	Mazama	Humboldt	Santa Fe	Blanca
1.7	■	■	■	■	■	■				■		■			■		■		
2.12a						■												■	
2.12b						■												■	
2.12c						■												■	
2.12d						■												■	
2.13						■												■	
4.2						■												■	
4.3						■												■	
6.14		■	■	■	■	■	■	■	■	■	■	■	■	■	■	■	■	■	■
6.15 *		■	■	■	■	■	■	■	■	■	■	■	■	■	■	■	■	■	■
8.8				■		■				■	■	■	■	■	■	■	■	■	■

\* Project 6.15 also participated in selected one-point safety test shots.

included documentation of: neutron flux and dose versus distance (2.12a, 2.13); initial and residual gamma-dose rate versus time and distance (2.12b, 2.13); total-gamma dose versus distance (2.12b, 2.13); neutron-induced-soil activity (2.12c, 2.13); and total-thermal exposure versus distance (2.12d). The field testing of a fallout detector, MG-3, was also included as a secondary objective of Project 2.13.

13.1.3 Background. Because of the anticipated tactical importance of very-low-yield nuclear weapons, information was needed to corroborate existing effects-prediction theories in this yield range or to provide sufficient data for the development of new prediction methods. Since previous experience indicated that nuclear radiation was the most far-reaching effect from very-low-yield bursts, it was particularly important that this effect be thoroughly documented. Neu-

tron flux and dose, gamma dose, and thermal-exposure measurements had been made on Shot Fig, a 21-ton detonation, during the EPG portion of Operation Hardtack. However, as this had been a surface burst, the radial extent of these effects could be expected to be different from those of an air burst of the same type device. Measurements made with a balloon-supported-instrument line during Shot Fig gave indication that the neutron and gamma doses would be higher in the case of an air burst. Thermal-exposure results could be expected to be affected in a similar manner.

Of particular importance was the definition of the essentially-immediate-lethality radius of low-yield bursts for biological specimens exposed in typical tactical-protective environments and the verification of safe stand-off distances for tactical-weapon delivery. This information was essential for evaluating the tactical capability of very-low-yield weapons and for development of safe weapon-delivery systems.

Studies of neutron-induced-soil activity for bursts of this yield category had not been previously performed, although such studies had been carried out for kiloton-range weapons during Operation Plumbbob (Reference 32). During the Operation Plumbbob experiment, an effort had been made to obtain empirical factors relating the dose rates induced in small samples of NTS soil with the gross free-field dose rates generated at the point of sample exposure. Subsequent to these experiments it was learned that the chemical composition of the soil in the samples used was substantially different from that of the field in which the exposures were made. For this reason the empirical factors established were subject to question, and it was considered necessary that new factors relating sample and field-dose rates for soils of identical composition be determined. Therefore, a neutron-induced-soil-activity experiment was included in the program to document the induced field generated by a tower burst of a fractional-kiloton device and to establish the empirical factors discussed above.

The possible employment of very-low-yield weapons in an air-to-air missile application generated problems with respect to aircrew dosage. Before delivery procedures and techniques could be formulated, experimental data on neutron doses and gamma-dose-rate variations with time, both as a function of distance, were required. This was the basis on which Project 2.13 was approved. The field testing of the MG-3 fallout detector was included in this project, as it represented a minimum effort consistent with the planned operations of the project.

13.1.4 Procedure. The program participated on two detonations during the NTS phase of Operation Hardtack, Shots Hamilton and Humboldt.

Shot Hamilton was fired on a 50-foot wooden tower on 15 October on Frenchman Flat and gave a yield of  $1.0 \pm 0.1$  ton. Shot Humboldt was detonated in Area 3 on a 25-foot wooden tower on 30 October, with a resultant yield of 5.2 tons.

Neutron-flux measurements were made by the Hurst threshold-detector technique (Reference 33). This method involves the use of small quantities of detector elements that are activated through nuclear transformations involving neutron capture or fission. The radioactive products of these transformations are directly proportional to the neutron flux to which the materials have been exposed and can be correlated directly. This method has been used in many nuclear-test operations by a number of agencies and has yielded excellent results. A more complete description of the detector system is included in Chapter 7.

For Shot Hamilton, neutron-detector systems were attached to two cable lines which extended radially from ground zero

Free-field measurements were made at slant distances from 23 to 800 yards. Detector systems were also installed in foxholes, tanks, and armored-personnel carriers (APC), in support of the biomedical experiment.

For Shot Humboldt, neutron-detector systems were attached to a single cable line

Meas-

urements were made at slant distances ranging from 13 to 300 yards. As during Shot Hamilton, detectors were located in foxholes and APC's to provide measurements in support of Project 4.2.

The use of cable lines facilitated early and safe recovery of the exposed detectors. Ten-ton dump trucks were used to pull the cables from the exposure area, immediately after the detonations. The detectors were then detached from the cables and transported to the neutron-counting trailer, located near the pig-pen area of the NTS.

Neutron-dose data was obtained by several means. The principal method involved calculation of dose from the measured-neutron flux, assuming a single-collision theory of dose contribution per neutron. The results of such dose determinations have agreed well with measurements made with more refined instrumentation. Other methods included the use of chemical dosimetry (Project 2.12a); resonance-threshold-foil (Indium) dosimeters (Project 2.13); Kodak personal-neutron-monitoring films (Project 2.13); and sulfur planchets and bags (Project 2.13). These various neutron detectors were placed at ground distances ranging between 55 and 1,600 yards, [REDACTED]

[REDACTED] Shot Hamilton. For Shot Humboldt, only the threshold-neutron detectors were used, and the instruments extended only to 300 yards.

Early gamma-dose rate as a function of time was measured during Shot Hamilton only. Stations were located at distances ranging between 100 and 800 yards from ground zero. For documentation of the initial gamma-dose rates versus time, Kaiser electronic-automatic-dose-rate instruments were utilized. These had dose-rate ranges to 40,000 r/hr and a recording time from 0 to 60 seconds after shot time. Incremental gamma-dose recorders (Emmett devices), wherein NBS film badges were mechanically exposed from a shielded location for specific time intervals, were used in an attempt to obtain gross dose-rate histories for the first 20 minutes after shot. These instruments had a resolution time of one minute, although the doses accrued in the first 3, 15 and 30 seconds were also measured by locating film badges in an initially exposed position.

Total gamma-dose measurements were made during Shot Hamilton at distances to 1,600 yards, utilizing various types of film badges, DT-60 and phosphate glass-needle dosimeters, and chemical dosimeters. NBS film badges were placed on stakes at 100-yard intervals on 12 radial lines extending from ground zero to a distance of 800 yards, while other instrumentation was placed at locations of interest to the supported projects [REDACTED]

For Shot Humboldt, total gamma-dose measurements were made through use of NBS and chemical dosimeters at ground distances ranging from 10 to 800 yards [REDACTED]

[REDACTED] For stations closer than 300 yards, instruments were attached to the neutron cable, while beyond this distance, NBS film badges were exposed on metal stakes.

Induced-activity measurements were made during Shot Hamilton only. Soil-sample stations were placed at distances of 25 to 200 yards from ground zero along one of the neutron-cable lines. Specially prepared soil samples were exposed in cylindrical containers buried in the ground. These cylinders were attached to the cable line and designed to eject automatically when the cable was withdrawn from the exposure area. Following recovery, the soil samples were to be reinstalled into the ground in an uncontaminated area where the dose-rate field generated by the activated samples could be measured. Simultaneously, the gross-field dose rates at the points of soil-sample exposure were documented by automatic dose-rate recorders and ground-survey teams. By correlating the dose-rate field demonstrated by the activated samples with the gross-rate field measured at the point of exposure, it was hoped that empirical factors could be determined whereby the activity of a gross field could be predicted from measurements made on small soil samples. This method would be of particular value in predicting the expected dose-rate levels for soils atypical to those found at nuclear test sites. An MG-3 fallout detector recorder, buried in a special neutron-shielded installation 30 yards from ground zero, was used to record the decay of the resultant field. This instrument served a dual purpose: it afforded an oppor-



tunity to document the very early decay of the induced field and provided a field test of the instrument itself. A second MG-3 instrument was placed 650 yards downwind from surface zero to measure any fallout that might occur at this location. Both instruments consisted of an ion-chamber detector, amplifier, recorder, and power supply. The detector threshold was 1 r/hr and the recording time was approximately  $4\frac{3}{4}$  hours.

Ground surveys were conducted after both shots at early times to document the resultant gamma-radiation fields and their decay. The AN/PDR-39 radiological-survey meters were hand-carried into the radioactive areas by personnel from the 1st Radiological Safety Survey Unit (RSSU). The procedure consisted of entering the area as early as possible and locating the 10 r/hr contour and then measuring the dose-rate levels at the stations of the film-badge lines external to this contour. Several teams were utilized to document the various radial lines. By performing a number of consecutive surveys, the collapse of the 10-r/hr line as well as the decay of the field at fixed locations could be documented.

Thermal-exposure measurements were made only during Shot Hamilton. To determine the total thermal-radiant exposure as a function of distance from a very-low-yield detonation, thermistor calorimeters were installed on a radial line extending from 175 to 700 feet from ground zero. Each station included two independent detectors to provide better reliability. Recorders were located in two transporters at 1,000 feet from ground zero.

Maps of the Hamilton and Humboldt arrays, showing locations of the various project instrumentation, are presented in Figures 13.2 and 13.3.

Gamma-dose rate versus time, induced activity, and thermal measurements were not attempted during Shot Humboldt. The neutron-flux dose and gamma-dose measurements were also significantly curtailed. This reduction in participation was a consequence of changing the shot location on the evening of D - 2 day, thereby precluding the relocation of essential instrumentation in time to permit participation.

13.1.5 Results and Discussion. Results as presented in this section pertain only to the documentation of the basic phenomena of free-field gamma and neutron radiations, neutron-induced soil activity, and thermal radiation. All results pertaining to measurements made in support of the biomedical experiment are presented in Section 13.2 of this report.

13.1.6 Shot Hamilton. The instrument array for Shot Hamilton was designed for an expected yield of 20 tons, although the predicted yield for the device ranged between 5 and 25 tons. For this reason, the unexpectedly low yield of 1 ton seriously reduced the amount and, in some cases, the quality of data obtained.

Neutron dose as a function of distance to 325 yards, as measured by the threshold-detector technique, is presented in Figure 13.4. The neutron dose measured at the 400-yard station was 15 rep, while at both the 600- and 800-yard stations the doses were below the 10-rep threshold of the detector system. Free-field neutron doses, as determined by sulfur activation to distances of about 1,300 yards, are presented for two lines at approximately right angles in Figures 13.5 and 13.6. In these latter figures, the dose data is presented as neutron dose times distance squared versus distance, thereby eliminating the geometrical attenuation effect.

Initial gamma-dose-rate-time histories, as recorded by the Kaiser dose-rate instruments located at 550 and 750 yards, are presented in Figures 13.7 and 13.8, respectively. The initial dose-rate station at 425 yards failed due to unknown causes. Total initial-gamma dose versus distance to 800 yards, measured for three radial lines extending from Shot Hamilton ground zero, are shown in Figure 13.9. A prediction curve, based on extrapolation of curves presented in TM 23-200 (Reference 15) to a yield of 1 ton, is also included for comparison purposes. Although twelve radial lines were instrumented for total gamma-dose documentation, the resultant exposed-film badges were rendered uninterpretable as a result of an accident which occurred during

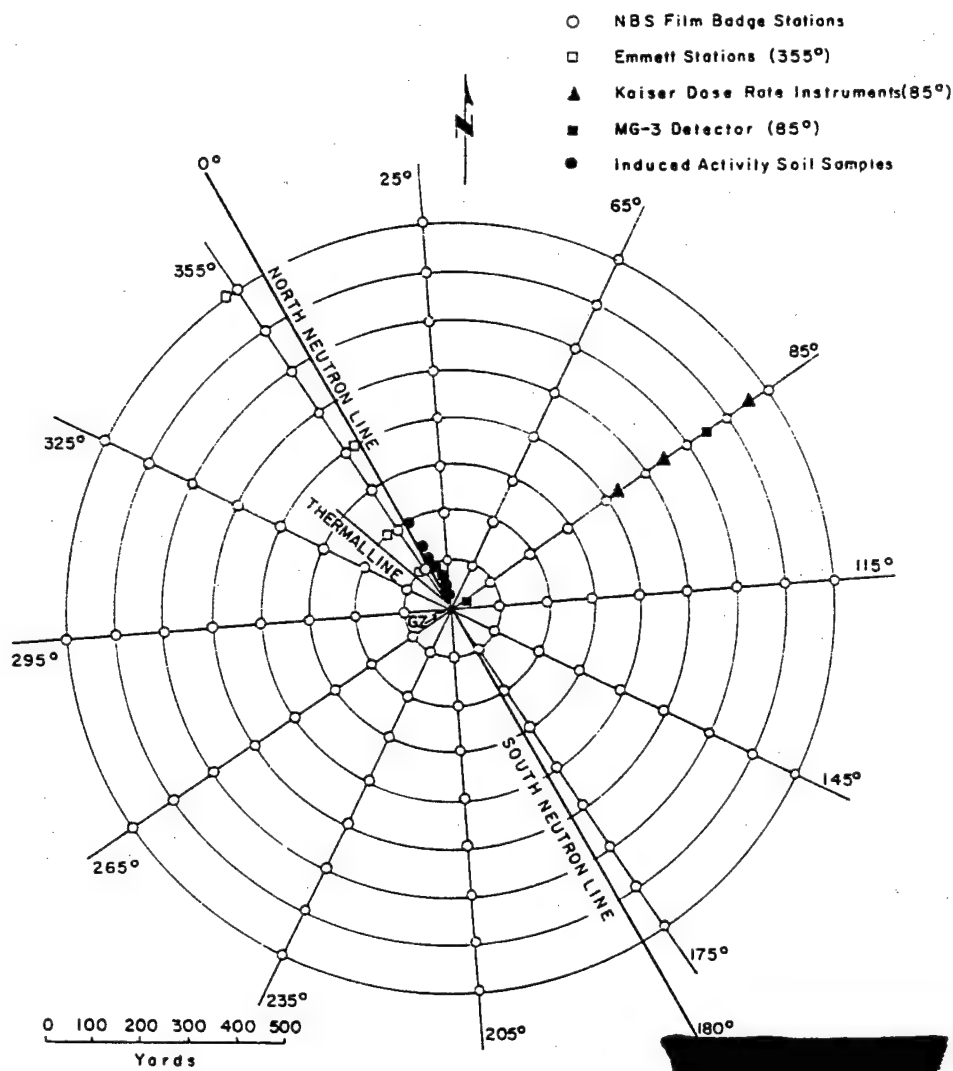


Figure 13.2 Station array, Shot Hamilton.

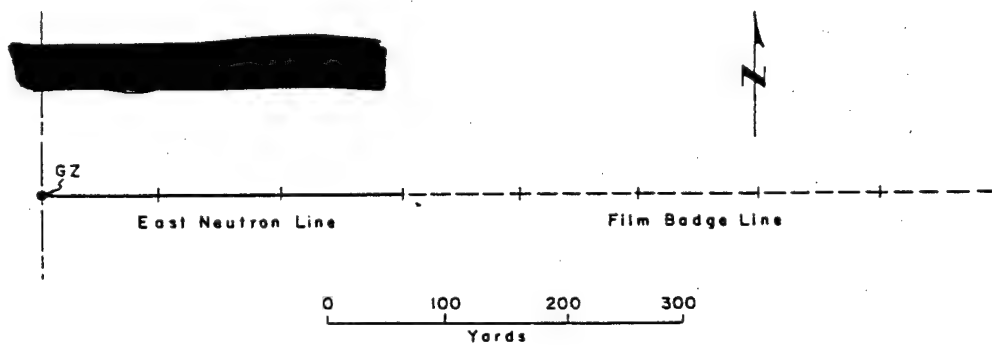


Figure 13.3 Station array, Shot Humboldt.

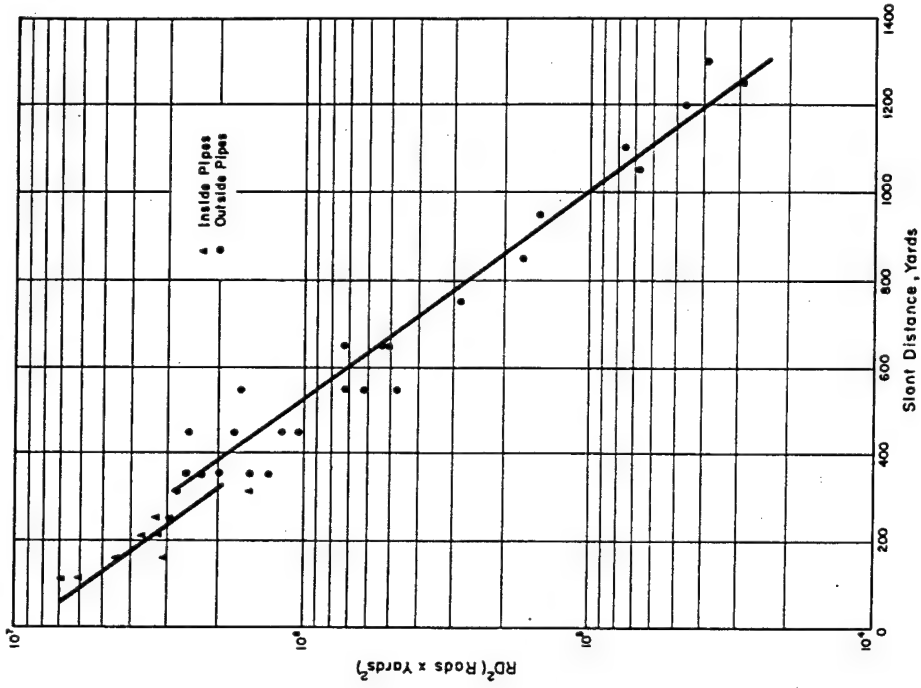


Figure 13.5 Neutron dose,  $RD^2$  versus slant distance, from sulfur activation on 0-degree axis.

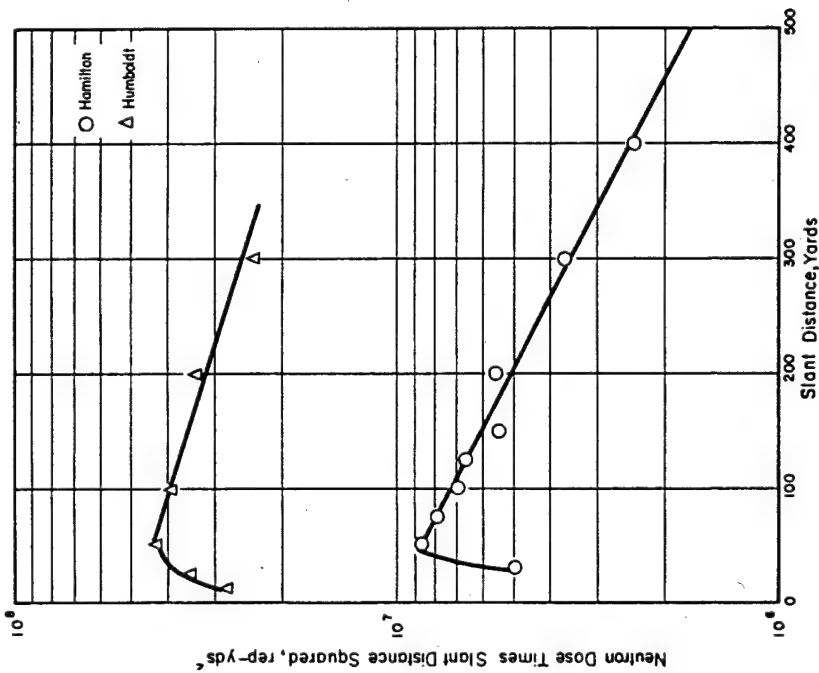


Figure 13.4 Neutron dose as measured by the threshold detector technique times slant distance squared versus slant distance for Shot Hamilton and Shot Humboldt.

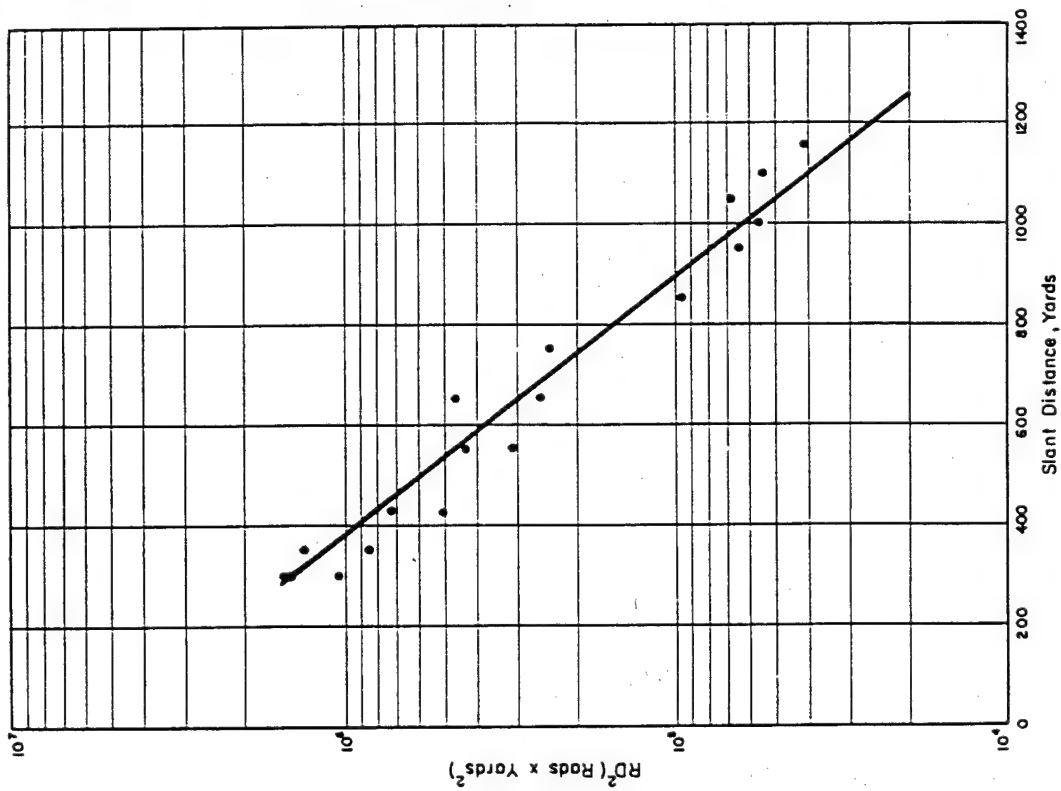


Figure 13.7 Initial gamma dose rate versus time at 550 yards, 85-degree axis.

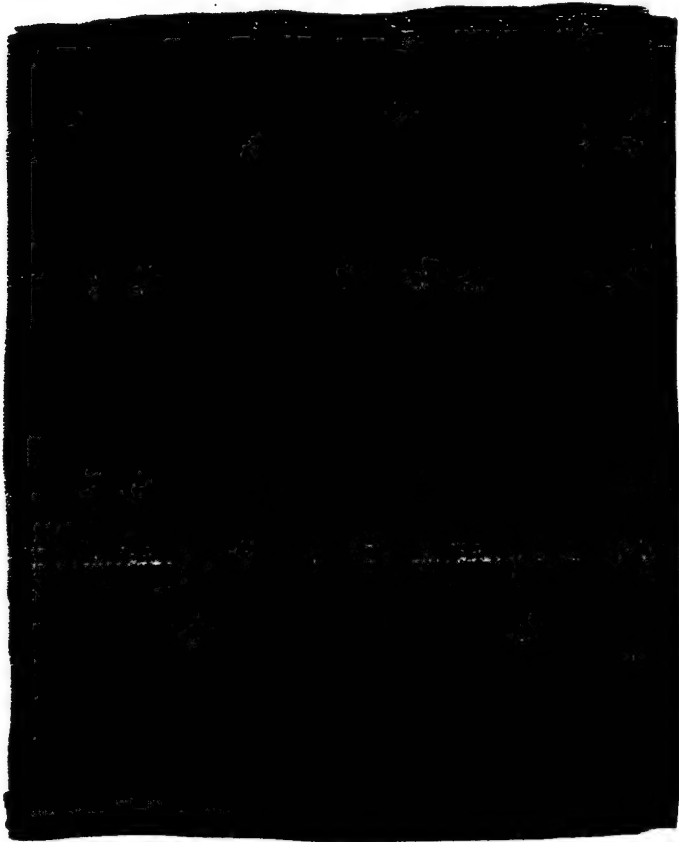


Figure 13.6 Neutron dose,  $RD^2$  versus slant distance, from sulfur activation on 85-degree axis.

their photographic development. All film badges employed in the Emmett devices were similarly damaged. High-range films were not affected by this processing accident. However, because of the low yield of the device the doses received were generally lower than the threshold limit of the film, resulting in only limited data being obtained. The data which was obtained came from films from three lines, which were processed separately. A summary of total gamma-dose data plotted as dose time distance squared versus distance, for two radial lines as obtained with the DT-60 dosimeters, NBS film badges, and LSD film stacks of Project 2.13 is presented in Figure

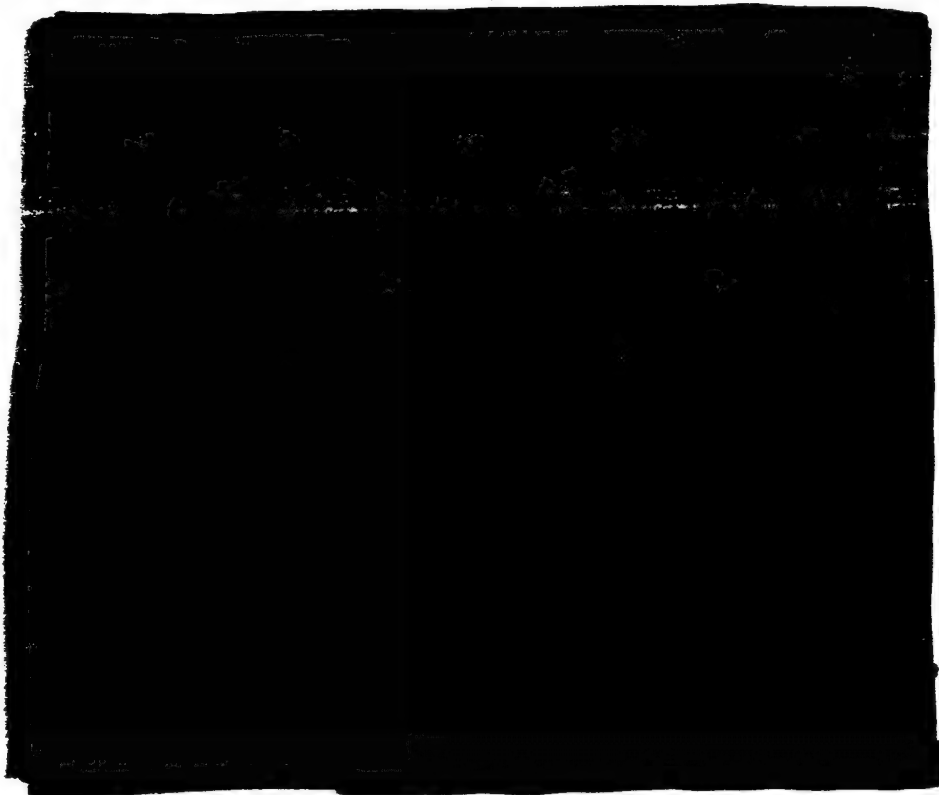


Figure 13.8 Initial gamma dose rate versus time at 750 yards, 85-degree axis.

13.10.

A theoretical initial gamma-dose curve as obtained from AFSWC-TR-58-13 (Reference 34) is also included for comparison.

Although the planned measurements for induced activity on Shot Hamilton were carried out, the unexpectedly low yield of the device resulted in soil-sample activity too low to permit successful measurement of the dose-rate fields generated by the samples. The induced activity was sufficient to permit spectral identification of  $\text{Al}^{28}$ ,  $\text{Mn}^{56}$ ,  $\text{Na}^{24}$ , and  $\text{Fe}^{59}$ . The gross-gamma field at the points of sample exposure was successfully documented; however, the field decay was characteristic of fission-product decay rather than that of induced activity. It appeared that fission products carried down by debris from the wooden tower were present in such quantities as to mask any induced activity that may have been produced. The fission-product nature of the residual-gamma field in the vicinity of the tower was also substantiated by the gamma-dose-rate record obtained with the buried MG-3 detector. This record showed a time exponential dose-rate decay with a time exponent of  $-1.25$ , indicative of fission-product decay. For

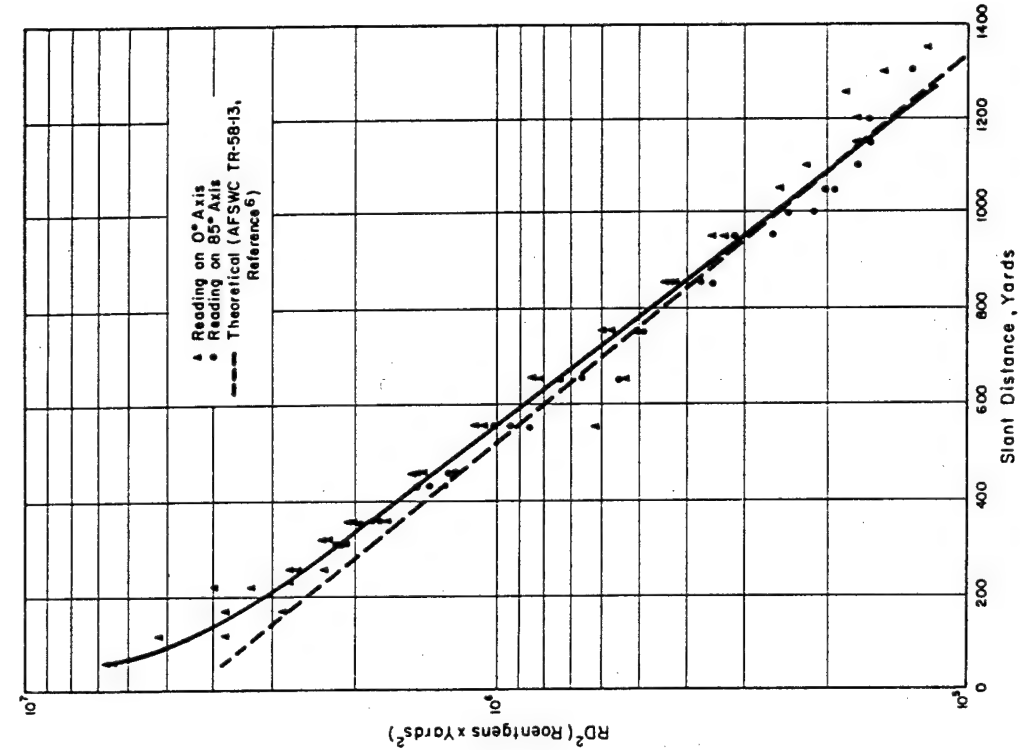


Figure 13.10 Summary of initial gamma,  $RD^2$  versus slant distance.

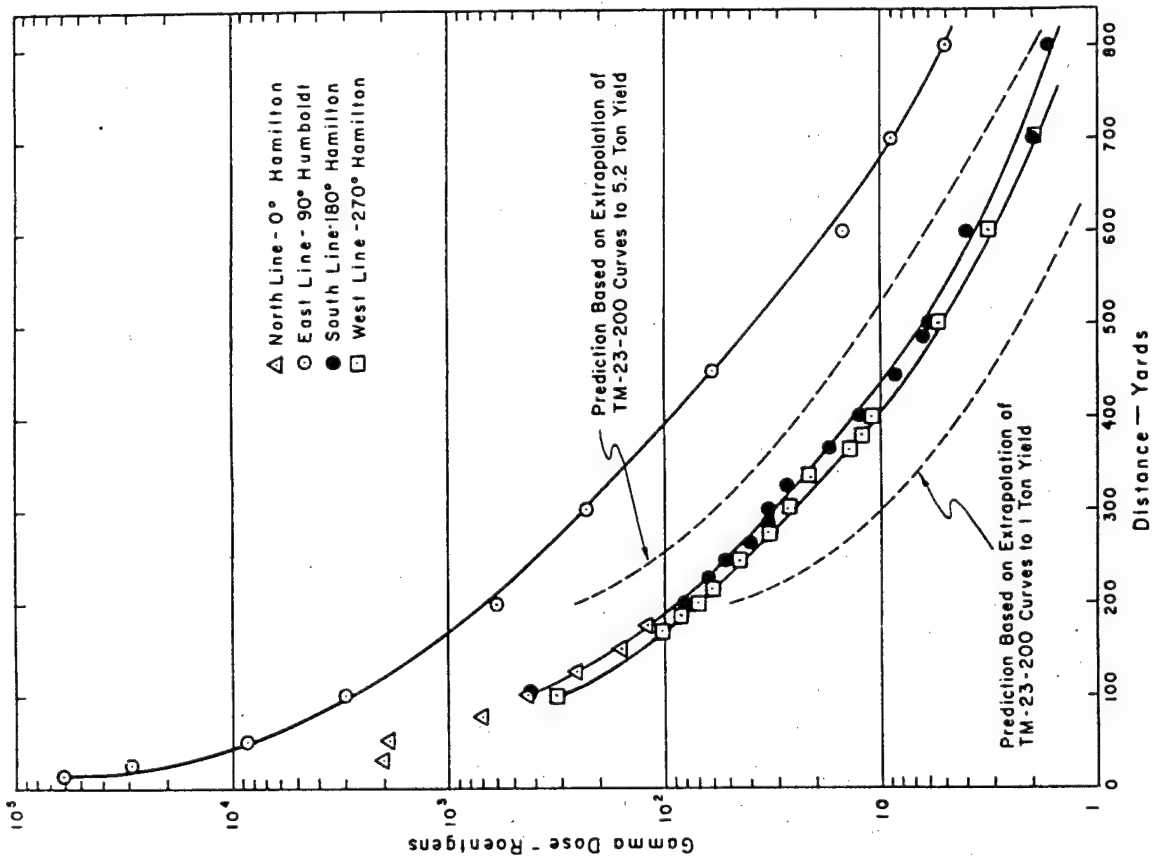


Figure 13.9 Initial gamma dose versus distance.

these reasons, the objectives of the induced-activity study were not realized.

Measurements of the total thermal-radiant exposure as a function of distance were made on Shot Hamilton. However, the results obtained were, in general, inconclusive. All stations except one registered less than  $1 \text{ cal/cm}^2$ , which was about the lowest detection limit for the thermistor calorimeter used. The lack of success in this experiment can be attributed to two factors, the very-low yield of the device and the fact that the line of sight from instruments to device was partially obscured by a diagnostic shield. This shield was installed at such a late time that the thermal instrumentation could not be relocated. The position of the shield was determined by consideration of its importance in the diagnostic effort and its effects on high-priority projects. Since the thermal effort had been approved on a strict noninterference basis, the partial obscuration of the thermal line had to be accepted by the program.

The MG-3 detector, located 650 yards downwind from the shot site, produced no data since the fallout activity at its location did not reach the threshold level of  $1 \text{ r/hr}$ . The successful operation of the buried detector, however, was sufficient to provide a valid field test of the instrument.

Reduction and analysis of the Shot Hamilton Data is incomplete as of the time of this writing. Calibration and analysis of chemical-dosimetry data, readout of neutron film, compilation of ground-survey data, and analyses of gamma spectra observed in soil samples are but a part of the work that remains to be accomplished.

**13.1.7 Shot Humboldt.** Due to the extremely short interval that existed between the time the decision was made to detonate Shot Humboldt in Area 3 and the actual firing date, only two sub-projects participated in this event, and even their participation was seriously curtailed. In general, participation was limited to those projects providing support measurements for the biomedical experiment. In Program 2, this consisted of Sub-Projects 2.12a and 2.12b, neutron- and gamma-dose measurements, respectively.

The free-field neutron dose versus distance results, as obtained by the threshold-detector technique, are shown in Figure 13.4 of the previous section. Because of the requirement to provide as complete a documentation of biomedical-animal-neutron exposure as possible, the free-field documentation was limited to a range of 300 yards. A comparison of the Shot Hamilton and Shot Humboldt neutron-dose curves gives a gross indication of the difference in yields of the two devices.

Since both the Kaiser dose-rate recorders and the Emmett devices could not be relocated in time to be used in Shot Humboldt, no time-based dose-rate data was obtained. Data on total initial-gamma dose versus distance for the one line along which measurements were made is presented in Figure 13.9 of the previous section. A prediction curve, based on extrapolation of the initial-gamma dose versus distance curves of Reference 15 to a yield of 5.2 tons, is also included in this figure. Although documentation of the resultant residual field by ground-survey parties was accomplished, the data has not been compiled and analyzed as of this writing.

**13.1.8 Conclusions.** Shot Hamilton. Satisfactory measurements of neutron dose by the threshold-detector technique were made in support of the biomedical experiment. Free-field neutron doses were successfully measured to 400 yards by the threshold-detector method and to approximately 1,300 yards with sulfur detectors. There was gross agreement between the values measured by the two methods, although the sulfur doses were consistently lower than those determined with threshold detectors. Free-field neutron doses, as determined by the threshold method, ranged from 5,490 rep at 25 yards slant range to 15 rep at 400 yards. As determined from sulfur-detector data, the neutron dose at 650 yards was approximately 1.5 rep, and doses beyond 700 yards were below 1 rep.

Initial gamma-dose-rate histories to approximately 40 seconds were obtained at two stations.

Measurements of total gamma dose in support of the biomedical experiment were successful. Free-field initial-gamma doses ranged from 2,000 r at 30 yards slant range to 1 r at 800 yards. At 400 yards, the total initial-gamma dose was approximately 15 r, while that at 600 yards was about 3 r.

No data on the dose-rate field generated by neutron-activated soil samples was obtained, although the presence of  $\text{Al}^{28}$ ,  $\text{Mn}^{56}$ ,  $\text{Na}^{24}$ , and  $\text{Fe}^{59}$  activities was confirmed by gamma spectroscopy. The results of documentation of the decay of the gross-residual field by both ground survey parties and special dose-rate recorders indicated that the radiation field was produced by fission-product contamination. The successful documentation of the decay of the residual field by a buried MG-3 fallout detector provided a sufficient field test of this instrument.

Data obtained on total thermal radiant exposure was inconclusive because of the low exposures sustained.

Shot Humboldt. Measurements of neutron and gamma-ray dose in support of the biomedical experiment were successfully accomplished. Free-field neutron doses ranged from 166,000 rep at 13 yards slant range to 260 rep at 300 yards slant range. Free-field total-initial-gamma doses ranged from greater than 60,000 r at 13 yards slant range to 5 r at 800 yards. At 600 yards, the total initial-gamma dose received was 15 r.

General. Program 2 was partially successful in achieving its assigned objectives during the NTS phase of Operation Hardtack. The primary objective of providing neutron and gamma-dose data to the biomedical experiment was successfully achieved. The documentation of neutron and gamma radii and initial dose-rate histories was generally successful. The neutron-induced soil activity and thermal-radiation-exposure experiments did not achieve their objectives. Failure to attain objectives can be attributed to the unexpectedly low yield of Shot Hamilton and the late decision which changed the firing site of Shot Humboldt.

## 13.2 EFFECTS OF A FRACTIONAL KILOTON SHOT ON A BIOLOGICAL SPECIMEN

13.2.1 Introduction. The [redacted] weapon system was conceived primarily to give the front-line soldier a nuclear capability not only in defense, but in a mobile tactical situation. An important potential use of the weapon would be in antipersonnel actions. In particular, proposed employment would include close-in delivery and immediate follow-up attack. Therefore, the weapon's effectiveness in producing immediate incapacitation in personnel was of considerable interest and resulted in the establishment of the primary objective, lethal response, listed below. Several secondary objectives were established to provide additional information pertinent to employment of the weapon system and to other matters. Direct study of effects on a biological specimen was considered necessary, because of great difficulty previously experienced in predicting biological response from physical measurements. The experiment was designed principally to study response of animals to radiation, although it was recognized that exclusion of other effects, particularly blast, from a normal tactical environment was not possible.

13.2.2 Objectives. The Project 4.2 experiment was divided into four separate, but related, objectives: (1) To determine the immediate lethal response of swine in an environment protected by normal tactical means (foxholes, tanks, and armored personnel carriers). (2) To obtain a relative biological effectiveness (RBE) for weapon neutrons through determination of the LD 50/30 in a biological specimen from both the gamma and neutrons, and gamma and fractional neutrons. (Response of small animals [mice] was also to be studied to provide additional backup informa-



tion to swine results.) (3) To evaluate additional radiation measurements and safety measures. (4) To determine the value of orally-administered aminoethylisothiuronium (AET) against weapon gamma and neutron radiation in mice.

13.2.3 Background. Because of the possible use [REDACTED] in close-in delivery and immediate follow-up attack, the need for information on immediate (within 15 minutes) personnel incapacitation was considered vital. Determination of incapacitation in an animal involves measuring specific functions performed by the specimen before and after exposure to the effects of the weapon. Unfortunately, the time in which the project was mounted was insufficient for training suitable animals. Therefore, a study of whether incapacitation could be produced was not feasible, and the primary objective was established as the determination of whether the weapon could produce immediate lethality in swine. Swine were selected because they were readily available, because they were adaptable to the temperatures of the NTS, and because considerable background existed as to their response to nuclear radiation.

The amount of a radiation dose which would cause immediate death in man or in swine is unknown. In a nuclear accident, a whole-body-radiation exposure of 1,900 r resulted in a man's death in nine days. There was no evidence of incapacitation in this case, until the sixth post-exposure day. As for swine, some have survived three days after 46,000 r whole-body radiation was received, at a rate of 100 r per minute, in a laboratory study. In an attempt to achieve immediate lethality, project plans called for at least 25,000 rad to be received by some swine on Shot Hamilton if the yield was 5 tons, with considerably higher doses expected if the more probable yield of around 20 tons were achieved. Project design on Shot Humboldt called for even higher doses to be received by the swine.

Specific information on the effects of neutrons from nuclear detonations on large biological specimens approaching man's physical size is not available. Previous attempts to obtain this information in the field were unsuccessful. During Operation Plumbbob, assuming an RBE of one for neutrons versus gamma, the LD 50/30 for combined gamma and neutron radiation was 486 r plus rep. Lethal dose range was from zero percent at 250 to 100 percent at 600 r plus rep. RBE estimates (assuming RBE for X-radiation to be one for lethality) vary from 0.3 to 1.7. In a single laboratory experiment, a group of forty dogs were exposed to 9 Mev cyclotron-produced neutrons. Single large doses were compared to 250 kilovolt potential X-radiation and resulted in an RBE for fast neutrons of 0.8. Comparative data on signs of illness, survival time, serial blood counts, and gross and microscopic pathology revealed no significant differences for the two types of radiation.

The mouse was selected as a backup to swine because of size, availability, and extensive field and laboratory data. Mice were used in the RBE studies and as the biological subjects of the AET protective experiments. The exact mechanism of action is not known, but the administration of certain chemical agents, prior to X-ray exposure, greatly reduce the lethality in mice. AET is one promising agent. A field test was considered desirable not only because the rate of dose delivery is much higher than in a laboratory, but also because knowledge of the agent's effectiveness against neutron radiation was limited.

13.2.4 Operational Procedure. The project participated on two shots, Hamilton and Humboldt.

Shot Hamilton. Seventy-one swine were placed in a simulated tactical environment for the immediate lethality objective: 64 in offset, open, and two-thirds-covered foxholes at slant ranges of 17.4 to 64 yards from the Hamilton device; and seven in five M-46 tanks and two M-59 armored personnel carriers (APC's) at slant ranges from 37 to 83 yards. Immediate lethality was to be determined by early re-entry parties and by instrumenting selected swine with vital sign-monitoring devices for pulse rate, respiratory sounds, and electrocardiograms. The Chemical Warfare Laboratories (CWL) Projects 2.12a and 2.12b installed dosimeters for free-air gamma and neutron measurements. Dosimeters were also installed in selected positions

to provide gamma- and neutron-dose data internal to swine, and within trenches and vehicles.

Installed in aluminum liners for the RBE (LD 50/30) experiments were 360 swine. They were placed along two mutually-perpendicular axes (150 degrees T and 240 degrees T) at ranges for which radiation doses of 250 to 700 rads were predicted. The doses instrumental in securing 50 percent lethality in 30 days were to be composed of different ratios of neutrons to gamma along the two axes. This was to be accomplished by a paraffin shield on the tower, which would reduce neutron doses on the 150 degrees T line in comparison to the 240 degrees T line. Mice were installed along the swine lines to provide additional backup information. Selected mice were inoculated for the AET experiment.

Twenty animals were placed at 600- to 800-yards slant range, where doses of around 25 r were expected, to evaluate the safe user distance. In addition, air sampling of air-borne plutonium to evaluate inhalation hazards was carried out at ground zero and at six downwind points at 600-yards radius from ground zero.

Shot Humboldt. Twenty-five swine were placed in trenches from 10 to 26 yards slant range from the shot, and 40 swine were equally divided between two APC's, whose midpoints were at 29.6 yards slant range. Foxholes were constructed in a fine, non-cohesive soil which was susceptible to collapse. Therefore, swine were placed in aluminum liners to provide some measure of protection from trench collapse. The APC's were attached to cables to enable early recovery and observation of the animals. Selected animals were equipped with vital sign-monitoring devices as on Shot Hamilton.

**13.2.5 Results. Shot Hamilton.** None of the objectives were achieved, because the shot yield of one ton was well below project design range of 5 to 25 tons. Information obtained on the various objectives was of value, however, and is listed below. In particular, results indicated there was no immediate lethality to swine protected by normal tactical means, at slant ranges as close as 18 yards to a one-ton shot.

It appears that maximum dose on the 71 swine installed in foxholes and vehicles was less than 5,000 rads. Maximum measured dose inside foxholes, 3,000 rads (gamma only), was obtained in the closest open trench, 22.4 yards slant range. In a second open trench, 26 yards slant range, a total dose of 2,500 rads (1,700 gamma plus 800 neutron) was measured. As expected, measured doses in two-thirds-covered and offset foxholes were considerably less than those in open foxholes. Maximum dose inside tanks and APC's was obtained in the closest APC, 57.5 yards slant range, where 2,200 rads (800 gamma + 1,400 neutron) was measured.

Sixty-nine of the 71 swine placed in protected positions were initially observed between H+10 and H+22 minutes and were alive and active. These swine were recovered on D and D+1 days. The two unobserved swine were buried by earth spalling from the sides of their foxholes; post-mortem examination indicated that they had died from suffocation. The response of the 69 recovered swine to radiation doses received was about as expected from previous studies. On D+1, these swine differed clinically from unexposed animals only in that they were less active; they were eating well and showed no evidence of gastrointestinal symptoms. Radiation-sickness symptoms were more pronounced on D+2, and the first animal died on D+4. Swine from offset trenches recovered rapidly and appeared normal by D+8.

Trenches of all types out to 55 yards from ground zero were affected by spalling, severity increasing with decreasing range from the shot. Spalling of the sides of the trenches occurred below the top 1 1/2 feet of the four-foot-deep foxholes. Most severely spalled open foxholes contained up to 20 inches of dirt, offset and two-thirds-covered foxholes up to 30 inches.

Swine on the RBE experiment were clinically observed for 14 days after the shot. There were no deaths and no clinical symptoms indicative of radiation sickness. Maximum free-air dose measured at RBE stations, 208 rads (120 gamma and 88 neutron), was much less than that required to produce 50 percent lethality in 30 days.

No conclusions could be drawn from the AET experiment, since radiation doses were too low to produce any appreciable effects.

Personnel engaged in early re-entry accumulated doses up to 9 r in approximately 12 minutes of observing animals. A reading of 340 r/hr was recorded at H+22 minutes at 5 yards from ground zero.

Results obtained from air-borne sampling indicated that alpha contamination is not an inhalation hazard at 600 yards downwind from ground zero. However, a hazard could exist to personnel engaged in activities around ground zero, in which appreciable dust is resuspended. Considerable fallout of alpha activity was indicated by the fact that horizontal surfaces of equipment such as tanks were contaminated (in excess of 20,000 counts/min per instrument probe), while the sides were relatively clean.

Shot Humboldt.

1. Dosimetry data inside foxholes and APC's is shown in Tables 13.2 and 13.3. From this data, it appears that swine in front of APC's received doses in excess of 50,000 rads and that swine in open foxholes received up to 188,000 rads.

2. Thirty-nine of 40 swine in the two APC's were recovered alive. The remaining swine was alive around H+30 minutes but was wedged in (because of blast damage to the APC) and was not

TABLE 13.2 FOXHOLE DOSIMETRY, SHOT HUMBOLDT

Station Number	Type	Slant Range *	EG&G Gamma †	NBS Film Gamma ‡	Fission Foil Neutron §
		yds	rads	rads	rads
3 NE	2/3-closed foxholes	10.8	47,400	23,200	13,400
8 SE	2/3-closed foxholes	13.3	43,900	19,100	7,100
13 NE	2/3-closed foxholes	16.5	25,800	11,100	7,300
18 SE	2/3-closed foxholes	19.9	10,200	8,600	2,600
23 NE	2/3-closed foxholes	23.5	4,000	4,600	2,100
2 SE	Open foxholes	10.8	Missing	35,200	75,200
9 NE	Open foxholes	13.3	Broken	44,600	144,000
12 SE	Open foxholes	16.5	Broken	18,600	93,000
19 NE	Open foxholes	19.9	49,300	12,700	38,400
22 SE	Open foxholes	23.5	20,400	10,700	11,200

\* True slant range calculated from tower height, ground distance, distance of the dosimeter off the surveyed axis, and depth below ground level.

† Chemical dosimeter, Edgerton, Germeshausen and Grier, Las Vegas, Nevada.

‡ Project 2.12b.

§ Project 2.12a.

recovered. The majority of the 39 recovered animals initially (around 15 minutes) exhibited ataxia and considerable apathy to any stimulus. There was scattered vomiting and diarrhea among them. A few animals, ultimately the first to die, demonstrated tetanic rigor, abnormal respiratory effects, and complete loss of response to any stimulus. Of the 39, the first died around H+2 1/2 hours, and all but two were dead by 21 1/2 hours after the shot.

3. Of 25 animals in the foxhole array, four from two-thirds-covered trenches were recovered alive: one around H+10 hours and three more by H+30 hours. All were alert and active on recovery but demonstrated no inclination to eat. Foxhole dosimetry indicated these animals received radiation doses up to 11,260 rads. Of the four, one was sacrificed, two died on D+3, and the fourth on D+4 days. The remaining 21 animals were in trenches so completely obliterated that early observation or recovery was not possible. Although cause and time of death of

these 21 swine were not specifically determined, early death may have occurred as a result of direct-blast effects, but more probably because of indirect effects (such as suffocation due to trench collapse) and crushing of the aluminum liners.

4. Autopsy of the four animals recovered from four two-thirds-covered foxholes indicated extensive pathology from blast, particularly in the lungs. These four foxholes were at slant ranges of 20 to 26 yards from the shot, a region within which peak free-air overpressure of up to 200 psi was recorded. The effect of blast on all foxholes was considerable. Loose fill, up to three feet in depth, made most of the trenches almost indistinguishable. In a few cases, alumi-

TABLE 13.3 M-59, ARMORED PERSONNEL CARRIER, DOSIMETRY, SHOT HUMBOLDT

	Slant Range *	EG&G Gamma †	LASL Gamma ‡	NBS Film Gamma §	Fission Foil Neutron ¶
	yds	rads	rads	rads	rads
66-SE APC					
Front	28.4	45,100	27,400	19,300	—
Middle	30.0	25,100	14,100	13,900	26,200 **
				12,600	
Rear	32.4	26,000	12,400	12,800	—
Outside, right front	27.0	—	34,900	—	—
Outside, left front	28.0	49,800	—	—	—
70-NE APC					
Front	28.5	43,700	—	18,800	—
Middle	30.0	27,700	15,000	15,100	26,400
				14,400	
Rear	32.4	35,300	—	13,100	—
Outside, right front	28.0	—	34,900	—	—
Outside, left front	27.0	48,400	—	—	—

\* True slant range calculated from tower height, ground distance, distance of the dosimeter off the surveyed axis, and depth below ground level.

† Chemical gamma dosimeter, Edgerton, Germeshausen and Grier, Las Vegas, Nevada.

‡ Chemical gamma dosimeter; Los Alamos Scientific Laboratories, Albuquerque, N. Mex.

§ Project 2.12a.

¶ Project 2.12b.

\*\* Pu valve from APC No. 70 used (foil recovered late).

num liners were visible and appeared to be severely crushed. Based on the general postshot appearance of the Shot Humboldt foxhole array and foxhole-dosimetry data, it is probably not possible to achieve radiation doses in normal tactical trenches sufficient to produce immediate lethality (>>50,000 rad) without associated serious damage due to direct blast or trench collapse.

### 13.3 OPERATIONAL ANALYSIS OF THE DAZZLE EFFECT ON COMBAT PERSONNEL

**13.3.1 Introduction.** A problem likely to be encountered by combat troops is temporary flash blindness or confusion of vision (dazzle) due to a nearby nuclear detonation. The project had as its objective the determination of the degree of dazzle to unprotected personnel at minimum-safe distances from ground zero and the duration of this effect.

**13.3.2 Operational Procedure.** Participation was limited to Shot Hamilton. Twenty-five personnel were positioned at 1,900 yards from ground zero, oriented from 90 to 180 degrees

with the line directly to the zero point. Each participant had been given an eye examination prior to the shot. Immediately after the detonation, from 10 seconds to 60 seconds, the group identified men and various-colored panels at distances of from 85 to 600 yards from their positions and individually recorded their impressions of identifications of these visual targets.

13.3.3 Results. No dazzle effect was observed in any individual. This could be attributed to the much lower-than-expected yield. Due to a combination of lack of satisfactory shots on which to participate and lack of personnel, no further activity by this project was attempted.

#### 13.4 EVALUATION OF AIR-BLAST GAGES AND SUPPORTING AIR-BLAST MEASUREMENTS

13.4.1 Objectives. The objectives of Project 1.7 were: (1) to evaluate newly designed VLP and BRL q gages and the Snob and Gregg gages for their ability to measure the blast-wave parameters; (2) to support projects under the Office of Civil Defense & Mobilization (OCDM) and the Civil Effects Test Organization (CETO) with structures instrumentation using self-recording gages for overpressure, displacement, and acceleration measurements as a function of time; and (3) to investigate the magnitude of tunnel air-blast pressures generated by the detonation and by piston action of tunnel walls.

The first objective was assigned to Project 34.3 under CETO and to Project 70.5 under OCDM. The third objective was assigned to Project 70.6 under OCDM.

13.4.2 Method of Experimentation. Shots Eddy, Mora, Hamilton, Socorro, and Rushmore were selected for evaluation of the new type very-low-pressure gage. The overpressure region of interest (below 1 psi) necessitated placement of these gages at ranges from approximately 3,500 to 50,000 feet. In addition, standard Ballistic Research Laboratories (BRL) pt gages were located along the blast line to document further the pressure-time histories from both fractional kiloton and kiloton-range bursts. Each of the pressure records obtained was studied to determine response accuracy and pressure repeatability. For comparison of instrument performance, a pt gage was placed at the same location as a VLP gage, and records were checked for magnitude of pressure and the wave shape of the pressure-time history.

Because the blast wave is drastically altered in low-overpressure regions by local weather conditions, information on wind direction and velocity, ambient barometric pressure, temperature, and relative humidity near the surface where the low pressure was being measured had to be obtained. Since such weather data could not be procured at outlying locations, the project maintained a portable weather station.

During Shot Hamilton, several gages were used to measure the flow characteristics behind the blast wave. The old type BRL q gage was placed adjacent to these gages and was used as a standard for comparing results. The type of gage employed in these measurements and the general design purpose are indicated in the following:

<u>General Gage Characteristics</u>		
<u>Gage</u>	<u>Measurement</u>	<u>Remarks</u>
Gregg	Wind and dust flow	
Snob	Wind flow	Two shapes used, one with a hemispherical nose, the other with a conical nose.
q	Wind flow and partial response to dust	Similar to old BRL q gage, but less sensitive to angle of flow because of conical nose.

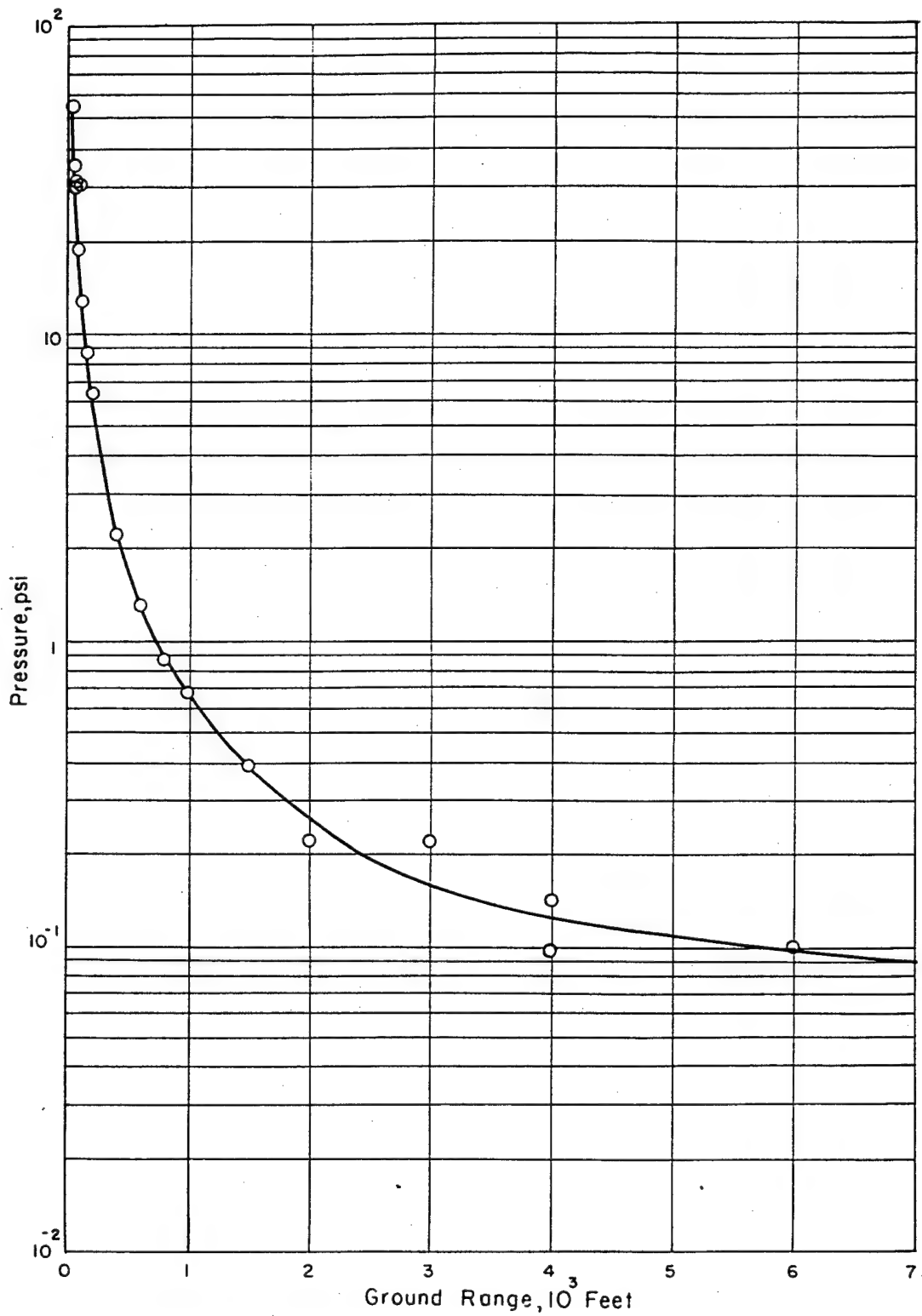


Figure 13.11 Overpressures versus ground range, Shot Hamilton.



Underground Shots Tamalpais and Evans were instrumented with air-blast-overpressure gages imbedded in the tunnel walls and floor at various distances from the point of detonation.

**13.4.3 Results.** The majority of the gages provided good records. Any failures could be attributed to either the noninitiation of a timing relay or to a malfunction of the gage itself. Even though the disk motor failed to operate, thus precluding the recording of pressure-time histories, both the pt and VLP gages were designed to register peak values of pressure.

On Shot Eddy, a balloon shot with a yield of approximately 83 tons, pressures varied from

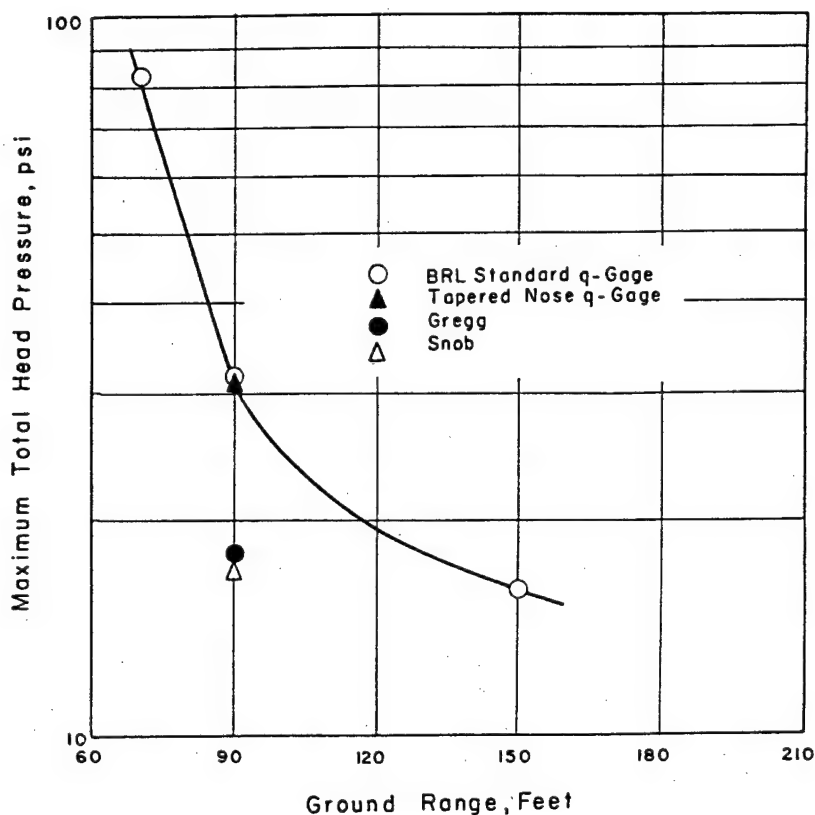


Figure 13.12 Maximum total head pressure versus ground range, Shot Hamilton.

2.80 psi at 1,500 feet to 0.93 psi at 3,500 feet, measured by a pt gage. Poor records were obtained by VLP gages at distances beyond 3,500 feet.

On Shot Mora, a balloon shot with an approximate yield of 2 kt, pressures from 10.0 psi at 195 feet to 0.34 psi at 47,500 feet were recorded.

Pressures from Shot Rushmore, a balloon shot with a yield of about 180 tons, were recorded on pt gages and ranged from 13.5 psi at 300 feet to 0.20 psi at 15,000 feet.

Figure 13.11 is a plot of the overpressures versus distance obtained on Shot Hamilton. A plot of the maximum-total-head pressure obtained during this shot is shown in Figure 13.12 to

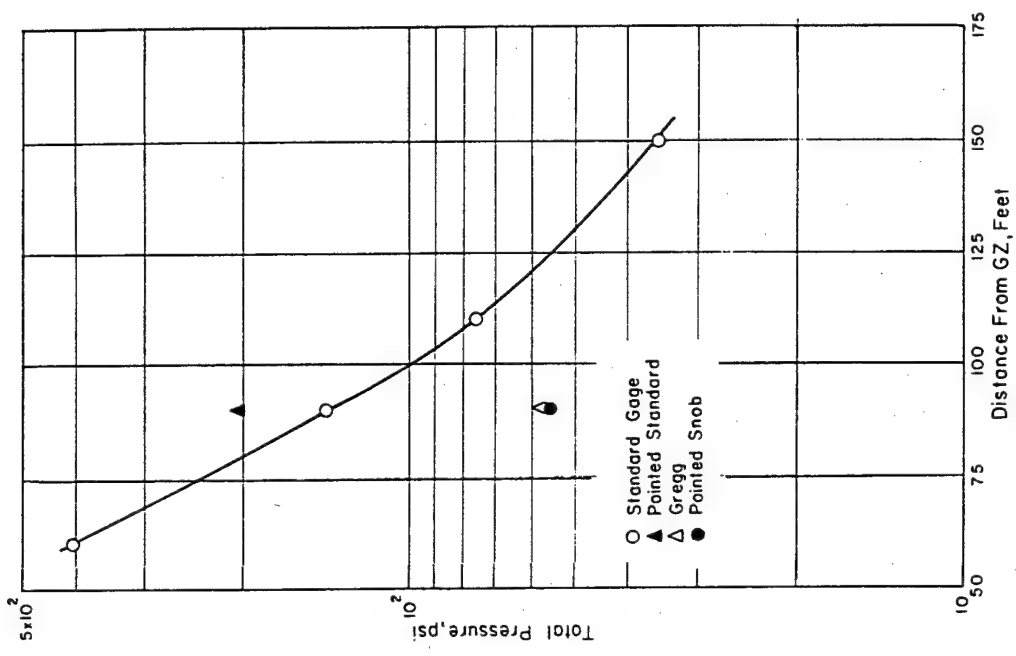
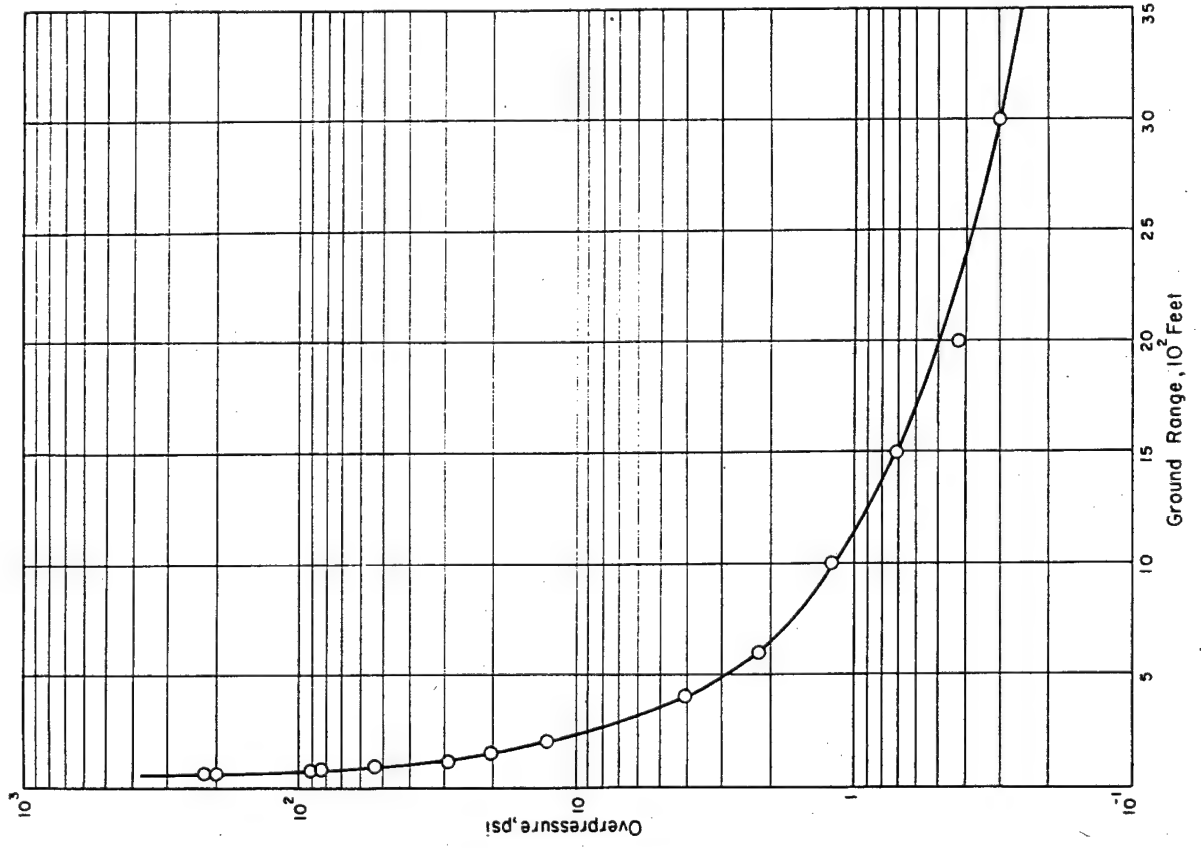


Figure 13.14 Maximum total head pressure versus ground range, Shot Humboldt.

Figure 13.13 Overpressures versus ground range, Shot Humboldt.



compare the value as measured by the different experimental gages used. The same two curves for Shot Humboldt are shown in Figures 13.13 and 13.14.

**13.4.4 Conclusions.** Any conclusions relative to the comparative performances of the several types of gages investigated and to a possible extension of existing TM 23-200 scaling laws to fractional-kiloton-range nuclear bursts will be provided following laboratory analyses of the data obtained. The presentation of this information is planned for the project's final report.

### 13.5 PROOF TEST OF AN/TVS-1 (XE-3) FLASH-RANGING EQUIPMENT

**13.5.1 Objectives.** The overall objective of Project 6.14 was to evaluate the Peerless flash-ranging set, AN/TVS-1 (XE-3), prior to its acceptance by the United States Army Signal Research and Development Laboratory (USASRDL).

The specific objectives were to determine the operational capability of two types of automatic shutter-activating units and to compile data on shutter speeds and filter values at different ranges from point of burst of various low-yield nuclear devices.

**13.5.2 Background.** In 1953 a Continental Army Command (CONARC) requirement called for the capability of determining the location and height of burst of friendly-delivered nuclear weapons. An electronic shutter-actuator (Blue Box Mark IV) was procured from Edgerton, Germeshausen and Grier (EG&G). During Operation Upshot-Knothole, U. S. Army Signal Research and Development Laboratory (ASRDL) and CONARC jointly evaluated a camera system employing this type of shutter actuator; these tests proved the feasibility of the device.

The bulk and weight of the actuator led to the design and development of a compact, lightweight, transistorized unit by ASRDL. This device was employed with earlier models of AN/TVS flash-ranging sets by Project 50.8 during Operation Plumbbob.

In the summer of 1955 a contract was let to Peerless Instrument Company for ten service-test models of the AN/TVS-1 (XE-3) flash-ranging set with an automatic shutter-actuation device. Peerless attempted to employ vacuum tubes in its first variation of the automatic shutter actuator. This version was poor because of the extremely short life and large power consumption of the vacuum tubes.

Test results of the transistorized, automatic actuator developed by ASRDL indicated that this lightweight and compact unit should be incorporated into the camera being fabricated by Peerless. Delivery of the first four completed models of the Peerless AN/TVS-1 (XE-3) flash-ranging set was made to ASRDL in September 1958 for engineer-acceptance tests.

**13.5.3 Theory.** By using a known baseline and predetermined orientation points, it is possible to detect targets, such as nuclear flashes, by triangulation-survey techniques. For accurate data reduction it is necessary to read to the center of the target's filmed image. The latter should be small; about  $\frac{1}{16}$  to  $\frac{1}{8}$  inch is considered ideal. To achieve a circumscribed impression of this size, the fireball must be photographed as near to time zero as possible with filtered lenses. The shutter-actuation system, therefore, must be automatically started with the initial time rise of the nuclear flash.

In order to reduce evenly the amount of light for all wave lengths of the visible spectra that entered the optical system, neutral density filters were used.

**13.5.4 Method of Experimentation.** The AN/TVS-1 flash-ranging set was a tripod-mounted, battery-operated, transportable, photographic-recording device, (Figure 13.15). Immediately in front of the film plane and at right angles to the optical axis was a lined, compensated grid

that was superimposed on the film when a picture was exposed through it.

The automatic shutter actuator was a photocell and amplifier combination responding to a fast time-rise pulse of light which was converted to a usable electrical pulse operating the shutter-tripping mechanism. During the NTS phase of Operation Hardtack, two types were used: one (unmodified) in which the electrical output corresponded to the light-input pulse in duration and the other (modified) which had a definite length-output pulse of about 50 msec, regardless of the



Figure 13.15 Peerless flash-ranging set, AN/TVS-1 (XE-3), showing camera with 5-inch lens, automatic actuator, camera mount, leveler, tripod, control box, and battery box.

duration of the light-input pulse. Both these units employed S4 response photocells and time constants that would accept only 50  $\mu$ sec or faster time light pulses.

Tests were conducted from ranges of 2 to 18 miles from ground zero for fractional kiloton-yield detonations and from 7 to 60 miles for the larger-yield bursts. For a given shot, specific locations on hilltop sites, with line of sight to ground zero, were determined by results obtained on a previous event. Shot participation included Shots Mora, Quay, Lea, Hamilton, Dona Ana, Rio Arriba, Wrangell, and Socorro. The burst was photographed by a Peerless flash-ranging camera employing the Land-Polaroid photographic process and equipped with either an ASRDL-modified or Peerless-unmodified shutter-actuating device.

**13.5.5 Results.** Data were obtained on the operational ranges of the shutter-activating device and on camera settings compatible with a selected ND filter for best image definition. Camera settings of f:32 at  $\frac{1}{200}$  second were used exclusively, a combination which provided the smallest diaphragm opening and fastest shutter speed possible with this camera.

The flash-ranging equipment functioned properly for all ranges up to 29,000 meters, except during Shot Hamilton, which had a yield much lower than predicted. At the greater distances up to 97,000 meters, performance was satisfactory on only one of five occasions. The failures (i. e., of nonoperation of the automatic actuators) were attributed to low-battery voltages resulting from the cold weather that persisted at the selected observations stations. A poor photograph

resulted from the first attempt at the longer range. This made clear the need for using a neutral density filter.

During the first test of the closer (3,600 to 29,000 meters) operations, it was noted that an ND-4 filter proved to be optimum. Subsequent participations at these ranges produced good photographic results. It was also noted that the two types of shutter actuators performed equally well.

13.5.6 Conclusions and Recommendations. Under conditions of high visibility, such as existed during these test participations, either type of automatic actuator would be acceptable. However, it is considered that the modified actuator would be more reliable should poor visibility conditions prevail.

The camera settings and filters employed were satisfactory at the ranges and for the yields involved. Specific recommendations in this regard can be made following further data analyses and will be reported in the final report.

Since the Peerless flash-ranging equipment, AN/TVS-1 (XE-3), operated as designed and results as anticipated were obtained, further field testing of the gear, in connection with nuclear detonations, is not required.

## 13.6 THERMAL RADIATION FROM LOW-YIELD BURSTS

13.6.1 Objective. The objective of Project 8.8 was to measure the thermal radiation resulting from the low-altitude detonation of low-yield devices. It was desired to obtain the values of irradiance as a function of time and wave length, as well as the total thermal radiation.

13.6.2 Background. Doubt had existed for some time as to whether the thermal-scaling laws for kiloton- and megaton-range detonations could be extended with any degree of accuracy to thermal predictions for fractional-kiloton-yield bursts. To resolve this problem, Project 8.8 was set up to measure the thermal radiation from the low-yield, low-altitude detonations of the NTS phase of Operation Hardtack.

The damage-producing effects of thermal radiation from a nuclear burst depend on the spectral distribution, rate of emission, and total amount of incident-thermal energy. Such information is important in tactical planning, since the probable degree of injury to personnel and damage to targets are, in turn, contingent on these effects. By comparison of this project's data with that measured from larger-yield bursts, thermal scaling laws may be extended to cover very-low yields.

13.6.3 Shot Participation. This project intended to participate in two shots, Hamilton and Quay. [REDACTED] authorization for further participation resulted in the measurement of thermal data from eleven shots, five of predicted fractional-kiloton yield (Quay, Hamilton, Rio Arriba, Mazama, and Humboldt) and six of predicted low-kiloton yield (Socorro, Wrangell, Rushmore, Sanford, DeBaca, and Santa Fe).

13.6.4 Method of Experimentation. Irradiance measurements were made utilizing four spectroscopic detectors, each being sensitive to a separate spectral range between 2,000 and 10,000 Å. A measurement of total irradiance as a function of time was obtained from a fast-response bolometer. A twenty-junction calorimeter was used to measure the total incident-thermal radiation. The data from these detectors were recorded on magnetic tape during the interval, H - 1 minute to H + 1 minute. Further thermal-spectral data were obtained by employing cameras photographing the burst through spectroscopic nosepieces.

Whenever practical, two sites were instrumented for each shot. For these station locations, blast and nuclear-radiation safety parameters were the main factors in range determination; minimum solar interference, radioactive-fallout pattern, and ease of access were taken into consideration in bearing selection. Table 13.4 indicates the bearing and range of each station from ground zero.

A mobile, instrumented trailer was positioned as the close-in station for all shots except Hamilton, Wrangell, and Sanford. For Shot Hamilton on Frenchman Flat, the trailer was the far site, while first-line motel room No. 11 housed the close-in station. Control Point 400,

TABLE 13.4 STATION BEARING, SLANT RANGE, ELEVATION, AND BURST ALTITUDE

Shot	Burst Altitude *	Near Station			Far Station		
		True Bearing †	Slant Range	Elevation *	True Bearing †	Slant Range	Elevation *
	km	deg	km	km	deg	km	km
Quay	1.355	212	2.75	1.25	—	—	—
Hamilton	0.949	260	0.97	0.94	266	1.83	0.94
Rio Arriba	1.244	325	3.47	1.25	193	12.38	1.29
Socorro	1.718	197	8.72	1.22	190	17.40	1.29
Wrangell	1.395	—	—	—	323	18.66	1.29
Rushmore	1.437	185	7.60	1.25	184	22.54	1.29
Sanford	1.395	—	—	—	323	18.66	1.29
De Baca	1.733	322	7.24	1.32	190	17.40	1.29
Mazama	1.295	293	3.18	1.32	184	21.63	1.29
Humboldt	1.234	206	1.79	1.22	192	13.14	1.29
Santa Fe	1.733	197	8.72	1.22	190	17.40	1.29

\* Altitudes and elevations above mean sea level. Elevations include detector height above terrain: motel, 6 feet; trailer, 8.5 feet; CP-400, 20 feet.

† True bearings from ground zero.

located above the main CP building, was instrumented with the equipment from the motel station and was used as the far site for all shots subsequent to Hamilton. Each station was manned by two personnel during each shot.

**13.6.5 Data Obtained.** From the thermal recordings of each shot, it was required to obtain the irradiance as a function of time for the four spectral ranges, far ultraviolet, near ultraviolet, visible, and infrared, and the total irradiance. The thermal pulse for each range was measured, giving the time and irradiance at first maximum, minimum (if any), and second maximum (if any). Computations could then be made to give the total integrated energy received in each spectral range and the percentage of the energy in each peak. By collating the measurements from each range, all quantities could be given roughly as a function of wave length.

The complete calculation of all the values was beyond the scope of the preliminary report. By comparison with identical measurements made from kiloton-range bursts, these factors can be correlated with the yield (planned for the final report), leading to a possible extension of existing scaling laws.

**13.6.6 Discussion.** The characteristics of the thermal pulse from fractional-kiloton-yield nuclear bursts, as functions of yield, wave length, and distance are given in the ITR. A preliminary analysis of these results is given below.

Table 13.5 gives the predicted and measured times to minimum and maximum for the five

fractional-kiloton-yield devices for which data reduction was accomplished at NTS. The measured times listed were approximate averages over the wave-length ranges and were weighted according to the value of thermal irradiance in each range, since the time measurements varied with wave length. The values indicate that the scaling laws for times to minimum and maximum may be extended reasonably well to bursts with yields as low as five tons. The measured values in each case were greater than the predicted, but never by a factor much greater than two. This deviation could possibly be due to the materials shielding the devices. No distinct second maximum was observed for Shot Hamilton, which had an actual yield of 1 ton.

Table 13.6 gives the approximate values of irradiance at first and second maxima as measured from each burst for the various spectral ranges. The shots are presented in order of increasing yield.

The extrapolated fireball radii (Table 13.5), based on preliminary measurements made by EG&G, agreed reasonably well with the predictions based on the scaling laws. Therefore, expected values of second maximum irradiance were computed from the scaling law for peak irradiance. These values are given in Table 13.6 as the unattenuated, predicted irradiance at second maximum for the bolometer. For every burst, these predicted quantities exceeded the measured, total irradiance. This scaling law, therefore, apparently fails to apply for yields in the indicated ranges, with the deviation increasing for decreasing yield. Using the measured fireball radii, such high values for irradiance at second maximum lead to apparent fireball tem-

TABLE 13.5 PREDICTED VERSUS MEASURED FIREBALL TIME HISTORY

Shot	Actual Yield	Predicted $R_{2max}$	Measured* $R_{2max}$	Predicted $t_{min}$	Predicted $t_{2max}$	Measured $t_{min}$	Measured $t_{2max}$
	tons	meters	meters	msec	msec	msec	msec
Hamilton †	1.0	3.5	4.4	0.08	1.0	—	—
Humboldt	5.2	6.7	8.5	0.2	2.3	0.5	1.7
Quay	84	20.4	22	0.78	9.3	1.4	12
Rio Arriba	92	21.1	27	0.82	9.7	1.6	12
Rushmore	180	27.6	41	1.1	13.6	2.0	18

\* Extrapolated from EG&G preliminary fireball growth data.

† Hamilton data to first maximum; see Figures 3.5 through 3.12, ITR-1675.

peratures that become increasingly excessive with decreasing yield. For comparison purposes only, the unattenuated spectral distributions at these high temperatures and the measured values are also given in Table 13.6.

Using the value for total irradiance at second maximum as measured during Shot Humboldt (approximately  $0.4 \text{ w/cm}^2$  at 1.8 km, unattenuated) and the extrapolated fireball radius, the apparent fireball surface temperature, estimated from the Stefan-Boltzmann law, was between 7,000 and 8,000 K.

The irradiance pulses can be integrated with respect to time, to give the percentage of total energy in each spectral range. Detailed integrations were not performed; however, a rough integration of the Shot Humboldt irradiance curves indicated that over 90 percent of the thermal energy incident at the detectors was at wave lengths greater than  $4,000 \text{ \AA}$  and that the percentage of energy received during the first peak was less than four percent of the total.

The curves from the fractional-yield devices consistently indicated a decreasing ratio of ir-

TABLE 13.6 MEASURED VERSUS SCALED IRRADIANCE

Slant Range	Detector Range	Measured $\phi_{1max}$	Measured $\phi_{2max}$	Measured $t_{min}$	Measured $t_{2max}$	Scaled* $\phi_{2max}$	Atmosphere $\bar{T}$
km		mw/cm <sup>2</sup>	mw/cm <sup>2</sup>	msec	msec	mw/cm <sup>2</sup>	pct
Shot Hamilton:							
1.0	Far ultraviolet	63	—	—	—	600	—
	Near ultraviolet †	75	—	—	—	1,500	91
	Visible	180	—	—	—	600	96
	Infrared	1,400	—	—	—	900	98
	Bolometer	—	—	—	—	4,400	97
1.8	Far ultraviolet	7.5	—	—	—	170	—
	Near ultraviolet †	8	—	—	—	440	83
	Visible	18	—	—	—	170	93
	Infrared	—	—	—	—	260	97
	Bolometer	—	—	—	—	1,300	95
Shot Humboldt:							
1.8	Far ultraviolet	28	—	—	—	400	—
	Near ultraviolet †	57	17	0.8	2.5	1,000	83
	Visible	90	68	0.5	1.2	400	92
	Infrared	290	250	0.5	1.7	600	96
	Bolometer	—	—	0.5	—	3,000	95
13.1	Far ultraviolet	—	—	—	—	7	—
	Near ultraviolet †	0.3	0.2	0.8	2.3	19	37
	Visible	—	0.6	0.5	1.5	7	57
	Infrared	—	—	—	—	11	81
	Bolometer	—	—	—	—	55	69
Shot Quay:							
2.7	Far ultraviolet	20	—	—	—	600	—
	Near ultraviolet †	70	25	2	8	1,500	77
	Visible	200	150	1.6	8	700	88
	Infrared	200	540	1.1	14	1,200	96
	Bolometer	—	—	—	—	5,100	92
Shot Rio Arriba:							
3.5	Far ultraviolet	3	0.8	1.6	11	430	—
	Near ultraviolet †	70	24	1.8	9.5	1,100	71
	Visible	170	100	1.7	9	540	86
	Infrared	220	410	1.2	12	860	95
	Bolometer	660	—	1.6	—	3,400	90
12.4	Far ultraviolet	—	—	—	—	32	—
	Near ultraviolet †	8	2.5	2	11.5	80	37
	Visible	10	8	1.8	10.5	46	58
	Infrared	20	48	1.5	12	75	82
	Bolometer	—	—	—	—	270	70
Shot Rushmore:							
7.6	Far ultraviolet	0.9	—	—	—	130	—
	Near ultraviolet †	40	29	2	17.5	340	51
	Visible	110	150	2	16.5	130	72
	Infrared	130	310	2	20	200	88
	Bolometer	360	—	2	—	970	80
22.5	Far ultraviolet	—	—	—	—	13	—
	Near ultraviolet †	3.7	2.7	2	17	30	26
	Visible	6	11	2	16.5	13	43
	Infrared	23	81	2	22	20	71
	Bolometer	—	—	—	—	110	57

\* As predicted by TM 23-200 scaling law, unattenuated by the atmosphere.

† Values of  $\bar{T}$  for the near ultraviolet ranges do not include ozone absorption (2,000 to 2,900 Å).

radiance at first maximum to that at second maximum with increasing wave length. This was consistent with measurements made on larger-yield bursts of previous operations.

It was felt that the data presented in the ITR, while preliminary in nature, gave a valid indication of the general thermal behavior of nuclear detonations with yields of less than a kiloton. It appeared that the large-yield scaling laws for times to minimum and maximum can be extended reasonably well to fractional-kiloton yields down to five tons; whereas, the TM 23-200 scaling laws generally gave values for irradiance at second maximum which deviated greatly from the measured quantities. Predicted values increasingly exceeded the measured values, as the yield decreased. For a five-ton yield, the bulk of the thermal energy was contained in the second peak and at wave lengths greater than 4,000 Å. The ratio of irradiance at the first maximum to that at the second maximum decreased with increasing wave length for fractional-kiloton-yield bursts.

Laboratory determination of the detector characteristics and a more exacting calculation of the atmospheric transmission will increase the accuracy of the data presented in the final report. Precision data-reduction techniques will minimize the limitations due to noise, lowered-frequency response, readout resolution, and curve plotting. Better correlation between measurements of identical pulses from different detectors and channels will give more accurate final results for each event. Reduction of the data from all shots will greatly improve the reliability of measurements and conclusions about the thermal behavior of fractional-kiloton bursts.

### 13.7 ELECTROMAGNETIC PULSE MEASUREMENTS OF LOW-YIELD BURSTS

13.7.1 Objectives. The objective of Project 6.15 during the NTS phase of Operation Hardtack was to obtain and analyze the wave form of the electromagnetic radiation from low-yield-nuclear bursts. In particular, broad-band measurements were to be made from 0 to 10 Mc at a range of 100 miles. It was also desired to determine the time of detonation. An attempt was to be made to detect exceptionally low-yield shots and underground shots. In addition, this participation by Project 6.15 afforded an opportunity to check out new components of a tactical system, known as Detonation Locator Central AN/GSS-5 (XE-1), for determining various burst parameters from both friendly and enemy nuclear detonations.

13.7.2 Background. Experiments during Operations Teapot and Plumbbob demonstrated the feasibility of locating the point of detonation of a nuclear device. Analysis of electromagnetic-pulse wave from data indicated a correlation between wave-form parameters and nuclear-burst information, such as yield and type of device. The Army has indicated a requirement for a tactical system, known as Pin Point, to determine various burst parameters from both friendly and enemy nuclear detonations. The first prototype electromagnetic-detection unit, a component of the Pin Point system, was expected to be completed by ASRDL in January 1959. This equipment is known as Detonation Locator Central AN/GSS-5 (XE-1).

13.7.3 Method of Experimentation. The receiving station was located on the outskirts of Boulder City, approximately 100 miles from the NTS. The equipment (consisting of broad-band receivers, associated components, oscilloscopes, and cameras) was housed in an M-348 semi-trailer and was essentially the same as that used in similar experiments during Operation Redwing and the EPG phase of Operation Hardtack.

The receivers differed primarily in the band widths covered. The several oscilloscopes employed were adjusted to various sweep speeds, and three types of cameras running at different speeds were used to record the oscilloscope traces.

Shot participation included Valencia, Mars, Mora, Hidalgo, Colfax, Tamalpais, Quay, Lea, Neptune, Hamilton, Logan, Dona Ana, Vesta, Rio Arriba, Socorro, and Wrangell.

13.7.4 Data Obtained. The only data recorded was obtained from three above-ground, kiloton-range nuclear detonations. The opportunity to observe electromagnetic pulses from very-low-yield and underground shots was lost because of thyratron-emitted pulses and a high ambient-noise level. Located in an area adjacent to electrical power transmission lines, the average noise level, a combination of sferics and man-made sources, was higher than encountered in previous tests. This limited the usable trigger level to about 0.1 v/m.

The equipment used proved to be adequate for the recording of known shot-time detonations in the kiloton range.



## *Appendix*

# PROJECT SUMMARIES

Brief summaries of each Hardtack project are given in this appendix, which is organized by projects, as a supplement to the program summaries given in the text of the report. Complete information about the projects is given in the individual reports thereof. Information on the availability of these complete project reports, all of which have been published in preliminary form, may be obtained from the Chief, Defense Atomic Support Agency, Washington 25, D. C.

### PROGRAM 1: BLAST MEASUREMENTS

**Project 1.1 "Underwater Pressures from Underwater Bursts"** (ITR-1606), U. S. Naval Ordnance Laboratory, Silver Spring, Maryland; E. Swift, Jr., Project Officer.

Free-field underwater pressures were measured during Shots Wahoo and Umbrella in order to provide basic data for the determination of critical damaging ranges and safe delivery distances of submarines and surface vessels in the vicinity of underwater nuclear detonations.

Pressures were recorded on magnetic tape from piezoelectric and electromechanical pickups in the water; the electronic recording equipment was self-contained and operated automatically. Backup was provided by mechanical gages; both self-contained pressure-time gages and ball-crusher gages measuring peak pressures were used.

For Wahoo, a 500-foot-deep shot in 3,200 feet of water, the measurements were to provide a check on results obtained during Operation Wigwam and to yield some information on refraction by thermal gradients, bottom reflections, the cavitation pulse, and the bubble pulse. Underwater pressures at depths down to 2,000 feet were obtained from the electronic recorders at a range of 2,390 feet and from the mechanical gages at depths down to 150 feet at 2,963, 3,465, and 15,000 feet from surface zero. The electronic equipment on two other target ships did not operate, due to failure in timing signals. Shock-wave pressures recorded at 800 feet and deeper were in agreement with Wigwam results, scaled down to 10 kt. At 300 feet and shallower, both pressure and duration of the shock wave were much less (approximately 15 percent) than would be expected in isovelocity water.

For Umbrella, a shot fired on the bottom in 148 feet

of water, the measurements were to provide information on the propagation of a shock wave in shallow water; in particular, it was intended to find peak pressures and durations of the shock wave as a function of distance and depth, the nature and magnitude of the associated ground wave, and the magnitude of the cavitation pulse. Underwater pressures were measured at sixteen stations. Records were obtained at distances of 500 to 8,000 feet from surface zero and at depths from 10 feet down to 130 feet. Most of the pressure-time recordings were at distances greater than 1,500 feet.

Middepth peak pressures of the shock wave were in agreement with the predictions made for 10 kt; for distances under 4,000 feet, they also agreed with scaled-down results from Operation Crossroads. At all distances, pressures were lower near the bottom than at middepth. The ground wave velocity was 10,600 ft/sec. The pressure in the water from this wave was lower than expected from results of high-explosive tests. A cavitation pulse was observed following the shock wave at all stations.

**Project 1.2 "Air-Blast Phenomena from Underwater Bursts"** (ITR-1607), U. S. Naval Ordnance Laboratory, White Oak, Silver Spring, Maryland; P. Hanlon, Project Officer.

Project 1.2 participated in the two underwater shots of Operation Hardtack. Shot Wahoo was a 10-kt burst at a depth of 500 feet in water 3,000 feet deep. Shot Umbrella was a 10-kt burst on the lagoon bottom at a depth of 150 feet.

The primary objective of this project was to determine air-blast overpressure as a function of time and distance for the two underwater shots of Operation Hardtack in order to provide data that could be used to establish safe delivery ranges for aircraft operating at low altitudes. Correlation between data from chemical (HE) and nuclear explosions was to be made to make use of more-extensive data from high-explosive bursts in water in determining overpressure fields that would exist for a shot of any yield in any configuration of water and weapon. This involved the determination of (1) the air-blast pressure and arrival times of the initial and any subsequent pulses, (2) the relative magnitudes of the blast transmitted across the water-air interface and that produced by the venting of the bubble, (3) the direction of the flow behind the front, and (4) the

positive impulse.

Measurements were made in two regions: The first region extended from the surface to an altitude of 1,000 feet, and the second extended from 1,000 feet to an altitude of 15,000 feet. The instrumentation for the low region, which consisted of Ultradyne gages (variable-inductance gage) and mechanical pressure-time gages supported by moored balloons was used during both shots. The higher-altitude instrumentation, mechanical pressure-time gages deployed by rockets and supported by parachutes, was used during Shot Umbrella only. High-speed photography was used during both shots to record early shock phenomena. Smoke rockets were used during Umbrella in conjunction with photography to determine the direction of flow behind the shock. There were two balloon and two surface stations established for Wahoo. Both balloon stations survived the shot, but one of the balloon strings was lost before recovery could be effected. The other balloon string was recovered, and both pressure-time systems (located at altitudes of 500 and 1,000 feet) produced records. Surface data were obtained from one station. The second surface station did not receive a timing signal.

There were five balloon stations, seven surface stations, and two rocket stations established for Shot Umbrella. Of the five balloon stations, four were lost as the result of high winds that arose prior to the shot. The two canisters of the balloon string recovered produced records. Records were produced at five of the seven surface stations. One of the stations lost, sank prior to the shot; the other failed as the result of an equipment malfunction. All of the rockets, 32 instrumentation rockets and 5 smoke rockets, were fired. The firing programmer and kindred equipment functioned in a normal manner. Twenty of the thirty-two instrument rockets were recovered. Seventeen of these rockets yielded recorder drums that had run through an entire cycle. Nine of the seventeen rockets produced usable data. A few of the remaining eight records, after further investigation, may produce data. The preliminary investigation of the rocket data indicated that the gage system did not vent properly. Corrections were made for this. Further investigations will be required. The positions of the canisters at zero time in this report are subject to change, because the positions given are based upon ballistic data only.

As a result of the data obtained, it appears as though all of the objectives of the experiment can at least be partially fulfilled.

It was found that, at least in a qualitative sense, the wave forms obtained from Shot Wahoo are those to be expected from high explosives detonated under similar scaled conditions. Further, the blast data obtained from Shot Wahoo are in close agreement with predictions based upon TNT, and the agreement is such that the use of a 100 percent efficiency in scaling TNT data

to nuclear data appears to be justified.

The surface data obtained from Shot Umbrella show that the wave forms are in reasonable agreement with TNT forms. The agreement between the surface Umbrella pressure-distance data and the extrapolated TNT data available indicates that the use of a 100 percent efficiency in scaling TNT data to the nuclear case appears to be reasonable. The Umbrella pressure estimates made on the basis of TNT data appear to be high, as compared with the pressure data obtained aloft for Shot Umbrella. Because of the uncertainties in these preliminary data, conclusions are very tentative.

Project 1.3 "Surface Phenomena from Underwater Bursts" (ITR-1608), U. S. Naval Ordnance Laboratory, White Oak, Silver Spring, Maryland; E. Swift, Jr., Project Officer.

The objectives of Project 1.3 were to study the visible surface phenomena from the underwater shots of Operation Hardtack. The results are to be used to improve the predictions for other operational conditions of interest to the Navy.

Timed technical photography from four surface stations and from aircraft flying around and directly over the burst was used to obtain the principal data. In addition, temperature and relative humidity were measured at a series of distances by automatic recorders.

For Wahoo, a 10-kt shot 500 feet deep in 3,200 feet of water, camera coverage of all important phenomena was satisfactory. The spray dome rose to about 900 feet and was immediately followed by a plume, which rose to about 1,750 feet. Smaller secondary plumes appeared at around 30 seconds. A surge cloud developed at around 30 seconds and spread out rapidly to around 14,000 feet in crosswind diameter and well over 1,000 feet in height at 2 minutes. All visible air-borne material fell back into the surge. The surge was irregular in size and consistency; it was carried downwind beyond the target vessels and was still visible at 12 minutes after the burst. Two temperature and humidity recorders operated; these showed a temperature change at the time of the passage of the base surge.

For Umbrella, a 10-kt shot on the bottom in 150 feet of water, camera coverage of all important phenomena was satisfactory. The spray dome developed rapidly into a columnar plume; the maximum height reached was about 5,800 feet. Except for a tenuous mist at the center, all visible material fell back into the base surge, which appeared in about 13 seconds. At 75 seconds the surge was about 1,850 feet high; at 7 minutes it reached a crosswind diameter of about 19,000 feet. It was still visible on the aircraft films at 24 minutes. Eight temperature and humidity recorders operated; the data shows clearly an early heating of the surge cloud by the

detonation and a cooling in the later stages.

**Project 1.4 "Physical Characteristics of Craters from Near-Surface Bursts" (ITR-1609), U.S. Army Engineer Research and Development Laboratory, Fort Belvoir, Virginia; A. W. Patteson, Project Officer.**

The objective of this project was to measure and analyze the physical characteristics (radius, depth, profile, lip height and width, throwout, and ground-surface displacement) of land or underwater craters.

Primary participation was on Shots Koa and Cactus, the only land-surface bursts of Operation Hardtack. Dimensions of the craters were to be determined by topographic, lead-line, and aerial-stereographic surveys. Secondary participation included aerial or fathometer surveys of barge Shots Fir, Oak, Nutmeg, Juniper, Poplar, Yellowwood, and Magnolia.

Results available for this report include preliminary data for Koa and Cactus. The data, in feet, include:

<u>Shot</u>	<u>Radius</u>	<u>Depth</u>	<u>Lip Height</u>	<u>Lip Width</u>
Koa	1,825	135	0	0
Cactus	185	36	Approx. 25	Approx. 250

The Cactus crater agreed with predictions and with the TM 23-200 crater curves and environmental factors, but the Koa crater did not. The Koa crater was considerably larger than expected; the water tank in which the device was fired is believed to have increased the transmission of energy to the ground.

**Project 1.5 "Refraction of Shock Waves from a Deep-Water Burst" (ITR-1610), U.S. Navy Electronics Laboratory, San Diego, California; C. J. Burbank, Project Officer.**

The objectives of this project were to check the validity of the theory of refraction of shock waves by determining the effect of refraction (resulting from temperature and salinity gradients) on peak pressures and on the wave shape and to obtain free-field underwater-pressure records as a function of distance, depth, and time for the support of other projects.

Gages were installed at five different stations, located at 2,036, 4,421, 7,702, 9,189, and 10,420 feet on a radial line from surface zero. Cables were suspended with sixteen gages evenly spaced at depths of from 50 to 800 feet at the first station and ten gages at depths of from 100 to 1,000 feet at the other stations. Data from the first station was telemetered to shore; at the other stations, data was recorded on magnetic tape and photographic film.

One pressure-time record was obtained from the station at 2,036 feet, and pressure-time records were obtained at ten depths from the station at 9,189

feet. The other stations failed to furnish data. The average overpressure for the gages at the 9,189-foot range was 126 psi; a single reading of 1,840 psi was obtained at the 2,036-foot range (100-foot depth).

The importance of shock-wave refraction is substantiated at the 9,189-foot station by the magnitude of the pulses for depths below 400 feet, by the absence of bottom reflections at the 100- and 300-foot depths, and by the absence of surface cutoff on the bottom reflections below 400 feet.

**Project 1.6 "Water Waves Produced by Underwater Bursts" (ITR-1611), Scripps Institution of Oceanography, University of California, La Jolla, California; L. W. Kidd, Project Officer.**

The objective was to document the water waves and inundation of nearby islands resulting from the two underwater shots, Wahoo and Umbrella. Basic data was to be used to study wave-generation mechanisms.

Six pressure-time gages were installed for Shot Wahoo, one near the shore line of Site James (8,100 feet from surface zero) and the others on deep sea moorings at ranges from 3,200 to 14,400 feet from surface zero. Two newly designed gyroscopically referenced systems were installed on target destroyers at ranges from surface zero of 2,900 feet and 8,900 feet. Photographs of wave action were taken from nearby islands referenced to wave poles installed on the reefs.

For Shot Umbrella, nine pressure-time gages were used; two near the shore lines of Sites Henry and Elmer, three on the lagoon bottom at ranges of 1,350 to 1,750 feet and four on the lagoon bottom at ranges from 4,000 to 6,700 feet. Photographs of wave poles and other ranged objects were taken.

Instrumentation failure for Shot Wahoo seriously limited early study of the water waves. The Wahoo waves were very similar to those resulting from Operation Wigwam. The first disturbance to propagate outward from surface zero was a trough. Waves following this trough increased in a regular manner until the passage of the highest and largest wave. Waves following the largest decreased in amplitude to background. The velocity of propagation of the water energy was higher than that of Wigwam water waves. Wahoo waves approaching the nearest islands and reefs in a direction perpendicular to the reef line increased in height by a factor of 1.9 and caused severe inundation and flooding of these areas.

The water waves from Shot Umbrella were very similar to those of Shot Baker of Operation Crossroads. The first disturbance was a crest which at ranges less than about 6,000 feet was the highest wave. Beyond 6,000 feet, the highest wave was found to move back in wave number with increasing range from surface zero.

At a range of 44,750 feet, the highest crest was 4.2 times the leading-crest height. Inundation effects at the nearby islands were negligible, because shoaling water and scattered coral heads caused the waves to break 2,500 feet from the shore line, thus dissipating their energy. The measured wave height at the 1,700-foot range agreed within 10 percent to the value calculated by scaling from high-explosive data in a manner developed by the Waterways Experiment Station. The rate of first-wave height decay at extended ranges cannot be determined at the present.

Project 1.7 "Air-Blast Phenomena and Instrumentation of Structures" (ITR-1612-1), Explosion Kinetics Branch, Terminal Ballistics Laboratory, Ballistic Research Laboratories, Aberdeen Proving Ground, Maryland; J. J. Meszaros, Project Officer.

The objectives of Project 1.7 were to document basic air-blast phenomena in the low- and high-pressure regions by measurements of free-field overpressure and dynamic pressure as a function of time and distance and to measure structural loading and response as a support to various Programs 1 and 3 projects, as well as to obtain full-scale shock-diffraction data to compare with results of future shock-tube studies. The project participated during eleven shots of Operation Hardtack. Electronic and self-recording gages and recording systems used by the Ballistic Research Laboratories again formed the basic instrumentation for obtaining the desired measurements.

Shots Cactus (17 kt) and Koa (1.37 Mt) afforded the opportunity to instrument essentially land-surface blast lines for both a kiloton-range and a megaton-range land-surface burst. Overpressure data was obtained in the range from 2 to 350 psi for Shot Cactus and 30 to 1,100 psi for Shot Koa. Structural-response measurements, including strain, acceleration, and free-field pressure inputs, were made for Projects 1.9, 3.2, and 3.6 on both of these shots.

Low-pressure measurements (pressure range from 0.05 to 1 psi) were obtained from eleven shots with various yields from the kiloton to the megaton range. The raw data is presented without correction for weather conditions existing at shot time.

Shock-wave-diffraction studies were made on the Project 3.2 structures during Shots Cactus and Koa at pressure levels ranging from 70 to 180 psi. Studies were also conducted on Station 1312 for Shots Yellowwood and Tobacco, with input pressures of 16 psi and 4 psi, respectively. Unfortunately, the pressures acting on the structure were far below preshot predictions, because of much-reduced yields. Thus, the high-pressure diffraction study on this structure was not realized; the information obtained will still be valuable for shock-tube comparison.

The instrumentation can be considered as having

operated successfully, in general. The major loss was the result of the accidental destruction of the magnetic-tape record from one recording system on Shot Koa during recovery operations. Information contained on sixteen electronic instrumentation channels were lost by this occurrence.

The results from the blast lines on Shots Cactus and Koa indicate that neither shot produced a precursor. All the pressure data, both low and high pressures, when scaled to 1 kt at standard sea-level conditions, agree favorably with a 1.6-kt free-air-pressure curve. This further verifies results obtained during Operations Castle and Redwing.

Project 1.7 (Supplement) "Air-Blast Phenomena and Instrumentation of Structures" (ITR-1612-2), Explosion Kinetics Branch, Terminal Ballistics Laboratory, Ballistic Research Laboratories, Aberdeen Proving Ground, Maryland; J. J. Meszaros, Project Officer.

The air-blast phenomena existing at or near the ground surface was measured during the very-high-altitude detonations of Shots Teak and Orange. Pressure-time measurements were made at three land stations and two sea stations. At two of the three land stations, instruments on a 34-foot tower yielded free-air-pressure data. Self-recording mechanical gages were used at all stations, and backup electronic gages were utilized at the two tower stations. There was moderately good agreement among gage records; however, pressures recorded were about half the values that would be obtained by scaling according to the modified Sachs scaling laws.

Project 1.7 (Second Supplement) "Air-Blast Phenomena and Instrumentation of Structures" (ITR-1612-3), Explosion Kinetics Branch, Terminal Ballistics Laboratory, Ballistic Research Laboratories, Aberdeen Proving Ground, Maryland; J. J. Meszaros, Project Officer.

Thirty-six Ballistic Research Laboratories (BRL) self-recording gages were utilized by Project 1.7 to record and document the pressure-time phenomena associated with Shots Quince and Fig. Data for pressure versus time with distance was recorded for Shot Fig, and a plot of the data shows that the established nuclear pressure distance curves and cube-root scaling law may be applied to fractional-nuclear detonations with reasonable accuracy.

Project 1.8 "Ground Motion Produced by Nuclear Detonations" (ITR-1613), Stanford Research Institute, Menlo Park, California; L. M. Swift, Project Officer.

Project 1.8 measured ground motion as it varied with input-pressure level, depth, and yield to corre-

late these data with similar data obtained in Nevada. Data were obtained at three stations (predicted pressure levels, 100, 200, and 600 psi) on two shots, Cactus (15 kt predicted) and Koa (2 Mt predicted). At each station (pressure level) air blast, relative displacement (between 0 and 50 feet and between 0 and 100 feet), and acceleration (at 1-, 10-, 30-, 50-, and 100-foot depths) were measured.

Measurements of air-blast pressure taken by the project indicate disturbed air blast wave forms and low overpressures at close ground ranges for Shot Cactus; clean wave forms, high pressures, and sharp early decay were observed at similar scaled ranges during Shot Koa.

Relative displacements were smaller than observed at Nevada at similar overpressure levels, with periods much longer than the duration of the blast waves.

Acceleration wave forms were complex, but they did indicate more-severe attenuation with depth of local air-induced accelerations than was the case during Operation Plumbbob. Earth-transmitted energy from direct ground shock and from refracted air-induced waves contributed significantly to the accelerations observed. For the earth accelerations measured during Plumbbob (at overpressures exceeding 100 psi), the direct and refracted earth shocks were not as pronounced.

Near-surface seismic velocities were found to be high at both Hardtack test sites, which contributed to early "outrunning" of earth-transmitted energy and the masking of local air-induced effects at depth.

The marked differences between these data and those obtained in Nevada from air bursts raise the question whether they were caused by the fact that the shots at the Eniwetok Proving Ground were surface detonations or by the difference in nature of the subsurface formations. This question is as yet unanswered; results of further study will be reported in the final (WT) report of the project.

Project 1.9 "Loading on Buried Simulated Structures in High-Overpressure Regions" (ITR-1614-1), Research Directorate, Air Force Special Weapons Center, Air Research and Development Command, Kirtland Air Force Base, Albuquerque, New Mexico; E. H. Bultmann, Jr., Capt, USAF, Project Officer.

This report describes one of a number of projects conducted to study the transmission of air-blast-induced ground pressure and the loading on buried structures produced by such pressure. This project was concerned particularly with the problem of the transmission of pressure to simulated buried structures in both dry and saturated sand.

The project employed 43 rigid cylinders, each having one deformable diaphragm end. Three thicknesses of diaphragm were used. The devices were buried at six depths, ranging from 0 to 20 feet, at each of two loca-

tions. The locations were chosen to give a predicted ground-surface overpressure of about 250 psi from each of two shots having a large difference in yield in order to study the effect of the length of positive-phase duration on air-blast-induced ground pressure.

The two shots in which this project participated were Cactus and Koa. For Shot Cactus, the yield was approximately 17 kt, which gave a peak ground-surface overpressure for the 23 drums used for this shot of from 305 psi to 245 psi. Shot Koa had a yield of approximately 1.4 Mt, which gave a variation in peak ground-surface overpressure for the 20 drums used for this shot of from 269 psi at the end of the trench nearest the shot to 240 psi at the opposite end.

Static measurements made on the diaphragms before and after the test consisted of strain-gage readings and permanent deflections. From these measurements the loadings on the diaphragms, in terms of maximum diaphragm pressures, were determined. Dynamic measurements of deformation, using both electronic recording and scratch gages, were made on the drums having the stiffest diaphragms. In addition, self-recording pressure-time gages were used at the ground surface.

Records were obtained from eight of nine transient strain-gage circuits for Shot Cactus and from one of eight for Shot Koa. A loss of records from Shot Koa was caused by the collapse of an instrument shelter during the test. The scratch gages and tide gages, which were developed for this test, performed very well; satisfactory records were obtained from all the scratch gages that were recovered.

Results indicate that the underground pressures were considerably different from those predicted on the basis of Plumbbob data. A fairly normal decay of maximum pressure with depth was observed down to the water table. Below the water table, however, ground pressures increased with depth; the largest value measured was over 500 psi, more than twice the surface level value.

Project 1.10 "Blast Overpressure from Very-High-Altitude Bursts" (ITR-1615), Air Force Cambridge Research Center, Laurence G. Hanscom Field, Bedford, Massachusetts; J. T. Pantall, Capt, USAF, Project Officer.

The objective of Project 1.10 was the measurement of time of arrival, peak overpressure, and pressure versus time at five balloon-borne canisters suspended at various distances below a low-yield device detonated at a very-high altitude. In order to circumvent telemetry blackout, the pressure data was to be stored on internal recorders and then played back into the telemetry transmitters, as well as telemetered directly. A power failure in the receiving station just before shot



time rendered the command transmitter inoperative; in consequence, the canister recorders could not be turned on, and no delayed telemetering was possible. Direct telemetering was blacked out at the three closest canisters and the transmitter in the fourth had not responded to the turn-on command signal before power failure occurred, but a direct telemetering signal was received from the most-distant canister. An apparent pressure signal was recorded; but the wave form was abnormal, and the time of arrival and peak overpressure appeared to be mutually inconsistent. It is believed that the signal was spurious and may have been produced by radiation damage to some circuit component. About 0.3 second after the arrival of the questionable pressure signature, the radio-frequency carrier from this canister was lost, and no further data was obtained. No conclusions are possible because of the lack of data.

Project 1.11 "Yield and Energy Partition of Underwater Bursts" (ITR-1616), Armour Research Foundation of Illinois Institute of Technology, Chicago 16, Illinois; F. B. Porzel, Project Officer.

The main objectives of Project 1.11 were to (1) determine the effective hydrodynamic yield for the bottom-burst geometry of Shot Umbrella, (2) measure the total energy release of Shots Wahoo and Umbrella, and (3) determine energy partition, shock velocity, and other hydrodynamic variables that contribute to knowledge of an underwater explosion.

The times of shock arrival were to be measured by means of pressure switches and a doppler system attached to the cable from which the nuclear device was suspended. The shock velocity was to be deduced from measurements of the time interval between closures of the blast switches and by the rate of phase change of a radio-frequency signal fed into the doppler cable. The data was to be received near surface zero and telemetered to another station at a safe location. From the shock-arrival data, the other hydrodynamic variables of interest were to be calculated, and correlations of the results by an analysis for strong shocks was to be made to obtain the total hydrodynamic energy released by the shot.

No data was obtained from Shot Wahoo, due to failure of the transmitters of the telemetering system. Data was obtained from Shot Umbrella from the pressure-switch systems, but the doppler cable broke, so no data was obtained from the doppler system.

The time-of-arrival measurements for Shot Umbrella extended for a distance of 14.8 to 115.6 feet from the bomb for a velocity range of 29,000 ft/sec to 8,500 ft/sec. Based on these measurements, the corresponding pressure-distance curve covers a range from 400,000 bars down to 21,400 bars.

Based on a theoretical calculation for the energy

split between water and coral regions of 80 percent to 20 percent, the Umbrella time-of-arrival measurements yielded a rough estimate for the total yield of 6.34 kt and an effective hydrodynamic yield of 10.1 kt. Data show, however, that the Umbrella blast wave behaved as though it were coming from a device of less than 10 kt at ranges up to 45 feet and of greater than 10 kt at ranges from 45 feet to 115.6 feet from the burst point. This fact makes the calculated yield very tentative, and a recalculation will be performed for the final (WT) report, which will very likely reduce the large bounds.

Project 1.12 "Ground-Shock Spectra from Surface Bursts" (ITR-1617), Air Force Ballistic Missile Division, Air Research and Development Command, Inglewood, California; J. F. Halsey, Project Officer.

The use of self-contained mechanical reed gages, capable of measuring the displacement shock spectrum in any one direction, provided an indication during Operation Plumbbob of the characteristics of blast-induced and ground-transmitted ground shock under conditions of low-yield loading. As a continuation of the Plumbbob effort, the Air Force Ballistic Missile Division (AFBMD), and the Ramo-Wooldridge Corporation (R-W), participated in two Hardtack shots, Cactus (low yield) and Koa (high yield), again using reed-gage instrumentation for determination of the displacement shock spectra. Each reed gage provided a reading of maximum displacement for a given frequency; frequencies from 3 to 300 cps were used. Canisters containing gages were installed with their tops flush to the ground level at predicted pressure levels from 75 to 200 psi on both shots. In addition, a number of canisters containing gages were installed in earth-confined arch structures of Project 3.2.

Satisfactory records were obtained for both shots. Limited comparisons have been made between low-yield and high-yield shots at the Eniwetok Proving Ground (EPG) and between low-yield shots at EPG and the Nevada Test Site. In general, vertical and radial displacements for the high-yield shot were much lower than expected on the basis of the extrapolation of Plumbbob data. Differences in soil conditions, surface versus raised bursts, and topography variations may have been contributing factors. Intensive parametric analyses and theoretical studies are being made in an attempt to establish suitable scaling laws; results will be reported in the final report.

In general, the vertical displacements at low frequencies (less than 10 cps) are lower and the high-frequency components (greater than 100 cps) higher from Shots Cactus and Koa than from Operation Plumbbob. Also, the ratios between radial and vertical components at various ranges tend to be

more nearly equal for the two Hardtack shots than for Plumbbob. Specifically, at 110 psi the vertical displacements of Shot Cactus were significantly less ( $\frac{1}{3}$  to  $\frac{1}{5}$ ) than for Plumbbob up to 20 cps, where they are almost equal. Above 50 cps, the vertical displacements for Cactus were two to four times greater than for Plumbbob. The radial displacements at 110 psi for Shot Cactus were about the same as for Operation Plumbbob up to 10 cps and two to four times greater at higher frequencies.

The vertical displacements at 90 psi for Cactus, as compared with those at 84 psi for Koa, were higher for Koa in the low-frequency range (twice as high at 3 cps), lower for the intermediate range (10 to 50 cps), and about equal for the high-frequency range. The radial displacements for Cactus at 90 psi were about the same as for Koa at 84 psi, except in an intermediate frequency range (10 to 50 cps) where the Cactus values were found to be greater.

**Project 1.13 "Characteristics of Ocean and Bottom for Shots Wahoo and Umbrella, Including Umbrella Crater (C)" (ITR-1618), Office of Naval Research, Washington, D. C.; J. W. Winchester, Project Officer.**

The primary objectives of Project 1.13 were to: (1) conduct an oceanographic and hydrographic survey of the Wahoo and Umbrella sites; (2) provide environmental data in support of other scientific projects; and (3) determine the magnitude of the crater from Shot Umbrella. The first objective had to be accomplished during the planning phase of Operation Hardtack and has been previously reported on. This pre-operational phase was conducted during September and October 1957, and the remaining work was accomplished during May and June 1958.

The operational phase was essentially intended to provide information on which to base an estimate of the temperature and density fields of the sea water at Wahoo shot time and to determine the magnitude of the Shot Umbrella crater. These objectives were fulfilled by using the Navy oceanographic survey vessel USS Rehoboth, simultaneous bathythermograph observations from platforms in the target array, and a Task Group 7.3 LCM equipped with a fathometer.

The USS Rehoboth worked in the vicinity of the Wahoo ship array from D-13 to H-5. During this time, oceanographic stations were occupied in a 150 mi<sup>2</sup> area, and current drogues were set in the vicinity of surface zero. Bathythermograph observations were made simultaneously, as weather and transportation permitted, from YC-4, YC-5, and YC-7 on D-6, D-5, and D-4. After the destroyers were placed in the array on D-1, a few simultaneous bathythermograph observations were made at approxi-

mately 3,000, 5,000, and 9,000 feet from surface zero. The three destroyers were provided with Edgerton, Germeshausen and Grier (EG&G) timing signals for use in dropping automatically a bathythermograph from each DD at M-15, M-5, and M-1. Installations on the DD-474 and the DD-592 failed to operate, because the timing signals did not get through to the units; but the equipment on the DD-593 functioned perfectly, and three excellent temperature traces were obtained. Positioning and control of the LCM for the crater survey was accomplished by cross bearings from Sites Glenn and Keith and by radio communications between the azimuth stations and the boat.

Vertical temperature distribution of the area consisted of a virtually isothermal layer from the surface to about 350 feet, but temperatures at 600 to 700 feet varied as much as 5 to 6 degrees Fahrenheit within 3 to 4 hours. Preliminary computations of the shot-time thermal structure indicate that the depth of the isothermal layer sloped upward from about 340 feet at the DD-593 to about 280 feet at the EC-2, and the thermal gradient between 300 and 600 feet was considerably greater at the EC-2 than at the DD-593. Below depths of about 900 feet, no significant changes in temperature as functions of either horizontal range or time were observed.

Preliminary results of the crater survey indicate that a crater of approximately 1,500 feet in diameter with a maximum depth of 15 to 20 feet was produced by Shot Umbrella.

## PROGRAM 2: NUCLEAR RADIATION

**Project 2.1 "Shipboard Radiation from Underwater Bursts" (ITR-1619) U.S. Naval Radiological Defense Laboratory, San Francisco, California; M. M. Bigger, Project Officer.**

The principal objectives of this project were: (1) the determination of gamma-radiation fields aboard three moored destroyers exposed to radiological environments at locations of possible operational interest about the surface zeros of two underwater nuclear detonations, Shots Wahoo and Umbrella; (2) estimation of transit (remote-source) gamma-radiation fields at exposed weather-deck locations aboard ship; (3) estimation of gamma-radiation fields in the water adjacent to the ships; and (4) measurement of gamma-ionization decay of a fallout sample collected on one destroyer a few minutes after each shot.

The destroyers, which were equipped with operating washdown systems, were instrumented with film badges and gamma-intensity-time-recorders (GITR's). Unshielded GITR's and the film badges supplied radiation data at locations representing major battle stations;

directionally shielded GITR's on the fantail of each destroyer supplied transit-radiation data; GITR's submerged in the water supplied some data on underwater radiation; and a fallout collector connected to a fully shielded GITR supplied gamma-ionization-decay data.

Radiation histories were obtained on only one destroyer for Shot Wahoo; and although radiation histories were obtained on all three destroyers for Shot Umbrella, some data was lost because of shock damage. Preliminary results from Shot Umbrella indicated that weather-deck dose buildup ranged between 600 r, received within 0.5 minute at 2,000 feet from surface zero, and 45 r, received within 2 minutes at 8,000 feet from surface zero. Dose-reduction factors less than 6.0 were obtained for all compartments above the waterline; factors greater than 9.0 were obtained only in machinery spaces below the waterline. Transit radiation appeared to represent a high percentage of the total radiation observed aboard the ships. In the one case where data was obtained, the underwater radiation did not contribute significantly to the total radiation aboard DD-593 after Shot Umbrella. Gamma-ionization decay was obtained for the period from 0.1 to 34.8 hours after Shot Umbrella.

The project had only limited success in meeting its objectives for Shot Wahoo, but met most of its objectives for Shot Umbrella. Improved readout of GITR records will be required before data adequate for use in an operations analysis can be presented.

Project 2.2 "Shipboard Contaminant Ingress from Underwater Bursts" (ITR-1620), U.S. Naval Radiological Defense Laboratory, San Francisco 24, California; M. M. Bigger, Project Officer.

The objectives were to obtain data in selected interior compartments of one destroyer (DD-592) located within the dynamic-radiological environment following two underwater nuclear detonations, from which it might be possible (1) to determine whether an inhalation hazard existed due to ingress of contaminants via ventilation or combustion air systems; (2) to estimate the external-gamma-radiation dose or dose rate due to ingress of contaminants; and (3) by measurement of particle-size distribution, to attempt correlation between biological dosimetry and physical measurements, as well as to provide information on these parameters for use in Item 2.

Three compartments with associated ventilation air systems, and the fireroom, in which a full-power air flow was maintained through an unfired boiler, were instrumented. Gamma-intensity-time recorders, incremental-air samplers, total-air samplers, surface (deposition) samplers, and small animals (mice and guinea pigs) were placed in selected locations within the compartments. Test conditions, simulating those

required of a ship under attack by nuclear weapons, included complete closure of the ship with the exception of test-ventilation systems and combustion-air systems. Twenty percent of rated-air flow was maintained through the test-ventilation systems to provide a maximum and known air-flow condition simulating the nuclear-attack condition with blowers off. An air sampler and animal station were also installed on top of a platform above the forward-gun director. This location was above the washdown.

Samples and animals were recovered at earliest permissible times after shot. Following recovery, the animals were sacrificed at various time intervals, and tissue activity counted. Air and surface samples were also counted.

Due to a ship-power failure, only animal data was obtained during Shot Wahoo. During Shot Umbrella, a circuit failure caused the loss of time-dependent air-sampler information; however, total-air samples were obtained.

Estimates of the internal dose due to inhalation in the test compartments during Shot Wahoo were below the threshold for acute exposure, but did indicate possible chronic effects. Similar estimates for Shot Umbrella were below the threshold for chronic effects, with the possible exception of the estimate for internal dose received in the engine room.

Shot Umbrella estimates of the external-radiation-dose rates in the test compartments due to the ingress of contaminants were a small fraction of total-dose rates of the compartment.

During both shots, the total-dose rates during the first few minutes were high, and due almost entirely to radiation sources external to the ship. It was evident that the ingress of contaminants could not have contributed significantly to the dose rates during this period.

Based on this preliminary information for the test situation existing for Shots Wahoo and Umbrella, the following tentative conclusions have been drawn: (1) For Shot Wahoo, an inhalation hazard that could produce chronic effects existed in the galley, after-crew's compartment, and after-engine room for an open-air system without fans operating. A similar hazard existed in the fireroom with full-combustion-power air flow. This hazard was not of such magnitude as to produce acute effects. (2) For Shot Umbrella, no inhalation hazard capable of producing either acute or chronic effects existed in the galley, after-crew's compartment, and fireroom. A possibility exists that chronic effects might result from exposures sustained in the engine room. (3) For Shot Umbrella, the deposited and air-borne contaminants in the test compartments did not contribute significantly to the total-dose rate. (4) Pending further refinement of air-sampler and animal data, no statement can be made concerning



correlation between biological dosimetry and physical measurements.

Project 2.3 "Characteristics of the Radioactive Cloud from Underwater Bursts" (ITR-1621), U.S. Naval Radiological Defense Laboratory, San Francisco 24, California; E. C. Evans III, Project Officer.

The principal objectives of the project were: (1) to measure the complex-gamma field at a number of positions within 10,000 yards of each of two underwater nuclear detonations; (2) to collect limited samples of air-borne debris resulting from these detonations; and (3) to expose a number of test panels to this same debris.

Gross-gamma fields were measured by means of gamma-intensity-time recorders (GITR's) installed on critically located floating platforms within a 10,000-yard radius of surface zero. Samples of radioactive material deposited from the cloud were obtained by incremental collectors installed with the basic GITR's. Using these gamma recorders in conjunction with NBS film packs, the gross-gamma fields and total doses were also measured at various positions aboard three destroyers and a liberty ship located within the area covered by the floating platforms, thus permitting a comparison between shipboard fields and the free field resulting from the unmodified radiating cloud. Some additional measurements of surface water activity and certain physicochemical parameters of the radioactive cloud were made, principally in order to correct the records obtained by the GITR's.

The project had success in meeting its objectives for both events. Nearly all of the total-gamma dose occurred within 15 minutes after zero time and was due to the passage of the air-borne radioactive material. However, the gamma-dose-rate traces from the two shots showed pronounced and characteristic differences in the transiting-gamma field. Gamma doses in excess of 100 r occurred within the first 15 minutes at downwind distances less than 16,500 and 11,000 feet from Shots Wahoo and Umbrella, respectively. In both instances, the dosage due to deposited radioactive material was light to insignificant.

A study of the downwind-gamma records would indicate the tentative conclusion that a distance of approximately 23,000 to 28,000 feet from surface zero should be maintained in order to assure a total free-field dose of less than 25 r. Radiation from deposited radioactive material presents little hazard when compared to free-field-gamma radiation hazards. Exposed test panels were recovered and some early decay information was obtained. Data from further analysis of these panels will be presented in the final report, only to the extent that they influence the basic gamma-field documentation.

Project 2.4 "Neutron Flux from Large-Yield Bursts" (ITR-1622-1), Chemical Warfare Laboratories, Army Chemical Center, Maryland; J. W. Kinch, Project Officer; and Project 2.4 (Supplement) "Neutron Flux from a Very-Low-Yield Burst" (ITR-1622-2), U.S. Army Chemical Warfare Laboratories, Army Chemical Center, Maryland; D. L. Rigotti, Project Officer.

The objectives of this project were to measure neutron flux and dose as a function of distance for two megaton-range detonations and for a fractional-kiloton-yield device, and to perform neutron flux and dose measurements as required by other DOD projects. The project participated in Shots Yellowwood, Walnut, Quince, and Fig.

The Hurst fission-foil method was used to measure neutron flux. Gold, plutonium, neptunium, uranium, and sulfur were employed as detecting materials, with zirconium also being used during the two thermonuclear shots. Steel buoys were used to support the detecting materials in Eniwetok Lagoon during the megaton events. Twenty-five stations were placed at distances varying from 917 yards to 4,100 yards for both Shots Yellowwood and Walnut. Eighteen stations located both on land and in the lagoon were at distances varying from 100 yards to 1,039 yards for Shots Quince and Fig. Neutron dose was calculated from the measured fluxes by using the single-collision theory of dose contribution per neutron. Neutron flux and dose measurements were also made in support of Projects 6.3 and 8.6.

The dose measured was lower than the values predicted by TM 23-200 by a factor of 2.3 for Shot Yellowwood, and a factor of 2.0 for Shot Walnut. This is considered good agreement.

[REDACTED] No results were obtained from Shot Quince, because of the absence of nuclear yield.

Within the ranges at which neutron measurements were made during Shot Fig, there was no variation of the neutron-energy spectrum above 3.7 kev with increasing distance from the point of detonation. However, as was expected, the total number of neutrons decreased with increasing distance from the point of detonation.

[REDACTED] Personnel stationed beyond 1,000 yards from this detonation would have received no significant neutron dose.

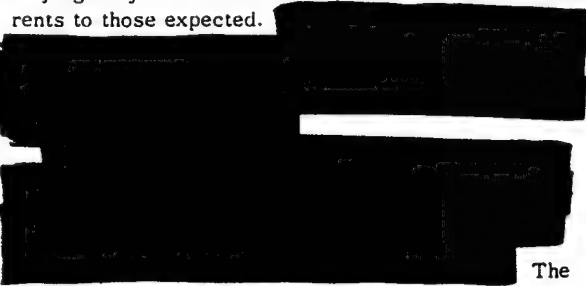
The effectiveness of the Hurst-fission-foil method of measuring neutron dose is limited by the long recovery time necessary at EPG. The buoy system of

placing passive detecting media over water is effective in areas with overpressures up to 90 psi, and can be made effective in higher-overpressure areas by minor modifications.

Project 2.6 "Neutron Flux from Very-High-Altitude Bursts" (ITR-1623), U.S. Naval Research Laboratory, Washington, D. C.; T. D. Hanscome, Project Officer.

The objective of Project 2.6 was to provide data on neutron flux (primarily 14-Mev neutrons) versus range from a megaton weapon detonated at very-high altitude. The instrumentation (in three pods for each shot) was carried aloft by the Redstone missile and ejected ballistically at predetermined ranges. The neutron spectrum was measured by the time-of-flight method with special attention being given to the 14-Mev neutron group. Various types of detectors measured fast- and slow-fission neutrons, background- and prompt-gamma rays, gamma-ray dose, and interference effects, such as electromagnetic disturbances. The detector outputs were electronically encoded, commutated, and recorded on a magnetic-tape recorder. The latter was programmed to record for 120 msec after the prompt-gamma-ray pulse and to switch repeatedly to a playback condition to telemeter the recorded information to a telemetry station in the missile-control bunker.

Gamma ray measurements were consistent from pod to pod. The neutron fluxes were approximately as calculated, but were a little low at some stations, as judged by the relation of the observed detector currents to those expected.

 The observed fluxes were within less than one order of magnitude of expected values.

The extraction of further data (including all that on the 14.2-Mev neutrons) required oscilloscope camera methods and film processing facilities not available in the field.

Project 2.7 "Nuclear Radiation from a Detonation at Very-High Altitude (C)" (ITR-1624), U.S. Naval Research Laboratory, Washington, D. C.; P. A. Caldwell, Project Officer.

The objective was to measure the neutron spectrum and total prompt-gamma-ray-flux produced by the deto-

nation of a nuclear device of low yield (approximately 2 kt) at an altitude of about 90,000 feet. This information was to be obtained by suitable detectors in the vicinity of the nuclear device and telemetered to the ground to be recorded and subsequently analyzed.

The theory and instrumentation for measurement of neutron spectrum and total prompt-gamma-ray flux from a nuclear device detonated at an altitude of 85,000 feet is described.

Measurement of neutron time of flight with a  $\text{Li}^6\text{I}$  scintillator-photodiode detector, with a similar  $\text{LiI}$  detector for gamma-ray correction of the  $\text{Li}^6\text{I}$  detector, was planned. The measurement was to have extended to plus 120 msec. A  $\text{CsI}$  scintillation detector, whose output was integrated for the first 10  $\mu\text{sec}$  after the zero time, and  $\text{KBr}$  crystal, whose darkening was measured as a function of time for 120 msec after zero time, were to be used to detect gamma flux.

The detector outputs were to have been electronically encoded and recorded on a magnetic-tape recorder programmed to record for 120 msec after zero time, reduce its speed to  $\frac{1}{16}$  of the recording speed, and continuously play back the data. The recorder output modulated a 70-kc voltage-controlled oscillator used in a standard frequency-modulated telemetering system. A ground station was to have received and recorded the signal.

The Bendix command system utilized by this project failed, and no data was obtained.

Project 2.8 "Aircraft and Rocket Fallout Sampling" (ITR-1625), U.S. Naval Radiological Defense Laboratory, San Francisco, California; R. R. Soule, Project Officer.

The general objective of the project was to estimate, by collection and analyses of cloud samples, the relative contribution of certain radionuclides to both local and world-wide fallout arising from megaton-range land- and water surface detonations. The specific objectives were to: (1) obtain air-borne particulate and gas samples by rocket and aircraft sampling techniques; (2) determine radionuclide distributions among particle groups that differ according to falling rates and that may be defined as major contributors to local and world-wide fallout; (3) attempt to determine an early-time radionuclide and particle-space distribution with respect to the upper and lower halves of the cloud and radially outward from the axis of the cloud in a vertical plane passing through ground zero; and (4) estimate the extent of separation of fallout particles from gaseous fission products by fission measurements on gas and particulate samples of the cloud collected near the top of the cloud and on particulate samples collected near the surface of the earth.

The project participated during Shots Koa, Walnut, and Oak. Rocket-borne and aircraft-borne cloud

samplers were used. The rocket, a new one of complex design, was a 20-foot-long unit consisting of a main motor, sustainer motor, parachute compartment, electronics compartment, and air-sampling nose section with closure system, and various items of auxiliary equipment. Two types of aircraft, B 57D and WB-50, were used. The B-57D aircraft were equipped with gross particulate and coincident gas-particulate samplers. These aircraft were used to collect coincident gas and particulate samples and, also, gross-particulate samples from altitudes around 55,000 feet, at times from about 2 hours to 26 hours after the detonation. The WB-50 aircraft were equipped with AFOAT-1 standard E-1 filter units and were used to collect fallout material at an altitude of 1,000 feet, at intervals of time from 4 to 12 hours after detonation.

Aircraft collections were successful on the three shots; however, there were some indications that samples for Shot Koa were contaminated by debris from Shot Fir. The actual extent of contamination is not presently known. The rockets, which the project had planned to utilize to collect early-time particulate samples, were not fully operational by the time of their planned participation. After an extensive field effort to correct difficulties encountered, the rocket portion of the project was terminated prior to Shot Oak.

It was concluded that sufficient aircraft samples were obtained during Shots Koa, Walnut, and Oak to provide the data required to meet the general objectives of the project.

Project 2.9 "Gamma-Dose Measurements from a Very-Low-Yield Burst" (ITR-1677), U.S. Army Chemical Warfare Laboratories, Army Chemical Center, Maryland; M. Morgenthau, Project Officer.

The objectives of this project were to: (1) document the initial gamma dose versus ground range, and (2) measure the total gamma dose as a function of time, at distances of military interest, for a fractional-kiloton nuclear surface burst. The project participated in Shots Quince and Fig.

Gamma dose was measured by film badges exposed at various ranges and azimuths on land, over water, and on balloon lines. Film badges were also used to measure the increments of gamma dose versus time, utilizing a modified Signal Engineering Laboratories' gamma dosimeter transport system (Emmett device). Emmett stations were located along a single radial line at distances of 100, 200, and 400 yards from ground zero.

Good correlation between the measured initial gamma doses and extrapolations of the gamma dose curves of TM 23-200 was noted. A soldier in the open must fire a weapon of this type from a range of at least 700 yards in order to avoid an initial gamma dose of

more than 15 r from a surface burst of a weapon similar to the Fig device. No marked variation of initial gamma dose with azimuth was observed. The initial pulse was of such short duration that most of the gamma radiation arrived at the stations in less than three seconds.

Project 2.10 "Residual Radiation from a Very-Low Yield Burst" (ITR-1678), U.S. Army Chemical Warfare Laboratories, Army Chemical Center, Maryland; M. Morgenthau, Project Officer.

The objective of this project was to determine residual-radiation intensities of contaminated areas resulting from a very-low-yield (fractional-kiloton) surface nuclear detonation. The project participated in Shots Quince and Fig.

The objective was accomplished by (1) remotely monitoring the crater and lip shortly after detonation; (2) performing helicopter-to-ground surveys at pre-selected points; (3) making a number of ground surveys during and after sample collection; (4) determining the gross gamma decay of the residual radiation from collected fallout samples; and (5) documenting the alpha contamination.

Shot Quince did not go nuclear, and the resultant residual activity was due entirely to alpha contamination. An area of approximately 20 yards in diameter around ground zero was contaminated to a level above 3,500  $\mu\text{g}/\text{m}^2$  and would have been uninhabitable until decontaminated. It would also have been necessary to decontaminate a 30-degree sector extending 300 feet downwind from ground zero. The high alpha concentration in the air was less than 2 percent of the emergency exposure of 50,000 (dis/min)/meter<sup>3</sup> for an hour.

The radiation intensities at the lip and crater of Shot Fig were above 10,000 r/hr at H+30 minutes, necessitating avoidance of such an area by troops advancing at an early time. The area contaminated by fallout to levels of military significance was less than expected by a factor of 2.5, according to the present scaling laws. A weapon similar to the Fig device probably can be used in close-support operations in ground warfare, as far as fallout is concerned, because of 100-r/hr contour at an hour after detonation extended only 40 yards crosswind, with an extrapolated downwind extension of 160 yards.

Although a conical volume approximately 30 feet in diameter and 8 feet deep was filled below the burst point with Nevada soil, the resultant fallout resembled coral island soil. The variety of material found in the fallout collectors indicated the probability of both fallout and throwout collection.

The early decay measurements show that the normal fission-product decay rate,  $t^{-1.2}$ , was not applicable for a period from H+1 hour to H+3 hours. Instead, the decay rate was  $t^{-1.35}$ . However, between

H+3 hours and H+24 hours, the decay rate was only  $t^{-0.94}$ , which is slower than the normal fission-product decay rate.

The alpha contamination resulting from the detonation of a weapon similar to the Fig device does not represent a military hazard.

As expected, the greatest amount of fallout was in the downwind area, and the amount collected decreased with distance.

Project 2.11 "Neutron, Thermal, and Gamma Measurements at Various Altitudes from a Very-Low-Yield Burst (U)" (ITR-1679), U.S. Army Chemical Warfare Laboratories, Army Chemical Center, Maryland; D. L. Rigotti, Project Officer.

The objective of this project was to measure neutron, thermal, and gamma radiation at altitudes up to 1,500 feet above a very-low-yield surface burst. The project participated in Shots Quince and Fig.

The threshold-detector technique was used to measure neutron flux, with gold, plutonium, neptunium, uranium, or sulfur being employed as detecting materials. Total gamma dose was measured using National Bureau of Standards (NBS) film badges. Chemical Warfare Laboratory thermistor calorimeters were used for thermal measurements. For Shot Quince, a General Mills Aerocap balloon was used to support the instrument line almost directly above ground zero and thirteen stations were instrumented for slant ranges from 40 to 500 yards. For Shot Fig, the balloon was tethered on a single cable at a lateral distance of 120 feet from ground zero. Due to bad weather conditions, which resulted in a loss in the lift of the balloon, the thermal detectors were eliminated, and neutron and gamma detectors were installed at slant ranges of 121 to 410 yards.

Satisfactory neutron and gamma measurements were made up to an altitude of 985 feet. Since the thermal detectors were eliminated, due to loss of balloon lift, no thermal results were obtained.

Using the threshold detector system, neutron doses of 6,654 rep at an altitude of 33.3 yards (121 yards slant range) to 353 rep at an altitude of 328.3 yards (346.7 yards slant range) were measured for Shot Fig. Gamma doses of 4,800 r and 350 r were measured at the same altitudes.

[REDACTED]

Neutron and gamma dose results for the balloon stations were higher by average factors of 1.5 and 2.0,

respectively, than those observed at equivalent distances along the ground.

The balloon technique is an effective method of exposing instrumentation to obtain free-air measurements.

Project 2.12 "Neutron Flux, Gamma Dose, Induced Activity, and Thermal Radiation from Low-Yield Bursts" (ITR-1680), U.S. Army Chemical Warfare Laboratories, Army Chemical Center, Maryland; E. H. Bouton, Senior Project Officer; D. L. Rigotti, J. C. Maloney, E. F. Wilsey, and J. J. Mahoney, Sub-Project Officers.

Project 2.12 was divided into four efforts, designated 2.12a, b, c, and d.

The objectives of Project 2.12a were to measure (1) neutron dose in support of the biomedical Project 4.2; (2) neutron flux and spectra in support of the induced-activity studies (Project 2.12c); and (3) neutron radii from Shots Hamilton and Humboldt.

The threshold-detector system and a chemical-dosimeter system were employed in obtaining these measurements. The threshold-detector system used gold, plutonium, neptunium, uranium, and sulfur detector elements. The chemical-dosimeter system consisted of two glass vials each filled with a saturated aqueous solution of trichloroethylene that differed by their dissolved oxygen content.

The detectors were attached at varying distances along cable lines extending radially from ground zero and recovered by using a truck to pull the cables out of the contaminated areas. Additional detectors were exposed on goal-post stations, vertical metal stakes driven into the bottom of foxholes, and within M-48 tanks and armored personnel carriers (APC). A number of chemical-dosimeter and threshold-detector systems, excluding plutonium and neptunium, were surgically inserted in pigs.

Installation and recovery of detectors along the cable lines was effected by Project 2.12 personnel, while installation and recovery of detectors in foxholes, on goal posts, inside vehicles, and inside animals was accomplished by Project 4.2 personnel.

Satisfactory neutron-dose measurements utilizing the threshold detector technique were made in support of the biomedical Project 4.2. The doses observed during Shot Hamilton under the different exposure environments had the following ranges: open foxholes, 894 rep at 26 yards to 486 rep at 36.5 yards; tanks, 1,094 rep at 37 yards to 538 rep at 50.3 yards; APC, 1,494 rep at 50 yards to 743 rep at 82 yards. The doses in offset foxholes was below the detection limit of the threshold system (10 rep). For Shot Humboldt the following ranges were observed: open foxholes, 155,000 rep at 13 yards to 12,000 rep at 26.4 yards; two-thirds-covered foxholes, 14,400 rep at 9.8 yards to 2,270 rep at 26.4 yards; APC, 28,400 and 28,200 rep at 33 yards.

Neutron- and gamma-dose measurements obtained by the chemical-dosimetry technique in support of Project 4.2 are inconclusive, since the response of the chemical dosimeter to the complete energy range of neutrons as well as to a combined neutron and gamma flux field has not as yet been completely evaluated. Further calibration work is being conducted at the Los Alamos Scientific Laboratory (LASL).

Satisfactory neutron flux and spectra measurements were made in support of Project 2.12c utilizing the threshold detector technique.

For both Shots Hamilton and Humboldt no qualitative variation of the neutron energy spectrum with increasing distance from the points of detonation was observed beyond 150 yards.

Free-field neutron doses from 5,490 rep at 25 yards to 15 rep at 400 yards using the threshold-detector system were measured for Shot Hamilton, and from 166,000 rep at 10 yards to 260 rep at 300 yards for Shot Humboldt.

Best preliminary estimates indicate that a man stationed without shielding at 600 yards from ground zero would have received 27 rep of neutron dose from Shot Humboldt and less than 10 rep from Shot Hamilton.

The primary objectives of Project 2.12b were to provide gamma-dose measurements in support of the biomedical Project 4.2 and to document gamma-dose radii for Shots Hamilton and Humboldt. Secondary objectives were to document residual-radiation intensities and decay near ground zero.

The biomedical project was furnished film badges for its stations at Shots Hamilton and Humboldt. Gamma radii were measured by film badges placed at various azimuths and distances from ground zero. The residual-radiation dose rates and decay were documented by repeated field surveys.

Initial-gamma-radiation doses at distances of 200 yards exceeded 70 r for Shot Hamilton and 600 r for Humboldt. To avoid a gamma dose of more than 15 r, a soldier in the open firing a weapon similar to the Hamilton and Humboldt devices must be at least 400 and 600 yards, respectively, from ground zero. No marked variation of dose with azimuth was observed. Measured gamma doses and extrapolations from curves in TM 23-200, "Capabilities of Atomic Weapons," agreed within a factor of two to three for both events. The alpha-contamination levels observed at distances greater than 100 yards are considered insignificant military hazards. The data on the resultant residual gamma field and its decay is undergoing further study and evaluation and will be presented in the final report.

The objectives of Project 2.12c were to (1) document the neutron-induced gamma field produced by a fractional-kiloton nuclear device detonated on a wooden tower 50 feet high and (2) determine empirical factors relating the gamma dose rates measured over this large neutron induced field with dose-rate measurements made over

small samples of the same activated soil. The soil samples were inserted into the ground at the project stations, exposed to a measured neutron flux, then ejected from the ground and pulled from the contaminated area by cables. Dose-rate measurements were made on the soil samples after they had been reinserted into the ground in an uncontaminated area. Ground survey parties and a recording dose rate meter measured the field dose rates. A 20-channel gamma-ray spectrometer was used to identify the major gamma activities in the soil samples. The spectrometer was also used to confirm the presence of fallout. The low-energy (less than 0.1-Mev) neutron flux in the ground area was determined by measuring the activity in copper strips inserted in each soil sample.

Induced activities were produced by Shot Hamilton, but could not be studied as planned because (1) the low yield of the device induced little activity in the soil and (2) an unexpected high level of fission-product contamination occurred in the vicinity of the project stations.

The presence of induced activity in the soil samples was determined by gamma spectrometer analysis. The major contributors to the gamma spectra in the soil samples were  $Al^{28}$ ,  $Mn^{56}$ , and  $Na^{24}$ , at H+ 16 minutes,  $Na^{24}$  and  $Mn^{56}$  at H+ 7 hours, and  $Na^{24}$  and  $Fe^{59}$  at H+ 54 hours.

The low-energy (less than 0.1 Mev) neutron flux was found to peak at 5 to 8 centimeters below the ground surface of normal Frenchman Flat soil and at the ground surface in more-moist Frenchman Flat soil.

Empirical factors relating field dose rates with sample dose rates could not be determined because of the low level of induced activity produced and the fission-product contamination of the project-station exposure area.

The presence of fission products was indicated by the typical fission-product dose-rate decay demonstrated by the residual field and by the presence of low-energy, fission-product-like peaks in the gamma spectra of a ground-surface soil sample recovered from the vicinity of ground zero at H+ 31 hours.

The objective of Project 2.12d was to determine the thermal radiant exposure versus distance for a fractional-kiloton bomb, and to compare the experimentally obtained radiant-exposure values with those calculated from existing scaling laws. Radiant exposures for Shot Hamilton were measured at horizontal distances of 175 feet to 700 feet from ground zero using thermistor calorimeters. The equipment operated very satisfactorily in that only two instruments failed out of a total of sixteen independent instruments and recorders. However, the results were in general inconclusive and unsatisfactory because of the very-low yield and some shielding material in the bomb tower partially obscuring the thermal line of sight. All except one station registered less than 1 cal/cm<sup>2</sup>, which was about the lowest



working limit of the detectors.

Project 2.13 "Gamma Radiation and Induced Activity from Very-Low-Yield Bursts" (ITR-1631), Air Force Special Weapons Center, Kirtland Air Force Base, New Mexico; D. R. Griesmer, Capt, USAF, Project Officer.

The primary objective of this project was to measure the initial nuclear radiation from a fractional-kiloton detonation. Specifically, this objective involved the measurement of: (1) initial gamma-dose rate; (2) total initial gamma dose in support of the dose-rate measurements; (3) total neutron dose in low-dose regions; and (4) rate of decay of induced activity in NTS soil. A secondary objective of this project was to field-test a prototype of the standard Air Force MG-3 gamma-radiation fallout detector. The project participated in Shot Hamilton.

Detectors and measuring devices were located along two surface lines at approximately right angles to each other.

Film badges, used to measure total initial gamma dose, were located from 0 to 600 yards from ground zero; they were placed inside standard 3-inch pipe holders for thermal and blast protection. These holders were attached to the Project 2.12a cable to permit their extraction from the contaminated area immediately after the shot. Other film badges were displayed on exposure stakes located from 300 to 1,600 yards from ground zero. Glass-phosphate dosimeters were exposed at distances from 55 to 650 yards.

Nuclear track emulsions, used to measure neutron dose, were displayed at distances of 850 to 1,600 yards from ground zero, while resonance threshold foil personnel neutron dosimeters were exposed at distances of 650 to 1,150 yards from ground zero. Sulfur and indium activation detectors for additional neutron dose measurements were exposed at all stations out to 1,600 yards.

Three Kaiser initial gamma dose-rate instruments were located at 425, 550, and 750 yards from ground zero. One low-resolution dose-rate detector head (MG-3) was buried 30 yards from ground zero, with the power supply and recorder located 320 yards from the detector head and connected to it by a protected cable. All components were shock-mounted and blast-protected. In addition, the buried low-resolution detector head was surrounded by 6 inches of boric acid and 12 inches of paraffin to minimize neutron-activation of the case itself. A second MG-3 was located 650 yards from ground zero, enclosed in a plywood box and staked to the ground.

The nuclear yield of 0.001 kt  $\pm$  10 percent (radiochemical) for Shot Hamilton was one-twentieth of that predicted. As instrumentation locations were estab-

lished assuming a higher yield, optimum utilization of the instrumentation was not obtained.

Measurements of initial gamma dose rate versus time from two locations as made with Kaiser electronic automatic-dose-rate instruments were obtained. After applying corrections for cloud rise, the observed average fission-product time-decay exponent was  $-0.72$  for times between H+0.4 and H+10 seconds and  $-0.33$  for times between H+10 and H+40 seconds.

Total-initial-gamma measurements made with films and glass-phosphate dosimeters were in substantial agreement with theoretical predictions. At 110 yards, an average dose of 360 r was measured, and at 310 yards 22 r was measured.

Neutron-dose measurements were made using sulfur and indium activation detectors and neutron films. The neutron dose on the high-neutron axis obtained by the sulfur-activation technique was 8 rads at 450 yards and 0.5 rad at 750 yards.

The decay rate detected by an MG-3 ion chamber buried at 30 yards from ground zero indicated only fission product decay. No neutron-induced activation of the soil was apparent from the data obtained.

Fallout was not recorded by the second MG-3 installation, because dose-rate levels resulting at this location were not sufficiently high to activate the instrument. Satisfactory operation of the buried instrument located at 30 yards proved to be a sufficient field test of this type instrument.

Project 2.14a/34.8 "Fallout Contamination from a Very-Low-Yield Burst" (ITR-1602), Sandia Corporation, Albuquerque, New Mexico; R. E. Butler, Project Officer; Project 2.14b/34.9 "Dimensions of Nuclear Cloud from a Very-Low-Yield Burst" (ITR-1603), Sandia Corporation, Albuquerque, New Mexico; H. G. Sweeney, Project Officer; and Project 2.14c/34.10 "Special Meteorological Measurements for Very-Low-Yield Fallout Studies" (ITR-1604), Sandia Corporation, Albuquerque, New Mexico; D. G. Palmer, Project Officer.

The primary objective of this project was to determine the military significance of fallout contamination from small-yield fission weapons.

The specific objectives were to: (1) make the necessary measurements to delineate the fallout gamma-radiation field produced by a land-surface detonation of a fission weapon with a yield between 10 and 100 tons; (2) use the above data, plus meteorological data concerning the wind structure and photographic data concerning the cloud dimensions, to construct a fallout model for use with any wind pattern, and evaluate extremes in militarily significant contamination intensities for the same yield range; and (3) define the attendant plutonium contamination problem. The project participated in Shots Quince and Fig.

The fallout field from Shot Fig was documented by monitoring an array of sticky-pans, located both on land and on buoys in the water, out to a distance of 2 miles downwind. Five barges, upon which coral soil was placed to simulate land stations, were placed to receive the maximum expected amount of fallout. The barges were instrumented with remote-area-monitoring systems which automatically recorded the full-field dose rates. The barges also carried a display of sticky pans and an air sampler.

The dose rate in the crater was measured by a remote-area-monitoring system which was mounted on a sled and towed into the crater after detonation by means of a cable extending to a safe area.

Dimensions of the cloud were documented by means of three camera stations located at varying azimuths and distances from ground zero out to about ten miles. Each camera station had a number of types of cameras arranged to photograph the cloud during all times of interest.

Meteorological measurements, obtained with two phototheodolite stations, provided information concerning temperature, wind speed and direction from the surface to 10,000 feet at times ranging from H-2½ hours to H+10 minutes. The shot was fired when the winds were determined to be most favorable for successful fallout sampling by the project, based on its instrumentation array. At shot time, the wind speed was about 15 knots, and the direction was directly over the barge fallout collecting stations. Good photographic data was obtained, and it showed that the cloud stabilized at about H+6 minutes with a maximum diameter and height of 1,900 and 5,400 feet respectively.

From the data obtained it was concluded that for the burst environment of Shot Fig, intensities greater than 1 r/hr measured at H+1 hour will not extend beyond 2,600 feet downwind. Levels greater than 100 r/hr at H+1 hour were estimated to extend less than 1,000 feet downwind and 150 feet crosswind.

From the data obtained, a fallout model will be constructed which will be used to estimate extremes in fallout intensity patterns caused by varying wind conditions and cloud dimensions.

### PROGRAM 3: STRUCTURES AND EQUIPMENT

**Project 3.1** "Tapered-Charge Testing of the DD-592" (ITR-1605), Underwater Explosions Research Division, Norfolk Naval Shipyard, Portsmouth, Virginia; H. M. Schauer, Project Officer.

As a preliminary Operation Hardtack effort, Project 3.1 consisted of a series of explosive tests, employing high-explosive tapered charges, against the destroyer DD-592. The tests were conducted in January 1958 off Santa Cruz Island, California.

The main objectives of Project 3.1 were: (1) to provide a pretest experimental check on the target-damage predictions in order that optimum placement of the ship targets could be achieved for Operation Hardtack; (2) to calibrate instrumentation and check out the adequacy of the recording installations and shock mountings designed by the various agencies for Operation Hardtack; and (3) to develop and check the high-explosive tapered-charge technique as a method of simulating and determining the effects of underwater nuclear detonations on ships.

This high-explosive tapered-charge technique should enable the Navy to obtain much effects data on ships, without recourse to future full-scale nuclear testing. The technique utilized specially formed high-explosive charges to simulate a reproduction of the shock-wave forms of underwater nuclear detonations against ships. It is hoped that much of the lethal and safe-delivery criteria for a variety of ships and burst conditions can be developed by the future use of large high-explosive tapered-charges and full-scale ships. The validity and limitations of the shaped-charge technique are expected to be given in the final WT report, which will be prepared after the full-scale underwater-nuclear-events results are available after Operation Hardtack.

For Project 3.1, a series of three large, special shaped (tapered), high-explosive charges weighing from 1,400 to 4,400 pounds were used to simulate underwater nuclear attack against the DD-592. This vessel was subsequently to be used as one of the target ships at the EPG on Shots Wahoo and Umbrella. All instrumentation on board the DD-592 which was to be used for the later full-scale events, was operative and calibrated for these shaped-charge tests.

Utilizing such instrumentation, the following Operation Hardtack Projects actually participated on the Project 3.1 test series:

- UERG Project 3.1 - Shaped Charge Studies.
- DTMB Project 3.3 - Shock Studies of Shipboard Machinery and Equipment.
- UERG Project 3.4 - Loading and Basic Target Response for Surface Ships.
- BuShips Project 3.8 - Damage Assessment.
- NOL Project 1.1 - Underwater Free-field Pressure Measurements.

A report of the effort of each of the above participating projects as related to Project 3.1, is included as a section of this report which documents the entire Project 3.1 test series.

The tests were tentatively planned to be a series of four shaped charges of successively increasing shock severity, starting with a mild attack corresponding to a peak underwater shock velocity of 2.5 ft/sec on the target. The tests were actually carried up to the threshold of shock damage, but stopped after

detonation of the third charge, to avoid the probability of serious damage to the DD-592 prior to the later main full-scale nuclear test effort at Eniwetok. The peak underwater-shock velocity on the target resulting from each of the successive three shaped charges tested was 2.3, 3.5 and 5.2 ft/sec, respectively.

Preliminary results of the Project 3.1 test series indicated that: (1) the shock-wave pressure histories obtained were approximately as expected and simulated a nuclear shock wave satisfactorily; and (2) the early shock response of the test area of the DD-592 target was in fair agreement with those predicted for corresponding nuclear attacks. However, the predictions were based on model tests, and a final evaluation of the shaped-charge technique will have to await confirmation of these predictions by the full-scale underwater nuclear detonations on Operation Hardtack.

Project 3.2 "Response of Earth-Confined Flexible-Arch-Shell Structures in High-Overpressure Region" (ITR-1626-1), U.S. Naval Civil Engineering Research and Evaluation Laboratory (NCEL), Port Hueneme, California; G. H. Albright, LTJG, CEC, USN, Project Officer.

The objective of the project was to determine failure criteria of prefabricated, corrugated steel, flexible arch-shell structures confined within non-drag-sensitive earthwork configurations of coral sand. Three structures were tested in the 80 to 180-psi peak-overpressure region from a 1.4 Mt surface shot, to empirically determine the response of such structures. A fourth structure was tested in the 90-psi peak-overpressure region from a 17 kt surface shot, to determine the effects of short-duration-blast loading upon a similar structure and environment.

Instrumentation of the test structures consisted of a total of 16 electronic channels measuring acceleration, 40 scratch gages and 15 rotating-drum gages measuring deflections, and 8 self-recording-pressure gages measuring internal pressures.

The 25-foot span by 48-foot 10-gage arch-shell structure subjected to 90-psi peak-overpressure from Shot Cactus, a 17 kt surface detonation, collapsed on the side away from ground zero. The collapse apparently was initiated by bearing failure of the shell plates at a bolted horizontal seam, approximately 5 feet above floor level on the collapsed side of the structure.

High radiation levels and the collapsed condition of the other three structures precluded major recovery operations and detailed observation immediately. However, the following results have been noted:

The 25-foot span by 48-foot 10-gage arch-shell subjected to 78-psi peak-overpressure from Shot Koa, a 1.4 Mt surface detonation, collapsed completely and filled with sand. The collapse appeared to be approximately symmetrical about the crown.

The 25-foot span by 48-foot 10-gage arch shell subjected to 180-psi peak-overpressure from Shot Koa collapsed completely with the crown touching the floor of the structure.

The 38-foot span by 40-foot 1-gage arch-shell subjected to 100-psi peak-overpressure from Shot Koa collapsed completely and filled with sand. The collapse appeared to be symmetrical about the crown.

A recovery excavation was planned for several months after shot day, when radiation levels would permit the collection of additional data.

Project 3.2 (Supplement) "Response of Earth-Confined Flexible-Arch-Shell Structures in High-Overpressure Region" (ITR-1626-2), U.S. Naval Civil Engineering Laboratory, Port Hueneme, California; J. C. LeDoux, LCDR, CEC, USN, Project Officer.

This supplementary report describes the excavation and data recovery operations for Project 3.2, which took place at the Eniwetok Proving Ground approximately 6 months after Structures 3.2b, 3.2c, and 3.2d were subjected to the effects of Shot Koa. The responses of the earth-confined arch shells are deduced from observations of the damaged structures and studies of the records of deflection and deflection versus time.

Both Structure 3.2b, located at the 78-psi overpressure region, and Structure 3.2c, located at the 180-psi overpressure region, had collapsed symmetrically about the crown, failed at the bottommost horizontal bolted seams, failed at certain transverse seams, and suffered severe damage and displacements of concrete foundation footings.

Structure 3.2d, located at the 100-psi overpressure region, had first deformed in the compression-bending mode, then further displaced downward at the crown, been subjected to a large infiltration of sand through the failure of nonstructural end walls, suffered displacements and severe damage to concrete foundation footings, and reached a final deformed peaked shape due to symmetrical reversal of curvatures of the arch shell on both sides of the crown.

Project 3.3 "Shock Loading in Ships from Underwater Bursts and Response of Shipboard Equipment" (ITR-1627), David Taylor Model Basin, Washington 7, D. C.; H. L. Rich, Project Officer.

The objectives of Project 3.3 included (particularly from the standpoint of shock damage to ship machinery and equipment important to ships combat capability): (1) the determination of safe range for delivery of an antisubmarine nuclear weapon by destroyers and submarines; (2) the determination of the intensity and shock motions on a submarine and on a merchantship under quasi-lethal attack from an underwater nuclear explosion; and (3) the acquisition of shock-motion data and the correlation of this data with other measurements and



with theory in order to extrapolate the Hardtack results to other attack geometries and ships.

Four unmanned target ships and three operating ships were instrumented with a total of approximately 325 velocity-time recorders, shock-spectrum recorders, and forty high-speed motion-picture cameras for measurement of shock motions from Shot Wahoo. The unmanned ships were USS Fullam (DD-474), USS Howorth (DD-592), USS Killen (DD-593), and SS Michael Moran (EC-2). Instrumented operating ships were USS Bonita (SSK-3), USS Mansfield (DD-728), and USS Orleck (DD-886).

From Shot Wahoo, complete shock-motion data were obtained on only five of the ships, owing to failure of radio-transmitted starting signals on the DD-474 and DD-592. There was lethal shock damage to main and auxiliary equipment on the SS Michael Moran at a range of [redacted] feet from surface zero, but only minor hull damage. There was only minor shock damage to DD-474, the nearest destroyer, at a range of [redacted] feet. Electronic and ordnance equipment were damaged on operating destroyers at ranges as far as [redacted] feet from surface zero. For ships located more than about 4,000 feet from surface zero, the shock motions produced by a pressure wave reflected from the ocean bottom were more severe than the motions produced by the shock wave transmitted directly from the burst. The operating submarine SSK-3 was safe at periscope depth at a range of [redacted] feet, and would doubtless have been safe at a range of [redacted] feet.

Seven unmanned target ships were instrumented for participation during Shot Umbrella, including DD-474, DD-592, DD-593, SSK-3, and the EC-2, which had previously participated during Shot Wahoo. In addition, Squaw 29, a  $\frac{1}{8}$ -scale short model of the SS-563 class of submarine, was placed in the array and submerged to periscope depth. Some instruments were installed to measure the shock motions of YFNB-12, the instrument barge used for housing recording and control equipment for Squaw 29.

Data were obtained on all targets during Shot Umbrella. There was moderate shock damage to equipment on DD-474 at a range of [redacted] feet, and no significant damage to DD-592, at a range of [redacted] feet. Additional damage occurred to SS Michael Moran at a range of [redacted] feet. Squaw 29, at a distance of [redacted] feet, was within the range of moderate shock damage; but only minor damage occurred on SSK-3, submerged to periscope depth at a range of [redacted] feet.

The following tentative conclusions, with respect to shock damage to machinery and equipment, were drawn from a preliminary examination of the Operation Hardtack data. It should be understood that Shot Wahoo conditions and Shot Umbrella conditions include the yield,

shot geometries, and (to a lesser extent) the bottom-reflection characteristics and water-temperature gradients for these tests:

The minimum-safe range for delivery of an anti-submarine weapon by destroyers is [redacted] feet for Shot Wahoo conditions and [redacted] feet for Shot Umbrella conditions. Damage or malfunction of particularly delicate equipment, e. g., some types of electronic equipment, may occur at greater ranges.

The range for moderate damage for delivery of an antisubmarine weapon by destroyers is between [redacted] and [redacted] feet for Shot Wahoo conditions and less than [redacted] feet for Shot Umbrella conditions.

The minimum-safe range for a submarine is [redacted] feet for Shot Umbrella conditions. For Shot Wahoo conditions, at a range of [redacted] feet at 50-foot depth, the estimated maximum submarine-hull velocity is about 2.5 ft/sec, which is considerably less than the hull-shock velocity necessary to cause significant equipment damage. Therefore, [redacted] feet is a conservatively safe range. Damage or malfunction of particularly delicate equipment may occur at larger distances. It is expected that an estimate of the minimum-safe range can be made in the final report.

The safe range and damage range for submarine and surface targets is determined by shock damage to ship's equipment, rather than by hull damage, for both Shot Umbrella and Shot Wahoo conditions.

Project 3.4 "Loading and Response of Surface-Ship Hull Structures from Underwater Bursts" (ITR-1628), Underwater Explosions Research Division, Norfolk Naval Shipyard, Portsmouth, Virginia; W. W. Murray, Project Officer.

Project 3.4 participated in Shots Wahoo and Umbrella to: (1) determine safe-delivery ranges for surface ships from the standpoint of hull deflections; (2) determine the lethal ranges for merchant ships from the standpoint of hull deflections; and (3) obtain basic information on hull response to provide check points for model tests and for high-explosive tapered-charge tests.

Gages and recording centers were installed in DD-474, DD-592, DD-593, and EC-2, and (for Shot Wahoo only) a barge (YC) in order to document the basic hull response of these surface ships. The gage choice and layout on the target ships was governed by a determination to measure: velocities, displacements, deflections, pressures, strains and rolling and pitching. The total number of gages employed on all ships was about 170. The system used for recording the gages placed primary reliance on magnetic-tape recordings with a frequency response flat up to 10 kc.

Measurements were obtained on the EC-2 and DD-593 during Shot Wahoo, and on the EC-2 and all three DD's during Shot Umbrella. Failures of the EG&G command

timing-signal system led to a complete loss of data during Shot Wahoo on DD-474, DD-592, and the barge. A hull damage survey of the EC-2 was conducted after each shot. Some of the test results secured both from the instrumentation effort and the hull damage survey are presented.

A preliminary examination of the raw data was made. Typical values are given for velocities, displacements, etc., of each of the target ships. The hull damage measured in the EC-2 after each test was slight: The only significant hull deformation was to be found in the attacked side where side-frame deformation amounted to about an inch, and hull-plating deformation to about  $\frac{3}{4}$ -inch.

The following are the tentative conclusions reached by this project. (It should be understood that Shot Wahoo conditions and Shot Umbrella conditions include yield, shot geometries, and, to a lesser extent, bottom reflections and thermal gradient characteristics.)

1. From the standpoint of hull deflection, the safe-delivery ranges for destroyers have been demonstrated to be [redacted] feet under Shot Wahoo conditions and [redacted] feet under Shot Umbrella conditions. No statement can be made at this time, from the viewpoint of hull deflections, concerning the minimum safe-delivery ranges except that they must be considerably smaller than the above values.

2. The lethal ranges for the EC-2, from the standpoint of hull deflections, may be estimated by use of the energy-density rule. The tentative assumption that  $1\frac{1}{2}$ -feet of deformation of the attacked side frames represents a lethal damage leads to the estimate that under Shot Wahoo conditions a horizontal range of [redacted] is lethal, and that under Shot Umbrella conditions a horizontal range of [redacted] is lethal.

3. Check points for small scale UERD model experiments were obtained from both Shot Wahoo and Shot Umbrella. However, no direct correlation with the UERD full-scale high-explosive tapered-charge tests (Project 3.1 of Operation Hardtack) is possible, due to the loss of data on the DD-592 during Shot Wahoo.

4. Basic information on hull response as related to free-field pressures and loading measurements was obtained, which, upon further analysis, is expected to prove valuable in extrapolating the results of Shot Wahoo and Shot Umbrella to other conditions.

Project 3.5 "Loading and Response of Submarine Hulls from Underwater Bursts" (ITR-1629), David Taylor Model Basin, Washington 7, D. C.; H. L. Rich, Project Officer.

Project 3.5 participated during Shots Wahoo and Umbrella in order to: (1) determine the lethal range for nuclear-weapon attack on submarines in shallow water; (2) measure pressures, hull strains, and hull deformations for correlation with theory; and (3)

determine the response of an operating submarine in simulated attack position.

The only submerged target in the ship array for Shot Wahoo was the USS Bonita (SSK-3), which was manned and located a [redacted] yards. The maximum compressional strain observed during the test was  $240 \mu$  in/in, which was well below the elastic limit. It was produced by a pressure wave reflected from the ocean bottom.

For Shot Umbrella, the USS Bonita was not manned, and was located bow-on a [redacted] feet. The maximum compressional hull strain was  $1,160 \mu$  in/in, which approximated the elastic limit. No permanent hull deformations occurred.

The principal submerged target for Shot Umbrella was the Squaw 29, a  $\frac{1}{3}$ -scale model of the SS-563 class submarine, placed a [redacted] feet. This target was heavily instrumented with 23 strain gages, 10 pressure gages, 4 deflection gages, 9 high-speed cameras, and roll, pitch, depth, and flooding indicators. The maximum compressional hull strain observed was  $13,000 \mu$  in/in, which was well above the elastic limit of approximately  $2,000 \mu$  in/in. The peak pressure applied to the hull was 1,150 psi, while the peak pressure in the water just below the Squaw was 1,530 psi. A maximum permanent deformation of at least  $\frac{1}{4}$ -inch in the pressure-hull plating between frames was measured in a preliminary inspection. The hull was plastically deformed, but did not rupture. Four of the 10 external ballast tanks ruptured, and all were seriously dished. This resulted in some loss of buoyancy.

The following conclusions are based on a preliminary examination of Hardtack data. It should be understood that Shot Wahoo conditions and Shot Umbrella conditions include the yield, shot geometries, and (to a lesser extent) the bottom-reflection characteristics and water-temperature gradients for these tests.

A range for moderate hull damage to a Squaw under Shot Umbrella conditions is [redacted] feet, at a depth of 50 feet. In order to estimate the safe or lethal ranges for Shot Umbrella conditions, the pressure field must be known, and an adequate theory correlating the plastic response of a submarine hull to pressure waves of short duration must be developed.

Based on a comparison of static collapse pressure of the hull with estimated applied dynamic pressure of the same magnitude, it is estimated that a safe range for the SSK-3 hull, under Shot Wahoo conditions, is [redacted] feet at a depth of 50 feet. This comparison is conservative and, therefore, is not to be considered the minimum-safe range. A better estimate will be made in the final report.

The SSK-3, under Shot Umbrella conditions a [redacted] foot range and at a depth of 50 feet, was shown to be well

beyond the minimum safe range for hull damage.

**Project 3.6 "Behavior of Deep Reinforced-Concrete Slabs in High-Overpressure Regions" (ITR-1630-1),** Research Directorate, Air Force Special Weapons Center, Air Research and Development Command, Kirtland Air Force Base, Albuquerque, New Mexico, and University of Illinois, Urbana, Illinois; E. H. Bultmann, Jr., Capt, USAF, Project Officer.

The objective of this project was to determine the dynamic behavior of deep (thick) reinforced-concrete slabs in the overpressure region of 175 to 600 psi, and thereby to provide the basis for establishing design criteria for massive reinforced-concrete structures under blast loads. Thirty one-way and fifteen two-way slabs placed flush with the ground surface were tested. The clear span was 6 feet, and the ratios of depth to span varied from 0.15 to 0.78. The test specimens were designed to study flexure strength and shear strength of slabs, both with and without shear reinforcement. The slabs were tested during Shot Koa, where the device yield was tentatively given as 1.4 Mt.

Instrumentation, provided by Project 1.7, included self-recording overpressure gages at each location, and self-recording acceleration gages on the supporting structures. Measurements before and after test were made to determine the magnitude and character of the permanent deformations. Because of excessive radiation at the project locations, data recovery has not been completed. The remainder of the data recovery, which includes removing the slabs from their supports for inspection, will be accomplished as soon as practicable.

No firm conclusions can be drawn from the limited amount of data currently available. However, preliminary results indicate that the resistance of the slabs to high-blast pressures was considerably higher than expected.

**Project 3.7 "Damage to Existing EPG Structures" (ITR-1631),** U.S. Army Engineer Waterways Experiment Station, Vicksburg, Mississippi; W. J. Flathau, Project Officer.

The objectives of this project were to document and evaluate the effects of blast forces, radiation, and water waves resulting from nuclear explosions on various support-type structures and previously exposed test structures located on the various islands of the EPG. The major effort of the project (a joint WES-H&N effort) was concentrated on the early shots, which were expected to yield the most significant information for this project. To cover any supplementary information from the later shots, because the project was to be a minimum effort of funds and personnel, arrangements were made with Holmes and Narver Inc., for the project to receive appropriate additional data from the later shots from the dam-

age survey normally conducted by that organization in the field. This report was submitted upon completion of the early shot effort, and thus before completion of collection of all data and analysis, in order to transmit the available data to interested agencies as soon as practicable.

No electronic recording was utilized; however, self-recording-type measurements of air overpressure and acceleration were made at several stations, along with some measurements of erosion due to water waves. The damage surveys were performed by visual inspection, photographs, and level surveys.

The curve used for predicting air overpressure, the most important parameter in determining blast damage, proved to be reliable. Observed pressure data obtained during this operation correlated well with the prediction curve which was based on data obtained from previous operations.

The curve used for predicting acceleration for floor slabs of structures appeared to give reasonable values. However, limited data was obtained, and the overall reliability of the prediction curve is uncertain.

It was found that a path-of-least-resistance method for predicting radiation within structures proved adequate. The method using the least slant distance did not give realistic values.

Damage to camps (light wood-frame type construction) was investigated. The damage data compared with, and amplified, the data contained in TM 23-200 (Reference 15) pertaining to wood-frame structures. Damage to antennas and radar reflectors also correlated well with data in the referenced manual.

A ground surface 21,000-gallon water tank of  $\frac{1}{8}$ -inch bolted steel plate, 8 feet high and 22 feet in diameter, suffered only light damage when exposed to pressures of 6.5- and 7.0-psi.

Heavily reinforced concrete, earth-mounded structures (walls 5 to 6-feet thick) survived air overpressures up to 450 psi.

Objects located close behind earth mounds, within a distance approximately equal to the height of the mound, received considerable protection from dynamic pressures at overpressures of 35 psi and lower.

Exposed standard 2-inch and 4-inch water pipes, including standard rising-stem valves, survived pressures up to 8 psi without any sign of damage.

**Project 3.8 "Assessment of Ship Damage and Preparation of Targets for Shots Wahoo and Umbrella" (ITR-1632),** Bureau of Ships, Washington 25, D. C.; J. J. Kearns, Project Officer.

The objectives of Project 3.8 included: (1) provision of competent technical and engineering personnel to survey damage occurring to the ship targets; (2) the determination and documentation of damage data from the ship targets and provision of this damage data to Proj-

ects 3.1, 3.3, 3.4 and 3.5; and (3) documentation by target. A related objective was to prepare the ship targets for inclusion in the shot arrays.

Three unmanned destroyers, USS Fullam (DD-474), USS Howorth (DD-592) and USS Killen (DD-593), were taken from the Naval Reserve Fleet and prepared for Shots Wahoo and Umbrella. The starboard-propulsion plants and all associated auxiliaries of these three ships were activated and put in operating condition. Controls were provided for automatic unmanned operation of the activated plants through both tests at 397-rpm shaft speed. Both propellers were removed, and a smooth disk with zero pitch was fitted on the starboard shaft to prevent forward thrust during operation of the ship's machinery. Washdown systems were installed on each of the ship targets to reduce radiological contamination.

An unmanned liberty ship, SS Michael Moran (EC-2), was prepared for the tests by: removal of the propeller; installation of three 60 kw diesel generators for laboratory and service power; reduction of floodable volume by use of flotation drums; installation of solid and water ballast for proper draft; and installation of a washdown system for reduction of radiological contamination.

A submarine, USS Bonita (SSK-3), was prepared for Shot Umbrella by rigging for the placement of concrete clumps (weights) forward and aft, to positioning the ship at a predetermined depth of submergence. Special small-vent valves were installed in the risers from all main ballast tanks for venting the tanks on submergence. To raise the ship, a diver closed these vent valves and blew the tanks by using the ship's high pressure air-bank by means of a special blow valve installed on the superstructure deck. This valve was operated, following the test, by a diver.

Some damage data were obtained on all ship targets; however, the damage was negligible on all but the DD-474 and EC-2. Damage from Shot Wahoo was thoroughly documented, but that from Shot Umbrella has only been done in a cursory manner at the EPG. Complete documentation will be made when ships arrive back at the shipyard.

The following tentative conclusions with respect to shock damage to machinery and equipment were drawn from a preliminary examination of the damage data. It should be understood that Shot Wahoo conditions and Shot Umbrella conditions include the yield, shot geometries, and (to a lesser extent) the bottom-reflection characteristics and water-temperature gradient for these tests.

The minimum-safe range for repeated delivery of an antisubmarine weapon by destroyers is [redacted] feet for Shot Wahoo conditions, and [redacted] feet for Shot Umbrella conditions. The minimum-safe range for single delivery with a shipyard availability soon thereafter, is [redacted] feet for Shot Wahoo and

[redacted] feet for Shot Umbrella conditions.

A safe range for delivery of an antisubmarine weapon from a submarine is [redacted] feet for Shot Umbrella conditions. The safe range for submarine delivery is obviously less than Bonita's [redacted] foot range during Shot Wahoo.

Crippling damage ranges for machinery and equipment in an EC-2 are [redacted] feet for Shot Wahoo conditions, and [redacted] feet for Shot Umbrella conditions.

From the standpoint of ship damage, the safe range for surface ships likely to deliver nuclear underwater weapons in the foreseeable future is determined by shock damage to machinery and equipment, rather than damage to the hull.

#### PROGRAM 4: BIOMEDICAL EFFECTS

Project 4.1 "Effects on Eyes from Exposure to Very-High-Altitude Bursts" (ITR-1633), School of Aviation Medicine, USAF, Randolph Air Force Base, Texas; J. E. Pickering, Col, USAF, Project Officer.

Within the limitations of biologic experimentation in the field, this project successfully explored the problem of limiting distances at which chorioretinal burns might be produced by exposure to very-high-altitude nuclear detonations. Additionally, the physical data obtained, with appropriate scaling factors, will permit the determination of reasonable exclusion radii for different yield devices at various altitudes.

Burns were produced in all animals at all stations where line-of-sight vision obtained. The severity and size of lesion correlated with distance from the burst. On Shot Teak (3.8 Mt at 250,000-foot altitude), minimal chorioretinal burns (0.1 mm or less in diameter) were produced in pigmented rabbits exposed behind plexiglass in an aircraft at 305 naut mi from relative ground zero. It was concluded that comparable burns would occur on the surface at approximately the same distance when viewed with no intervening attenuator (plexiglass).

On Shot Orange (3.8 Mt at 141,000-foot altitude) similar lesions were produced in pigmented rabbits (exposed behind plexiglass at 15,000-foot altitude) at a distance of 225 naut mi from relative ground zero. The limiting-surface distance for comparable lesions in this shot was considered to be 225 naut mi when viewed directly. All retinal burns produced within 160 naut mi from ground zero, if occurring in man, would cause a serious permanent scotoma. For macular involvement, visual acuity would be reduced to 20/100 to 20/200.

Project 4.2 "Effects of Very-Low-Yield Bursts on Biological Specimens (Swine and Mice) (U)" (ITR-1663), Walter Reed Army Institute of Research, Walter Reed Army Medical Center, Washington 12, D. C.; W. H. Moncrief, Jr., Lt Colonel, MC, Project Officer.

During Shots Hamilton and Humboldt, [REDACTED]

[REDACTED] swine placed in a tactical environment were used as a biological target, with immediate lethality as the principal objective. The animals were exposed in three different types of foxholes, M-46 tanks, and M-59 armored personnel carriers at distances where lethal levels of radiation might be expected without complete destruction of the environment. Also included in the experiment was an exposure array designed to extend the data for median dose in 30 days ( $LD_{50-30}$ ) for swine obtained at Operation Plumbbob and also to determine the relative biological effectiveness (RBE), with death as an end point, of neutrons and gamma. The  $LD_{50-30}$  study in swine was supported by a parallel mouse-exposure program to exploit past experience with mice.

Another experiment was designed to evaluate chemical pre-protection with aminoethylisothiuronium (AET) against radiation fluxes. In addition, a technique of neutron dosimetry,  $Na^{24}$  induced activity in blood, was used in the field.

Because of failure of the Hamilton device to give a yield in the range expected, the biological objectives were not obtained.

For Shot Humboldt, with a yield of 5.2 tons, immediate lethality was the only objective. Immediate lethality occurred only at ranges where the environment was destroyed by blast; precise cause of death in the swine exposed could not be determined.

Swine protected from blast and thermal radiation in M-59 armored personnel carriers at 27 yards slant range from Shot Humboldt received doses in excess of 50,000 rads, gamma plus neutrons, and survived in excess of two hours. Four swine were recovered alive from the two-thirds-covered foxholes at 20, 21, 22, and 26 yards, slant range, having received in excess of 7,000 rads, gamma plus neutrons. Doses in all two-thirds-covered foxholes were much less than 50,000 rads, and early death of the swine was primarily due to blast and suffocation. In a normal tactical environment it is probably not possible to achieve doses above 50,000 rads without introducing serious complicating factors due to direct blast or trench collapse.

It appears that measurement of neutron-induced  $Na^{24}$  activity in the blood is a feasible method for estimating the neutron dose received.

Project 4.3 "Temporary Visual Impairment (Dazzle) of Combat Personnel from Very-Low-Yield Bursts" (WT-1664), Headquarters U. S. Continental Army Command, Fort Monroe, Virginia; R. H. Verheul, Col, Inf, USA, Project Officer.

The general objective of Project 4.3 was to evaluate the dazzle effect on unprotected combat personnel at a minimum safe distance from Shot Hamilton, a fractional-kiloton nuclear detonation.

The experimental procedure required personnel of three test groups, who were oriented at 90, 135 and 180 degrees away from ground zero at a distance of 5,700 feet, to determine and record visual acuity immediately following the shot and, in rapid sequence, form and color perception of test objects at successively greater distances from the groups. The results showed no significant degradation of vision from dazzle under the conditions of this study.

From review and analysis of previous studies of dazzle and dark adaptation, it is concluded that loss of combat effectiveness as a consequence of dazzle will not constitute a major hazard for combat personnel.

#### PROGRAM 5: EFFECTS ON AIRCRAFT STRUCTURES

Project 5.1 "In-Flight Structural Response of a B-52 Aircraft to Side Loading from Nuclear Detonations" (ITR-1634), Wright Air Development Center, Wright-Patterson Air Force Base, Dayton, Ohio; W. R. Lounsbury, Captain, USAF, Project Officer.

The primary objective was to determine the structural response of the B-52 aircraft when subjected to side loads imposed by blast effects from nuclear explosions in order to verify the delivery capability of the aircraft for multiple-delivery tactics.

The test aircraft was a production model B-52D, with the exception of modifications to ensure that secondary items would not be a limiting factor in the test series; also, certain items of equipment not essential to the tests were deactivated or removed. The aircraft configuration was similar to the test aircraft used during Operation Redwing, with the exception of the addition of full 3,000-gallon external wing fuel tanks.

In instrumenting the B-52D (AF56-591) the principal emphasis was on measurement of blast inputs and aircraft structural responses to blast-induced loads. The blast inputs associated with the shock wave were determined from overpressure transducers located at a number of positions on the aircraft. Aircraft structural responses to the blast were recorded from the response of calibrated strain-gage circuits located along the span of the left and right wings, on the left and right stabilizers, on the fin, and on the aft body. Supplemental data was obtained from stress and acceleration measurements. The aircraft was also instrumented to record thermal input and thin-skin temperature responses.

To accomplish the objective of the program, the aircraft was exposed to blast effects that approached the aircraft from various orientations. The aircraft orientation was varied by the selection of bearing angles from the aircraft to the point of burst (measured from the aircraft nose) of 35, 90, 125, 150, and 180 degrees. Test missions were flown at altitudes of 25,000 to 30,000 feet, and the horizontal distance from the point of detonation



was selected to give the desired aircraft responses.

The spatial location of the aircraft was determined on the basis of structural responses predicted from an analytical study of the calculated gust response of the aircraft. Positioning methods were modified as the response data from successive shot participations became available.

Actual positioning of the B-52 relative to the detonation was accomplished by the use of the aircraft bombing-navigation system (BNS) or by a ground-radar tracking system (MSQ).

During the side-load evaluation, the airplane was exposed to and data were recorded from a total of ten "successful" nuclear detonations. Preliminary measured yields of the devices ranged from 200 kt to 9.5 Mt. All test missions flown were successful from an operational and positioning standpoint; however, three tests in which the B-52 participated, in addition to the ten mentioned above, were considered unsuccessful because of yields that were much lower than predicted.

There was no evidence of damage from thermal energy or blast effects as a result of participations in the side-loading program. The B-52D capability was successfully demonstrated for structural responses up to 73 percent of allowable limit on the wing, 103 percent on the horizontal stabilizer, 94 percent on the fin, and 65 percent on the fuselage and for 100 percent of the allowable overpressure. These comprise the primary considerations in defining the nuclear-weapon-delivery capability of the aircraft. Complete analysis and application of the data obtained will permit verification of the delivery capability of the B-52D for multiple-delivery tactics.

Project 5.2 "In-Flight Structural Response of A4D-1 Aircraft to Nuclear Detonations" (ITR-1635), U. S. Naval Air Special Weapons Facility, Kirtland Air Force Base, Albuquerque, New Mexico; P. A. Anderson, LCDR, USN, Project Officer.

Two A4D-1 airplanes were used by Project 5.2 in order to: (1) measure the structural response of the A4D-1 aircraft when subjected to the effects of high-yield nuclear detonations; (2) measure the effects input; and (3) correlate the response and input data obtained by this project with the data obtained from the A4D-1 participation in Operation Plumbbob to define and verify the high-yield (megaton-range) weapon delivery capability of this aircraft.

With dual airplane participation, the general procedure was to place one airplane at as low an altitude as possible (to a minimum of 3,000 feet) and the other airplane at a higher altitude. The aircraft were positioned to obtain the desired predicted inputs and, where possible, mission speed, test altitude, and paint color of critical surfaces were varied in order

to obtain as high a response level as possible at both the times of detonation and of shock arrival. Positioning was accomplished by the use of a modified M-33 gun-tracking radar. Each airplane had separate radar control. In all cases, the airplanes were in straight-and-level flight with the tail toward the detonation at both time zero and time of shock arrival. Instrumentation was installed to obtain the overpressure and thermal inputs and the aircraft response to these inputs.

Project 5.2 participated during eight shots. With dual aircraft participation for each shot, this gave sixteen successful test participations. The altitudes were all comparatively low, ranging from 3,000 to 11,000 feet. Aircraft orientation angles to the detonation ranged from 8.7 to 84.9 degrees at time zero and 4.9 to 60.3 degrees at time of shock arrival. The overpressures measured ranged from 0.333 to 2.69 psi.

During the course of the tests, the aircraft experienced the following maximum inputs and responses: overpressure, 2.69 psi; temperature rise, 229 F; maximum temperature, 297 F; maximum wing-bending moment, 1,190,000 in-lb; percent allowable wing-bending moment, 54; and incremental load factor at the center of gravity, 3.71.

From the participation of Project 5.2, the following can be concluded: (1) The data obtained from Operations Hardtack and Plumbbob, when combined with the aircraft-performance characteristics, will permit a definition of the delivery capability of the A4D airplane. (2) The correction applied to the thermal radiation calculation for orientation to the fireball of a surface burst may be nonconservative. (3) In resolving the direct radiant exposure to its vertical component, the actual orientation angle gave good correlation with the measured results. (4) The scattered radiation phenomena will require further study. (5) The methods of calculating free-stream overpressure gave good correlation with the measured results if a conservative factor of 10 percent was applied to the basic curve. (6) The methods for calculating the time of shock arrival gave excellent correlation with the measured values. (7) The theory developed to predict the aircraft structural response gave good correlation with the measured results. (8) Satisfactory wing chordwise-pressure-distribution data were obtained. The data are sufficient that, from a careful analysis, the separate effects of overpressure propagation and gust velocity approaching from the trailing edge can be obtained. (9) The method of obtaining the heat-transfer coefficient by means of the boundary-layer shear-stress probes appears promising.

Project 5.3 "In-Flight Structural Response of FJ-4 Aircraft to Nuclear Detonations" (ITR-1636), U. S. Naval Air Special Weapons Facility, Kirtland Air Force

Base, Albuquerque, New Mexico; M. A. Esmiol, Jr., LCDR, USN, Project Officer.

The objectives of Project 5.3 were to: (1) measure the effects input and structural response of the FJ-4 aircraft when subjected in flight to the effects of high-yield nuclear detonations; (2) correlate the data obtained with that data obtained from the FJ-4 participation during Operation Plumbbob; and (3) define and verify the Class D delivery capability of this aircraft.

Radiant exposure, nuclear radiation, and overpressure were the phenomena limiting the proximity of the test aircraft to the detonations. Positioning an aircraft for the collection of data was accomplished by the use of a race-track flight pattern with the final leg traversing surface zero so that the aircraft was tail-on or directly over the detonation point at time of shock arrival. The primary positioning equipment was the same as that used during Operation Plumbbob, modified M-33 gun-tracking radars on the ground with X-band radar beacons in the aircraft to insure positive lock-on.

A variety of instrumentation, including calorimeters, radiometers, strain gages, pressure transducers, thermocouples, film badges, and oscillographs, was used to measure and record the inputs and responses.

Each of two aircraft participated in eight surface shots with yields ranging from 14.6 kt to 1.5 Mt. Maximum weapon effects and responses measured were: 37.0 cal/cm<sup>2</sup> measured normal radiant exposure, 50.6 cal/cm<sup>2</sup> measured direct radiant exposure, 2.50 psi overpressure measured on the aircraft fuselage, and 64.7 percent of limit allowable stress at the critical wing station. Test conditions varied from 4,000 to 16,000 feet in altitude and from 9,100 to 24,000 feet in slant range at time zero. Elevation angles of the aircraft at shock arrival varied from 6 to 88 degrees. The only damage sustained during the tests was non-structural, consisting of scorching of paint and miscellaneous seals during Shot Walnut.

The following are considered to be the most significant of the conclusions made from preliminary analysis of the test data: (1) Effect inputs and structural responses were measured on the FJ-4 aircraft when subjected in flight to yields up to 1.5 Mt. (2) Although correlation of the data obtained from Hardtack with that previously obtained during Plumbbob must await more complete analysis and review, no major difficulties are anticipated. Extension of thermal and overpressure limitations were possible during Hardtack, due to Plumbbob experience and analysis, and an improved structural dynamic response analysis was developed and utilized, which was based upon the Plumbbob results. These factors tend to prove the compatibility of the respective data. (3) In conjunction with the data obtained from Plumbbob, blast, thermal, and structural response data have been obtained over

a sufficiently wide range of yields and incidence angles to permit subsequent definition of the Class D delivery capability of FJ-4 model aircraft. (4) All of the methods for predicting maximum temperature rise of the aircraft structure using measured radiant exposure gave good correlation with the measured maximum temperature rises. However, the methods for predicting radiant exposure are conservative. (5) The theoretical dynamic response analysis has been verified within the range of the test conditions by the accurate prediction of the most critical stress level within the airframes on sixteen test flights. (6) The correlations obtained justify the use of the present thermal and dynamic response prediction methods in future delivery-capability studies of similar aircraft.

#### PROGRAM 6: TESTS OF SERVICE EQUIPMENT AND MATERIALS

Project 6.3 "Effects of Nuclear Radiation on Electronic Fuze Components and Materials (U)" (ITR-1637), Diamond Ordnance Fuze Laboratories, Washington, D. C.; Edward E. Conrad, Project Officer.

The objectives of this experiment were to: (1) expose electronic component parts and materials used in ordnance electronic-fuze circuitry to the same radiation environment that will be experienced by the various fuzes when they are tactically operated or stored in the vicinity of a nuclear detonation; (2) perform measurements on these component parts and materials before, during, and after a detonation; and (3) evaluate the behavior of an operating captive typical guided-missile (Corporal) fuze system when exposed to the same radiation environment as the individual electronic component parts.

Transistors, electron tubes, solid-state diodes, resistors, capacitors, and an epoxy encapsulating resin were exposed to neutron doses ranging from 10<sup>12</sup> to 4 × 10<sup>14</sup> neutrons/cm<sup>2</sup> and gamma doses ranging from 10<sup>4</sup> r to greater than 10<sup>5</sup> r.

It was found that some transistor parameters underwent transient changes greater than 84 times their initial value without ensuing permanent damage.

Vacuum tubes exhibited changes in plate current of up to 120 percent for periods of 200 μsec after a detonation. Gas diodes, when biased as much as 70 percent of their firing voltage, reliably fired at distances up to 4,500 feet from ground zero in a detonation of 20 kt.

The reverse resistance of a silicon-alloy-junction diode fell to less than a tenth of its normal value.

Resistors exhibited decreases in resistance which ranged from 10 to greater than 20 percent for periods of 1 msec.

All capacitors tested showed increases in capacitance and dissipation factor which ranged from zero to 13 percent for periods of 10 msec.

The Corporal fuze system exhibited transient disturbances that indicate a strong possibility of firing when it was exposed to a neutron dose as low as  $10^{12}$  neutrons/cm<sup>2</sup> and a gamma dose as low as  $10^4$  r. This occurred at a distance of 2,000 feet from a detonation of approximately 20 kt.

Project 6.4 "Wave Form of Electromagnetic Pulse from Nuclear Detonations" (ITR-1638), U. S. Army Signal Research and Development Laboratory, Fort Monmouth, New Jersey; F. Lavicka, Project Officer.

The objective was to obtain and analyze the wave form of the electromagnetic pulse resulting from nuclear detonations. Broad-band measurements were made over the frequency range from 0 to 10 Mc. Two sites were used: Kusaie, 460 miles from Bikini and 420 from Eniwetok; and Wotho, 100 miles from Bikini and 240 from Eniwetok.

The measurements were not designed to be radically new. Although improvements in equipment were incorporated wherever possible, the primary concern of this project was to increase the cataloging of electromagnetic-pulse wave forms. The additional signature information is expected to be useful in the Pin Point system.

Measurements were made during Shots Yucca, Cactus, Fir, Butternut, Koa, Holly, and Nutmeg. Signals were picked up by short whip-type antennas and fed via cathode followers and delay lines to high-frequency oscilloscopes. Photographs were taken at five sweep time bases: 0.2, 0.25, 1, 2, and 10  $\mu$ sec/cm.

The shot characteristics were compared to the actual wave-form parameters.

The data is in good agreement with that obtained during Operation Redwing.

Project 6.5 "Radar Determination of Fireball Phenomena" (ITR-1639), U. S. Army Signal Research and Development Laboratory, Fort Monmouth, New Jersey; E. Baker and T. Viars, Project Officers.

The objectives of this project were to: (1) determine whether radar echoes can be received from the fireball produced by nuclear detonations; (2) investigate the nature of these echoes, if received; and (3) determine the feasibility of determining ground zero, height of burst, and yield, by using ground radar.

Radar observations of nuclear burst had been made during a number of earlier tests; however, information on detection of radar echoes from the fireball itself was lacking.

Operations were conducted on Eniwetok and Rongelap Atolls and on U. S. Navy destroyers located at known distances from Johnston Island.

Radar Sets AN/MPG-1 and SCR-584 were used at Eniwetok and Rongelap and Radar Set SRb on the Navy destroyers. The B-scope presentations of the AN/MPG-1 were photographed by motion-picture cameras. PPI and A-scope presentations of the SCR-584 were photographed by means of Automax Camera Model GIR and Dumont Type 321 strip camera, respectively. The SRb scope presentations were photographed using a Fairchild Model 015 camera with a specially-designed mount.

Data was obtained for Shots Butternut, Koa, Wahoo and Teak. Radar signals were obtained from the surface and underwater shots, beginning shortly after time zero, and were still visible as late as H+5 minutes. It appears that these returns were caused by water vapor, interaction of the shock front with the surface, and the water wave, rather than by the fireball. However, the radar returns received from Shot Teak were of short duration and did not appear until about H+1 minute, which indicates initial absorption, followed by reflection from the region of high-electron density caused by the fireball.

Although there are problems relative to the use of ground radar for determining the location and yield of nuclear bursts, the data obtained from the low-altitude shots of Operation Hardtack indicate that this objective is feasible. Due to the inability of this project to participate fully with the SRb radar in the Johnston Island high-altitude tests, it appears that insufficient data was obtained to completely satisfy the objectives of radar detection and examination of a fireball produced by a nuclear burst.

Project 6.6 "X-Band Radar Determination of Nuclear-Cloud Parameters" (ITR-1640), U. S. Army Signal Research and Development Laboratory, Fort Monmouth, New Jersey; C. W. Bastian, Project Officer.

The objective of Project 6.6 was to make observations with Radar Set AN/CPS-9 in order to determine what parameters of an atomic detonation are detectable with X-band radar. Previous radar observations of atomic clouds had been made during Operations Greenhouse, Redwing and Plumbbob.

Equipment was located at Eniwetok, Rongelap, and Kwajalein; the console was mounted in a V-51 van with a small photographic darkroom; and a second V-51 van was used as the communications, repair shop, and logistics van. The Eniwetok radar was used in the existing fixed-station equipment of the Air Weather Service. The AN/CPS-9's were modified to give range height indicator (RHI) scales of 150,000 and 300,000 feet, in addition to the normal 50,000-foot height, and also to allow surveillance to ranges of approximately 400 miles.

The data was reduced with the aid of a microfilm viewer, and enlarged prints of the film recordings.

A surface burst of a megaton device was observed



at a maximum range of 200 miles with the AN/CPS-9. The rate of rise, rate of growth, maximum height, maximum diameter, and range and azimuth were detected with X-band radar of shots of different yields at different ranges. A number of comparisons were made, and the results presented in the forms of graphs and photographs.

Three observations were made of high-altitude shots. No radar returns were received by any of the AN/CPS-9 stations at detonation time or thereafter, except in the case of Shot Orange. The echo observed at the Johnston site at the detonation time of Shot Orange was attributed to the appearance of the Redstone missile in the beam of the antenna, prior to detonation time.

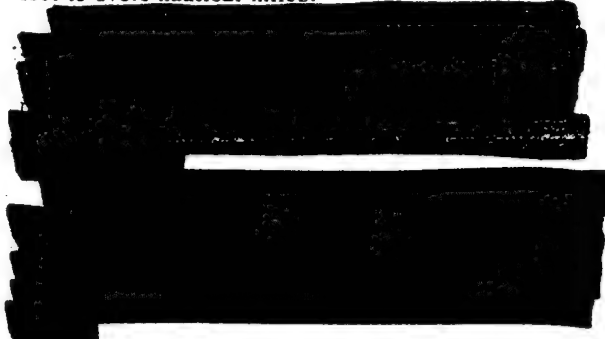
Project 6.7 "Naval Mine Field Clearance by Underwater Bursts" (ITR-1641), U.S. Naval Ordnance Laboratory, White Oak, Silver Spring, Maryland; G. M. Davidson, Project Officer.

A field of 120 naval mines, consisting of Marks 25-2, 39-0, 50-0, 52-1, 52-2, 52-3, and 52-6, was laid due north of surface zero for Shot Umbrella in order to study the feasibility of clearing a mine field with shallow-water kiloton-range nuclear bursts. The mines were planted at distances from surface zero ranging from 1,400 feet to 8,100 feet. The operation of 23 of the mines, planted at distances greater than those at which damage was expected, were monitored during the shot by means of a system of internal recorders designed to begin recording when the mines were armed and to continue recording until the mines were recovered. The depth of water at the mine field varied between 120 and 150 feet. The results of the test indicate that 100 percent clearance of mines may be expected at distances of less than 1,600 feet from ground zero for weapons comparable in yield to the Umbrella device. At distances between 1,600 feet and 2,000 feet, 67 percent of mines Mark 25-2 suffered component damage sufficient to render the mines inoperative. At distances between 2,000 and 2,800 feet, 43 percent of mines Mark 25-2 suffered component damage sufficient to render the mines inoperative. The probability of clearing mines by actuations produced by kiloton-range nuclear detonations at distances greater than those at which damage occurs was found to be extremely low for all mine types.

Project 6.8 "Feasibility of Wide-Area Clearance of Naval Influence Mines by Nuclear Weapons" (ITR-1642), U.S. Navy Mine Defense Laboratory, Panama City, Florida; R. E. Lee, LCDR, USN, Project Officer.

Measurements of mine-actuating influences (pressure, magnetic, and acoustic) generated by Shot Umbrella were recorded to obtain information on the feasibility of using nuclear weapons for wide-area

mine clearance by influence means. Instrumented mines, Mark 25 Mod 0, 25 Mod 2, 36 Mod 2, and 50 Mod 0, were monitored to determine the effect of the influences generated on the mine mechanisms. Influence and mine-reaction data were obtained at each of three platforms located in Eniwetok Lagoon. Mine-reaction data was obtained from Shots Wahoo, Yellowwood, Tobacco, Sycamore, and Umbrella. Preliminary yields of the shots varied from 10 kt to 343 kt. Ranges from surface zero varied from 3,290 feet to 173.5 nautical miles.



This report is based primarily on go-no-go data. Before the full significance of the data with respect to mine countermeasures can be realized, the influence measurements, together with the mine-reaction data obtained, will require additional reduction and analysis. A thorough reduction and analysis of the influence data obtained is planned for the final report.

Project 6.9 "Effects of Nuclear Detonations on the Ionosphere" (ITR-1643), U.S. Army Signal Research and Development Laboratory, Fort Monmouth, New Jersey; B. D. Jones, 1/Lt, USA, Project Officer.

The original objectives of this experiment were to determine the effects of very-high-altitude, large-yield nuclear detonations on the ionosphere and on signals propagated via the ionosphere. However, the location of the shots (Teak and Orange) was so changed that it was not possible to obtain suitable project sites. Therefore, the original objectives no longer applied, and the experiment became an attempt to increase the store of knowledge about ionospheric effects of large-yield ground-level detonations (using the sites that had already been instrumented for Shots Teak and Orange).

To accomplish the original objectives, two ionosphere recorders had been installed, one at Kusaie and one at Wake (1,600 km apart), so located that the great-circle path between them lay nearly along a meridian and with a midpoint about 100 km northwest of Bikini Atoll. Attempts to operate the two recorders synchronized for oblique-incidence-propagation data proved unsuccessful, due to malfunctioning of the synchronizers. Ionospheric observations were then made



at vertical incidence only. However, no useful data was obtained at Wake, due to failure of three generators. Recordings of vertical data were made as the frequency was swept through the range from 1 to 25 Mc each 15 seconds.

At Kusaie, to the south of the detonations, effects were observed for Shots Fir and Koa that were very similar to those obtained during Operation Redwing at the same site. The average velocity from shot time until the arrival of the first disturbance overhead was again found to be 20 km/min. A second disturbance, with an indicated velocity of about 13 km/min, also was observed again.

Project 6.10 "Ionization Produced by Very-High-Altitude Bursts (U)" (ITR-1644), Geophysics Research Directorate, Air Force Cambridge Research Center, Air Research and Development Command, Laurence G. Hanscomb Field, Bedford, Massachusetts; George J. Gassmann, Project Officer.

The objective of Project 6.10 was to investigate the ionization and associated effects of nuclear detonations at high altitude. The project participated in Shots Teak (3.8 Mt at 250,000 feet) and Orange (3.8 Mt at 141,000 feet).

Two ionospheric recorders were used, one (Type C-4) on Sand Island and the other (Type C-3) aboard a C-97 aircraft. Also on the aircraft was magnetometer (sensitivity  $\pm 10\gamma$ ) and an all-sky camera with a field of view of 165 degrees. Radio receivers tuned to 9, 15, and 20 Mc frequencies were used, both on the aircraft and Sand Island to monitor field strengths of signals sent from Oahu.

On Oahu, receivers recorded field strengths of signals from Kwajalein, Christmas Island, and Guam.

[REDACTED]

The all-sky camera recorded visual phenomena on both shots. On Shot Teak, it showed an expanding luminescent reddish sphere which passed over the aircraft, 110 miles from ground zero, about one minute after the shot. The air-borne magnetometer did not record either long- or short-term variation of the earth's geomagnetic field on either Shot Teak or Shot Orange.

Project 6.11 "Effects of Very-High-Altitude Bursts on Radio-Wave Reflection and Attenuation (U)" (ITR-1645), Stanford Research Institute, Menlo Park, California; L. T. Dolphin, Project Officer.

The objective of this project was to measure the absorption and induced-ionization effects of high-altitude nuclear detonations with an aim to resolving the anticipated problems of high-power ICBM detection radars.

Five special radars encompassing the frequency range from approximately 10 to 1,000 Mc (in five discrete frequencies) were constructed, installed, and tested in the 125-foot M/V Acania. Arrangements were made for simultaneous operation with as much flexibility as possible. Each of the two lowest frequencies employed steerable Yagi antennas and the upper three frequencies were operated simultaneously in a steerable 30-foot-diameter parabolic reflector.

Riometers were operated at three locations: Johnston Island, Wheeler Air Force Base, Oahu, Territory of Hawaii, and French Frigate Shoals. These devices essentially provided a constant measure of the integrated cosmic noise from overhead. Since the cosmic noise pattern is constant from one day to the next, it is possible to detect absorption to an accuracy of better than  $\pm 1$  db, by noting depressions in the record. Three frequencies are generally used at each site (30, 60 and 120 Mc) to enable absorption to be measured over a wide range.

A number of lesser experiments were included: (1) monitoring of Explorer IV satellite for telemetered GM tube and scintillation-counter counts and, (2) operation of K-band and X-band radiometers pointed at shot zero (by EG&G). All of this equipment was operated at EPG prior to Shots Teak and Orange.

No echoes or serious perturbations were observed from Shot Yucca at EPG with the Acania located at Wotho Atoll, although marked absorption was obtained with a riometer located at Eniwetok.

Echoes from the rising cloud and the resulting aurora were observed during Shot Teak. Serious absorption was observed at Johnston Island for hours after the shot, and lesser absorption was observed at French Frigate Shoals, and Wheeler Air Force Base, Territory of Hawaii.

Shot Orange gave numerous echoes long after the shot, although the effects appeared to be less than those of Shot Teak. Absorption shown by the riometers at Johnston Island lasted several hours.

Excellent satellite recordings were made, but analysis of the recordings has not been completed.

A burst of noise was observable from the above shots, and from many surface shots at EPG by the K- and X-band radiometers.

Increasing the altitude of the shot appeared to radically increase the ionization and absorption effects observable in the 10-to-1,000 Mc region. Shot Teak, (and to a lesser extent, Shot Orange) strikingly resembled a man-made auroral display, observable both visually and with radio equipment, not unlike the natural

aurora which has been studied by the same techniques in Alaska.

When altitudes such as those of Shot Teak are reached, considerable high-frequency communication blackout occurs. Furthermore, absorption, on the order of minutes, occurs near the shot at even ultra-high-frequencies. Clutter from shot-caused aurora would also be of concern to a radar operating in the vicinity.

Project 6.12 "Effects of Very-High-Altitude Bursts on Pulsed Electromagnetic Transmissions (U)" (ITR-1646), U.S. Army Signal Research and Development Laboratory, Fort Monmouth, New Jersey; S. E. Bania, Project Officer.

The objective of Project 6.12 was to investigate the extent and nature of the attenuation of radio frequency transmissions through the ionized region produced by a high-altitude nuclear detonation.

Radio-frequency transmissions through the ionized region were accomplished by placing transmitters above burst altitude with Nike Cajun rockets and receiving the emissions at ground stations. Four receiver stations were equipped to record transmissions through the Teak and Orange fireballs; one on Johnston Island; one on each of two ships located on an azimuth of 020 degrees True, at distances of the order of 75 and 150 naut mi; and one near the summit of Mt Haleakala, Maui, T. H., approximately 715 naut mi from Johnston Island.

The rocket-launcher site at Johnston Island was capable of firing six Nike-Cajun sounding rockets, each of which contained L and S band-pulse-carrier-radio transmitters. The launchings were controlled from the Johnston Island receiving station.

Each receiver station contained L- and S-band receiving equipment and recording equipment. The Johnston Island and Maui stations were equipped to record the received signals on strip paper, film, and magnetic tapes. The two ship stations recorded signals only on paper and magnetic tape.

For Shot Teak, two rockets were fired. The first rocket was to be at apogee at burst time. However, its transmitter failed, prior to burst. Since the second rocket was not fired until after burst, data was not obtained at burst time. Signal records were obtained at Johnston Island, Maui, and on one ship. The Johnston Island record began 55 seconds after burst, and lasted about 3.5 minutes. It showed definite changes in transmission, when compared with similar recordings taken during rehearsal rocket firings.

Six rockets were launched during Shot Orange. The first rocket was approximately at apogee at burst time. One minute after burst, the second rocket was launched. The remaining rockets were fired singly at intervals of several minutes. Data was recorded at all sites through-

out the entire period of transmission. Preliminary review of the records obtained from the ship stations showed that signal attenuation occurred as the rocket entered the ionized region near the burst. The Johnston Island recordings showed violent changes in signal, although the signal was not completely lost. The Maui station recorded small groups of amplitude-signal bursts during the Nike-Cajun launchings.

It is concluded that signals are attenuated, although not to the extent that prior theoretical calculations predicted. More definite conclusions cannot be drawn before the data is thoroughly reduced.

Project 6.13 "Effects of Very-High-Altitude Bursts on Air-Borne Radar (R)" (ITR-1659), Lincoln Laboratory, Massachusetts Institute of Technology, Lexington, Massachusetts; V. L. Lynn, Project Officer.

The high-altitude, high-yield detonations, Shots Teak and Orange, were observed using two UHF, air-borne radars. In addition, the aircraft were instrumented for rocket-borne beacon reception and noise observations. The radar of lower frequency (425 Mc) detected strong returns from both bursts for a period slightly under an hour. The other radar (675 Mc) received returns from both shots, but substantially weaker and of shorter duration. Stronger returns were received from the lower-altitude shot (Orange) at both frequencies. In each case, the development of the returns on the PPI scopes indicated three separate periods. Little or no return was observed for a period of the order of a minute. Thereafter, the return built rapidly to strong signals over a wide area that took an oval shape oriented in the north-south direction. This period lasted for several minutes. The final period was characterized by breaking and fading of the return, and sporadic, weak or medium returns from an area oriented along an east-west line somewhat to the north of the actual burst point.

A missile-borne beacon of Project 32.3 was received on 222 to 224 Mc, and a blackout effect for a few tens of seconds was observed on each shot. No noise effects were observed at the higher frequencies, but minor changes were noted at lower frequencies.

Project 6.14 "Proof Test of AN/TVS-1 (XE-3) Flash-Ranging Equipment" (ITR-1661), U.S. Army Signal Research and Development Laboratory, Fort Monmouth, New Jersey; G. D. Scarborough, Maj, USA, Project Officer.

This project participated in Shots Mora, Quay, Lea, Hamilton, Dona Ana, Rio Arriba, Wrangell and Socorro of the NTS phase of Operation Hardtack. The objective was to evaluate the Peerless flash-ranging set, prior to its acceptance by USASRD. Consistent, reliable operation was obtained at 18 miles from burst. This distance was the maximum line of sight range that was

available for a suitable observation point. Two types of automatic shutter-activators (components of AN/TVS-1) were tested with equally good results. Camera settings of f:32 at 1/200 second were used exclusively, and a selected neutral density filter was employed for best image definition. Specific recommendations as to best filter usage for various ranges and yields can be made following further data analyses and will be included in the WT report.

Project 6.15 "Electromagnetic Pulse Measurements of Low-Yield Bursts" (ITR-1662), U. S. Army Signal Research and Development Laboratory, Fort Monmouth, New Jersey; G. Cantor, Project Officer.

This project participated in Shots Valencia, Mora, Tamalpais, Quay, Lea, Hamilton, Logan, Dona Ana, Rio Arriba, Socorro, Wrangell, and five one-point safety test shots.

Data was collected to verify a method for estimating yields and to analyze the wave form of the electromagnetic pulse radiated from a nuclear detonation. A component of the detonation locator central AN/GSS-5 (XE-1) was also evaluated. Measurements were made over a frequency band of 0 to 10 Mc at a range of about 100 miles.

In each of the three systems employed in this operation, the method of detection consisted of a probe antenna located on the roof of the instrument trailer. The roof was used as the ground plane and was physically grounded to the earth. The probe was coupled to oscilloscope inputs through an impedance-matching device, a cathode follower receiver. The output of the cathode follower was fed through a delay line to oscilloscopes. A photographic record was made of the data presented in the oscillograms.

The only data recorded was obtained from three aboveground, kiloton-range nuclear detonations. The opportunity to observe electromagnetic pulses from very-low-yield and underground shots was lost because of thyatron-emitted pulses and a high ambient noise level. Located in an area adjacent to electrical power transmission lines, the average noise level, a combination of sferics and man-made sources, was higher than encountered in previous tests. This limited the usable trigger level to about 0.1 v/m.

The equipment used proved to be adequate for the recording of known shot-time detonations in the kiloton range.

#### PROGRAM 8: THERMAL RADIATION AND EFFECTS

Project 8.1 "Effects on Materials of Thermal Radiation from Nuclear Detonations" (ITR-1647), Naval Material Laboratory, New York Naval Shipyard, Brooklyn 1, New York; W. L. Derksen, Project Officer.

The objective of Project 8.1 was to determine the radiant exposure, in calories per square centimeter, at each of Project 4.1's stations during Shots Teak and Orange. In addition to this information, Project 8.1 obtained some information on the variation of irradiance with time during the shot, and on the probability of burns of human skin at the Johnston Island station.

The instruments used for the radiant exposure measurements were flat copper calorimeters of a type used successfully in a number of previous weapon tests by Project 8.1 personnel and others. For the time-variation of irradiance, photocells with maximum spectral response at 0.8 micron were used. Skin-simulant assemblies developed by the Naval Material Laboratory were used for determining the probability of human skin burns at the Johnston Island station.

Only the radiant-exposure measurements have been reduced for the ITR. The reduction of the remainder of the measurements will be left for the WT report, because of the necessity of further laboratory measurements. The WT will also include a study of the attenuation and scatter of the thermal radiation by the atmosphere.

During Shot Teak, all of the stations except the USS Hitchiti had a clear line of sight to the fireball. The results for each station were as follows: Johnston Island, 1.2 cal/cm<sup>2</sup>; USS DeHaven, 0.27 cal/cm<sup>2</sup>; USS Cogswell, 0.066 cal/cm<sup>2</sup>; USS Hitchiti, 0.0007 cal/cm<sup>2</sup>; and C-97 aircraft, 0.015 cal/cm<sup>2</sup>.

During Shot Orange, only stations USS Epperson and C-97 had a clear line of sight. The results for each station were: USS Boxer, 0.07 cal/cm<sup>2</sup>; USS Epperson, 0.075 cal/cm<sup>2</sup>; USS DeHaven, 0.007 cal/cm<sup>2</sup>; and C-97 aircraft, 0.0035 cal/cm<sup>2</sup>.

Project 8.2 "Thermal Radiation from Very-High-Altitude Bursts" (ITR-1648-1), Air Force Cambridge Research Center, Laurence G. Hanscom Field, Bedford, Massachusetts; R. M. Brubaker, Maj, USAF, Project Officer.

The objective was to measure, analyze, and report on thermal radiation resulting from the detonation of a nuclear device at a very-high altitude. Measurements were made during Shot Yucca, a balloon-borne device detonated at 85,250 feet.

To measure thermal radiation as a function of time, wave length, and distance, two RB-36 aircraft and three canisters were instrumented with spectroscopic thermal-radiation detectors.

Each of the aircraft carried spectrally flat thermal-radiation detectors covering the range from 2,000 to 10,000 Å in four bands, a bolometer to measure the total thermal radiation, gun-sight-aiming-point (GSAP) cameras with spectroscopic nosepieces, and a Traid camera with a spectroscopic nosepiece. The data were

recorded on fourteen-channel magnetic-tape recording systems.

The three canisters were spaced at predetermined intervals on the instrument dragline of the balloon. Each canister was instrumented with spectroscopic thermal-radiation detectors similar to those in the aircraft and, in addition, carried a radiometer to measure total thermal radiation. A six-channel magnetic-tape recording-and-playback system was employed in each canister to store the data for delayed transmission by a very-high-frequency (VHF) transmitter to a ship-based frequency modulation (FM) telemetry receiving station.

A complete set of data was obtained from the aircraft instrumentation from which the irradiances and times of maxima and minima have been computed for each wave-length range and for total thermal radiation. Total energy at the aircraft was approximately 50 mwatt-sec/cm<sup>2</sup> with about eight percent of this being emitted before minimum. A power surge disabled the ship-based command transmitter, which was required to initiate the canister recorder and playback systems; therefore, no data were received from this instrumentation. A VHF ionization blackout, beginning at zero time and lasting approximately 4 seconds at the nearest canister, prevented any direct transmission of thermal-radiation data.

Project 8.2 (Supplement) "Thermal Radiation from Very-High-Altitude Bursts (A)" (ITR-1648-2), Air Force Cambridge Research Center, Laurence G. Hanscom Field, Bedford, Massachusetts; R. M. Brubaker, Maj, USAF, Project Officer.

The objective was to measure and analyze thermal-radiation phenomena resulting from the detonation of thermonuclear devices at very-high altitudes. Measurements were made during Shots Teak and Orange, both missile-borne nuclear warheads. Teak was detonated at 250,000 feet, and Orange was detonated at 141,000 feet.

To measure the thermal radiation as a function of time, wave length, and distance, the same two RB-36 aircraft used earlier during Shot Yucca were used as instrument platforms. Each aircraft carried spectrally-flat thermal-radiation detectors covering the range of 2,000 to 10,000 Å in four bands, a bolometer to measure the total thermal irradiance, gun-sight-aiming-point cameras with spectroscopic nosepieces, and a Traid camera with spectroscopic nosepieces. The data were recorded on dual fourteen-channel tape recording systems.

A complete set of data was obtained for each shot, from which an irradiance-versus-time analog record was made and the peak values computed. The thermal pulses of the two shots differed, in that Teak had only one principal maximum, while Orange showed some of

the characteristics of lower-altitude shots—an indication of a minimum followed by a second pulse of considerable magnitude. The first principal maximum occurred at approximately one-half millisecond on each shot, having a value of about 160 w/cm<sup>2</sup> for Teak and 12 w/cm<sup>2</sup> for Orange.

Project 8.3 "Growth of Fireball Radii at Very-High Altitudes (A)" (ITR-1649-1), Edgerton, Germeshausen and Grier, Boston, Massachusetts; Lewis Fussell, Project Officer.

The purpose of Project 8.3 was to determine, by photographic means, the modes by which energy is propagated and dissipated from nuclear explosions at very-high altitudes. A corollary objective was to document all visible aspects of the detonations for later analysis of any unforeseen phenomena.

The project analyzed the films from Shot Yucca, a very-high-altitude burst, detonated on 28 April 1958 at 1440 hours, 00.256 ± 2 msec. Records from five 70-mm streak cameras and two 35-mm Fastax cameras, which photographed the burst from two RB-36 aircraft, were analyzed to obtain a plot of diameter versus time for the fireball growth. A fireball diameter of about 40 meters was attained initially, becoming 136 meters by the time of the normal (third) minimum, and 260 meters by 20 msec.

Three light maxima were observed at approximately 0.1, 0.5, and 3.0 msec. A microdensitometer trace of one streak record revealed preliminary information concerning variations in brightness and temperature over the first 20 msec.

No attempt was made to calculate a yield, because of the uncertainties in scaling for high-altitude bursts.

Project 8.3 (Supplement) "Growth of Fireball Radii at Very-High Altitudes" (ITR-1649-2), Edgerton, Germeshausen and Grier, Boston, Massachusetts; Lewis Fussell, Project Officer.

The phenomena visible during the early stages of Shots Teak and Orange were photographed, and fireball diameter as a function of time was obtained from measurements of the photographic records. Yield was not calculated for either shot because of uncertainties in scaling for very-high-altitude bursts.

The diameter-time data, as recorded on Shots Teak and Orange, provide further information for an analysis of energy partition and propagation accompanying the detonation of nuclear weapons at high altitudes. Additional data from these films, including light intensity as a function of time and auroral phenomenology, will be analyzed for the final, WT, report.

Project 8.4 "Early-Time Spectra of a Very-High Altitude Nuclear Detonation (A)" (ITR-1650-1), U. S. Naval Radiological Defense Laboratory, San Francisco,



California; Edward C. Y. Inn, Project Officer.

Time-resolved bomb-light spectra at early times were photographed for a nuclear detonation at an altitude of about 90,000 feet (VHA). The 1.7-kt weapon was balloon-borne to altitude, and the spectra were photographed from two RB-36 aircraft cruising at an altitude of about 40,000 feet and a horizontal range of 12 naut mi. Each aircraft was equipped with a high-speed streak spectrograph. The time resolution of one of the modified quartz-prism spectrographs was adjusted to be about 50  $\mu$ sec, the other to about 225  $\mu$ sec. Two unusual features of the first pulse were noted, namely, the first pulse consisting of two maxima prior to the minimum and the presence of discrete absorption during the first 100  $\mu$ sec, extending from the ultraviolet cutoff at 3,000  $\text{\AA}$  into the infrared.

Project 8.4 (Supplement) "Early-Time Spectra of a Very-High-Altitude Nuclear Detonation" (ITR-1650-2), U. S. Naval Radiological Defense Laboratory, San Francisco, California; Edward C. Y. Inn, Project Officer.

The objective of this project was to photograph time-resolved bomb-light spectra from nuclear detonations at altitudes of about 250,000 feet (Shot Teak) and 141,000 feet (Shot Orange). The 3.8 Mt-weapon for each shot was missile-borne to altitude, and the spectra were photographed from two RB-36 aircraft cruising at an altitude of about 30,000 feet and a horizontal range of 70 naut mi. Each aircraft was equipped with a high-speed streak spectrograph, which consisted of a modified small-prism spectrograph. The time resolution of one was adjusted to about 20  $\mu$ sec and the other to about 115 to 130  $\mu$ sec.

The marked differences in the spectra of the two shots were highly indicative of the effect of ambient density and therefore the phenomenology associated with the formation of the fireball. Teller emission consisting of  $N_2$  and  $N_2^+$  bands was observed in both shots. The important difference was that for Teak Teller light the first positive system of  $N_2$  appeared strongly and the second positive only weakly, while for Orange, only the second positive system of  $N_2$  was present.

The Teak spectra indicated that the radiant energy was emitted in a single short pulse peaking at about 500  $\mu$ sec and dropping down to about 10 percent of the peak at about 10 msec. That for Orange consisted of a short first pulse peaking at about 500  $\mu$ sec and followed by a flat pulse with a duration of about 170 msec.

The Teak spectra appeared to consist only of strong molecular emission bands of  $N_2$ ,  $N_2^+$ , and possibly  $O_2^+$ , with no apparent emission continuum.

The Orange spectra during the maxima of the thermal pulse consisted essentially of a strong emission continuum superposed by discrete absorption bands of

$N_2^+$ , atmospheric  $O_3$ , and possibly other constituents. This was then followed by molecular band emission of  $N_2$ ,  $N_2^+$ , and possibly other constituents.

Project 8.5 "Narrow-Band Infrared Spectral Irradiance of Very-High-Altitude Bursts" (ITR-1651), Bureau of Aeronautics, Department of Navy, Washington, D. C.; R. Zirkind, Project Officer.

The objective of this project was to measure narrow-band infrared spectral irradiance from very-high-altitude nuclear detonations.

An air-borne station was equipped with an infrared monochromator, Perkin-Elmer Model 108A, and a modified AN/AAS-4 (XA-2) infrared mapping device. Each instrument had a single liquid-helium-cooled, zinc-doped germanium detector to measure the region of 2 to 12 microns with high sensitivity. The project participated in the high-altitude shots, Teak, Orange, and Yucca and in a sea-level shot, Koa, for correlation purposes. The monochromator provided spectra from 2 to 12 microns every 11 msec. The mapping device provided information on the diameter of the fireball every 1.3 seconds in the spectral bands,  $2.25 \pm 0.25$ ,  $3 \pm 0.4$ ,  $3.5 \pm 0.5$ ,  $3.9 \pm 0.4$ ,  $4 \pm 2$ , and  $7 \pm 5$  microns. Detailed analysis will be required to obtain final results. No observable infrared emission was obtained during Yucca. For Teak and Orange, the observable emission terminated at 2 and 18 seconds, respectively. In the case of Koa, infrared radiation was observed from 0.3 second to 3 seconds. The fireball radii for Teak and Orange were about 100,000 feet.

Project 8.6 "Vulnerability of Missile Structures to Nuclear Detonations" (ITR-1652), Aircraft Laboratory, Wright Air Development Center, Wright-Patterson Air Force Base, Ohio; C. J. Cosenza, Project Officer.

The work of Project 8.6 was divided into three studies, the first two conducted during Shot Cactus (ablation studies within the fireball) and the third during Shots Teak and Orange (destructive effects of very-high-altitude bursts). The basic objective was the collection of data to assist in the prediction of ICBM vulnerability to a nuclear detonation.

For the first study, four specimens were exposed inside the fireball of Shot Cactus, two of these to determine the rate of surface melting of a steel hemispherical surface, and the other two to measure the speed of sound within the fireball as a function of time. All of the time-history data were recorded by magnetic-tape recorders designed specifically to record electrical-instrumentation signals inside the fireball. In addition to the time-history instrumentation for the measurement of temperatures, pressures, and accelerations, passive gages were used

to record specimen velocity and the angle at which the specimens were hit by the shock wave. The specimens have been recovered and returned to Dayton, Ohio; however, due to the high radiation level, only a limited amount of analysis has been performed. The magnetic tapes have been removed from the four recorders. Three of the recorders apparently operated normally and a preliminary playback of the tapes indicates that there are signals on the tapes.

The second study had as its objective experiments of the ablation of materials exposed in Shot Cactus. The blow-off pressure of the ablating vapors was measured. Measurements were also made of the radiant energy from the fireball incident on objects immersed in the plasma, and of the effect of ablating vapors in filtering this radiation. The effects of neutron bombardment on a number of materials was observed. The radiation level of the general area after the detonation was unexpectedly high, so that immediate recovery was precluded. A thorough search was conducted when the radiation level had declined; however, the instrument carrier was not located.

For the third study, a jettisonable instrument pod was affixed to each of the (Teak and Orange) Redstone missiles. These pods were ejected prior to burnout, and were in the vicinity of the device at burst time. The pod exposed to the Teak detonation (250,000 feet) operated as programmed, was tracked by radar to burst time, and was recovered. A flashing light was the principal aid to recovery. There is strong evidence of X-ray-induced structural failure of the Teak pod. Measurements were made of the X-ray-induced mechanical impulses, neutron intensities, and thermal fluxes. The measured X-ray impulses, of the order of  $10^4$  dyne-sec/cm<sup>2</sup>, may be somewhat larger than anticipated.

The thermal neutron albedo of the atmosphere at this high-burst altitude was measured. Thermal damage to the pod was negligible, although iron surfaces on the pod were melted. The Orange pod was not recovered.

Project 8.7 "Thermal Radiation from a Very-Low-Yield Burst" (ITR - 1676), U. S. Army Chemical Warfare Laboratories, Army Chemical Center, Maryland; J. J. Mahoney, Project Officer.

The objectives of Project 8.7 were to determine the thermal radiant exposure versus distance from ground zero for a very-low-yield (fractional-kiloton) burst and to compare these values with theoretical results obtained from existing thermal scaling laws.

The radiant exposure for Shot Fig was found to range from 11.1 cal/cm<sup>2</sup> at 150 feet to 0.28 cal/cm<sup>2</sup>

at 900 feet from surface zero.

Values for thermal radiant exposure obtained from the regular scaling laws agree closely with the experimental values obtained from this test.

Project 8.8 "Thermal Radiation from Low-Yield Bursts" (ITR-1675), Air Force Cambridge Research Center, Laurence G. Hanscom Field, Bedford, Massachusetts; J. W. Reed, 1st Lt, USAF, Project Officer.

The objective of Project 8.8 during the NTS phase of Operation Hardtack was to measure the thermal phenomena resulting from the detonation of fractional-kiloton-yield nuclear devices. Measurements were made on six bursts with yields less than 1 kt. To provide correlation with these data, additional measurements were made on four bursts of greater than a kiloton yield.

In order to measure thermal irradiance as a function of time, wave length, and distance, two stations were instrumented with spectroscopic-radiation detectors covering the spectrum from 2,000 to 10,000 Å in 4 bands. A bolometer was used to measure total thermal irradiance, and a calorimeter to measure total thermal radiation. The data were recorded using multi-channel magnetic-tape recording systems. To supplement the electronically recorded information, cameras registered spectroscopic and documentary data.

Thermal data were obtained from each of the ten shots. The predicted and measured times to minimum and maximum for 5 fractional-kiloton bursts are furnished. In addition, the approximate values of irradiance at first and second maxima as measured from each burst for the various spectral ranges are presented. The large-yield scaling laws for times to minimum and maximum appeared to extend reasonably well to yields down to 5 tons; however, the scaling law for irradiance at second maximum failed to hold for the fractional-kiloton-yield bursts investigated. Second maxima generally were much lower than predicted values, and the deviation increased with decreasing yields.

#### PROGRAM 9: SUPPORT PHOTOGRAPHY

Project 9.1d "Temperature, Density, and Pressure of Upper Atmosphere During a Very-High-Altitude Nuclear Detonation" (ITR-1653), Cooper Development Corporation, Monrovia, California; R. E. Loftman, Project Officer.

In an effort to obtain supporting atmospheric data for Shot Teak, instrumented Nike-Asp sounding rockets were fired, using the falling-sphere technique to determine density, pressure, and temperature as a function of altitude between 200,000 and 300,000 feet.

The sphere contained a transit-time accelerometer to measure drag acceleration, a telemetry system to relay accelerometer-transit times to a ground station, and a DPN-19 beacon to provide, in conjunction with an MSQ-1A tracking radar, space-position data. An IBM 650 computer was available to resolve this raw data to solutions for density, temperature, and pressure.

All four soundings were unsuccessful, and firing of subsequent rounds was cancelled. Component failures within the sphere were the primary reason that upper atmospheric data were not obtained. It is recommended that the system be perfected and tested, pursuant to any future participations.

Project 9.2 "Shot Yucca: A Very-High-Altitude Nuclear Detonation" (ITR-1654), Office of the Deputy Chief of Staff, Weapons Effects Tests, Field Command, Armed Forces Special Weapons Project, Sandia Base, Albuquerque, New Mexico; Harry C. Henry, Lt Col, USAF, Special Assistant, Task Unit 7.1.3.

On 28 April 1958 at 1125:05 hours a 128-foot-diameter, 2-mil polyethylene balloon supporting a low-yield nuclear device and effect-measuring instrumentation was launched from the deck of the USS Boxer (CVS-21) within the Eniwetok Proving Ground. The objective of the program was to measure the effects of the detonation at an altitude of approximately 92,000 feet by means of close-in canister instrumentation and by means of instrumented aircraft. The device was successfully detonated at 1440 hours on 28 April 1958 by radio command at a pressure altitude of 85,000 feet or a radar-measured altitude of 85,500 feet. The burst yielded an estimated 1.7 kt and provided the necessary conditions for measuring the partition of energy and extending the scaling laws for low-yield weapons to 100,000 feet.

Due to command-transmitter failure prior to zero, no significant weapon-effect data was received from the five suspended canisters. Aircraft instrumentation is reported to have been successful.

Project 9.2b "Operation of Balloon Carrier for Very-High-Altitude Nuclear Detonation" (ITR-1655), Balloon Development Laboratory, Geophysics Research Directorate, Air Force Cambridge Research Center, Air Research and Development Command, Laurence G. Hanscom Field, Bedford, Massachusetts; A. E. Gilpatrick, Maj, USAF, Project Officer.

The project provided a platform for a nuclear device and measurement instrumentation at a pressure altitude of 85,000 feet (16 1/2 millibars) by means of a large plastic balloon. The original plan called for a development program based on a pay load of 600 pounds and a floating

altitude of approximately 90,000 feet. The actual weight was increased in small increments to a final weight of 761.5 pounds, with a corresponding decrease in altitude to 85,500 feet. The balloon system was launched from the deck of the USS Boxer (CVS-21). Prior to reaching ceiling altitude, the nuclear device was separated from the balloon a distance of 568 feet by a hydraulic load-lowering device, and the measurement instrumentation was additionally deployed along a nylon line at specific intervals totaling 3,000 feet below the nuclear device. Both the load-lowering device and the instrumentation-deployment system were developed by the project. Because of the support nature of the project mission, this report does not contain weapon-effect data.

It is concluded that the large, plastic, constant-volume balloon vehicle provided a stable and reliable platform for the very-high-altitude nuclear detonation, Shot Yucca.

Project 9.2c "Aircraft Modification and Instrumentation for High-Altitude Technical Photography" (ITR-1656), Weapons Effects Test Group, Field Command, Armed Forces Special Weapons Project, Sandia Base, Albuquerque, New Mexico; Jack G. James, Lt Col, USAF.

Operational requirements necessitated the test of effects of very-high-altitude nuclear detonations on Operation Hardtack. The report covers, in summary, the planning, design, and modification of two RB-36 aircraft as high-altitude-instrumentation platforms for Projects 8.2, 8.3, and 8.4.

Project 9.3a "Operation of Missile Carrier for Very-High-Altitude Nuclear Detonations" (ITR-1657), U.S. Army Ballistic Missile Agency, Redstone Arsenal, Alabama; Glenn P. Elliott, Col, USA, Project Officer.

Project 9.3a, with personnel from the U.S. Army Ballistic Missile Agency, Picatinny Arsenal, and Fort Belvoir, participated in Operation Hardtack by firing two Redstone missiles with [REDACTED]. The first firing, Shot Teak, took place on 31 July 1958, with a burst altitude of approximately 76 km; the second firing, Shot Orange, took place on 11 August 1958, with a burst altitude of approximately 38 km.

In addition to providing the carrier for these detonations, the U.S. Army Ballistic Missile Agency designed, mounted on the missile, and delivered to prescribed locations in space, four instrument carriers (pods), which were mounted on the surface of the thrust unit and expelled explosively from the thrust unit during the powered phase of the trajectory.

Certain indications of missile performance were provided the Missile Flight Safety Officer, as well as means of taking corrective action in the event of mal-



function. These were command destruction of the fuel tanks, command cutoff, and, in the case of Orange, a means of preventing warhead arm. Flight-performance data for both shots were recorded and are presented herein, as well as day-by-day records of preflight preparations.

Project 9.4 "Shots Wahoo and Umbrella: Two Underwater Nuclear Test Detonations" (ITR-1658), Office of the Deputy Chief of Staff, Weapons Effects Tests, Field Command, Armed Forces Special Weapons Project, Sandia Base, Albuquerque, New Mexico; Corwin G. Mendenhall, Jr., CAPT, USN.

Two underwater detonations were planned for Operation Hardtack: Shot Wahoo, to simulate a 10-kt weapon detonated 500 feet below the surface in water 3,000 feet deep and Shot Umbrella, to simulate a 10-kt weapon detonated on the bottom in about 150 feet of water. Shot Wahoo was detonated 16 May 1958 and Shot Umbrella was detonated 9 June 1958. The shots were fired against a target array composed of three destroyers, an EC-2 liberty ship, a submarine, and a submarine model.

The objectives of the tests were to document (1) the basic effects with regard to initial and residual radiation, air overpressures, underwater shock pressures, crater characteristics, mechanics of the base surge, and radiological contamination and (2) the response of selected targets to underwater shock pressures.

The objectives were met in all except a few areas, wherein they were partially met. It appears that, for the conditions of these tests, radiological effects will dictate safe delivery ranges for nuclear antisubmarine weapons by surface ships; for submarines, underwater pressures will dictate safe delivery ranges.

From the data obtained, it is expected that the following general results will follow: (1) a determination of safe minimum standoff distances for delivery of nuclear antisubmarine-warfare weapons by existing vehicles; (2) an improvement in predictions of lethal range of nuclear antisubmarine-warfare weapons against submarine and surface targets in shallow and in deep water; and (3) a determination of the mine field clearance capability of underwater nuclear bursts.

## REFERENCES

1. Special Weapons Test Planning Group, SWET 5, Report Number 5.
2. C. G. Mendenhall, Jr.; "Shots Wahoo and Umbrella: Two Underwater Nuclear Test Detonations"; Project 9.4, Operation Hardtack, ITR-1658, March 1959; Office of the Deputy Chief of Staff, Weapons Effects Tests, Field Command, Armed Forces Special Weapons Project, Sandia Base, Albuquerque, New Mexico; Secret Formerly Restricted Data.
3. V. L. Lynn and others; "Effects of Very-High-Altitude Bursts on Air-Borne Radar (S)"; Project 6.13, Operation Hardtack, ITR-1659, October 1958; Lincoln Laboratory, Massachusetts Institute of Technology, Lexington, Massachusetts; Secret Restricted Data.
4. E. Swift, Jr.; "Surface Phenomena from Underwater Bursts"; Project 1.3, Operation Hardtack, ITR-1608, January 1958; U. S. Naval Ordnance Laboratory, White Oak, Silver Spring, Maryland; Confidential Formerly Restricted Data.
5. C. J. Aronson and others; "Underwater Free-Field Pressures to Just Beyond Target Locations"; Project 1.2, Operation Wigwam, WT-1005, May 1957; Explosives Research Department, Naval Ordnance Laboratory, White Oak, Silver Spring, Maryland; Confidential Formerly Restricted Data.
6. G. K. Green; "Gamma Ray Intensities Measured by Radio Telemetry"; Crossroads Project IV-8, dated April 1947.
7. J. L. Tuck; "Radiation Intensity Versus Time Inside Target Ships"; Crossroads Project V-11, dated September 1946.
8. W. E. Strobe; "Investigation of Gamma Radiation Hazards Incident to an Underwater Atomic Explosion"; Operation Wigwam, Buships Report, March 1948; Bureau of Ships, U. S. Navy, Washington, D. C.
9. G. G. Molumphy and M. M. Bigger; "Proof Testing of Atomic Weapons Ship Countermeasures"; Project 6.4, Operation Castle, WT-927, October 1957; Naval Radiological Defense Laboratory, San Francisco, California; Confidential Formerly Restricted Data.
10. H. R. Rinnert; "Ship Shielding Studies"; Project 2.71, Operation Redwing, ITR-1321, October 1956; Naval Radiological Defense Laboratory, San Francisco, California; Confidential.
11. M. B. Hawkins and others; "Determination of Radiological Hazard to Personnel"; Project 2.4, Operation Wigwam, WT-1012, July 1956; Naval Radiological Defense Laboratory, San Francisco, California; Official Use Only.
12. F. R. Holden and others; "Radioactive Contamination of Ventilation Supply System, USS Crittenden, from Baker Explosion, Operation Crossroads"; Report No. AD-200 (X), 14 February 1950; Naval Radiological Defense Laboratory, San Francisco, California; Confidential.
13. G. Carp and others; "Initial Gamma Radiation Intensity and Neutron-Induced Gamma Radiation of NTS Soil"; Project 2.5, Operation Plumbbob, ITR-1414, November 1957; Army Signal Engineering Laboratories, Fort Monmouth, New Jersey; Secret Restricted Data.

14. F. B. Porzel; "Close-in Time of Arrival of Underwater Shock Wave"; Project 4.4, Operation Wigwam, WT-1034, June 1956; Armour Research Foundation of the Illinois Institute of Technology, Chicago, Illinois; Confidential Formerly Restricted Data.
15. "Capabilities of Atomic Weapons"; TM 23-200, Revised Edition, November 1957; Armed Forces Special Weapons Project, Washington, D. C.; Confidential.
16. "USNMCS Report No. 46"; Navy Mine Countermeasure Station (now U. S. Navy Mine Defense Laboratory), Panama City, Florida.
17. T. D. Hanscome and D. K. Willet; "Neutron Flux Measurements"; Project 2.2, Operation Teapot, WT-1116, July 1958; U. S. Naval Research Laboratory, Washington, D. C.; Secret Restricted Data.
18. Wayne C. Hall; "Neutron Measurements, Part III, High-Energy Spectrum (Time-of-Flight Method)"; Annex 1.5, Operation Greenhouse, WT-37, September 1951; Naval Research Laboratory, Washington, D. C.
19. P. A. Caldwell, T. D. Hanscome, and W. E. Kunz; "Attenuation of High Frequency and Ultra High Frequency by Ionization Resulting from Nuclear Explosions"; Project 6.6, Operation Redwing, ITR-1346, July 1956; Naval Research Laboratory, Washington, D. C.; Secret Restricted Data.
20. T. D. Hanscome and others; "Parameters Affecting Design of Instrumentation to Measure Gamma and Neutron Fluxes from a Very-High-Altitude Nuclear Detonation"; Project 2.7, Operation Plumbbob, ITR-1416, April 1959; Naval Research Laboratory, Washington, D. C.; Secret Restricted Data.
21. C. J. Cosenza and F. E. Barnett; "Vulnerability of Missile Structures to Nuclear Detonations"; Project 8.6, Operation Hardtack, WT-1652 (to be published); Aircraft Laboratory, Wright Air Development Center, Wright-Patterson Air Force Base, Ohio; Secret Restricted Data.
22. E. H. Bultman, G. F. McDonough and G. K. Sinnamon; "Loading on Simulated Buried Structures at High Incident Overpressures"; Project 1.7, Operation Plumbbob, ITR-1406, October 1957; Research Directorate, Air Force Special Weapons Center, Air Research and Development Command, Kirtland AFB, Albuquerque, New Mexico; Confidential Formerly Restricted Data.
23. J. F. Halsey and M. V. Barton; "Spectra of Ground Shocks Produced by Nuclear Detonations"; Project 1.9, Operation Plumbbob, ITR-1487, February 1958; Air Force Ballistic Missile Division, Air Research and Development Command, Inglewood, California; Confidential.
24. G. S. Hurst, R. H. Richie, and H. N. Wilson; Science Instr 22, 981; 1951; Unclassified.
25. David L. Rigotti, John W. Kinch, and Herbert O. Funsten; "Neutron Flux from Selected Nuclear Devices"; Project 2.3, Operation Plumbbob, ITR-1412, March 1958; Chemical Warfare Laboratories, Army Chemical Center, Maryland; Secret Restricted Data.
26. Gifford H. Albright; "Evaluation of Earth-Covered Prefabricated Ammunition Storage Magazines as Personnel Shelters"; Project 3.3, Operation Plumbbob, ITR-1422, November 1957; Department of the Navy, Office of the Chief of Civil Engineers, Research Division, Bureau of Yards and Docks, Washington, D. C.; Confidential Formerly Restricted Data.
27. Norman A. Haskell and Richard M. Brubaker; "Free-Air Atomic Blast Pressure Measurements"; Project 1.3, Operation Upshot-Knothole, AFCRC Technical Report 54-20, Novem-

ber 1953; Air Force Cambridge Research Center, Bedford, Massachusetts; Secret Restricted Data.

28. R. M. Chapman and M. H. Seavey; "Preliminary Report on the Attenuation of Thermal Radiation from Atomic or Thermonuclear Weapons"; AFCRC Technical Report 54-25, November 1954; Air Force Cambridge Research Center, Bedford, Massachusetts; Secret Restricted Data.

29. "Nuclear Radiation Handbook"; AFSWP-1100, March 1957; Armed Forces Special Weapons Project, Washington, D. C.; Secret Restricted Data.

30. M. Morganthau and others; "Land Fallout Studies"; Project 2.65, Operation Redwing, ITR-1319, December 1956; Radiological Division, Chemical Warfare Laboratories, Army Chemical Center, Maryland; Secret Restricted Data.

31. E. N. York, R. E. Boyd, and J. A. Blaylock; "Initial Neutron and Gamma Air-Earth Interface Measurements"; Project 2.10, Operation Plumbbob, ITR-1419, December 1957; Air Force Special Weapons Center, Kirtland Air Force Base, Albuquerque, New Mexico, Confidential, Formerly Restricted Data.

32. Philip W. Krey, Doris D. Peterson and Edward F. Wilsey; "Soil Activation by Neutrons"; Project 2.1, Operation Plumbbob, ITR-1410, December 1957; Chemical Warfare Laboratories, Army Chemical Center, Maryland; Secret Restricted Data.

33. C. W. Luke and others; "Neutron Flux Measurements"; Project 2.51, Operation Redwing, ITR-1313, December 1956; Chemical Warfare Laboratories, Army Chemical Center, Maryland; Secret Restricted Data.

34. P. I. Richards; "Prompt Doses and Dose Rates from Nuclear Weapons"; AFSWC-TR-58-13, May 1958; Air Force Special Weapons Center, Kirtland Air Force Base, Albuquerque, New Mexico; Secret Restricted Data.

35. M. A. Esmiol, Jr., and others; "In-Flight Structural Response of FJ-4 Aircraft to Nuclear Detonations"; Project 5.3, Operation Hardtack, ITR-1636, September 1958; U. S. Naval Air Special Weapons Facility, Kirtland Air Force Base, Albuquerque, New Mexico; Secret Restricted Data.

36. J. W. Reed and others; "Thermal Radiation from Low-Yield Bursts"; Project 8.8, Operation Hardtack, ITR-1675, January 1959; Air Force Cambridge Research Center, Laurence G. Hanscom Field, Bedford, Massachusetts; Secret Restricted Data.

37. F. Lavicka and G. Lang; "Wave Form of Electromagnetic Pulse from Nuclear Detonations"; Project 6.4, Operation Hardtack, ITR-1638, July 1958; Army Signal Research and Development Laboratory, Fort Monmouth, New Jersey; Secret Restricted Data.

## DISTRIBUTION

### Military Distribution Category 100

#### ARMY ACTIVITIES

- |   |  |
|---|--|
| <p>1 Deputy Chief of Staff for Military Operations, D/A, Washington 25, D.C. ATTN: Dir. of SW&amp;R</p> <p>2 Chief of Research and Development, D/A, Washington 25, D.C. ATTN: Atomic Div.</p> <p>3 Assistant Chief of Staff, Intelligence, D/A, Washington 25, D.C.</p> <p>4- 5 Chief Chemical Officer, D/A, Washington 25, D.C.</p> <p>6 Chief of Engineers, D/A, Washington 25, D.C. ATTN: ENGNB</p> <p>7 Chief of Engineers, D/A, Washington 25, D.C. ATTN: ENGB</p> <p>8 Chief of Engineers, D/A, Washington 25, D.C. ATTN: ENGTB</p> <p>9- 10 Office, Chief of Ordnance, D/A, Washington 25, D.C. ATTN: ORDIN</p> <p>11 Chief Signal Officer, D/A, Comb. Dev. and Ops. Div., Washington 25, D.C. ATTN: SIGCO-4</p> <p>12 Chief of Transportation, D/A, Office of Planning and Int., Washington 25, D.C.</p> <p>13 The Surgeon General, D/A, Washington 25, D.C. ATTN: MEDNE</p> <p>14- 16 Commanding General, U.S. Continental Army Command, Ft. Monroe, Va.</p> <p>17 Director of Special Weapons Development Office, Headquarters COMARC, Ft. Bliss, Tex. ATTN: Capt. Chester I. Peterson</p> <p>18 President, U.S. Army Artillery Board, U.S. Continental Army Command, Ft. Sill, Okla.</p> <p>19 President, U.S. Army Infantry Board, Ft. Benning, Ga.</p> <p>20 President, U.S. Army Air Defense Board, U.S. Continental Army Command, Ft. Bliss, Tex.</p> <p>21 President, U.S. Army Aviation Board, Ft. Rucker, Ala. ATTN: ATEG-DC</p> <p>22 Commanding General, First United States Army, Governor's Island, New York 4, N.Y.</p> <p>23 Commanding General, Second U.S. Army, Ft. George G. Meade, Md.</p> <p>24 Commanding General, Third United States Army, Ft. McPherson, Ga. ATTN: ACofS G-3</p> <p>25 Commanding General, Fourth United States Army, Ft. Sam Houston, Tex. ATTN: G-3 Section</p> <p>26 Commanding General, Fifth United States Army, 1660 E. Hyde Park Blvd., Chicago 15, Ill.</p> <p>27 Commanding General, Sixth United States Army, Presidio of San Francisco, San Francisco, Calif. ATTN: AMGCT-4</p> <p>28 Commanding General, Military District of Washington, USA, Room 1543, Bldg. T-7, Gravelly Point, Va.</p> <p>29 Commandant, Army War College, Carlisle Barracks, Pa. ATTN: Library</p> <p>30 Commandant, U.S. Army Command &amp; General Staff College, Ft. Leavenworth, Kansas. ATTN: ARCHIVES</p> <p>31 Commandant, U.S. Army Air Defense School, Ft. Bliss, Tex. ATTN: Dept. of Tactics and Combined Arms</p> <p>32 Commandant, U.S. Army Armored School, Ft. Knox, Ky.</p> <p>33 Commandant, U.S. Army Artillery and Missile School, Ft. Sill, Okla. ATTN: Combat Development Department</p> <p>34 Commandant, U.S. Army Aviation School, Ft. Rucker, Ala.</p> <p>35 Commandant, U.S. Army Infantry School, Ft. Benning, Ga. ATTN: C.D.S.</p> <p>36 The Superintendent, U.S. Military Academy, West Point, N.Y. ATTN: Prof. of Ordnance</p> <p>37 Commandant, The Quartermaster School, U.S. Army, Ft. Lee, Va. ATTN: Chief, QM Library</p> <p>38 Commandant, U.S. Army Ordnance School, Aberdeen Proving Ground, Md.</p> <p>39 Commandant, U.S. Army Ordnance and Guided Missile School, Redstone Arsenal, Ala.</p> <p>40 Commanding General, Chemical Corps Training Comd., Ft. McClellan, Ala.</p> <p>41 Commandant, USA Signal School, Ft. Monmouth, N.J.</p> <p>42 Commandant, USA Transport School, Ft. Eustis, Va. ATTN: Security and Info. Off.</p> | <p>43 Commanding General, The Engineer Center, Ft. Belvoir, Va. ATTN: Asst. Cmdt, Engr. School</p> <p>44 Commanding General, Army Medical Service School, Brooke Army Medical Center, Ft. Sam Houston, Tex.</p> <p>45 Director, Armed Forces Institute of Pathology, Walter Reed Army Med. Center, 625 16th St., NW, Washington 25, D.C.</p> <p>46 Commanding Officer, Army Medical Research Lab., Ft. Knox, Ky.</p> <p>47 Commandant, Walter Reed Army Inst. of Res., Walter Reed Army Medical Center, Washington 25, D.C.</p> <p>48 Commanding General, Qm R&amp;D Comd., QM R&amp;D Cntr., Natick, Mass. ATTN: CBR Liaison Officer</p> <p>49 Commanding General, Qm. Research and Engr. Comd., USA, Natick, Mass.</p> <p>50- 51 Commanding General, U.S. Army Chemical Corps, Research and Development Comd., Washington 25, D.C.</p> <p>52- 53 Commanding Officer, Chemical Warfare Lab., Army Chemical Center, Md. ATTN: Tech. Library</p> <p>54 Commanding General, Engineer Research and Dev. Lab., Ft. Belvoir, Va. ATTN: Chief, Tech. Support Branch.</p> <p>55 Director, Waterways Experiment Station, P.O. Box 631, Vicksburg, Miss. ATTN: Library</p> <p>56 Commanding Officer, Office of Ordnance Research, Box CM, Duke Station, Durham, North Carolina</p> <p>57 Commanding Officer, Picatinny Arsenal, Dover, N.J. ATTN: ORDBB-IX</p> <p>58 Commanding Officer, Diamond Ord. Fuze Labs., Washington 25, D.C. ATTN: Chief, Nuclear Vulnerability Br. (230)</p> <p>59- 60 Commanding General, Aberdeen Proving Grounds, Md. ATTN: Director, Ballistics Research Laboratory</p> <p>61 Commanding General, Frankford Arsenal, Bridge and Tacony St., Philadelphia, Pa.</p> <p>62- 63 Commanding Officer, Watervliet Arsenal, Watervliet, New York. ATTN: ORDEF-RR</p> <p>64- 65 Commanding General, U.S. Army Ord. Missile Command, Redstone Arsenal, Ala.</p> <p>66 Commander, Army Rocket and Guided Missile Agency, Redstone Arsenal, Ala. ATTN: Tech Library</p> <p>67 Commanding General, White Sands Proving Ground, Las Cruces, N. Mex. ATTN: ORDES-OM</p> <p>68 Commander, Army Ballistic Missile Agency, Redstone Arsenal, Ala. ATTN: ORDAB-HT</p> <p>69 Commanding Officer, Ord. Materials Research Off., Watertown Arsenal, Watertown 72, Mass. ATTN: Dr. Foster</p> <p>70 Commanding General, Ordnance Tank Automotive Command, Detroit Arsenal, Centerline, Mich. ATTN: ORDMC-RO</p> <p>71- 72 Commanding General, Ordnance Ammunition Command, Joliet, Ill.</p> <p>73 Commanding General, Ordnance Weapons Command, Rock Island, Ill.</p> <p>74 Commanding Officer, USA Signal R&amp;D Laboratory, Ft. Monmouth, N.J.</p> <p>75 Commanding General, U.S. Army Electronic Proving Ground, Ft. Huachuca, Ariz. ATTN: Tech. Library</p> <p>76 Commanding Officer, USA, Signal R&amp;D Laboratory, Ft. Monmouth, N.J. ATTN: Tech. Doc. Ctr., Evans Area</p> <p>77 Commanding Officer, USA Transportation R&amp;E Comd., Ft. Eustis, Va. ATTN: Chief, Tech. Svcs. Div.</p> <p>78 Commanding Officer, USA Transportation Combat Development Group, Ft. Eustis, Va.</p> <p>79 Director, Operations Research Office, Johns Hopkins University, 6935 Arlington Rd., Bethesda 14, Md.</p> <p>80 Commandant, U. S. Army Chemical Corps, CBR Weapons School, Dugway Proving Ground, Dugway, Utah</p> <p>81 Commanding General, U.S. ORD Special Weapons-Ammunition Command, Dover, N.J.</p> <p>82 Commander-in-Chief, U.S. Army Europe, APO 403, New York, N.Y. ATTN: Opt. Div., Weapons Br.</p> |
|---|--|

83 Commanding General, Southern European Task Force, APO 168, New York, N.Y. ATTN: ACofS G-3  
 84 Commanding General, Eighth U.S. Army, APO 301, San Francisco, Calif. ATTN: ACofS G-3  
 85 Commanding General, U.S. Army Alaska, APO 942, Seattle, Washington  
 86 Commanding General, U.S. Army Caribbean, Ft. Amador, Canal Zone. ATTN: Cml Office  
 87 Commander-in-Chief, U.S. Army Pacific, APO 958, San Francisco, Calif. ATTN: Ordnance Officer  
 88 Commanding General, USARFANT & MDPB, Ft. Brooke, Puerto Rico  
 89 Commander-in-Chief, EUCOM, APO 128, New York, N.Y.  
 90 Commanding Officer, 9th Hospital Center, APO 180, New York, N.Y. ATTN: CO, US Army Nuclear Medicine Research Detachment, Europe

NAVY ACTIVITIES

91 Chief of Naval Operations, D/N, Washington 25, D.C. ATTN: OP-03EG  
 92 Chief of Naval Operations, D/N, Washington 25, D.C. ATTN: OP-31  
 93 Chief of Naval Operations, D/N, Washington 25, D.C. ATTN: OP-75  
 94 Chief of Naval Operations, D/N, Washington 25, D.C. ATTN: OP-91  
 95 Chief of Naval Personnel, D/N, Washington 25, D.C.  
 96-97 Chief of Naval Research, D/N, Washington 25, D.C. ATTN: Code 811  
 98-99 Chief, Bureau of Aeronautics, D/N, Washington 25, D.C.  
 100-104 Chief, Bureau of Aeronautics, D/N, Washington 25, D.C. ATTN: AER-AD-41/20  
 105 Chief, Bureau of Medicine and Surgery, D/N, Washington 25, D.C. ATTN: Special Wpns. Def. Div.  
 106 Chief, Bureau of Ordnance, D/N, Washington 25, D.C.  
 107 Chief, Bureau of Ordnance, D/N, Washington 25, D.C. ATTN: S.P.  
 108 Chief, Bureau of Ships, D/N, Washington 25, D.C. ATTN: Code 423  
 109 Chief, Bureau of Supplies and Accounts, D/N, Washington 25, D.C.  
 110 Chief, Bureau of Yards and Docks, D/N, Washington 25, D.C. ATTN: D-440  
 111 Director, U.S. Naval Research Laboratory, Washington 25, D.C. ATTN: Mrs. Katherine H. Cass  
 112-113 Commander, U.S. Naval Ordnance Laboratory, White Oak, Silver Spring 19, Md.  
 114 Director, Material Lab. (Code 900), New York Naval Shipyard, Brooklyn 1, N.Y.  
 115 Commanding Officer and Director, Navy Electronics Lab., San Diego 52, Calif.  
 116 Commanding Officer, U.S. Naval Mine Defense Lab., Panama City, Fla.  
 117-120 Commanding Officer, U.S. Naval Radiological Defense Laboratory, San Francisco, Calif. ATTN: Tech. Info. Div.  
 121 Officer-in-Charge, U.S. Naval Civil Engineering R&E Lab., U.S. Naval Construction Bn. Center, Port Hueneme, Calif. ATTN: Code 753  
 122 Superintendent, U.S. Naval Academy, Annapolis, Md.  
 123 Commanding Officer, U.S. Naval Schools Command, U.S. Naval Station, Treasure Island, San Francisco, Calif.  
 124 President, U.S. Naval War College, Newport, Rhode Island  
 125 Superintendent, U.S. Naval Postgraduate School, Monterey, Calif.  
 126 Officer-in-Charge, U.S. Naval School, CEC Officers, U.S. Naval Construction Bn. Center, Port Hueneme, Calif.  
 127 Commanding Officer, Nuclear Weapons Training Center, Atlantic, U.S. Naval Base, Norfolk 11, Va. ATTN: Nuclear Warfare Dept.  
 128 Commanding Officer, Nuclear Weapons Training Center, Pacific, Naval Station, San Diego, Calif.  
 129 Commanding Officer, U.S. Naval Damage Control Tng. Center, Naval Base, Philadelphia 12, Pa. ATTN: ABC Defense Course  
 130 Commanding Officer, Air Development Squadron 5, VX-5, China Lake, Calif.  
 131 Director, Naval Air Experiment Station, Air Material Center, U.S. Naval Base, Philadelphia, Pa.  
 132 Commander, Officer U.S. Naval Air Development Center, Johnsville, Pa. ATTN: NAS, Librarian  
 133 Commanding Officer, U.S. Naval Medical Research Institute, National Naval Medical Center, Bethesda, Md.  
 134 Commander, U.S. Naval Ordnance Test Station, China Lake, Calif.

135 Commanding Officer and Director, David W. Taylor Model Basin, Washington 7, D.C. ATTN: Library  
 136-137 Commanding Officer and Director, U.S. Naval Engineering Experiment Station, Annapolis, Md.  
 138 Officer-in-Charge, U.S. Naval Supply Research and Development Facility, Naval Supply Depot, Bayonne, N.J.  
 139 Commander, Norfolk Naval Shipyard, Portsmouth, Va. ATTN: Underwater Explosions Research Division  
 140-141 Commander-in-Chief, U.S. Atlantic Fleet, U.S. Naval Base, Norfolk 11, Va.  
 142-145 Commandant, U.S. Marine Corps, Washington 25, D.C. ATTN: Code AO3H  
 146 Commanding General, Fleet Marine Force, Atlantic, Norfolk, Va.  
 147 Director, U.S.M.C. Development Center, U.S.M.C. Schools, Quantico, Va.  
 148 Director, U.S.M.C. Educational Center, U.S.M.C. Schools, Quantico, Va.  
 149 Commandant, U.S. Coast Guard, 1300 E. St., NW, Washington 25, D.C. ATTN: (OIN)  
 150 Commanding Officer, U.S. Naval CIC School, U.S. Naval Air Station, Glynco, Brunswick, Ga.  
 151 Commander-in-Chief, Pacific, c/o Fleet Post Office, San Francisco, Calif.  
 152-153 Commander-in-Chief, U.S. Pacific Fleet, Fleet Post Office, San Francisco, Calif.  
 154 Commanding General, Fleet Marine Force, Pacific, Fleet Post Office, San Francisco, Calif.

AIR FORCE ACTIVITIES

155 Assistant for Atomic Energy, HQ, USAF, Washington 25, D.C. ATTN: DCS/O  
 156 Deputy Chief of Staff, Development, HQ, USAF, Washington 25, D.C. ATTN: AFDDP  
 157 Deputy Chief of Staff, Operations, HQ, USAF, Washington 25, D.C. ATTN: AFOOP  
 158 Deputy Chief of Staff, Operations HQ, USAF, Washington 25, D.C. ATTN: Operations Analysis  
 159 Director of Civil Engineering, HQ, USAF, Washington 25, D.C. ATTN: AFOCE  
 160-161 Assistant Chief of Staff, Intelligence, HQ, USAF, Washington 25, D.C. ATTN: AFCIN-3B  
 162 Deputy Chief of Staff, Plans and Programs, HQ, USAF, Washington 25, D.C. ATTN: War Plans Division  
 163 Director of Research and Development, DCS/D, HQ, USAF, Washington 25, D.C. ATTN: Guidance and Weapons Div.  
 164 The Surgeon General, HQ, USAF, Washington 25, D.C. ATTN: Bio-Def. Pre. Med. Division  
 165 Commander-in-Chief, Strategic Air Command, Offutt AFB, Neb. ATTN: OAWS  
 166 Commander, Tactical Air Command, Langley AFB, Va. ATTN: Doc. Security Branch  
 167 Commander, Air Defense Command, Ent AFB, Colorado. ATTN: Atomic Energy Div., ADLAN-A  
 168 Commander, Air Material Command, Wright-Patterson AFB, Dayton, Ohio. ATTN: MCSM  
 169 Commander, Air Force Ballistic Missile Div. HQ, ARDC, Air Force Unit Post Office, Los Angeles 45, Calif. ATTN: WDSOT  
 170 Commander, Hq. Air Research and Development Command, Andrews AFB, Washington 25, D.C. ATTN: RDRWA  
 171 Commander, Second Air Force, Barksdale AFB, La. ATTN: Operations Analysis Office  
 172 Commander, Eighth Air Force, Westover AFB, Mass. ATTN: Operations Analysis Office  
 173 Commander, Fifteenth Air Force, March AFB, Calif. ATTN: Operations Analysis Office  
 174 Commander, Air Proving Ground Center, Eglin AFB, Fla. ATTN: PCTRL  
 175-176 Commander, AF Cambridge Research Center, L. G. Hanscom Field, Bedford, Mass. ATTN: CRQST-2  
 177-181 Commander, Air Force Special Weapons Center, Kirtland AFB, Albuquerque, N. Mex. ATTN: Tech. Info. & Intel. Div.  
 182-183 Director, Air University Library, Maxwell AFB, Ala.  
 184 Commander, Lowry AFB, Denver, Colorado. ATTN: Dept. of Sp. Wpns. Tng.  
 185 Commandant, School of Aviation Medicine, USAF, Randolph AFB, Tex. ATTN: Research Secretariat  
 186 Commander, 1009th Sp. Wpns. Squadron, HQ, USAF, Washington 25, D.C.  
 187-189 Commander, Wright Air Development Center, Wright-Patterson AFB, Dayton, Ohio. ATTN: WCOSI  
 190-191 Director, USAF Project RAND, VIA: USAF Liaison Office, The RAND Corp., 1700 Main St., Santa Monica, Calif.  
 192 Commander, 3535th Navigator Wing, Mather AFB, Calif.  
 193 Chief, Ballistic Missile Early Warning Project Office, 220 Church St., New York 13, N.Y. ATTN: Col. Leo V. Skinner, USAF

**SECRET**

- 194-195 Commander, Air Technical Intelligence Center, USAF, Wright-Patterson AFB, Ohio. ATTN: AFCIN-4B1a, Library
- 196 Assistant Chief of Staff, Intelligence, HQ. USAFE, APO 633, New York, N.Y. ATTN: Directorate of Air Targets
- 197 Commander, Alaskan Air Command, APO 942, Seattle, Washington. ATTN: AAOTN
- 198 Commander-in-Chief, Pacific Air Forces, APO 953, San Francisco, Calif. ATTN: PFCIE-MB, Base Recovery

OTHER DEPARTMENT OF DEFENSE ACTIVITIES

- 199-200 Director of Defense Research and Engineering, Washington 25, D.C. ATTN: Tech. Library
- 201 Executive Secretary, Military Liaison Committee, P.O. Box 1814, Washington 25, D.C.
- 202 Executive Secretary, Joint Chiefs of Staff, Washington 25, D.C.
- 203 Chairman, Armed Services Explosives Safety Board, DOD, Building T-7, Gravelly Point, Washington 25, D.C.
- 204 Director, Weapons Systems Evaluation Group, Room 1E880, The Pentagon, Washington 25, D.C.
- 205 Commandant, The Industrial College of The Armed Forces, Ft. McNair, Washington 25, D.C.
- 206 Commandant, Armed Forces Staff College, Norfolk 11, Va. ATTN: Secretary
- 207-214 Chief, Defense Atomic Support Agency, Washington 25, D. C.
- 215 Commander, Field Command, DASA, Sandia Base, Albuquerque, N. Mex.

- 216 Commander, Field Command, DASA, Sandia Base, Albuquerque, N. Mex. ATTN: FCTG
- 217-226 Commander, Field Command, DASA, Sandia Base, Albuquerque, N. Mex. ATTN: FCWT
- 227 Commander, JTF-7, Arlington Hall Station, Arlington 12, Va.
- 228 U.S. Documents Officer, Office of the United States National Military Representative - SHAPE, APO 55, New York, N.Y.

ATOMIC ENERGY COMMISSION ACTIVITIES

- 229-231 U.S. Atomic Energy Commission, Technical Library, Washington 25, D. C. ATTN: DMA
- 232-233 Los Alamos Scientific Laboratory, Report Library, P.O. Box 1663, Los Alamos, N. Mex. ATTN: Helen Redmar
- 234-238 Sandia Corporation, Classified Document Division, Sandia Base, Albuquerque, N. Mex. ATTN: R. J. Smyth, Jr.
- 239-241 University of California Lawrence Radiation Laboratory, P.O. Box 808, Livermore, Calif. ATTN: Clovis G. Craig
- 242 Essential Operating Records, Div. of Infor. Services for Storage at ERC-H. ATTN: John E. Hans, Chief, Headquarters Records and Mail Service Branch, U.S. AEC, Washington 25, D.C.
- 243 Weapon Data Section, Technical Information Service Extension, Oak Ridge, Tenn.
- 244-280 Technical Information Service Extension, Oak Ridge, Tenn. (Surplus)

**SECRET**  
**RESTRICTED**